AD-A150 653 PROCEEDINGS OF THE INTERNATIONAL CONFERENCE ON THE PERFORMANCE OF OFF ROAD (U) INTERNATIONAL SOCIETY FOR TERRAIN VEHICLE SYSTEMS M J DWYER AUG 84 1/4

UNCLASSIFIED [illegible] F/G 13/6 NL

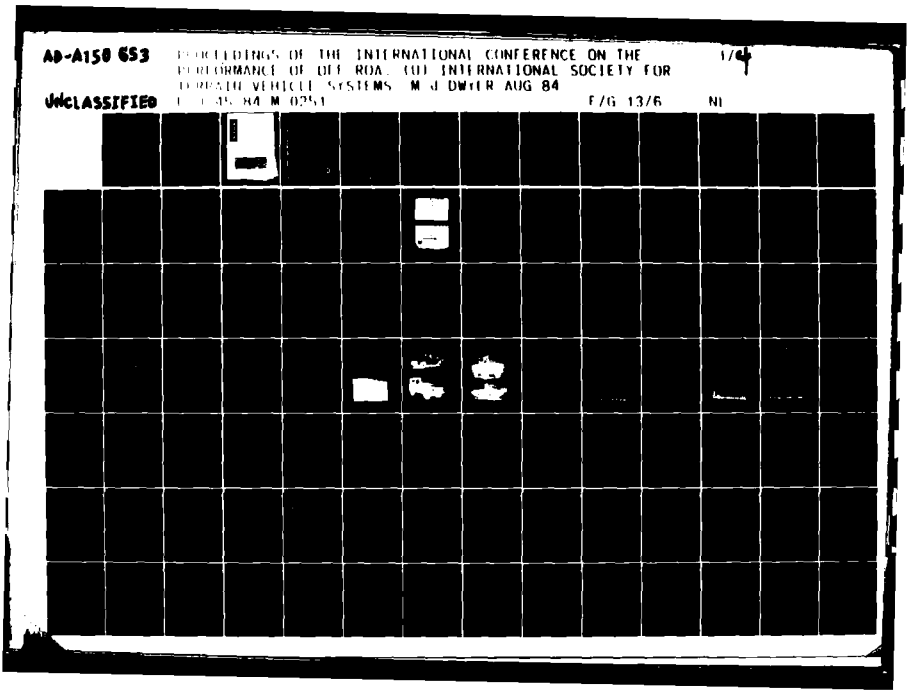

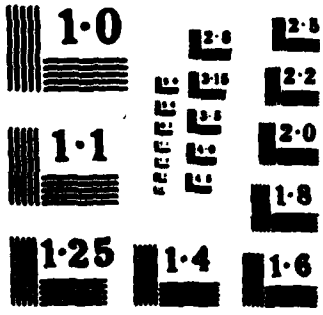
1·0
1·1
1·25
1·4
1·6
1·8
2·0
2·2
2·5

Unclassified

SECURITY CLASSIFICATION OF THIS PAGE (When Data Entered)

REPORT DOCUMENTATION PAGE		READ INSTRUCTIONS BEFORE COMPLETING FORM
1. REPORT NUMBER	2. GOVT ACCESSION NO.	3. RECIPIENT'S CATALOG NUMBER
4. TITLE (and Subtitle) PROCEEDINGS: 8th INTERNATIONAL CONFERENCE INT. SOC. FOR TERRAIN VEHICLE SYSTEMS		5. TYPE OF REPORT & PERIOD COVERED FINAL MAY - AUG 1984 6. PERFORMING ORG. REPORT NUMBER
7. AUTHOR(s) ED: MICHAEL J. DWYER		8. CONTRACT OR GRANT NUMBER(s) DAJA45-84-M-0251
9. PERFORMING ORGANIZATION NAME AND ADDRESS INT. SOC. FOR TERRAIN VEHICLE SYSTEMS NIAE, WREST PARK, SILSOE BEDFORD MK45 4HS, U.K.		10. PROGRAM ELEMENT, PROJECT, TASK AREA & WORK UNIT NUMBERS 61102A-It161102-BH57-01
11. CONTROLLING OFFICE NAME AND ADDRESS USARDSG-UK PO Box 65 FPO NY, NY 09510-1000		12. REPORT DATE AUG 84 13. NUMBER OF PAGES 1304 (3 vols)
14. MONITORING AGENCY NAME & ADDRESS(if different from Controlling Office)		15. SECURITY CLASS. (of this report) Unclassified 15a. DECLASSIFICATION/DOWNGRADING SCHEDULE

16. DISTRIBUTION STATEMENT (of this Report)

Approved for public release; distribution unlimited.

17. DISTRIBUTION STATEMENT (of the abstract entered in Block 20, if different from Report)

18. SUPPLEMENTARY NOTES

19. KEY WORDS (Continue on reverse side if necessary and identify by block number)

MOBILITY; CROSS-COUNTRY MOBILITY; OFF-ROAD MOBILITY; SOIL-VEHICLE INTERACTION; VEHICLE DYNAMICS.

20. ABSTRACT (Continue on reverse side if necessary and identify by block number)

The three volumes consist of a collection of all significant papers presented at the 8th International Conference. Subjects include; Tyre-soil interaction; theoretical aspects of ride dynamics; track-soil interaction; practical aspects of ride dynamics; operation in paddy fields; operation on steep slopes; soil compaction; steering; computer modelling; vehicle component design; measurement of soil and snow properties and soil bin facilities; and vehicle design. Other keywords include:

DD FORM 1 JAN 73 1473 EDITION OF 1 NOV 65 IS OBSOLETE

Unclassified

SECURITY CLASSIFICATION OF THIS PAGE (When Data Entered)

INTERNATIONAL SOCIETY FOR TERRAIN VEHICLE SYSTEMS

USACRREL, 72 Lyme Road, Hanover, New Hampshire, 03755, USA

SFM/FOA 2, Box 27322, S-102 54, Stockholm, Sweden

8th International Conference

The Performance of Off-Road Vehicles and Machines

August 5-11, 1984

Churchill College, Cambridge University, England

Proceedings

Volume III of III

VOLUME III

TOPIC 9

COMPUTER MODELLING

ENERGY FOR FIELD OPERATIONS IN DEVELOPING COUNTRIES

C.P. CROSSLEY

SILSOE COLLEGE, SILSOE, BEDFORD, U.K.

1. INTRODUCTION

Oil prices have risen from 2 dollars per barrel in 1972 to over 30 dollars per barrel in 1982/83. After adjusting for inflation the 1972 price would be equivalent to about 14 dollars in 1982, so it can be seen that prices have more than doubled in real terms in ten years, (Figure 1).

The effect of such a price increase has been particularly severe in those developing countries having no oil supply sources of their own. Agricultural production of cash crops for export is very often an important source of foreign exchange for the purchase of fuel, and in many cases world prices of exported commodities have not increased substantially over the same period. Some countries are fortunate in having oil supply sources of their own or, like Brazil, have agricultural conditions suitable for the provision of large quantities of non fossil-based fuel from commodities such as sugar, sunflower seed and cassava. Other countries however have relatively little opportunity for the economic development of alternative fuel sources and will continue to rely heavily on external supplies of fuel.

Since agricultural production is an important aspect of the economy of most developing countries and usually involves a large proportion of the population in subsistence or cash crop agriculture, there is likely to be a continuing need for engine powered mechanization in the agricultural sector, using both large and small scale equipment. Traditional hand and animal power sources overcome the fuel supply problem and should be the preferred alternatives where they are suitable, but due in part to the limited power available from these sources it is necessary to utilize field machinery in many situations. This paper identifies the stages of energy use associated with engine powered field equipment, and investigates the possibilities for energy reduction within the various stages.

2. AN EXAMPLE OF THE SCOPE FOR ENERGY REDUCTION

From work carried out in semi-arid conditions in Botswana it has been established that the use of four tines spaced at 750 mm in a cultivation technique known as precision strip tillage (PST) resulted in a total draught requirement of 12.2 kN compared with 12.6 kN for 3 mouldboard ploughs. Due to the increased width of work the energy required at the implement in precision strip tillage was reduced to 40.3 MJ/ha compared with 105 MJ/ha using conventional 400 mm mouldboard ploughs (Willcocks, 1981). This illustrates the effect that a change in cultivation practice can have on energy requirements. For the purpose of this paper, the above implement energy requirements were used to enable predictions of tractor energy consumption to be made. Losses due to wheel slip, rolling resistance, transmission inefficiency and turning time increased the predicted tractor energy consumption during cultivation to 65 MJ/ha

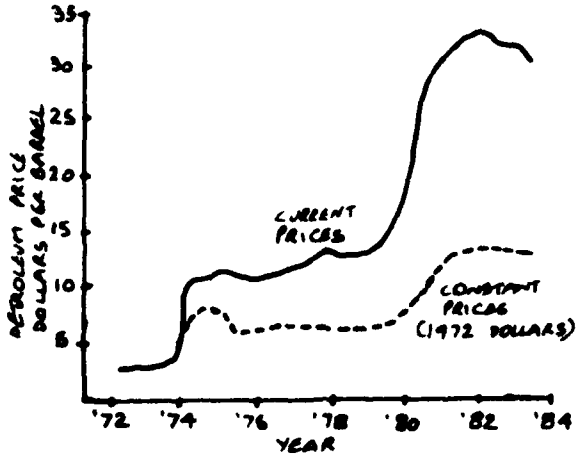

Fig 1. Petroleum prices 1972 - 83

Source: World Development Report 1983, IBRD

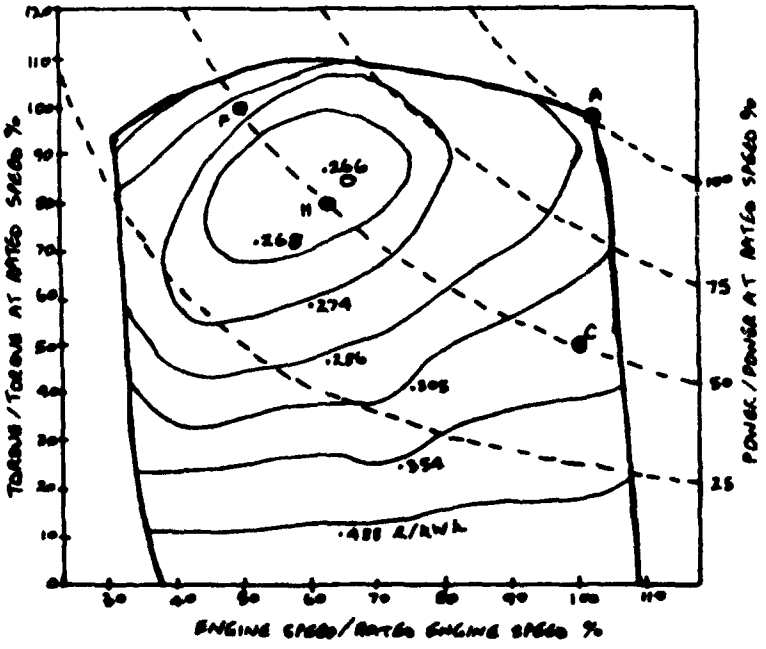

Fig 3. Typical tractor engine specific fuel consumption map.

After Mathews, The Agricultural Engineer, (1982) 37,3

for PST and 169 MJ/ha for mouldboard ploughing. The corresponding predicted fuel consumptions were 6.39 l/ha and 16.2 l/ha respectively, while the predicted rates of work were 1.28 h/ha and 3.21 h/ha. The speed used in the calculations (based on the data from Botswana) was 0.9 m/s and only around one-third of the engine power of a 50 kW tractor would then be used. Depending on the combination of torque and engine speed selected by the operator this may give either better or worse specific fuel consumption than is achieved at near full power, but it does not represent an efficient utilization of a high powered machine. Changing the implement to five tines and running the tractor at 1.8 m/s gave a predicted rate of work of 0.51 h/ha and the predicted fuel consumption fell to 5.1 l/ha, due to a more efficient torque/speed combination. For detailed calculations see Appendix.

The above considerations indicate the complexity of the choices involved in attempting to reduce energy consumption. The various stages of energy use in a cultivation operation are now examined. The procedure described may also be applied in principle to other field operations such as crop husbandry or harvesting. Primary cultivation is usually the single most energy-intensive operation however and is considered for that reason.

3. STAGES OF ENERGY USE AND THE SCOPE FOR IMPROVEMENT

Figure 2 shows the process by which energy in the form of fuel is used in cultivation operations to provide a required change in soil conditions, and also identifies seven main areas in which energy requirements could be reduced. These are:

(i) To increase the efficiency with which the engine uses fuel. This is an engine design problem.

(ii) To improve the engine operation efficiency, ie. endeavouring to work at the lowest specific fuel consumption available at the particular power demand. This is traditionally an operator training/motivation problem, but recent advances in commercial vehicle transmissions could eventually provide aids to tractor operation.

(iii) To improve the overall transmission efficiency. This is taken to include all stages between the engine flywheel and the wheels, and involves problems of gear design and power absorption.

(iv) To reduce energy consumption in the ground drive system caused by rolling resistance and slip losses at the wheels.

(v) To reduce the energy requirement of the implement. This involves detailed implement redesign to reduce specific draught forces.

(vi) To reduce the required amount of soil disturbance. Here there are opportunities for techniques such as precision strip tillage, minimum or zero tillage, bed systems, etc.

(vii) To improve the efficiency of field operation. Here the problem comes from a combination of machine management and operating conditions. It includes aspects of tractor scheduling, transport time and field efficiency.

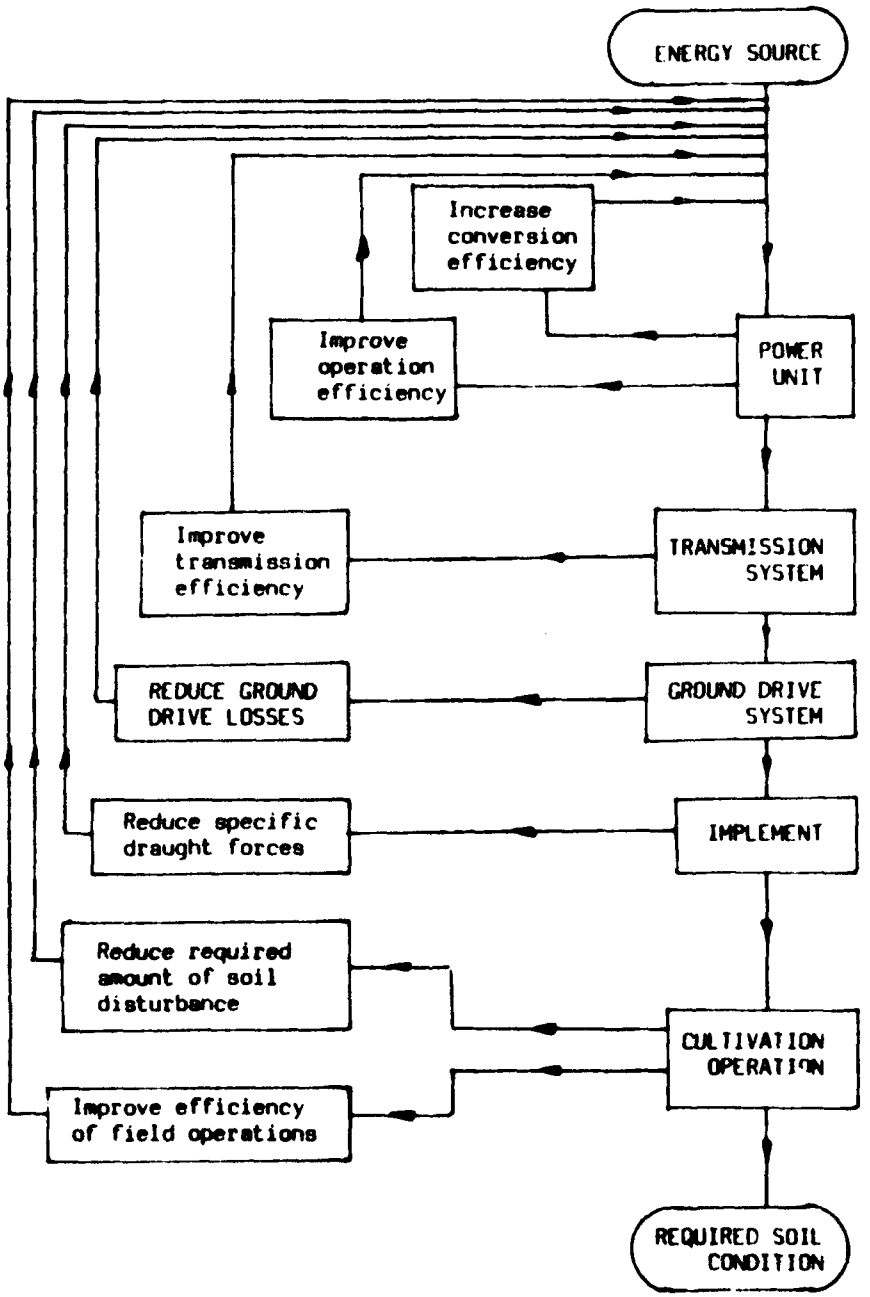

Figure 2. Scope for reducing energy requirements in field operations

The above seven areas are now examined in more detail.

3.1 Engine Efficiency

A useful way to express engine efficiency is in terms of specific fuel consumption (SFC) at full rated power. This specifies fuel quantity used (volume or mass) per unit of energy obtained (power multiplied by time) and is conveniently expressed in l/kWh. Measures such as higher compression ratios, improved combustion chamber design, lower piston and bearing friction losses, higher operating temperatures through the use of new materials, multi-valve heads and other techniques can contribute small but measurable gains in economy with spark ignition and/or compression ignition engines as appropriate, (King, 1983). For engines not operating at full rated power the selection of optimum part load specific fuel consumption probably affords more opportunity for improved economy, as described in section 3.2.

Even a well designed engine can consume excess fuel if it is not maintained in optimum condition during its working life. Dynamometer tests carried out by ADAS in Wales showed specific fuel consumptions varying over a period of three years by as much as 14% greater than the standard OECD test result. Power outputs also varied considerably, being affected mainly by the condition and accuracy of adjustment of the fuel injection system (ADAS/MOAD, 1983). In many developing countries the level of operator skill, maintenance procedures and spares back-up is usually less than ideal, all of which will tend to reduce engine efficiency.

3.2 Engine Operation

Power from an engine is obtained from the product of torque and rotary speed. From consideration of an engine fuel consumption map (Figure 3), it is evident that the decisions of the operator can have a very significant effect on the amount of fuel consumed at a given power level. At point A on the map (full rated speed, full rated torque) specific fuel consumption is a constant at about 0.29 l/kWh. At half power however there is a choice. Point C (full rated speed, half rated torque) gives an SFC of 0.334 whereas point F (half rated speed, full rated torque) produces a lower SFC of 0.280 and point H (62% rated speed, 80% rated torque) is even lower at 0.267 l/kWh.

With 25 kW of power being used (in a 50 kW engine), operation at points C and H would consume 8.35 l/h and 6.67 l/h respectively, affording a potential reduction of 20% in fuel consumed. Current machinery design leaves the selection of the speed/torque combination to the operator, who is advised to run in the highest practicable gear in order to reduce engine speed. Assistance is provided by one tractor manufacturer in the form of a two needle display of exhaust gas temperature and engine speed where the aim is to encourage improved fuel economy through tractor operation with the crossed needles intersecting in the "economy" zone. Work at the East of Scotland College of Agriculture has suggested that exhaust gas volume measurement should also be incorporated to improve the derived specific fuel consumption data (Witney et al, 1983).

Possibilities exist in the longer term for a more automatic control of the torque/speed combination. Continuously variable transmissions (CVT) are under development by a number of motor vehicle manufacturers.

Variable vee belt arrangements have existed for many years. Development is also currently taking place at Leyland Vehicles of a design based on the Perbury inclined roller arrangement. Control is by microprocessor, enabling a complete automatic transmission system to be achieved at high efficiency (Engineering, 1983). With a microprocessor programmed with the specific fuel consumption map of a tractor engine, there may be possibilities for controlling transmission ratios and engine speed to provide the required levels of power for field operations at constant forward speed and at the optimum torque/speed ratio for good fuel consumption.

3.3 Transmission Efficiency

A tractor fitted with drive tyres of diameter 1.5 metres will typically have a maximum forward speed in bottom gear of 0.72 m/s. This requires a wheel rotation speed of 9.2 revs/min, whereas the maximum engine speed will be about 2200 revs/min. The total reduction required in the transmission system is therefore nearly 240:1. This reduction will usually be achieved in not less than four stages, each having its own inefficiency. Nevertheless, the efficiency of individual gear sets is high, so the total losses will not usually amount to more than a few percent, making the scope for improvement very limited. Hydrodynamic and hydrostatic transmission systems are significantly less efficient but are not usually found in tractors except for specialized applications.

3.4 Ground Drive Losses

Losses occur when a drive wheel is used in agricultural soils to provide tractive effort. The losses comprise rolling resistanceand slip. In a given soil, rolling resistance decreases with increasing tyre diameter and so does slip, but while increased weight generally reduces slip it will tend to increase rolling resistance. For maximum economy it is necessary to operate at the maximum tractive efficiency, which typically occurs at around 12-15% slip for a conventional tractor (see Figure 4). From work performed by members of the NIAE Tyre Study Group, ADAS has provided a guide to farmers, relating engine power, P, forward speed, S, and wheel loading, W, by the formula

$$W = \frac{1.6\,P}{S}$$

where W is in kN
P is in kW
S is in m/s

It is shown that by fitting 23.1-26 tyres loaded to 2.54 tonnes instead of 13.6-38 tyres loaded to 1.52 tonnes, an increase in work rate of up to 14% can be achieved with a typical tractor (ADAS, 1983).

Considerable scope therefore exists for improving fuel economy by working at values of slip which accord with maximum tractive efficiency, and by reducing rolling resistance through the use of larger tyres running at the optimum inflation pressure. Towed wheels are often responsible for high levels of rolling resistance, particularly when equipment such as trailers and combine harvesters are fitted with small diameter, high pressure tyres (Gee-Clough, 1980). Larger tyres can be run at lower inflation pressure, leading to lower ground pressures and less risk of

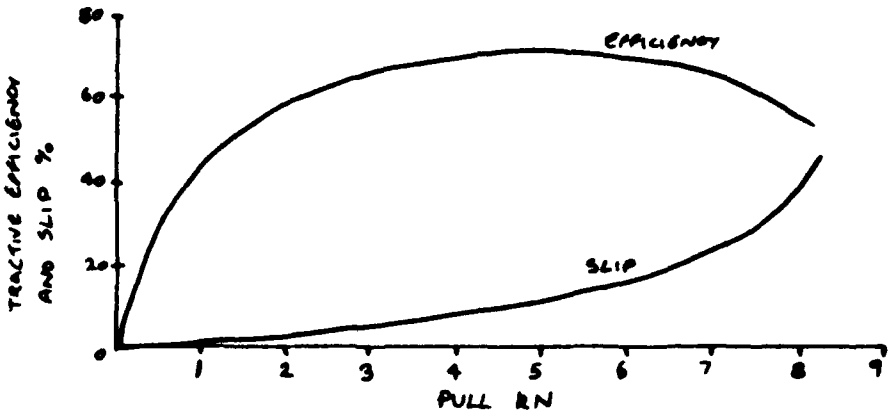

Fig 4. Tractive efficiency and slip for a 13.6/12-38 tractor driving wheel with 1370 kg load and 0.8 Bar inflation pressure in average field conditions. Source: Dwyer, NIAE Report 18

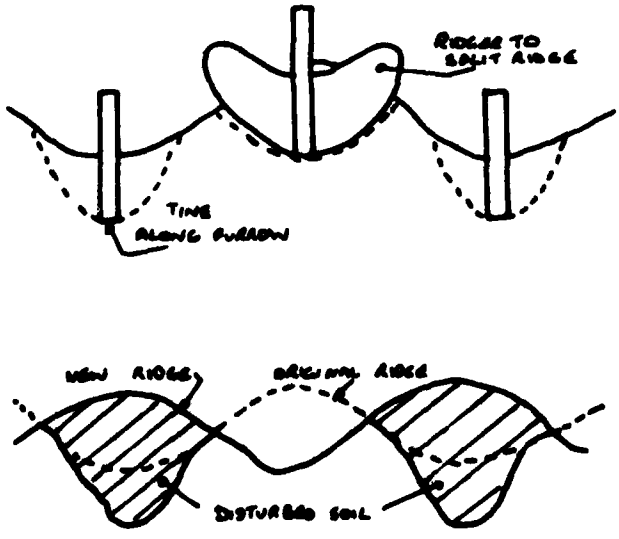

Fig 5. Ridge splitting operation using a ridging body to split the ridge after tines in the previous furrow.

soil damage. Work is in progress at various centres on the development of automatic on-the-move adjustment of tractor tyre pressures.

Where implement draught forces are not provided by direct traction the amount of slip and rolling resistance associated with small, lightly loaded wheels can be reduced significantly, improving fuel efficiency. This is particularly the case with small scale equipment, and the development of two winch-based tractors is described in section 4 of this paper.

3.5 Implement Draught Forces

Work carried out by Spoor and Godwin has shown that the addition of inclined wings to a subsoiler tine together with shallow leading tines significantly increases the degree of soil disturbance, particularly at depth, and reduces the specific draught, (Spoor and Godwin, 1978).

Ploughing at higher speeds is an effective way of utilizing high tractor power without the need for high drawbar pulls (since drawbar power equals drawbar pull multiplied by forward speed). However, the draught of a conventional mouldboard plough increases with speed, reducing the advantages of high speed ploughing. The development of a high speed mouldboard plough which requires a draught force similar to conventional ploughs is an area being investigated in a number of centres. Other problems also associated with high speed ploughing are those of tractor ride and implement control system response.

3.6 Soil Disturbance Reduction

Reference was made in section 2 to the work of Willcocks in Botswana, where precision strip tillage using tines at 750 mm spacing reduced the energy requirements per hectare compared with conventional mouldboard ploughing by a factor of 2.6. In suitable semi-humid conditions in tropical areas, possibilities exist for zero-tillage techniques based on herbicide sprayers and rolling jab planters. The energy requirement for field operations is said to be reduced from 300 MJ/ha for conventional cultivation operations to 35 MJ/ha (Wijewardene, 1978). The use of wide bed systems at 1.5 metre spacing in conjunction with animal drawn toolbars has been developed at ICRISAT in India and shows useful reductions in energy consumption for field operations (Binswanger et al, 1979).

The technique of ridge cultivation practiced in a number of developing countries also fits the pattern of concentrating cultivation operations in the vicinity of the crop. Disturbing the bottom of the old furrow with a tine prior to splitting the adjacent ridges onto it provides useful soil depth for the new ridge by mechanical means (Figure 5). Cultivation then comprises two operations at one metre spacing instead of close spaced tillage followed by ridging (Crossley and Kilgour, 1978).

3.7 Efficiency of Field Operations

A certain proportion of the energy consumed in relation to field operations is not used directly in disturbing the soil. Previous sections of this paper have identified areas of energy loss during actual soil cultivation. Further losses occur during associated activities such as turning, headland travel and transport to and from the field. The use

of a reversible plough (mouldboard or disc), or tines will substantially reduce the need for headland travel. Implements arranged in gangs one behind the other will reduce the number of passes required for a series of low draught operations, and hence will reduce fuel consumption.

Indifferent scheduling of tractor operations, particularly in tractor hire schemes, can increase the amount of travel associated with each cultivation activity. Low standards of operator training will tend to lead to inefficient field operations with consequent increases in fuel consumption. Tractors maintained in poor condition will also not operate efficiently. Small and irregularly shaped fields increase the amount of lost travel. All these factors are typical of operation at the smallholder level in developing countries and help to account for the very high costs per unit area associated with almost all tractor hire schemes in these conditions.

Other factors contributing to high costs are the high spares and repairs costs consequent upon operation in difficult conditions under poor maintenance regimes; low rates of work due to operation at low drawbar powers (going too slowly with too small an implement); and low availability of tractors because of delays in obtaining spare parts required after breakdown (Mdee, 1983). These factors do not increase direct energy costs but any reduction in effective use or availability of an expensive machine will result in increased indirect costs in that more machines are required to perform a given set of tasks. However, the energy costs associated with the manufacture and supply of machinery, chemicals and other inputs are not within the scope of this paper.

4. WINCH TRACTORS FOR DEVELOPING COUNTRIES

An increase in agricultural productivity in developing countries is vital, and, because in the majority of countries the smallholder sector is dominant, it is this sector which requires the major effort. Improving small farm yields is certainly feasible but this requires a package of inputs such as seeds, fertilizers, management and mechanization, of which mechanization is one of the most challenging.

Smallholder conditions are such that large, conventional tractors cannot work effectively, due to such factors as small field size, difficult access, field obstructions, scattered holdings and limited spares/service infrastructure. Therefore it has been considered necessary to attempt to develop special small tractors which can work effectively in these conditions, can be made locally, are simple to operate and repair and can be owned by the individual farmer.

Yet, of the large number of prototypes and limited production small tractors which have been developed over the years, only a tiny handful has made any real progress and none can really be regarded as a success story. A major reason is that compromises between the conflicting requirements of performance, durability and cost have resulted in tractors which, although fairly cheap, have poor tractive ability, a low rate of work, very high fuel consumption per unit area and an effective component life which is often measured in hundreds of hours rather than in thousands.

Section 3.4 of this paper outlined the losses incurred in normal tractor operation due to rolling resistance and slip. When performing

cultivation operations in hard soil such as is encountered in the dry season in many developing countries, it is found that many small tractors experience high levels of wheel slip, particularly when surface conditions are poor due to high trash levels, or where surface layers are loose after harvesting or slippery following early rains. Values of fuel consumption of three times those experienced with conventional tractors have been recorded with some small tractors used in these conditions (Crossley and Kilgour, 1978).

Two small-scale winch based machines have been developed at Silsoe College. The SNAIL is a two wheeled machine while the SPIDER is a fairly small, four wheeled, ride-on machine having a diesel engine, good ground clearance and a transport platform. The SPIDER can carry out secondary cultivation and transport operations like a normal small tractor. However, to achieve the high pulls required for primary cultivation both machines make use of the winch principle, using a separate implement which is controlled by a second operator. The machine is driven forward while the cable runs out and then, when the winch is engaged and while a self operating anchor prevents the machine from sliding backwards, the implement is drawn towards the tractor on its cable. Upon the implement reaching the tractor the cycle is repeated. (Figures 6 and 7).

The mode of operation is very unconventional but there are special reasons why it is desirable. First it provides a high drawbar pull (in the range 5-8 kN depending on the engine power), from a fairly small light machine. Second, it does so very efficiently compared with a normal small tractor, so that fuel consumption per unit area is similar to that of large, conventional tractors (around 20 litres per hectare) instead of as much as 60-70 litres per hectare with some small tractors. Third, because it is not used for direct traction for high draught operations, components such as the tyres are relatively small and not as expensive as those on a small tractor of equivalent performance.

Two prototype SNAIL machines were tested in Malawi in 1975 and 1976 (Crossley and Kilgour, 1978). A prototype SPIDER machine has also been tested in Tanzania (Crossley and Kilgour, 1983). It has been concluded that using the winch principle it is possible to produce machines which are technically satisfactory for operation in the small farm sector of developing countries and which utilize fuel more efficiently than existing small tractors.

5. REFERENCES

ADAS (1983). Tyres and traction. Ministry of Agriculture, Fisheries and Food/Central Office of Information.

ADAS/MDAD (1983). Power output and fuel usage by tractors on the farm. Mechanization Department, ADAS, Wales.

Binswanger, H.P., Chodeka, R.D. and Thierstein, G.E. (1979). Observation on the economics of tractors, bullocks and wheeled tool carriers in the semi-arid tropics of India. ICRISAT Workshop, 19-23 February.

Crossley, C.P. and Kilgour, J. (1978). Field performance of a winch-powered cultivation device in Central Africa. J. Agric. Engng. Res. 23, 385-396.

Fig 6. Prototype SNAIL machine under test in Malawi

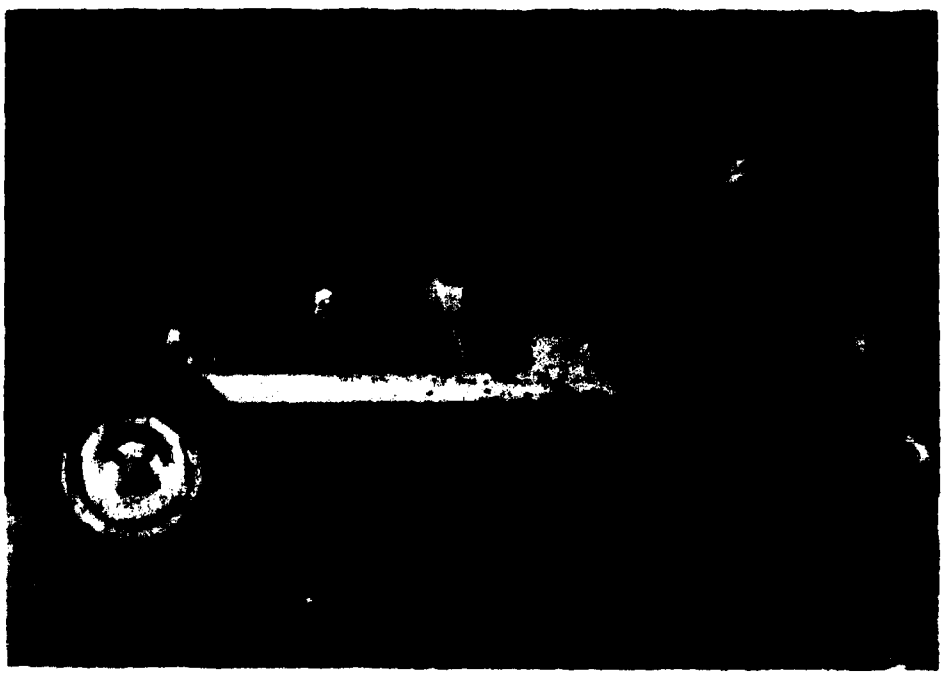

Fig 7. Prototype SPIDER machine nearing completion

Crossley, C.P. and Kilgour, J. (1983). The development and testing of a winch-based small tractor for developing countries. J. Agric. Engng. Res. 28, 149-161.

Engineering (1983). Getting rid of the gearbox. April.

Gee-Clough, D. (1980). Selection of tyre sizes for agricultural vehicles. J. Agric. Engng. Res. 25, 261-278.

King, C.S. (1983). A car for the nineties: BL's energy conservation vehicle. Institution of Mechanical Engineers. Proceedings 1983 Vol. 197 No. 64.

Mdee, M.R.M. (1983). Effectiveness of hire operations at Mkongo agronomy centre, Tanzania. M.Sc. Thesis, Silsoe College, Silsoe, U.K.

Spoor, G. and Godwin, R.J. (1978). An experimental investigation into the deep loosening of soil by rigid tines. J. Agric. Engng. Res. 23, 243-258.

Willcocks, T.J. (1981). Tillage of clod-forming sandy loam soils in the semi-arid climate of Botswana. Soil and Tillage Research 1 (1980/81), 323-350.

Witney, B.D., Copland, T.A. and Milne, F. (1983). Tractor performance monitor. East of Scotland College of Agriculture leaflet, October.

6. APPENDIX

6.1 Large Tractor + Three Mouldboards

Individual width 400 mm. Total width 1200 mm.
Individual pull 4.2 kN. Total pull 12.6 kN. Speed 0.9 m/s.
Implement power 11.34 kW.
Slip 15%. Transmission efficiency 0.94.
Rolling resistance 2.5 kN. Engine power used is $(12.6 + 2.5) \times .9 / (.85 \times .94)$
ie. 17 kW.
Maximum engine power 50 kW. Proportion of power used .34.
At 85% speed, torque used is 40%.
From map SFC is 0.337 l/kWh.
Rate of work is 1.08 m^2/s, ie. 2.57 h/ha.
Fuel used is $0.337 \times 17 \times 2.57 = 14.75$ l/ha.
Turning time is 25%, ie. 0.64 h/ha.
At 10% power and 0.400 l/kWh fuel used in turning is 1.56 l/ha. ∴
total fuel used is 16.2 l/ha.
Total time is 3.21 h/ha.
Tyres 13.6-38 loaded to 2740 kg total. Coefficient of traction 0.47.
Implement energy during cultivation $11.34 \times 2.57 \times 3.6$, ie. 105 MJ/ha.
Tractor energy: during cultivation $17 \times 2.57 \times 3.6$ ie. 157.4 MJ/ha;
during turning $5 \times 0.64 \times 3.6$ ie. 11.57 MJ/ha; total 168.97 MJ/ha.
Proportion of implement energy to tractor energy 0.62.

6.2 Large Tractor + Four Tines

Individual width 750 mm. Total width 3000 mm.
Individual pull 3.025 kN. Total pull 12.1 kN. Speed 0.9 m/s.
Implement power 10.89 kW.
Slip 14%. Transmission efficiency 0.94.
Rolling resistance 2.5 kN. Engine power used is $(12.1 + 2.5)\ 0.9 / (0.86 \times 0.94)$
ie. 16.25 kW.
Maximum engine power 50 kW. Proportion of power used .325.
At 85% speed, torque used is 38%.
From map SFC is 0.345 l/kWh.
Rate of work is 2.7 m^2/s, ie. 1.029 h/ha.
Fuel used is $0.345 \times 16.25 \times 1.029 = 5.77$ l/ha.
Turning time is 25%, ie. 0.257 h/ha.
At 10% power and 0.488 l/kWh fuel used in turning is 0.627 l/ha. ∴ total fuel used is 6.39 l/ha.
Total time is 1.286 h/ha.
Tyres 13.6-38 loaded to 2740 kg total. Coefficient of traction 0.45.
Implement energy during cultivation $10.89 \times 1.029 \times 3.6$, ie. 40.34 MJ/ha.
Tractor energy: during cultivation $16.25 \times 1.029 \times 3.6$ ie. 60.196 MJ/ha; during turning $5 \times 0.257 \times 3.6$ ie. 4.626 MJ/ha; total 64.822 MJ/ha.
Proportion of implement energy to tractor energy 0.62.

6.3 Large Tractor + Five Tines (high speed)

Individual width 750 mm. Total width 3750 mm.
Individual pull 3.025 kN. Total pull 15.125 kN. Speed 1.8 m/s.
Implement power 27.22 kW.
Slip 20%. Transmission efficiency 0.94.
Rolling resistance 2.7 kN. Engine power used is $(15.125 + 2.7)\ 1.8 / (0.8 \times 0.94)$
ie. 42.7 kW.
Maximum engine power 50 kW. Proportion of power used 0.85.
At 85% speed, torque used is 100%.
From map SFC is .279 l/kWh.
Rate of work is 6.75 m^2/s, ie. 0.411 h/ha.
Fuel used is $42.7 \times .279 \times .411 = 4.9$ l/ha.
Turning time is 25%, ie. .102 h/ha.
At 10% power and 0.488 l/kWh fuel used in turning is 0.251 l/ha. ∴ total fuel used is 5.15 l/ha.
Total time is 0.513 h/ha.
Tyres 13.6-38 loaded to 3000 kg total. Coefficient of traction 0.51.
Implement energy during cultivation $27.22 \times 0.411 \times 3.6$, ie. 40.27 MJ/ha.
Tractor energy: during cultivation $42.7 \times 411 \times 3.6$, ie. 63.17 MJ/ha; during turning $5 \times .102 \times 3.6$, ie. 1.836 MJ/ha; total 65 MJ/ha.
Proportion of implement energy to tractor energy 0.62.

COMPUTER MODELS TO PREDICT THE PERFORMANCE OF AGRICULTURAL TRACTORS ON HEAVY DRAUGHT OPERATIONS

M.J. DWYER

NATIONAL INSTITUTE OF AGRICULTURAL ENGINEERING, SILSOE, ENGLAND.

SUMMARY

It would be of benefit to users of agricultural vehicles to have available computer models to compare the performance of different machines. Such models are already widely available to prospective purchasers of military vehicles. The main difficulty in developing similar models for agricultural vehicles is the wide variety of operations which are carried out on farms. One important area, however, where such models can be developed are for heavy draught operations such as ploughing, cultivating, subsoiling etc. This paper describes models of varying complexity which can be used to predict the power output or workrate of a tractor on such operations. The simpler models need only a programmable calculator, but the more "user-friendly" versions would require a microcomputer. The programs can be used to compare the workrates of tractors of different design and these results can then be used in linear programs of the general farm management system to determine the effects on overall profitability.

Introduction

The British agricultural industry spends approximately £250M per year on new tractors. The cost of operating all the tractors working on British farms is probably about four times this figure. Similar statistics would undoubtedly apply to other developed countries of similar size. Therefore, in terms of national economics it is worthwhile devoting some effort to ensuring that, as far as possible, the agricultural industry has available to it the most appropriate vehicles and that they are operated as efficiently as possible.

To the individual farmer the importance of selecting the right vehicle is even more critical. His choice may affect his profitability for the following two or three years. Similarly, the efficiency with which he operates his vehicles can have a crucial effect on his income. Delays

in cultivating land and sowing crops beyond the optimum time, or inability to apply fertilizer or herbicides at the appropriate stage can easily reduce the value of a crop by several thousands of pounds.

Clearly, therefore, there are benefits to be had from making available to farmers and their advisers data which will enable them to make the right choice of vehicles for their particular situation. Engineering data on tractors have been available from independent sources for many years. The first was the University of Nebraska in USA[1], followed by the OECD[2] in Europe. Tractor test reports from both of these sources now circulate worldwide. However, they are designed primarily to provide reproducible engineering data, which cannot, therefore, be applied directly to predict field performance. Drawbar performance, for example, is measured on a concrete or tarmacadam surface of specified characteristics, rather than on a field surface, which could obviously not be reproduced exactly for a subsequent test or in another country.

The original aims of these test procedures were to help to eliminate from the market poor quality products and to provide prospective purchasers with an unbiased comparison between different manufacturers' products. Some element of this remains, but normal commercial pressures have very largely removed manufacturers of low quality vehicles from the scene and considerably narrowed the differences between the products of the major manufacturers. On the other hand the range of models produced by each manufacturer has expanded greatly in recent years. A very wide range of power levels is available, two or four-wheel drive on most models, usually a choice of transmissions and a host of other options. Therefore, even though a user may quite justifiably make his choice of manufacturer based on the service he receives from his local dealer, he is still in need of expert independent advice on the most suitable model to choose for his particular requirements.

Data from official test reports are still a valuable starting point in assessing the relative merits of different tractors. However, more objective techniques than reliance on judgement and experience are necessary if these data are to be used to the greatest benefit of the user and ultimately the community.

When seeking computer models to aid the selection and use of agricultural vehicles it is natural to look at what has been done in a similar way for military vehicles. For some years there have been available to prospective buyers of military vehicles computer models which can be used to compare the specification of competitive vehicles[3,4,5]. It would clearly be attractive to have something similar available to prospective buyers of agricultural vehicles.

Scope of the models

Before devising an appropriate model the first essential is to define the vehicle mission and the criterion which will be used to compare performance. For a military or transport vehicle this is usually fairly straightforward. An area of appropriate terrain can be chosen from suitable maps or by surveys and the time taken for a vehicle to travel between two selected points can be computed, with a pre-set limitation on the maximum vibration level permitted to be transmitted to the driver. It is much more difficult to devise a representative mission for an agricultural vehicle.

Although agricultural tractors are designed primarily for carrying out heavy draught operations, the majority probably spend less than half their working hours on such tasks. A typical tractor probably carries out more than a dozen different operations in a year. For some of these, such as sub-soiling, ploughing, cultivating, harrowing and drilling, workrate may be limited by tractive performance. For others, such as transporting, spraying, fertiliser distribution and mowing, workrate may be limited by driver comfort. However, for many others, such as planting, harvesting and baling, workrate will be determined by the limitations of the machine being used in conjunction with the tractor rather than by the performance of the tractor itself. It may, therefore, be impracticable to realise the ideal of simulating the whole annual cycle of farming operations carried out by one tractor.

An alternative approach is to consider the traction-limited tasks and the driver-comfort-limited tasks separately. Other papers at this conference deal with models for predicting the effects of vehicle design on driver comfort[6,7]. This paper is restricted to performance on heavy draught operations, where traction is likely to be the limiting factor.

A simple model for predicting drawbar power

The minimum tractor data required for prediction of drawbar power are the engine torque-speed relationship, the transmission efficiency, the ratios of the driving wheel speeds to the engine speed in each gear, the weight on each axle and the tyre dimensions. These can be found in an official test report or the manufacturer's specification and the tyre manufacturer's data book. The field conditions must be defined by the average cone penetrometer resistance measured through the top 250 mm depth of soil.

Tyre performance is determined either from the empirical relationships developed by Wismer and Luth in the USA[8] or from the following derived by Gee-Clough in UK[9].

$$M = \frac{Cbd}{W}\sqrt{\frac{\delta}{h}}\left(\frac{1}{1+\frac{b}{2d}}\right) \quad \ldots\ldots (1)$$

$$C_{RR} = \frac{R}{W} = 0.049 + \frac{0.287}{M} \quad \ldots\ldots (2)$$

$$(C_T)_{max} = \frac{T_{max}}{W} = 0.796 - \frac{0.92}{M} \quad \ldots\ldots (3)$$

$$k(C_T)_{max} = 4.838 + 0.061\ M \quad \ldots\ldots (4)$$

$$C_T = \frac{T}{W} = (C_T)_{max}\ (1 - e^{-ks}) \quad \ldots\ldots (5)$$

where M = mobility number
C = average cone penetrometer[10] resistance through the top 250 mm of the soil surface
b = tyre width
d = tyre diameter
W = vertical load on the tyre
δ = tyre deflection
h = tyre section height
C_{RR} = coefficient of rolling resistance
R = rolling resistance
$(C_T)_{max}$ = maximum coefficient of traction

T_{max} = maximum thrust
k = a constant
C_T = coefficient of traction
T = thrust
s = slip

These equations may be used to calculate the rolling resistance of the wheels and the thrust available from the driving wheels as a function of slip. The drawbar pull, D, is then the difference

$$D = T \text{ (driving wheels)} - R \text{ (undriven wheels)} \quad \ldots\ldots (6)$$

The torque, Q, required at the driving wheels is

$$Q = [T \text{ (driving wheels)} + R \text{ (driving wheels)}]\, r \quad \ldots\ldots (7)$$

where r = rolling radius of the driving wheels
and the input power, P_i, required is

$$P_i = Q\omega = \frac{QV}{r} \quad \ldots\ldots (8)$$

where ω = rotational speed of driving wheels
and V = theoretical forward speed without slip

Therefore, $P_i = (T + R)V \quad \ldots\ldots (9)$

The corresponding output power, P_o is

$$P_o = D\,V(1 - s) \quad \ldots\ldots (10)$$

The problem therefore, is to find the maximum value of P_o which is possible in each gear without exceeding the maximum available value of P_i.

It is now necessary to distinguish between two possible situations. In the higher gears output power will be limited by the engine power available, whereas in the lower gears output power will be limited by slip. For each gear, therefore, the maximum output power possible with either of these limitations must be calculated and the lower of the two is the actual maximum power available in that gear.

The calculation of engine-limited maximum power is very straightforward. The engine torque at maximum power is multiplied by the transmission efficiency and the appropriate gear ratio to find the torque available at the driving wheels. This torque is divided by the rolling radius and the total rolling resistance is subtracted to find the drawbar pull, D.

The engine speed at maximum power is divided by the gear ratio to give the rotational speed of the driving wheels and this is multiplied by the rolling radius to give the no-slip forward speed, V.

The thrust from the driving wheels is calculated from the drawbar pull plus the rolling resistance of the undriven wheels, equation 6, and the slip, s, is calculated from equation 5. In doing this it is necessary to take account of the weight transfer from the front axle to the rear axle due to the torque required to overcome the rolling resistance of the driving wheels. It may be assumed that the rolling resistance of the undriven wheels, the thrust from the driving wheels and the implement draught force all act in the same horizontal plane and do not, therefore, affect the weight distribution between the axles.

The weight on the rear wheels, W_R, is given by

$$W_r = W_{Rs} + \frac{Q_D}{l}$$

where W_{Rs} = static weight on rear wheels

Q_D = torque required to overcome the rolling resistance of the driving wheels

l = tractor wheelbase

For a two-wheel drive tractor

$$W_R = W_{Rs} + W_R(C_{RR})_R \frac{r}{l} \qquad \ldots\ldots (11)$$

where $(C_{RR})_R$ = coefficient of rolling resistance of rear wheels

For a four-wheel drive tractor

$$W_R = W_{Rs} + \left[W_R (C_{RR})_R + W_F (C_{RR})_F \right] \frac{r}{I} \quad \ldots\ldots (12)$$

where W_F = weight on front wheels

and $(C_{RR})_F$ = coefficient of rolling resistance of the front wheels

Since $W_F = W - W_R$

where W = total weight of the tractor

these equations may be solved for W_R and W_F.

If the tractor is two-wheel drive, W_R is then used in equation 5 to find the slip, s.

The true forward speed is then

$$V(1 - s)$$

and P_o is calculated from equation 10.

If the tractor is four-wheel drive, there will be two equations 5, one for each axle. An iterative procedure will then be necessary to find the slip, which will normally be the same, or be in some fixed relationship for the two axles.

The calculation of maximum slip-limited power is slightly more complicated. Combining equations 5, 6 and 10, for a two-wheel drive tractor,

$$P_o = \left[W_R (C_T)_{max} (1 - e^{-ks}) - W_F C_{RR} \right] V (1 - s) \quad \ldots\ldots (13)$$

For maximum P_o, $\frac{dP_o}{ds} = 0$

$$W_R (C_T)_{max} (e^{-ks} + ke^{-ks} - kse^{-ks}) = W_R (C_T)_{max} - W_F C_{RR} \quad \ldots\ldots (14)$$

For a four-wheel drive tractor

$$P_o = \left[\left(W(C_T)_{max}\ (1 - e^{-ks})\right)_R + \left(W\ (C_T)_{max}\ (1 - e^{-ks})\right)_F\right] V\ (1 - s)$$

When $\frac{dP_o}{ds} = 0$

$$\left(W\ (C_T)_{max}\ (e^{-ks} + ke^{-ks}{}_{-kse}{}^{-ks})\right)_R$$

$$+\left(W\ (C_T)_{max}\ (e^{-ks} + ke^{-ks} - kse^{-ks})\right)_F = \left(W\ (C_T)_{max}\right)_R + \left(W\ (C_T)_{max}\right)_F \quad ..(15)$$

These equations can be solved for s. The thrust at the driving wheels, T, may be calculated from equation 5 and the torque at the driving wheels, Q, from equation 7. This may then be divided by the gear ratio and the transmission efficiency to give the engine torque and the engine speed can be read from the engine torque-speed relationship.

The engine speed can be divided by the gear ratio to give the rotational speed of the driving wheels and multiplied by the rolling radius to give the no-slip forward speed, V. The output power, P_o, can then be calculated from equation 13.

This model is simple enough to be run on a small programmable calculator, but can be quite effective in, for example, comparing two and four-wheel drive or showing the effects on drawbar power output of changing parameters such as tyre size, ballasting or gear ratios. The model can be made easier to use by storing data on tyre dimensions and typical tyre sizes, speed-torque relationships, transmission efficiencies, gear ratios and weight distributions related to maximum engine power. Some of these values can then be used by default when the effects of changing others is being investigated. The amount of storage space required would probably then necessitate a micro-computer, however. This also enables a "user-friendly" program to be written which prompts the user for the appropriate data.

A simple model for predicting tractor workrate on heavy draught operations

The model described above predicts drawbar power. To convert this to workrate requires some knowledge of the relationship between draught force and working width. The simplest approach is merely to assume a linear relationship so that drawbar power can be converted directly to workrate in, for example, hectares per hour. This will give a "spot" rate of work, which could then be multiplied by a field efficiency factor depending on the size and shape of the field to determine true rate of work, allowing for turning and stoppages.

In practice, however, this modification does nothing more than convert the dimensions of the output to a form which may be more meaningful to a farmer. For example, the model might give the maximum power outputs of two tractors as 45 and 50 kW respectively and one could merely multiply these by a typical figure for mouldboard ploughing such as 0.025 (ha/h)/kW to give 1.125 and 1.25 ha/h respectively. This would not alter the comparison, but might be more easily understood by a farmer.

In practice, however, the widths of implements are not continuously variable. They can only be changed in increments, by adding or removing bodies or tines, for example. Also, changing the width of the implement will alter its weight and, therefore, the weight on the driving wheels of the tractor. To take account of this, the model input must include the minimum width of implement to be considered, the increments of increase in width, the corresponding weights and positions of the centre of gravity behind the hitch points, the horizontal and vertical components of soil force per increment of width and the distances of the point of application of the resultant of the vertical components of soil force behind the hitch points.

The method of calculation, for each gear ratio, starts with the minimum width of implement. The corresponding weight of the implement, position of centre of gravity, vertical component of soil force and position of the point of application of the vertical component of soil force are used to calculate the weights on the axles of the tractor. These must be checked against the maximum values permitted by the tractor and tyre manufacturers. Equation 1 is used to calculate the mobility numbers of the wheels and

equations 2, 3 and 4 to calculate the rolling resistances, $(C_r)_{max}$ and k values.

For two-wheel drive tractors the rolling resistance of the undriven wheels is added to the implement draught force to determine the total thrust, T, required from the driving wheels. Equation 5 is used to ensure that the necessary thrust can be produced and, if so, to calculate the slip, s. The torque required at the driving wheels, Q, is calculated from equation 7 and divided by the gear ratio and transmission efficiency to give the engine torque required. This is then checked against the torque available from the engine and the engine speed is read from the torque-speed relationship. This speed divided by the gear ratio and multiplied by the rolling radius gives the theoretical forward speed, which, when multiplied by (1 - s) gives the true forward speed. Workrate is then the true forward speed multiplied by the implement width. This procedure is repeated with increasing increments of implement width until some limiting factor is reached, such as overloading of an axle, 100% slip or engine stall.

For four-wheel drive tractors, the total thrust equals the implement draught, but the distribution of the thrust between the axles and the corresponding slip must be determined by an iterative process using equation 5. Otherwise the method of calculation is the same as for two-wheel drive.

This model is a closer simulation of the real field situation and, because the changes in draught force are incremental, it is more useful for comparing the effects of changes in gear ratios and spacing. Also, taking account of implement weight and its effect on weight distribution will show up any limitations on the size of implement necessary to enable full power to be utilised in a particular gear.

The model is probably adequate for most comparisons which one would want to make between tractors. Its main limitations, however, are in its very simplified simulation of the implement characteristics. It would not, therefore, be suitable for studying the effects of implement design on tractor performance.

A more complex model for predicting tractor workrate on heavy draught operations

The main limitation of the simple model described above is that it does not take account of the effect of forward speed on the soil forces on the implement. Including this in the analysis complicates the calculations, but extends the scope of the model to studying the tractor-implement interaction more effectively.

The effect of speed on the draught force of implements has been studied for many years, notably by Goryachkin[11] and Söhne[12]. More recently Gee-Clough[13] used dimensional analysis, as previously proposed by Krastin[14], to develop the following equation for the specific draught of a plough.

$$\frac{D}{aw} = 13.3\ \gamma a + 3.06\ \frac{\gamma V^2}{g}$$

where a = plough depth
w = plough width
γ = soil density
and g = gravitational constant

Subsequently Oskoui et al[15,16] found better agreement with experimental results by using cone penetrometer resistance in the first term of this equation and introducing the plough mouldboard tail angle, θ, in the second term, to take account of different plough body shapes.

$$\frac{D}{aw} = K_1 C + K_2\ \frac{\gamma V^2\ (1 - \cos\theta)}{g}$$

where K_1 and K_2 = empirical constants

The American Society of Agricultural Engineers' Agricultural Machinery Management Data[17] quotes typical values of specific draught for a range of soil types which are all of the form

$\frac{D}{aw} = A + B V^2$ for mouldboard ploughs

and $D = C + D V$ for chisel ploughs and cultivators

where A, B, C and D are empirical factors. Typical values for different North American soil types are as follows:

A	20–70 kN/m^2
B	0.13–0.49 $(kN/m^2)/(km/h)^2$
C	0.48–0.527 kN/tine at 82.6 mm depth
D	0.0361–0.0492 (kN/tine)/(km/h) at 82.6 mm depth

In general, greater depths of cultivation and higher values of draught force would be encountered in Europe.

Far less data exist on the effect of speed on the vertical soil forces on implements. For mouldboard ploughs this can probably be ignored for most purposes since, in general, vertical soil forces are small anyway. The upward forces on the coulter and landside generally approximately balance the downward forces on the mouldboard, so that the net vertical force applied to the tractor from the plough is normally close to the weight of the plough alone. Therefore, any variations due to speed are likely to be negligible.

For tined implements such as subsoilers, chisel ploughs and cultivators, the vertical force is normally approximately a fixed proportion of the draught force, dependant on the tine rake angle. It will, therefore, vary with speed in the same way as does the draught force.

When the effect of forward speed on implement draught is included in the analysis it is no longer possible to calculate engine torque from implement draught, read off the corresponding engine speed and convert this to forward speed. This speed will not coincide with the speed for which the draught was originally calculated. Therefore, an iterative procedure must be used starting with the zero speed draught force, calculating the corresponding forward speed, using this speed to form a new estimate of draught and repeating the procedure until a satisfactory level of accuracy is attained. Even introducing this added complexity, however is unlikely

to put the calculations beyond the scope of a programmable calculator, provided a simple relationship between speed and torque is accepted. If an exact speed-torque relationship is required, however, because this must now be included in the iteration procedure and, therefore, stored in the program, at least a micro-computer is likely to be needed.

Further refinements of the model

The model may be further improved, if necessary, by inclusion of other factors which may affect tractive performance such as slopes, wheel tracking, operation with wheels in the furrow and use of the differential lock. Of these the effect of working on slopes is probably the easiest to incorporate. Going directly up or down a slope has two effects. Firstly, there is a shift in weight distribution towards the downhill axle. This may be calculated initially from the angle of the slope, the height of the centre of gravity and the wheelbase. It then appears in the calculations as a change in the value of the static weight on the rear axle, W_{Rs}. Secondly, the component of the combined weights of the tractor and implement acting down the hill appear as a constant term in the equation for the drawbar pull:

$$D = (MC_T)_{\text{Driving wheels}} - (MC_{RR})_{\text{Undriven wheels}} \pm (W \sin \beta)_{\text{Tractor + implement}}$$

where β = angle of slope.

The effect of wheel tracking is that a leading wheel compacts and strengthens the soil on which a following wheel runs. This may be included in the model by choosing a higher value of cone penetrometer resistance for a wheel which runs in the track of a preceding wheel. The problem is to decide how much increase to allow. The only data which are available[18] are for tyres following each other which are of the same size and carrying the same load at the same inflation pressure. For any other situation it is only possible to estimate a likely figure from these data, which imply an increase in cone penetrometer resistance of 2-3 times for the second tyre.

In Europe most tractors plough with two wheels in the furrow. This has two effects. Firstly, weight is transferred from the land-side wheels to the furrow-side wheels. This is the same as the effect of working across a side-slope. It may be dealt with in the model by calculating the weight transfer from the height of the centre of gravity of the tractor and the track width and predicting the performance of each wheel individually. The second effect, however, is that the cone penetrometer resistance in the furrow bottom is likely to be higher than that on the surface. Again there are very little data available apart from those of Gee-Clough[19] which showed a typical increase in cone penetrometer resistance of about 35% between the furrow bottom and the surface.

When two wheels on the same axle carry different weights or are running in different soil conditions the overall performance depends on whether the differential is operating or locked. When it is operating the thrust from both wheels must be the same. Therefore the thrust required from the axle must be halved and equation 5 used for each wheel individually to determine the slip for that wheel. The overall slip for the axle is then the average of the slip values of the two wheels. If the differential is locked then the slip is the same for both wheels and it is necessary to use an iterative procedure to determine from equation 5, for each wheel, a value of slip which will produce values of thrust which add up to the required total.

Example 1 - Simple model for a David Brown 1390 two-wheel drive tractor

The following input data are taken from the appropriate OECD test report[20], except that only half of the available gears are included for convenience.

Front tyre size 7.50-16
Static weight on each front tyre 6.19 kN
Rear tyre size 16.9-34
Static weight on each rear tyre 12.08 kN
Wheelbase 2.108 m

Gear	L1	L2	H1	L3	H2	H3
Engine speed / Wheel speed	134.1	80.8	67.2	46.8	40.5	23.5

Engine torque at maximum power x transmission efficiency = 198.5 Nm

Engine speed at maximum power = 2200 rev/min

Assuming a value of cone penetrometer resistance, C = 1000 kN/m^2 and using the tyre manufacturer's data book for tyre dimensions, from equations 1, 2 and 11,

Dynamic weight on front wheels = 11.81 kN

Dynamic weight on rear wheels = 24.73 kN

Mobility number of front wheels = 9.03

Mobility number of rear wheels = 16.66

From equation 2,

Rolling resistance of front wheels = 0.95 kN

Rolling resistance of rear wheels = 1.64 kN

From equation 3, 4 and 5

Maximum coefficient of traction, $(C_T)_{max}$ = 0.741

Maximum thrust = 18.32 kN

k $(C_T)_{max}$ = 5.85

k = 7.90

Thrust = 18.32 $(1 - e^{-7.90s})$ kN

Gear	L1	L2	H1	L3	H2	H3
Torque available at driving wheels at maximum engine power, kNm	26.62	16.04	13.34	9.29	8.04	4.66
Drawbar pull, kN	33.41	19.10	15.44	9.96	8.27	3.70
No-slip forward speed, km/h	4.57	7.59	9.12	13.10	15.13	26.08
Thrust from driving wheels, kN	34.36	20.05	16.39	10.91	9.22	4.65
Slip, %	>100	>100	28.49	11.46	8.86	3.71
True forward speed, km/h	0	0	6.52	11.60	13.79	25.11
Drawbar power, kW	0	0	27.96	32.09	31.68	25.81

From equation 14, slip for maximum output power = 25.15%
From equation 5, thrust from driving wheels = 15.81 kN
From equation 6, drawbar pull = 14.86 kN
From equation 7, torque at driving wheels = 12.90 kN m

Gear	L1	L2	H1	L3	H2	H3
Engine torque, Nm	96.16	159.60	191.90	275.55	318.41	548.75
Engine speed, rev/min	2260	2240	2220	above max. torque		
Speed of rear wheels, rev/min	16.85	27.72	33.04			
No-slip forward speed, km/h	4.69	7.73	9.20			
Drawbar power, kW	14.49	23.88	28.42			

Therefore the highest drawbar power available in each gear, the forward speeds and the equivalent rates of work at 0.025 (ha/h)/kW are as follows.

Gear	L1	L2	H1	L3	H2	H3
Drawbar power, kW	14.49	23.88	28.42	32.09	31.68	25.81
Equivalent rate of work, ha/h	0.362	0.597	0.711	0.802	0.792	0.645
Forward speed, km/h	3.51	5.79	6.89	11.60	13.79	25.11
Equivalent implement width, m	1.03	1.03	1.03	0.69	0.57	0.26

Example 2 - Simple model for a David Brown 1390 four-wheel drive tractor

The following input data are taken from the appropriate OECD test report[21]. Data not given below are the same as for the two-wheel drive tractor.

Front tyre size 11.2-24
Static weight on each front tyre 7.35 kN
Rear tyre size 16.9-34
Static weight on each rear tyre 9.83 kN
Wheelbase 2.14 m
Dynamic weight on front wheels = 13.91 kN
Dynamic weight on rear wheels = 20.45 kN
Mobility number of front wheels = 14.98
Mobility number of rear wheels = 18.36

Rolling resistance of front wheels = 0.95 kN
Rolling resistance of rear wheels = 1.32 kN
Maximum coefficient of traction of front wheels = 0.735
Maximum coefficient of traction of rear wheels = 0.780
Maximum total thrust = 26.17 kN
k $(C_T)_{max}$ of front wheels = 5.75
k $(C_T)_{max}$ of rear wheels = 5.96
k of front wheels = 7.82
k of rear wheels = 7.64
Thrust of front wheels = $10.22\ (1 - e^{-7.82s})$ kN
Thrust of rear wheels = $15.95\ (1 - e^{-7.64s})$ kN

The total torque required at the driving wheels to transmit the full engine power is the same as for the two-wheel drive tractor.

Gear	L1	L2	H1	L3	H2	H3
Total thrust, kN	33.75	19.43	15.78	10.30	8.61	4.04
Slip, %	>100	17.68	11.99	6.49	5.20	2.18
True forward speed, km/h	0	6.25	8.03	12.25	14.34	25.51
Drawbar power, kW	0	33.73	35.20	35.05	34.30	28.63

From equation 15,

Slip for maximum output power = 24.85%
Thrust from front wheels = 8.76 kN
Thrust from rear wheels = 13.56 kN
Total thrust = 22.32 kN
Total torque at driving wheels = 18.17 kN m

Gear	L1	L2	H1	H3	H2	H3
Engine torque, N m	135.51	224.90	270.42	388.29	448.69	773.28
Engine speed, rev/min	2260	1440	above maximum torque			
No-slip forward speed, km/h	4.69	4.97				
Drawbar power, kW	21.85	23.16				

Therefore, the highest drawbar power available in each gear, the forward speeds and the equivalent rates of work at 0.025 (ha/h)/kW are as follows.

Gear	L1	L2	H1	L3	H2	H3
Drawbar power, kW	21.85	33.73	35.20	35.05	34.20	28.63
Equivalent rate of work, ha/h	0.546	0.843	0.880	0.876	0.855	0.716
Forward speed, km/h	3.52	6.25	8.03	12.25	14.34	25.51
Equivalent implement width, m	1.55	1.35	1.10	0.72	0.60	0.28

Conclusions

The performance of agricultural tractors carrying out heavy draught operations can be predicted from data available from standard test reports together with tyre performance data. Predictive equations previously developed from single wheel tests, using cone penetrometer resistance as a measure of soil strength, are particularly suitable for this purpose.

Models of varying complexity may be developed depending on the main variables of interest. In particular, models which predict output in terms of drawbar power can be kept relatively simple, whereas those which predict rate of work with implements whose draught is dependent on forward speed are inevitably more complex.

Even simple models can be effective in quantifying the benefits of design features such as four-wheel drive, tyre size or power/weight ratio. This is illustrated by the examples given in this paper, where the four-wheel drive version of the tractor gave a 10% higher maximum power output than the two-wheel drive version. However, of equal significance is the fact that the two-wheel drive version had to be operated in L3 gear at 11.6 km/h to develop maximum power, whereas the four-wheel drive version could develop maximum power in H1 gear at 8.03 km/h. Therefore, if the operation being carried out demanded that the forward speed be restricted to H1 gear, the output of the four-wheel drive version would have been 24% higher than the two-wheel drive, or, in L2 gear, 41% higher.

More complex models can be programmed on a microcomputer to be "user-friendly" so that they can be run by farmers or their advisers without the need for a detailed understanding of the theory behind them.

References

1. SPLINTER, W.E., STEINBRUEGGE, D.E., LANE, D.E. and LARSEN, L.F. Nebraska tractor test - programs and philosophy. SAE Paper No. 730763, 1973.

2. MANBY, T.C.D. and MATTHEWS, J. Development and operation of OECD tractor test code. SAE paper 730762, 1973.

3. JURKAT, M.P., NUTTALL, C.J. and HALEY, P.W. The US Army Mobility Model (AMM-75). Proceedings of the 5th International ISTVS Conference, Detroit, 1975.

4. MELZER, K.-J. Analytical methods and modelling; state-of-the-art report. Journal of Terramechanics, vol. 19, no. 1, 1982.

5. MELZER, K.-J. Possibilities of evaluating the traction of tires for off-road transportation vehicles. Proceedings of the 2nd European ISTVS Conference, Ferrara, 1983.

6. HORTON, D.N.L. and CROLLA, D.A. The design of off-road vehicles with good ride vibration qualities. Proceedings of the 8th International ISTVS Conference, Cambridge, 1984.

7. STRAUSS, C. Comparison of measured and simulated ride comfort for an agricultural tractor and influence of travel speed on dynamic response. Proceedings of the 8th International ISTVS Conference, Cambridge, 1984.

8. WISMER, R.D. and LUTH, H.J. Off-road traction prediction for wheeled vehicles. Journal of Terramechanics, vol. 10, no. 2, 1973.

9. GEE-CLOUGH, D. Selection of tyre sizes for agricultural vehicles. Journal of Agricultural Engineering Research, vol. 25, no. 3, 1980.

10. A.S.A.E. Soil penetrometer. A.S.A.E. recommendation R313, 1968.

11. GORYACHKIN, V.P. Collected works. Sel' khoagiz, Moscow, 1940.

12. SÖHNE, W. Suiting the plough body shape to higher speeds. Grundlagen der Landtechnik, vol. 12, 51-62 (NIAE translation no. 101), 1960.

13. GEE-CLOUGH, D., MCALLISTER, M., PEARSON, G. and EVERNDEN, D.W. The empirical prediction of tractor-implement field performance. Journal of Terramechanics, vol. 15, no. 2, 1978.

14. KRASTIN, E.N. The use of methods of theory of dimensional analysis for the evaluation of the draft characteristics of the plow during operation in different conditions, Doklady MIISP, vol. 8, no. 61, 1973. (Translation Gill/333, National Tillage Machinery Laboratory, Auburn, Alabama, USA).

15. OSKOUI, K.E. and WITNEY, B.D. The determination of plough draught - Part I. Prediction from soil and meteorological data with cone index as the soil strength parameter. Journal of Terramechanics, vol. 19, no. 2, 1982.

16. OSKOUI, K.E., RACKHAM, D.H. and WITNEY, B.D. The determination of plough draught - Part II. The measurement and prediction of plough draught for two mouldboard shapes in three soil series. Journal of Terramechanics, vol. 19, no. 3, 1982.

17. A.S.A.E. Agricultural machinery management data. Agricultural Engineers Yearbook, A.S.A.E. D230.3.

18. DWYER, M.J., MCALLISTER, M. and EVERNDEN, D.W. Comparison of the tractive performance of a tractor driving wheel during its first and second passes in the same track. Journal of Terramechanics, vol. 14, no. 1, 1977.

19. GEE-CLOUGH, D., MCALLISTER, M. and EVERNDEN, D.W. Tractive performance of tractor drive tyres, III. Running in the furrow bottom. Journal of Agricultural Engineering Research, vol. 22, no. 4, 1977.

20. O.E.C.D. Report on test of David Brown 1390 two-wheel drive tractor. O.E.C.D. Approval No. 827, 1982.

21. O.E.C.D. Report on test of David Brown 1390 four-wheel drive tractor. O.E.C.D. Approval No. 826, 1981.

DIFFERENTIAL EQUATIONS OF THE VEHICLE'S LINEAR MOTION MATHEMATICAL SOLUTION AND EXPERIMENTAL APPROACHES

R. FACCHINI

Lt. Col eng/ MINISTERO DIFESA — D.G. Mot.Comb. - ROMA - ITALIA

1 FOREWORD

With reference to fig. 1 which shows three oriented cartesian axes constrained to the vehicle and with the origin coinciding with the center of mass, it will be taken in consideration only the horizontal straight longitudinal motion along the axis of x.

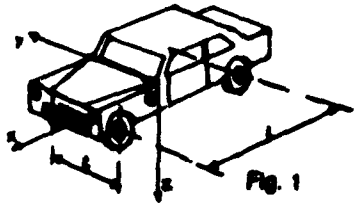

Fig. 1

In this case, the vertical components of support reaction will balance the weight, while the orizontal components of the forces involved will be only the drawbar forces, the motion resistances and the inertial masses.

The rolling resistance and drag have a fairly complex nature; in practice they are difficult to separate because this requires complicated devices and procedures.

For this reason, on the basis of theoretical considerations and numerous tests, many authors have formulated several synthetic expression for the combined calculation of the rolling resistance and drag.

With the well known meaning of the symbols, among the many formulas it is remembered:

1. $R = \frac{1}{p^{0.8}} \left(20 + \frac{V^{2.5}}{129 \cdot 10^3 \cdot W^{0.44}}\right)$ ANDREAU

2. $R = 5{,}1 + \frac{55}{p_c} + \frac{(8.5 + 5W)(V/160)^2}{p_c}$ KAMM

3. $R = \frac{K}{10^3}\left[5{,}1 + \frac{5.5 + 9W}{p_c} + \frac{(8.5 + 3W)(V/160)^2}{p_c}\right]$ SAE

4. $R = (f_o + KV^2)\,W$ MORELLI- ZIGNOLI

The last expression, normally used today, will be kept as a base of this study.

Introducing the value of K and the mean density of air ($0{,}13 \frac{Kg \cdot s^2}{m^4}$) with the international system measurement unit,

it becomes $R = f_o W + (6.5 \cdot 10^{-2} W + 0{,}65 \cdot Cx \cdot S)\,V^2$

with:

f_o = rolling resistance dimensionless coefficient

W = vehicle weight
Cx = drag coefficient
S = vehicle cross section

giving

- $r_c W = A^2$ (N) and
- $6.5\ 10^{-6} W + 0.65\ Cx\ S = B^2 (N \frac{s^2}{m^2})$

the following expression will be obtained
$R = A^2 + B^2 V^2$

2. DIFFERENTIAL EQUATIONS OF THE MOTION INTEGRATION AND MATHEMATICAL SOLUTIONS

a *Vehicle in neutral driving*

In general, the differential equation of the vehicle motion in vectorial form is:

$$\bar{F} + \bar{R} + Me \frac{d\bar{v}}{dt} = 0$$

where
$\bar{F}$ = drawbar force
$\bar{R}$ = total motion resistance
Me = equivalent translating mass of the vehicle

$$Me = \frac{W}{g} + \frac{1}{R_o} \sum_i \lambda_i^2 J_i \qquad \text{where:}$$

W = vehicle weight
R_o = rolling height
λ_i = i^{th} speed reduction
J_i = i^{th} equatorial moment of inertia of rotating mass

$\frac{d\bar{v}}{dt}$ = momentary longitudinal acceleration

In the case of the vehicle in neutral, it results
$F = 0$, while as already seen:
$R = A^2 + B^2 V^2$

Then the differential equation in scalar form becomes:

$$A^2 + B^2 V^2 + Me \frac{dv}{dt} = 0$$

from which through simple passages:

$$-\frac{dt}{M_o} = \frac{dv}{A^2 + B^2 V^2} = \frac{dv}{B^2 (A^2/B^2 + V)}$$

giving

$$\frac{A}{B} = c \quad e \quad \frac{M_o}{B^2} = n$$

it results

$$-\frac{dt}{n} = \frac{dv}{c^2 + v^2} \quad \text{integrating:}$$

$$\frac{-t}{a} + K = \int \frac{dv}{c^2 + v^2} = \frac{1}{c} \operatorname{arctg} \frac{v}{c}.$$

$K - t = \frac{a}{c} \operatorname{arctg} \frac{v}{c}$, with K = arbitrary constant

giving as boundary conditions that for v = 0,
t = m = vehicle stopping time, it results
K = m; and therefore:

$$m - t = \frac{a}{c} \operatorname{arctg} \frac{v}{c}$$

As it can be freely choosen the instant of test beginning, it results for t = 0, v = v_o.
Then the other constant "a" can be eliminated.
In fact with the shown condition, it results

$$a = \frac{mc}{\operatorname{arctg} v_o/c}$$ and replacing

$$t = m\left(1 - \frac{\operatorname{arctg} v/c}{\operatorname{arctg} v_o/c}\right) \quad (2)$$ or making explicit versus V:

$$\operatorname{arctg} \frac{v}{c} = \frac{m-t}{a} c\, a\,; \quad \frac{v}{c} = \operatorname{tg} \frac{m-t}{a} \cdot c$$

at last

$$v = c \operatorname{tg}\left[\left(1 - \frac{t}{m}\right) \operatorname{arctg} \frac{v_o}{c}\right] \quad (3)$$

The equation of motion found in the formulas (2) and (3), is perfectly defined up to three constants:

c = $\frac{f}{k}$ = rate between the square root of the components of motion resistance
m = vehicle stopping time starting from the beginning of the test
V_o = momentary speed at the same time

On two cartesian axes v - t, once established the test values of m and V_o, the equation (3) defines a family of infinite trigonometrical tangents.

Each of them has a different trend in function of parameter "c" yet all passing through the nodes of cordinates (t = 0, v = v_o) and (t = m, v = o).

In this way, once defined, either experimentally or analitically, the value of the parameter c,a curve is identified which graphically and analytically, through the eq. (3) determines perfectly the motion law of a specific vehicle.

b. Vehicle driven by constant torque

In this case the forces acting on the vehicle are:

- $F = \frac{M}{R_o}$ = force expressed by driving torque being R_o the rolling height

- $R = A^2 + B^2 \cdot v^2$ with the known meaning of symbols.

Then from the general equation of motion (1) it is obtained the following differential scalar equation:

$F - R = M_a \frac{dv}{dt}$, or

$$Me \frac{dv}{dt} = B^2 \left(\frac{M}{R_o \beta^2} - \frac{A^2}{\beta^2} \cdot v^2 \right)$$

$$\text{giving } \frac{M}{R_o \beta^2} - \frac{A^2}{\beta^2} \cdot c^2 = K^2 \qquad (4)$$

$$\text{it results } \frac{M_e}{B^2} \frac{dv}{dt} = K^2 - v^2$$

separating the variables

$$\frac{B^2 dt}{M_e} = \frac{dv}{K^2 - v^2} \quad \text{and integrating, it results}$$

$$\frac{B^2}{M_e} t + h = \int \frac{dv}{K^2 - v^2} = \frac{1}{K} \operatorname{sett\,tgh} \frac{v}{K} \qquad (5)$$

with h = *arbitrary constant*

Giving as boundary condition the standing start of vehicle, that is:
for $t = 0$, $v = 0$ we have $h = 0$
Then it results

$$\frac{B^2 \cdot K}{M_e} t = \operatorname{sett\,tgh} \frac{v}{K}$$

at last

$$v = K \operatorname{tgh} \frac{B^2}{M_e} K \cdot t \qquad (6)$$

Therefore the (6) defines a family of hyperbolic tangents.

Each tangent is identified by a well precise value of K and torque at the wheels.

Then it gives the analytical explanation of graphical trend of $v - t$ in acceleration test in constant torque of any vehicle.

It is a series of infinitesimal hyperbolic tangents with K variable continously in function of the variation of the torque at the engine (if there is no change of gear).

Any way, the (6) is valid only in the case of standing start, as this condition was given to eliminate the integration constant.

Therefore in general, from the equation:

$$\frac{B^2 \cdot t}{M_e} + h = \frac{1}{K} \operatorname{sett\,tgh} \frac{v}{K} \qquad (5)$$

it results.

$$\frac{B^2 K}{M_e} t + K \cdot h = \operatorname{sett\,tgh} \frac{v}{K}, \text{ and if } K \cdot h = n$$

it will be obtained:

$$v = K \operatorname{tgh} \left(\frac{B^2}{M_e} \cdot K t + n \right) \qquad (7)$$

Where n depends on the used gear and we have $n = 0$ for the gear employed for the standing start.

The hyperbolic tangent, which is shown analytically by the equation (6), is identified perfectly up to three constants:

B^2 (N $\frac{s^2}{m^2}$) = efficency parameter of the vehicle, known by previous point

n (dimensionless) = parameter which depends on the used gear

Me (N $\frac{s^2}{m}$) = equivalent translating mass of the vehicle in the used gear

K (m/s) = coefficient which depends on the torque at wheels and on the efficiency parameters A^2 and B^2

Then for each couple of coordinates v - t of an acceleration graph in a certain gear, from the equation (7) it can write a hyperbolic equation where the unknown quantities are: Me, n, K.

Considering 3 couple of values v - t in the same section of graph (same gear), it will be possible to write consistent equations of 3 independent equations with 3 unknown quantities.

As such consistent equation included hyperbolic equations, the theoretical solution is impossible, yet we can go on (trial and error) inserting many term s of values Me, n, K. so that we can verify the 3 equations.

3. EXPERIMENTAL APPROACHES - VALIDATION TESTS

a Carried out tests

In order to provide experimental validation, many tests in neutral driving and of ac celeration have been carried out with 4 meaningfull vehicles.

To assure the uniformity, significance and repeatability, such tests have been carried out on road and on a special "standard" running track of the Proving Ground of the Italian Army at P. Corese (Rome).

Photo (1) Aerial photograph of running track

Tested vehicles

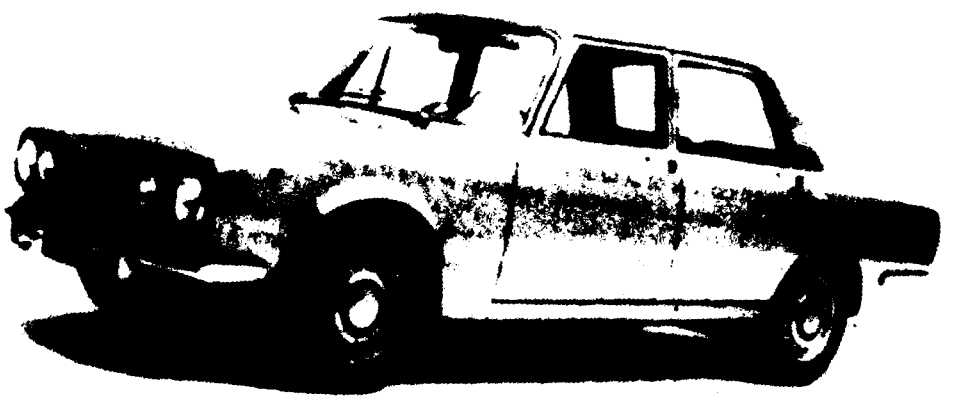

Photo 2: Alfa Romeo 1750

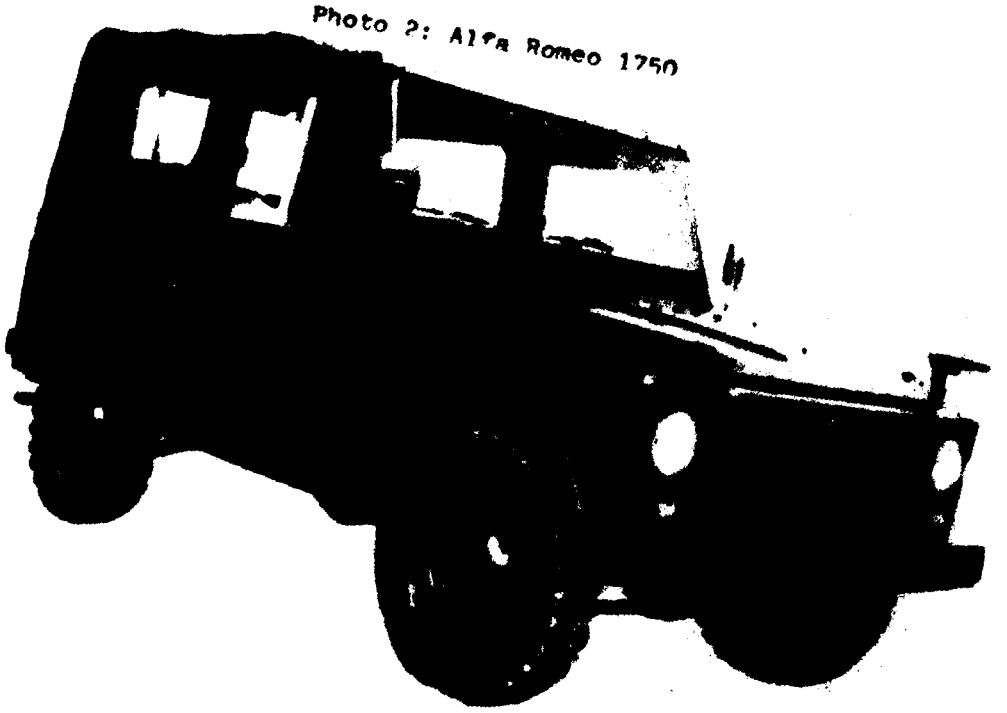

Photo 3: AR 76

Tested vehicles

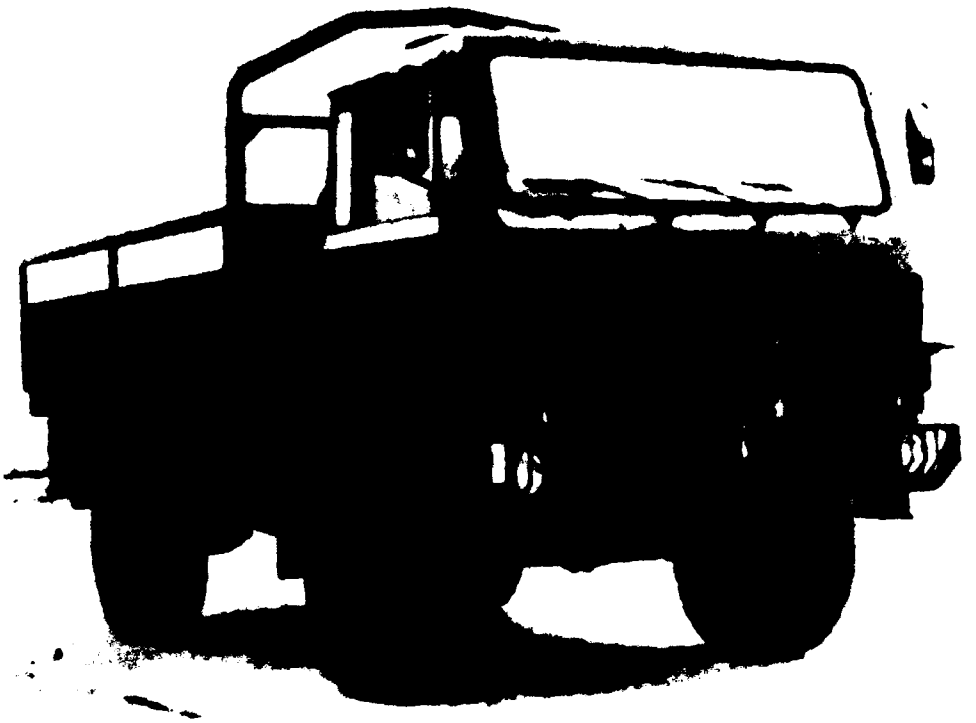

Photo 4: ACL 75

Photo 5: ACL 75 Amphibious

The following vehicles have been tested

· Alfa Romeo 1750	civilian car vehicle
· AR/76	reconnaissance military vehicle
· ACL/75	light utility military truck
· ACL/75 amphibious	light utility military amphibious truck

For the sake of brevity, the peculiarities of recording devicies of graph v - t are omitted

The procedures and the redundance of the tests have got rid of casual errors, wind effect, slight slopes etc as much as possible.

b Vehicle in neutral driving

1) Test result

The results of the test are synthetized in fig. 2.

The scattering has been insignificant and in any case included in the graphic error.

2) Calculation of the efficiency parameters: A^2 and B^2.

Considering the tested vehicle data, the values of experimental coefficient "c" obtained from the graphs and the analitycal expressions given in the theoretical part, the following parameters (A^2 and B^2) of the vehicle inclusive efficiency have been obtained:

Vehicle	Alfa Romeo 1750	AR/76	ACL/75	ACL/75 amphibious
weight (Kgp/N)	1500/14715	2340/22932	6925/67865	5120/50176
S (m^2)	1,88	2,75	5,72	5,54
R_0 (m)	0,28	0,37	0,48	0,53
Me (N $\frac{s}{m}$)	1545	2434	7271	5376
m (s)	110	122	146	124
V^0 (m/s)	20	25	20	20
c (m/s)	19,6	11,5	11,8	14
a (m)	2710	1232	1660	1808
B^2 ($\frac{M \cdot g^6}{W^2}$)	0,57	1,975	4,379	2,973
A^2 (N)	219	261,2	609,8	582,7

3) Checking of rolling and drag coefficients.

The calculation of the coefficients r_0 and Cx has been made only in order to get validation and comparison data with the generally used quantities in locomotion mechanics.

Making use of the known data and expressions, we obtain the following results:

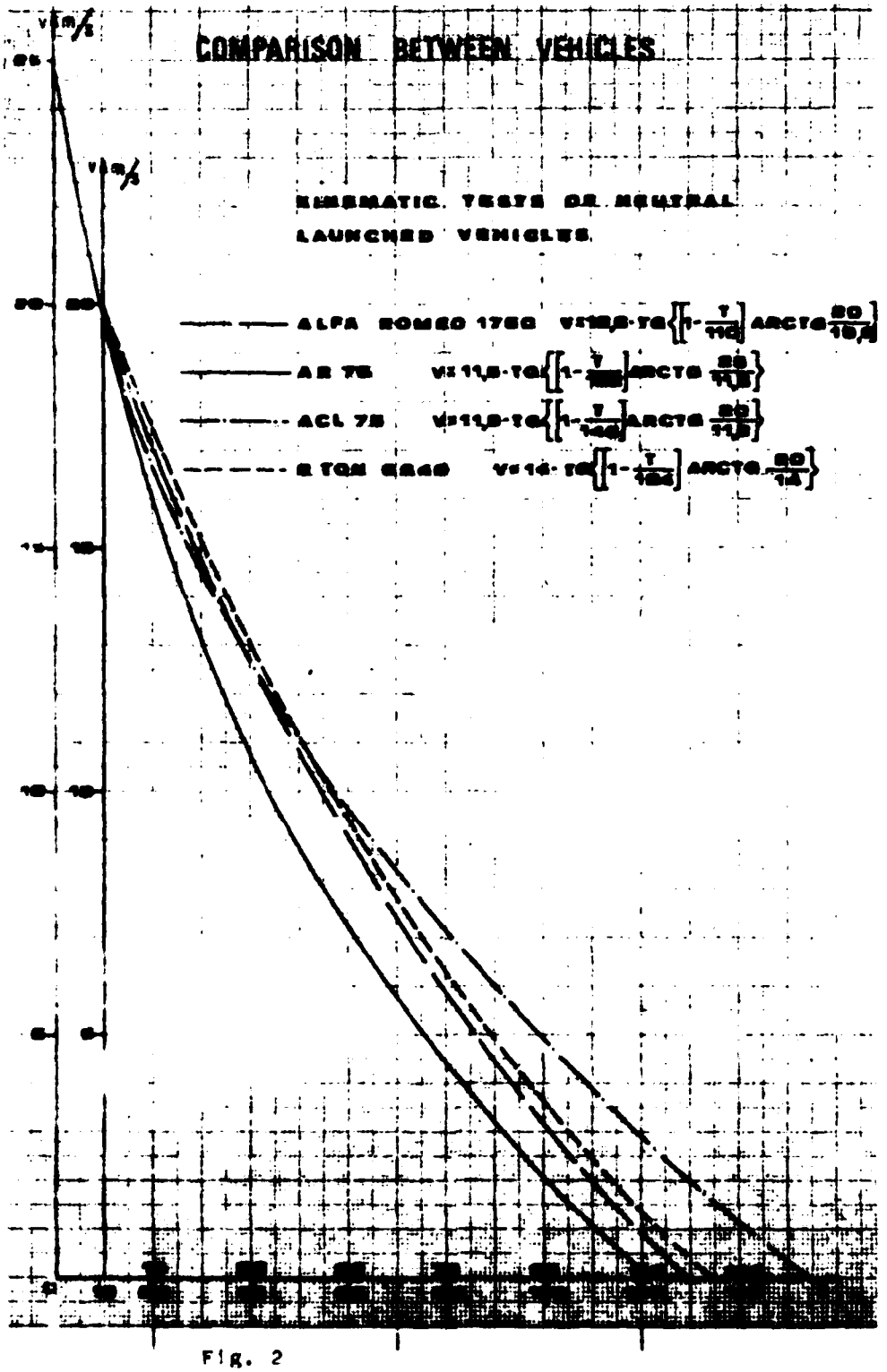
COMPARISON BETWEEN VEHICLES
KINEMATIC TESTS OF NEUTRAL LAUNCHED VEHICLES
ALFA ROMEO 1750
AR 75
ACL 75
2 TON CARGO

Fig. 2

Vehicle	Alfa Romeo 1750	AR/76	ACL/75	ACL/75 amphibious
A^2 (N)	219	261	609,8	582,7
B^2 ($\frac{N\ s^2}{m^2}$)	0.57	1,975	4,379	2,973
W (Kg)	1500	2340	6925	5120
S (m^2)	1,88	2,75	5,72	5,54
ro	0,0149	0 0114	0,0089	0 0116
Cx	0.388	1,094	1,164	0,816

The found values of r_0 and Cx are quite congruous to the test condition and suitable to them provided by the experience and by other methods (in particular the highest r_0 of Alfa romeo is due to the fact that only for this car the tests have been carried out on road)

It is necessary to point out besides, that the good Cx of amphibious truck is due to his lower fairing

c Vehicle driven by constant torque

1) Test result

The results of the acceleration tests are synthetized in fig 3 and 4

2) Determination of the parameters Me n and K

The following calculation is not completly correct as the torque is not constant in the same gear, but it changes with the speed (r p m) of the engine

It can be regarded roughly good, if we consider that such variations are much lower than the changes due to the speed gear, besides in the diesel engines this couple range is fairly moderate

The maximum error due to the couple range of engine

$(\frac{C_{max} - C_{min}}{C_{max}} 100)$ is

Alfa Romeo = 9,6 % AR/76 = 19.1 %

ACL/75 = 10.5 % ACL/75 amph = 10.5 %

For each vehicle and for each used gear, the calculation of unknow values Me, n, K, has been carried out casting, trial and error, the following hyperbolic consistent equations

$V_0 = K \operatorname{tgh} (\frac{\beta^2}{M_e} \cdot K\,t_0 + n)$

$V_1 = K \operatorname{tgh} (\frac{\beta^2}{M_e} \cdot K\,t_1 + n)$

$V_g = K \operatorname{tgh} (\frac{\beta^2}{M_e} \cdot K\,t_g + n)$

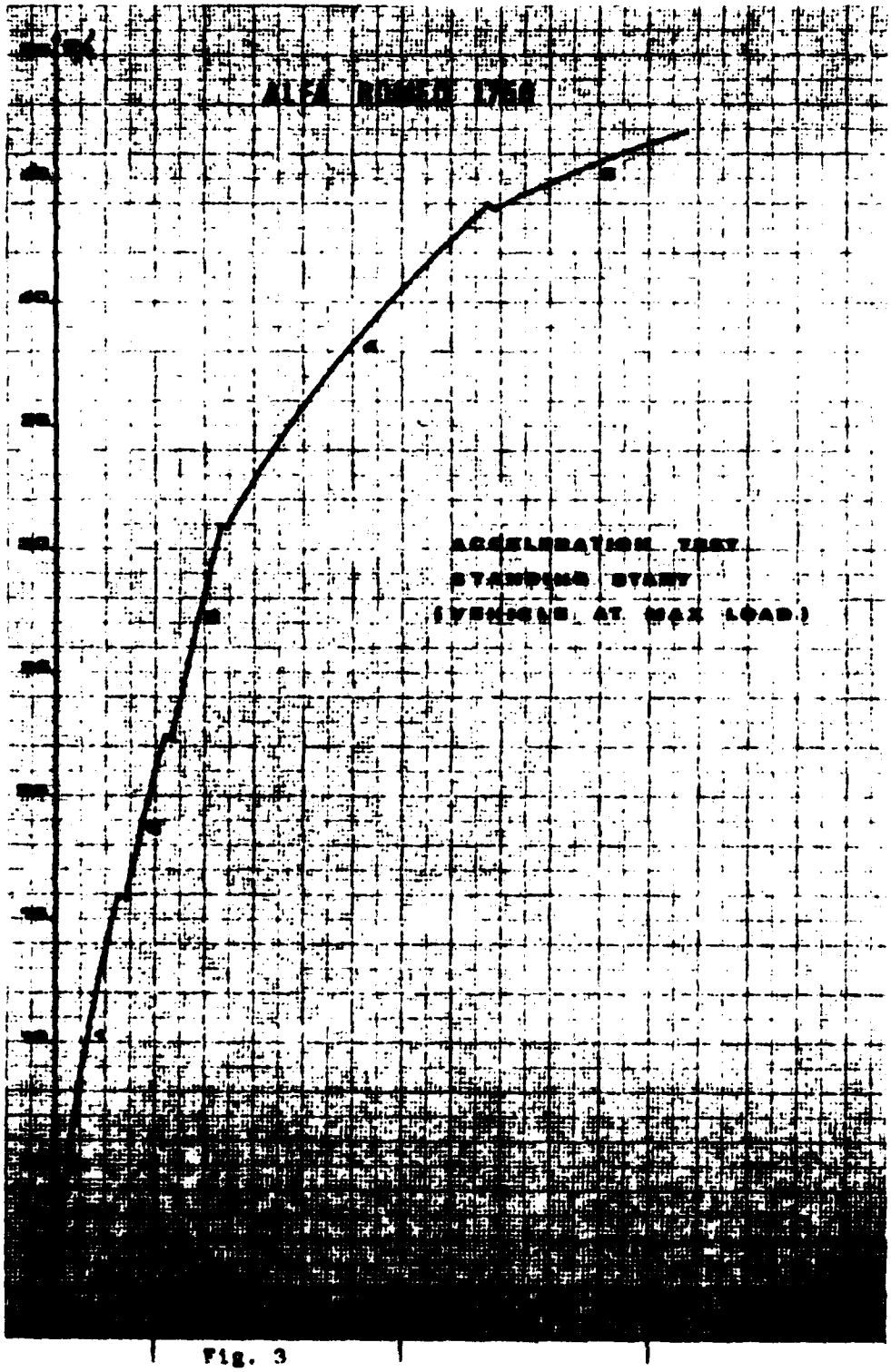

Fig. 3

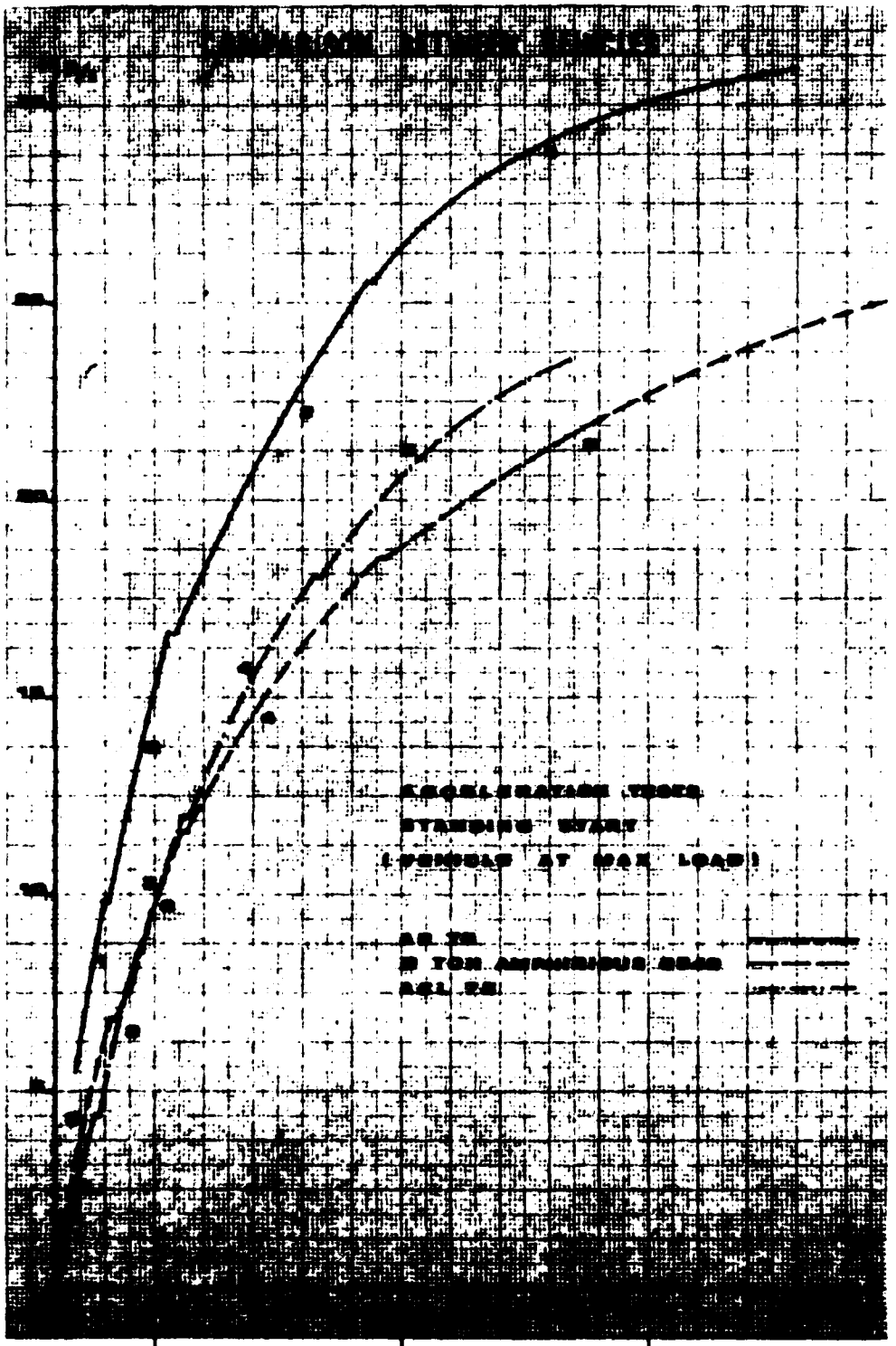

Fig. 4

where, known the meaning of other symbols, we have

V_o. V_i. V_g = speed at gear engaging at an intermediate instant and at gear disengaging respectively

t_o. t_i. t_g = relating instants to previous speeds

The results are reported in the following tables

Alfa Romeo 1750 W = 1500 Kg, B^2 = 0,57

Gear	ρ	Me	n	K
1°	11	1810	0	101
2°	8,065	1670	0,06	77
3°	5,848	1600	0,11	71
4°	3,246	1560	0,21	51
5°	4,31	1540	0,65	51

ACL/75 W = 6925 Kg. B^2 4,38

Gear	ρ	Me	n	K
1°	45,498	21700	0	73
2°	25,87	12800	0,01	54
3°	16,48	9400	0,05	42
4°	10,29	8400	0,18	33
5°	7,583	8100	0,31	26

AR/76 W 2340 Kg. B^2 = 1,975

Gear	ρ	Me	n	K
1°	23,102	4200	0	64
2°	13,23	3360	0,04	49
3°	8,57	3080	0,29	35
4°	6,30	2700	0,41	32

ACL/75 amphibious 6640: W = 5120 Kg; B^2 = 2,973

Gear	ρ	Me	n	K
2°	23,393	10200	0	63
3°	14,805	8200	0,04	48
4°	9,303	6600	0,17	34
5°	6,856	6100	0,36	26

3) Determination of the working torque and the inclusive efficiency

From the obtained values it is possible to arrive to the working torques at wheels Mr and at engine Mp with the expressions

$Mr = (K^2 + C^2) B^2$ Ro and $Mp = M_r/\rho$

The calculation has been carried out in the following tables:

Alfa Romeo 1750: $C^2 = 384$; $B^2 = 0{,}57$; $R_O = 0{,}281$

Gear	K	$K^2 + C^2$	M_r	φ	M_p
1	101	16584	1695	11	154
2	77	6313	1011	8,065	125
3	71	5425	869	5,848	148
4	51	2985	478	3,246	147
5	51	2985	478	4,31	111

AR/76 $C^2 = 132$; $B^2 = 1{,}975$; $R_O = 0{,}37$

Gear	K	$K^2 + C^2$	M_r	φ	M_p
1	64	4228	3098	23,102	133
2	49	2533	1850	13,23	139
3	35	1357	991	8,57	116
4	32	1156	845	6,30	134

ACL - 75 : $C^2 = 139$; $B^2 = 4{,}38$; R_e 0,48

Gear	K	$K^2 + C^2$	M_r	φ	M_p
1	73	5468	11495	45,498	252
2	54	3056	6422	25,87	248
3	42	1903	4000	16,48	242
4	33	1228	2581	10,29	251
5	28	923	1940	7,583	256

2 TON amphibious : $C^2 = 196$; B^2 2,973; $R_O = 0{,}51$

Gear	K	$K^2 + C^2$	M_r	φ	M_p
2	63	4165	6315	23,393	269
3	48	2500	3790	14,905	254
4	34	1352	2049	9,303	220
5	28	980	1486	6,856	216

At last, comparating the values of M_p to the output torques at engine test stand, in the corrisponding speeds, we are able to determine the inclusive efficiencies (ηt):

Vehicle \ Gear	1°	2°	3°	4°	5°
Alfa Romeo	0,826	0,670	0,793	0.788	0,565
AR 76	0,880	0,920	0,768	0,887	---
ACL 75	0,856	0,842	0,822	0,852	0,869
2 TON Amphibious 6640	---	0,914	0,863	0,747	0,733

This values consider both the mechanical efficiency of the trasmission and the energy dissipation during the motion, for the water, fuel and lubricating oil pumps, fan, air suction, exhaust gas, electric generator, etc..

A further step would be the determination of the total efficiency (thermic engine included) of the vehicle during the motion with the expression

$$\eta_t = \frac{A^2 + B^2 \cdot V^2}{C_s \, C_{sv} \, R} \qquad (7)$$ where:

C_s = volumetric fuel consumption versus to run unit ($10^5 \frac{dm^3}{100\ Km}$)

C_{sv} = specific heat versus volume unit ($\frac{Kcal}{dm^3}$)

R = mechanichal equivalent of heat = 4187 $\frac{J}{Kcal}$

E.g. the calculus carried out on the ground of consumption remarks of Alfa Romeo travelling at 100 Km/h, has provided a total efficiency $\eta t = 0,23$, with a thermic engine efficiency of 0,29.

These data are congruous and, with a very good approximation, they correspond to those obtained from other sources and experiences.

4. CONCLUSIONS

It is not wished to leave out the limits of reliability in the proposed methods, that is :
- partial inadequacy of the binominal expression of motion resistance,
- incomplete fuel induction in the engine;
- error on considering the torque constant at the same gear.

In any case we believe that the application of the described methods is useful in the study of the vehicle and his motion; in particular it should provide the following benefits;
- only kinematical remarks are carried out with devices which have a good level of precision and reliability,
- measurements regard only two tests (in neutral and acceleration) with a small scattering;
- field tests (more onerous for the organization) are very much reduced , whereas we make larger use of calculation;
- particular and expensive devices (wind tunnel, "big inertial wheel", "aerodynamic protection" etc..) are not requested,so we avoid difficulties and errors connected to their use;

-it is possible to perform checks choosing on the graphs the desired number of point (t,v) and statistical elaborations can be made by computer;
- they allow to do an analitycal study of vehicle/soil parameters.

This is possible by changing the considered parameter (e.g. tyre inflation pressure), calculating again the coefficients on which that parameter is acting, and, at last comparing the obtained values so that we shall reach the opimization of the tested parameter.

Coming to the fact, the method with the vehicle in neutral allows the determination of:
- vehicle efficiency parameters: A^2 e B^2,
- rolling coefficient r_0 and consequent optimization of:
  - rolling height
  - kind, width and structure of the tyre
  - tyre inflation pressure according to speed and load on the tyre
- equivalent translating mass in neutral
- vehicle cross section
- drag coefficient C_x and minimization of its components:
  - head effect: C_a
  - tail effect: C_c
  - side friction resistance: C_i
  - drag on the wheels = C_r
  - resistance caused by lift: C_l

Even if, the method based on acceleration test, is less reliable for its larger scattering, it could provide usefull factors of check verification and valutation, with regard to:
- momentary torque at wheels
- equivalent translating mass in each gear: M_e
- power losses in order to supply additional but indispensable vehicle members: electric, hydraulic, pneumatic , lubrication system.

In conclusion the limited achieved tests have provided quite encouraging results.

TRACTOR-SOIL-IMPLEMENTS FUNCTIONAL INTERACTIONS AND MODELS

G. JAHNS* AND H. STEINKAMPF**
FAL, BRAUNSCHWEIG-VÖLKENRODE, WEST GERMANY

INTRODUCTION

Tractors and machinery have evolved to high technical levels, however this advanced level of technology results in system complexities making it difficult and expensive to further improve quality. Also, it may be more difficult for farmers to realize the total potential of these higher quality systems.

Computer models are powerful aids for identifying and evaluating the numerous machine and operational parameters that affect tractor and implement efficiency. They can allow engineers to optimize their design more cheaply and quickly than by using field trials only, and they can also show them which system parameters must be displayed to the operator to enable him to make best use of the total potential that is engineered into the system and for which the farmer has paid.

The models introduced and explained in this paper help to analyze technical and agricultural parameters, such as soil condition, ploughing speed and depth, wheel load, etc. (see Table 1).

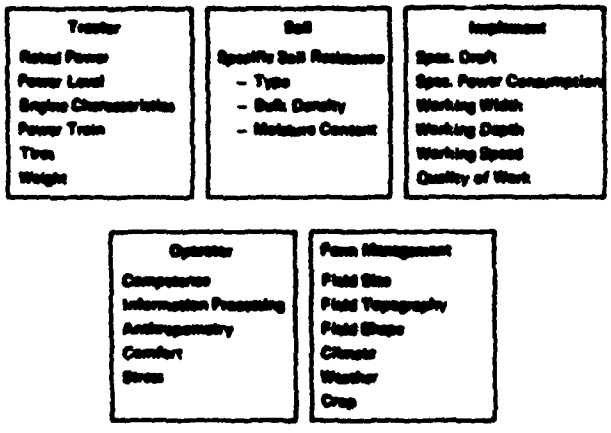

Table 1. Parameters effecting the efficiency of tractor-soil-implement systems.

* Dr.-Ing. Gerhard Jahns is a scientist at the Institute for Basic Research in Agricultural Engineering (director: Prof. Dr.-Ing. W. Batel)

** Dr.-Ing. Heinrich Steinkampf is a scientist at the Institute for Production Engineering (director: Prof. Dr. agr. H. Schön)

Unfortunately not all parameters can be investigated by computer models e.g. the desired result of tillage operations or the stress on the operator are important criteria which cannot be satisfactorily quantified by physical values and are therefore not computable. In the following, ploughing as a time and fuel consuming tillage operation, is used as an example. The theoretical field capacity is the main criteria evaluated.

MODELING STRATEGY: COMPUTING PRINCIPLE AND DATA ACQUISITION

Computer models are used to investigate sophisticated systems by means of mathematical descriptions and to arrange and clearly display the results. The real link between the physical and the mathematical system is provided by data from field tests, such as, for example, the drawbar pull requirement of ploughs, the rolling resistance and tractive coefficient curves of tires, etc. To save computer time and memory it is desirable to describe this field data by equations instead of storing them and interpolating intermediate values. Often reversible equations are desirable so as to prevent the need for interations. It is one of the advantages of computer models, as well as a risk, that in contrast to physical reality, the admissible range of parameters can easily be exceeded. In those cases the validity of the results has to be observed particularly carefully. The form and extent of each model should be related to the questions to be answered. Even though high computer power is available, no model should be more complicated than is necessary.

Dividing the tractor-soil-implement system into modules (Figure 1 - upper section) gives the advantage that the intersections of the model can be the same as in the real system. Therefore, calculated and measured values can easily be compared and the individual modules can be exchanged and be of different complexity. The characteristics of the modules are schematically indicated at the bottom of Figure 1.

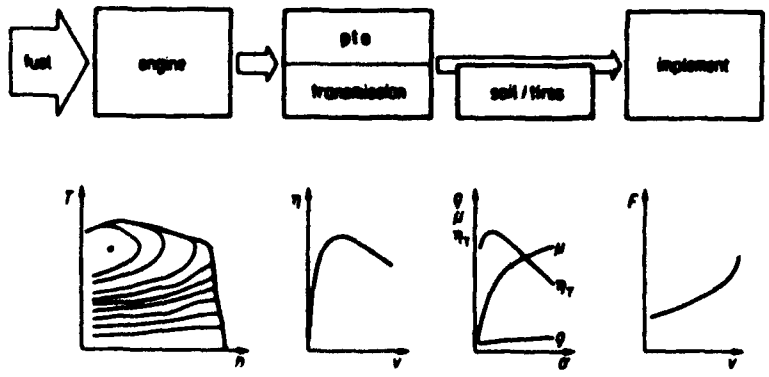

Figure 1. Tractor-soil-implement model schematic.

The characteristics of tractor engines are well described by their performance maps. To avoid time and memory consuming computation, an equation has been developed to calculate the fuel consumption of an engine in relation to speed and torque or to speed and power. This equation is universal for all engines while its coefficients are specific to the engine under investigation. To calculate these coefficients values for speed, fuel consumption and torque or power for 9 working conditions are required. They are available for many tractors from test reports, or can be measured using a suitably instrumented dynamometer. The results discussed first are based on an engine and tractor as described in OECD-Test Report No. 809 with a rated power of 44,2 kW and a mass/power ratio of 68,9 Kg/kW to 149 Kg/kW.

The description of the power train is the weakest point in this and all known tractor models. Even though there are data available that describe parts of the power train, there are no overall efficiency data available for power trains of tractors. Therefore, in this model, as a first approach, a constant overall power train efficiency of 0.8 is used.

The traction of tires for different soil and working conditions has been measured in numerous field tests. Data from more than 2500 tests at the FAL are available and have been prepared for computer use. Figure 2 shows the results of the data processing. In this case the data were obtained by five test runs established under identical conditions. For certain values of slip σ the traction coefficients κ ($\hat{=}\ \mu$ in USA) indicated by x and the gross traction coefficients μ ($\hat{=}\ \mu_g$ in USA) indicated by + are plotted versus slip. The edged lines connect the averages of these values. The rolling resistance coefficient ρ is calculated as the difference between the traction coefficients $\rho = \mu - \kappa$. The smooth lines represent the approximations as:

$$\mu = a_0\sigma + b_0 e^{c_0\sigma} + d_0 \tag{1}$$

$$\kappa = a_1 + b_1 e^{c_1\sigma} \tag{2}$$

$$\rho = a_2 + b_2\sigma \tag{3}$$

and the traction efficiency as:

$$\eta_t = \frac{\kappa}{\mu} = \frac{\kappa}{\kappa + \rho} \tag{4}$$

The values of the parameters of the equations for the tires and soils used in the following are given in Table 2.

Versuchs-Nr.	3132 A-E	Einzelversuche	5
Versuchsjahr	1982	Versuchsort	Salzdahlum
Bild-Nr.	0		
Reifen	18.9 R 34	Felge	DW14 X 34
Hersteller	Continental	Fermer 804	
Karkassenfestigkeit	8 PR	Stollenhöhe	100 %
Rollradius	74.22 cm	Stollenzahl	40
		Stollenwinkel	45 Grad
Radlast	19.73 KN	Laufrichtung	vorwaerts
Luftdruck	1.10 bar	Fahrgeschwind.	3.40 km/h
Auslastung	109.90 %		
Bodenart	sand.-schluff.- Lehm	Porenvolumen	35.50 - 44.20 %
Zustand	gefr.-geg.,t=10-12cm	Bodenfeuchte	15.70 - 17.90 %
Oberfläche	Stoppel	Vorfrucht	Getreide

$\mu = a\sigma + b\sigma\exp(c\sigma) + d \quad \kappa = a + b\sigma\exp(c\sigma) \quad \rho = a + b\sigma$

	a	b	c	d
μ :	0.3156148E-02	-0.6103078E 00	-0.7319605E-01	0.6524163E 00
κ :	0.6763928E 00	-0.7504138E 00	-0.7022065E-01	
ρ :	0.8423895E-01	0.4910573E-03		

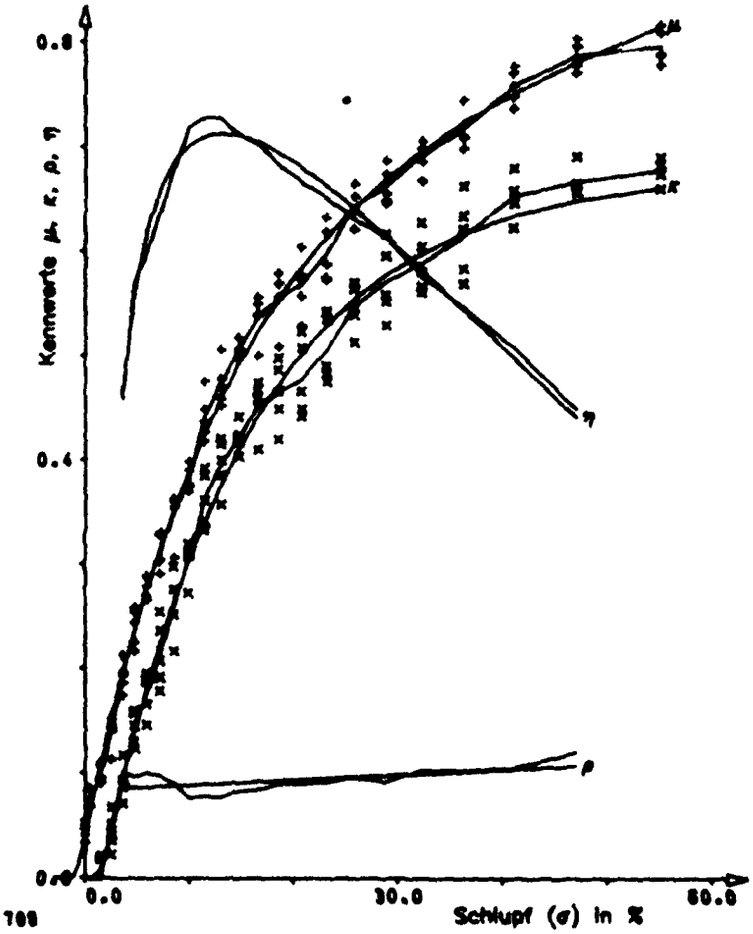

Figure 2. Data from field tests for evaluation of traction efficiency.

Parameter	Units	loamy Clay	sandy Loam
a_1	–	0.713	0.521
b_1	–	- 0.884	- 0.524
c_1	–	- 7.803	- 8.299
a_2	–	0.0575	0.076
b_2	–	0.025	0.205
a_3	kN/m^2	67.273	33.539
b_3	$\frac{kN}{m^2} \cdot \frac{h^2}{km^2}$	0.464	0.223

Table 2. Parameters of traction and rolling resistance coefficients and of required drawbar pull for two different soils.

As in reality, for computer models the data for the implements and the tires must be related to the same soil. Many attempts have been made to describe soil conditions e.g. by cone index or soil textural triangle etc; however, as yet there is not any satisfactory method of rating soil conditions with respect to tire performance and draft requirements of implements using physical values and verbal descriptions are used. Without these descriptions of the soil conditions draft or power requirements of implements are meaningless. Unfortunately, many publications dealing with draft and power requirements of implements measure only one specific working condition, e.g. draft for only one speed and working depth, etc. Data necessary to enable computer models to describe the draft and power requirements of implements must cover the expected speed range and working conditions and include a precise description of the soil.

In this model the required tractive effort for the plough has been measured under similar soil conditions and was described by Zach /1/. The required traction can be calculated for a speed range of V = 2 to V = 8 km/h by the equation:

$$F = b \cdot t \, (a_3 + b_3 v^2) \qquad (5)$$

with the ploughing width b and the ploughing depth t both in m. The parameters are listed in Table 2. The mass in kg of the plow can be calculated /2/ as a function of the ploughing width:

$$m = - 21 + 803 \, b \qquad (6).$$

It is assumed that 60 % of the weight of the plough is transferred on to the tractor.

Parameters Effecting Tractor Efficiency

The theoretical field capacity is used as a measure to calculate the effects of different parameters in respect to tractor

efficiency. It is further assumed that the tractor is ploughing with a conventional plough at a depth of 25 cm on level ground at a constant speed. For this first discussion, a temporary simplification is assumed that equal conditions exist for all four wheels and that the gear ratio and the ploughing width are continuously changeable.

Effect of Ploughing Width and Speed

Figure 3 shows the theoretical field capacity, the fuel consumption and the true ground speed of the tractor on a loamy clay for different ploughing widths.

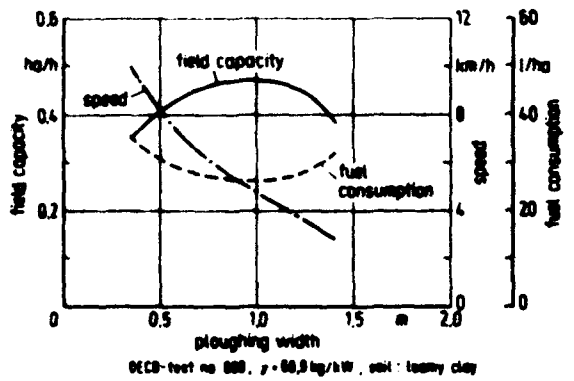

Figure 3. Field capacity, speed and fuel consumption versus ploughing width.

All three curves are boundary lines. That means for a given ploughing width these lines indicate the highest field capacity, highest speed and lowest fuel consumption possible. The field capacity has a maximum at a ploughing width of about one meter, where the fuel consumption has its minimum. The results show that for each optimum field capacity and plough width there is only one unique speed. Therefore, maximum field capacity is only achieved with a certain ploughing width and speed. If either one of them is changed the field capacity is lowered, or the tractor can't work because the boundary line has been exceeded.

Effect of Tractor Mass and Engine Power

Increasing the mass of a tractor, e.g. by ballasting the tractor, gives higher field capacity as can be seen from Figure 4. This is a well known effect but has limitations for a real tractor. These limits, the lower one for the tractor without ballast, and the upper one for the tractor with maximum recommended ballast, are indicated in Figure 4 by the hatched region. The tractor under investigation allows exceptional hight ballasting more than once its own weight. It can be seen from Figure 4 that by ballasting a tractor the maximum field capactiy increases with a decreasing rate of improvement. The same is true for the ploughing width. The field capacity curve

itself becomes less convex with higher mass, respectively the mass/power ratio. That means at high mass/power ratio the reduction in field capacity is not as significant if the ploughing width does not exactly match the optimal ploughing width than it would be at a low level of power/mass ratio.

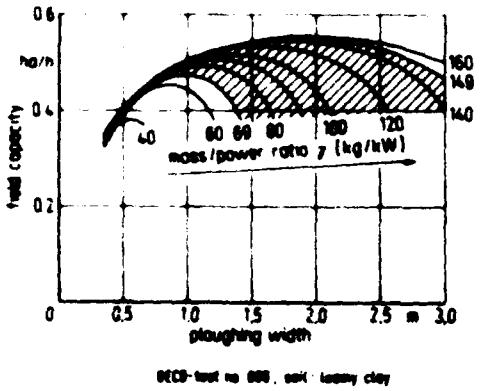

Figure 4. Influence of mass/power ratio on field capacity and ploughing width.

Figure 5 shows that for a constant mass/power ratio of 60 Kg/kW the theoretical field capacity increases linearly with engine power. The same is true for ploughing width. Figure 5 also shows that with higher engine power the field capacity curves become less convex. This means that as mentioned before, if the plough width does not exactly match the optimum the reduction in field capacity is not as significant and matching the right plough width is more critical with lower powered tractors.

While for Figure 5 constant mass/power ratio was assumed, it can be learned from Figure 6 showing the mass/power ratio versus rated power of today's tractors, that the mass/power ratio of tractors in use is declining with increasing rated engine power. In consequence, the increase of field capacity by increasing the power is partly compensated by the decrease of the mass/power ratio of today's high powered tractor.

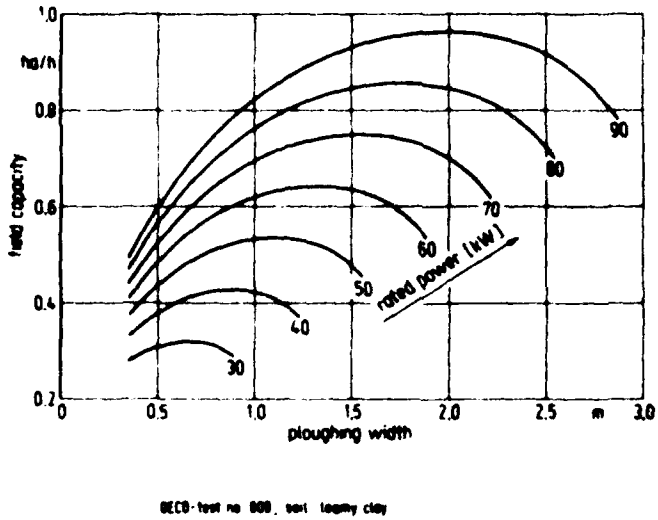

OECD-test no 808, sort loamy clay

Figure 5. Influence of rated power on field capacity and ploughing width.

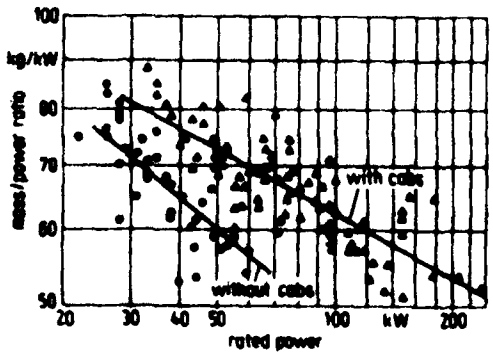

Figure 6. Mass/power ratio versus rated power /3/.

Effect of Soil

Figure 7 clearly shows why farmers with fields of different soil conditions have trouble matching the plough width to their tractors. The light soil, the sandy loam, has a flatter curve and a higher maximum occurring at a greater ploughing width than for the heavy soil, the loamy clay. The plough width can only be a compromise in these cases. Because there is no ranking system for soil available, it is only possible to compare individual soil types and conditions as in Figure 7 which shows two different soils as described in /1/.

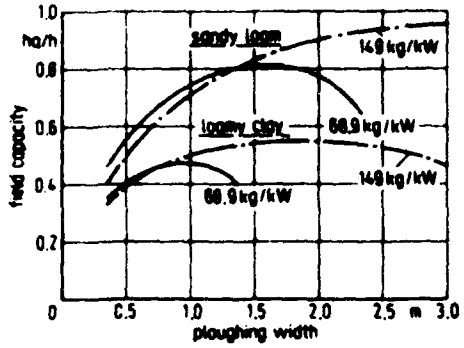

OECD-test no. 000.

Figure 7. Influence of soil types on field capacity and ploughing width.

Comparisons

Figure 8 shows the changes in field capacity and fuel consumption per hectare if one parameter is changed. For this comparison it is assumed that the tractor-soil-implement systems as defined in the beginning is working at the point of maximal theoretical field capacity, (see Figure 3). Ploughing 10 % deeper reduces the field capacity and raises the fuel consumption by approximately the same amount, and visa versa. The same holds true for the stationary component of the ploughing resistance (see Equation 5). If slip increases by 10 % the field capacity will drop and the fuel consumption rises slightly by more than 1 %. An increase of power and mass simultaneously by 10 % causes an increase of field capacity of about the same amount and a negligible rise in fuel consumption per hectare. If only the power is increased by 10 %, field capacity (7 %) and fuel consumption (2 %) increase. A + 10 % change in the tractor mass, e.g. by ballasting the tractor, causes a 2 % higher traction efficiency. As it is assumed that the comparisons of Figure 8 are related to maximum field capacity and minimum fuel consumption per hectare, obtained only at optimal ploughing width, every change of plough width will decrease the field capacity and increase fuel consumption.

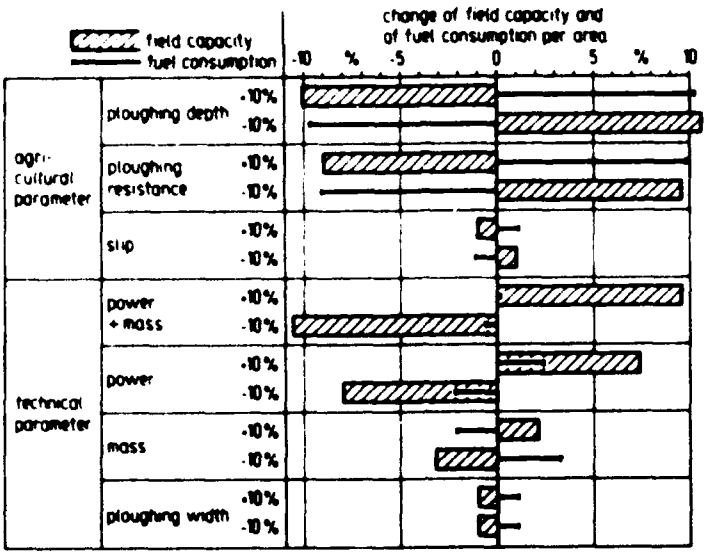

Figure 8. Comparison of field capacity and fuel consumption related to different parameters.

Optimal Field Capacity or Optimal Fuel Consumption

This question, often discussed enthusiastically, can easily be answered using a computer model. Figure 9 shows a comparison of the performance characteristics of a tractor (OECD No. 536) operating at rated power and when the specific fuel consumption reads 250 g/kWh (left curves), and the same tractor operating at its point of optimal fuel consumption of 224 g/kWh where it delivers 53 % of rated power (right curves). Calculations show that a reduction in fuel consumption of 19 % is achieved at the expense of a 40 % reduction in field capacity.

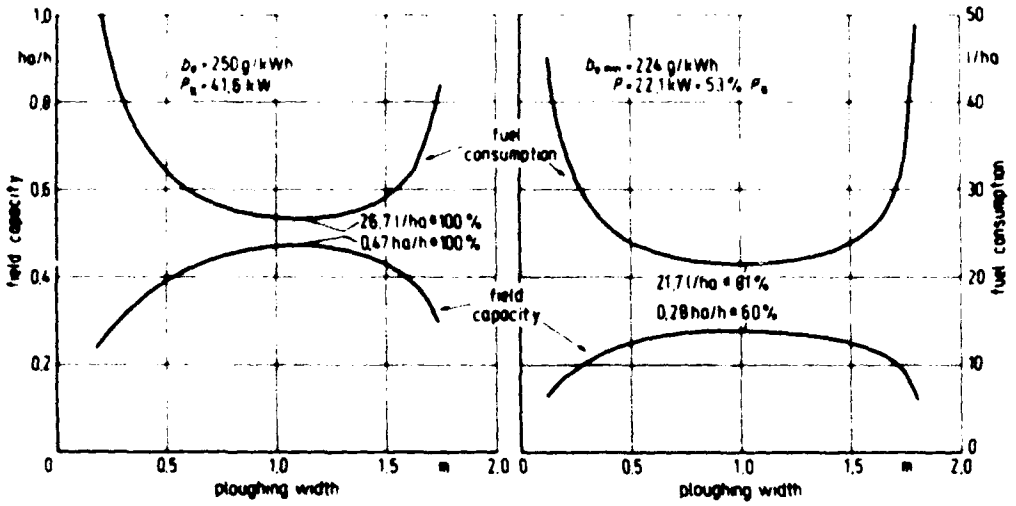

Figure 9. COMPARISON: Optimal field capacity (left) or optimal fuel consumption (right)

EXTENDED MODEL

As discussed previously, this model is not suitable for evaluating the effect of different conditions under all four wheels. Consequently, to investigate the effects of:

- 2 or 4-wheel drive
- different wheel speeds on 4-wheel drives
- locking differentials
- uneven or sloping areas

the model must be extended.

Figure 10 shows the schematic of this extended tractor-soil-implement model. The modular structure is maintained but the number of required data are greatly increased. In some parts of the model, for example to describe the different conditions under all four wheels, four sets of data are required instead of one. To describe the efficiency of every gear relative to torque and speed, efficiency maps similar to engine performance maps are required. Consequently, the computing time also increases. Effort, therefore, is made to describe the maps and graphs of the models for equations /4, 5/, or better yet, by reversible equations so as to prevent the need for iteration, and to reduce computing time and memory requirements.

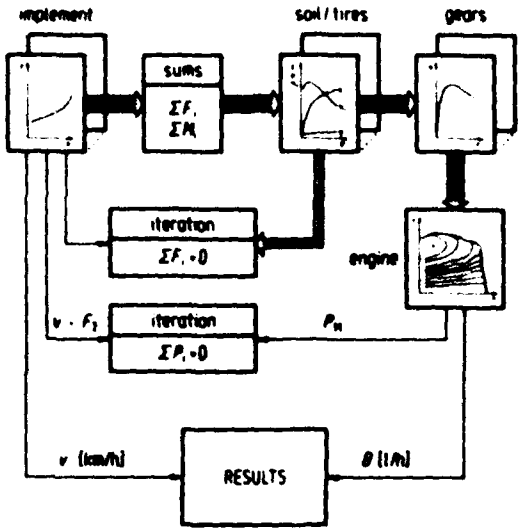

Figure 10. Extended tractor-soil-implement model schematic.

The foregoing, the non-realistic assumption of a continuously changeable gear ratio was made. Using an extended model now, and replacing the module representing the continuous gear type transmission with a modul of the conventional gear type transmission, and using data obtained from the tractor (OECD 536) under investigation the validity of the assumptions made and results obtained can be checked.

Figure 11 shows the results provided by the two models. The thin lines show the field capacity for the gears 5 to 12 (extended model), the solid lines the field capacity for the continuous gear type transmission applying 100 % (λ = 1), and 89 % (λ = 0,89) of the rated power of the tractor. The results show that with the conventional gear type transmission only at rated speed and power the lines for the single gears reach the previously calculated line of optimum field capacity for 100 % of the rated power. Below the line representing the field capacity for 89 % of the rated power that is for a continuous gear type, every field capacity can be achieved with the conventional transmission. How well the area between the lines for 100 % and 89 % is covered by the conventional gear type transmission depends on the gear ratios and number of gears. From Figure 11 also can be discerned that the effects on field capacity of the previously discussed parameters are not affected by the type of the transmission as long as its efficiency is the same.

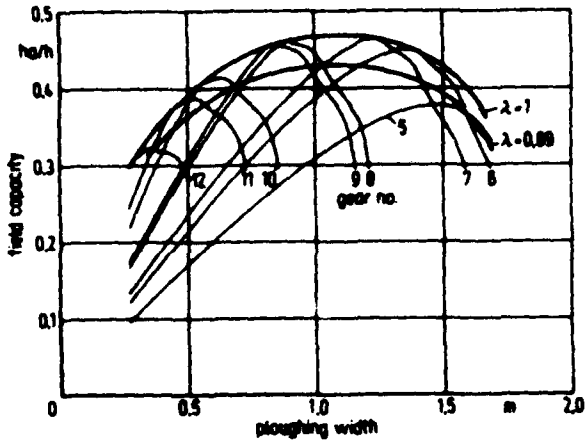

Figure 11. Field capacity on loamy clay for different gears.

Effect of Farm Management

The foregoing was only concerned with the technical parameters that influence the theoretical field capacity, but farmers are also faced with many more parameters that influence the overall work time and fuel consumption. To investigate the influence of the operator or the farm management and structure, an additional model has been developed using the results from the foregoing - it makes it possible to evaluate and compare e.g. the effects of field size and shape. The data and assumptions for this evaluation are given in Table 3.

field	
headland width	5 m
number of idle trips	2
speed of idle trips	16 km/h
tractor	OECD-Test No. 536
tractor loading	85 % of rated power
plough	two way moldboard
theoretical field capacity	0.46 ha/h - loamy clay 0.81 ha/h - sandy loam
times	
trips to and from field	15 min
one headland turn	0.5 min
breaks per area	1.5 min/ha
breaks per total time	4 %
preparation at the farmstead	15 min
preparation in the field	5 min

Table 3. Initial condition to calculate total work time and fuel consumption.

The results displayed in Figure 12 show that the smaller the fields are, the higher is the work time per hectare which mainly is effected by times which are independent from the field size, such as set up time, fixed time losses, etc. A large part of the total work time is related to the time used for headland turning, which itself is determined by the way the headland turning is accomplished. This mainly depends on the type of implement used and the skill of the driver.

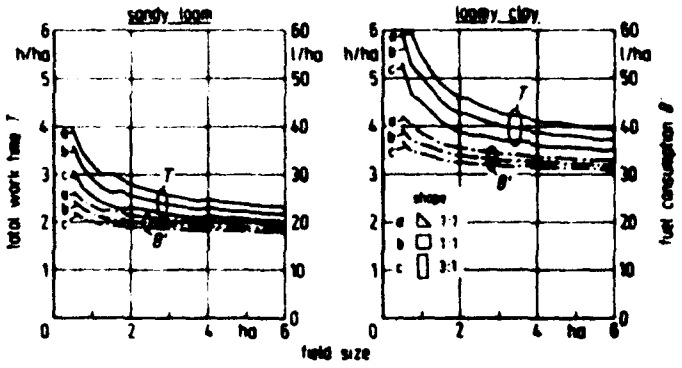

Figure 12. Influence of field size and shape on total work time and fuel consumption for two different soil types /6/.

Field measurements showed /7/ that the skill of the driver influences the time for headland turning by ± 20 %. In Figure 13 the total time versus field size of a skilled driver using 0.4 min (KTBL - standard time 0.5 min) for headland turning and a 80 kW tractor and an unskilled driver using 0.6 min and a 90 kW tractor are shown. The results show that the skill of the driver with the smaller tractor (9 % less theoretical field capacity than the 90 kW tractor) overcompensates this by up to about 1.5 ha. Only above 1.5 ha, when the ratio of the time for headland turnings to total time drops under a certain value, will the unskilled driver with the bigger tractor be quicker.

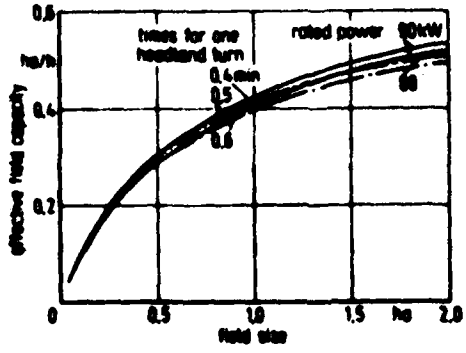

Figure 13. Influence of rated power and driver skill.

Conclusion

In the foregoing ploughing as one of the most time and fuel consumption tillage operations was used to show how, by computer models, the influence of different technical and agricultural parameters on field capacity, fuel consumption or work time can be evaluated. As a matter of economics the extent of the models discussed had been matched to the questions posed. While the first examples were related to technical parameters the last examples showed how non technical parameters e.g. the skill of the driver, the farm structure or the farm management can greatly influence the success of farming even if the technical parameters are equitable.

Literature

/1/ Zach, M.; Steinkampf, H. and C. Sommer: Arbeitseffekte und Leistungsbedarf eines Kreiselpfluges. Landbauforschung Völkenrode Bd. 23 (1973) Nr. 1, S. 29/40.

/2/ Stroppel, A.: Eine Methode zur Beurteilung von Bodenbearbeitungsverfahren im Hinblick auf die Schlagkraft. Grundl. Landtechnik Bd. 27 (1977) Nr. 4, S. 108/14.

/3/ Söhne, W. and K.Th. Renius: Überblick über die Gesamtentwicklung des Ackerschleppers. In 25 Jahre VDI-Fachgruppe Landtechnik, VDI, Düsseldorf 1983.

/4/ Jahns, G.: Auswertung und Darstellung von Reifenversuchen. Institutsbereicht Nr. Ja 21, 1984.

/5/ Jahns, G.: A Method of Describing Diesel Engine Performance Maps. ASAE-Paper No. MCR 83-103, 1983.

/6/ Jahns, G.; Steinkampf, H.; Olfe, G. and H. Schön: Einfluß landwirtschaftlicher Parameter auf Zeit- und Energiebedarf bei Schlepperarbeiten. Grundl. Landtechnik Bd. 33 (1983) Nr. 4, S. 85/90.

/7/ Rosegger, S. and F.-P. Sörgel: Ermittlung von technischen und arbeitswissenschaftlichen Planungsdaten für die pflanzliche Produktion. Landbauforschung Völkenrode, Sonderheft 32 (1976).

AREAL EVALUATION OF VEHICLE MOBILITY

W. KOEPPEL, C. STRAUSS

BATTELLE-INSTITUT E.V., FRANKFURT AM MAIN, FEDERAL REPUBLIC OF GERMANY

INTRODUCTION

Evaluation of the mobility performance of wheeled off-road transportation vehicles is still considered to be under debate within the research as well as the design and user communities. Methodologies and design tools have not quite permitted a kind of standardized approach so far, although much progress has been achieved through the past five years. K.-J. Melzer has been discussing various possibilities of evaluating the traction of tires for off-road transportation vehicles in a position paper presented at the 2nd European Conference; ~~Rennes /1/~~ this paper concentrated on a mission-based analysis of mobility performance characteristics for a case study vehicle. Based on this case study, the authors will describe some evaluation tools relating to areal mobility performance characteristics of the vehicle under consideration. Such an approach requires comprehensive terrain data bases to be dealt with while applying computer-aided methods. The evaluation procedure will provide performance data which have to match the user's requirement data which are defined in terms of characteristic speeds, immobilization percentages, ~~etc. (Table 3)~~ that are achieved by a vehicle in an area under investigation.

APPROACH

The overall system of vehicle, driver and terrain is modeled by a simulation mobility model /2/, which consists of three independent computational modules as shown in Fig. 1. Out of these modules, only the areal (off-road) module and the on-road module are being applied to our problem. Linear features (creeks, rivers, etc.) do not constitute the type of terrain that is negotiated by commercially operated wheeled vehicles.

Terrain Conditions

Terrain conditions usually are heavily influenced by soil and surface characteristics in terms of soil strength and slipperiness. Thus, seasonal changes of soil moisture and strength as well as short-term changes of surface conditions are crucial terrain parameters governing a cross-country vehicle's performance data. Considering these facts, it was decided to define characteristic terrain conditions for the simplified case study being discussed here and referring to K.-J. Melzer's traverse mode approach /1/. It is suggested to run simulations across an operational area of the size of a

1:50,000-scale topografic quadrangle sheet for the weather conditions

- o dry,
- o extremely wet,
- o slippery surface (original soil strength corresponds to dry condition).

Terrain data of the quad sheet comprise both off-road and on-road data required by the mobility model /2/. These data have been assembled on the basis of thematic maps (soil maps, geological maps, land-use maps, forestry maps, topografic maps), aerial photos and ground truth data. The resolution cell size is 100 x 100 m for off-road terrain and 10 x 10 m for on-road segments.

Statistical data on some key parameters such as soil strength, slope and surface micro-roughness in terms of RMS are given in Table 1 for off-road and on-road terrain. The area consists of 2700 terrain units [1], while the road and trail network is made up of 1500 road/trail units [2]. The frequency distributions indicate that the off-road terrain constitutes a rather hilly environment with severe slopes being accompanied by comparatively low soil strengths in extremely wet condition. The road conditions do not exhibit extreme difficulties, as the average slopes do not exceed 5 %, for example.

Table 1 also gives an overview on the soil types and road types encountered within the area under investigation. The absolute and relative frequencies of the various terrain units encountered are also indicated. Most of the soils in the off-road environment are fine-grained soils (MH, SM, SC, ML, CL) with some rarely occurring organic soils and fat clays (CH). More than 50 % of the road network is made up of secondary roads (light-surface roads), while about 30 % consist of agricultural and forest trails with soil surfaces. Only 15 % primary roads (federal highways) are contained in the existing network.

Vehicle Configuration

The vehicle configurations of the case study are equivalent to those in Ref. /1/. A 1.5-t truck (4x4) with the following characteristic data has been chosen:

The gross vehicle weight equals 4.4 t; the tires are of a 10.50-R20 size and have a standard tire deflection of 15 % (100 x deflection/section height).

The above data are being modified such as to permit investigation of the effects of a central tire inflation pressure system (CTIPS). Tire deflections of 25 % and 35 %

---

1) defined as areas of homogeneous terrain
2) defined as stretches of homogeneous roads/trails

with respect to their impact on mobility are being evaluated in a first modification step. Next, a variation of tire size using a 14.00-R20 radial is made, also allowing for deflections of 15 %, 25 % and 35 %. This covers two essential variables controlling wheeled vehicles' performance in off-road terrain from a running gear point of view - tire size and tire inflation pressure. The study aims at determining whether the given requirement data (Table 3) quantifying the user's needs are being met by either of the vehicle systems described in terms of tire size and CTIPS.

EVALUATION

Mobility evaluation tools for areal and mission-oriented mobility quantification are

- o mobility profiles,
- o speed-limiting factors,
- o speed/speed-limiting factor maps (areal evaluation),
- o characteristic mission speeds.

These - preferably as combined information - provide a comprehensive description of a vehicle's mobility capabilities in a specific terrain.

Mobility Profiles

The mobility profile is generated from the basic output data of the computer simulation - the maximum speed of the vehicle investigated within an off-road or on-road terrain unit. It indicates an accumulated average speed which the vehicle can maintain within the off-road terrain area or road network under consideration. The speed may be defined as a function of the percentage of the total area or network of terrain units that it avoids; here, the assumption is made that the vehicle avoids such terrain which exhibits the maximum impediment to its motion. Immobilization is defined by a theoretical speed close to zero in order to allow continuous computation of the profile. Fig. 2 shows a typical mobility profile for a specific vehicle and a given weather condition within (off-road) terrain; the vehicle gets immobilized within 14 % of the area under consideration.

Speed-limiting Factors

As a second descriptor, the reasons for the simulation output speeds or no-goes are given in the evaluation process. These include:

No-go:	Speed:
o Traction	o Ride comfort
o Obstacles	o Power
o Vegetation	o Visibility
	o Vegetation
	o Obstacles
	o Curvature (on-road)

Speed Maps

Speeds can be plotted into maps for the area under investigation. The information may be further specified by means of plotting comparative speed analyses of two vehicle candidates or by plotting the associated speed-limiting factors in their areal distribution.

Characteristic Mission Speeds

By incorporating both off-road and on-road terrain data into a statistical data base which may be negotiated by the vehicle at a given ratio of off-road vs. on-road travel, it is possible to derive "characteristic mission speeds" (v_m) from both the off-road and on-road mobility profiles. These speeds characterize the mobility performance of the vehicle in such a way that at a given percentage of both off- road and on-road terrains a theoretical speed can be obtained which the vehicle can maintain. If the user defines a specific off/on-road terrain mix to be negotiated by his vehicle, the characteristic mission speed indicates whether this is possible or not.

Evaluation Results

The mobility evaluation for both off-road terrain and roads/trails of the investigated area yielded the following results:

a) Off-road terrain:

In dry weather conditions, both tire formats show practically identical mobility profiles (Fig. 3); at the soil strength values concerned (not shown here), also variation of the tire deflection does not influence the vehicle performance.

In extremely wet conditions, however, the 1400-R20 tire shows a better performance than the 10.50-R20 tire, both at 15 % deflection (Fig. 4); nevertheless, the speeds differ by only 2 to 4 km/h and the immobilization magnitudes are almost equivalent (16 % for the 14.00-R20 tire and 18 % for the 10.50-R20 tire).

When applying a central tire inflation pressure system (CTIPS), it can be seen from Fig. 5 that - at a deflection of 35 % - the 10.50-R20 tire provides almost the same mobility as the 14.00-R20 tire. Fig. 6 shows the range of mobility increase for inflation of the 10.50-R20 tire from 15 % to 35 %, whereas Fig. 7 clearly indicates that the 14.00-R20 tire does not gain much from this variation. A comparison of the performance data under dry and extremely wet conditions is provided in Figs. 8 and 9 with a constant deflection rate of 15 %. The speeds achieved on dry and extremely wet soils differ by 10 to 15 km/h.

If slipperiness effects due to rainfall are introduced for soils of high strength, drastic mobility deficiencies occur, as is shown by Figs. 10 and 11. Immobilization also increases tremendously from 14 % to 33 %.

A comprehensive compilation of the frequency distributions of speed-limiting factors for the investigated vehicle configurations is given in Table 2. The related characteristic speeds v_{a50}, v_{a90} and v_m are listed in Table 3, which also includes the road & trail performance data discussed below.

b) Roads and trails:

By analogy to the off-road results, the mobility profiles of the two tire formats do not differ at all under dry conditions (Fig. 12).

Fig. 13 provides the comparative results for dry and extremely wet conditions, indicating an average speed difference of about 5 km/h. The 14.00-R20 tire format does not bring about any mobility increase within the investigated road network.

Slippery condition substantially reduces the mobility of the two vehicles in the most difficult road units and leads to approx. 3 % immobilizations for both tire formats (Fig. 14).

The frequency distributions of the speed-limiting factors are listed in Table 3.

On the basis of the given mobility requirements (Table 3) which are defined in terms of maximum immobilization percentages and an average speed of v_{a90}, it is then determined whether the vehicle performance data satisfy the given boundary conditions. The areal mobility requirement data are described by the following values (cf. Table 3).

a) v_{a90} = 10 / 5 / 5 km/h for off-road conditions during dry/extremely wet/slippery weather scenarios

v_{a90} = 35 / 30 / 30 km/h for on-road conditions during dry/extremely wet/slippery weather scenarios

b) Immobilization tolerance = 10 / 15 / 25 % for off-road conditions during dry/extremely wet/slippery weather scenarios

Immobilization tolerance = 0 / 0 / 5 % for on-road conditions during dry/extremely wet/slippery weather scenarios

Generally, the evaluation data show that under extremely wet weather conditions the off-road immobilization results of the 15-% deflection tire (original vehicle), which amount to approximately 18 %, are not much reduced (16 %) by applying 35 % deflection. Nevertheless, the given requirements of 15 %

maximum immobilization are roughly met. Slipperiness, however, does seriously affect the performance data as the immobilization rate increases up to 33 %. This has to be taken into account while planning operations of the vehicles under these weather conditions. Necessarily, mobility aids like tire chains have to be taken into consideration if specific operational goals are to be met by the vehicles. Speeds of v_{a90} are not reached; however, 85 % of the terrain may be negotiated with a minimum speed above the required speed of 5 km/h under extremely wet conditions by both tires, the 10.50-R20 format having to be inflated to 35 %, however; thus, a CTIPS is needed to fulfil the requirements set.

The results of a combined on/off-road task obtained for the vehicles on a statistical basis, i.e. assuming a defined ratio of on-road to off-road movements, are shown in Fig. 15 in terms of the characteristic mission speeds discussed earlier. The data are based on the respective off-road and on-road mobility profiles for wet conditions and 15 % deflection. The larger tire provides advantages for any given terrain mix; however, the advantages are of a magnitude of 2 to 4 km/h only. This must not constitute a major reason in favor of a 14.00-R20 equipment, especially when taking into account the capabilities of a CTIPS; the 35-% deflection data yield even less discrepancies between the two tire formats (Fig. 16).

Fig. 17 illustrates again the extremely big problems being created by slipperiness effects plotted for both off- and on-road terrain conditions in a combined graph.

The final selection of the tire format and of the CTIPS equipment has to be based on the results of the areal overall analysis of the terrain-vehicle-operator system in a defined operational area for different weather conditions and defined procurement cost data.

Table 3 indicates the requirements to be met by the vehicle that are derived from the user's needs and the performance data achieved by the vehicle systems obtained through the simulation results.

The data indicate that none of the vehicles entirely satisfies the conditions set by the user's demands. However, the vehicle configurations with CTIPS almost reach the required performance data; the immobilisation values are almost equalling 15 %, whereas the v_{a90} speed requirements are fulfilled by v_{a85} values of both 10.50-R20 and 14.00-R20 tire formats at 35 % deflection. Characteristic speeds (Table 3), immobilisation percentages and the entire mobility profiles do not allow major preferences to be given to the tire format 14.00-R20. Nevertheless, the required performance data call for equipment with CTIPS in order to be able to negotiate the most difficult terrain with sufficient traction.

It has to be taken into account, however, that slippery surface conditions create serious mobility problems. It is probably necessary to use chains in order to increase

traction under these weather conditions. Otherwise, the vehicles will be immobilized within 1/3 of the entire off-road area to be negotiated.

If the entire road/trail network is considered in connection with off-road travel on a statistical mix basis, "characteristic mission speeds" at a defined ratio of off-road and on-road travel can be obtained on the basis of the off-road and on-road mobility profiles (Figs. 15 to 17). Table 3 gives an example of reducing these data to a v_{m50} value which characterizes the curves by an average speed at which 50 % of the terrain mix (roads and off-road areas) may be travelled. This 50 % constitutes those terrain areas and network segments which are the "easiest" ones for the vehicle (in other words: the most "difficult" terrain and road network segments are avoided).

The v_{m50} values indicate that the performance of the two tire formats is quite similar again. Even under slippery conditions, an average speed of 32 km/h may be maintained if the most difficult off-road and on-road terrain units are avoided. Again, preferences can be allocated to neither the smaller nor the bigger tire format.

In an attempt to make a final vehicle system selection, the following evaluation results are compiled:

As the procurement cost of the 10.50-R20 tire (100 points, Table 4) is below that of the 14.00-R20 tire (102.4), it is concluded to recommend the vehicles to be equipped with the 10.50-R20 tire format and a CTIPS. This will enable the user to operate his vehicles in the above terrain conditions with a maximum efficiency in terms of mobility and cost involved.

As already mentioned above, traction problems under slipperiness conditions have to be countered by suitable measures like equipping the tires with chains, etc.

CONCLUSIONS

The investigations reported in this paper were intended to provide a quantitative decision aid to the user of vehicles to be equipped with a specific running gear (tire format, central tire inflation pressure system). Both vehicle performance and procurement cost involved were taken into account during the process of defining the best-suited vehicle system solution for given terrain and weather conditions.

The results obtained have to be understood as a broad performance evaluation of the overall terrain-vehicle-driver system. If the user roughly defines the actual mission profile in terms of terrain and weather to be negotiated by his vehicles, a mobility evaluation model - as the one applied here - can provide comprehensive data on the vehicle performance to be expected within extensive areal terrain.

LITERATURE

/1/ Melzer, K.-J.: Possibilities of Evaluating the Traction of Tires for Off-Road Transportation Vehicles. Proceedings 2nd European Conference on Terrain-Vehicle Systems, "Off-Road Transportation and Soil Working", Ferrara, 1983, p. 63

/2/ Jurkat, M.P.; Huttall, C.J.; Haley, P.: The US Army Mobility Model, Proc. 5th Intern. Conf. on Terrain-Vehicle Systems, Detroit, Vol. IV, p. 1-1, 1975

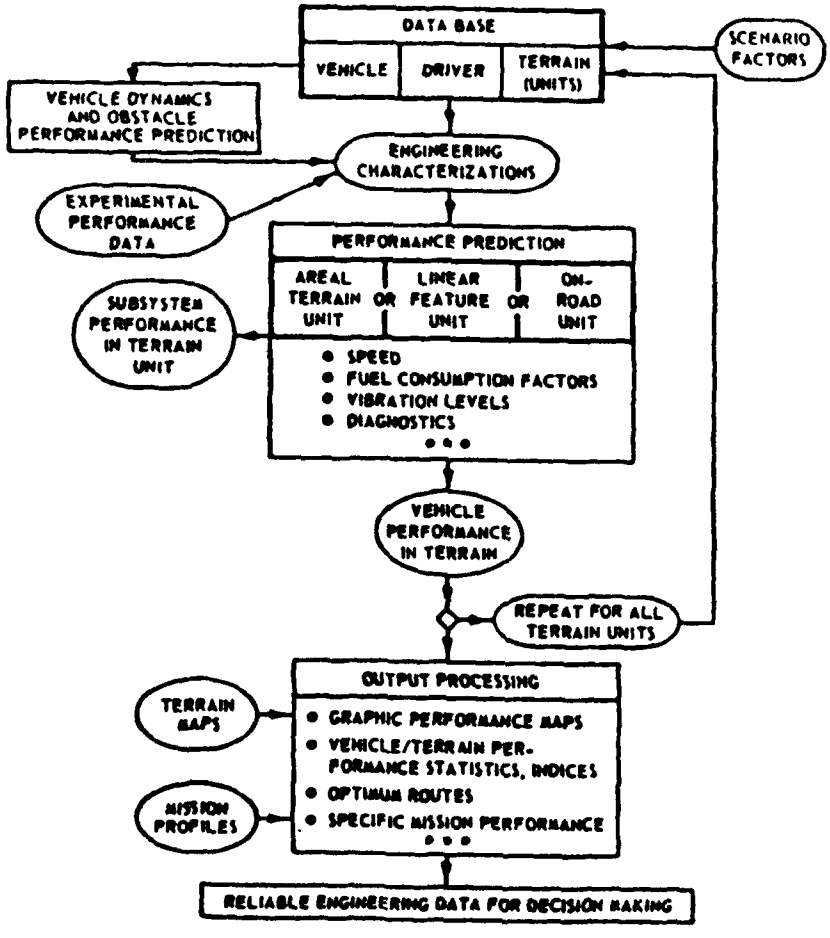

Fig. 1: Principle of the Mobility Model /2/

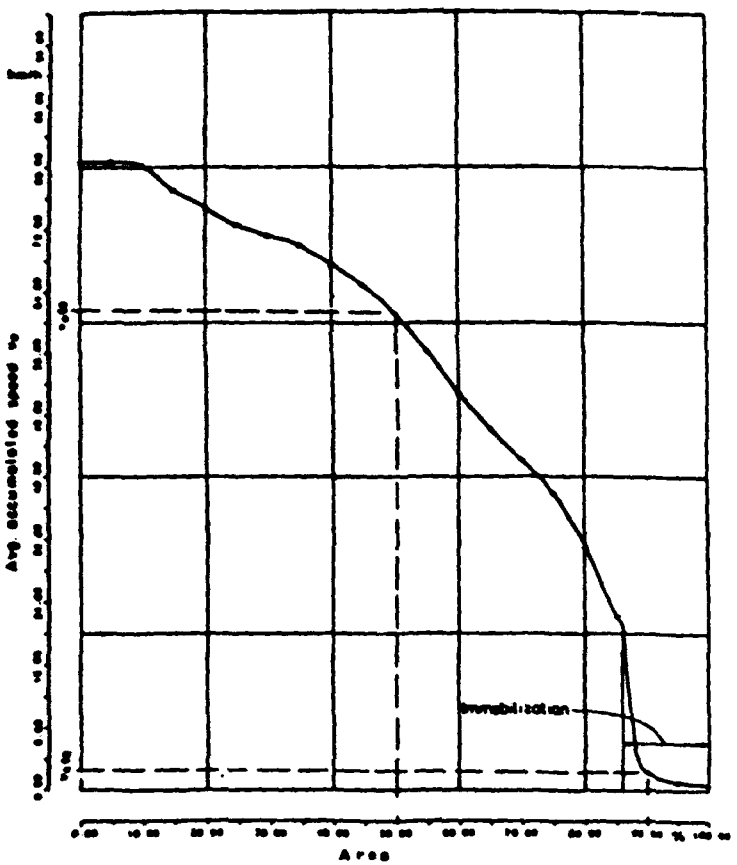

Fig. 2: Typical Mobility Profile for a Vehicle in an Area Under Investigation

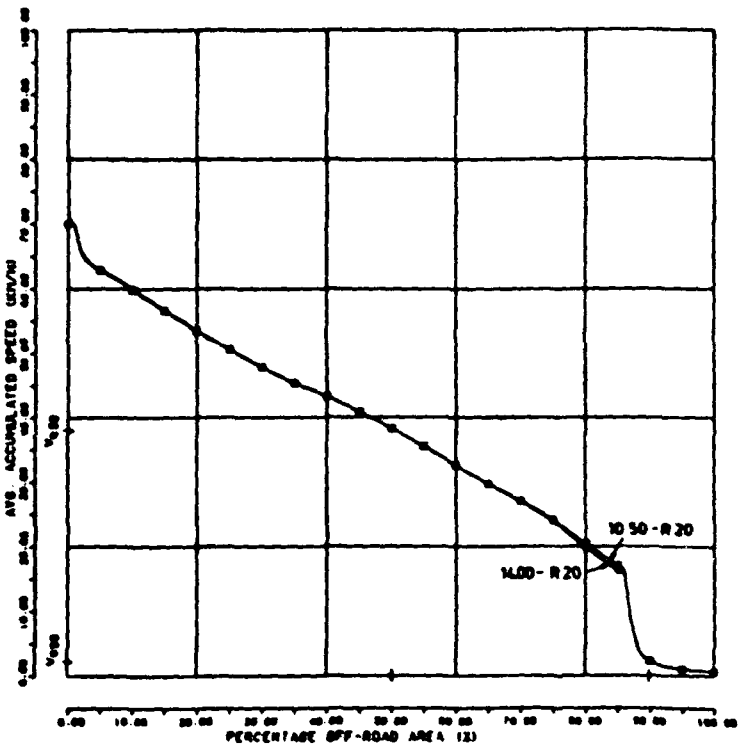

Fig. 3: Mobility Profiles for the 4x4 Truck with 10.50-R20 and 14.00-R20 Tires at 15 % Deflection Rate Under Dry Weather Conditions (Off-Road)

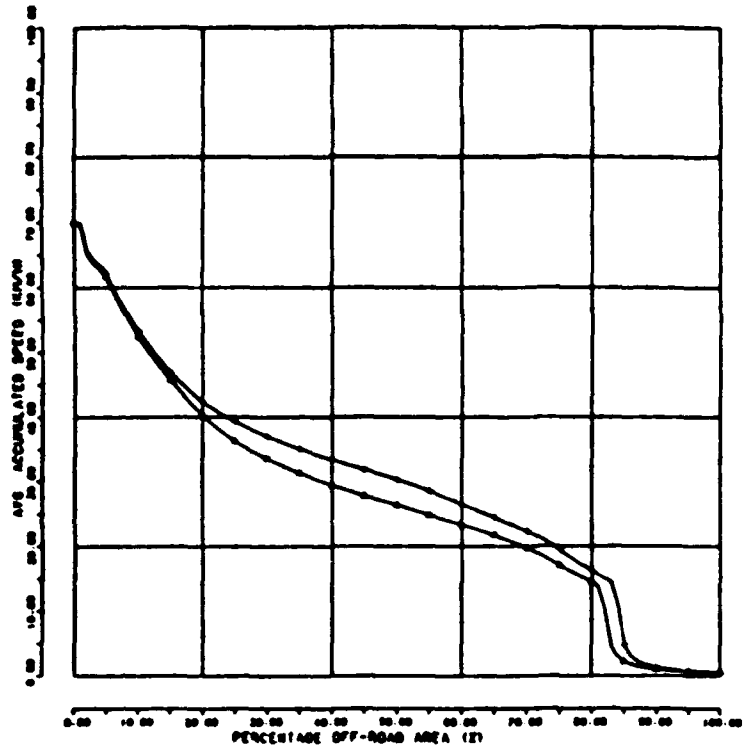

▲ 4X4 / 10.50-R20 (15%) / E. WET
+ 4X4 / 14.00-R20 (15%) / E. WET

Fig. 4: Mobility Profiles for the 4x4 Truck with 10.50-R20 and 14.00-R20 Tires at 15 % Deflection Rate Under Extremely Wet Weather Conditions (Off-Road)

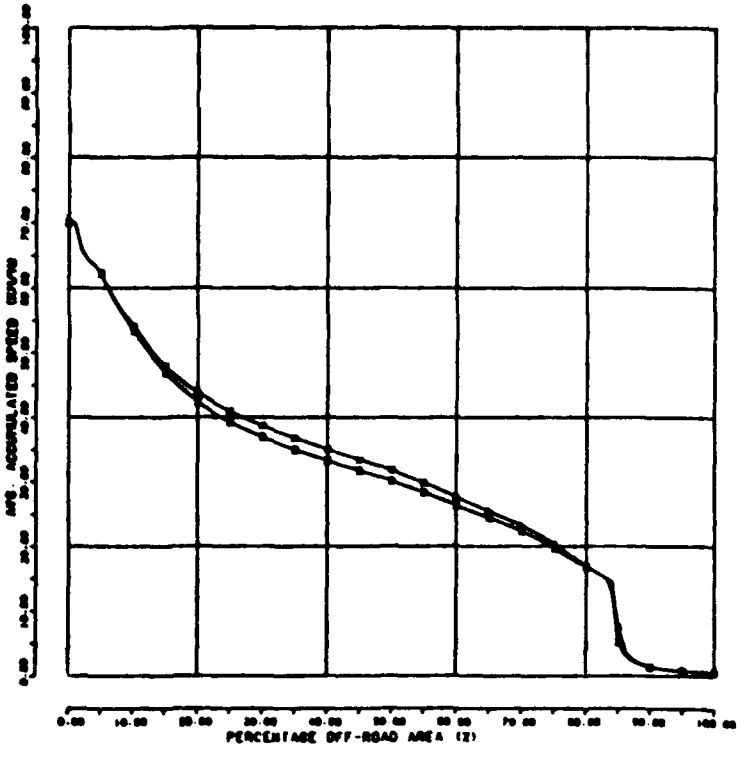

⧗ 4X4 / 10.50-R20 (35%) / E. WET
✱ 4X4 / 14.00-R20 (35%) / E. WET

Fig. 5: Mobility Profiles for the 4x4 Truck with 10.50-R20 and 14.00-R20 Tires at 35 % Deflection Rate Under Extremely Wet Weather Conditions (Off-Road)

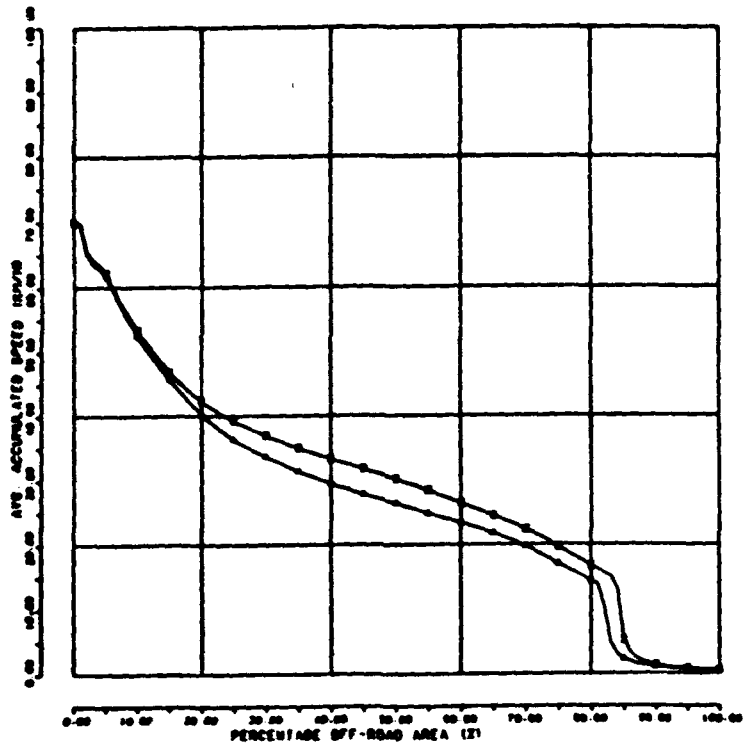

▲ 4X4 / 10.50-R20 (15%) / E. WET
⧗ 4X4 / 10.50-R20 (35%) / E. WET

Fig. 6: Mobility Profiles for the 4x4 Truck with 10.50-R20 Tires at 15 % and 35 % Deflection Rate Under Extremely Wet Weather Conditions (Off-Road)

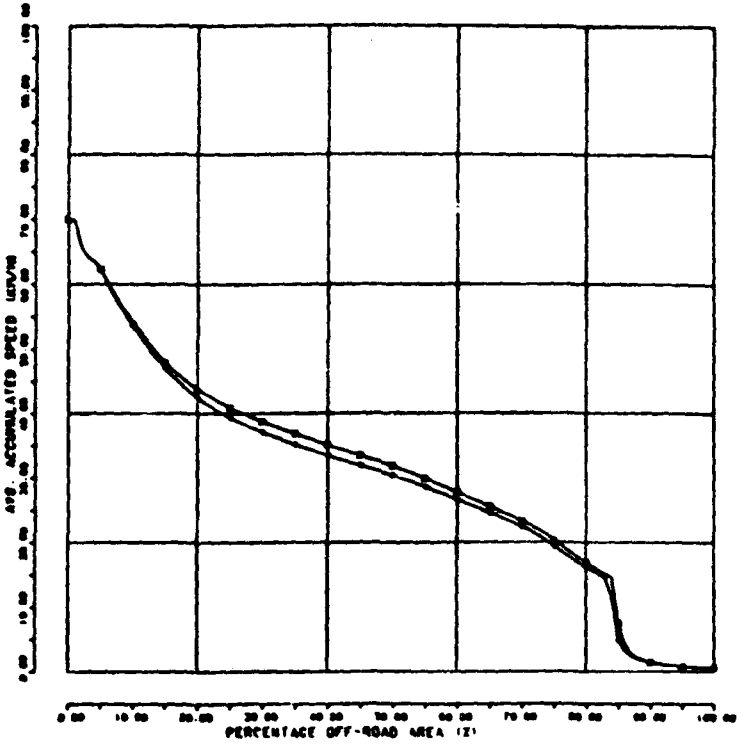

+ 4X4 / 14.00-R20 (15%) / E. WET
※ 4X4 / 14.00-R20 (35%) / E. WET

Fig. 7: Mobility Profiles for the 4x4 Truck with 14.00-R20 Tires at 15 % and 35 % Deflection Rate Under Extremely Wet Weather Conditions (Off-Road)

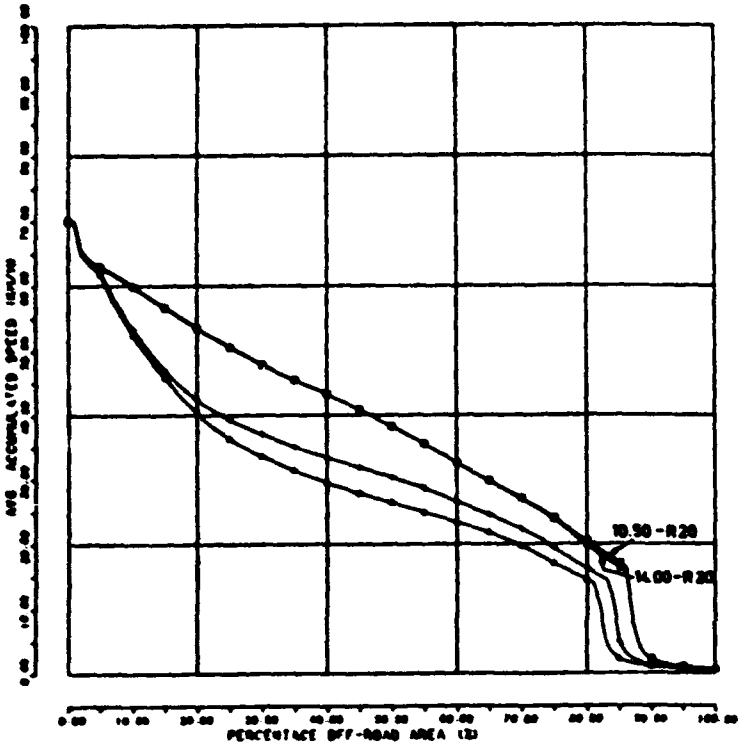

□ 4X4 / 10.50-R20 (15%) / DRY
△ 4X4 / 10.50-R20 (15%) / E. WET
⊠ 4X4 / 14.00-R20 (15%) / DRY
+ 4X4 / 14.00-R20 (15%) / E. WET

Fig. 8 Mobility Profiles for the 4x4 Truck with 10.50-R20 and 14.00-R20 Tires at 15 % Deflection Rate Under Dry and Extremely Wet Weather Conditions (Off-Road)

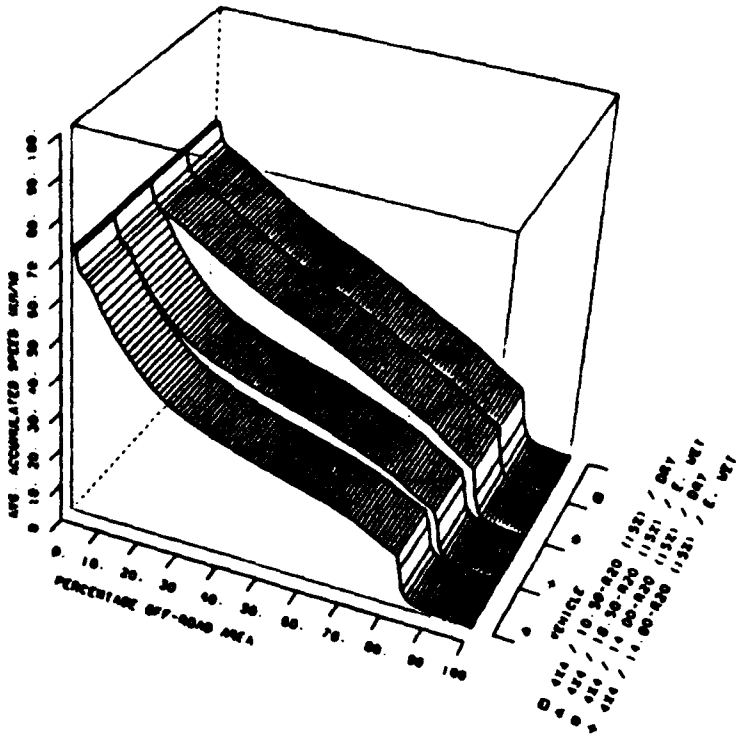

Fig. 9: Mobility Profiles for the 4x4 Truck with 10.50-R20 and 14.00-R20 Tires at 15 % Deflection Rate Under Dry and Extremely Wet Weather Conditions (Off-Road, Three-Dimensional Plot)

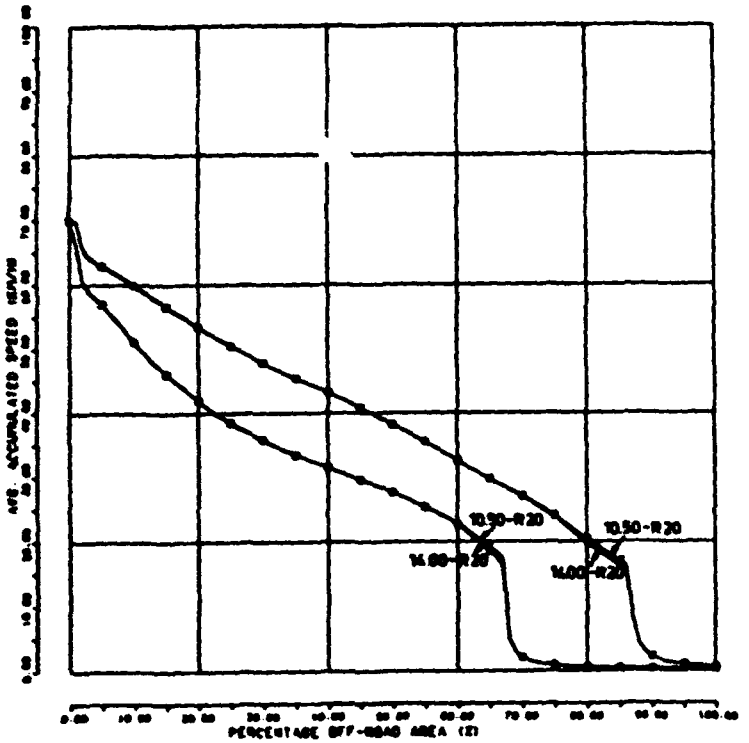

× 4X4 / 10.50-R20 (15%) / DRY-SLIP
○ 4X4 / 10.50-R20 (15%) / DRY-SLIP
□ 4X4 / 14.00-R20 (15%) / DRY
◎ 4X4 / 14.00-R20 (15%) / DRY

Fig. 10: Mobility Profiles for the 4x4 Truck with 10.50-R20 and 14.00-R20 Tires at 15 % Deflection Rate Under Dry and Slippery Weather Conditions (Off-Road)

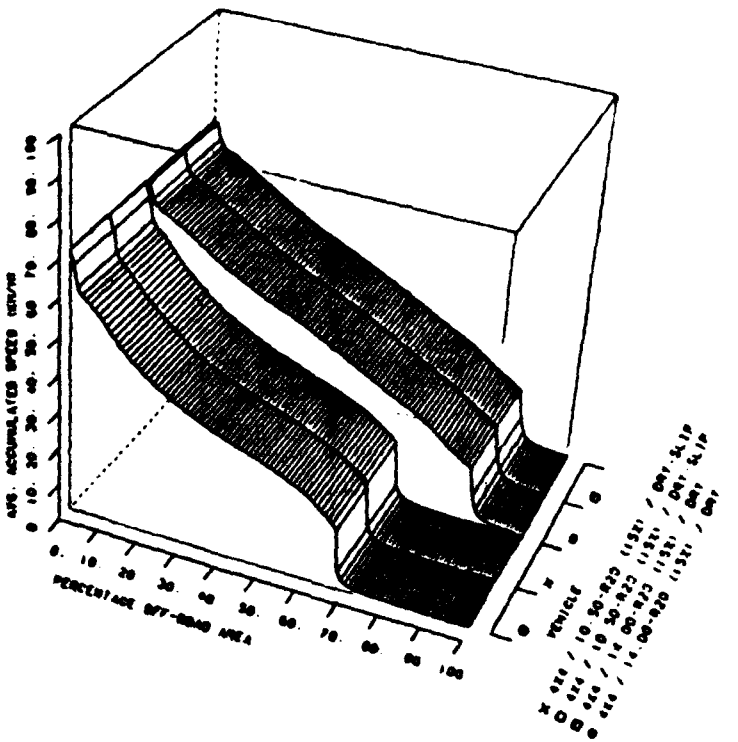

Fig. 11: Mobility Profiles for the 4x4 Truck with 10.50-R20 and 14.00-R20 Tires at 15 % Deflection Rate Under Dry and Slippery Weather Conditions (Off-Road, Three-Dimensional Plot)

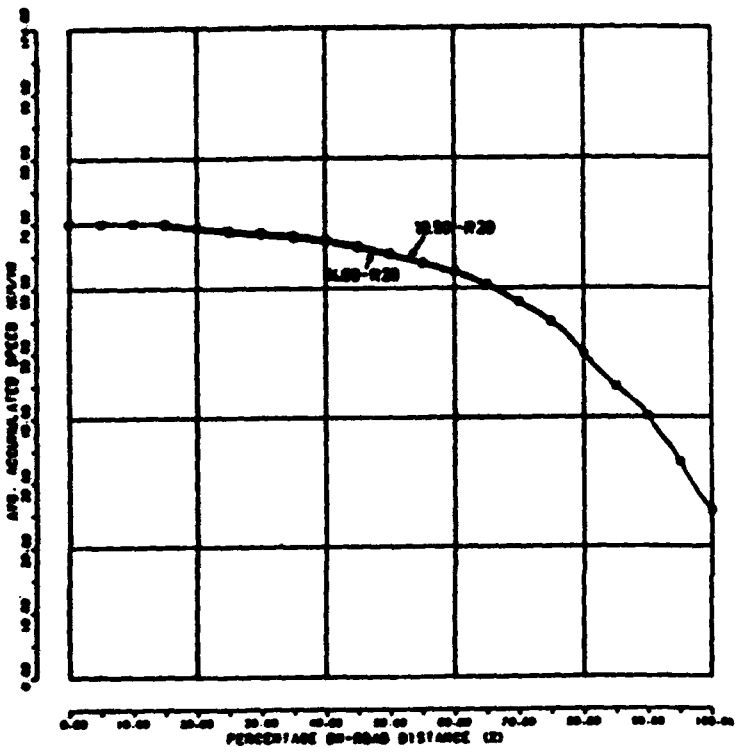

■ 4X4 / 10.50-R20 (15%) / DRY
● 4X4 / 14.00-R20 (15%) / DRY

Fig. 12: Mobility Profiles for the 4x4 Truck with 10.50-R20 and 14.00-R20 Tires at 15% Deflection Rate Under Dry Weather Conditions (On-Road)

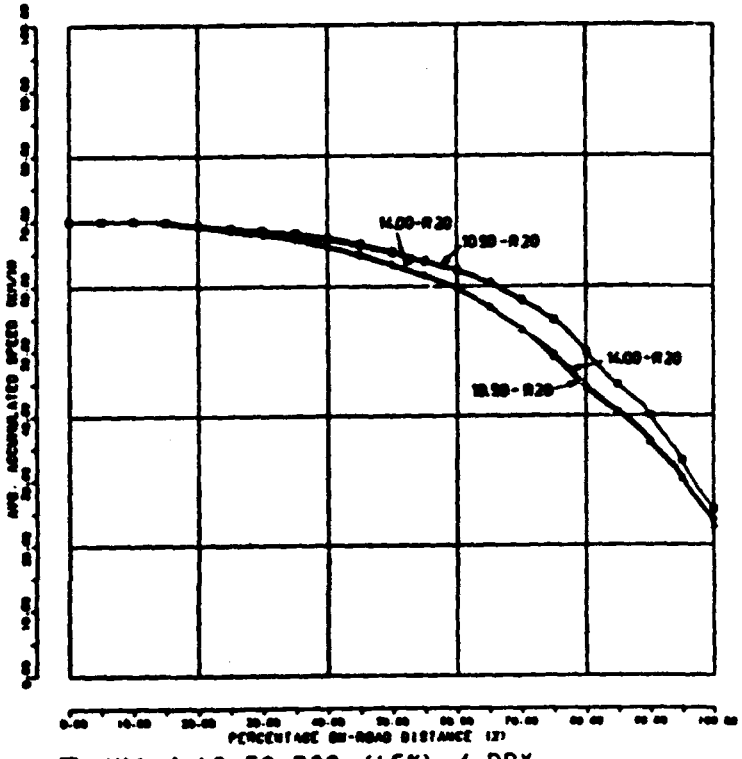

■ 4X4 / 10.50-R20 (15%) / DRY
▲ 4X4 / 10.50-R20 (15%) / E. WET
● 4X4 / 14.00-R20 (15%) / DRY
+ 4X4 / 14.00-R20 (15%) / E. WET

Fig. 13: Mobility Profiles for the 4x4 Truck with 10.50-R20 and 14.00-R20 Tires at 15% Deflection Rate Under Dry and Extremely Wet Weather Conditions (On-Road)

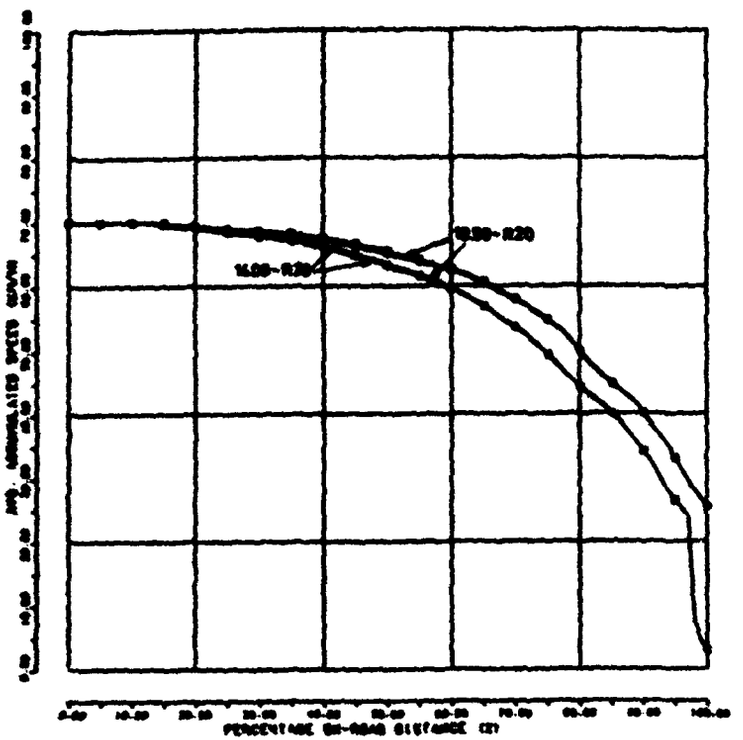

X 4X4 / 10.50-R20 (15%) / DRY-SLIP
O 4X4 / 14.00-R20 (15%) / DRY-SLIP
□ 4X4 / 10.50-R20 (15%) / DRY
✱ 4X4 / 14.00-R20 (15%) / DRY

Fig. 14: Mobility Profiles for the 4x4 Truck with 10.50-R20 and 14.00-R20 Tires at 15% Deflection Rate Under Dry and Slippery Weather Conditions (On-Road)

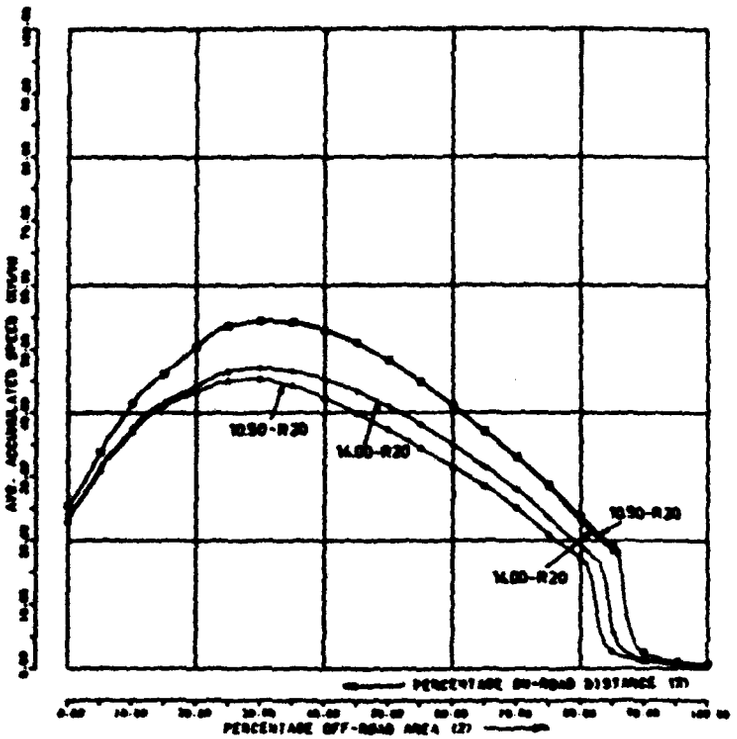

□ 4X4 / 10.50-R20 (15%) / DRY
△ 4X4 / 10.50-R20 (15%) / E. WET
✱ 4X4 / 14.00-R20 (15%) / DRY
+ 4X4 / 14.00-R20 (15%) / E. WET

Fig. 15: Characteristic Mission Speed Profiles for the 4x4 Truck with 10.50-R20and 14.00-R20 Tires at 15% Deflection Rate Under Dry and Extremely Wet Weather Conditions

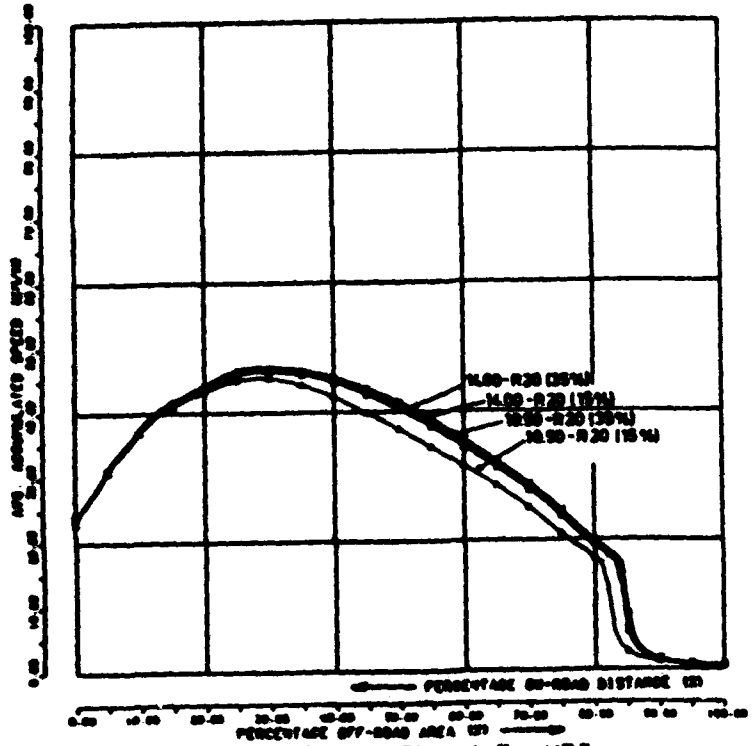

▲ 4X4 / 10.50-R20 (15%) / E. WET
⧗ 4X4 / 10.50-R20 (35%) / E. WET
+ 4X4 / 14.00-R20 (15%) / E. WET
⧗ 4X4 / 14.00-R20 (35%) / E. WET

Fig. 16: Characteristic Mission Speed Profiles for the 4x4 Truck with 10.50-R20 and 14.00-R20 Tires at 15% and 35% Deflection Rate Under Extremely Wet Weather Conditions

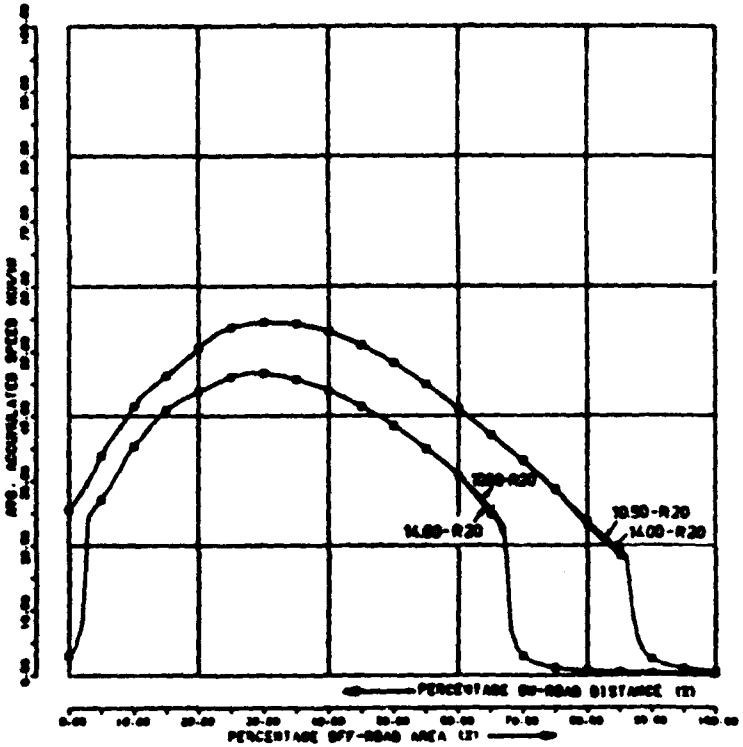

□ 4X4 / 10.50-R20 (15%) / DRY
X 4X4 / 10.50-R20 (15%) / DRY-SLIP
✱ 4X4 / 14.00-R20 (15%) / DRY
○ 4X4 / 14.00-R20 (15%) / DRY-SLIP

Fig. 17: Characteristic Mission Speed Profiles for the 4x4 Truck with 10.50-R20 and 14.00-R20 Tires at 15% Deflection Rate Under Dry and Slippery Weather Conditions

Table 1: Key Parameters for Off-Road and On-Road Terrain in the Area Investigated

Off-Road

	Surface Roughness, RMS	Slope	Soil Strength, RCI			
			Dry Weather	Average	Wet	Extr. Wet
	(cm)	(%)	(psi)			
Mean	2.1	14.0	281	233	88	82
Stand. Dev.	1.3	16.9	29	46	80	79
Range	0.3-7.9	1-104	36-300	19-296	36-296	19-296

Soil Type	Absolute Frequency of Terrain Units	Relat. Frequency of Terrain Units (%)
Fine-Grained Soil	2582	96.9 %
Organic Soil	32	0.4 %
Fat Clay	93	2.7 %

On-Road

	Surface Roughness, RMS	Slope	Soil Strength, RCI			
			Dry Weather	Average	Wet	Extr. Wet
	(cm)	(%)	(psi)			
Mean	1.8	4.6	293	278	243	240
Stand. Dev.	1.8	5.0	18	55	94	99
Range	0.3-7.1	0-44.0	130-300	80-300	36-300	36-300

Road Type	Absolute Frequency of Terrain Units	Relat. Frequency of Terrain Units (%)
Primary Road	181	15.8 %
Secondary Road	411	56.4 %
Trail	918	27.8 %

Table 2: Frequency Distribution of Speed-limiting Factors for the Investigated Area

			No-Go Reasons (%)		Speed-limiting Factors (%)						
			Obstacle Inacces.	Total Resist.	Side Gradient	Soil/Slope Resistance	Visibility	Maneuvering	Total Resistance	Obstacles	Road Curvature
	15 t	Off-Road	4.3	9.2	10.3	30.8	0.2	16.9	9.8	18.6	-
	35 t		4.4	9.2	10.3	30.7	0.2	16.9	9.8	18.6	-
	15 t	On-Road	-	-	15.3	74.5	-	-	-	-	10.2
	15 t	Off-Road	4.4	9.2	10.3	30.7	0.2	17.0	9.8	18.4	-
	35 t		4.4	9.1	10.4	30.7	0.2	17.0	9.8	18.4	-
	15 t	On-Road	-	-	15.3	74.7	-	-	-	-	10.0
	15t	Off-Road	5.9	12.3	5.8	33.4	0.1	17.6	9.3	15.6	-
	35 t		5.0	10.6	6.6	34.2	0.2	17.2	9.6	16.6	-
	15 t	On-Road	-	-	12.1	76.1	-	-	-	-	11.8
	15 t	Off-Road	5.2	11.0	6.6	33.7	0.2	17.1	9.6	16.6	-
	35 t		4.9	10.6	7.0	33.5	0.2	17.0	9.7	17.1	-
	15 t	On-Road	-	-	13.1	75.2	-	-	-	-	11.7
	15 t	Off-Road	12.3	20.6	6.8	25.2	2.3	13.5	6.9	12.4	-
	35 t		12.3	20.6	6.9	25.0	2.4	13.5	6.9	12.4	-
	15 t	On-Road	-	2.9	12.0	71.0	-	-	-	-	14.1
	15 t	Off-Road	12.3	20.6	6.9	25.0	2.4	13.6	6.9	12.3	-
	35 t		12.3	20.7	6.9	24.9	2.4	13.5	6.9	12.3	-
	15 t	On-Road	-	2.9	12.4	70.9	-	-	-	-	13.8

Table 3: Requirement Data and Performance Data Achieved by the Investigated Vehicle Systems

				Areal Performance											
				Dry Weather Condition				Extr. Wet Weather Condition				Slippery Surface			
				V_{a50}	V_{a90}	V_{m50} **)	Immob.	V_{a50}	V_{a90}	V_{m50}	Immob.	V_{a50}	V_{a90}	V_{a50}	Immob.
				km/h	km/h	km/h	%	km/h	km/h	km/h	%	km/h	km/h	km/h	%
Requirement Data		Off-Road		-	10	-	10	-	5	-	15	-	5	-	25
		On-Road		-	35	-	0	-	30	-	0	-	30	-	5
Achieved Data	10.50-R20	Off-Road	15 % Deflection	38.2	2.3 *) (17.0)	41.2	13.5	26.4	1.0 (2.2)	33.0	18.2	27.6	0.4	32.4	32.9
			35 % Deflection	38.2	2.3 (17.0)		13.5	30.1	1.4 (5.2)		15.6	27.6	0.4		32.9
		On-Road	15 % Deflection	65.4	40.1		0	63.4	35.7		0	63.4	34.1		2.9
	14.00-R20	Off-Road	15 % Deflection	38.2	2.2 (16.2)	41.2	13.5	30.3	1.3 (4.8)	36.0	16.2	27.6	0.4	32.4	32.9
			35 % Deflection	38.2	2.3 (16.3)		13.5	31.8	1.5 (7.5)		15.5	27.6	0.4		32.9
		On-Road	15 % Deflection	65.0	40.0		0	63.1	36.3		0	63.1	34.1		2.9

*) v_{85} values are included in parentheses for dry/extr. wet off-road conditions

**) v_{m50} values at 15 % deflection

Table 4: Nominal Procurement Cost for the 4x4 Truck with 10.50-R20 Tires and 14.00-R20 Tires and for the CTIPS

	Truck A	Truck B
10.50-R20 tire	100	-
14.00-R20 tire	-	102.4
Central tire-inflation-pressure system (CTIPS)	107.2	109.6

PREDICTING THE PERFORMANCE OF FAST CROSS COUNTRY VEHICLES.

J.C. LARMINIE.
CONSULTANT: LYTCHETT MATRAVERS, POOLE, DORSET, ENGLAND.

INTRODUCTION.

This paper describes the practical application of ISTVS work to help the user describe to the designer the requirements of his vehicle, and to help them both assess what performance can be expected from that vehicle over various types of terrain. In the past, statements of requirements have necessarily been loosely worded for lack of any agreed criteria for defining the characteristics of the vehicle. Sometimes this has led to the designer misinterpreting the user requirement. If this is then compounded by a lack of opportunity to run prototypes on realistic trials, a potentially unsatisfactory vehicle may come into service, and shortcomings only become apparent later with perhaps disastrous, or at least expensive results. The criteria and assessments methods to be described have applications to any cross-country vehicle where speed is relatively high, but their development has been primarily for use in designing Armoured Fighting Vehicles (AFVs). For AFVs there are a wide range of options for mobility standards. These arise from differing priorities for mobility in relation to the payloads of firepower, protection and crew. Military vehicles are usually stretching technology. To save development time and the expense of test vehicles, it is usually necessary to make major decisions on some characteristics from paper studies at the design stage. Even when test vehicles are available, the test areas likely to be available in peacetime are of soil and topography very different from likely battlefields, and performance is often misleading. Soldiers are intensely practical, and do their best with whatever they are given, and have little opportunity to complain.

AIM.

The author has been involved in the practical applications of various methods for predicting performance. It has been necessary to supply actual predictions to the best possible accuracy within reasonable bounds of time, and cost. The user and the designer have needed answers, not theories. The aim of this paper is to describe the methods used, and why they appear to be the best: or the least bad. It is also necessary to give warnings on the limitations of the methods, and from this to draw conclusions as to where future efforts should be devoted to improving the methods. Experience has shown these methods to be, within their bounds of accuracy (and these bounds are admittedly quite wide), to be reliable.

The future work of ISTVS and elsewhere is going to improve methods of prediction. For instance, at present the suitability of a cone penetrometer for soil strength measurement is under scrutiny. But until some new method has been proved, and a fund of information gathered by it built up, the current methods must be supported.

MAJOR INFLUENCES ON MOBILITY

Statements of mobility can be split between two very different forms of expression:

a. Criteria. There can be fairly precise statements of the levels needed of the various vehicle design characteristics. These characteristics include ground pressure, engine power, transmission efficiency and effectiveness, suspension capacity, and vehicle shape and size.

b. Performance Assessments. Real trials or paper studies can show the implications of various levels of vehicle characteristics defined by the criteria, and under various stated ground conditions: aspects such as journey average speed.

There are four major influences which constrain vehicle performance:

a. Vehicle Characteristics.

b. Route chosen by the user: for AFVs the commander.

c. Soil, vegetation, contours, and the effects of human activity along that route.

d. Reactions of the driver to the three previous influences.

The first stage of assessment is to establish whether the vehicle has the basic ability to move along that route at all: traction must exceed all resistances, especially that due to sinking into the soil. Then there is the instantaneous acceleration and resulting speed which build up over time to a complete journey.

Vehicle characteristics can be stated in reasonable detail and with reasonable accuracy. Fairly simple assessment methods allow predictions to be made speedily, and with confidence that the accuracy of these methods is much greater than the greatest sources of possible error. These major areas of doubt are:

a. Variations in soil strength from occasion to occasion.

b. Choice of route, and driver reactions along that route.

SINKAGE AND TRACTION

Ground Pressure Criteria.

Tracked vehicles for a long time were assessed by the relationship of track ground contact area to vehicle weight: the Nominal Ground Pressure (NGP). This proved a useful guide to soft ground performance, provided comparisons were between vehicles of generally similar running-gear. NGP makes no allowance for variations in loading due to the number and diameter of the wheels, and the pitch of the track link. There is no practicable relationship between soil strength and NGP, for calculating sinkage. Performance has had to be gauged by practical trials. Many demonstrations of apparent mobility have been misleading, due to ill defined vehicle parameters and ignorance of soil influences.

It was not possible to compare wheeled with tracked vehicles. The NGP quoted by the tyre manufactures for pneumatic tyres is the oval imprint on a flat plate, whereas the fairer comparison would be after some sinkage.

The United States Army developed the Vehicle Cone Index and Rating Cone Index (VCI and RCI) system to meet these requirements. The VCI is a measure of vehicle ability and has formulae for tracked or wheeled vehicles. The RCI is a rating of soil strength measured with a cone penetrometer. From these criteria traction and hill climbing can be forecast. The VCI was derived empirically from the results of mobility tests, and is predominantly NGP with some correcting factors. It contains an unlikely combination of expressions. The wheeled vehicle VCI formula has no tyre deflection term. The formula for tracked vehicles has no wheel diameter term, and is very insensitive to wheel numbers and to track pitch. It also has arbitrary factors of limited extent for weight and for aggressiveness of grip. The wheeled and tracked formulae are unweildy, and having sums and products, slow to recalculate variations of parameters. The limitations are emphasised by later US Army work to derive soils numerics, discussed later.

Since the VCI was so unwieldy the author, when in the British Army at the School of Tank Technology (now the Armour School) derived a simple NGP formula for wheeled vehicles that was comparable to that for tracks.

$$NGP = \frac{\text{Vehicle Gross Weight}}{\text{No of wheels} \times \text{tyre radius} \times \text{section width}}$$

Limited trials showed that this formula put wheeled vehicles into a fair relationship with NGP for tracked vehicles, and that any error was dominated by that due to ignoring the aggressiveness of the track shoe or tyre tread. It provided a readily calculated and useful yardstick until such time as the Mean Maximum Pressure system was developed.

Mean Maximum Pressure.

The measurement of actual ground pressures as a tracked vehicle passes over a point will show the peak pressures as each wheel passes. It is these maximum pressures that are the major factor controlling sinkage. Weight distribution will normally not be equal on all axles, but taking the mean of these maximum pressures under each wheel station will give

a measure of the expected sinkage. A formula relating mean maximum pressures (MMP) to running gear parameters was explained and published by Rowland in 1972 (Ref 1). This paper also gave an equivalent MMP for pneumatic tyred wheeled vehicles. Also in the paper were some initial relationships of MMP to trafficability. At the same time much the same information was published for internal use of the British Ministry of Defence in MVEE Report 72031.

Rowland took this work further in 1975 (Ref 2). This paper gave further guidance on soil strengths required for suitable performance for various levels of ground pressure described by MMP, and gave design aims. Most important were revisions and refinements of the formula for MMP for wheeled pneumatic tyred vehicles. (See Fig. 1). It is thus important not to use the outdated formula given in Ref 1 and the contemporary MVEE Report. This phase of work was completed by Rowland and Peel with Ref 3. This related the MMP formula for wheeled vehicles to the underlying dimensionless analysis by Freitag, as further refined by Turnage. (US Army Waterways Experimental Station). MMP is the equivalent to the dimensionless wheel numeric, but expressed as a vehicle parameter and a pressure, rather than a limiting soil strength. The MMP system still uses RCI derived by cone penetrometer for soil measurement. Thus MMP is not a new system, but draws on both the British and US Army work, and puts it in terms easy for the layman to understand and use.

Credibility of MMP.

Examination of the formulae show that the expressions are what might be expected from pure abstract consideration of the controlling factors. The originators of MMP accept that it does have limitations. The formulae imply assumptions that in fact are seldom met:

a. Weight is evenly distributed.
b. The vehicle is travelling slowly in a straight line.
c. The vehicle has sufficient ground clearance to avoid bellying.
d. It assumes the soil is homogeneous, and thus ignores any effect of tread on a cohesive soil.

The expression of ground pressure by the MMP system is considered the most reasonable criteria for vehicle ground pressure. Its limitations are fewer than those of other systems. It is accurate enough to give a clear indication of potential performance. The MMP formula for wheeled vehicles has variations for the type of soil: cohesive (clayey) or frictional (sandy). Since a vehicle is more likely to find a cohesive soil critical than a frictional one, it is normal to use the formula for cohesive soil.

Trafficability from MMP.

Rowland explained in Ref 1 and 3 the inter-relationships between MMP and soil strength, and these are shown in Fig. 1 c, d, and e. It is thus possible from MMP to calculate tractive effort, and resistance to motion due to sinkage and ultimate failure, for various soils.

AD-A150 653 PROCEEDINGS OF THE INTERNATIONAL CONFERENCE ON THE PERFORMANCE OF OFF ROA. (U) INTERNATIONAL SOCIETY FOR TERRAIN VEHICLE SYSTEMS M J DWYER AUG 84

2/4

UNCLASSIFIED F/G 13/6 NL

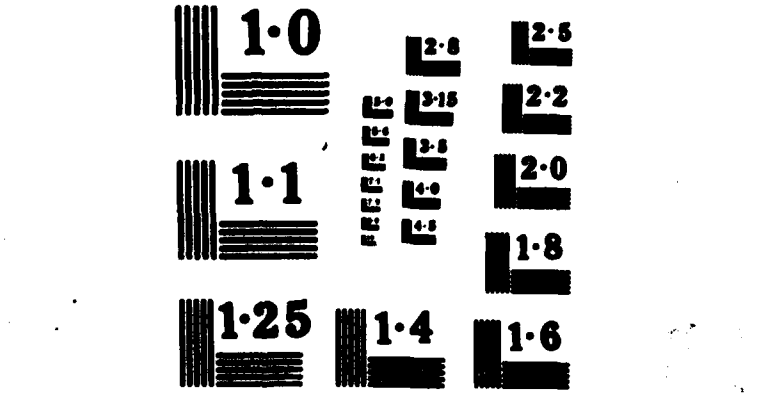
1·0
1·1
1·25
1·4
1·6
1·8
2·0
2·2
2·5

MMP as Design Aid.

In Ref 2 is demonstrated how a study of vehicle running gear design can give the best MMP for a given NGP. A crawler tractor can have this relationship, 'Q' of about 1.5. Typical AFV can expect to have 'Q' about 2.5, though with special features such as the overlapping wheels of Panther, 'Q' can be 1.7. Some typical MMPs are given in Fig. 2.

Twinned Rear Wheels.

When running straight, twinned rear wheels cannot give their full value, since half their width will be in fresh soil, and half in the ruts left by the front wheels. Rowland suggests twinned rear wheels could be treated as singles. But since actually vehicles find the turns the critical parts of a journey, when the rear wheels will be clear of the ruts of the front, this seems severe. It has therefore been recent practise to calculate MMP by counting the four twinned wheels on a rear axle as 3. (Thus for a 4x4 vehicle, with twinned rears, the factor 2m in the MMP formula becomes 5).

Half-Tracks.

A vehicle of wheeled front axle and tracks at the rear can be assessed in two parts. The MMP for the front is calculated using K=3.32 in the wheels formula. For the rear the MMP tracks formula is used. The weights on each are as distributed. The two MMPs are averaged to give a vehicle MMP with weighting to allow for that weight distribution.

Trailers.

Provided the towing vehicle and trailer have tyres the same size, and weight distribution is approximately even, MMP can be calculated treating the train as one vehicle of partial wheel drive. If these provisos are invalid, limiting conditions must be calculated for the towing vehicle from MMP, and the resistance of the trailer from Soil Numerics (Ref 3).

Experience with MMP.

The MMP formulae have now been in practical use by the British Ministry of Defence and their contractors for some eight years. Over this period there have been further minor developments of the system. These have been incorporated in the presentation of the expressions and their derivatives shown in Fig. 1.

The wheeled vehicle formula has the term δ/h, for the tyre deflection. This reflects the improvement that can be got by deflating tyres. To allow simple comparison of vehicles under the same conditions, it has been normal to quote MMP at tyre deflection $\delta/h = 0.18$; typical road inflation pressure.

Experience with MMP suggests that in the range of MMP common for military vehicles, between 100 and 450 kPa, some 20 kPa is the minimum significant difference of MMP.

Requirements for Further Definition.

One important use of MMP is for comparisons between tracked and wheeled vehicles. To give a satisfactory performance a vehicle with skid steering, as are most track-

layers, will need some excess of traction when running straight, so that it can still move when the steering is applied to give negative traction on the inside. The normal wheeled vehicle with ackerman steering, or tracked steering by bowing tracks, or an articulated vehicle, does not suffer this disadvantage, and thus can be expected to perform under some condition with a worse MMP than a skid-steer vehicle. In search of improved performance, skid-steer wheeled vehicles have been built (eg AMX10 RC) since this allows large tyres. Limited trials indicate a penalty of skid-steering equivalent to a 15% increase in ground pressure.

Soil is seldom homogeneous, and thus a large vehicle will find it easier to operate on deeper firmer layers. Also obstructions such as tree roots, boulders and other humps are relatively smaller for the large vehicle. Thus is appears that a larger vehicle can operate in some particular going with a higher MMP than can a smaller vehicle. This subject is highly complex, with wide variations on the gradient of soil strength with depth. In some conditions a vehicle of high ground pressure can dig in to get grip, and pass, while one of light pressure floats less deep, and cannot find traction. At present there is no figure as to the extent of this scale effect.

An aggressive track link or tyre tread has long been accepted as generally beneficial on non-homogeneous cohesive soils. Tank tracks are now generally fitted with rubber pads in an attempt (often counter-productive) to limit damage to roads. Some pads are removable, but this is a slow job, and leaves a cavity in the track-link, which then packs up with soil, and ruins the grip to much the same extent as the pad. A particularly difficult condition is on turf, which shears off. Very limited trials by the author indicate that an aggressive steel tread (eg Centurion) may give a benefit equivalent to a 25% reduction in ground pressure, compared to a large flat pad. Maclaurin (Ref 4) gives details of improvements to tractive coefficients due to tread pattern and tyre deflation. For tyres with dual purpose road and cross country treads as used on military vehicles, a reasonable approximation of the improvement of grip compared with a road tread, or a smooth padded track, is equivalent to some 10% reduction in MMP.

Dry Sand.

Operation in dry sand is usually less of a problem than on cohesive clayey soils. Cohesive soils predominate in critical parts of temperate and tropical areas. Therefore it is usual to quote MMP using the cohesive soil formula for wheeled vehicles. (For tracked vehicles the one formula is used for both soil types). However, where a wheeled vehicle is being specifically assessed for use on dry sand as in some deserts, the appropriate formula should be used (see Fig.1.g). The flotation of the tyre in dry sand is reflected in the relative increase in the benefit of tyre breadth and deflection. Sinkage and thus resistance will depend on sand density. This varies across any one dune according to recent sorting of the sand by the wind, and any subsequent disturbance. The sand gives increasing strength with depth, due to surcharge. There is thus an effect of scale aiding larger

vehicles. Dry sand is disturbed by an aggressive tread which would be considered an advantage on clay. Correction factors for the detrimental effect are in Fig. 1.g. The sand MMP formula has only recently been taken into use. It is derived from the sand soil numeric (Ref 3). Trials have yet to confirm the constant 'S' to make the wheels sand MMP fully comparable with tracks MMP. The present use of the wheels sand MMP is for comparisons between different wheeled vehicles, and different tyre sizes on the one vehicle. Wet inland sandy soil can to a limited extent be considered a cohesive soil when using MMP. Most peacetime testing and training areas are sandy soils.

The Effect of Speed on Sinkage.

The MMP expressions assume slow movement, so that sinkage is complete. High speed denies time for full sinkage, and thus resistance is lessened. Speed can provide the kinetic energy to overcome the severe resistance of a short soft patch. Power and low ground pressure are inter-related, and lack of one can to some extent be compensated by the other.

Traction.

The traction from the ground to overcome air, gradient, hard-ground rolling resistance, and soil sinkage will, on cohesive soils (clay), depend on the soil strength and the vehicle ground contact area. Where the soil is frictional, as in sand or on a hard surface, traction is by frictional forces, so proportional to weight. Most soils are a mixture of cohesive and frictional types. Apart from deserts, an aggressive tread generally pays. The traction will have some proportionality to weight. A "coefficient of adhesion" can be used like a coefficient of friction, to give a total traction force which is proportional to weight. Some examples are:

Coefficient of Adhesion	Cross-country tyre	Steel track
Dry rough concrete	0.8-1.0	0.45
Dry clay loam	0.5-0.7	0.9
Wet clay loam	0.4-0.5	0.7
Damp gravelly sand	0.3-0.4	0.35
Loose dry sand	0.2-0.3	0.3
Dry snow	0.2	0.15-0.35
Ice	0.1	0.1-0.25

Trackslip.

A vehicle near the limit of traction will have significant track or wheel-slip. Peak traction often occurs at about 20% slip: with negligible slip at only very low tractive efforts. Thus a vehicle will often be suffering slip of some significance without being near failure, and without the crew being aware of it. This slip must be allowed for in calculations of speed made good. Little data is available for the amount at higher speeds, and thus slip is seldom taken into account in performance assessments.

ACCELERATION AND SPEED.

Available and Effective Power.

Considerable losses are involved for an engine installed in a vehicle compared with on a test bed. There are further losses in the transmission. A definite statement is needed of power actually available at the sprockets or wheels.

If the transmission is continuously variable (CVT) the engine can run all the time at its peak speed. If there are a series of gear steps, for much of the speed range the engine will be giving less than its peak power. A graph of power against ground velocity shows a saw-tooth shape as power rises to a peak in each gear. The relationship of the area under this saw-tooth shape to the whole area gives the power available effectively over the whole speed range: the Effective Power. The closeness of effective power to peak power will depend on the torque/speed characteristics of the engine, and the number of gears. Some examples of efficiencies and effectiveness affecting net power are given below:

Engine Installation Losses: about 15%

Transmission Losses:

Gearbox:	Spur Gears:	Epicyclic gears:	CVT
	7%	10%	22%

Final Drive losses: about 4%

Gearbox Effectiveness: (diesel engine)	4 gears:	6 gears:	8 gears:	CVT.
	81%	87%	91%	100%

Thus for a 1000 HP engine with 6 epicyclic gears:
1000x.85x.9x.96 = 734 peak HP at sprocket,
734x0.87 = 639 effective HP over whole speed range.

The running gear will have inertia resistance when accelerating. There are very few published records of running gear inertias. If complete vehicle data is not available, the rotational inertia of an AFV running gear may be taken as equivalent to 10% of vehicle gross weight if tracked, and 15% if wheeled.

The tracked running gear will give a hard-road resistance to motion of 3½ to 5% dependent on track weight, pitch and tension. Resistance increases marginally with front sprocket rather than rear. A typical figure for hard road resistance would be 4%.

An all-wheel-drive wheeled vehicle has a hard road resistance of about 2% with full differential action. When off the road the wheeled vehicle will usually have greater sinkage resistance. These hard ground resistances should be added to the sinkage resistances shown in Fig. 3. In Fig. 3 is a line marking the combination of soil softness and ground pressure where sinkage resistance reaches about 20%. This is suggested as the realistic maximum if, after allowing for the additional hard ground resistance, there is to be sufficient traction available to use for acceleration, hill climbing, and manoeuvering.

Size and Manoeuverability.

A big vehicle in a small space must move cautiously, so speed cannot be used to the full. At other times, obstacles such as ditches are smaller to the large vehicle, so speed is helped. In limiting conditions size will often help: thus soft tilth is less deep. Turning circle is often important in reaching confined spaces. In good going the sharp turning circle of skid steering is a great asset, though in limiting conditions full use of it may halt the vehicle. Ground clearance, side-slope stability, approach and departure angles of the vehicle, and for wheeled vehicles the under-vehicle clearance between axles, are other important secondary characteristics. The characteristics of past vehicles give guidance as to satisfactory levels.

ASSESSMENT OF JOURNEY TIME.

Portrayal of Performance.

This section describes the methods used to forecast performance over a journey by simulation using a computer based model. Ideally, real vehicles would be driven over real routes, but this is seldom possible. Tests would need to be done in all seasons. In Europe, trial and test areas are often on unrepresentative heathland, since its infertility makes it unwanted for farming, and thus available. Its firm sandy soil stands up well to the continuous traffic it must bear. Rich cohesive clayey soil would become a quagmire. It is therefore necessary to cull all the information possible from whatever realistic tests there may be, and extrapolate this by modelling. The experienced person has always done this mentally to a certain extent. The modelling merely does it more formally and thoroughly.

The simulation allows "runs" by vehicles yet to be built, and these runs can be readily repeated with various vehicle parameters altered, different route conditions, and drivers of different aptitudes. The use of a computer allows information to be logged on a scale that would be impracticable without a comprehensively instrumented test vehicle. The computer program can sort, process and print the information in a form ready for use. The results from the simulation can show the user performances for various options of concepts, with the current equipment for comparison. The designer can try out various ideas. The results from the simulation can be transposed into test routines. They allow calculation of component lives and fuel consumption. Peacetime tests and training will be on heathland. Both peacetime and war routes must be modelled. The results of the simulation can have a wide use. An enemy tank can be simulated to provide details of target behaviour for use in fire control study. Both own and enemy movements can be used in war gaming.

Basic Constraints.

The external influences can affect vehicle performance just as much as its own mechanical characteristics. It is not possible to get realistic results for all phases of vehicle use, since there are so many assumptions that would have to be made on these external constraints. However,

there are many circumstances when a vehicle will be driven as fast as possible, and when the assumptions can be defined and justified, and from these can be got a good guide to vehicle ability. There are conditions of traffic or tactical constraint under which the driver does not drive as fast as possible, and personal interpretations of the most suitable speed vary widely. If the driver is holding the vehicle back, the simulation ceases to be vehicle assessment, and becomes a study of human factors. The mobility of the vehicle is important for those moments when it will be fully extended, and thus the simulation must model them. Even so, variations in ground conditions and driver behaviour can produce much greater ranges of performance variation than vehicle attributes. Furthermore, a good driver will take great trouble at critical moments to mitigate the worst shortcomings of the vehicle. Thus, with a diesel engine with turbo-charger, or a gas-turbine, with marked lag in throttle response, the driver anticipates power demand, if necessary dissipating early weaker response by the brakes. Thus an intricate model to simulate extreme detail of vehicle reaction may not be warranted by the relative size of errors due to outside conditions, and also may be confounded by the reactions of the driver. It is thus possible to take a simple approach to the model.

The Mathematical Model.

The simulation monitors vehicle position along the route, noting from the stored data the instantaneous gradient and surface resistance. It looks ahead along the route to measure the distance to the next hazard, such as a bump or a bend, and from its record of speed limits at hazards on the route, and knowledge of instantaneous speed, applies the brakes, and then limits engine power demand to hold the required speed limit through the hazard. The journey is a large number of flat-out sprints ended by braking for a hazard, and interspersed by the hazard speed limits. The model refers to the stored data for engine torque, gear ratios (including any torque converter or other coupling effects) appropriate to ground speed, takes account of losses and inertias, and derives instantaneous acceleration. Minor sub-routines operate during gear changes, or when tractive effort exceeds grip. The calculation is reiterated at a rate which is a compromise between cost and accuracy. A regular 1/10th second gives sufficient accuracy bearing in mind the other large uncertainties.

Route Selection.

Actual routes from real pieces of ground must be recorded and used for the simulation. The user will confound any statistical handling of route parameters. The natural landscape pattern, and mans' subsequent use gives trends to the ground characteristics. The prime task of the driver is to make the best use of the ground: minimising any handicaps. There are some models, and some receiving some favour, which treat areas of similar characteristics as "patches", for which averaged criteria for matters such as gradient and surface roughness are used. This can be misleading. The work vehicle fetching and carrying will choose the easiest route, and the farmer working the soil the most appropriate. The AFV crew choose a route to keep themselves in sight of their friends

giving covering fire, and out of sight of the enemy, and to avoid any risk of getting bogged. A so called "cross-country" journey will in Europe run much of the distance on roads or tracks. When near the axis these make it worth a small detour to use them for greater speed, with firmer smoother surfaces, and culverts over ditches.

An example of the difficulty in interpreting statistical statements on terrain is the oft quoted characteristic of percentage trafficability. This gives no guidance as to the ease with which a route might be picked between patches that are impassable. An area might have say 10% non-trafficable due to one deep fast-flowing river with steep high banks. To somebody trying to move across the river it is a complete stop to mobility, but perhaps little penalty if moving astride the river. Another area could also be 10% non-trafficable due to water obstacles, but with it in small lakes and ponds with firm ground inbetween, allowing a route to be picked with little difficulty in any direction to any part of the area.

Route Features.

Attributes such as soil and gradient control the resistance which the vehicle must suffer, and roughness gives the suspension speed limit. Modelling of an AFV in NW Europe can be limited to open country, since in towns and semi-urban areas, and in woodland, tactical constraints will often limit speed. The open farmland is the good tank country, where a tank will move as fast as possible from one tactical bound to the next, and where automotive performance will be critical. The arable land has been subject to many years of tilling, and so is quite smooth: smooth enough for a tank, even with relatively poor suspension, to move with speed unlimited by roughness; even downhill in the dry season. Valley pasture is also usually smooth due to its origins as silted scoured valleys. For drainage or demarcation, fields tend to be bounded by ditches, banks or walls, which form quite severe bumps, and a block to vision beyond. Thus they form quite a severe hazard that must often be taken quite slowly. During the season of standing crops, the driver in a low vehicle may not be able to see hazards until close, and must rely on his commander telling him when it is safe to go at full speed.

On roads and tracks the two speed limits are bends and traffic. For an AFV in actual combat, the "traffic" will be in the form of destroyed vehicles, and if there is any risk of delay or ambush, such hazards would be detoured.

Route Preparation.

It is only by collecting routes chosen in realistic scenarios that the trends for route characteristics will emerge. It would be exceedingly difficult to choose routes without first visiting the area, since maps do not show enough topographical detail, and photographs need to be taken at driver eye level. The area must also be visited to record details of the profile and soil. The length of route needed is considerable. For any one landscape pattern routes totalling a few hundred kilometres must be chosen and recorded. Analysis of those routes will show the behaviour of route parameters such as gradients, soils, use of road and tracks,

and the unimpeded movement distance between hazards (UMD). Once this pattern is known, a sample route can be selected for modelling, some 10km long, containing representative distributions of the parameters. Such samples must be collected for each area of a particular landscape pattern, and for each type of use. Thus for a tank, attack routes have trends different to those for withdrawal.

Route preparation is an expensive, protracted, but critical part of the simulation. In default of the realistic routes, short representative routes of about 1km can give preliminary indications of performance. Experience with the simulations has shown the importance of the choice of route, the need for long samples, and the misleading results that arise when the route is dealt with less realistically.

Interactive Events.

The effect of a hazard on the vehicle or driver depends on its position along a route, and will provoke different reactions. Thus if still going slowly having just moved forward from a fire position, a ditch oblique to the axis might be crossed at once, because it would cause little delay. But if the ditch was met at speed, a detour might be made to cross it later. Changes in gradient and changes in soil softness are highly interactive. With a normal gearbox, a timely down hill stretch can allow the engine to pull away after a gear change. Any attempt to simplify route selection could be misleading. Synthetic routes can only be used for very limited parametric variation to check modelling sensitivity, not for actual assessment. There seems to be no statistical justification for using anything other than routes taken from natural terrain, chosen for their realism by knowledgeable users.

The Driver.

Drivers vary in boldness, appreciation of ground, and skill at the controls. The cautious driver will slow right down at a bump that could be "flown" at speed. The injudicious will not slow down as required at a hazard, and then will have to slow when he could have been going fast again to allow the other crew members to recover, and to recover his own nerve. The skilled driver will make perfect manual gear changes, or override the automatic box just where needed to inhibit unwanted gear changes: others loose time and punish the vehicle.

It would be very difficult to get accurate details of driver behaviour over the very routes used for simulations, and thus assumptions have to be made. A thoroughly obedient, consistent but timid driver has been used in the modelling that forms the background to this paper. Hazards are never "flown", but always approached with caution. Braking and cornering are always done at the speeds to ensure the crew are not discomfitted. This allows consistent and simple interpretation of route information.

It has been found for NW Europe that UMD of some 500m might be typical. The different interpretations by the drivers of hazard severity will tend to alter UMD. However, for the sorts of powers being considered for AFVs of some 25 HP/Ton the results are not very sensitive to UMD. (See Fig. 4).

Suspension.

Bumps are a frequent hazard which limits speed. These speed limits must be included in the simulation. Before a run is modelled the route must be previewed, and suspension speed limits established throughout its length. The suspension preview needs considerable detail of the route. The whole micro-profile must be plotted. Account must be taken of the extent this will be flattened as the vehicle deforms the soil, and the extent to which remaining bumps will be bridged by track links. The soil deformation takes time, and acts as additional bump absorption adding to that of the suspension. The driver can also help the vehicle over a severe bump. All this must be accounted for.

At present so little information is available on route micro-profile that any attempt to model suspension behaviour as part of the simulation would be misleading: as it is on some models that do so. Luckily it is possible to prepare bump limiting speeds beforehand, and incorporate them in the model input.

For NW European farmland, as already described, for an AFV within a field, or on roads and tracks, it can be assumed suspension is not a speed limit. The bump speed limits come at field boundaries, or banks when joining a road. Taking into account the limits to vision from crops, and the caution of the assumed driver, these will usually be taken at a very slow speed. Due to the high speeds that are attained at other points along the route, the results are not sensitive to the actual speed that might be considered "slow". See Fig. 5. Thus speed at bumps can be chosen arbitrarily: say 2 m/s.

For other terrain such as Savanna and Heathland, where this assumption is unsound, during the dry season high powered vehicles representative of various suspension ability can be driven down the routes to establish limiting speeds. These vehicles need not necessarily be of the right type: thus a High Mobility Load Carrier, the Alvis Stalwart, running with a little ballast at the rear can set a good standard. At the slower limits, an unladen truck with leaf springs can be used.

Steering.

Speed limits on bends on roads are set by limiting side force, with crew comfort the criterion. Power absorption then is insignificant. Cross-country, sharp turns are normally made going slowly, so the power used will not affect speed. At speed, turns are usually relatively small, and thus power dissipated in steering insignificant. Thus power consumed in the steering can normally be ignored. However, when taking evasive manoeuvres, such as weaving to avoid being hit, the power needed is a major consideration, and account must be taken of power used.

VALIDATION

Magnitude of Errors.

The major output of the simulation is the average speed. Examples are shown in Fig. 6. It will be seen that relatively minor changes in soil strength are the equivalent of major changes in vehicle potential. Thus the major constraint in

accuracy is the lack of information in detail on the variation of soil strength from occasion to occasion.

Performance Matching.

A simple model is most vulnerable to inaccuracy during strong acceleration from a standing start. The simulations with which the author has been concerned had good confirmation of realism by the close match of standing-start sprints by relatively high powered AFVs on a hard surface. Further validation is got by driving a vehicle along the whole routes modelled, to compare actual results with those of the simulation. However, this needs a fair sample of drivers, and a large recording team to take soil strength measurements before there could be any changes. Thus for practical reasons, validation is dependent on circumstantial evidence. However, as an example of the order of accuracy, the validation of standing-start sprints showed that the match was sensitive to the aerodynamic form factor: and this for AFVs limited to 90 km/h. Confirmation of assumptions on driver behaviour has been possible by monitoring their performance in a driving simulator. This has been on a complex one, with a full landscape model allowing the driver to pick a route. The vehicle characteristics can be adjusted to assess driver behaviour over a range of performances.

CONCLUSIONS.

The mobility simulations can give realistic results and allow the derivation of detailed data. The key issues are the route, and the strength of the soil along it, and the interpretation of the route by the driver. By comparison, vehicle characteristics are known in finer detail, and a complex model can simulate the vehicle very thoroughly. Such detailed modelling has its uses for the study of component behaviour. However, to give detailed forecasts of performances in service, there must be good samples of truly representative routes, with full knowledge of the variations of the soil strengths, and of driver behaviours. Since the collection of such information is a lengthy task, simulations will perforce have to be done on route samples shorter than ideal, and with ground conditions known for only a limited number of occasions, with little knowledge of true distributions. Knowledge of driver reaction is also likely to be limited.

With such a wide margin of uncertainty due to these influences, a simple model can simulate the vehicle characteristics with commensurate accuracy. This can be quick and cheap to run. It also allows most effort to be put to collecting more accurate information on those compelling external influences. Indeed, should some vehicle have an idiosyncrasy that at times penalises it, and which might show up in a detailed model, the modelling could mislead, since the idiosyncrasy is likely to be alleviated by the driver making allowances for it.

The simulations have their uses where the vehicle is driven fully extended without the driver holding back for any constraining circumstances, and where the vehicle is not at risk of getting bogged.

When comparing vehicles of very different ground pressures, simulations which include sections of route where vehicles are liable to get stuck can be misleading, since drivers would be likely to choose routes to suit the vehicle ground pressures. To assess performance in heavy going a clearer judgement can be got by consideration of the basic criteria of ground pressure, expressed in the MMP system, and with knowledge of the power to weight ratio. Secondary criteria, such as size, shape, and turning circle are also important.

ACKNOWLEDGEMENTS.

Specific details of performances or equipments have not been quoted in this paper to avoid publication of any classified or proprietary information. However, much of the experience and knowledge on which this paper is based has come from the British Ministry of Defence. The MMP system was prepared by the Military Vehicles and Engineering Establishment at Chobham, and the simulations done under their aegis. The Defence Operational Analysis Establishment, West Byfleet have developed the methods for route selection. Figures 2a, 4, 5 and 6 have been published with the kind permission of EASAMS Ltd., of Camberley and it is in the devising, developing and running their mobility simulation MOBTANK on behalf of MOD and for Vickers Defence Systems of Newcastle that much of the modelling experience described in this paper has been gained. Opinions and judgements made in this paper are those of the author.

REFERENCES.

1. ROWLAND, D. Tracked Vehicle Ground Pressure and its Effect on Soft Ground Performance. Paper to ISTVS Conference 1972.

2. ROWLAND, D. A Review of Vehicle Design for Soft Ground Operation. Paper to ISTVS Conference 1975.

3. ROWLAND, D. and PEEL, J.W. Soft Ground Performance: Prediction and Assessment for Wheeled and Tracked Vehicles. Proc I Mech E 205/75.

4. MACLAURIN, E.B. The Effect of Tread Pattern on the Field Performance of Tyres. Paper to ISTVS Conference 1981.

a. **Tracked Vehicles**

$$MMP = \frac{1.25W}{2n\ c\ b\sqrt{pd}}\ kPa$$

W = Vehicle Weight (kN)
n = number of axles
c = track link profile factor (area/pd)
b = track width (m)
p = track pitch (m)
d = wheel diameter

b. **Wheeled Vehicles** (Wet fine-grained soils (Cohesive) (Clays)).

$$MMP = \frac{KW}{2n\ b^{0.85} d^{1.15} \sqrt{\delta/h}}\ kPa$$

W = Vehicle Weight (kN)
n = number of axles
K = Factor given below
Tyres: unladen
b = breadth (m)
d = diameter (m) less tread
δ/h = deflection (%) (hard ground)

Number of Axles n	Proportion of Axles Driven						
	1	$\frac{3}{4}$	$\frac{2}{3}$	$\frac{1}{2}$	$\frac{1}{3}$	$\frac{1}{4}$	$\frac{1}{5}$
2	3.65	-	-	-	4.4	-	-
3	3.9	-	4.35	-	-	5.25	-
4	4.1	4.44	-	-	4.95	-	6.05
5	4.32	-	-	4.97	-	-	-
6	4.6	-	5.15	-	5.55	6.2	-

Differential Locks. If these are in use, equivalent MMP is improved:- 4 x 2 Vehicle: MMP x 0.98.
4 x 4 or 6 x 6: MMP x 0.97.

c. **Resistance from Soil Sinkage**

$$\frac{R}{W} = 0.28\left(\frac{M}{C}\right)^{1.95}$$

R = resistance
W = Weight
M = MMP
C = CI = $\frac{RCI}{0.8}$

NB. All units must be the same.

Fig. 1. MEAN MAXIMUM PRESSURE EXPRESSIONS

d. **Trafficability Limits** (Wet fine grain (Cohesive) (Clay) soils).

1 pass RCI = 0.096 MMP (Rating Cone Index of soil strength in lbf/in^2). MMP in kPa.

Multiple Passes: Multiply 1 pass RCI by

	1	2	5	10	25	50
RCI x	1	1.2	1.53	1.85	2.35	2.8

e. **Vehicle Design Aims**
MMP required for satisfactory performance (Ref 1)

Condition	Performance Importance		
	Ideal	Satisfactory	Maximum Acceptable
Temperate, wet, fine-grain	150	200	300
Tropical, wet, fine-grain	90	140	240
European bogs	5	10	15
Muskeg	30	50	60
Over-snow	10	25-30	40

f. **Gradient Ability or Draw bar Pull.**
To find limiting soil strength for gradients or draw-bar pull, multiply level ground limiting RCI by factor below.

	Grade or DBP/GVW: 1 pass			
	0	0.1	0.2	0.3
Wet fine-grained: with diff	1.0	1.2	1.6	2.0
: locked differential	1.0	1.1	1.25	1.4
Dry coarse-grained: with diff	1.0	1.5	2.4	4.7
: locked differential	1.0	1.3	1.7	2.3
Wet coarse-grained: with diff	1.0	1.2	1.5	2.5

Fig. 1. (continued) MMP TRAFFICABILITY EXPRESSIONS

g. MNP (Wheels) (*Dry coarse-grained soils (frictional) (Sands)*).

$$MNP = \frac{S \cdot T \cdot W}{2a\, b^{1.5} d^{1.5} \delta/h} \text{ kPa}$$

W = Vehicle Weight (kN)

T = tread factor = 1 smooth tyre
1.4 road tyre
2.8 non directional road/ec
3.3 earth mover

S = Constant for proportionality to tracked MNP. Take S = 0.60

b = tyre breadth (m) (unladen)

d = tyre diameter (m)

δ/h = tyre deflection (S) (hard ground)

Notes: 1. The relationship of MNP (sand) to RCI in sand is not yet established.
2. For wet sand, MNP (Clay) gives fair indication.

h. Typical Radial Tyre Deflections on Hard Ground.

Inflation suitable for	δ/h
Hard Road : Fast speeds	0.17
Grit tracks: about 30km/h	0.19
Soft Ground: about 15km/h	0.25

For pure comparisons of MNP, use of δ/h=0.18 allows standardisation. For trafficability limit *use deflection for proposed inflation.*

Fig. 1 (continued) *MNP EXPRESSIONS*

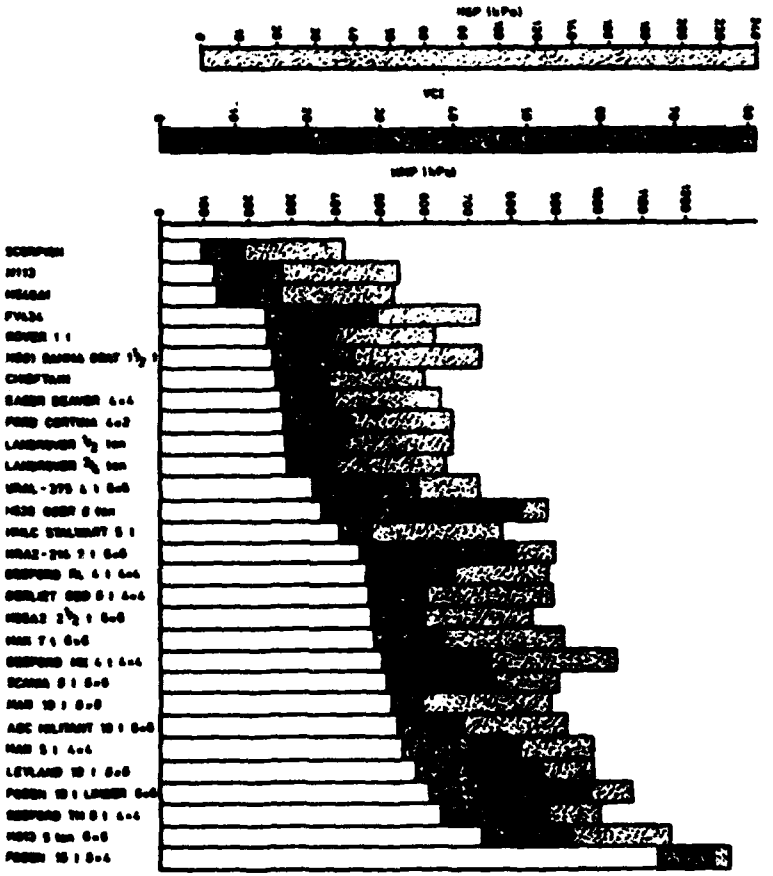

Courtesy BASANS Ltd

Fig 2a. RELATIVE MERIT AND CHANGING ORDER OR MERIT WITH GROUND PRESSURE CRITERIA: MGP, VCI, MNP.

	TYRES				MNP		MNP
	Size	Breadth b(m)	Diameter d(m)	d/b	Clay kPa	Sand kPa	
SMALL VEHICLE 4x4 W= 2.03t	6.00x16	0.175	0.704	4.0	282	537	81
	6.50x16	0.181	0.718	3.97	270	496	77
	7.50x16	0.205	0.778	3.8	220	364	62
	9.00x16	0.252	0.882	3.5	160	221	45
LARGE VEHICLE 4x4 W= 14t	14.00x20	0.370	1.204	3.25	556	539	154
	16.00x20	0.419	1.289	3.08	462	403	127
	24.00x20.5	0.595	1.340	2.25	328	224	86
Notes	Radials	unladen	less tread		δ/h = 0.18 c/c tread	Road tread	

Fig. 2b. EXAMPLES OF TYRE ASPECT RATIOS AND SCALE EFFECTS COMPARING MNPs FOR CLAY AND SAND

GROUND PRESSURE MNP kPa	SOIL STRENGTH: RCI 25 172	35 241	45 310	60 414	70 483	105 724	lbf/in^2 kPa
110	7.6	3.9	2.4	1.4	1.0	0.5	Very Light AFV
140	12.	6.3	3.8	2.2	1.6	0.7	Light tracked AFV
185	21.	10.8	6.6	3.8	2.8	1.3	
230	32.	16.5	10.1	5.8	4.3	1.9	Light MBT
285	48.	25.1	15.4	8.8	6.5	2.9	Heavy MBT Motor car
310	57.	29.5	18.1	10.3	7.6	3.5	Good wheeled AFV
350	72.	37.4	22.9	13.1	9.7	4.4	Normal wheeled AFV
450	118.	61.1	37.4	21.4	15.8	7.2	Good all-wheel drive truck
Farming	>——Increasing time since last ploughed——>						For total resistance: add hard ground resistance: eg:- Car 1.7 Wheeled AFV 2.6 Tracked AFV 4.1
Weather	>——Decreasing amount of recent rain——>						
Soil	Almost boggy	Very soft	Soft	Medium	Good	Firm	
Walking	Sticky Boots sucked off	Heavy	Tiring Mud works up legs	Easy but boots needed	Normal Shoes		

Fig. 3. RESISTANCE TO MOTION. (S) DUE TO SINKAGE INTO SOIL (Wet fine-grained: Cohesive: Clayey)

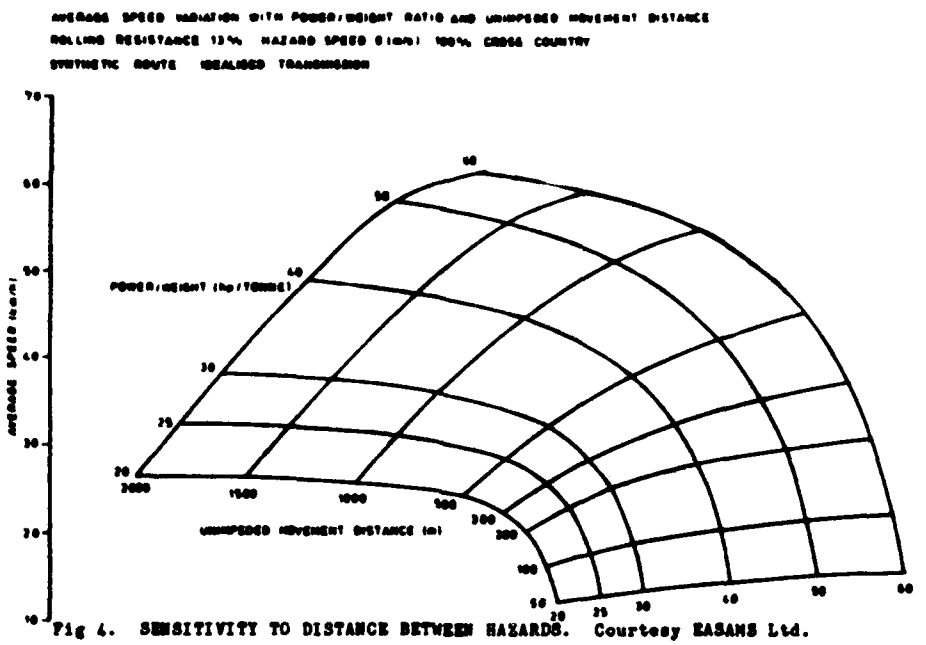

Fig 4. SENSITIVITY TO DISTANCE BETWEEN HAZARDS. Courtesy HASANS Ltd.

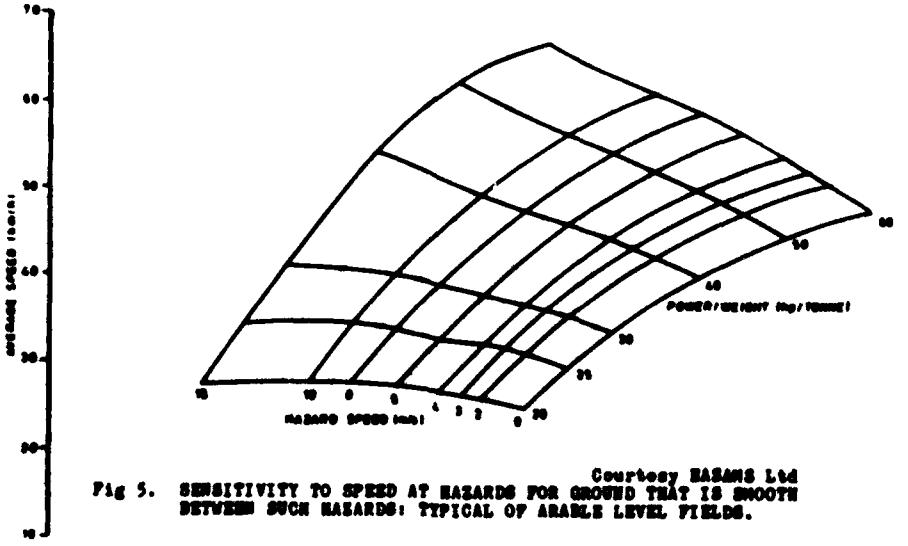

Courtesy HASANS Ltd

Fig 5. SENSITIVITY TO SPEED AT HAZARDS FOR GROUND THAT IS SMOOTH BETWEEN SUCH HAZARDS: TYPICAL OF ARABLE LEVEL FIELDS.

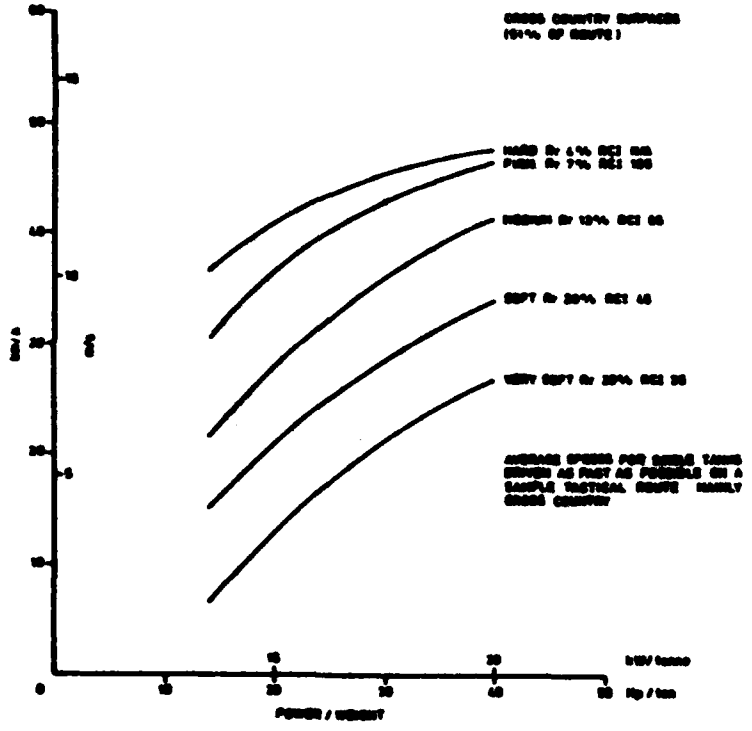

Courtesy HASANS Ltd

Fig 6. AVERAGE SPEEDS FOR NET POWERS FOR TEN CROSS COUNTRY ROUTE, FOR VARIOUS GROUND CONDITIONS. ROUTE SHORTNESS GIVES BIASSES.

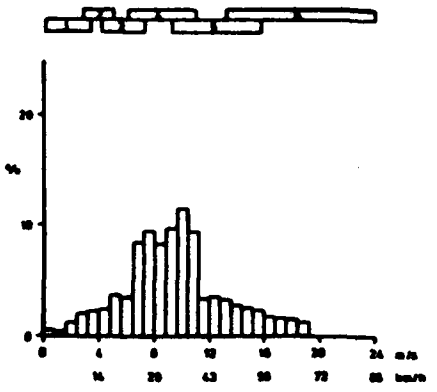

a. Record of velocities, with speed range for each gear. Peaks indicate where heavy going prevented pulling away in next gear.

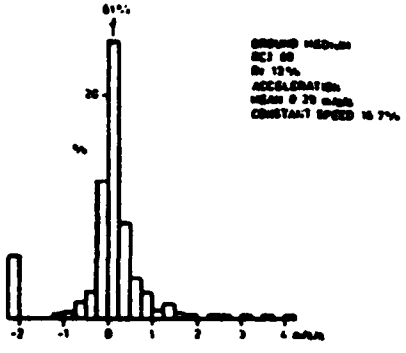

b. Record of Accelerations. All braking was at -2m/s/s.

Courtesy HASANS Ltd

Fig 7. EXAMPLES OF HISTOGRAMS

TOPIC 10

VEHICLE CONFORMAL DESIGN

MICROPROCESSOR BASED SPEED GOVERNING OF DIESEL ENGINES USED IN MOBILE APPLICATIONS FOR BEST ALL ROUND PERFORMANCE

B.S. CHITTAWADGI*, H.C. DHARIWAL**, R.S. BHATKOKESHWAR***
INDIAN INSTITUTE OF TECHNOLOGY, BOMBAY, INDIA

SYNOPSIS

The fluctuating loads encountered in all mobile applications give rise to the oscillations of speed of diesel engines which are the main cause of deterioration of the performance of these engines. This lowers the power output and fuel economy of engines used in mobile applications. Various attempts made to apply the control engineering to the engine governing problems have made it clear that an optimum matching of the parameters of engine, governor and load is necessary to achieve the best fuel economy and power parameters of the engine.

The large number of parameters encountered which do not remain constant for the full speed and power range as well as during the entire service life of engine make the task of governing difficult in spite of all the complexities introduced in mechanical governors. It is shown here that the microprocessor application to the governing of diesel engines is alone capable of providing the optimum control using the PID and other advanced algorithms for various applications during the entire service life of engine.

INTRODUCTION

Diesel engines have established themselves in all heavy duty applications due to their higher fuel economy. They however, have a very serious shortcoming of instability of working under certain speed and load ranges [1]+ which may lead to its runaway beyond safe speed limits and therefore a safety hazard or to another extreme of stalling (Fig. 1). This was realised in the early years of invention of diesel engines and centrifugal governor used for the governing of speed of steam engines was adapted to control the speed of diesel engines also. The same principle is used even today extensively for speed governing of diesel engines.

The required stability of working of engines was not obtained in many instances and difficulties in the proper selection of parameters of the governor were experienced. Hunting used to result in many cases. The necessity of scientific investigation of the process of governing was felt in order to provide the solution to the problems encountered.

The attempts of the English astronomer Eric in 1840 and Maxwell in 1868 [2] are worth mentioning here who applied the methods of mathematical analysis to the problems encountered when using centrifugal governors. Their work

---

+ Numbers in parentheses indicate the references at the end of the paper.

* Professor, Department of Aeronautical Engineering.
** Asstt. Professor, Department of Mechanical Engineering
*** Research Scholar, Department of Aeronautical Engineering

has served as a practical mathematical tool in control engineering and has helped in the development of control engineering as a separate branch of engineering.

Theoretical contributions to the theory of governing were made by various other scientists like Chebyshev in 1871, Vyshnigradski in 1877 and Stodola, Rouse, Hurvitz, Mikhailovsky and Liapunov later to name a few. Vyshnigradski published in his paper graphical representation of the regions of stable, unstable and indeterminate stability in 1877 [2] which are widely used in analysing the engine governor system and are known as Vyshnigradski diagrams.

All the above efforts as well as later advances in control engineering have not been able to provide the mathematical solution required to the engine governing problems and the design and development of engine governors have largely remained experimental and empirical in nature. This is due to the large number of variables of the engine as well as that of the loads to which the diesel engines are subjected to in their numerous mobile applications (transport, agriculture, construction and road making machines, military locomotives etc.).

The centrifugal governors used even today have some of the serious shortcomings which give rise to increase in specific fuel consumption and decrease in power output of these units when subjected to dynamic loading in comparison with the corresponding values under static operation under laboratory conditions.

The main reason for the deterioration of performance of diesel engines is the appearance of oscillations of speed of engine crankshaft when subjected to fluctuating loads in mobile applications. It has been shown in this paper that only microprocessor control is capable of taking all the variables into account encountered in various applications to which diesel engines are subjected to and provide all round best performance by keeping the speed fluctuations to the minimum. The mechanical governors in spite of all the complexities introduced (like double sensing loops, feed back links, indirect governing, torque and speed correction, variable spring stiffness) are not capable of meeting the requirements of dynamic loading in various applications in an optimum manner. The loss of power and fuel economy can be upto 25 percent (Fig. 2).

LITERATURE REVIEW

Many attempts have been made in the post war years to apply the theory of control engineering in order to understand the erratic behaviour and improve the performance of engine governor systems.

Thus Bujak's paper in 1945 [3] outlines the necessity of treating the problem of governing of diesel engines dynamically instead of statically. He has pointed out to the importance of the effect of friction, inertia, flywheel effect and time lag on the performance of governor. He has suggested approximate expressions for the transfer function of engine. As agreed by the author himself the theory presented is greatly abridged and has emphasised the need for detailed analysis.

Welbourn and others [4] published a paper in 1959 on the investigation of the problems encountered in the operation of hydraulic speed governors. Working of an unstable engine governor was investigated by the authors. An attempt in this paper has been made to apply the theory of control engineering to the problems of governing. Derivations of some of the equations and application of control engineering to the problems has been illustrated and necessity

of collaboration between engine industry, and academic institutions has been emphasized by the authors.

The necessity of taking the effect of various parameters of the engine governor system on its operation has been highlighted by Oldenburger in a paper presented to the American Society of Mechanical Engineers in 1965 [5]. He has suggested a design of the hydraulic governor with a dash pot which makes it possible to adjust the various parameters and thus change the time lag of the governor to improve the performance of the system. He has shown how with the change of parameters of the system the frequency response and transient response characteristics can be varied to achieve the desired results.

The improvement of the performance with load sensing has been proposed by Webb and Janota [6] and Blair [7]. This has been found useful in diesel generating set application in order to meet their exacting speed requirements.

It should be pointed out here that in almost all the cases, the frequency response curves for the engine and load system were obtained either experimentally or through approximate analysis of the system and the engine transfer function arrived at using Bode's plot.

The approach cited above has limited uility from engine governor synthesis point of view since it does not take into account the basic constructional and operational parameters of the system and cannot therefore be of practical value for developing engine governor system.

Bowns [8] in departure from the above authors who have used the continuous control theory, tried to apply the sampled data control theory to the engine governor system in order to take into account the pulsed nature of working of engine. It is to be pointed out here that the sampled data control theory is not quite valid to centrifigual speed control since the speed is continuously sensed by it and the time lag of engine is not a fixed quantity and may vary from zero to the duration of one cycle depending on at which instant of engine cycle has the rack adjustment taken place.

Krutov [9,10,11,12,13] in his various books and papers published has presented an integrated approach to the engine-governor-load system. He has given a detailed derivation of the differential equations of the engine and governors. The equations have been derived from the first principle and therefore the various coefficients contained in the equations can be calculated from the constructional and operational parameters of the engine and governor.

The use of Routh Hurvitz criteria, Vyshnigradski diagrams, root locus plots, frequency characteristics and logarithmic frequency characteristics etc. has been amply illustrated to achieve optimum design and synthesis of the governing system. The methods of calculations and plotting of transient speed characteristics has been shown which is necessary for judging the quality of dynamic characteristics (Fig. 3) of the system.

The equations of engine and its various elements presented below clearly show the interaction of various parameters of system of importance which have to be taken into account for achieving a quality governing [11] :

DIFFERENTIAL EQUATIONS OF VARIOUS ELEMENTS OF A TURBO-CHARGED ENGINE

The Equation of the Engine

$$T_d \frac{d\varphi}{dt} + K\varphi = q + \theta_1 \rho - \theta_2 \alpha_e$$

where,

$$\varphi = \frac{\Delta\omega}{\omega_0} \quad q = \frac{\Delta g_c}{g_{co}} ; \quad \rho = \frac{\Delta P_c}{P_{co}} ; \quad \alpha_e = \frac{\Delta M_L}{M_{Lo}} ;$$

$$T_d = \frac{J\omega_o}{\frac{\partial M}{\partial g_c} \cdot g_{co}} ; \qquad K = \frac{F_s \omega_o}{\frac{\partial M}{\partial g_c} \cdot g_{co}} ;$$

$$F_S = \left(\frac{\partial M_L}{\partial \omega} - \frac{\partial M}{\partial \omega}\right) \qquad \theta_1 = \frac{\partial M}{\partial P_c} \cdot \frac{P_{co}}{\frac{\partial M}{\partial g_c} \cdot g_{co}} ;$$

$$\theta_2 = \frac{\partial M_L}{\partial M_L} \cdot \frac{M_{Lo}}{\frac{\partial M}{\partial g_c} \cdot g_{co}} ;$$

$$\frac{\partial M}{\partial g_c} = k \left(\eta_e - \alpha \frac{\partial \eta_e}{\partial \alpha}\right) ;$$

$$\frac{\partial M}{\partial P_c} = k . g_c . \alpha \left(\frac{1}{\eta_c P_c} + \frac{1}{\eta_v} \frac{\partial \eta_v}{\partial P_c}\right) . \frac{\partial \eta_e}{\partial \alpha} ;$$

$$\frac{\partial M}{\partial \omega} = k . g_c . \left(\frac{\partial \eta_e}{\partial \omega} + \frac{\alpha}{\eta_v} . \frac{\partial \eta_e}{\partial \alpha} - \frac{\partial \eta_v}{\partial \omega}\right)$$

here, $k = \frac{H_g . J . 10^3}{\pi . \tau}$

The Equation of the Turbocharger

$$T_c \frac{d\varphi_c}{dt} + k_c \varphi_c = \xi + \theta_q . q - \theta_\rho . \rho + \theta_T . x_T - \theta_c x_c$$

where,

$$\varphi_c = \frac{\Delta\omega_c}{\omega_{co}} ; \quad \xi = \frac{\Delta P_T}{P_{To}} ; \quad x_T = \frac{\Delta h_T}{h_{To}} ; \quad x_c = \frac{\Delta h_c}{h_{co}}$$

$$T_c = \frac{J_T \cdot \omega_{co}}{\frac{\partial M_T}{\partial P_T} \cdot P_{To}} \quad ; \qquad k_c = \frac{F_c\, \omega_{co}}{\frac{\partial M_T}{\partial P_T} \cdot P_{To}}$$

$$F_c = \left(\frac{\partial M_c}{\partial \omega_c} - \frac{\partial M_T}{\partial \omega_c}\right) \quad ; \qquad \theta_q = \frac{\partial M_T}{\partial g_c} \cdot \frac{g_{co}}{\frac{\partial M_T}{\partial P_T} \cdot P_{To}}$$

$$\theta_p = \frac{\frac{\partial M_c}{\partial P_c} \cdot P_{co}}{\frac{\partial M_T}{\partial P_T} \cdot P_{To}} \quad ; \qquad \theta_T = \frac{\frac{\partial M_T}{\partial h_T} \cdot h_{To}}{\frac{\partial M_T}{\partial P_T} \cdot P_{To}}$$

$$\theta_c = \frac{\frac{\partial M_c}{\partial h_c} \cdot h_{co}}{\frac{\partial M_T}{\partial P_T} \cdot P_{To}}$$

Equation of the Inlet Manifold

$$T_1 \frac{dp}{dt} + k_1 p = \varphi_c - \theta_1 \varphi + \theta_{1h} \cdot x_c$$

where,

$$T_1 = \frac{V_1 \rho_c}{n_c \frac{\partial G_c}{\partial \omega_c} \cdot \omega_{co}} \quad ; \qquad k_1 = \frac{F_1 P_{co}}{n_c \cdot \frac{\partial G_c}{\partial \omega_c} \cdot \omega_{co}}$$

$$F_1 = \left(\frac{\partial G_e}{\partial P_c} - \frac{\partial G_c}{\partial P_c}\right) \quad ; \qquad \theta_1 = \frac{\partial G_e}{\partial \omega} \cdot \frac{\omega_o}{n_c \cdot \frac{\partial G_c}{\partial \omega_c} \cdot \omega_{co}} \quad ;$$

$$\theta_{1h} = \frac{\frac{\partial G_c}{\partial h_c} \cdot h_{co}}{n_c \cdot \frac{\partial G_c}{\partial \omega_c} \cdot \omega_{co}} \quad ;$$

Equation of the Exhaust Manifold :

$$T_e \frac{d\xi}{dt} + k_e \xi = \varphi + \theta_e \rho - \theta_c \cdot q - \theta_{xT} x_T$$

where,

$$T_e = \frac{V_e \cdot \rho_T}{n_e\left(\frac{\delta C_e}{\delta \omega} + \frac{\delta C_f}{\delta \omega}\right) \cdot \omega_o} \; ; \quad k_e = \frac{F_e \cdot P_{To}}{n_e\left(\frac{\delta C_e}{\delta \omega} + \frac{\delta C_f}{\delta \omega}\right) \cdot \omega_o}$$

$$F_e = \left(\frac{\delta C_T}{\delta P_T} - \frac{\delta C_e}{\delta P_T}\right); \quad \theta_e = \frac{\delta C_e}{\delta P_c} \cdot \frac{P_{co}}{n_e\left(\frac{\delta C_e}{\delta \omega} + \frac{\delta C_f}{\delta \omega}\right) \cdot \omega_o}$$

$$\theta_c = \frac{\left(\frac{\delta C_T}{\delta g_c} - \frac{\delta C_f}{\delta g_c}\right) \cdot g_{co}}{n_e\left(\frac{\delta C_c}{\delta \omega} + \frac{\delta C_f}{\delta \omega}\right) \cdot \omega_o}$$

$$\theta_{xT} = \frac{\frac{\delta C_T}{\delta h_T} \cdot h_{To}}{n_e\left(\frac{\delta C_e}{\delta \omega} + \frac{\delta C_f}{\delta \omega}\right) \cdot \omega_o}$$

Equation of the Fuel System :

$$k_q \cdot q = x + \theta_\varphi \cdot \varphi$$

where,

$$x = \frac{\Delta h}{h_o} \; ; \qquad k_q = \frac{\frac{g_{co}}{\delta gc}}{\frac{\delta h}{h_o}} \; ;$$

$$\theta_\varphi = \frac{\frac{\delta C_c}{\delta \omega} \cdot \omega_o}{\frac{\delta g_c}{\delta h} \cdot h_o}$$

Equation of the Load :

$$M_L = M_{Lo} + \Delta M' \cos \frac{2\pi}{t} \Delta T + \Delta M'' \cos \frac{2\pi t'}{t^2} \cdot \Delta T$$

Equation of the Direct Acting Mechanical Governor with Dash Pot :

$$T_g^2 \cdot \frac{d^2\eta}{dt^2} + T_k \frac{d\eta}{dt} + (\delta_z + \theta_\eta U_r)\eta = \varphi + \theta_\eta Y - \theta_g a_g$$

where,

$$T_g = \sqrt{\frac{IZ_o}{2E_o}} \; ; \qquad T_k = \frac{\nu \; Z_o}{2E_o} \; ;$$

$$\delta_z = \frac{F_g Z_o}{2E_o} ; \qquad F_g = \left(\frac{\delta E}{\delta z} - \omega^2 g \frac{dA}{dz}\right)$$

$$\eta = \frac{\Delta Z}{Z_o} ; \quad \gamma = \frac{\Delta y_k}{y_{ko}} ; \quad \alpha_g = \frac{\Delta \Psi}{\Psi_o}$$

$$E_o = U_g^2 A\omega_o^2 ; \qquad \theta_n = \frac{b_k \cdot y_{ko}}{2E_o} ;$$

$$\theta_g = \frac{dE}{d\Psi} \cdot \frac{\Psi_o}{2E_o} ; \qquad U_r = U_A \cdot \frac{Z_o}{y_{ko}}$$

SYNTHESIS AND DYNAMICS OF ENGINE-GOVERNOR SYSTEM

The synthesis and investigation of the dynamics of diesel engine is carried out by the simultaneous solution of the above differential equations of the engine and its various elements, governor and load. Besides verifying the stability of working of engine-governor system, the quality of governing is ascertained by the nature of variation of speed during transient operation. The system of governing of engine should be such that the maximum overshoot of speed, settling time and degree of insensitivity of governor do not exceed the design values under all possible working conditions.

An examination of the above equations makes it clear that the system of engine, governor and load comprises of a large number of interacting parameters. Many of these parameters change in a wide range for the variation of load and speed encountered and do not remain constant during the service life of engine due to the wear and tear of the engine, fuel system and governor parts.

Frequency Response Characteristics of Engine-Governor System :

The results of investigations carried out by Krinetski [14] to study the effect of various parameters of engine, governor and load for unsupercharged engines on the amplitude of fluctuation of speed of engine with the variation of frequency of variation of load is shown in Fig. 4. It can be seen that the amplitude of fluctuation of speed varies widely for different engines, fuel system, transmission and load parameters. The optimum matching of the parameters of engine, control system and load is therefore essential to achieve minimum amplitude of oscillation of speed of engine. The fluctuation of speed of engine under varying loads is responsible for the deterioration of its power and fuel economy parameters.

Fig. 5(a) shows the variation of amplitude of oscillation of engine with the frequency of variation of load for different values of time constants occurring in the equation of direct acting governors. It can be seen that the values of these parameters have a very significant effect on the amplitude of fluctuation of speed and sharply expressed resonance of frequency of oscillation of speed can occur for certain values of these parameters.

Fig. 3(b) shows the same for indirect acting governors with acceleration sensing, flexible feed back connection and astatic governor with broken characteristic of servomotor. It can be seen that this improves the quality of governing considerably under certain conditions.

It was concluded on the basis of the above investigations that with proper matching of the parameters of engine, load and indirect acting governors with automatic control of transmission can achieve the minimum fluctuation of speed of engine under dynamic loading. The design of governor however becomes very complicated and costly and cannot meet the requirements of all the applications in which the engines are used.

DETERIORATION OF PERFORMANCE OF ENGINES SUBJECTED TO VARYING LOADS [1]

The fluctuation of speed of engine under varying loads affects the quantity of fuel and air supplied and the thermal conditions of the engine. The injection timing for the varying speed and load conditions also does not remain optimum. The quick change of positive and negative accelerations of crankshaft leads to over regulation causing sharp decrease of brake parameters of engine and even to its stalling.

The deterioration of fuel injection characteristics, charging and scavenging of cylinders and changing thermal conditions during speed fluctuations of crankshaft together with the varying velocity and nature of motion of fresh charge in the combustion chamber leads to the deterioration of air fuel mixing and combustion inside the cylinder, which leads to higher smoke density.

The inertia of mechanical devices for automatic control of injection advance to quickly changing loads and speeds lead to deviation of injection advance from its optimum value. This leads either to increased roughness of combustion or late burning during expansion stroke.

In the case of turbo charged engine the air supplied is not sufficient for complete combustion of fuel due to inertia of the rotor of turbocharger and mismatching of the characteristics of the turbocharger and the engine results during transient working.

The friction losses during transient working change due to the change in the hydrodynamic lubrication conditions and thermal lag. This coupled with the power required to increase the kinetic energy of moving parts during accelerations, greater losses during gas exchange processes and decrease of mean indicated pressure of cycle leads to lower brake power output of the engine when working under varying loads than when the load is constant.

The wear of various parts of engine also intensifies under dynamic loading in comparison to the stable working conditions due to deterioration in lubrication conditions, increased maximum force and rate of rise of these forces on various bearings. The wear under dynamic loading can be 50-60 percent higher than under stable working conditions. The fuel consumption may thus be higher by upto 20% when working on fluctuating loads and the engines are derated by 10-25% by power output and 10-15% by speed in order to maintain identical service life. This can be clearly seen in Fig.6.

It is therefore clear that the speed fluctuations of engine when subjected to dynamic loads should be kept as minimum as possible.

EFFECT OF THE PARAMETERS OF TORQUE SPEED AND GOVERNING CHARACTERISTICS ON PERFORMANCE OF ENGINE

TORQUE SPEED CHARACTERISTIC [1]

The torque speed characteristic of a diesel engine has a flat shape and is one of the reasons which necessitates the mounting of governor on a diesel engine. The parameters characterizing the torque speed characteristic are:

$$\mu = \frac{M_{max} - M_r}{M_r} \text{ - coefficient of reserve of turning moment,}$$

and $$K_n = \frac{n_M}{n_r} \text{ - coefficient of speed}$$

where,

M_{max} - maximum torque developed by the engine

M_r - torque developed at the rated power output,

n_M - speed at maximum torque,

n_r - rated speed of engine.

Coefficient of Reserve of Turning Moment : The maximum allowable loading and the mean speed of operation of engine subjected to dynamic loading has to be reduced as discussed earlier and the value of the optimum loading coefficient,

$$K_{Lopt} = \frac{M_{mopt}}{M_r};$$

the coefficient of brake specific fuel consumption

$$K_{geopt} = \frac{g_{em}}{g_{er}}$$

the coefficient of power output, mean and minimum speed at optimum loading point vary with μ as shown in Fig.7.

It can be seen that with increase of μ the power output and fuel economy parameters improve and the optimum torque speed correction is therefore necessary for an engine for a given application.

Coefficient of Speed : The power and economy parameters of diesel engines have maximum values at an optimum value of speed coefficient and decrease with an increase or decrease of the value of the speed coefficient (Fig. 8). The decrease is more the higher is the loading and the oscillations of speed of the engine. At higher values of coefficient of speed not only power output of engine decreases but its control also becomes more difficult. The speed coefficient should therefore have an optimum value depending on the type of application and the loading cycle encountered.

GOVERNING CHARACTERISTICS [11,1]

The coefficient of non-uniformity of speed and the degree of insensitivity of governor affect the working of engine to a great extent. The values of

these parameters do not remain constant for the complete speed range encountered in various applications and increase as speed decreases. The various measures adopted for overcoming this drawback like using idle spring, main spring with variable inclination and variable stiffness etc. only partly solve the problem.

Degree of insensitivity : For a high degree of insensitivity of governor, the speed does not correspond to the instantaneous value of load. This leads to the reduction of output of engine, overconsumption of fuel and makes the control of engine more difficult.

When the degree of insensitivity is very small, the high frequency oscillations of load on the engine crankshaft may give rise to oscillations of fuel pump rack under certain conditions. The oscillations affect the working of governing system, may even lead to over regulation and increase the wear of parts of governor.

Coefficient of Non-uniformity of Speed of governor is determined by its constructional features and in particular the stiffness of spring. Very small values of this parameter may give rise to instability of working of diesel engine under fluctuating loads and greater values may induce high oscillations of speed and impermissibly high maximum idling speed. This makes the control of engine more difficult and increases wear of engine.

MICROPROCESSOR CONTROL OF DIESEL ENGINES

It is clear from what has been said above that the mechanical governors developed for a given application are not capable of providing the flexibility necessary for meeting the requirements of the wide ranges of speeds and loads encountered in mobile applications for the entire service life of engine. When using the same engine in a different application, the mechanical governing system cannot provide the optimum control of engine and deterioration of performance of engine usually results.

The microprocessor control of speed can be most sophisticated by incorporating the PID and other advanced control algorithms [15]. The coefficients of these algorithms can be changed for varying loads and speeds as well as condition of engine. The torque speed correction can be introduced in the software thus flexibly changing the coefficients of reserve of torque and speed depending on the requirements of loads encountered in a particular application. The control of optimum injection advance when added to the speed control can ensure maximum fuel economy and power output with minimum emissions and keeping the speed fluctuations to a minimum under all operating conditions.

Microprocessor control can be introduced for various types of fuel systems like accumulator, distributor and jerk pump. It is easier to introduce the injection advance control on distributor and accumulator type fuel systems. The adaptive control strategy can reduce the tolerance across the vehicle population and deterioration factors during the service life of engine with less margin for emission control. The modelling of control algorithms and implementation of microprocessor programs can significantly reduce engineering development time to approach an optimum design. The turn around time for electronic systems development is measured in hours and minutes rather than days required for the reworking of mechanical components.

The electronically controlled fuel system becomes a highly standardized product compared to the endless variety of mechanical calibrations required for various

engines and applications encountered. Thus a single pump can be mass produced with a simple zero calibration and the individual engine calibrations are contained in the software.

There is also the potential to program the system to diagnose and correct malfunctions and EGR control, altitude compensation, starting control, transmission control, idle speed control, and various other information on vehicle cruise and fuel consumption can make the microprocessor control the most cost effective solution.

CONCLUSION

It is clear from the above discussion that the mechanical controls are not in a position to meet the requirements of various mobile applications in which diesel engines are used. The microprocessor control is capable of providing the flexibility necessary for the optimum control of speed and keep the fluctuation of speed to a minimum thus ensure all round best performance of diesel engines used in mobile applications.

Nomenclature

- A - coefficient of disturbing force of governor;
- b_k - stiffness of dashpot spring;
- E - restoring force of governor;
- g_c - cyclic fuel delivery;
- G_c - rate of flow of air through the compressor;
- G_e - rate of flow of air through the engine;
- G_f - rate of consumption of fuel;
- G_T - rate of flow of gases through the turbine;
- h_c - compressor blade angle setting;
- h_T - turbine blade angle setting;
- H_l - lower calorific value of fuel;
- i - number of cylinders in the engine;
- J - mass moment of inertia of the moving parts of engine
- J_T - mass moment of inertia of rotating parts of turbo-compressor;
- n_c - index of polytropic compression in compressor;
- n_e - index of polytropic expansion in turbine;
- N_L - load setting;
- P_c - pressure of air after compressor;
- P_T - pressure of gases before turbine;
- t - arithmetic mean period of micro-fluctuation of load;
- T - arithmetic mean period of macro-fluctuations of load;
- U_g - ratio of speeds of governor and engine;
- U_A - ratio of dashpot lever;
- V_e - volume of exhaust manifold;
- V_i - volume of inlet manifold;

y_k - displacement of dashpot;

Z - displacement of governor sleeve;

α - coefficient of excess air;

α_e - non-dimensional parameter of change of load setting;

α_g - non-dimensional parameter of change of position of speed setting lever;

M' - arithmetic mean value of the amplitude of micro-fluctuations of load;

M'' - arithmetic mean value of the amplitude of macro-fluctuations of load;

ΔT - time interval;

η_e - brake thermal efficiency of engine;

η_v - volumetric efficiency of engine;

ν - coefficient of viscous drag;

ρ_c - density of air in the inlet manifold;

τ - number of strokes per cycle of engine;

ω - angular speed of rotation of engine crankshaft;

ω_c - angular speed of rotation of turbocompressor;

μ - reduced mass of the moving parts of the governor;

REFERENCES

1. Khatchian A.S., and others, Internal Combustion Engines, Vysshaya Shkola, Moscow, (1978).
2. Krutov V.I., Automatic Control of I.C. Engines, Mashgiz, Moscow, (1958).
3. Bujak, J.Z., The variable speed hydraulic governor, Proc. of Instn. of Mech. Engrs., (1945), V.153, pp.153.
4. Welbourn, D.B. and others, Governing of C.I. Engines, Proc. of the Instn. of Mech. Engrs., (1959), V. 173, 1.
5. Oldenburger, R., Hydraulic Speed Governor with major governor problems solved, Journal of Basic Engg., Trans. Am. Soc. of Mech. Engrs., (1965), V. 87, pp. 575.
6. Webb, C.R. and Janota, M.S., Governors with load sensing, Proc. Instn. of Mech. Engrs., (1969-70), 184 (Pt. 1), 161.
7. Blair, J.R., Governing : An examination of a Torque Feed Forward Loop, Proc. Instn. of Mech. Engrs., V.186, pap.n.47, (1972), pp. 603.
8. Bowns D.E., The Dynamic Transfer Characteristics of Reciprocating Engines, Proc. Instn. of Mech. Engrs., (1970-71), 185.
9. Krutov V.I., Collection of problems in the Automatic Control of I.C. Engines, Mashinostroeniye, Moscow, (1972).
10. Krutov, V.I., Sporysh, I.P., and Unoshev, V.D. Fundamentals of the Theory of Controls, Mashinostroeniye, Moscow (1969).
11. Krutov, V.I., Governing of I.C. Engines, Mashinostroeniye, Moscow (1979).
12. Krutov, V.I. and others, Frequency Method of Evaluation of Dynamic Characteristics of Governing Systems of Diesel Engines, 'Izv. Vuzov', Mashinostroeniye (1978), No. 7, 76-79.

13. Krutov, V.I. and others, Local Degree of non-uniformity of Governing Characteristics of Diesel Engines, 'Avtomobilnaya Promyshlennost', (1976), No.2, 12-13.

14. Krinetski, I.I., Governing of I.C. Engines, Mashinostroeniye, Moscow (1965).

15. Deshpande, P.B., Ash, R.H., Elements of Computer Process Control, Instrument Society of America, (1981).

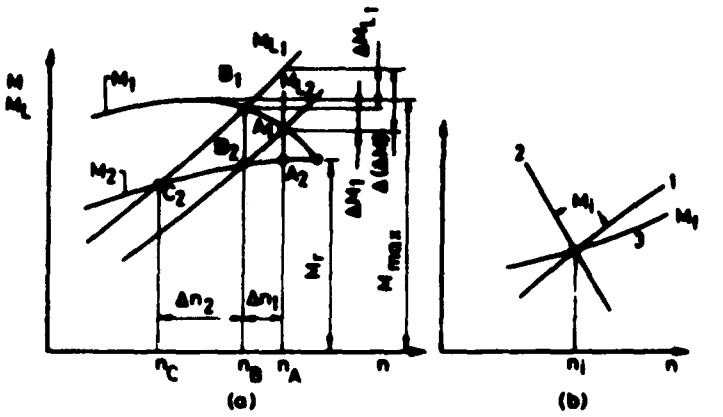

FIG.1 — STABILITY OF WORKING OF AN I.C.ENGINE
(a) AT RATED SPEED (b) AT IDLING SPEED [1]

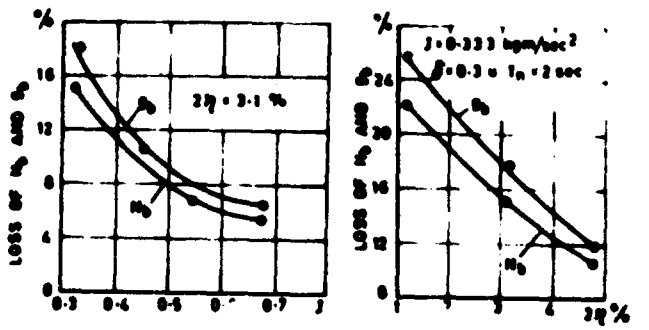

FIG.2 — VARIATION OF LOSS OF POWER AND FUEL CONSUMPTION IN PERCENT WITH MOMENT OF INERTIA OF THE ENGINE AND THE ZONE OF INSENSIVITY OF GOVERNOR FOR TRANSIENT LOADING [16]

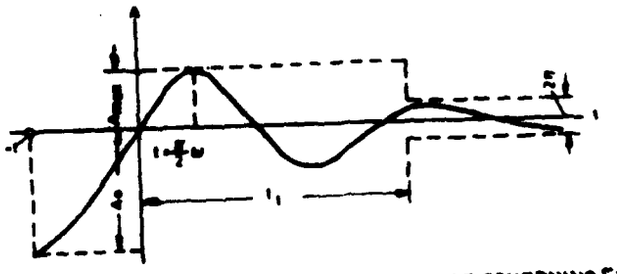

FIG. 3 - PARAMETERS OF THE QUALITY OF GOVERNING [14]
t_1 - Transient period, A_{max} - Maximum overshoot
A_0 - Initial deviation, $2n$ - Zone of insensitivity

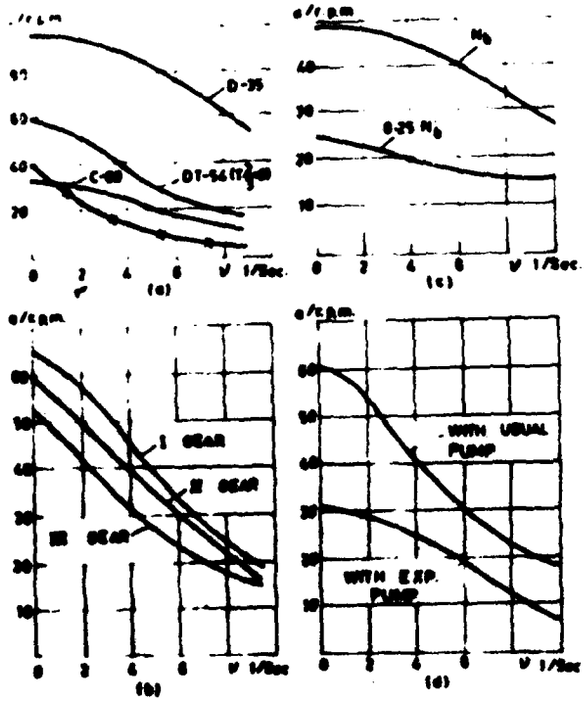

(a) FOR VARIOUS TRACTORS (b) FOR VARIOUS GEAR RATIOS (DT-54) (c) FOR VARIOUS LOADS (TD-35)
(d) WITH VARIOUS FUEL PUMPS (DT-54)

FIG. 4 - FREQUENCY RESPONSE OF TRACTOR ENGINES [14]

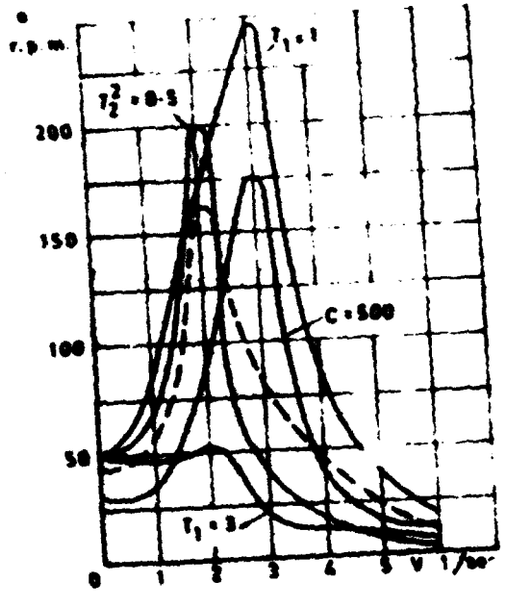

FIG.5(a)-FREQUENCY RESPONSE OF DIRECT ACTING MECHANICAL GOVERNORS [14]

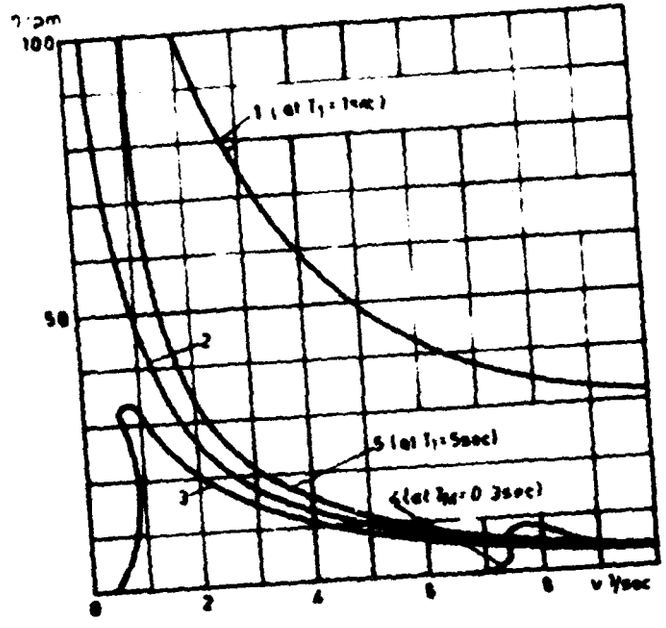

FIG 5(b) FREQUENCY RESPONSE OF INDIRECT ACTING MECHANICAL GOVERNORS [14]

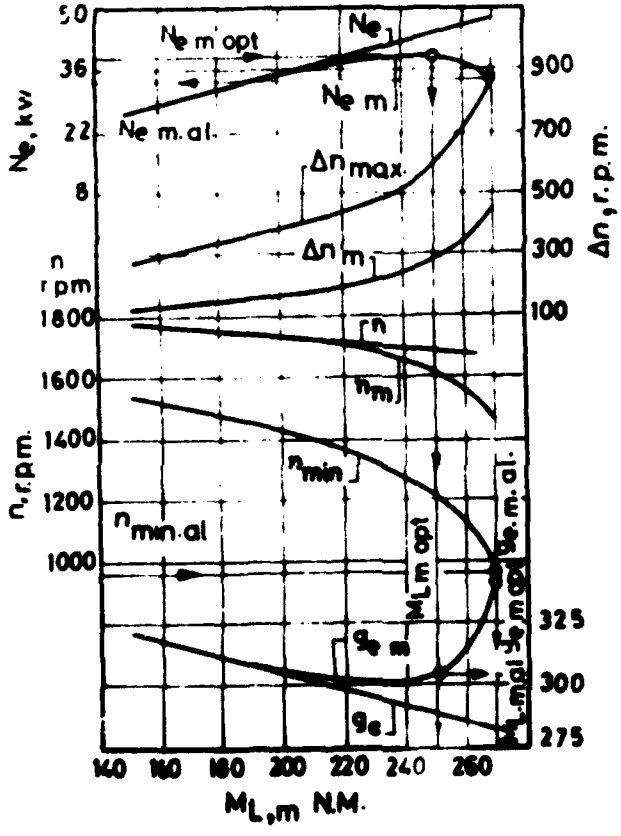

FIG. 6 – VARIATION OF THE PARAMETERS OF DIESEL ENGINE SMD-4 WITH LOAD ON A BULLDOZER[1]

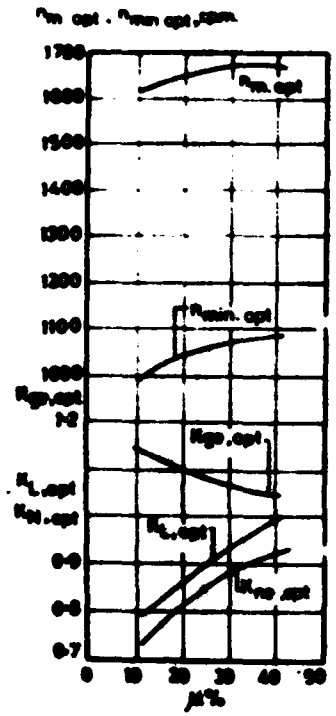

FIG. 7 – VARIATION OF THE PARAMETERS OF THE DIESEL ENGINE A-41 WITH THE COEFFICIENT OF RESERVE OF TURNING MOMENT IN BULLDOZER OPERATION [1]

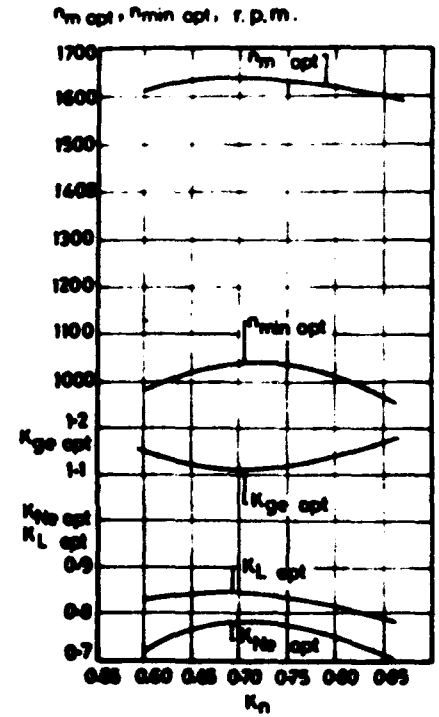

FIG. 8 – VARIATION OF THE PARAMETERS OF THE DIESEL ENGINE A-41 WITH SPEED COEFFICIENT IN BULLDOZER OPERATION [1]

ELECTRONIC-COMMUTATOR AC/DC MOTOR-DRIVEN TRACKED ALL-TERRAIN VEHICLES WITH EXTREMELY HIGH MOBILITY

B.T. FIJAŁKOWSKI

M.G. Bekkero dedicatum

THE THADDEUS KOSCIUSZKO* MEMORIAL CRACOW POLYTECHNIC, CRACOW, POLAND

INTRODUCTION

'Tracked all-terrain vehicles' is a general term which includes all types and sizes of soft wet land- and snow-traversing vehicles. All such equipment must meet the highest standards of safety, comfort, reliability, flexibility, durability and mobility and work under the most arduous operating conditions. Because of their unique all-terrain capabilities, the tracked all-terrain vehicles are also used for nonmilitary purposes, particularly in those cases where extremely high mobility over difficult terrain is required. For example, these vehicles can be used in conjunction with electrical power transmission- and natural gas or oil pipe-line erection and the servicing and maintenance of existing transmission- and pipe-lines.

The key to the exceptional all-terrain capabilities of the tracked all-terrain vehicles are their low specific ground pressures. These are as little as 100 hPa when fully loaded, which are less than half the specific ground pressure of an adult and about twice the value of person moving over snow on skis. This means that fully loaded tracked all-terrain vehicles can negotiate soft wet land ie swamps, which will be impossible for any wheeled off-road vehicle and extremely difficult for anybody on foot. Their outstanding oversnow capabilities make them equally mobile over land covered by deep snow. Besides, the tracked all-terrain vehicles in their standard versions, with normal tracks are fully amphibious without any special preparations having to be taken.

At present, greater and greater demands are being placed on manufacturers not only for safety, comfort, reliability, flexibility, durability and mobility but also for energy saving, particularly liquid fuel economy of all vehicles.

Today's complicated energy situation will make it necessary to give greater priority in the use of electrical energy in modern newly designed energy-saving propulsion systems for tracked all-terrain vehicles with extremely high mobility. In most cases these propulsion systems permit the feeding back electrical energy to the energy store in conjunction with braking of the vehicle.

In different parts of the world today there is a lot of activity going on with construction of such energy-saving propulsion systems for tracked all-terrain vehicles with extremely high mobility. Among many proposed ideas, those of hybrid-electric propulsion systems are dominant. Hybrid-electric propulsion systems are hybrids in which at least one of the energy stores, sources or convertors can deliver electrical energy[1].

---

* *Thaddeus Kobciuszko, 1746-1817. Polish patriot and general. Having studied engineering and military tactics in France, he joined American revolutionary forces; supervised bldg of W Point fortifications.*

Modern newly designed energy-saving hybrid-electric propulsion systems work on tracked all-terrain vehicles are being done with only two energy sources and therefore are considered only internal-combustion (IC) engine/ traction-duty (TD) storage battery - hybrid-electric propulsion systems in which there are liquid fuel for the IC engine, and a secondary TD storage batteries for the traction electric motors or motorized wheels driving the vehicle tracks.
In the 'series' hybrids they use an IC engine-driven brushless and commutatorless alternating-current (AC) generator ie alternator or brushless electronic-commutator direct-current (DC) generator which recharges TD storage batteries and supplies traction brushless electronic-commutator AC/DC motors or motorized wheels.
In the 'parallel' hybrids they use an IC engine-driven/supercharging brushless electronic-commutator DC dynamotor which acting as a DC generator recharges TD storage batteries and acting as a DC motor supplied by TD storage batteries supercharges IC engine. It is a simple method of obtaining a very considerable increase in power and liquid fuel economy.
The productivity of these tracked all-terrain vehicles is determined by the amount of electrical energy available in the storage batteries and propulsion system efficiency.
Electronic-commutator AC or DC motors and motorized wheels can be widely used in modern newly designed energy-saving hybrid-electric propulsion systems for tracked all-terrain vehicles. With torque and speed control it is possible to vary the power input to AC or DC motors and motorized wheels using modern power electronics. The rapid development of power electronics and contemporary monocrystal and amorphous semiconductor electrical valves during the last two decades allows one to select either an AC propulsion system (eg, AC generator ie alternator and three- or five-phase electronic--commutator AC motors) or a DC propulsion system (eg, electronic-commutator DC generator and electronic-commutator DC motors), in these cases where speed control with low losses is desired.

STATE-OF-THE-ART, 1980

As an historical side-light, it can be mentioned that tracked all-terrain vehicles were used for nonmilitary purposes in the begining of 20th century. An early 1900s 'Rolls-Royce' half track vehicle (snowmobile), in which Vladimir Ilich Ulyanov - Lenin was driven (Fig. 1) is at the Lenin Museum in Gorki (30 km from Moscow), USSR.
A 1970s small half track snow-traversing vehicle manufactured in the USSR is shown in Figure 2.
In 1970s, the traditional method, particularly before the oil crisis, was to control the speed of the propulsion system for tracked all-terrain vehicles with conventional transmission toothed gears, usually providing for selection of only three or four specific rotational speeds of the IC engine's crankshaft for a given ground speed; with hydraulic or magnetic couplings, etc.
The present inability to harness the IC engine's peak power at all ground speeds should soon be remedied with the introduction of continuously variable transmission (CVT), which in combination with some single gearing makes it possible to choose a continuous range of IC engine's crankshaft rotational speeds associated with a given power output, which can be selected automatically by a microprocessor-based propulsion controller. In most cases these were good solutions to the torque and speed control problem in view of the low investment costs and moderate operating costs then prevailing. While conventional transmission toothed gears had high efficiencies, the CVT of that day employed a torque convertor for coupling the

Fig. 1 'Rolls-Royce' snowmobile, circa 1918

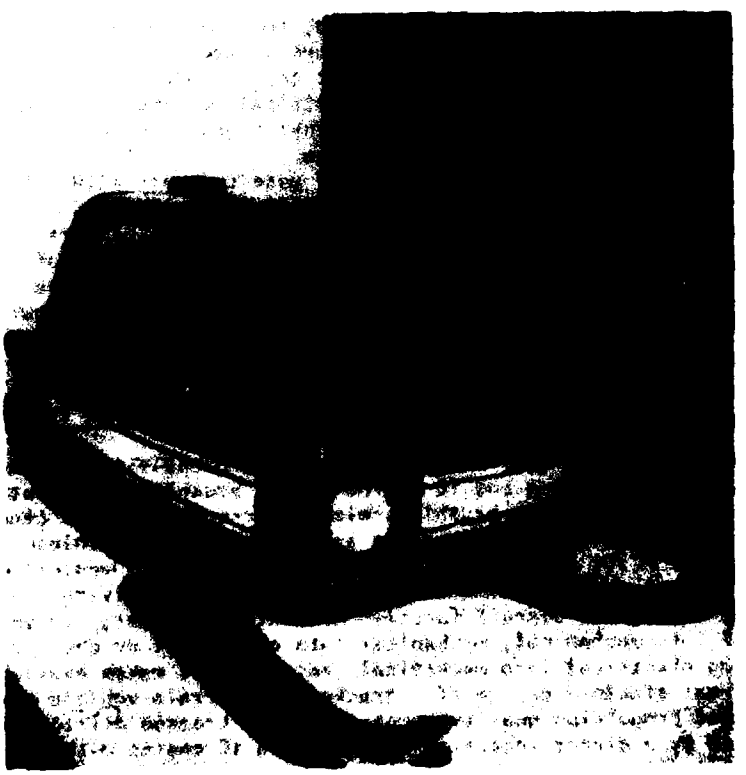

Fig. 2 Contemporary small snow-traversing vehicle

IC engine's crankshaft to the transmission gear sets, which introduced energy losses that were tolerable for the IC engine powered tracked all-terrain vehicles, but significantly increased the energy consumption of the electronic-commutator AC/DC motor-driven vehicles. Now that the costs of energy have increased a calculation of the investments made today shows that the costs representing losses constitute a considerable proportion of the total costs.

Energy-saving hybrid-electric propulsion systems using microprocessor-based propulsion controller for tracked all-terrain vehicles with extremely high mobility then become an attractive alternative.

Till now propulsion systems for tracked all-terrain vehicles operate through transmission toothed gears, which can be integral with vehicle assembly. There is no doubt that from the viewpoint of the energy-saving toothed-gearless hybrid-electric propulsion systems for tracked all-terrain vehicles themselves the use of a separate, low-frequency brushless electronic-commutator AC or DC motor on each driving axle preferably directly driving the tracked vehicle wheel without any reduction gear or motorized wheel directly driving the vehicle track is the ideal. This arrangement will produce the minimum maintenance and the most robust equipment. Unfortunately the need for variable torque and speed operation of these energy-saving toothed gearless hybrid-electric propulsion systems has in the past made this ideal difficult to realize. It has necessitated the use of variable low-frequency IC engine-driven rotating generating plant. In itself has this plant proved to be either expensive or difficult to maintain. It is not surprising, therefore, to find that when static electronic commutators for electrical machines became available in the 1960s, capable of fulfilling this need, that they should be tried. These early static electronic commutators for electrical machines used monocrystal semiconductor controlled valves called thyristors in bridge connected circuit using forced commutation technique.

The rapid development in the performances of gate turn-off (GTO) thyristors called trigistors during early 1970s significantly changed this picture as it was clear that electronic commutators using trigistors in a matrix connected circuit could be considered, the turn-off time of trigistors being at least an order better than thyristors. Turn-off time of trigistors $t_{off} \leq 1$ μs. In the nearest future the electronic commutators using S. Ovshinsky's amorphous semiconductor controlled valves called ovonics in a matrix connected circuit will be considered and used.

ENERGY-SAVING TOOTHED-GEARLESS HYBRID-ELECTRIC PROPULSION SYSTEMS

The energy-saving toothed-gearless hybrid-electric propulsion system represents an interface between the IC engine-driven brushless commutatorless AC generator ie alternator or brushless electronic-commutator DC generator and/or the on-board TD storage batteries and the traction brushless electronic-commutator AC/DC motors directly driving the tracked vehicle wheels without any reduction gears or motorized wheels directly driving the vehicle tracks, having the overall function of controlled energy conversion from chemical into mechanical, mechanical into electrical or chemical into electrical and electrical into mechanical. Recently, it makes available solution for satisfactory design of a tracked all-terrain vehicle having performance and propulsion quality comparable with tracked all-terrain vehicles powered by a direct injection turbocharged IC engine with the CVT. Because of their simple and robust design traction brushless electronic-commutator AC or DC motors and motorized wheels, would be preferable to the traction rotating-mechanoelectrical-commutator AC or DC motors and motorized wheels for any torque and speed control applications, particu-

larly in modern newly designed energy-saving toothed-gearless hybrid-electric propulsion systems for tracked all-terrain vehicles with extremely high mobility. The torque and speed control of traction brushless electronic-commutator AC or DC motors and motorized wheels using direct AC-AC (cycloconverter-type) and indirect AC-AC (DC link-type) or direct DC-AC (inverter-type) electronic commutators gives large benefits for these propulsion systems.
In recent years a very rapid development of direct and indirect electronic commutators has taken place. It is now technically possible to use such electronic commutators for torque and speed control of traction brushless electronic-commutator AC or DC motors and motorized wheels in new energy--saving toothed-gearless hybrid-electric propulsion systems. The use of direct and indirect electronic commutators has already been automatically accepted in these propulsion systems and as the costs of contemporary electrical valves fall their use will be extended.

IC engines. Today's most efficient IC engine for electronic-commutator AC/DC motor-driven tracked all-terrain vehicles is the diesel (D) engine (it is difficult to find a more efficient energy source). One of the inherent advantages of this IC engine and of some other IC engines in which liquid fuel is injected directly into the cylinder is that the efficiency falls more slowly then the efficiency of otto engines, in which the fuel and air are mixed before being drawn into the cylinder. Another advantage is that, unlike otto engines, they do not have to be fed extra fuel when they are started cold. In calculating the fuel economy of modern newly designed energy-saving toothed-gearless hybrid-electric propulsion systems for tracked all-terrain vehicles it is assumed that the vehicles will be equipped with direct-injection turbocharged D engines. The rotational speed of the IC engine's crankshaft can be regulated by an electro-hydraulically (or, as an alternative electro-pneumatically) controlled engine speed controller. The control shaft of the latter is coupled to the engine fuel pump by means of an adjustable linkage system and the angular position of the control shaft determines the rotational speed of the IC engine's crankshaft. Special attention has been devoted to coping with IC engine exhaust fumes in order to reduce the impurities in the ambient air as far as possible. The IC engine exhaust fumes are thus filtered in a catalytic cleaner and then in a scrubber. From the latter, the exhaust gases are carried through a pipe down under the vehicle. The IC engines are in themselves very silent and in combination with the systems used for cleaning exhaust gases, the total noise is strikingly low.
The IC engines drive the following units:

- the brushless commutatorless AC generator ie alternator or brushless electronic-commutator DC generator which supplies current to the brushless electronic-commutator AC/DC motors or motorized wheels and charges on-board TD storage batteries;
- the auxiliary storage battery charging DC generator with an integral electronic commutator;
- the cooling-air fan blower or cooling oil pump for cooling of the traction electric motors or motorized wheels;
- the hydraulic pump for the hydraulic-motor-driven radiator fan;
- the pump for the cooling-water system for the IC engine.

IC engine-driven AC/DC generators. When a special source of alternating or direct current must be provided for such applications as energy-saving toothed-gearless hybrid-electric propulsion system operations or in general explosive or extremely wet ambient conditions prevail, it is desirable or even essential that a brushless type of AC or DC generator be em-

ployed. This eliminates all sliding contacts and avoids the destructive effects that result from electrical arcing.
The unique feature of brushless commutatorless AC generator ie alternator or brushless electronic-commutator DC generator is its use of an auxiliary exciter electronic commutator which, mounted on the shaft of rotating machine, connects the AC output of a rotating electronic-commutator DC exciter-generator to the rotating field of the energy convertor.
The entire excitation circuit, ie, an auxiliary exciter electronic commutator, and DC field, therefore, relates as a unit and eliminates the need for slip rings and brushes.
The primary source of mechanical power for the brushless commutatorless AC generator or brushless electronic-commutator DC generator in energy-saving toothed-gearless hybrid-electric propulsion systems for tracked all-terrain vehicles is generally an IC engine which drives the field - electronic commutator - exciter assembly, while the stationary DC field of the electronic-commutator DC exciter-generator, energized from the output terminals of the AC or DC generator, builds up through a bridge-connected rectifier or DC chopper.
A bridge-connected controlled rectifier or DC chopper in the latter circuit is used to adjust the voltage output of the DC exciter-generator which in turn, regulates the DC excitation and the AC or DC output voltage of the AC or DC generator.
IC engine-driven brushless commutatorless AC generators ie alternators or brushless electronic-commutator DC generators for energy-saving toothed--gearless hybrid-electric propulsion systems have a polyphase (three- or five-phase) armature winding and one or more pairs of magnet poles, generating a magnetoelectric (permanent rare-earth magnet poles) or an electromagnetic (electromagnet poles) field. The latter have a self- and a separately-excited field winding. The armature and field windings are designed with class F insulation. The AC and DC generators are self-ventilated and designed with two bearings, feet and two shaft-ends. Through the one shaft-end, the AC or DC generator is directly coupled to the flywheel of the IC engine by means of a disc couplings. On the other shaft-end is fitted the wheel for the centrifugal fan blower or oil pump which supplies cooling air or oil to the traction brushless electronic-commutator AC/DC motors or motorized wheels. The rated current of the AC and DC generators can be overloaded by 100 per cent over a short period.
The sinusoidal induced armature voltages generated by the IC engine-driven AC or DC generator are of equal magnitute and phase-displaced by $2\pi/m$ (m - armature winding phase number) owing to the fact that the armature winding phases have an equal number of turns and are equally spaced.
An IC engine-driven brushless commutatorless AC generator ie alternator or brushless electronic-commutator DC generator can supply the brushless electronic-commutator AC/DC motors or motorized wheels.
IC engine-driven DC generators have undergone considerable change in recent years. In the past DC generators with a rotating mechanoelectrical commutator have been universal. These have a polyphase armature winding which rotates between fixed field electromagnetic poles, also a rotating mechanoelectrical commutator which rectifies armature induced voltages generated in the polyphase armature winding to an armature induced DC voltage and lets it be picked up by a pair of carbon brushes. It has become difficult for DC generators with a rotating mechanoelectrical commutator to meet the modern newly designed energy-saving toothed-gearless hybrid-electric propulsion system's heavy demand for rating power without being made larger and heavier, and the trend is to use brushless type DC generators with a static electronic commutator, which size for size, can generate more power.

The armature induced AC voltages generated by the machine's armature winding can be converted into armature induced DC voltage in order to charge the TD storage batteries and to supply the brushless electronic-commutator AC/DC motors or motorized wheels, and this can now be done by a static electronic commutator using only diode type electrical valves. An advantage of the brushless type DC generators with a static electronic commutator is that, having field magnetoelectric (permanent rare-earth magnet) poles rotating between a fixed three- or five-phase armature winding, it can be made a brushless design without an exciter and in that case it is equally easy to service as a contemporary squirrel-cage subsynchronous (induction) AC motor.

On-board traction-duty storage batteries. Electronic-commutator AC/DC motor-driven tracked all-terrain vehicles with extremely high mobility can be fitted with a choice of traction-duty (TD) storage batteries of various capacities. The capacity can be adapted to the requirements of acceleration, gradient ability, ground speed and operational intensity. TD lead-acid storage batteries are normally used in the tracked all-terrain vehicles and the battery compartment is adapted to this. Generally, they are placed in the vehicle body under the floor. Apart from supplying operating current to traction electronic-commutator AC/DC motors or motorized wheels and control equipment, the storage batteries also feed current to all auxiliary equipment such as the hydraulic pump or air compressor for the braking systems, retarders, etc.
Severe demands are imposed on TD storage batteries, since they operate under arduous conditions from both the electrical and mechanical points of view. Apart from being mechanically strong so as to be able to withstand shocks and vibrations, such batteries must also have a long life, for example, withstand a large number of discharges. They must also have a low internal resistance so that a high voltage is maintained during discharges. The TD lead-acid storage batteries used in tracked all-terrain vehicles satisfy these requirements and, furthermore have a high capacity per volume unit. Experience has also shown that these batteries are insensitive to the pulsating current resulting from the use of the traction electronic-commutator AC/DC motors or motorized wheels.
However, electronic-commutator AC/DC motor-driven tracked all-terrain vehicles with extremely high mobility require simple on-board TD storage batteries having a capacity that is at least ten times that of present lead-acid storage batteries. The appearance of new lithium-sulphur and sodium-sulphur-type storage batteries in the next few years may profoundly affect tracked all-terrain vehicle design. Technically, the energy density of these new storage batteries is five to ten times greater than the conventional lead-acid batteries. Practically, what this means is that the modern newly designed energy-saving toothed-gearless hybrid-electric propulsion systems for tracked all-terrain vehicles will have acceleration and speed capability of present conventional compact.

Static electronic commutators. The idea to design fully static electronic commutator for conversion of AC or DC voltage to a variable frequency AC voltage in order to be able to control the voltage and frequency of an AC or a DC generator and the torque and speed of an AC or a DC motor is by no means new. If one studies old literature on the static converters, one can observe that such electronic commutators were described as early as the begining of the 1920s[2-4]. However, such electronic commutators did not gain wide acceptance and most of the ideas did not leave the laboratory.
The fact that this was so may be attributed to the characteristics of the electrical valves available to the scientists in these days.

It was not until the 1960s that scientists were given the possibility to solve this problem by introduction of the semiconductor controlled rectifier (SCR) called thyristor. At the same time, it has been possible to introduce the rapid integration of electronic components in the controllers included in static electronic commutators.
In this way, the static electronic commutator has evolved from a power amplifier to advanced process equipment incorporating microprocessors for fully automatic control, monitoring and protection.
In the 1980s, as static electronic commutators for electrical machines are developed and put into practical use, the demands for fast-switching thyristors with high performances, such a higher blocking voltage, shorter turn-off time, and larger current capability, are increasing in order to make more efficient, more compact, and more economical. However, as it is well known, it is very difficult to design fast-switching thyristors with high blocking voltage and high-current capability as well as short turn--off time.
Recently attention has been focused on the reverse-conducting (RC) gate turn-off (GTO) thyristor, called the RC trigistor and the symmetrical (S) gate turn-off (GTO) thyristor, called the GTO symistor or S trigistor as fast-switching semiconductor controlled valves which have the feasibility of overcoming this difficulty. The electrical valves proved to be successfulfor practical electronic commutator applications, and important application data were obtained. These S and RC trigistors have been used in energy-saving toothed-gearless propulsion systems with regenerative braking for electronic-commutator AC/DC motor-driven tracked all-terrain vehicles and have the advantage of making them more compact, less expensive, and of lighter mass than conventional reverse-blocking thyristors with freewheeling diodes.
Static electronic commutators can be divided into two main groups: direct and indirect commutators. The direct electronic commutator is input line--commutated cycloconverter and technically is closely related to the reversible electronic commutator for DC electrical machines. A cycloconverter was originally developed as a frequency changer for rail-traction supplies at $16\frac{2}{3}$ cps in the 1920s and 1930s[4]. Its greatest shortcoming is the moderate frequency range (0 to about $\frac{1}{3}$ of the input-line frequency). This make it of interest especially for three- or five- phase electronic-commutator AC electrical machines which may be used for energy-saving toothed-gearless hybrid-electric propulsion systems. The cycloconverter is the most flexible of the electronic commutators. It transfers active and reactive power in both directions, allowing a driven machine to operate at any power factor, motoring and generating. It is particularly useful for reversible propulsion systems in arduous situations, eg, for tracked all-terrain vehicles where the robustness of the traction electronic-commutator AC motor or motorized wheel makes it desirable alternative to the more common traction rotating mechanoelectrical-commutator DC motor or motorized wheel.
The indirect electronic commutator, where the frequency conversion takes place in two stages (via rectification) may be divided in their turn into two subgroups: electronic commutators with current source DC link (without storage batteries) and electronic commutators with voltage source DC link (with storage batteries or capacitors). Finally, electronic commutators with voltage source DC link are available in two kinds: these with variable DC link voltage and these with constant DC link voltage. A characteristic feature of an electronic commutator with voltage source DC link is that the output impedance from DC link filter is low, because it includes storage batteries or capacitors. Storage batteries are acting as capacitors. An electronic commutator with current source DC link, as a rule only have an inductor as filter.

During the 1970s a research group at the Thaddeus Kościuszko Memorial Cracow Polytechnic (Politechnika Krakowska im. Tadeusza Kościuszki) - Institute of Automotive Vehicles and Internal Combustion Engines (the leader of the research group, Dr B.T. Fijałkowski) has developed static electronic commutators of a cycloconverter-type and all three variants of the DC link-type for low-frequency traction three- or five-phase syn- and asynchronous brushless electronic-commutator AC motors and motorized wheels. Besides, this research group has developed an electronic commutator for DC dynamotors (DC generator/motor). All these electronic commutators can be used in energy-saving toothed-gearless hybrid-electric propulsion systems for tracked all-terrain vehicles with extremely high mobility.

Traction electronic-commutator AC/DC motors and motorized wheels. A mass of the traction brushless electronic-commutator AC motor or motorized wheel with a lowered rating frequency is greater than the mass of the same AC motor or motorized wheel with the rating frequency of 50 cps or 60 cps. An optimum rating frequency for the AC motor or motorized wheel with the lowered rating frequency is equal $16\frac{2}{3}$ cps to 25 cps. At further lowering of the rating frequency the mass of the AC motor or motorized wheel is quickly increased. The power and the efficiency of traction AC motors or motorized wheels depend on frequency which the motor or motorized wheel normally operated at. For example, the $16\frac{2}{3}$ cps traction AC motors or motorized wheels have a power factor of .96 to .97 at rated operating conditions, and their efficiencies are about 90 per cent, whereas motors and motorized wheels of the same type operating at 50 cps have a power factor of .86 to .89 and efficiencies of about 85-89 per cent.
The traction three- or five-phase syn- or subsynchronous (induction) electronic-commutator AC motors or motorized wheels with a lowered rating frequency are the most usual occuring. In energy-saving toothed-gearless hybrid-electric propulsion systems for tracked all-terrain vehicles with extremely high mobility these traction AC motors or motorized wheels generally run with an adjustable speed. One control method then is frequency control of traction AC motors or motorized wheels. This means that the output-line frequency of the electronic commutator (proportional to the speed) may be varied. These propulsion systems are suitable for those tracked all-terrain vehicles where the advantages of the traction AC motor or motorized wheel as high reliability, low maintenance, low mass and small size as well as the absence of rotating sliding contacts with carbon brushes and generally also a shaft transducer (tachometer) are particularly appreciated.
Because of their simple and robust design traction brushless electronic-commutator AC motors and motorized wheels, and then above all magneto-electric (permanent rare-earth magnet poles) syn- and subsynchronous (induction squirrel-cage) AC motors and motorized wheels would be preferable to the traction rotating mechanoelectrical-commutator DC motors and motorized wheels for a torque and speed control application, particularly in modern newly designed energy-saving toothed-gearless propulsion systems.
Traction synchronous electronic-commutator AC motors and motorized wheels will be frequently used in road and off-road hybrid-electric tractions requiring toothed-gearless propulsion system having a high output in combination with a high speed.
The principal reasons for the choice of this AC motor or motorized wheel type are:

- A traction synchronous electronic-commutator AC motor or motorized wheel with a power factor, eg, .96 or more generally has a considerable higher efficiency (up to 1 per cent higher) than the corresponding trac-

tion subsynchronous (induction) electronic-commutator AC motor or motorized wheel.

- A traction synchronous electronic-commutator AC motor or motorized wheel can generate reactive power unlike all traction subsynchronous AC motors and motorized wheels, which consume reactive power.

- A traction synchronous electronic-commutator AC motor or motorized wheel is very robust and well protected against mechanical damage, which could be caused by sudden load or electronic-commutator output-line variations.

- The rotor of a traction synchronous electronic-commutator AC motor or motorized wheel is considerably more rigid than that of a traction subsynchronous electronic-commutator AC motor or motorized wheel because of its design with permanent rare-earth magnet poles.

- A large air-gap and permanent rare-earth magnet poles make it easy to mount, dismantle and align the machine. Since the traction synchronous electronic-commutator AC motor or motorized wheel is also available in a brushless design, it is equally easy to service as a traction subsynchronous (squirrel-cage) electronic-commutator AC motor or motorized wheel.

- The torque versus current characteristic during acceleration is considerably better for a traction synchronous electronic-commutator AC motor or motorized wheel than for traction subsynchronous (squirrel-cage) electronic-commutator AC motor or motorized wheel. A traction synchronous electronic-commutator AC motor or motorized wheel has both a lower current and a higher torque during acceleration. In addition, the lower current implies a smaller voltage drop. This makes the acceleration performance of a traction synchronous electronic-commutator AC motor or motorized wheel still more superior to that of a traction subsynchronous electronic-commutator AC motor or motorited wheel, since the voltage influences the breakaway torque as a square.

- Owing to the permanent rare-earth magnet poles the rotor has a large thermal capacity. A traction synchronous electronic-commutator AC motor or motorized wheel therefore withstands longer transient times than a traction subsynchronous (squirrel-cage) electronic-commutator AC motor or motorized wheel.

Traction synchronous electronic-commutator AC motors and motorized wheels can generate reactive power (through overexcitation), which make them particularly suited for electronic-commutator acceleration. From the torque versus current characteristic viewpoint electronic-commutator acceleration is equivalent to traction rotating mechanoelectrical-commutator DC motor or motorized wheel acceleration, whose good characteristics are well known from existing hybrid-electric propulsion systems for tracked all-terrain vehicles.

Since its introduction in the 1890s, the subsynchronous induction squirrel-cage AC motor have been the paragon of a robust and reliable source of propelling power. Over the years, however, traction subsynchronous (squirrel-cage) electronic-commutator AC motors and motorized wheels have undergone rather considerable changes. To begin with, they were overdimensioned, both mechanically and electrically. They were naturally expensive to manufacture and purchase. Recently, traction subsynchronous (squirrel-cage) AC motors and motorized wheels are being manufactured rationally. They are subject to international standards, are carefully dimensioned and are inexpensive.

One of the most valuable characteristics of the existing rotating mechano-electrical- or modern newly designed electronic-commutator DC motor or motorized wheel is it ability to provide a wide range of easily adjustable speeds. This benefit is particularly important because a high degree of speed control is often essential to electric motor-driven tracked all-terrain vehicles. To control the speed of traction electronic-commutator DC motors and motorized wheels steplessly and over a considerable range the adjustable-voltage and frequency system offers many advantages. Generally, reffered to as electronic-commutator control after the author, the method requires two separate sources of supply, one of which is a main adjustable--voltage and frequency static electronic commutator (fed by the constant-voltage source eg, TD storage batteries) that supplies AC power to the armature three-phase winding of the DC motor and the other a small adjustable-voltage controlled rectifier or DC chopper (fed by the constant-voltage source eg, TD storage batteries) that excites the DC motor field. The speed range is much greater than that obtainable with a traction subsynchronous (squirrel-cage) electronic-commutator AC motor or motorized wheel. It is the same that obtainable with a traction synchronous electronic-commutator AC motor or motorized wheel. A brushless electronic-commutator DC dynamotor (generator/motor) is used in the energy-saving parallel hybrid--electric propulsion system for tracked all-terrain vehicles with extremely high mobility.
Modern newly designed traction brushless electronic-commutator AC or DC motors and motorized wheels can be sealed environment-free units which have the significant advantage of an oil-cooling system by which both stator and rotor are cooled. The same coolant oil can be used to provide oil mist lubrication for the motor bearings. They can be fitted with thermistors for measuring the winding and electrical-valve temperature and heaters to prevent condensation when AC/DC motors or motorized wheels are at a standstill.

EXPERIMENTAL ENERGY-SAVING PROPULSION SYSTEMS FOR TRACKED ALL-TERRAIN VEHICLES

In the field of energy-saving hybrid-electric propulsion systems for tracked all-terrain vehicles examples of study are represented by three experimental prototype propulsion systems, which are developed by a research group at the Thaddeus Kościuszko Memorial Cracow Polytechnic, Cracow, PL. The first experimental prototype energy-saving toothed-gearless series hybrid-electric propulsion system for the track vehicle (Fig. 3) is acting as a smooth, silent and oil-free torque convertor. This comprises a separately-excited three-phase synchronous brushless type AC generator ie alternator with constant output, solidly coupled to the D engine, which feeds three-phase currents to the trigistor direct electronic-commutator AC motors input lines. The trigistor direct electronic commutator is input-line-commutated cycloconverter, which uses only 9 S trigistors. Here each input line is connected to each output line via S trigistor. A three--phase - three-phase cycloconverter can transfer active and reactive power in both directions, allowing two driven traction low-frequency three-phase subsynchronous (induction squirrel-cage) AC machines to operate at any power factor, motoring and generating. The alternator constant output is determined by controlling the excitation current to the AC generator. This is done steplessly with the aid of trigistorized half-controlled rectifier. The electric torque convertor also makes it possible to distribute steplessly and without wear D engine output for driving. The ground speed is determined by controlling the pulse-width (pulse-width modulation) and

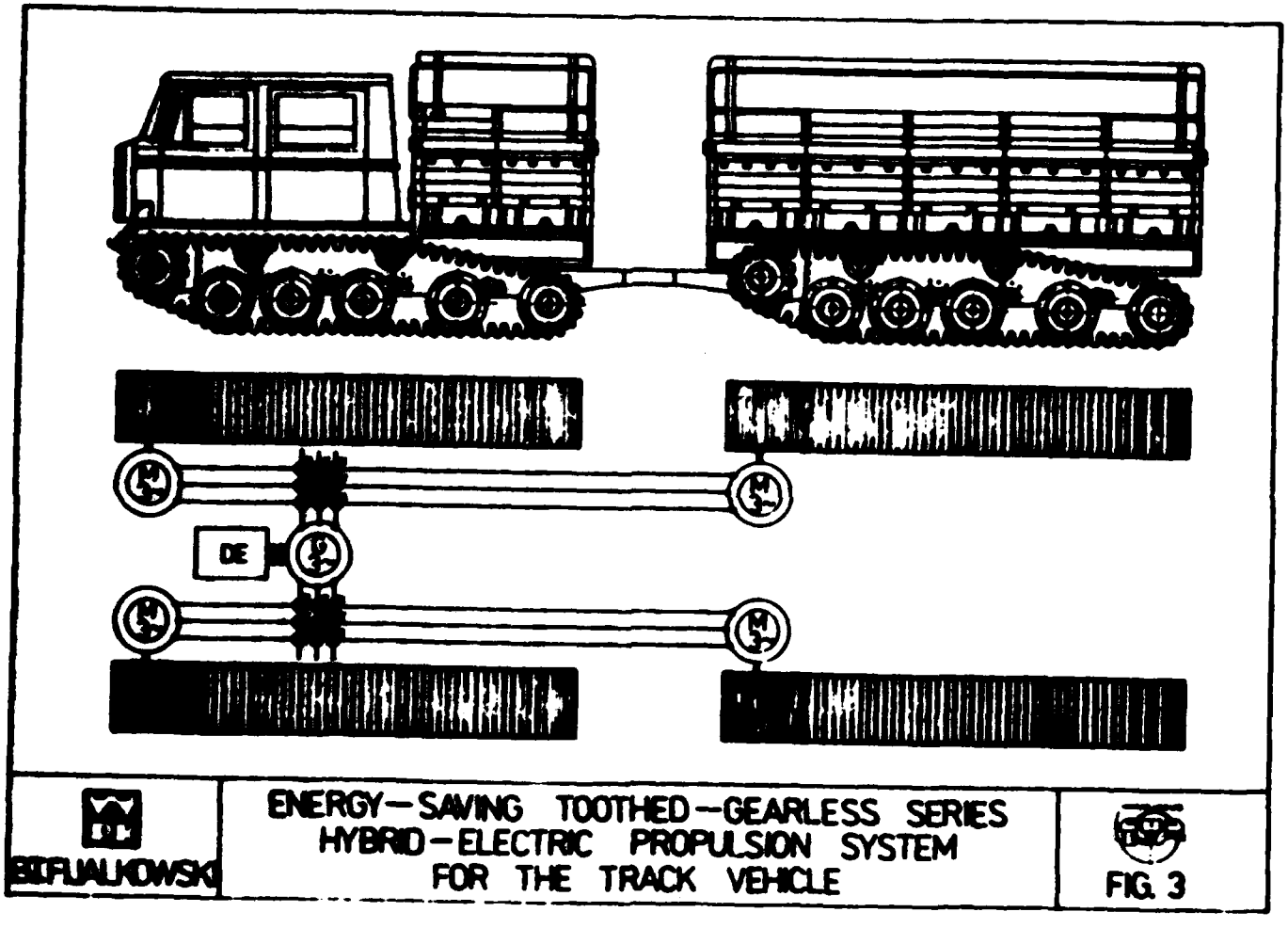

BIELAWSKI

ENERGY–SAVING TOOTHED–GEARLESS SERIES HYBRID–ELECTRIC PROPULSION SYSTEM FOR THE TRACK VEHICLE

FIG. 3

1088

phase-shift (phase-shift modulation) of triggering pulses to the trigistor direct electronic commutator. This is done steplessly with the aid of microprocessor-based propulsion controller connected to the accelerator mechanism of the track vehicle. The matching of the torque convertor relative to the acceleration or gradient ability is obtained automatically in the traction low-frequency subsynchronous electronic-commutator AC motors. The first experimental prototype propulsion system has no transmission gear and reduction gear. This energy-saving toothed-gearless series hybrid-electric propulsion system consists of traction low-frequency subsynchronous electronic commutator AC motors directly coupled to the front driving wheels. The propulsion system is operated at an electronic commutator output voltage of 400 V. At this voltage a high total efficiency can be obtained.Figure 4 shows the oscillograms of the electronic commutator output voltage to neutral waveforms for three different output frequencies.

Fig. 4 Electronic commutator output voltage to neutral for different output frequencies.

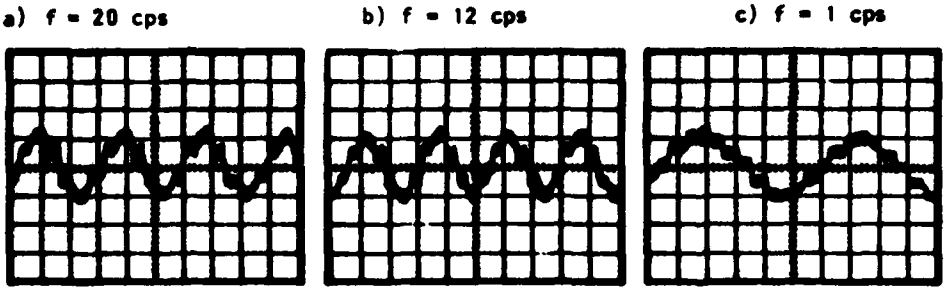

The first experimental prototype energy-saving toothed-gearless series hybrid-electric propulsion system (Fig. 3) can be used for the track vehicle, which is an articulated tracked all-terrain vehicle with extremely high mobility, where both the front and the rear cars are driven by two wide rubber tracks, ie all four tracks are driven. This track vehicle is intended as a transport unit for material and personnel, capable of carrying up to 2500 kg of equipment and 4 persons in addition to the driver. On level ground the track vehicle can run satisfactorily at about 50 km/h and it can have a range of action of 300 km. For example, this vehicle can be used in conjunction with natural gas pipeline erection and the servicing and maintenance of existing pipelines.
The second experimental prototype energy-saving toothed-gearless series hybrid-electric propulsion system for the all-terrain carrier with extremely high mobility (Fig. 5) is also acting as a silent electric torque converter. This comprises a separately-excited three-phase synchronous brushless type AC generator ie alternator with constant output, solidly coupled to the D engine, which feeds three-phase currents to the trigistor indirect electronic commutator AC motors input lines. The trigistor indirect electronic commutator is voltage source DC link-type (with TD storage batteries), where the frequency conversion takes place in two stages (via rectification). The first stage using 6 diodes is acting as an uncontrolled rectifier with constant DC link voltage. It feeds current to

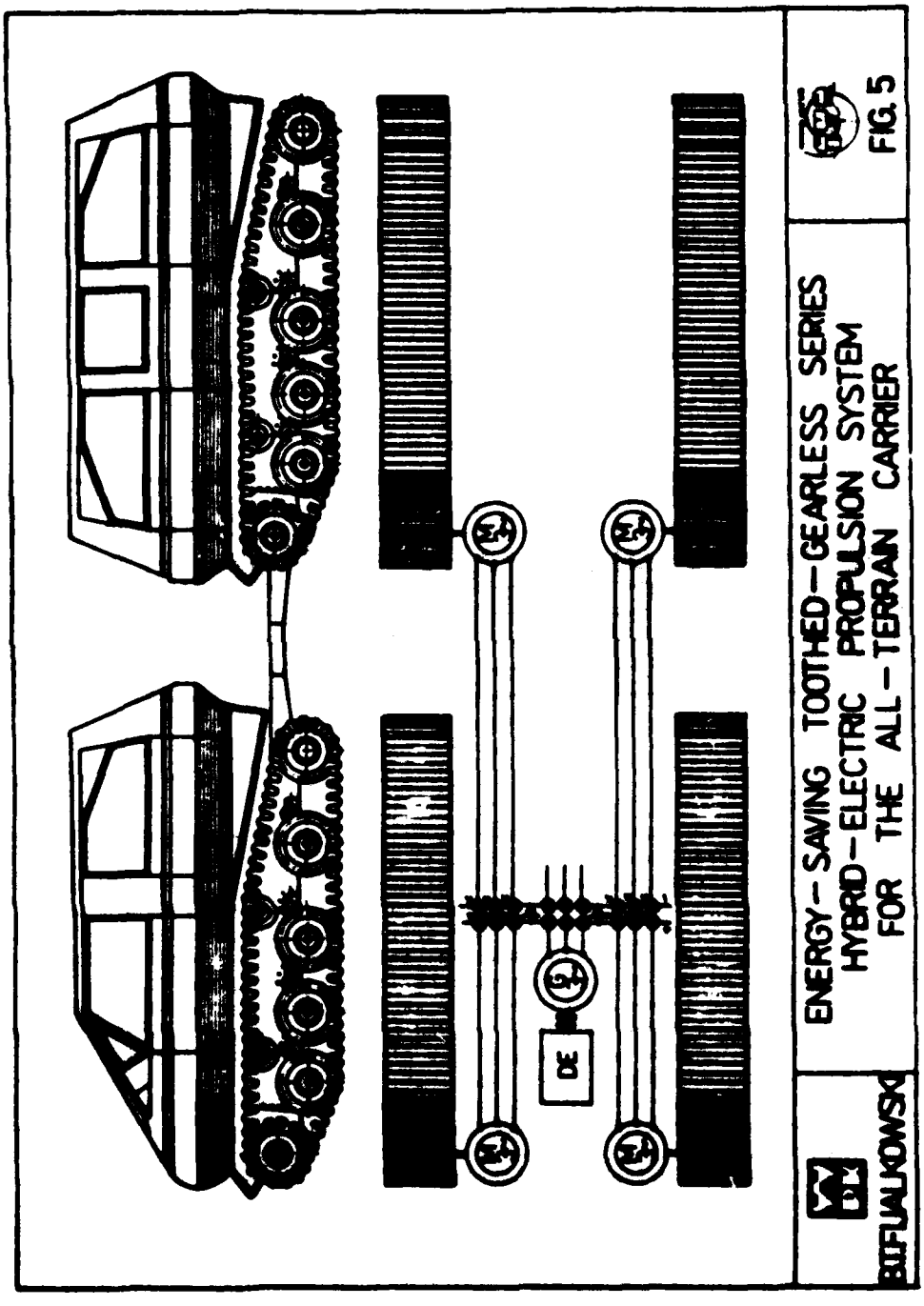
ENERGY-SAVING TOOTHED-GEARLESS SERIES
HYBRID-ELECTRIC PROPULSION SYSTEM
FOR THE ALL-TERRAIN CARRIER
FIG. 5
BUFFALKOWSKI
DE

the TD storage batteries and the second stage using only 6 RC trigistors and acting as an inverter. Here each input line of a rectifier is connected to each output line via diode and each input line of an inverter is connected to each output line via RC trigistor. Conversion from direct--voltage to alternating-voltage takes place in such a way that the three--phase output lines are switched in turn with a $2\pi/3$ phase shift to the plus or minus poles ie input lines of the direct-voltage with the aid of the RC trigistor triode parts. Since the phases of the AC motor currents are displaced in relation to the voltage, currents will flow through the RC trigistor diode parts during this interval of the cycle. To commutate the current from one DC pole ie input line to the other, a special gate turn-off commutating circuit in the microprocessor-based propulsion controller has to be arranged for each phase. When full output voltage is obtained, the RC trigistor triode parts are conducting for π and the output line-to-line voltage then consists of voltage pulses of $2\pi/3$ width, separated by dead intervals of $2\pi/6$. In practice, the maximum output voltage of the trigistor indirect electronic commutator is approximately the same as the actual alternator AC voltage. The neutral of the three-phase system is not fixed, but will oscillate with three times the output frequency. This means the voltage to neutral will have a staircase shape. The system used is to rectify (by means of diodes) the alternator induced AC voltages to produce constant voltage DC link and then invert (by means of RC trigistor triode parts) the DC to produce AC of desired frequency. For the flow of load reactive current feedback RC trigistor diode parts are provided. TD storage batteries connected to DC link are used to alloy regenerated energy to be fed back to them and to provide all-electric operation of the experimental prototype propulsion system. Because of the need to operate at zero speed and to obtain smooth acceleration or deceleration and reversal of the traction low-frequency synchronous electronic--commutator AC motors, the trigistor inverter is operatesin pulse width modulation (PWM) mode to produce sinusoidal output line current waveforms of desired frequency. Operation of the trigistor indirect electronic commutator under this mode is of particular importance to the energy--saving toothed-gearless series hybrid-electric propulsion system for the all-terrain carrier with extremely high mobility. Traction low-frequency synchronous electronic-commutator AC motors will not operate smoothly at low-speeds unless magnetomotarce waveforms within the machine is sinusoidal; this can only be produced by supplying the machine's armature winding with sinusoidal currents. Inherently an electronic commutator is only a switching device and cannot produce smooth voltage waveforms. Normally an electronic commutator is arranged to switch once or twice per cycle only producing square waveforms. This waveform is far from sinusoidal and only a suitable for high speed propulsion systems with main transmission gear and reduction gear. If the electronic commutator can be arranged to switch many times per cycle for differing periods of time a nearly sinusoidal output waveforms can be produced. This contains a large fundamental component and only very high harmonics which effect on the traction low-frequency synchronous electronic-commutator AC motor current. Oscillograms of voltage and current waveforms of the traction low-frequency synchronous electronic-commutator AC motor for three different indirect electronic commutator output frequencies are shown in Figure 6.

The second experimental prototype energy-saving toothed-gearless series hybrid-electric propulsion system (Fig. 5) can be used for all-terrain carrier with extremely high mobility, where both the front and the rear cars are also driven by the same two wide rubber tracks. All four tracks are consequently driven. This all-terrain carrier is primarily intended as

a transport unit for personnel or material, capable of carrying up to 2000 kg of equipment or 19 persons in addition to the driver. A special purpose superstructure for loads up to 2500 kg may be easily fitted in place of the cab on the rear car. On level ground the all-terrain carrier can run in a satisfactory manner at about 50 km/h and can reach a maximum speed of 60 km/h. It can have a range of action of 500 km.

Fig. 6 Electronic commutator output line-to-line voltage (top) and motor current (bottom) for different electronic commutator output frequencies.

a) f = 10 cps, U = 60 % b) f = 5 cps, U = 30 % c) f = 1 cps, U = 10 %

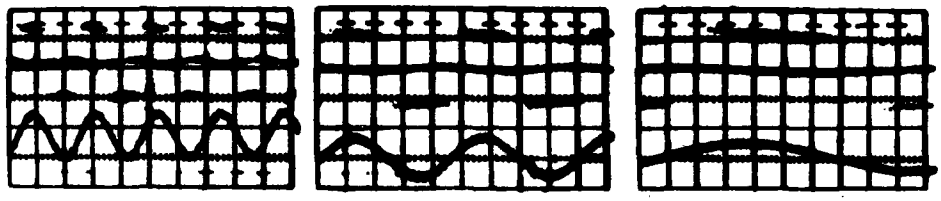

The third experimental prototype energy-saving parallel hybrid-electric propulsion system for the tracked snow-traversing vehicle (snowmobile) with extremely high mobility (Fig. 7) uses a D engine-driven/supercharging brushless type electronic-commutator DC dynamotor (generator/motor) which acting as a DC generator recharges TD storage batteries and acting as a DC motor supercharges D engine. It has a CVT which helps reduce liquid fuel consumption not only by providing an efficient transmission but by allowing D engine and DC dynamotor to be run at or near maximum efficiency independent of ground speed. The D engine and separately-excited brushless electronic-commutator DC dynamotor are mechanically coupled with the one-way clutch. The DC dynamotor's electronic commutator mainly consists of a circuit which controls the armature supply DC voltage by means of the trigistor direct DC - AC electronic commutator control and a circuit which controls the field current by means of the trigistor DC chopper control also in case of pure traction electronic-commutator DC motor driving. In the case of D engine driving with recharging, the separately-excited electronic-commutator DC dynamotor changes its function to the DC generator with an electronic commutator acting as a RC trigistor diode part uncontrolled rectifier and recharges the TD storage batteries which connection may be changed from series of 440 V to parallel of 220 V, and the charging current is indirectly controlled by the trigistor DC chopper which controls only the field current. A separately-excited brushless type electronic-commutator DC motor with an electronic commutator acting as a RC trigistor inverter, having power electronics armature and field controls would provide the best combination of efficiency, performance and production cost for this propulsion system. For maximum range stop-and-go driving the tracked snow-traversing vehicle would utilize regenerative braking to recover kinetic energy.

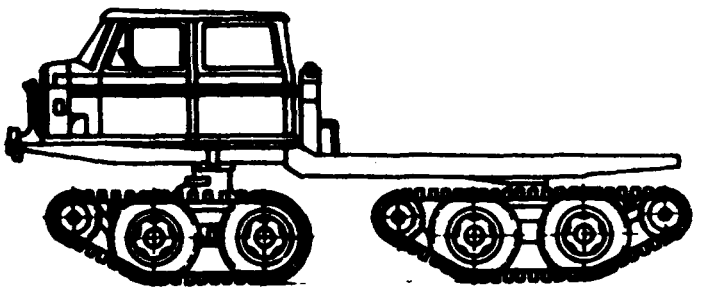

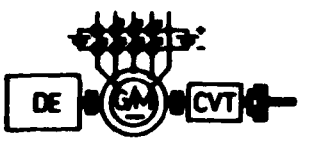

BIFUALJOWSKI	ENERGY – SAVING PARALLEL HYBRID – ELECTRIC PROPULSION SYSTEM FOR THE TRACKED SNOW – TRAVERSING VEHICLE	FIG. 7

Besides, the third experimental prototype energy-saving parallel hybrid-electric propulsion system has two same type clutches, one is acting as a damper built between D engine and one-way clutch and the other is between electronic-commutator DC dynamotor and CVT. These are of the dry single--disc and coil-spring type clutches operated electro-hydraulically.
The third experimental prototype energy-saving parallel hybrid-electric propulsion system for the tracked snow-traversing vehicle has following six propelling modes:

- D engine and DC motor driving;
- D engine driving with D engine-driven DC generator recharging;
- pure D engine driving;
- pure DC motor driving;
- regenerative braking with a driving-wheel-driven DC generator recharging;
- D engine-driven DC generator recharging during stoppage.

An energy-saving snow-traversing-vehicle hybrid-electric propulsion system built up from combination of a brushless electronic-commutator DC dynamotor and CVT offers many advantages, such as stepless ground speed control, low losses and fast control of the recharging voltage or both the torque and the speed of the D engine-driven/supercharging DC dynamotor. Power electronics for the third experimental prototype propulsion system shown in Figure 7 consists of a RC trigistor electronic commutator, acting as an adjustable frequency inverter for motoring or uncontrolled rectifier for generating of the electronic-commutator dynamotor; a RC trigistor DC chopper; an on-board TD storage battery charger and a multiple output isolated DC power supply. The propulsion system power source can be specially developed TD lead-acid storage batteries. The propulsion system signal microelectronics consists of a microprocessor-based propulsion controller and local power electronics interface circuitry.
The third experimental prototype energy-saving parallel hybrid-electric propulsion system (Fig. 7) can be used for the tracked snow-traversing vehicle (snowmobile) with extremely high mobility, where both the front and the rear wheel-axles are driven. This tracked snow-traversing vehicle can be intended as a transport unit for cutting-down trees in the forest or polar expedition.

CONCLUSION

Brushless electronic-commutator AC or DC motors and motorized wheels are well established today in energy-saving toothed-gearless hybrid-electric propulsion systems for tracked all-terrain vehicles with extremely high mobility. Growing attention is being shown in the use of trigistor electronic-commutator AC or DC motors for these propulsion systems. The trigistor electronic commutators presented here are very simple in design and have features making them technically superior to thyristor electronic commutators of conventional types. They should have a given place as the technically and economically best solutions in electrical machines in the future. These propulsion systems have good dynamic properties and are highly efficient. In addition the problem of high acceleration currents of traction electronic-commutator AC or DC motors and motorized wheels does not arise. The difference between the costs of existing traction AC or DC motors and motorized wheels and brushless electronic-commutator AC or DC motors and motorized wheels has substantially narrowed, but the latter alternative is still more expensive. However, there are examples of users who in their investment calculations have also taken into account estimated maintenance costs and then found that the brushless electronic-com-

mutator AC or DC motor propulsion system is the most favourable alternative. Another case, where the electronic commutator is clearly competitive is for double- or multi-motor propulsion systems and double- or multi-motorized-wheel propulsion systems that is when several traction AC/DC motors or motorized wheels are to be run with the same speed and can be connected to a common electronic commutator (see Figs 3 and 5).
An excellent way to control the torque and speed of a doubly fed supersynchronous and synchronous or single fed subsynchronous (induction) electronic-commutator AC/DC motor or motorized wheel is to vary the frequency of the supply armature voltage. With this method it is, of course, necessary to provide a direct or indirect electronic commutator whose output frequency and voltage can be adjusted simultaneously. Speed adjustment is virtually stepless over an extremely wide range. When several AC/DC motors or motorized wheels are connected to the common electronic commutator, all will change speed simultaneously as the frequency is varied.
It is impossible to make any general recommendations for energy-saving toothed-gearless series or parallel hybrid-electric propulsion systems for the tracked all-terrain vehicles with extremely high mobility, but each individual application must undergone a technical and economic evaluation. A number of factors should then be taken into account, of which the most important are nature of the energy source, the torque and speed requirements, utilisation of an existing AC or DC motor or purchase of a modern newly designed electronic-commutator machine, the environment, etc.
Special demands will be made on traction electronic-commutator AC or DC motors and also motorized wheels, including a high accelerating torque and robust mechanical and electrical design. Further, for tracked all-terrain vehicles with extremely high mobility they must stand up to frequent accelerations, the severe traction environment and the most widely varying weather conditions.
Energy-saving toothedgearless series and parallel hybrid-electric propulsion systems for tracked all-terrain vehicles with extremely high mobility have been growing attention throughout the world as part of the measure for preserving the environment and energy saving, which is now a worldwide problem. Methods for lowering energy consumption in electronic-commutator AC/DC motor-driven tracked all-terrain vehicles with extremely high mobility give two important benefits: reduced dependence on liquid fuel and higher profitability.

REFERENCES

1. 'International Electrotechnical Commission', 'Technical Committee 69' - 'Working Group No. 5' (Hybrid Electric Road Vehicles), September 17-18, 1981, London, England.
2. MARTI, O.K. und WINOGRAD, H.: Stromrichter. R. Oldenbourg, Muenchen und Berlin 1933 (Hier eine Zusammenstellung der Stromrichterarbeiten von 1922 bis 1932).
3. GLASER, A. und MUELLER-LUEBECK, K.: Einfuehrung in die Theorie der Stromrichter. Bd. 1, J. Springer, Berlin 1935.
4. RISSIK, H.: Mercury Arc Current Convertors. Pitman, 1935.

ROTARY HYDRAULIC SUSPENSION DAMPER FOR HIGH MOBILITY OFF-ROAD VEHICLES

T.J. HOLMAN B. Sc.

Senior Project Engineer, Horstman Defence Systems Ltd.

ABSTRACT

In order to achieve high mobility over off-road terrain, a vehicle suspension system should combine adequate wheel travel with a high level of damping force. The device described is a suspension damper which utilises the rotational movement inherent in most vehicle suspension systems to generate large damping forces proportional to vertical wheel velocity. By use of modern hydraulic technology a compact design with high level of thermal dissipation and immunity from foreign object damage has been achieved.

The device was developed, in the first instance for use with a torsion bar suspension system on a military tracked armoured personnel carrier. In this application, high levels of performance and reliability have been demonstrated. However, the technology is readily applied to other types of suspension typically used on wheeled or tracked vehicles and examples of such applications are described.

INTRODUCTION

When considering the performance and economy of a vehicle on good roads the performance of the suspension system is not normally of prime importance. However, in the off-road environment, the performance of the suspension is an essential factor. Examples of vehicles having good power/weight ratios (and hence good "on road" performance) but very poor off-road performance are manifold. Such vehicles are commonly unable to utilise their available power due to the level of discomfort induced by traversing even modest terrains. Fuel economy under these circumstances is obviously unsatisfactory as the drivers reaction will be to decelerate when pitching becomes excessive and to accelerate again once relative stability is restored. It is arguable that in such cases a more satisfactory vehicle would be one that used a lower rated power pack together with an improved suspension system.

What then constitutes a good suspension system for an off-road vehicle? Off-road terrain is typically a random series of of undulations of varying pitch, the amplitude of which is significant as compared to the diameter of the road wheel. Vehicles designed to cope with typical off-road terrain,should maximise available road wheel travel and incorporate a high level of damping.

The function of a damper is to absorb energy imparted to the road wheel. Analysis of a spring-mass-damper system show that damping should be proportional to the velocity at which the wheel is being displaced. However, if a high damping rate is to be used, in the case of a very large wheel velocity, excessive suspension forces may be generated. In order to prevent such excessive forces it is normal to incorporate a relief valve or similar device to limit the magnitude of the damping force induced. It is generally accepted that in order to give adequate ride characteristics, this limit should exceed the static wheel load by a factor of 1.5 to 2. This means that the vast majority of suspension events will result in proportional levels of damping force and only the rare "high-speed excursions" will result in constant force due to relief valve "blow-off".

Damping forces of the order described infer very large energy levels to be absorbed. The damper converts the mechanical energy into heat. Therefore, in order to prevent overheating, a high performance damper for an off-road vehicle must dissipate such heat very effectively.

The main source of ride discomfort is vehicle pitching. This results from excitation of the pitch mode natural frequency of the vehicle. This is typically very low (c 1 Hz). Oscillation of this type must be adequately damped. However, it is undesirable that a damper should respond positively to the higher frequency, small amplitude oscillation induced by passage over cobblestone surfaces (or, in the case of tracked vehicles, track links.) Response to these would result in unwanted energy dissipation.

Current Suspension Systems

Most vehicle suspension systems involve linkages which convert the vertical motion of the roadwheel into an angular movement. Common examples of this are the trailing arm and the wishbone types of suspension. However, most suspension dampers currently in use are of the linear, piston type. Thus the angular movement of the suspension member is reconverted to a linear motion. (Fig 1)

Fig 1. Linear telescopic damper installation (Typical)

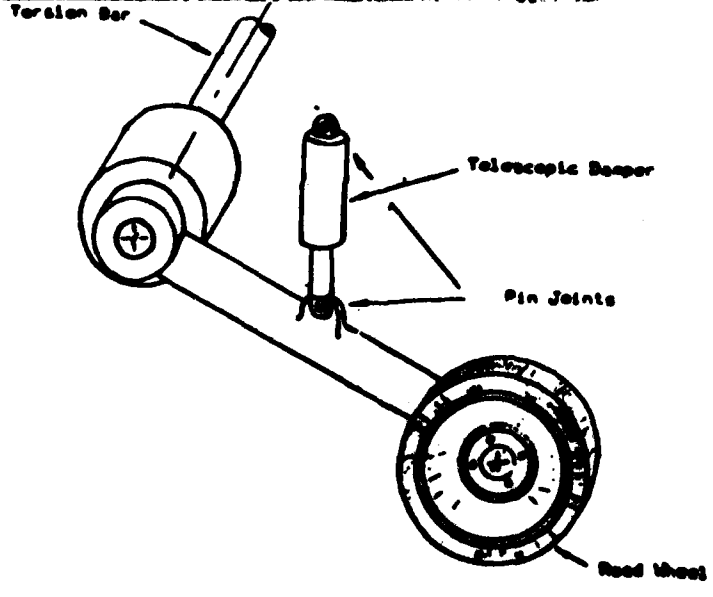

The most common linear suspension damper is the hydraulic telescopic unit which is pin-jointed to the suspension arm and to a fixed point on the vehicle. Although this type of unit is adequate for most road vehicle applications it suffers from a number of disadvantages when considered for off-road operation:

(i) In order to provide damping forces of the order required it is necessary to have either very high internal pressures or a very large piston area. This, combined with the large amplitudes over which damping is required, results in a very bulky unit which may be difficult to engineer into a vehicle installation.

(ii) As mentioned above, the large damping forces which are required result in a large amount of thermal energy to be dissipated. This can only be conducted away via the pin joints, and any radiation heat loss, particulary when the unit is covered with mud, is very small. Thus, sustained operation over typical cross-country terrain is liable to result in overheating and failure.

(iii) The typical location of telescopic dampers means that, dampers are exposed to debris being dislodged by the roadwheels and damage to the damper due to ingress of such debris is common.

Linear dampers may be used with any type of spring e.g. coil springs, torsion bars, leaf springs etc. A recent development of the piston principle is, however, the hydro-pneumatic unit which incorporates a gas "spring" with a hydraulic damper. A unit of this type has been developed for the latest British Main battle tank "Challenger". Although this type of unit overcomes some of the problems encountered with the telescopic, it is not immune from overheating problems and can only be produced within a viable space envelope by the use of very high hydraulic pressures (9000lbf/in^2-62MPa)
This requires the use of complex (and expensive) technology to achieve acceptable levels of reliability and durability.

ROTARY DAMPERS

In view of the above, the development of a damper which would utilise the inherent angular movement of suspension systems, has been considered desirable for some time. this is particularly true in the fields of tracked military vehicles where a large number of vehicles utilise transverse horizontal torsion bars as a springing medium connected to the road wheel by a trailing arm. It is believed that rudimentary rotary damping has been used on some Soviet tracked vehicles and indeed the West German Leopard II is fitted with rotary friction damper. However, the first known use of a hydraulic rotary damper is the U.S. Abrahams M.1. tank.
Horstman Defence Systems Ltd have been involved in vehicles and subsystems for almost 70 years. Indeed, the company's founder, Mr. Sidney Horstmann patented and gave his name to a bogey-type suspension which has been used on many types of vehicle up to and including the "Chieftain" tank.

Rotary Damper for MCV 80

In 1978 Horstman won a contract to design and develop a rotary suspension damper for the MCV80 vehicle. This vehicle has a design weight of 23.5 tonnes and is tracked with 12 road wheels. It is required to carry a section of ten infantrymen including driver, commander and a gunner for the turret mounted 30mm. cannon. It is intended that in service the vehicle would operate in consort with battle tanks and as such must display comparable mobility. This is no mean requirement, as the battle tank's greater overall length renders it less susceptible to pitching over a given course. Thus, in suspension terms, the requirements for MCV80 exceed those required of its accompanying battle tanks.

Design Requirements

In order to give MCV80 the required mobility a wheel travel of 400mm was specified. The design requirement to be met by Horstman was to design a damper capable of allowing wheel travel of this order, whilst providing the required damping rate up to the blow-off level necessary for the specified mobility.
The vehicle has been designed and developed by GKN Sankey Fighting Vehicle Operations. Their specification called for a hydraulic damper to be mounted at the axle arm pivot and to include the necessary bearings. (Fig2) Springing is provided by a horizontal torsion bar passed thro the centre of the damper. The bar is anchored by the housing of the corresponding wheel station on the opposite side of the vehicle.

Fig 2 Integral Rotary Damper.

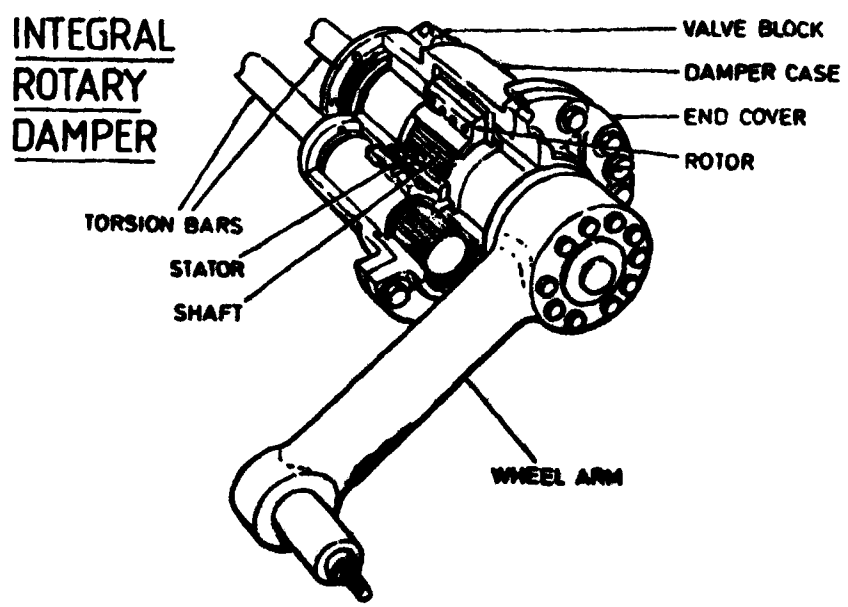

Description of Unit

The Horstman Rotary Hydraulic Suspension Damper is in concept similar to a two vane rotary actuator. Two vanes are attached to a rotating hub and a further two to an annular stator casing. This effectively creates four discrete fluid cavities. (Fig 3). Whereas, in an actuator,pressure is applied to diagonally opposite cavities to generate rotational movement, in the damper, rotation of the hub results in pressure being generated in the two cavities which are diminished by the rotational movement. The damping rate is determined by the rate at which fluid is allowed to leak from the pressurised chambers across the rotor vanes, via seals, orifices and valves.

Fig 3. Section through Damper Cartridge.

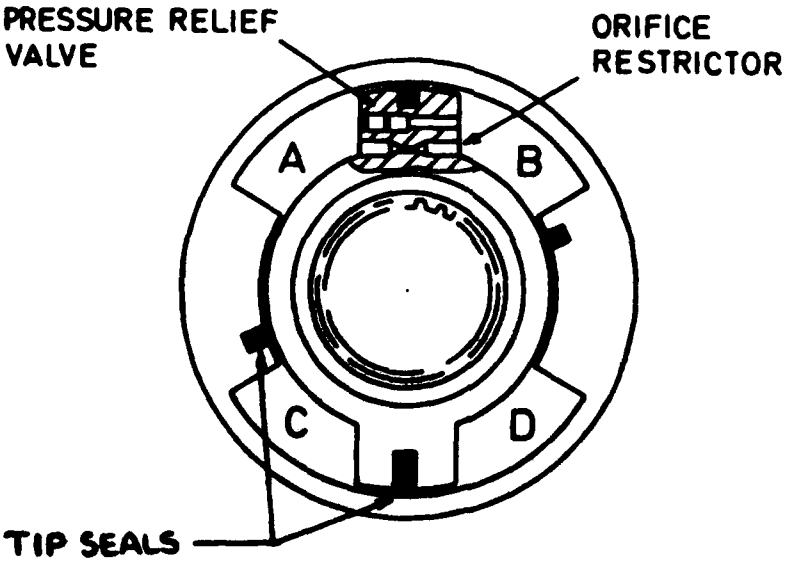

Conventional rotary actuators require near-perfect sealing. This is achieved by complex elastomeric elements and an extremely rigid structure. This results in a relatively heavy unit which must function at modest pressures and angular velocities in order to achieve adequate seal life. However, in a rotary damper application, perfect sealing is not of paramount importance. Angular velocities may also be an order of magnitude higher than those generally specified for actuators. Further, as this is a vehicle application, it is desirable to minimise weight and hence to design the structure for the required life and not to preserve rigidity underall circumstances. These requirements demand a sealing system different from those used in rotary actuators.

Horstman Defence Systems have developed a sealing system capable of satisfying these somewhat unusual requirements. This system does not give perfect sealing, allowing a small rate of leakage across the vane. this leakage flow is laminar and therefore highly temperature dependent.

In order to minimize this dependence a fixed orifice is incorporated in the rotor vane producing a substantially temperature independant flow path. The combination of the "parasitic" leakage around the vanes and the orifice flow gives an almost linear damping rate. This rate is only dependant on fluid temperature to a small extent. By close attention to the detailed engineering of the seal system, it has been possible to achieve a damping rate which satisfies the stiff damping characteristic considered necessary for this vehicle.

Fig 4. Typical Rotary Damper Performance Characteristics.

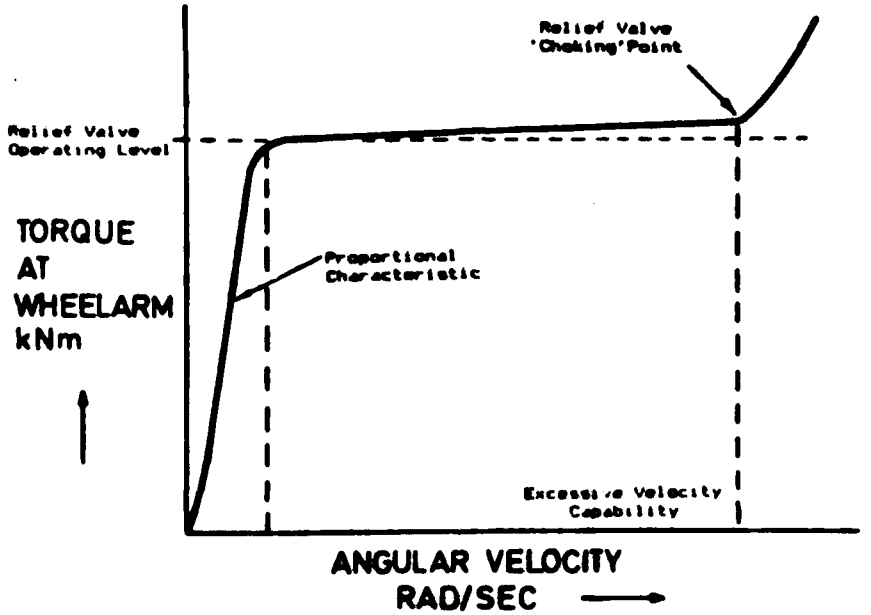

One of the significant advantages of an annular working area is that a relatively large swept volume can be contained within a modest space envelope. This means that large damping torques can be generated by hydraulic pressures of the order considered normal in industrial systems, typically 3000-4000 bf/in² (200-300 Bar). Obviously this is highly advantageous in designing seal systems, however, it does impose severe requirements on the valve system instituted to give "blow-off" at excessive angular velocities. (Fig 4.) It is clear that in order to achieve a relatively "flat" characteristic, at vertical wheel velocities of several metres per second, a very large volume of oil must be transferred across the rotor vane once the blow-off pressure has been achieved.

This function has been satisfied by the use of a number of pressure relief valves incorporated in the rotor vane. A further benefit of this is that dampers can be differentially rated to give higher blow-off in a desired direction. On tracked vehicles it is desirable to have lower blow-off forces in the rebound direction in order that road-wheels do not "hang-up" (i.e. can return quickly to their normal position following a bump, when the only force restoring them is that imposed by the torsion bar or spring.) In order to prevent build-up of internal hydraulic pressure due to rapid cyclic actuation or thermal expansion of the damping fluid, a spool type change over valve is used to vent the non-pressurised chambers to an externally mounted reservoir. (Fig 5)

Fig 5. Rotary Damper Oil System (schematic).

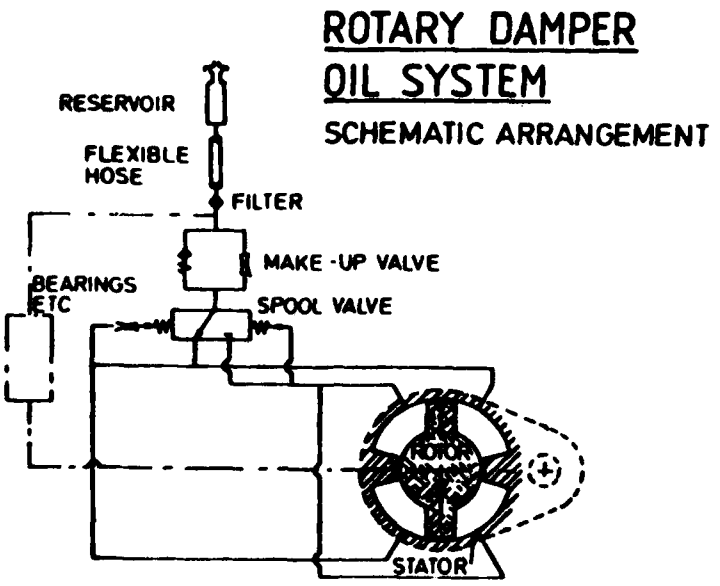

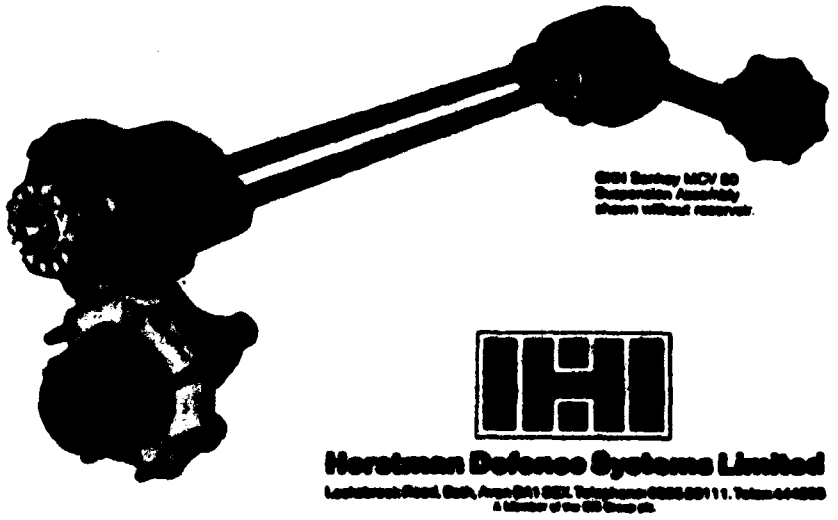

The damper unit is flange mounted to the vehicle hull. This is important for two reasons: Firstly, a large area of contact is maintained between the damper unit and the vehicle hull. This permits the vehicle hull to function as a very effective heat sink, dissipating the energy absorbed by the damper. Secondly, this type of mounting allows a very "clean" outside profile such that the damper is well protected from damage due to ballistic attack or terrain debris thrown up by roadwheels and trackwork.

Rig Testing

In order to fully test the rotary suspension damper, Horstman Defence Systems have commissioned a number of special purpose test rigs. The most significant of these is a large electro-hydraulic test stand which is capable of exercising dampers over the entire service range of torques and speeds. In a damper the highest torques are generated by the highest angular velocities. Thus, this test stand has an instantaneous power rating in excess of 300 KW. Other rigs are a performance test rig of more modest rating, and a general purpose, hydraulic, test bench for component evaluation.

Over 4000 hours of rig testing has now been completed. This has covered investigation into all aspects of functional performance, structural integrity and long term durability. Damper units have been fully evaluated against a test cycle compiled from actual vehicle data, covering the prescribed duty cycle. Several such tests of 600 hours duration have been satisfactorily completed, and most recently such a test was continued to 1000 hours without failure. This duration equates to two vehicle "overhaul" lives.

Although it is recognised that such testing cannot replace actual vehicle testing, it allows the damper to be evaluated in terms of durability and performance. This has enabled a high level of confidence to be established prior to the installation of rotary dampers on the customers vehicles.

Vehicle Testing

The first damper units were delivered to the customer in mid 1979 and since that time over 150 dampers have been supplied for testing on prototype vehicles. Over 100,000 Km vehicle testing has been carried out on Ministry Of Defence testing grounds, and very high levels of reliability have been achieved.

Many independent authorities have commented most favourably on the level of ride comfort that is achieved, even when traversing severe cross country terrain. The suspension performance is reported to be such that the vehicle may be driven at constant throttle and speeds considered to be very high for the type of terrain.

The basic function of an armoured infantry vehicle is to carry infantry, and, as mentioned above, MCV80 carries a section of ten men. It is therefore of great importance that the men being transported should arrive at their dismounting point in a fit state to fight. The suspension of the MCV80 has been fully evaluated in instrumented vehicle testing which has been reported elsewhere. This testing suggests that, in the service environment MCV80's complement will cover the ground more quckly and in more comfort than in other vehicles of this type.

Frequency response testing has shown that, although the damper responds very effectively to frequencies normally associated with pitch oscillation, energy dissipation at high frequencies (30HZ) is very low. Vehicle testing has shown that the suspension is free from the harshness frequantly experienced in telescopic dampers at high frequency.

Thermal performance has also been shown to be very good even when operating in high ambient temperatures, and this has permitted conventional elastomeric seals to be used extensively without thermal degradation.

Fig 6. GKN-Sankey MCV80 Vehicle.

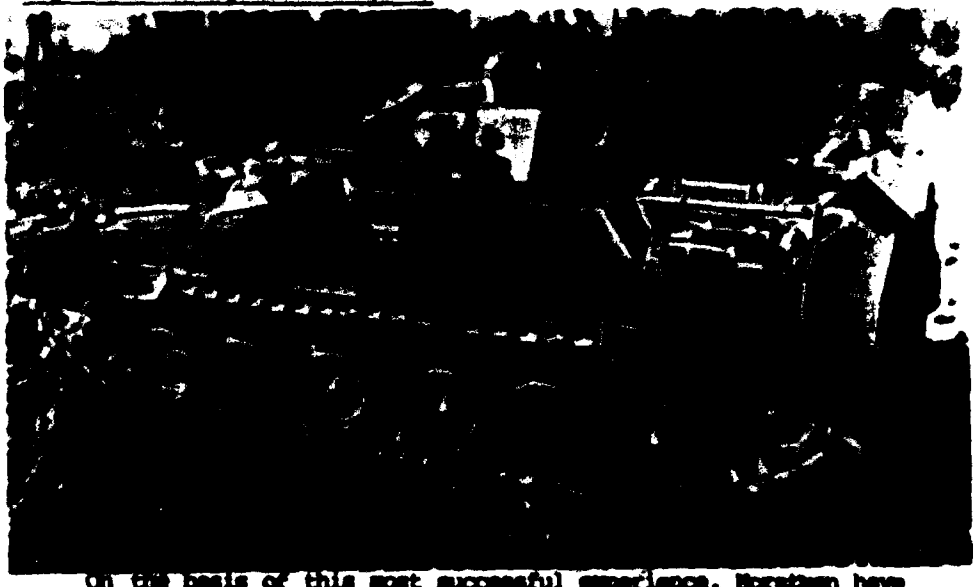

On the basis of this most successful experience, Horstman have now designed a range of similar Integral damper/axle arm units for vehicles across the range of weight from 10-60 tonnes. Of course, each of these designs are applicable to vehicles having horisontal, lateral torsion bar springing, together with trailing arm type suspension. Thus they are most applicable to new designs of vehicle or those where substantial redesign can be undertaken. Obviously this is of little interest to vehicle manufacturers with established designs where the space such a damper might require is already filled. In view of this, Horstman have addressed themselves to the problem of producing a design of damper which is capable of being fitted to an existing vehicle without significant change.

Lever Arm typeRotary Damper

To satisfy this requirement, Horstman have designed a lever-arm rotary damper. Again the concept of lever arm damping is not novel, such units being prevalent on cars and commerical vehicles during the 1950's. However, such units converted the rotary motion of the arm into the linear motion of piston-type units. The Horstman lever-arm rotary unit utilises the sealing technology previously developed for the integral damper units to produce a compact, high performance damper, which can be readily atached to the side wall of a vehicle. The damper lever is attached to the suspension member by a link which may be cranked to allow latitude in locating the mounting face. Also as there is no necessity to pass the torsion bar spring through the centre of a lever-arm damper, the overall size for a given rating can be substantially reduced, particularly at the smaller end of the range.

Obviously, an externally mounted unit cannot be as invulnerable to foreign object damage as the integrated version. However, the rounded shape and detailed design of the external seal render this unit much less vunerable than a more traditional piston type unit. The flat face on the inboard side of the damper is readily mounted onto the side plate or chassis member to ensure effective heat dissipation.

Fig 7. Horstman Lever-Arm Rotary Damper.

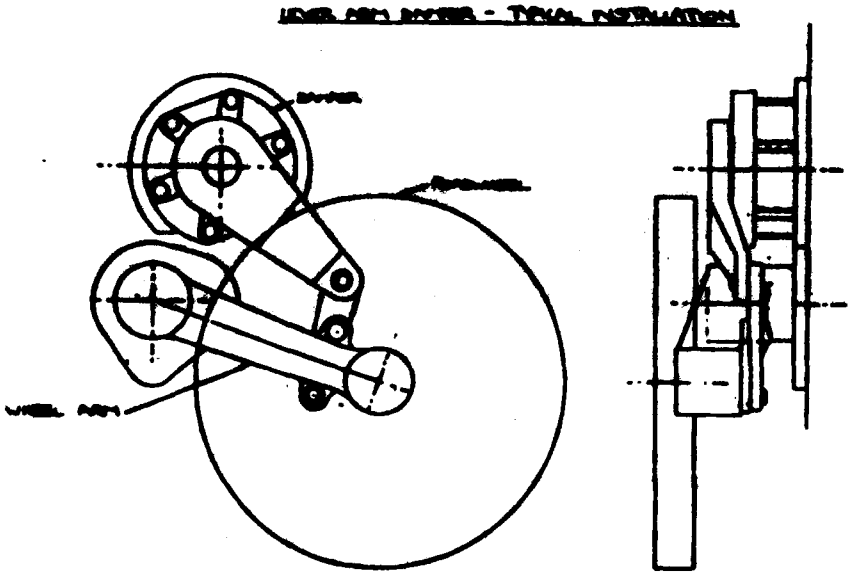

Although this unit has, in the first instance, been designed for installation on tracked vehicles. In principle there is no reason why it could not be installed on wheeled vehicles. Indeed, since angular movement is just as apparent in the suspension of wheeled vehicles,the technology or rotary suspension dampers is of equal relevance. Detailed design of the lever arm unit has now been completed and it is intended to evaluate its performance on several vehicles during 1984.

Horstman Defence Systems Ltd have designed and developed a rotary suspension damper which is capable of providing large damping forces on large wheel travel suspension systems. By the use of modern hydraulic technology a compact design with a high level of thermal dissipation and immunity from foreign object damage has been achieved. The design concept has been fully demonstrated on the GKN-Sankey MCV80, a high mobility armoured infantry carrier.

The technology involved can be applied in various designs to vehicles over a very large weight range utilising the angular movement inherent in most common suspension systems.

The Horstman Rotary Damper provides levels of performance normally only associated with more sophisticated (and expensive) types of suspension. Furthermore, because of the high levels of reliability and durability achieved by this type of unit, a very low "whole-life" cost suspension system can be created.

References

1. B. MacLaurin "Progress in British Tracked Vehicle Suspension Systems" SAE Paper 830442 1983

2. R.M. Orgorkiewicz "MCV 80 the new British infantry combat vehicle" International Defence Review 6/1982

3. D.H.C. Jenkins "Driving the MCV 80" International Defence Review 6/1982.

ACKNOWLEDGEMENTS

The successful development of the Horstman rotary damper for MCV80 could not have been achieved without very close co-operation with the staff of GKN-Sankey(Fighting Vehicle Operations). Horstman Defence Systems are proud to have contributed to the success of MCV80, which has shown itself to be a most impressive vehicle.

Horstman Defence Systems Ltd is a member of the EIS Group p.l.c .

QUICK CONNECT INTERVEHICLE COUPLING SYSTEM

I. O. Kamm, G. Wray, and J. Nazalewicz

Stevens Institute of Technology, Castle Point Station, Hoboken, NJ

SUMMARY

This paper covers the design, fabrication and operational testing of an electronically controlled, hydraulically powered, articulated intervehicle coupling joint which permits rapid vehicle coupling without external assistance and with substantial intervehicle misalignment.

A microprocessor based control system will be added to coordinate the individual engine and transmission operations and to optimize and simplify the control of the articulation joint.

Tests to date have shown that the vehicles can be coupled in less than one minute even with substantial misalignment between the two units; and that obstacle climbing capability is greatly improved. A field test program is being planned to determine the gains in mobility obtainable with this coupling system as compared to a single vehicle.

INTRODUCTION

Vehicles connected by an intervehicle joint are not new. Some are connected by passive joints, such as trailers. In others, such as earthmovers, the two halves are connected by a powered joint which is then used for steering. Tracked vehicles, using power articulated joints for steering without detracting from the propulsive effort, have shown superior mobility in soft soils and snow for some time. Lately, control of the pitch attitude between vehicles has been added for superior obstacle crossing capability. Adding this third dimension can pose control problems for the driver, often detracting from, sometimes negating, the advantages of the coupled system.

Side-by-side performance comparisons of coupled versus identical single machines demonstrate that the gains in mobility can be significant, and should be of benefit in tactical situations. But, on the other hand, the single machines are adequate for most of the everyday operations for which they are designed.

The coupling system presented here allows the vehicles to be used in the usual way as long as there are no particular mobility problems; but to be connected quickly, without exposure of personnel to external hazards, when increased mobility is needed. The versatility which this approach offers permits us to re-think the applications of coupled vehicle systems.

At the time of this writing, a coupling joint has been designed, fabricated, and installed on two M-113 APC's. The system is operational with relatively simple controls. The vehicles can be quickly coupled and uncoupled. The joint can accomodate large initial misalignments of the two vehicles in the process of coupling. The development is now underway of a microprocessor based control system which optimizes the performance of the coupled vehicle system by coordinating the forces that are generated by the joint with those generated by the traction elements. Further, the possibilities will be explored that exist for an automatic coupler using a target homing device, and for incorporating a terrain sensing device in the vehicle control system.

Finally, a field test program will be conducted to determine tradeoffs between system size and sophistication needed and the mobility gains that can be made. It is expected that the technology developed here can be transferred to other vehicle systems and applications.

OPERATIONAL REQUIREMENTS

The coupling system is designed to satisfy the following operational philosophy:

The individual vehicles will operate as single units as far as their mobility permits. The added coupling components should not impair normal operation. The vehicles will be coupled when an operator anticipates that the single vehicle cannot handle a certain terrain or obstacle, or failing that judgement, after a vehicle becomes immobilized. This requires that coupling can be accomplished even after one vehicle is stuck in an awkward attitude. (Envision here a vehicle stuck in a creek bed, unable to climb out either in forward or reverse.) The coupling process will be controlled by the driver in the rear vehicle, because he can see the joint. (Later, a homing device could be used for that purpose.) The hydraulic actuators will position and latch the mating parts of the coupler. No one is needed outside the vehicle for the coupling process.

When coupled, the assist given to the immobilized vehicle will utilize, to the maximum extent possible, the traction forces that can be generated by both vehicles. The attitude control generated by power articulating the joint will direct these forces to the most advantageous line of application, the intervehicle forces generated by the joint will augment the traction forces that are lacking.

(For distinction: articulated vehicles usually can only operate in tandem, with one power plant for both; coupled machines are individually powered and can be used solo.)

The coupled vehicles are expected to have mobility superior to that of the single M-113, when: climbing steps greater than two feet in height, crossing ditches wider than seven feet, entering and exiting bodies of water, negotiating short, very steep, slopes (greater than 60% for one vehicle length), and steering in very soft soils and snow. Remaining in the coupled mode during normal operations will allow higher cross-country speeds over rough terrain and improve directional control.

The coupling system has to accomodate the necessary combined freedom of motion in pitch, yaw and roll; provide the correct, timely and coordinated action of the joint and traction forces; and force the correct co-axial alignment of the coupler during the coupling process, all as dictated by terrain-vehicle interaction.

In the detailed design of the coupling system the following major guidelines were followed:

1. *The ability to quickly couple and uncouple the vehicles is of first priority.*

2. *The quick coupling should be accomplished in less than one minute and from within the vehicle.*

3. *The coupling system should cause minimum interference with the performance and usefulness of the single vehicles.*

4. *The quick coupling system is to be sized for a two unit machine.*

5. *Intervehicle assist will be used to supplement normal traction.*

6. *The driver's task will be kept simple, in line with normal skills. The tasks of intervehicle and traction control coordination are to be done by microprocessors.*

7. *Allow for the maximum yaw and pitch angles that intervehicle clearances permit.*

DESCRIPTION OF THE SYSTEM

A. Mechanical

The coupler consists of a plug, mounted on the rear of the forward vehicle, which is latched inside the socket attached to the rear vehicle. This assembly is force articulated in yaw and in pitch by hydraulic cylinders.

Figures 1 and 2 show the details of the coupler, attached to M-113 APC's including the latching arrangement between the socket and plug. The dotted lines in Figure 1 show the components in the stowed position.

The stowed plug prevents the ramp from being completely lowered on hard ground. However, the resulting step up onto the ramp is less than the floor height of the vehicle. Photographs of the respective side and top views of the coupler installed on the vehicles are shown in Figures 3 and 4.

The working range of the pitch articulation of the coupler with respect to the forward unit are 45° up and 45° down from the horizontal. The socket attached to the rear unit can be pitched up 45° and down 20°. Most of this motion can be utilized during operation without mechanical interference of the two vehicle hulls depending on combined yaw and pitch attitudes. Further upward motion (60° and 65°) of the joint halves is used for stowing purposes only.

The primary pitch motion is about the forward pitch axis, secondary motion is about the rear axis. Thus, the vehicles are permitted to assume angular and parallel misalignment simultaneously. The yaw articulation limits are 45° to the right and left from the centerline. The yaw and pitch motions are independent. Yaw motion occurs only between the forward unit and the coupler plug; the socket is fixed in yaw to the rear unit. The coupler plug rotates freely in the socket permitting free roll motion between units.

B. Hydraulics

The hydraulic schematic is shown in Figure 5. The system consists of a variable displacement pump, which supplies both the yaw cylinders and the pitch cylinders through two separate servovalves to produce a pitch or yaw rate of 15°/second maximum. Pressure relief valves and cross port reliefs provide overload protection. The rear unit has the identical pump installed, to actuate the rear pitch cylinder and the latching mechanism.

C. Controls

For the present purpose of demonstrating the quick coupling capability the hydraulics are analog controlled. The engines and transmissions are controlled either manually or with the master/slave servo controls. At the present time, intervehicle signals are transmitted via umbilical cord, to be replaced by radio (or similar) transmission links later.

Under the next phase of this effort a microprocessor control system will be implemented to coordinate the utilization of traction and articulation forces to the best advantage of the system, and at the same time protect the joint against overloads. The tentative control schematic with its supporting subsystems is shown in Figure 6.

RESULTS

To date, the check out of the coupling system installed on the two vehicles has shown the following:

1. *The mechanical and hydraulic components of the coupling system function as intended.*

2. *Coupling can be achieved with substantial misalignment between units.*

3. *The coupling system assists in obstacle climbing.*

In the operational tests performed to date, all of the design goals were either met or exceeded.

Coupling and uncoupling can be achieved without external assistance in less than ten seconds under ideal conditions, but it may take up to one minute with severe misalignment of the vehicles. Coupling has been accomplished with a difference in elevation of 42" (appx. 1 meter) between the machines and an angular misalignment of up to 60°. The coupled machines have climbed a 45" (115 cm.) step (the height of a loading platform), compared to the 2' (60 cm.) step possible with the single vehicle.

The wall to wall turning diameter is 44' (13.5 m) with a combination of joint and track steering and with the vehicles at a pitch-up attitude to reduce ground contact length.

CONCLUSIONS

A quick coupling feature can be incorporated into a coupling joint system which is capable of providing substantial mobility assistance to the vehicles. The ability to provide such assistance when needed, but also to allow use of the vehicles in the customary sense at other times, provides new opportunities for applications where an expanded need exists for:

- *obstacle negotiation*
- *platform stability*
- *platform attitude control*
- *intervehicle assistance*
- *traction augmentation*
- *vehicle survivability.*

ACKNOWLEDGMENT

This work is supported by the Defense Advanced Research Projects Agency and monitored by the U.S. Army Tank-Automotive Command. Dr. C. W. Kelly, III, Chief of the System Science Division, DARPA provides direct technical supervision; Mr. Tibor Czako of the Tank-Automotive Concepts Laboratory is Scientific Program Officer.

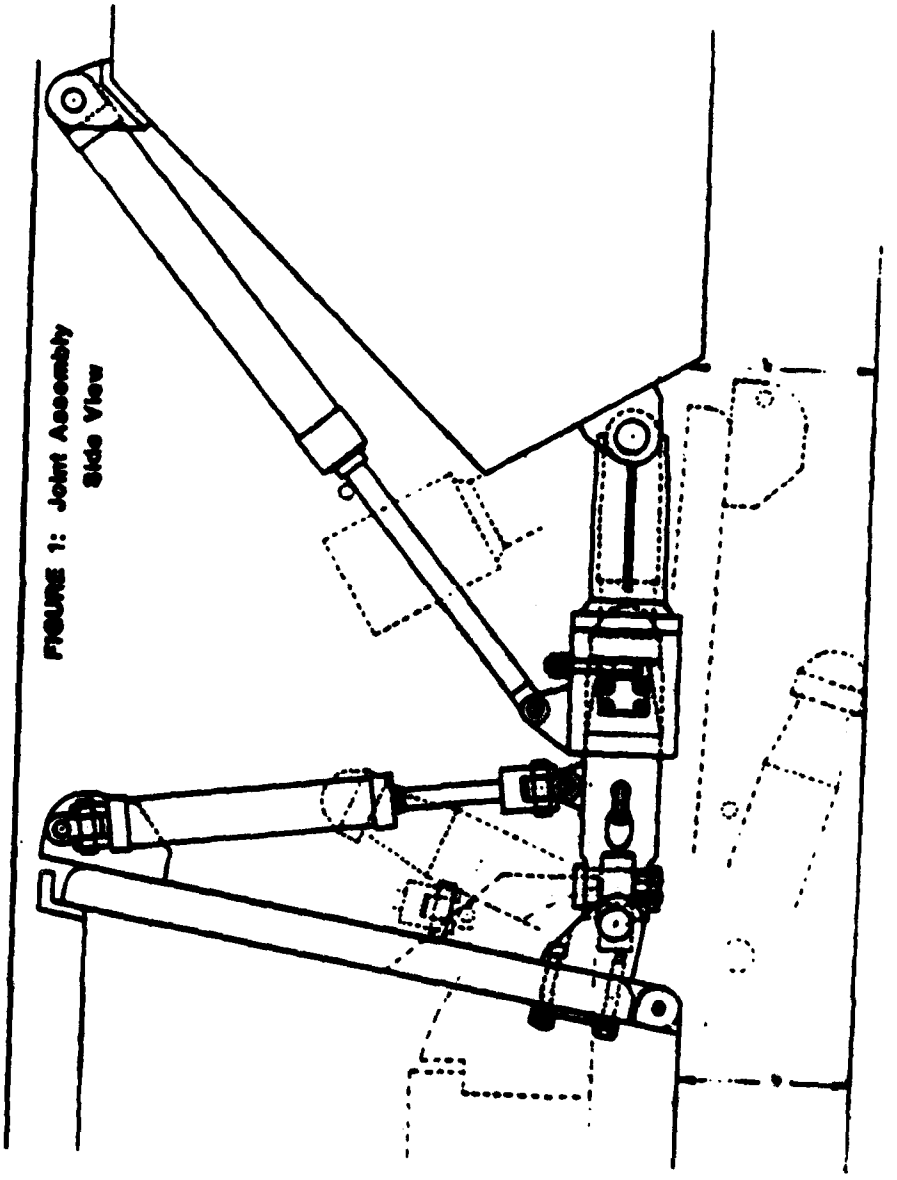

FIGURE 1: Joint Assembly
Side View

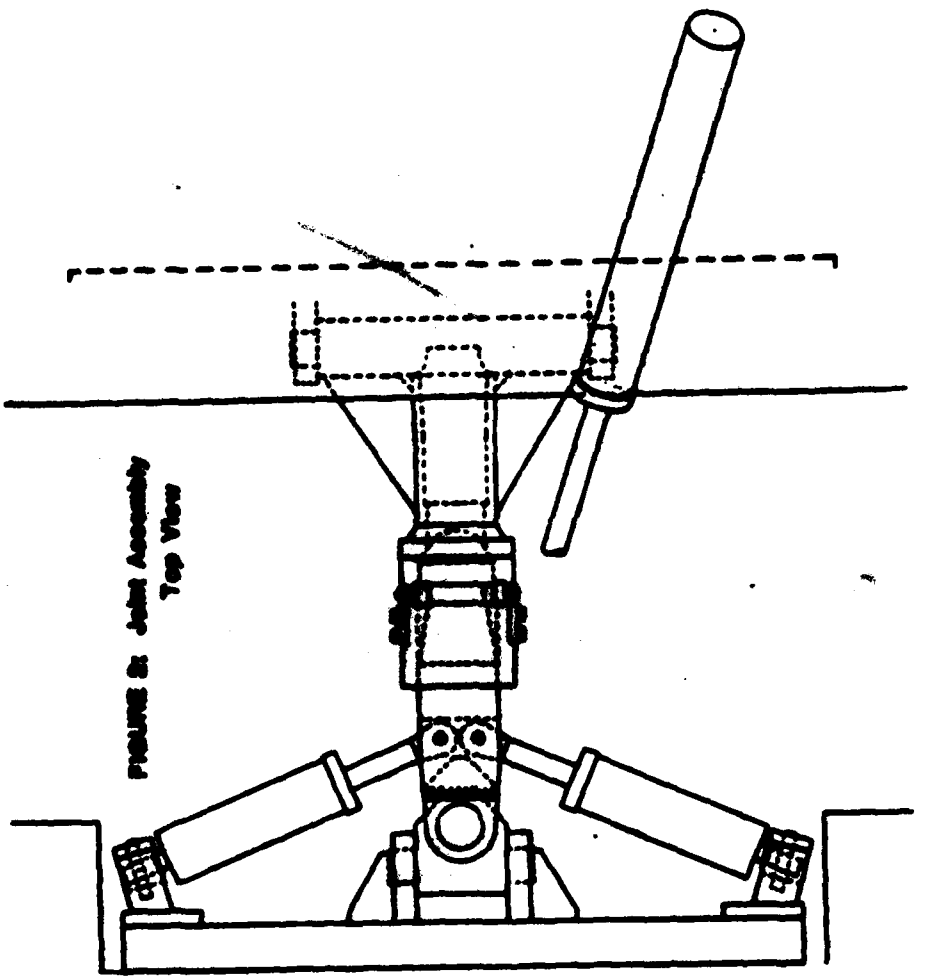

FIGURE 8: Joint Assembly Top View

FIGURE 3: Assembled Joint From Left Side

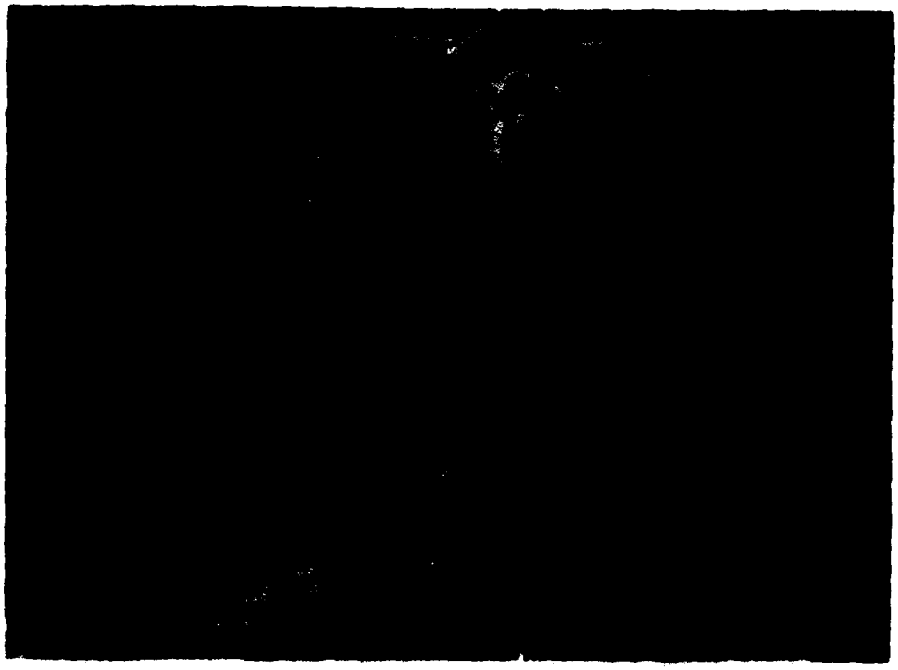

FIGURE 4: Assembled Joint From
Deck of Rear Unit

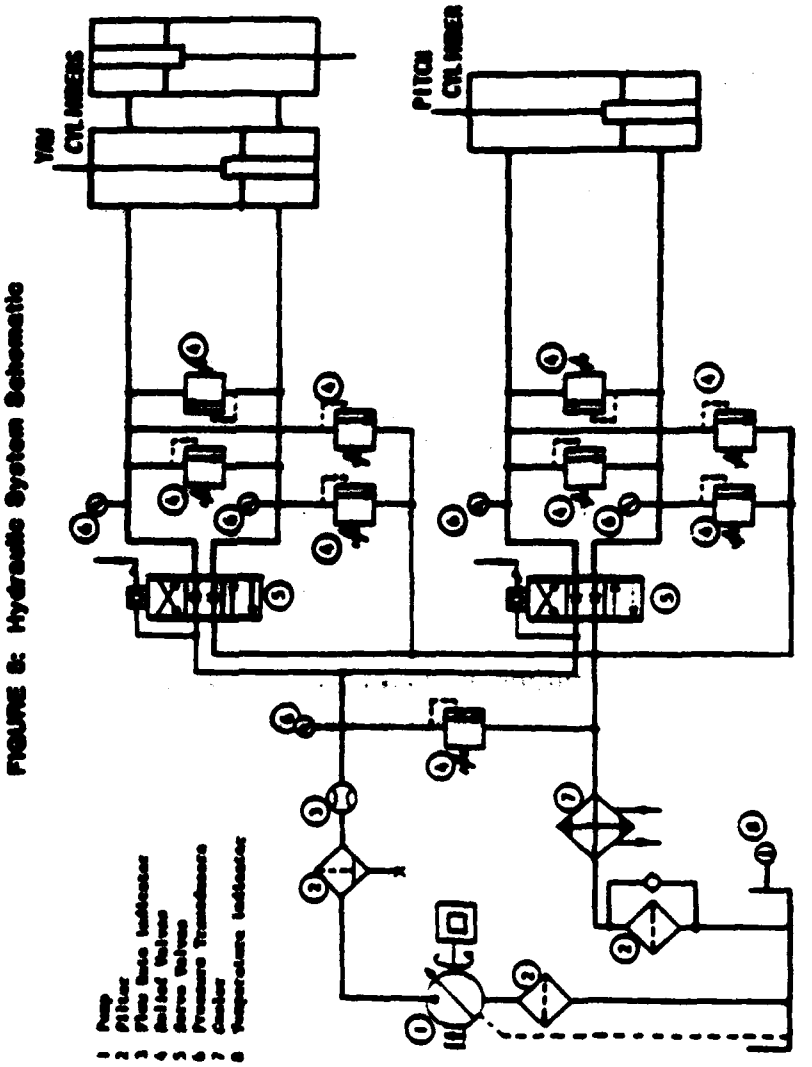

FIGURE 6: Hydraulic System Schematic

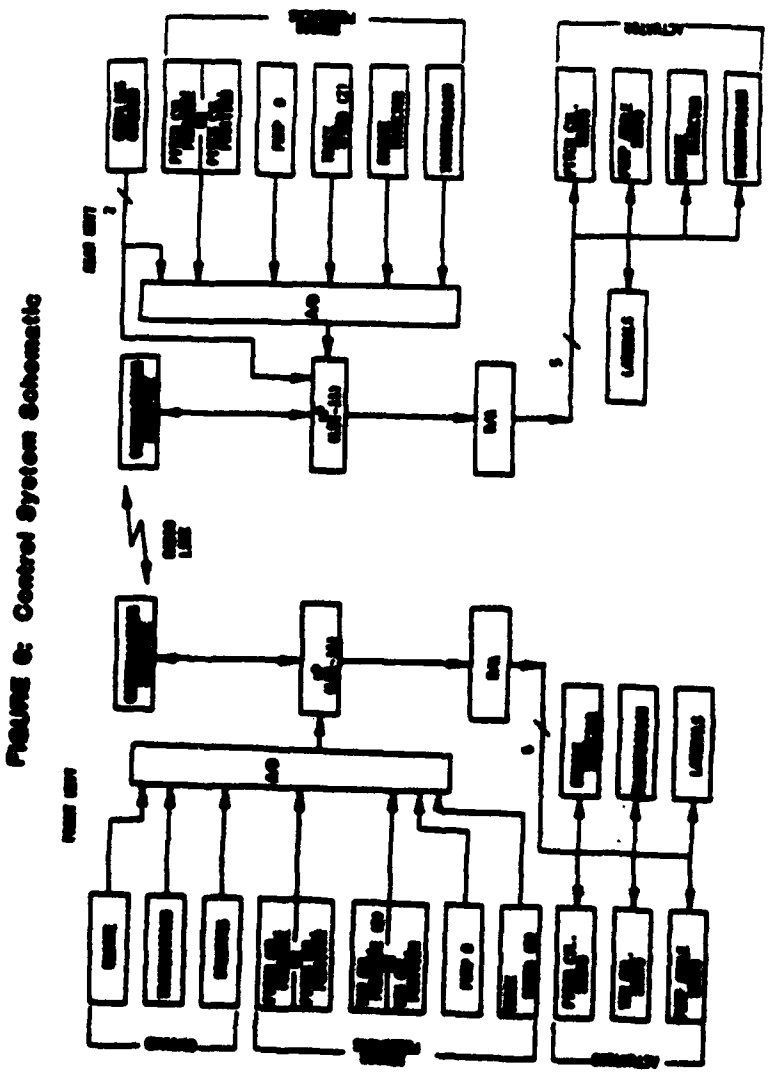

FIGURE 6: Control System Schematic

ESTIMATION OF WEAR LIFE OF HEAVY DUMP TRUCK TYRE

T. MURO *, S. HATA ** and R. FUKAGAWA **

* Ehime Univ., Matsuyama, JAPAN ** Kyoto Univ., Kyoto, JAPAN

SYNOPSIS

A frictional work of each tyre has been calculated by means of rigorous mathematical analysis and practical approximate method at cornering site.

To estimate a wear life of each tyre, a relation between amount of wear and frictional work has been investigated for some period, and then another relation between residual depth of tread and operation time has been measured in-situ for several tyres of a capacity 45 tons heavy dump truck.

As a result, the change of amount of wear of tyre with the passage of operation time can be expressed by an exponential function as

$$x = d_a \left[1 - \exp \left(- \frac{a}{d_a - x_c} \cdot AW_c \cdot t \right) \right] .$$

Here, x is a length of wear of tread, t is an operation time, a is a length of wear per unit frictional work of tyre, AW_c is a frictional work per unit operation time, d_a is a converted depth of tread from tyre deformation, x_c is the length of wear of tread when a relation between coefficient of friction and slip ratio of tyre has been measured.

Then, the wear life of tyre t_E(hr) for $x = x_E$ (mm) is calculated as follows ;

$$t_E = \frac{\ln d_a - \ln (d_a - x_E)}{a \cdot AW_c} (d_a - x_c) .$$

KEY WORDS

Tyre, Wear, Dump truck, Friction

INTRODUCTION

In recent years, heavy dump truck has been supersized more and more as an earth moving transportation vehicle at large scale earthwork site, such as earth fill dam, land reclamation work or soil excavation site, and it has been contributed to increase an efficiency of construction. Here, as an important durability problem of construction machinery, a change of amount of wear of heavy dump truck tyre with the passage of operation time and a wear life of each tyre have been analysed theoretically. And the aim of this study is to build up a rational method to estimate the wear life of tyre, and to improve a construction system by means of increasing the durability of heavy dump truck tyre.

To analyse the wear mechanism of OR tyre, a systematic study concerning with trail conditions, i.e. slope, radius of curvature, and relation between coefficient of friction and slip ratio etc., operational conditions, i.e. vehicle speed, acceleration at driving, and retardation at braking etc., and vehicle dimensions, i.e. size, weight, inertia of tyre and vehicle, and position of gravity center etc. should be taken. That is, a frictional work of each tyre should be calculated by means of rigorous mathematical analysis and practical approximate method, from the equations of motion of vehicle and tyre which are introduced at driving and braking for straight and cornering motion on several slopes.

Especially on cornering site, the amount of wear of tyre increases remarkably. The dependance of radius of curvature of trail and vehicle motion on each slip ratio and coefficient of friction of tyre should be analysed in detail for each position, and then the characteristics of frictional work of each tyre will be clarified.

Next, the change of amount of wear of each tyre should be analysed with the passage of operation time, considering the trail conditions and various vehicle motions. In-situ test, the amount of wear of each tyre of a heavy dump truck (Capacity 45 tons) has been measured in every month. At the same time, the shape of trail, slope, radius of curvature at cornering site, the vehicle motion, and the relation between coefficient of friction and slip ratio have been measured. After the relation between amount of wear and frictional work of each tyre has been investigated for some period, the method of estimation of wear life was established.

EQUATION OF MOTION

Coefficient of Friction and Slip Ratio

Fig. 1 (a) shows several vectors of frictional force and velocity at driving and braking , which occur on a cornering tyre. $\vec{u}$ is a vector of velocity in the moving direction of tyre. $R\vec{\omega}$ is a vector of circumferential velocity of tyre, in which R is a radius of tyre and $\vec{\omega}$ is a rotational angular velocity of tyre. And the vector of slip velocity $\vec{v}_s$ can be expressed as $\vec{u} + R\vec{\omega}$. Here, the angles between F, u, v_s and rotational plane of tyre are given as α, β, γ, respectively. β is a slip angle of tyre which is given as an angle between rotational plane and moving direction of tyre. Slip ratio S_{lon} in the longitudinal direction (or rotational plane), and another slip ratio S_{lat} in the lateral direction (or normal direction to rotational plane) of tyre are expressed approximately for small slip angle β as follows. [1]

At driving ($0 \leq u\cos\beta < R\omega$)

$$S_{lon} = \frac{(R\omega - u\cos\beta)\cos\beta}{R\omega} \geq 0 \qquad (1)$$

$$S_{lat} = -\sin\beta \qquad (2)$$

At braking ($u\cos\beta \geq R\omega$)

$$S_{lon} = \frac{R\omega - u\cos\beta}{u} < 0 \qquad (3)$$

$$S_{lat} = -\sin\beta \qquad (4)$$

Here, when the value of S_{lat} is negative for positive(or clockwise)slip angle, the tyre turns counterclockwise to left hand side.

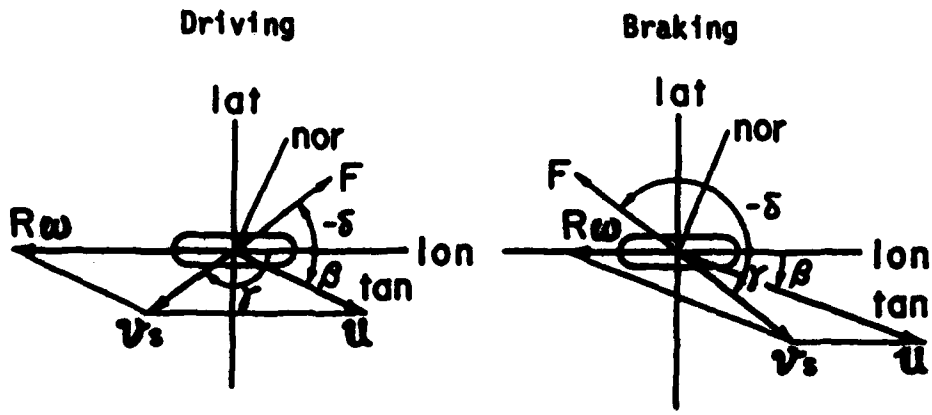

Fig. 1 (a) Force and slip velocity developed on tyre at cornering

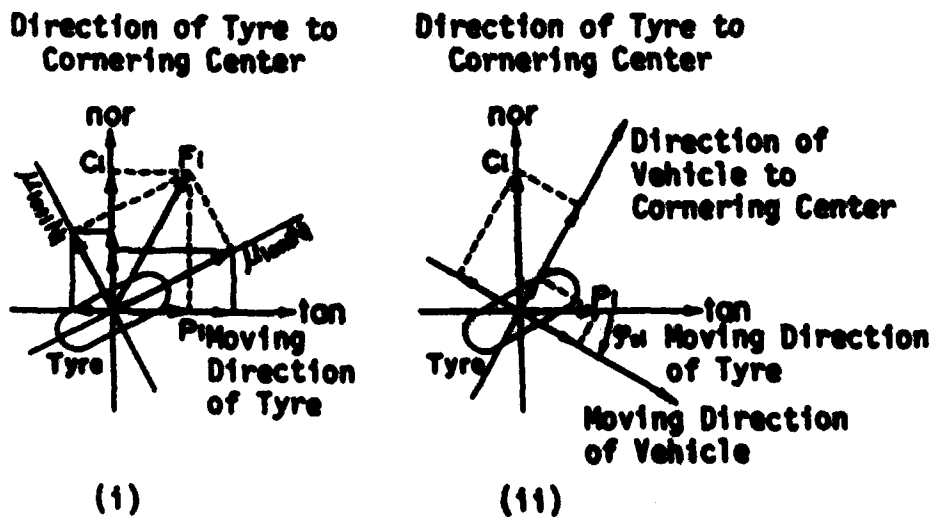

Fig. 1 (b) Forces developed on tyre

The relation between coefficient of friction μ and slip ratio S of tyre depends on rubber tread material, carcass and tread structure, and surface condition of roughness or material of trail. It is cleared that the coefficient of friction is directly proportional to slip ratio for initial slip of tyre. [1] That is,

$$\mu = c \cdot s \tag{5}$$

where c is a constant.

In-situ test results concerning with an unisotropic friction of tyre were reported for N type tread tyre. [1] It was cleared that both frictional phenomena in longitudinal and lateral direction of tyre are almost isotropic in a region of static friction, the shape of ellipse of friction [2] approaches to circle, and both directions of slip and frictional force of tyre are situated on a straight line.

Equation of Vehicle Motion

Fig. 2 (a) shows a model of heavy dump truck which is running on a slope. Slope angle I is positive for ascending motion. ℓ is a distance from front to rear wheel axis, ℓ_f and ℓ_r is a distance from front and rear wheel axis to gravity center G of vehicle, respectively. R_i and ω_i is a radius and angular velocity of each tyre, in which suffix i shows a tyre position, i.e. 1: front left wheel, 2: front right wheel, 3: rear left wheel, 4: rear right wheel. W is a total vehicle weight, N_i is a normal load acted on each tyre, and U is a velocity of vehicle.

Fig. 2 (b) is a plan of vehicle running on X-Y plane, in which both moving direction of vehicle and each tyre and direction of forces acted on them are shown, respectively. b_f is an interval between left and right front tyre, and b_r is an interval between left and right rear tyre. K_f or K_r is a distance from front or rear wheel to gravity center of vehicle respectively. γ_s is an angle from X-axis to vehicle axis, and θ_s is an angle from X-axis to moving direction of vehicle. ε_{si} is an angle between X-axis and moving direction of each tyre. Here, all the clockwise angle from X-axis are defined to be positive. β_s is a slip angle of vehicle from its axis to moving direction of it, β_{si} is a slip angle of each tyre from its longitudinal direction to moving direction of it, α_{si} is a steering angle of front tyre from vehicle angle to longitudinal direction of tyre, ϕ_{si} is an angle from moving direction of tyre to that of vehicle, and all the clockwise angle are positive.

The mutual relations of each angle are shown as follows ;

$$\beta_s = \theta_s - \gamma_s \tag{6}$$

$$\phi_{si} = \theta_s - \varepsilon_{si} \tag{7}$$

$$\beta_{si} = \varepsilon_{si} - \alpha_{si} - \gamma_s = \beta_s - \alpha_{si} - \phi_{si} \tag{8}.$$

γ_f or γ_r is a constant which is calculated as $\tan^{-1}(b_f/2\ell_f)$ or $\tan^{-1}(b_r/2\ell_r)$ respectively.

As shown in Fig. 1 (b-i) , force F_i acted on each tyre is composed of a force P_i acted in its moving direction and another force C_i acted in its direction to cornering center. Forces P_i and C_i are given as follows ;

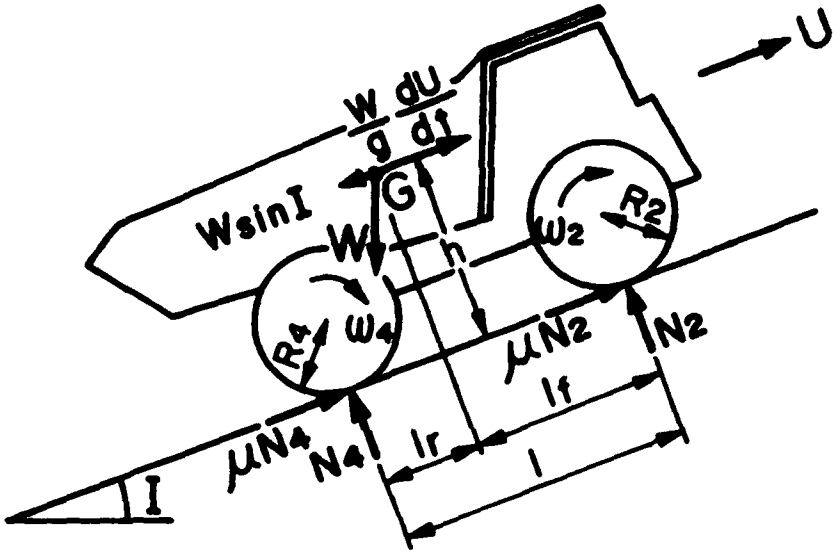

Fig. 2 (a) Dimension of heavy dump truck

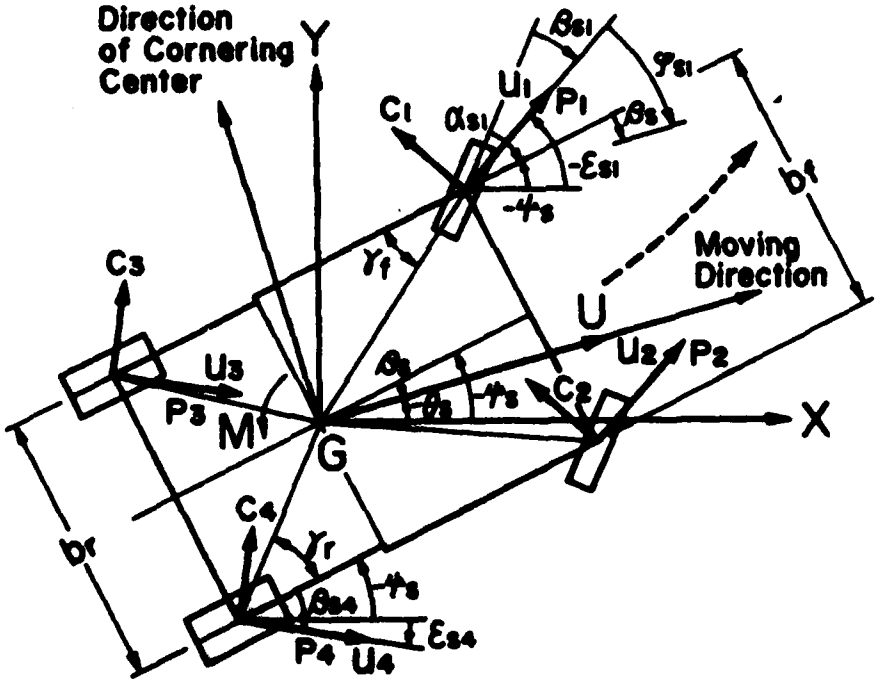

Fig. 2 (b) Movement of vehicle

$$P_i = \mu_{tani} N_i = (\mu_{loni} \cos\beta_{si} + \mu_{lati} \sin\beta_{si}) N_i \quad (9)$$

$$C_i = \mu_{nori} N_i = (\mu_{loni} \sin\beta_{si} - \mu_{lati} \cos\beta_{si}) N_i \quad (10)$$

And those forces P_i and C_i are divided to another forces in a moving direction of vehicle and its direction to cornering center, as shown in Fig. 1 (b-ii).

Next, 3 equations of motion of vehicle in its moving direction, in its direction to cornering center, and in its rotational direction are introduced in terms of its gravity center as follows,

$$\frac{W}{g} \frac{du}{dt} = \sum_{i=1}^{4} (P_i \cos\phi_{si} - C_i \sin\phi_{si}) - W \sin I \quad (11)$$

$$\frac{W}{g} \frac{U^2}{r} = \sum_{i=1}^{4} (P_i \sin\phi_{si} + C_i \cos\phi_{si}) \quad (12)$$

$$\begin{aligned} -J_Z \frac{d^2\psi_S}{dt^2} = {} & K_f \{ P_1 \sin(\beta_S - \phi_{s1} + \gamma_f) - C_1 \cos(\beta_S - \phi_{s1} + \gamma_f) \} \\ & + K_f \{ P_2 \sin(\beta_S - \phi_{s2} - \gamma_f) - C_2 \cos(\beta_S - \phi_{s2} - \gamma_f) \} \\ & + K_r \{ -P_3 \sin(\beta_S - \phi_{s3} - \gamma_r) + C_3 \cos(\beta_S - \phi_{s3} - \gamma_r) \} \\ & + K_r \{ -P_4 \sin(\beta_S - \phi_{s4} + \gamma_r) + C_4 \cos(\beta_S - \phi_{s4} + \gamma_r) \}. \end{aligned} \quad (13)$$

Here, g is gravitational acceleration, J_Z is moment of inertia of vehicle. N_i is a normal load acted on each tyre which is calculated from both equilibrium equations of moment in terms of gravity center of vehicle in its longitudinal and lateral direction, and condition of 4 lowest parts of each wheel to be positioned on a same plane after deformation of spring and tyre. Therefore, the normal load N_i is directly varied by acceleration or retardation of vehicle.

Fig. 3 is an approximate model of heavy dump truck, of which 4 wheels are replaced by 2 single wheels. As an approximate practical method, next equations of motion are established for this approximate model.

$$\begin{aligned} F_t &= \frac{W}{g} (\frac{du}{dt} + g \sin I) \\ &= \mu_{lonf} \cos(\beta - \alpha) \cdot N_f - c \sin\beta_f \sin(\beta - \alpha) \cdot N_f \\ &\quad + \mu_{lonr} \cos\beta \cdot N_r - c \sin\beta_r \sin\beta \cdot N_r \end{aligned} \quad (14)$$

$$\begin{aligned} F_n &= \frac{W}{g} \frac{U^2}{r} \\ &= \mu_{lonf} \sin(\beta - \alpha) N_f + c \sin\beta_f \cos(\beta - \alpha) \cdot N_f \\ &\quad + \mu_{lonr} \sin\beta \cdot N_r + c \sin\beta_r \cos\beta \cdot N_r \end{aligned} \quad (15)$$

$$\begin{aligned} M &= J_Z \frac{d^2\psi_S}{dt^2} \\ &= \mu_{lonf} \sin\alpha \cdot N_f \ell_f + c \sin\beta_f \cos\alpha \cdot N_f \ell_f - c \sin\beta_r \cdot N_r \ell_r \end{aligned} \quad (16)$$

Here, f or r means front and rear respectively. The difference between rigorous mathematical analysis and approximate practical method does not appear for straight motion, but increases gradually with an increase of steering angle of tyre for cornering motion.

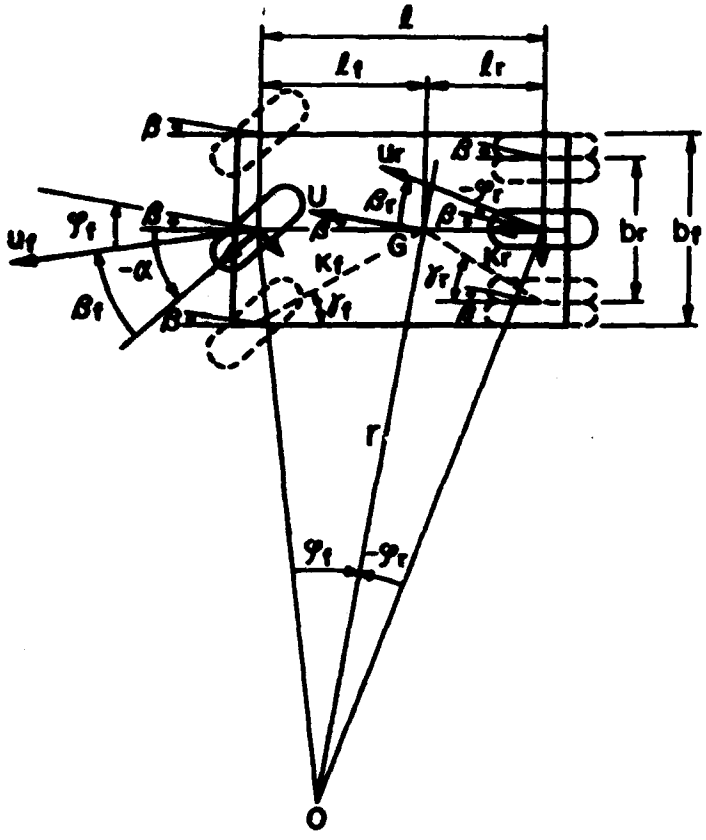

Fig. 3 Approximate model of heavy dump truck

Table 1 Dimensions of tyre and heavy dump truck

State		Empty	Loaded
R	Turning radius of tyre (m)	1.01	0.96
ℓ	Distance from front to rear wheel axis (m)	4.19	4.19
ℓ_f	Distance from front wheel axis to gravity center(m)	2.44	2.73
ℓ_r	Distance from rear wheel axis to gravity center(m)	1.75	1.46
b_f	Interval between left and right front tyre (m)	3.16	3.16
b_r	Interval between left and right rear tyre (m)	2.74	2.74
h	Height of gravity center of vehicle (m)	2.11	2.91
J_z	Moment of inertia of vehicle (kgm^2)	89970	240800
E_f	Modulus of elasticity of front wheel (t/cm)	0.884	0.884
E_r	Modulus of elasticity of rear wheel (t/cm)	2.053	2.053
K_f	Distance from front wheel to gravity center (m)	2.91	3.27
K_r	Distance from rear wheel to gravity center (m)	2.22	1.91
I_f	Moment of inertia of front wheel (kgm^2)	510	510
I_r	Moment of inertia of rear wheel (kgm^2)	2510	2510
W	Total weight of vehicle (kgf)	39200	104900
μ_R	Coefficient of rolling friction	-0.02	-0.02

Equation of Tyre Motion

Defining a moving direction and a clockwise rotation of each tyre to be positive, the following equation of rotational motion of tyre is derived from moment equilibrium condition.

$$I_i \frac{d\omega_i}{dt} = (\mu_{loni} - \mu_R) N_i R_i - T_i \qquad (17)$$

Here, μ_{loni} is a coefficient of friction occurred in each tyre by driving or braking torque T_i . μ_R is a rolling coefficient of friction. I_i is a moment of inertia of each tyre.

Next, the equations of rotational motion of front and rear tyre derived from previous approximate model are as follows ;

$$I_f \frac{d\omega_f}{dt} = (\mu_{lonf} - \mu_R) N_f R_f - B T \qquad (18)$$

$$I_r \frac{d\omega_r}{dt} = (\mu_{lonr} - \mu_R) N_r R_r - T \qquad (19)$$

Here, B is a torque ratio of front to rear wheel.

In the above equations, the terms of inertia are negligibly small values from the result of observation of movement of practical heavy dump truck tyre. Assuming that R_f is nearly equal to R_r , the following relation is derived.

$$\mu_{lonf} = B (\mu_{lonr} - \mu_R) N_r / N_f + \mu_R \qquad (20)$$

Now, the method of rigorous mathematical analysis is to transform the coordinate system of equations (11) (12) (13) and (17) to another one expressed a sloping terrain, and to simulate a slip ratio S_{loni} , S_{lati} , velocity of tyre u_i , and normal load N_i , calculating a velocity and rotational angular velocity of vehicle and tyre for a given steering angle α_{si} and torque T_i of tyre in each time Δt . In previous report [3], the values of frictional work of each tyre at straight or cornering motion of vehicle on a flat or inclined terrain were compared with each other for several representative examples. As a result, this method has a weak point which needs a lot of time for calculation. On the other hand, the practical approximate method is to calculate a slip ratio of front and rear tyre by solving the unknown values μ_{lonr} , β_f and β_r in equations (14) (15) (16) and (20) for measured value F_t , F_n and M , and to compute the coefficient of friction mobilized on each tyre by means of division of these slip ratios.

IN-SITU TEST

Test Vehicle

Table 1 shows the dimensions of tyre and heavy dump truck at empty or loaded state. In this table, coefficient of rolling friction, modulus of elasticity of front and rear wheel, height of gravity center of vehicle, and total weight of vehicle have been directly measured in-situ.

Characteristics of Course and Movement of Vehicle

Fig. 4 (a) is a plan of courses of heavy dump truck at some soil and rock excavation site. There are 9 kinds of course from A1 to A9 , and

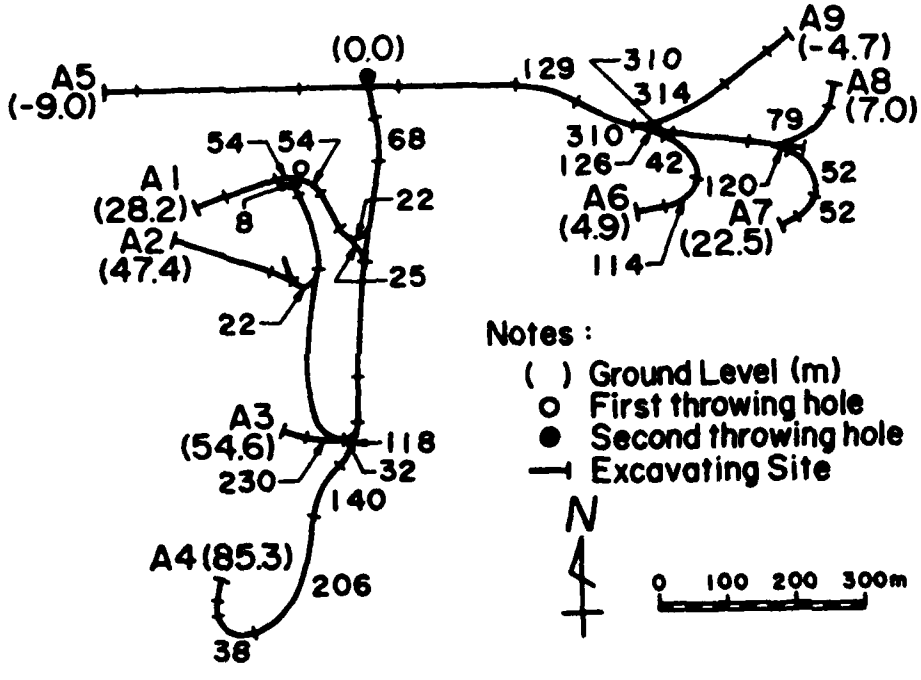

(a) Plan and Radius of curvature (m)

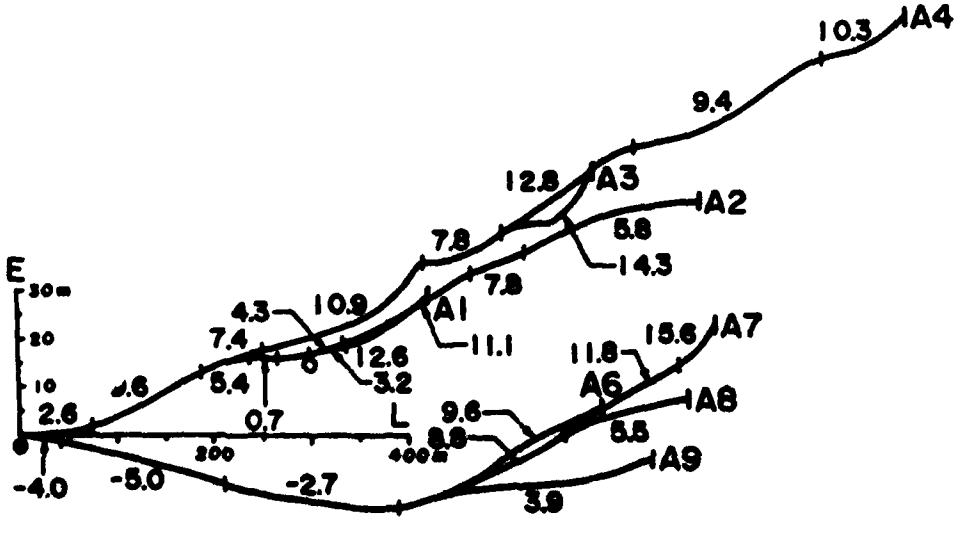

(b) Elevation and Slope (%)

Fig. 4 General view of courses of heavy dump truck

several heavy dump trucks run up and down between first or second throwing hole and each excavating face. Total round distance of each course is about 10.2 Km. Average longitudinal slope is 9.2 %, and maximum one is 15.6 %. The geographical feature of this district is comparatively gentle as shown in Fig. 4 (b) . And the roadbed is composed of weathered granite, of which elastic wave velocity is 690 m/sec for P wave and 405 m/sec for S wave. The road surface is kept in good condition by means of compaction of decomposed granite soils, and it has been justified to be put in a good maintenance from the results of power spectrum analysis [4].

On the other hand, the characteristics of movement of heavy dump truck, i.e. distance, slope, radius of curvature, velocity, acceleration and retardation of vehicle for each section of courses were measured by use of 8 mm movie camera and they have been analysed precisely.

Measurement of Wear Amount of Tyre

All the tyres measured in-situ test are earth moving service tyre 21.00 - 35 - 36 PR ; N type tread of initial depth 68 mm. And it is an off-the-road tyre which is well manufactured for cut resistance. Its standard dimension is as follows ; outer diameter 2050 mm, width 591 mm, height 504 mm, and inner pressure 5.6 kgf/cm^2 (548.8 kPa). As the heat resistance of tyre is comparatively low, the temperature of front tyre which is severely used at carrying down on a slope exposed to the sunshine in summer time was controlled not to be over the critical temperature of tyre 112°C. The amount of wear of tyre was measured every month, and it was expressed as an average value of 4 residual depths of tread which were measured by use of depth gauge at each point of one fourth of tread width.

Fig. 5 (a) shows the measured wear histories of front left tyre FL , front right tyre FR , rear left tyre RL , and rear right tyre RR , which relate residual depth with operation time. Here, the residual depths of tread of FR and RR are calculated as averaged values of inner and outer tyre respectively. Then, an amount of wear of tyre is given as a difference of initial depth of tread and residual depth of it.

In general, rear tyre tends to be worn more than front tyre [5),6)]. But, in this case, the amount of wear of front tyre approached to the same value as that of rear tyre, because the front wheel load increased due to carrying down motion of vehicle and the large braking torque acted on front wheel at braking. The variation of residual depth of tread was remarkable at initial operation time, and the change of amount of wear of tyre with the passage of operation time tended to be expressed by an exponential function. The wear life of each tyre was long enough and it was estimated to be from 4,000 hours to 5,000 hours.

RELATION BETWEEN FRICTIONAL WORK AND AMOUNT OF WEAR

The frictional work per one round movement of each front and rear tyre positioned at right or left hand side of heavy dump truck f_W has been calculated for each course from vehicle motion, and distance, slope and radius of curvature of trail measured in-situ. In this calculation, it is assumed that only rear wheel is drived at driving and both front and rear wheel is braked at braking as the torque ratio B equals 0, 0.5 and 1.0. Next, the frictional work of tyre positioned in k for some period of measurement of amount of wear of tyre $F_W(k)$ is able to calculate as a summation of the product of number of round movement of vehicle n_j on each course j and frictional work per one round movement of each

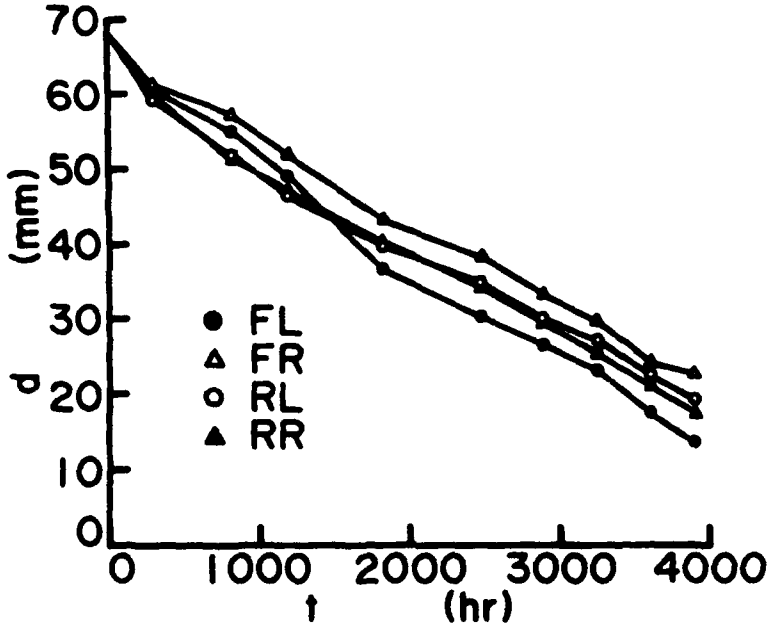

Fig. 5 (a) Measured wear history which relates residual depth d with operation time t

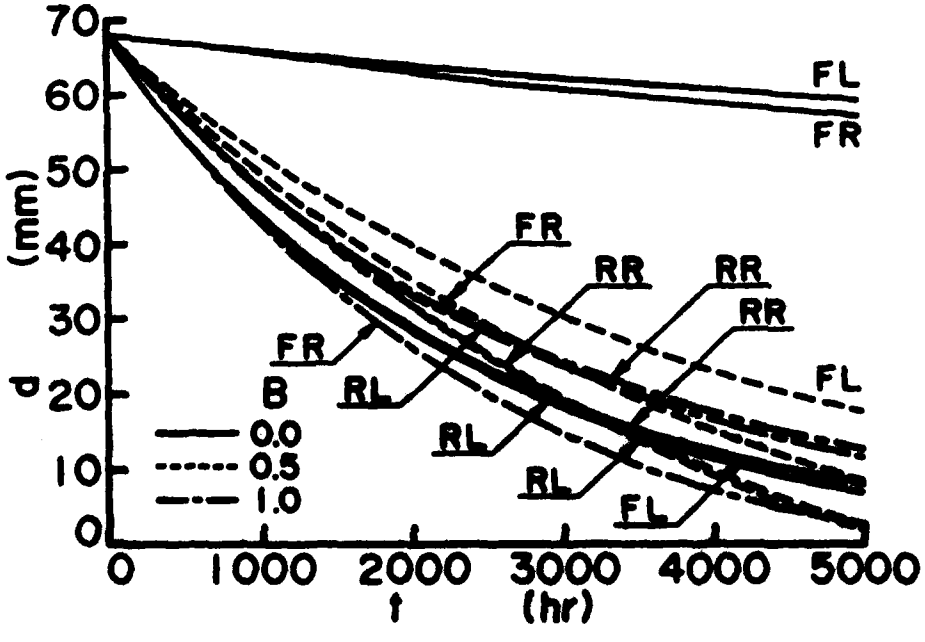

Fig. 5 (b) Residual tread depth d and operation time t calculated for the test heavy dump truck tyre

tyre on each course $f_w(k)_j$.

That is, $$F_w(k) = \sum_j n_j \cdot f_w(k)_j \quad . \tag{21}$$

As the frictional work of each tyre $F_w(k)$ for some period of wear measurement has been calculated by use of μ - s curve determined for a tyre of wear length x_c , it should be modified for the tyre of average wear length x within that period of wear measurement. Assuming the modulus of elasticity in shear of tread is equal to that of carcass, the relation between slip ratio S for a tyre of wear length x and slip ratio S_c for a tyre of wear length x_c is given as follows ;

$$S = \frac{d_0 + d_c - x}{d_0 + d_c - x_c} S_c \quad . \tag{22}$$

Here, d_0 is initial depth of tread, and d_c is converted height of carcass which contributes to tread deformation.

Therefore, the modified frictional work $F'_w(k)$ is given as follows ;

setting $d_0 + d_c = d_a$,

$$F'_w(k) = \left(\frac{d_a - x}{d_a - x_c}\right)^2 F_w(k) \quad . \tag{23}$$

Now, the relations between calculated frictional work $F'_w(k)$ and measured amount of wear $M(k)$ for some period of vehicle operation are shown in Fig. 6 (a) (b) (c) . The frictional work has been calculated for each tyre positioned in FL , FR , RL and RR of the test vehicle for the period of wear measurement at the braking torque ratio $B = 0$, 0.5, and 1.0 respectively. As a result, the frictional work seems to be proportional to the amount of wear. That is,

$$M(k) = a(k) \cdot F'_w(k) \tag{24}$$

Here, $a(k)$ is an amount of wear per unit frictional work of tyre positioned in k , and it takes a constant value determined by tyre structure, tread pattern and rubber material etc.. As the average value of $a(k)$ is defined to be $\bar{a}$ for 6 test tyres, $\bar{a}$ equals 0.928×10^{-6} mm/kgf·m for $B = 0$, $\bar{a}$ equals 1.524×10^{-6} mm/kgf·m for $B = 0.5$, and $\bar{a}$ equals 1.268×10^{-6} mm/kgf·m for $B = 1.0$.

WEAR HISTORY CURVE AND WEAR LIFE

As mentioned previously, the frictional work of tyre F'_w has been given as,

$$F'_w = \int \frac{d_a - x}{d_a - x_c} S_c \mu N v \, dt \quad . \tag{25}$$

Therefore, the variation of wear length of tread Δx with the passage of operation time Δt is able to calculate as follows ;

$$\Delta x = a \, \Delta F'_w = a \cdot \frac{d_a - x}{d_a - x_c} S_c \mu N v \cdot \Delta t \tag{26}$$

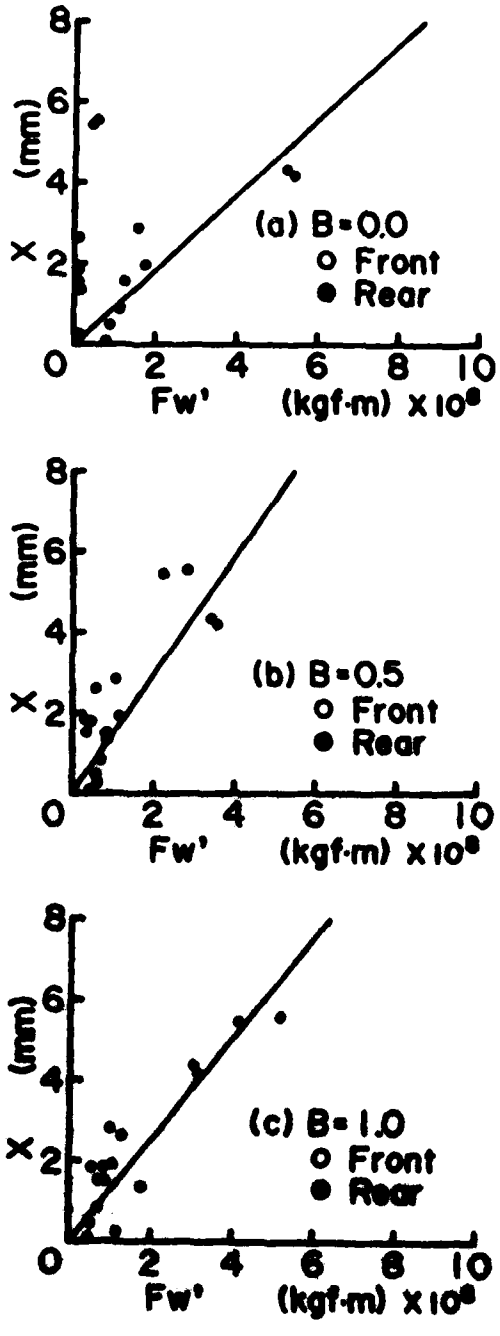

Fig. 6 Relations between amount of wear X and frictional work F'_w of front and rear tyre

Integrating above equation with time for the boundary condition, i.e. $x = 0$ at $t = 0$, it is cleared that the wear history curve of tyre is expressed by an exponential function. That is,

$$x = d_a \left[1 - \exp \left(- \frac{a}{d_a - x_c} \int_0^t S_c \mu N v \, dt \right) \right] \qquad (27)$$

In general, the frictional work of tyre F_w is propotional to the operation time t. That is,

$$F_w = \int_0^t S_c \mu N v \, dt = A W_c \cdot t \quad . \qquad (28)$$

Here, AW_c is a constant. Substituting this relation into equation (27), next equation is introduced as,

$$x = d_a \left[1 - \exp \left(- \frac{a}{d_a - x_c} \cdot A W_c \cdot t \right) \right] \quad . \qquad (29)$$

Then, a wear life of tyre i.e. a total operation time of vehicle t_ξ until a tyre is worn out perfectly, is able to calculate as follows ;

$$t_\xi = \frac{\ell n \, d_a - \ell n \left(d_a - x_\xi \right)}{a \cdot A W_c} \left(d_a - x_c \right) \qquad (30)$$

, where x_ξ is a limit of wear length of tread of tyre.

The estimated wear history curves are drawn smoothly by use of equation (27) or (29) for different braking torque ratio B. Fig. 5 (b) shows the estimated wear history curves of each tyre of test vehicle for $B = 0$, 0.5 and 1.0 respectively. The wear length of front tyre seems to be larger than that of rear tyre when braking torque ratio B varies from 0.5 to 1.0. Furthermore, comparing this estimated wear history curve with that measured one, the value of B is estimated to be about 1.0. That is, the test vehicle is considered that the braking torque of front wheel is nearly equal to that of rear wheel.

In the above calculation, $d_o = 68$ mm, $d_c = 30$ mm, $d_a = 96$ mm, $x_c = 30$ mm, $x_\xi = 58$ mm, and a wear life of tyre is calculated as an operation time when a residual depth of tread becomes 10 mm. For an example, AW_c of left and right rear tyre is calculated to be 1.285×10^6 kgfm/hr and 1.264×10^6 kgfm/hr respectively for $B = 0$, then the wear life of left and right rear tyre becomes 5,125 hours and 5,212 hours respectively.

Therefore, the wear history curve and wear life of tyre is able to estimate properly, if the braking torque ratio is measured accurately.

Furthermore, the relation between wear life of OR tyre and coefficient of its trail condition has been analysed in detail [7].

CONCLUSIONS

To estimate a wear history curve and a wear life of tyre of heavy dump truck, it is necessary to find the relation between amount of wear of tyre measured in-situ and frictional work of tyre calculated during some

operational period for its trail condition and vehicle operational conditions. Afterwards, the total characteristics of wear history curve of tyre should be analysed by means of these relations. Then, the wear life of each tyre is able to estimate properly.

The obtained results are summarized below ;

1) The amount of wear of tyre increases remarkably at the time of driving up a slope or braking down a slope, and especially at driving or braking at cornering site. The wear amount of tyre driving up a slope increases parabolically with its slope angle.

   To decrease the amount of wear of tyre, it is necessary not to drive or brake suddenly on a slope, to design a slope angle as small as possible, to construct a flat cornering site, and to design its radius of curvature as large as possible.

2) The amount of wear of tyre at cornering is inversely proportional to the radius of curvature of trail. When driving or braking torque acts on rear wheel only, the rear tyre is worn away by a large acceleration or retardation of vehicle at a higher slope angle and also by a large centrifugal force to be directly proportional to a square of vehicle speed. At cornering site, the amount of wear of rear tyre turning inside is the greatest of all tyres.

3) In general, the wear history curve of tyre is expressed by a next exponential function.

$$x = d_a \left[1 - \exp \left(- \frac{a}{d_a - x_c} \cdot A W_c \cdot t \right) \right]$$

   Here, x (mm) is a wear length of tread, t (hr) is an operation time, a (mm/kgfm) is a wear length per unit frictional work of tyre, AW_c (kgfm/hr) is a frictional work per unit operation time, d_a (mm) is a converted depth of tread from tyre deformation, x_c (mm) is the wear length of tread when a relation between coefficient of friction and slip ratio of tyre has been measured.

4) The wear life of tyre t_E (hr) for $x = x_E$ (mm) is calculated as follows ;

$$t_E = \frac{\ln d_a - \ln (d_a - x_E)}{a \cdot AW_c} (d_a - x_c) .$$

   Estimating a wear life of tyre by means of the above method may be evaluate to be useful for a management of OR tyre.

REFERENCES

1) T. Muro, M. Enoki ; Characteristics of friction of OR tyre at cornering site, Memoirs of the Faculty of Eng., Ehime Univ., 10, 2, pp. 285 - 297, 1983. (In Japanese)

2) A. Gračenko ; Some applications of slip and drift theory of the wheel, Proc. 5th Int. Conf., I.S.T.V.S., 2, pp. 449 - 472, 1975.

3) T. Muro, M. Enoki and M.Toyotaka ; Characteristics of friction and

wear of OR tyre at driving and braking time, Memoirs of the Faculty of Eng., Ehime Univ., 10, 1, pp. 295 - 313, 1982. (In Japanese)

4) T. Muro, M. Enoki ; Wear of ORtyre —— several measurement in situ test ——, Japanese Terramechanics, 2, pp. 11 - 17, 1982. (In Japanese)

5) T. Muro, M. Enoki ; Relation between trail alignment and wear life of heavy dump truck tyre, Memoirs of the Faculty of Eng., Ehime Univ., 10, 2, pp. 299 - 309, 1983. (In Japanese)

6) T. Muro, M. Enoki ; Wear characteristics of heavy dump truck tyre, Japanese Terramechanics, 3, pp. 90 - 96, 1983. (In Japanese)

7) T. Muro, M. Enoki ; Wear life of OR tyre and coefficient of its trail condition, Japanese Terramechanics, 3, pp. 97 - 104, 1983. (In Japanese)

RUD INTRODUCES A CHAIN DEVICE TYPE "TERRA" - THE NEW COMBINATION OF POLYURETHAN AND ALLOY STEEL FOR SNOW, SAND AND OFF-THE-ROAD TERRAIN

DR.-ING. HANSJORG RIEGER

The increasing expenses in the development of tracked armoured vehicles and thus resulting trend for armoured wheel vehicles has led to the idea to develop an "off-the-road chain". This new design guarantees the maneuverability of a wheeled vehicle and is compatible with a tracked vehicle.

the new developed RUD off-the-road chain type "TERRA" is made of breaking resistant and tough polyurethan in combination with a very robust chain mesh made of alloy steel. Special chain elements allow quick and easy fitting.

Thorough-going tests with leading manufacturers of armoured vehicles have proved that the maneuverability in heavy muddy terrain is identical with the results of a tracked vehicle.

The bearing surface of the tire is increased by approx. 50 %, therefore, the tendency of sinking in of the vehicle is considerably reduced.

The specific arrangement of the single plates guarantees good traction and self-cleaning of the chain.

The result is an improvement of the climbing power and stability on slippery underground as well as on sand.

This new chain device can be used on roads up to max. speed of 60 km/h without damaging the road surface. The tires are protected by the chain and, therefore, their economy is increased.

Please allow us to sum up again in details the main advantages of the "off-the-road chain" as well as to indicate the most popular tire sizes for which this chain device is available.

* plates made of breaking resistant and tough polyurethan in combination with a very robust chain mesh made of alloy steel
* increase of maneuverability in "off-the-road" terrain up to the fielt of (tracked) armoured vehicles
* the bearing surface of the tire is increased by approx. 50 %
* increase of climbing power by approx. 50 %
* stability on underground is guaranteed when firing a cannon
* it is possible to drive on roads up to a max. speed of 60 km/h without damaging the road surface
* tires are protected by the chain
* special chain elements allow quick and easy fitting
* economy of the chain is guaranteed by easy exchange of the plates

Available tire sizes (for single wheels):

11.00-16	20 179
205 R - 16	20 146
7.50-16	20 153
12.00-20	20 202
12.5-20	20 187
13.00-20 Pilote X	20 211
14.5-20	20 201
14.00-20	20 220
18-22.5	20 217
16.9-30	20 619
18-20 EB	20 213
18.00-25	20 249
20.5-25	20 244
22-20	20 676

For dual tires on demand !

Of course, there is the possibility to supply chains for tire sizes not listed above. The question of clearance on the vehicle is very important. To answer the question whether chains can be fitted, the following schedule indicates the minimum clearance required if TERRA chains are used.

Minimum clearance required for fitting the TERRA off-the-road-chain

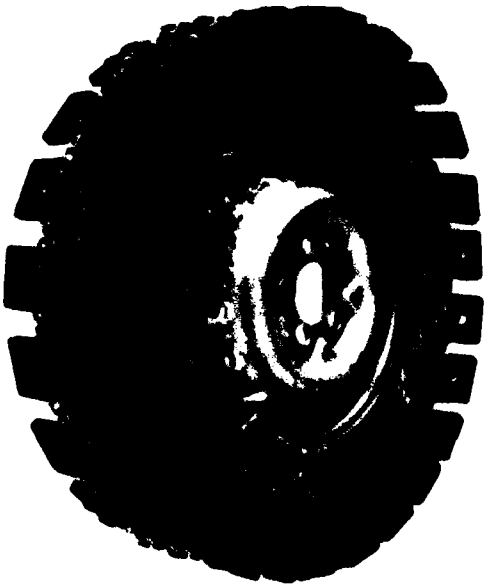

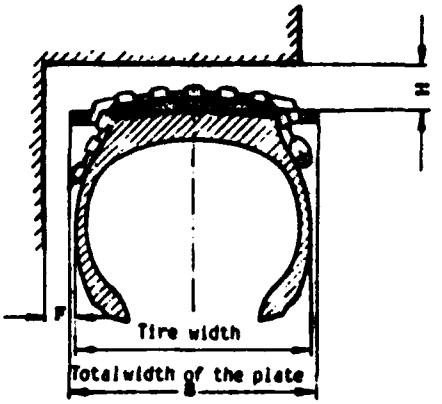

Tire Size	Part No.	B	H	F	Number of plates
11.00 - 16	20 179	355	45	26	21
205 R - 16	20 146	246	30	16	22
7.50 - 16	20 153	295	45	15.5	17
12.00 - 20	20 202	420	50	25	18
12.5 - 20	20 187	420	50	25	16
13.00 - 20 Pilote X	20 211	420	50	25	18
14.5 - 20	20 201	420	50	25	20
14.5 - 20	20 214	420	50	25	22
14.00 - 20	20 220	462	50	28	20
16 - 22.5	20 217	550	56	28	21
16.9 - 30	20 619	550	56	28	26
18 - 20 BS	20 213	590	56	28	20
18.00 - 25	20 249	590	56	28	29
20.5 - 25	20 244	590	56	28	26
22 - 20	20 676	590	56	28	17
12.00 - 20 Zwill.	20 390	792	56	28	21
12 R 22.5 Zwill.	20 386	654	56	28	18
18.00 - 33 Zwill.	20 443	1212	60	60	24

Minimum clearance required on the inner side wall F + 20 mm

Minimum clearance required on tire tread H + 35 mm

The technical details and data are shown in the following information sheet. The material for the plates is a high quality polyurethan with resistance of more than 90 shore. After many and thorough-going tests this material proved to be the most suitable one. The plate is made in a mould or if the quantity will allow it in a more economic way of injection die-casting. During tempering the plates are bended. This bending is important for a better fit of the chains on the tires. The share of cost of the polyurethan plate compared to the chain can be described as approx. 70 : 30 %. Damaged plates can be exchanged at any time with very simple tools.

The chain mesh is made of compact round steel chains made of alloy steel, breaking and wear resistant. The chain mesh can be fitted and closed without any tools thanks to very simple construction elements.

Thanks to the particular design there is no fixed connection between chain and plate. This guarantees above all the realization of such a design.

The chain is covered by patents in most countries of the world.

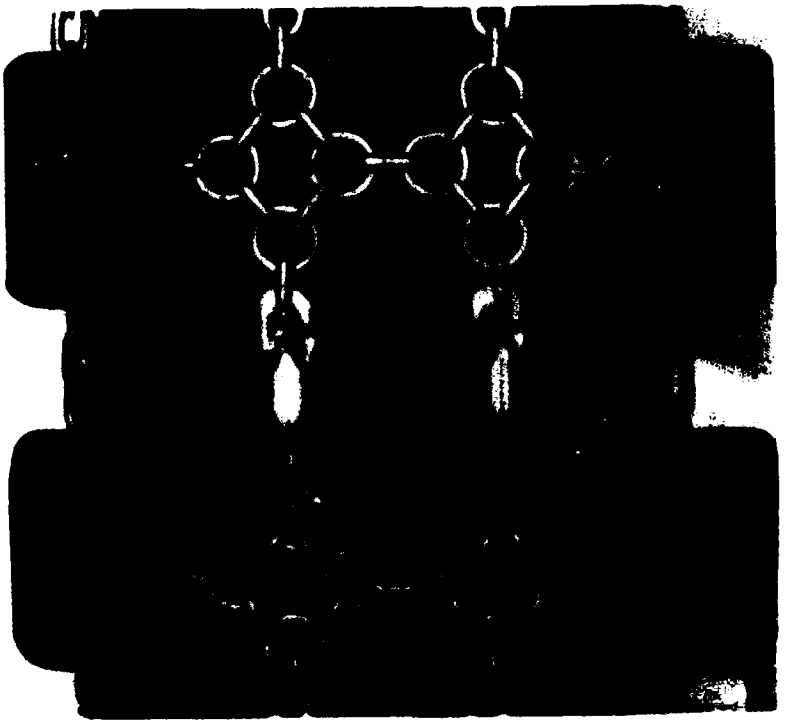

AD-A150 653 PROCEEDINGS OF THE INTERNATIONAL CONFERENCE ON THE PERFORMANCE OF OFF ROA.. (U) INTERNATIONAL SOCIETY FOR TERRAIN VEHICLE SYSTEMS M J DWYER AUG 84 3/4

UNCLASSIFIED [illegible] F/G 13/6 NL

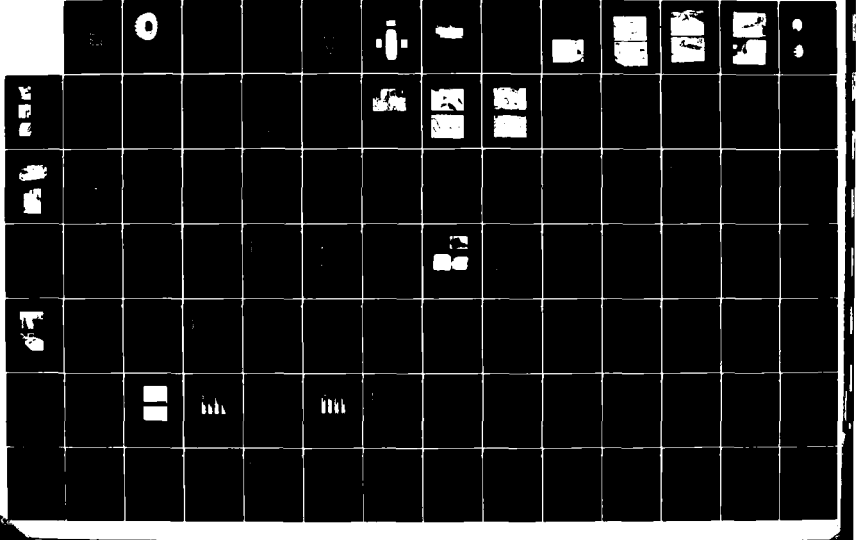

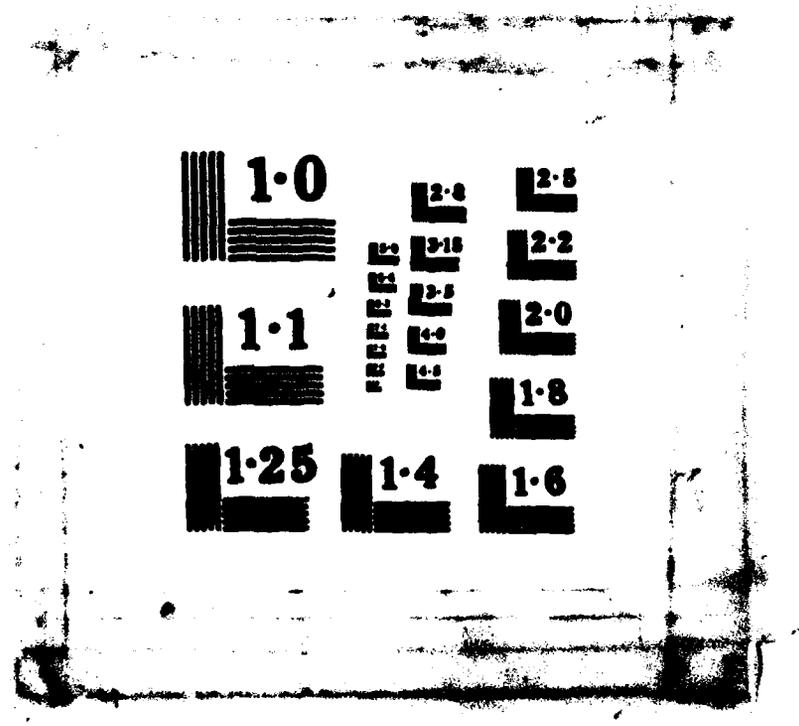
1·0
1·1
1·25
1·4
1·6
1·8
2·0
2·2
2·5

Off-the-road chain, type "TERRA" for working machines

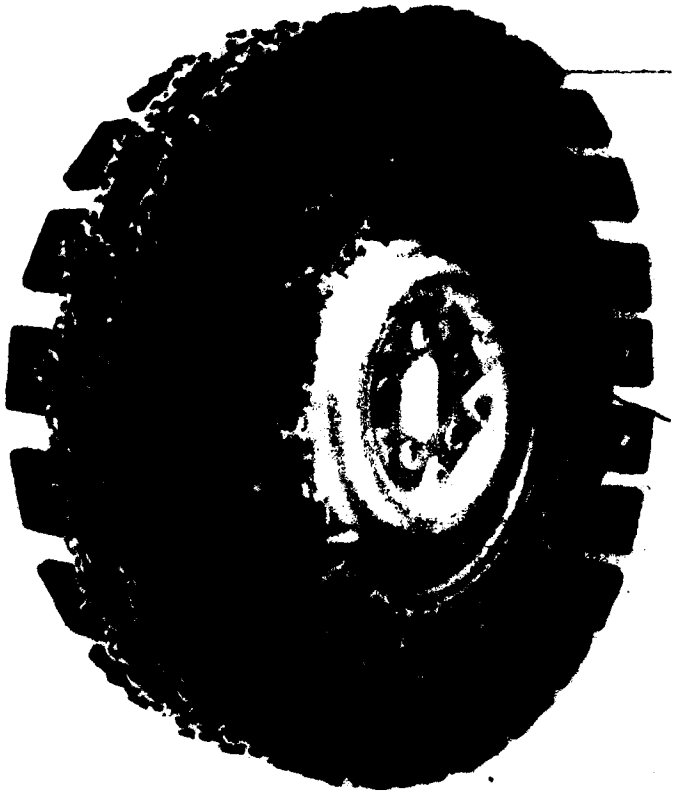

Plates made of elastic, wear resistant polyurethan, in order to protect the road and to enlarge the bearing surface.

Robust round steel chain links made of alloy steel, breaking and wear resistant, meant as additional gripping- and wear elements.

Technical dates

* round steel chain links, protecting tyres and road
* chain mesh also closed without gaps at the connectin point by means of the RUD - central lock
* breaking strength of the chain mesh 350 N/mm²
* the bearing surface of the tyre will be increased on an average by 50 %
* prevents a sinking down
* protects the road an the tyres
* will guarantee an economic application of the device beyond the road
* due to the permission of the design, movable on solid roads also in case of changing the position

Field of application

Cross-country vehicles and machines in off-the-road chains, type "TERRA", have been released by the Kraftfahr-Bundesamt for being used on roads. The only exception are roads paved with clinker cement. With regard to roads paved with black pitch, the chains are only allowed to be used in the period from the 1st October to the 30th April.

The following diagrams demonstrate efficiency of the off-the-road chain type "TERRA". The comparison tests had been made with a non skid chain type DH 74 F, made in our works; this type of chain is introduced with several Nato countries as non skid chain and listed for procurements.

To enable you to have a comparison between a standard non skid chain and the off-the-road chain type "TERRA" we enclose a summary on page 8 of an article published in the magazine "Wehrtechnik", where you can find the most important data for a comparison.

The enclosed diagrams will show you that the main advantage of the "TERRA" chain is the increased bearing surface, which prevents the vehicle to sink. At the same time the traction is essentially increased to compare with a standard tire. The main advantages of the "TERRA" chain are evident: increased bearing surface and traction.

View of tire bearing surface

Enlargement of the bearing surface, which prevents the cave in by using MUD-traction chain type TERRA (off the road application)

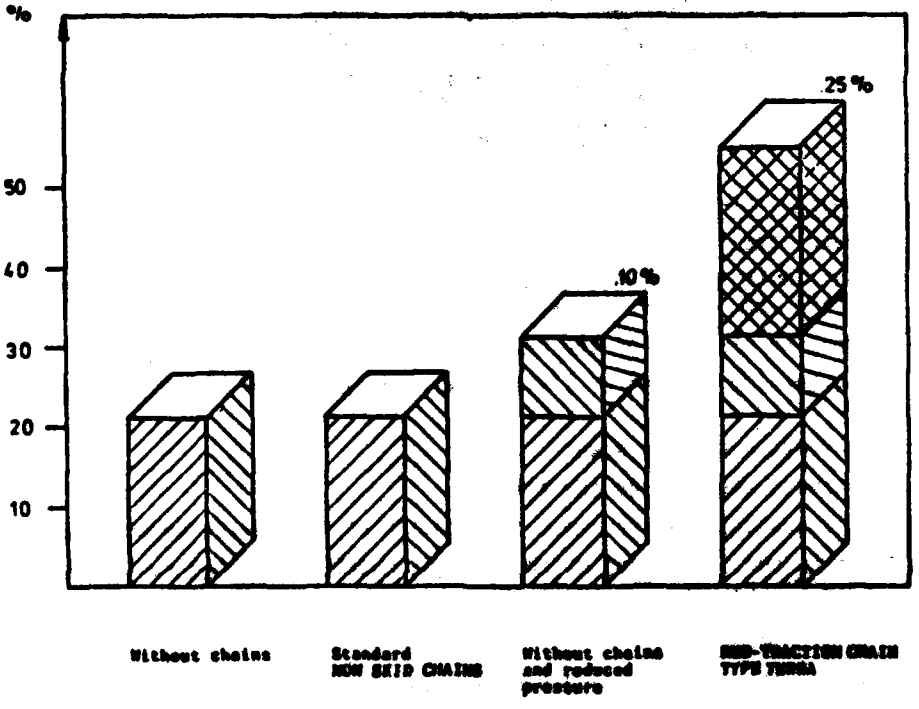

Pulling force RUD traction chain type TERRA (off the road application)

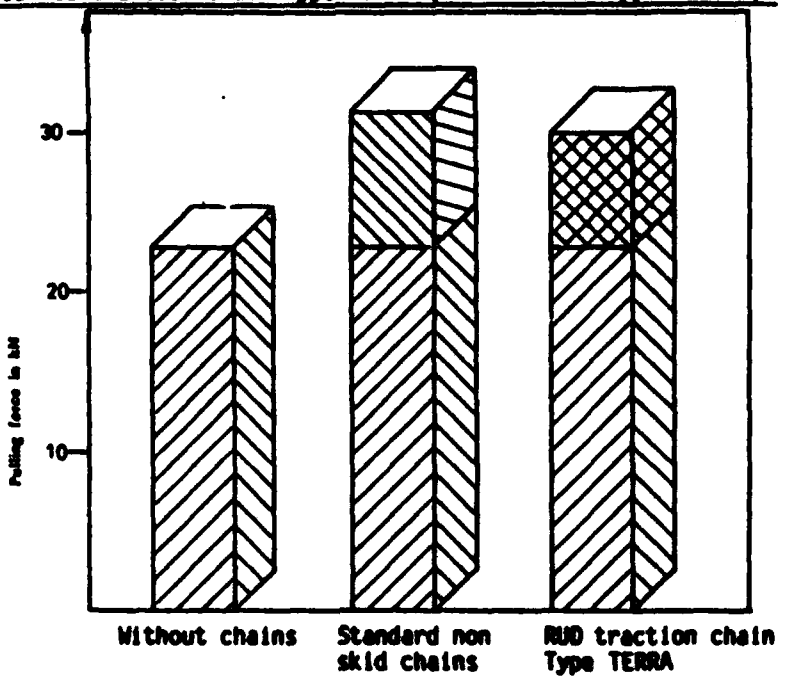

Climbing capability RUD traction chain type TERRA (in muddy underground)

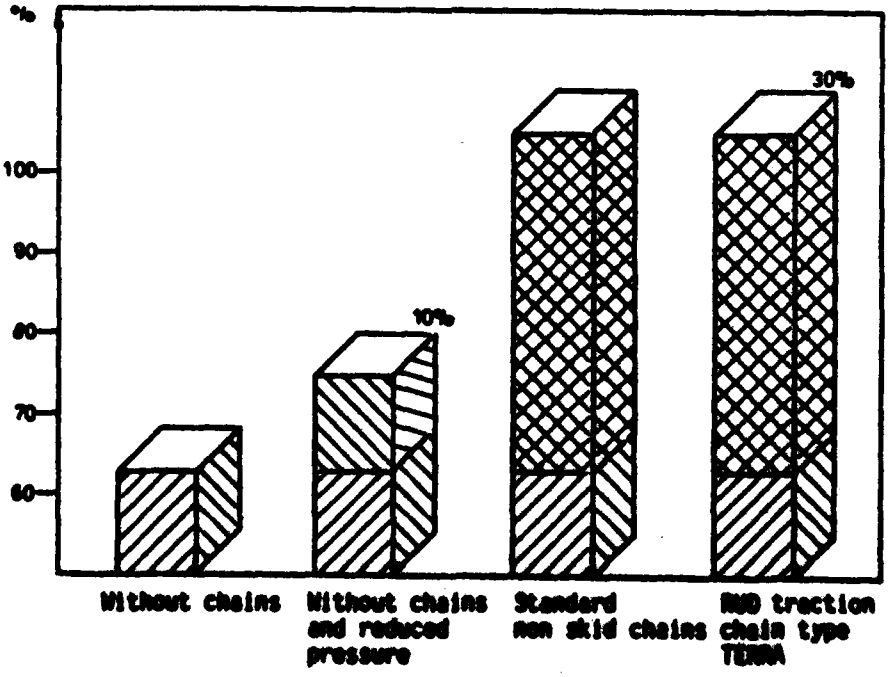

THE NEW TRACTION CHAIN

Articel published in the German Magazine "Wehrtechnik" Issue 8/76

The development of new vehicles with a higher motor force (higher h.p./t) and the application of tires with larger width and higher capacity for both civil and military use requested development of the so far know non skid chains. In addition to this it was alos requested to have chains with a longer service time. During the last ten years RUD-Kettenfabrik Rieger & Dietz GmbH u. Co. of Aalen, West Germany, developed a completely new traction chain device. The tests were made not only in off-the-road duty but also in winter duty and in user tests where chains were used more than 15 000 km (appr. 9 000 miles) on concrete surface. In addition to this the German Bundeswehr made their own tests on non skid chains of different make and construction to find the ideal chain for the vehicles of the second generation. As a result the German Bundeswehr has selected the "Gleitschutzkette DH 74 F" (non skid chain DH 74 F).

The chain mesh is made out of a center strand running in the direction of the wheel circumference. In addition to the longitudinal sections to insure stability against side slips there are oblique chain portions to insure the transfer of the traction forces. The chain mesh of a chain suitable for twin wheels consists out of two parallel designed "single spur-chains".

Contrary to the spur-chain so far used with the German Bundeswehr the inner length of chain links was reduced from the former pitch of five times diameter to a new pitch of only three times the diameter of the chain link. This has considerably increased the resistance against bending and wear. In connection with a change in the raw material the minimum breaking resistance in relation to the link cross-section had been increased from 240 kp/mm² to 320 kp/mm². Additional so-called grip links or wear links are welded to the chain links to make the links "tilt free", which means that the chain links equipped with wear links protect the adjacent chain links. The grip links ideally absorb against all forces. Besides additional wear and grip links provide for manifold up to sixfold higher wear protection.

The off-the-road tire chain [illegible] (for ice, snow, off-the-road and snow-free road) DH 74 F [illegible] chain-free coupling-lever; it is possible to adjust [illegible] according to the ground conditions. The chain can be [illegible] without any additional tools.

The traction force of the chain was [illegible] in Sweden on a snow-covered road by measuring the torque of the driving-axle of a 16-t-truck and a 22-t-trailer. The [illegible] twin wheels 12.00-20 M+S. The results: tire chains fitted on the outer wheels of the twin tires increased the [illegible] chains fitted on twin wheels even 60 %.

To underline how important non skid chains can be, we have to recall that the tire grip on snow-covered roads is approx. 25 % reduced compared with a dry asphalt road. The reduced driving-force does not allow to move the vehicle or to keep it on the road.

In soft and swampy terrain the traction of vehicles can be increased by 100 up to 200 % by using non skid chains DH 74 F. This means in far more than a "snow chain" but a many-purpose device of the vehicle.

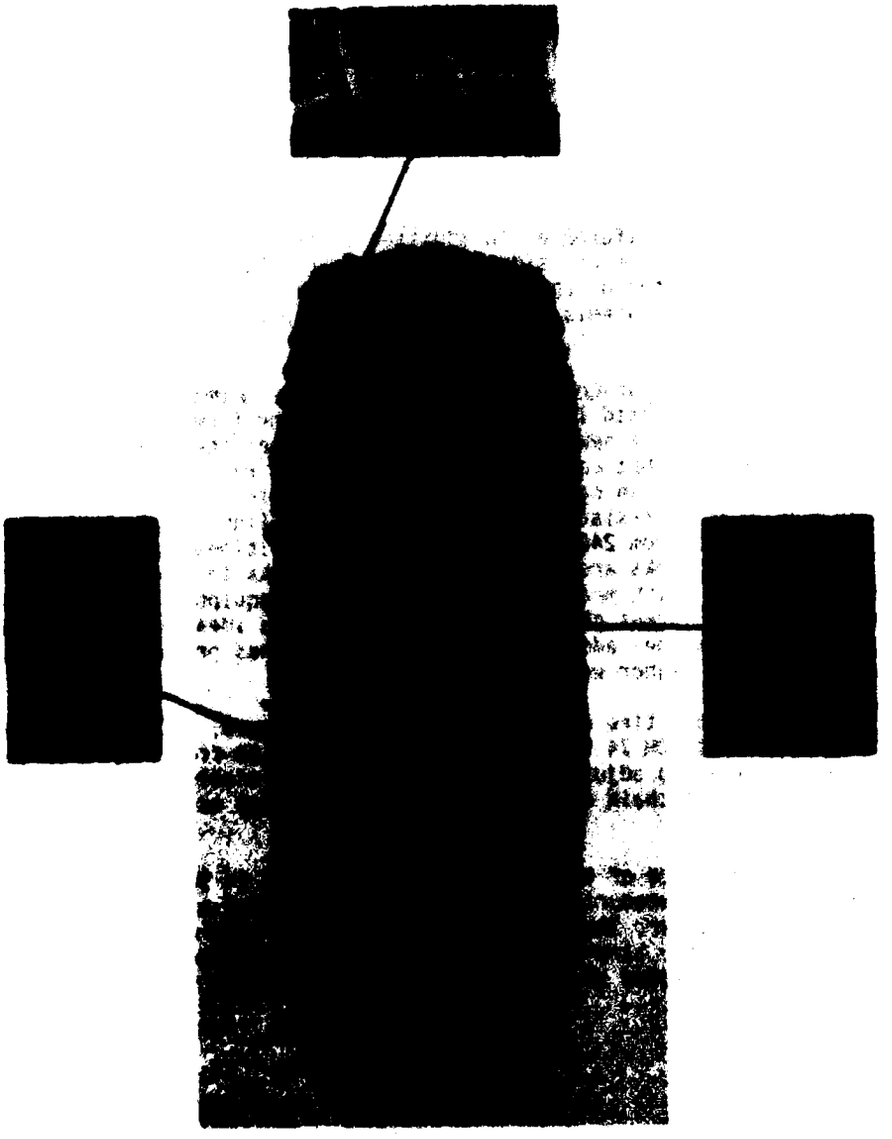

OFF-THE-ROAD CHAIN TYPE "TERRA" FOR USE ON SAND

Besides using the off-the-road chain type "TERRA" in muddy conditions a great advantage could be found for application in sand. The vehicle is much easier to manoeuvre.

Instruction of use for RUD off-the-road chain Type TERRA on sand:

* fit the chain according to fitting instruction
* then reduce tire pressure to 1,5 atü
* after sand operation increase tire pressure to standard.

The summary of a test report of an important French car manufacturer indicates:

The manoeuverability of a chained vehicle in pulverized sand is increased compared to an unchained vehicle, because of the strong reduction of the ground pressure.

Please find below the summary of a test report of a large French manufacturer for armoured wheeled vehicles for your information. These tests had been made by this company by their own and, therefore, can be considered to be neutral.

Tests with TERRA chains in muddy terrain

Objective of the test: to find out whether the TERRA chain made by RUD will increase the maneuverability of the vehicle.

Time and place of the test: April 13/14, 1982 in Mailly

Test vehicles:

Vehicle no. 08, total weight 7,9 t
2,8 l motor capacity, mixture 8,2
260 service hours reached
front and rear wheels chained with TERRA.

Vehicle no. 00, total weight 7,8 t
2,6 l motor capacity, mixture 8,2
230 service hours reached.

Conditions of test:

Terrain very muddy with deep water holes
street covered with asphalt

Tests of the TERRA chain:

To find its purpose, the description, the fitting and the advantage of the TERRA type chain.

Dimensions:

The chain is fitted to the tire having an air pressure like under normal conditions; if the thickness of the chain is added, the ground clearance is increased by more than 100 mm, compared with a ground clearance of a vehicle which tires have a tire pressure of 3,5 bars in muddy terrain.

Due to the fact that on a test in sand the ground pressure area of a chain wheel is one third higher than the ground pressure area of the tire, the ground pressure is reduced by 33 %.

Dynamic tests:

Terrain: The dynamic tests were made over 3 hours. The vehicle no. 08 fitted with TERRA chains had no difficulties at all to overcome the obsticles at one. The other vehicle no. 00 was forced several times to overcome the difficult spots and was blocked five times. The tests are continued on a different terrain. The greater maneuverability of the vehicle no. 08 results in three reasons:

1. Ground clearance more than 100 mm
2. Ground pressure reduced by one third
3. Grip of the TERRA chain,
   the individual plates of which are flexible against each other and, therefore, they are self-cleaning; contrary to this the profile of the tire will be filled with mud and consequently, the tread of the tire remains even and slippery.

Road:

A distance of 40 km was driven on a road covered with asphalt. Maximum speed was 60 km/h. This speed can be reached without damaging the cover of the road.

Off-the-road terrain:

The chain can be easily repaired in muddy terrain

Summary:

In muddy and marshy terrain the use of the TERRA chain will considerably increase the manouverability of the vehicle and enable that vehicle to climb over obsticles and difficulties, which would not be possible with an unchained vehicle.

The tests were realized in deep mud, however, with a solid underground. The output of a TERRA chain in rice fields in the Far East can only be confirmed. The easy maintenance guarantees a quick repair.

A few photographs will demonstrate the manifold possibilities for the use of the off-the-road chain type TERRA.

Last but not least we would like to show you in short the different phases of the fitting of the TERRA type chain.The fitting is made in a very simple way, no tools are required. To fit chains on 4 tires approx. 15 - 20 minutes are required.

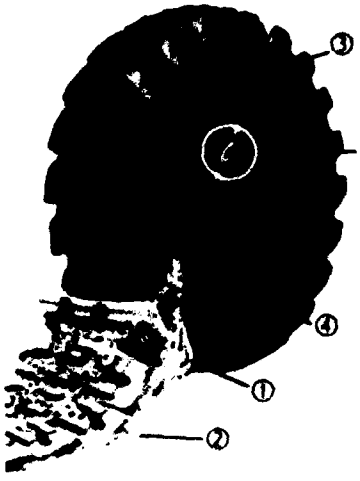

Fitting and taking off the RUD corss country chain is done in the same sequence and handling as with RUD non-skid chains. Lay out the cross country chains closely in front or behind of the wheel and arrange them. Coupling lever ① and tensioning chain ② outwards. Put fitting chain ③ across the tyre and close by fastener (arrow). Attach side chain by hooks ④ or by copperplated fitting hooks.

Drive slowly for about one wheel revolution. Thereby the chain will creep across the tyre.

Starting inside close side-chain ⑤ with hook ④ then outside of the wheel.

Remark: If tyres are badly worn, you may fit side-chain shorter.

Fit central fastener together in an angle of 90°.
See picture.

Tighten tensioning chain outside of wheel and introduce the hook ① into the next link within reach of the tensioning chain ②. Close hook.
Remark: Retension chain after short drive (approx. 10 m). Chain should be strongly tightened on the tyre.
Dismanting of Terra chains to be done the other way round.

USE OF MICROCOMPUTER TECHNOLOGY TO IMPROVE THE PERFORMANCE OF TRACTOR/IMPLEMENT COMBINATIONS

J.M. WILKES, S.W. BURRAGE, M.J. VARLEY

WYE COLLEGE (UNIVERSITY OF LONDON), WYE, NR. ASHFORD, KENT, ENGLAND

ABSTRACT

With the steady increase in the size of tractors and implements, it is becoming important that the operator has more information on performance to provide improved opportunity for maximising productivity of machinery and labour while maintaining the quality of work. This paper discusses the application of microcomputer technology in monitoring the performance of tractor/implement combinations in the field. A package installed on a tractor and used in research projects at Wye College is described. Details are given of sensors that are used to measure performance parameters including engine speed, governor setting, pto torque, drive wheel speed, forward speed, and the forces on the three point linkage. Engine power, pto power, drawbar pull and power, wheel slip and dynamic weight can also be derived by the computer for immediate display. While all these parameters may be important for research and development work, many would also be useful in normal tractor operation. The problems of developing simple tractor based packages are discussed.

INTRODUCTION

What information does the operator require to maximise the productivity of machinery and labour while maintaining the quality of work? With the steady increase in the size of tractors and implements and the relative increase in the cost of skilled labour, much more information on performance parameters is needed to improve the efficiency of field operations. For many years tractor drivers only had information on engine speed from which approximate forward speed and pto speed could be derived, and on parameters which could indicate pending equipment failure such as engine oil pressure, coolant temperature and fuel level. However, since the mid-seventies and the rapid development of micro-electronics, many monitoring systems have been developed to improve the performance of particular field operations such as combine harvesting, seed drilling and crop spraying (Wilson, 1983).

More and more information is being made available by research workers on the effects of changing parameters on tractor and implement performance. If much of this information is going to be of value, more information must be available to the driver during operation. A microcomputer can provide the heart of the information system. It could monitor the required parameters and derive others for immediate display. The development of display technology will be very important in providing the information in an effective way (Wright, 1983). The microcomputer can provide the versatility to cater for the wide variety

of operations by using different programmes for different types of operation. Changes in software may also be made as machinery developments occur.

In recent years work at Wye College has concentrated on the development of sensors for use in research on the performance of tractor/implement combinations in the field; particularly tillage operations which utilise both drawbar and pto power. A microcomputer was introduced in 1982 to act as a data logger but also to provide the operator with instant feed-back from each sensor. This meant that data could be studied as it was being collected and recorded and any equipment failure was immediately apparent.

THE DATA LOGGING PACKAGE

The data logging system is fully mounted on the tractor under test (Fig. 1) and is powered by a 900 W generator and tractor batteries. Figure 2 illustrates the architecture of the system. Sensors with an analogue signal are linked to the computer through a 12 bit, 32 channel, analogue to digital interface. Sensors with a digital pulsed signal are linked through a 4 channel, 12 bit, counter interface. The counters are re-set to zero immediately following a computer scan.

The computer can be programmed to scan all channels with a choice of scanning frequency from 1 per second to 1 per 255 seconds. If a more detailed study of an individual channel is required, the scanning frequency can be increased to a maximum of 1000 readings per second. The output of each channel is indicated on the screen. To enable rapid data storage, readings are stored in the computer's memory during a test run. At the end of each run the data are transferred to cassette tape and the memory cleared ready for the next run. The screen is very important for keeping a check on the performance of each channel and for early detection of equipment failure or malfunctions.

The data stored on cassette tape are transferred to diskette for storage using a second microcomputer. The recorded data can be easily examined either as individual or groups of channels using graphical displays on the screen or printer.

The data logging software can include the calibrations of the sensors to engineering units. This means that displayed data can be more easily related to the parameters being measured than if it were in the form of voltages and frequencies.

SENSORS

Sensors are mounted on the tractor to measure and record performance parameters including engine speed, drive wheel speeds, forward speed, governor setting, pto torque and the forces on the three point linkage.

Engine Speed and Forward Speed

The sensors for engine speed and forward speed use miniature magnetic pick-ups with digital output. The device responds to movement of ferrous parts past the pole piece at the end of the unit. A toothed wheel gives an output of one pulse per tooth as it rotates past the

sensor. The engine speed sensor is fixed in close proximity to the timing gear on the camshaft. The forward speed sensor is fixed in close proximity to a disc fixed to the inside of a 'fifth' wheel which is mounted on the tractor or implement under test. The disc has 180 perforations evenly spaced in a circle close to its outer edge so that the sensor has an output of 180 pulses per revolution of the wheel.

Drive Wheel Speeds

A different type of sensor was selected for drive wheel speed due to the slow rotation involved. Slotted opto-switches are used in conjunction with discs mounted on the inside of each drive wheel (Fig. 3). The slotted opto-switch has an infra-red source and sensor housed in a moulding which incorporates an infra-red filter to minimise ambient light effects and also give dust protection. Each disc has 180 teeth around its circumference which pass through the infra-red beam and give an output of 180 pulses per revolution of the wheel.

Governor Setting

The position of the governor control lever is sensed using an angle encoding potentiometer with 12 bit resolution mounted on the injector pump (Fig. 4).

Pto Torque and the Forces on the Three Point Linkage

A British Hovercraft Corporation strain gauged transducer incorporating slip rings and brushes is mounted on the tractor's pto shaft (Fig. 5) to indicate pto torque. A modified 'Scholtz' linkage (Fig. 6) is used to sense the forces on the three point linkage. The length of the pto transducer and 'Scholtz' linkage are basically the same so that the geometry of implement attachment is maintained except for the extra spacing required. This results in more weight transfer and reduces the maximum weight which may be carried on the linkage.

The Scholtz linkage has 7 strain gauge bridges: 3 sensing the horizontal (draught) forces on each link; 2 sensing the vertical forces on the two lower links; and 2 sensing the sideways forces on the two lower links. The top link is mounted in such a way as to eliminate vertical and sideways forces.

DERIVED PARAMETERS

Figure 7 illustrates some other parameters which may be derived from those measured and recorded. Pto power, drawbar power and wheel slip are derived using straight forward calculations from the parameters shown.

The calculation of engine power uses the principal of governor control which senses engine speed to adjust fuel input and thus power developed. At each setting of the governor control lever there is a relationship between engine speed and power developed. After calibration on a pto dynamometer and an adjustment for pto transmission losses, power developed by the engine can be calculated from accurate measurement of engine speed and the position of the governor control lever.

The dynamic weight on the drive wheels can only be calculated from the horizontal and vertical forces on the three point linkage, if there is also a knowledge of the tractor wheelbase, static axle weights, the position of the three point linkage and the slope of the land on which the tractor is working.

DEVELOPMENT OF TRACTOR BASED PACKAGES

The system so far described has been designed for use in research and development relating to the field performance of tractor and implement combinations. A requirement for this system has been the ease of transfer of the equipment from one machine to another. A system built into a tractor to provide the driver with more information on performance parameters would be part of the integral design of the tractor and associated implements. Transducers would be built into the body of the tractor and would probably be less complex than those used in the Wye R and D package.

The main problems of installing such a system on a tractor are maintaining enough flexibility and adaptability to cater for all the different types of operation in which tractors are involved and standardising the interface between transducers on implements, machinery and the tractor system.

The microcomputer provides the necessary flexibility by permitting changes in software for different types of operation. It enables a suite of programmes to be available to fit the range of operations to be carried out. Further programmes may be added as advances in technology and equipment changes occur, reducing the likelihood of obsolescence.

A system would need to cope with different types, numbers and positions of transducers. In order to facilitate interchangeability and mixing of equipment from different sources, some standardisation would be necessary. This would particularly apply to the link between the tractor and implements in relation to the power supply to the transducers and the nature of the output signals from them.

Another very important area will be the development of display technology to present the information in an effective way preferably colour coded to indicate good or bad performance at a glance. The provision of audible information may also be of use where direct observation is not possible. However this area should be approached with caution as additional noise can have a negative effect.

A record for analysis at a later time might be an advantage for the operator to assess his overall performance.

SUMMARY

There is no doubt that the tractor driver requires more information available to him in order to have the opportunity to carry out field operations most efficiently in relation to both rate of work and quality of work. More information may also reduce the risk of accidents and equipment failure. The best way by which this information can be communicated to him is an area worthy of exploration.

A microcomputer based system built into the tractor offers a flexible and adaptable system to cater for all types of field operation and has obvious advantages over the current trend towards separate monitoring systems for each type of operation. The cost of the microcomputer based system is likely to be small relative to the cost of the tractor, implements and labour. A system should pay for itself quickly through increased rates of work, quality of work and fewer breakdowns.

This paper has discussed the provision of information to the operator of a tractor. However, the microcomputer is also capable of carrying out control functions such as the control of forward speed, tyre pressures, weight transfer, the differential lock and the depth control of implements. In fact any complex operation which is difficult to perform with any accuracy under human control.

REFERENCES

1. An update on automotive electronic displays and information systems, p 129, SAE International Congress and Exposition, 28 February - 4 March, 1983.

2. SCHULZ, B.G. (1966). A three-point linkage dynamometer for restrained linkages. J. agric. Engng Res. 11 (1): 33-37.

3. WILSON, R.J. (1983). A history of instrumentation on agricultural equipment. SAE paper 830322, p 181-189 of 1.

4. WRIGHT, P. (1983). Display concepts for agricultural vehicles. SAE paper 830323, p 191-198 of 1.

Figure 1. The data logging system on the tractor

Figure 2. The architecture of the data logging system

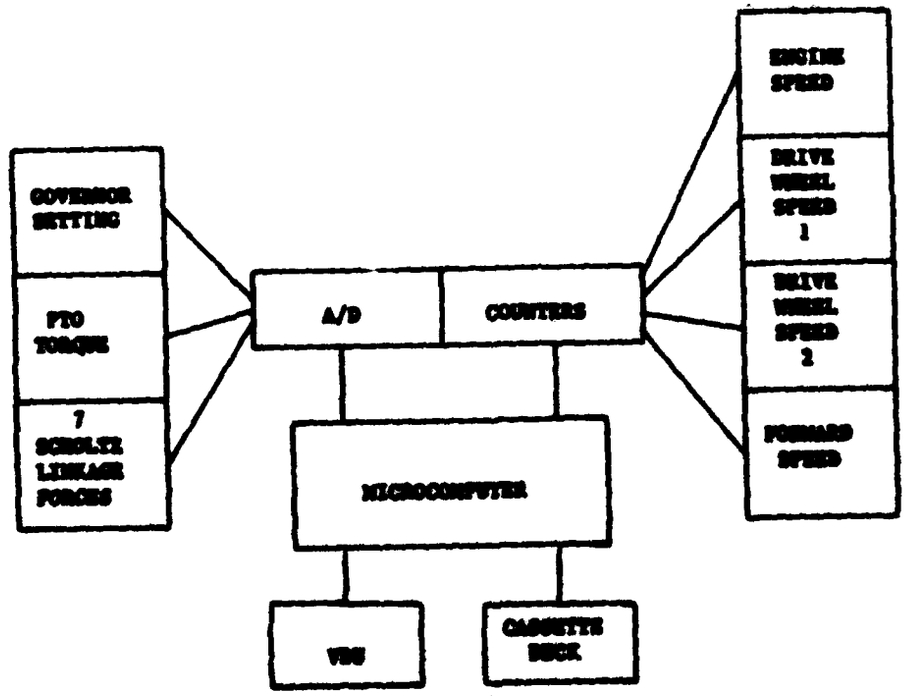

Figure 3. The position of a drive wheel speed transducer

Figure 4. The potentiometer indicating governor control setting

Figure 5. The pto torque transducer

Figure 6. The three point linkage transducer

Figure 7. Parameters which may be derived from those measured and recorded

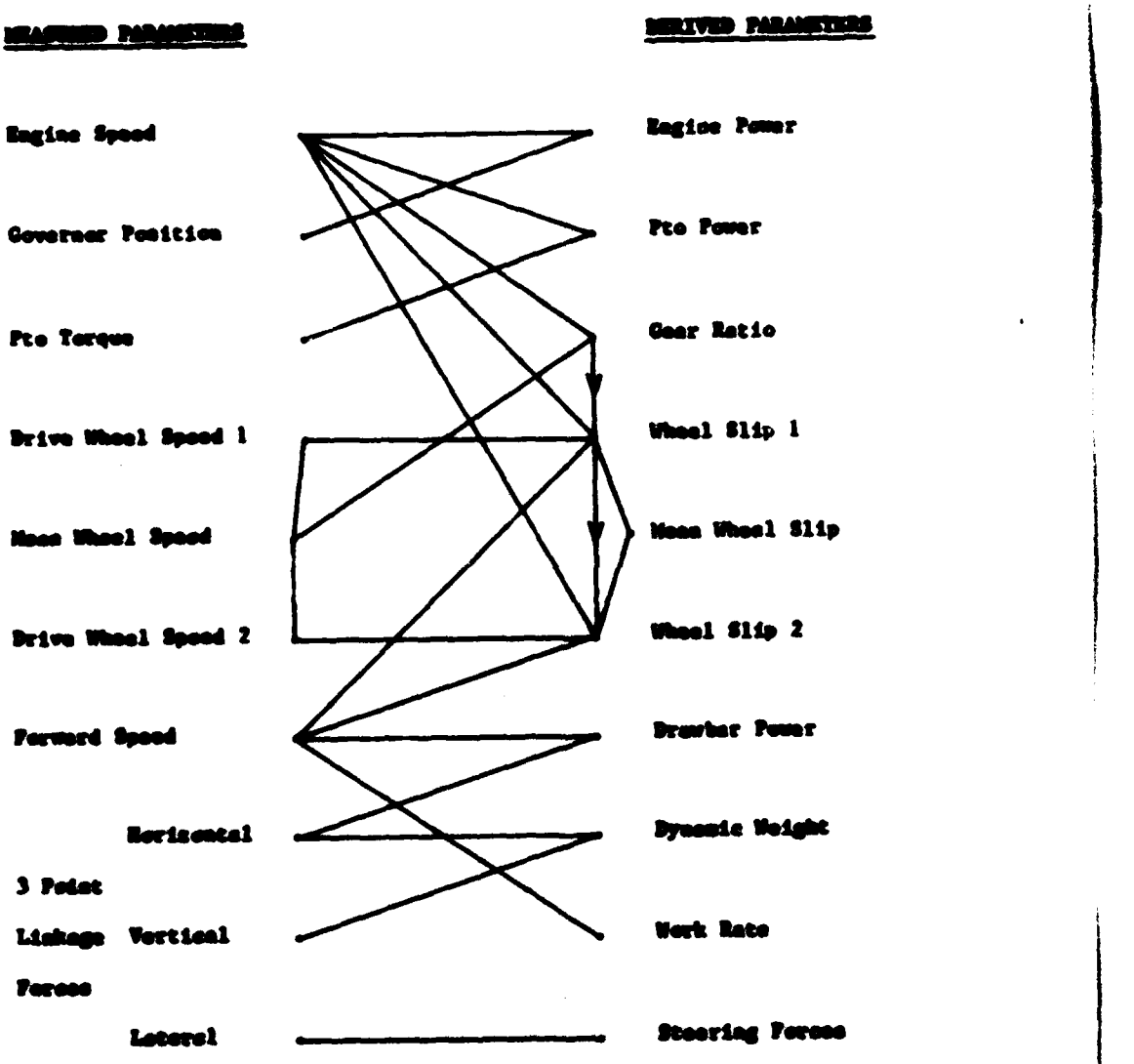

TOPIC 11

MEASUREMENT OF SOIL AND SNOW PROPERTIES
AND SOIL ICE FACILITIES

MEASUREMENT OF SOIL PROPERTIES IN DRYLAND AND WETLAND CONDITIONS

D. GEE-CLOUGH, M.A. SARGANA

AGRICULTURAL AND FOOD ENGINEERING DIVISION, ASIAN INSTITUTE OF TECHNOLOGY, P.O. BOX 2754, BANGKOK, THAILAND.

The effect of deformation rate on cone index value, plate sinkage parameters, cohesion and internal friction angle was measured in a dry, sandy loam soil and in a saturated, puddled clay soil. The effect of normal pressure on calculated values of cohesion and internal friction angle in the sandy loam soil was also investigated. Deformation rate did not greatly affect any of the soil properties in the sandy loam soil but significantly affected almost all of them in the puddled clay soil. In the sandy loam soil it is shown that normal pressure in the ring shear test must be close to that exerted by the vehicle on the soil otherwise large errors can occur in calculating cohesion and internal friction angle.

1. INTRODUCTION

The main soil properties used in terramechanics theories are cohesion, internal friction angle, cone index value and plate sinkage parameters. The way in which cohesion, internal friction angle and plate sinkage parameters are measured is meant to simulate the passage of vehicles through the ground. Cone index is simply something which is easy to measure and has been found to correlate reasonably well with tractive performance. Even though the method of measurement is meant to simulate the passage of vehicles it is unlikely in fact that it does with the instruments now in use. Wong[1] states that shear rates of 2-25 cm/s are common in off-road vehicles. There are very few shear meters in existence which can be worked at 25 cm/s. It is likely that many devices now in use, particularly the hand-held devices, work at one-fifth of this rate or less. In addition the rate of shear is very rarely even measured. Similarly this rate of 25 cm/s is roughly the rate at which a 1.6 m dia. wheel travelling at 1.6 m/s and making a 4 cm deep rut is compacting the soil. There are very few plate sinkage meters which can be used at this rate. The A.S.A.E. standard penetration rate for cone penetrometers is 3 cm/s which is only one-eighth of this rate. Similarly the pressure which off-road vehicles can exert on the soil can frequently be 150 kPa or higher. There are few shear meters which can provide pressures as high as this while maintaining adequate contact area.

This study was undertaken to find out the likely errors in measuring soil properties due to failing to simulate the conditions caused by the passage of vehicles. It was conducted in a dry, sandy loam soil and a saturated, puddled clay soil.

2. PREVIOUS WORK

Freitag[2], in experiments in clay soil, measured by how much the cone index value increased or decreased when penetration speed was changed from the "standard" 3 cm/s value. He found that below this speed the cone index value decreased rapidly, but that above 3 cm/s the cone index value tended to level off and that at a speed 13 times the standard value the cone index value had increased by approximately 30%. In similar tests in sand he reported that no speed effects were apparent other than those which could be explained by inertia effects.

Emori and Schuring[3] stated that the force required to push a plate into the soil should be able to be modelled using the following equation:

$$F = f_1(z) + f_2(z, \dot{z}) + f_3(z, \ddot{z}) \qquad \ldots\ldots (1)$$

where F = force acting on the plate

z = penetration depth

$\dot{z}$ = plate velocity

$\ddot{z}$ = plate acceleration

They did not however produce any experimental evidence to support the model.

El-Domiaty and Chancellor[4] measured the influence of strain-rate on soil cohesion and internal friction angle of a saturated clay soil using a triaxial testing machine. They found for both overconsolidated and normally consolidated specimens that cohesion was strongly dependent on strain-rate but that internal friction angle was independent of strain-rate.

Flennikan et. al.[5] used an apparatus in which a guided weight was dropped onto an unconfined soil sample. Strain rate was varied by varying the height from which the weight was dropped. They reported that dynamic peak stresses in the soil were from 100 to 500 percent greater than the maximum stresses obtained in quasi-static tests.

Stafford and Tanner[6] used a shear annulus to measure the effect of rate of deformation on soil shear strength in a sandy clay loam and a clay soil at different moisture contents. They reported a logarithmic relationship between cohesion and deformation rate with only small increases in cohesion above a rate of 1 m/s. Large increases in cohesion with increasing deformation rate were measured in the range 0-1 m/s however. There was no clear relationship between deformation rate and internal friction angle in these experiments.

Wong[1] states that measurement of soil properties for terramechanics analysis should be made using, for example, loading pressures and deformation rates similar to those exerted on the soil by the passage of vehicles. He does not quantify the errors which can be caused if these conditions are not simulated adequately. In fact with many devices for measuring soil properties in common use today, particularly the hand-held devices, it is almost impossible to simulate these conditions. The

following experiments were therefore carried out with three devices now in common use, namely a cone penetrometer, plate sinkage meter and shear annulus to measure the effect on soil properties of deformation rate. In addition the effect of normal pressure on cohesion and friction angle measured using the shear annulus was also investigated.

3. APPARATUS USED

A Bevameter was designed to be mounted on the A.I.T. soil bin carriage (Fig. 1). The carriage is basically a remote controlled tractor with forward speed, lift arm position and power-take-off speed able to be varied continuously during a run. A 50 kW diesel engine drives two hydraulic pumps, one of which powers the drive wheels (primary circuit) and the other the p.t.o. and lift arms (secondary circuit). When using the Bevameter the flow from the secondary circuit pump was diverted through the Bevameter hydraulic system. This consisted of a hydraulic ram, the fluid flow to which was controlled by a manual control value which was pressure and temperature compensated. The system was designed so that ram speed could be pre-set anywhere between 1-25 cm/s and would stay constant whether the ram was loaded or unloaded. The Bevameter is shown in Fig. 2 and a schematic of the system showing also the instrumentation used is shown in Fig. 3.

The cone penetrometer had a standard sized cone of 3.2 sq.cm base area. The plate sinkage tests were carried out using a 6 x 12 cm plate. The shear annulus had an outside diameter of 30 cm and inside diameter of 20 cm.

Two soils were used, a sandy loam soil with moisture content 3% (d.b.) and a saturated, puddled, clay soil. The clay soil was prepared so that it simulated a rice field ready for seedling transplanting. The sandy loam soil was in a similar condition to a dryland seedbed.

4. RESULTS

4.1 Cone Index

Results from the cone penetrometer experiments are shown in Fig. 4. The saturated clay soil was seen to have a distinctive layered pattern with the zone 0-15 cm being much different than the zone 15-30 cm. Consequently the cone index value was calculated separately for each zone. The cone index value for the sandy loam was the average cone penetrometer resistance in the zone 0-30 cm.

Cone index in the sandy loam soil was independent of rate of penetration in these experiments but cone index in both layers of the clay soil was strongly dependent on penetration rate. The best fitting straight lines to the data for the clay soil were:

$$C = 10 + 31\,V \quad \text{(upper layer)}$$

$$\text{and } C = 86 + 101\,V \quad \text{(lower layer)} \qquad \ldots\ldots (2)$$

where C = cone index value (kPa)

V = penetration rate (m/s)

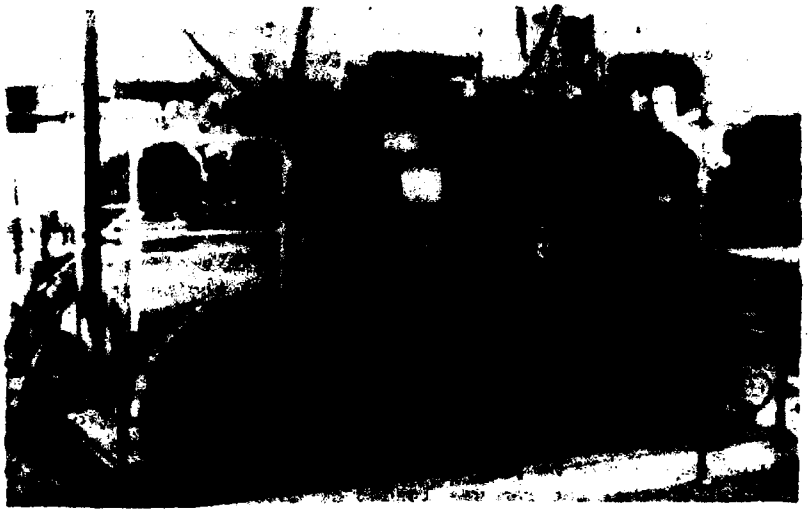

Fig. 1. AIT Soil Bin Carriage

Fig. 2. Dynamometer Used in Experiments

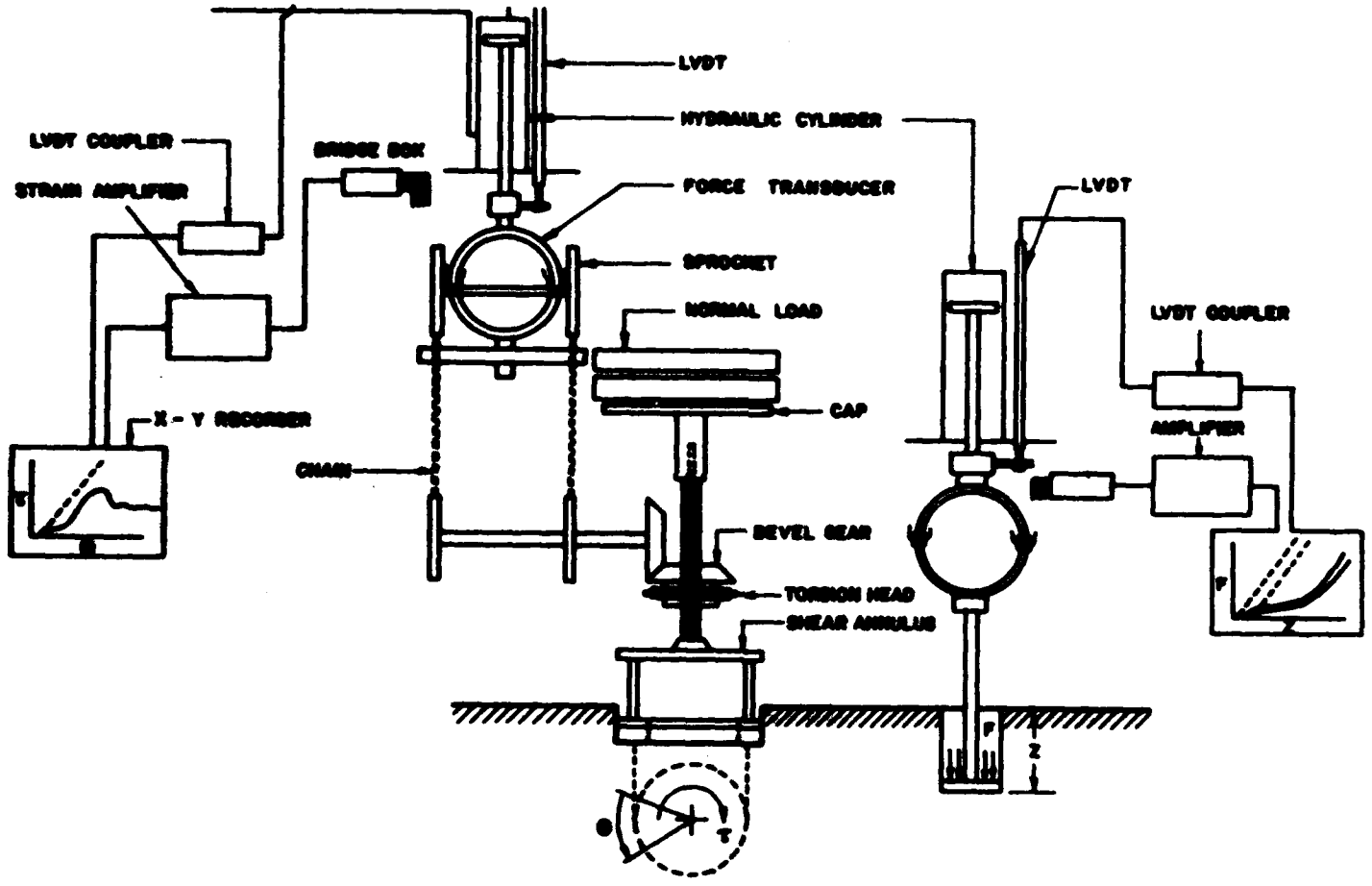

FIG. 3 SCHEMATIC OF BEVAMETER SYSTEM

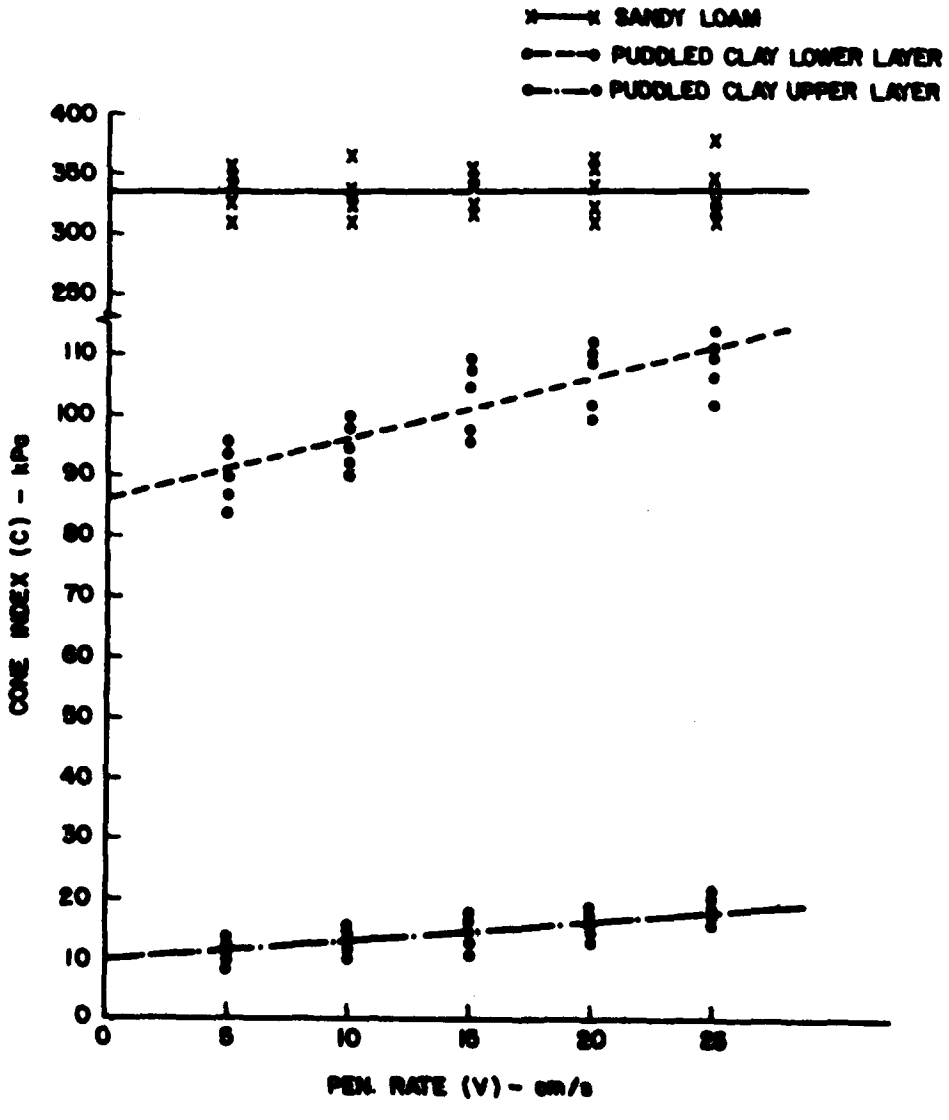

FIG. 4 EFFECT OF PENETRATION RATE ON CONE INDEX

Using these equations the cone index values at the ASAE standard rate of penetration of 3.05 cm/s are 11 kPa and 89 kPa for the upper and lower layers respectively. At a penetration rate of 25 cm/s these values become 18 kPa and 111 kPa respectively. These values are, of course, very low but the increase in cone index values measured at 25 cm/s compared to those at 3.05 cm/s was 64% for the upper layer and 25% for the lower layer.

4.2 Plate Sinkage Parameters

The pressure-sinkage relationship for the plate was assumed to be of the form:

$$P = kz^n \quad \text{..... (3)}$$

where P = pressure on plate (kPa)

k = sinkage modulus (kN/m^{2+n})

z = sinkage (m)

n = exponent of sinkage

The effect of penetration rate on k and n is shown in Figs. 5 and 6. The data were obtained by repeating each test at a particular penetration rate 5 times, calculating the mean pressure at particular sinkages and then computing mean values of k and n. Once again in the clay soil the layer 0-15 cm was treated separately from the layer 15-30 cm.

In the sandy loam soil both k and n decreased as penetration rate increased. The equations to the lines shown are:

$$k = 540 - 440\ V$$

and $$n = 0.32 - 0.4\ V \quad \text{..... (4)}$$

In the clay soil, k increased with increasing penetration rate in both upper and lower layers, the relationships being:

$$k = 15 + 12\ V \quad \text{(upper layer)}$$

and $$k = 186 + 449\ V \quad \text{(lower layer)} \quad \text{..... (5)}$$

n for the lower layer was independent of deformation rate but n for the upper layer decreased as deformation rate increased and the relationship was

$$n = 0.5 - 0.48\ V \quad \text{..... (6)}$$

Wong[1] states that most existing plate sinkage meters have a penetration rate of from 2.5 to 5 cm/s. Using the higher value, the difference in k and n values at 5 and 25 cm/s is shown in Table 1.

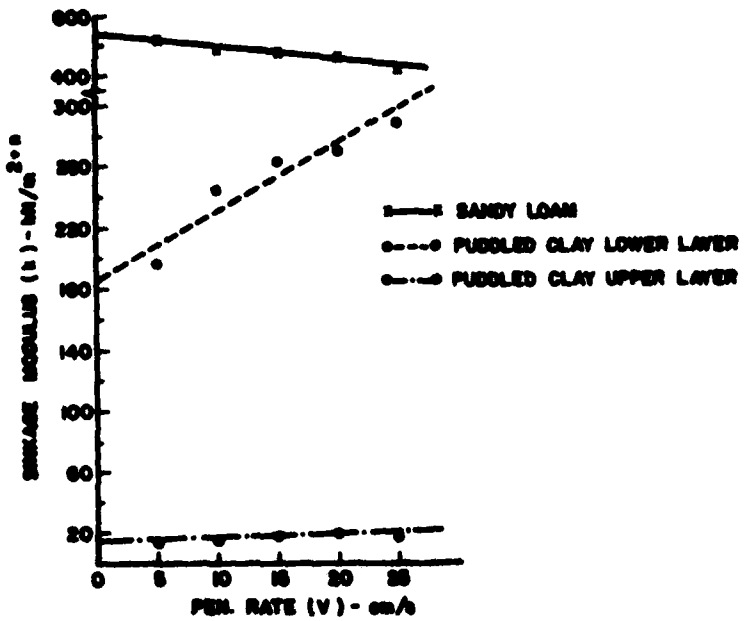

FIG. 5 EFFECT OF PENETRATION RATE ON SINKAGE MODULUS

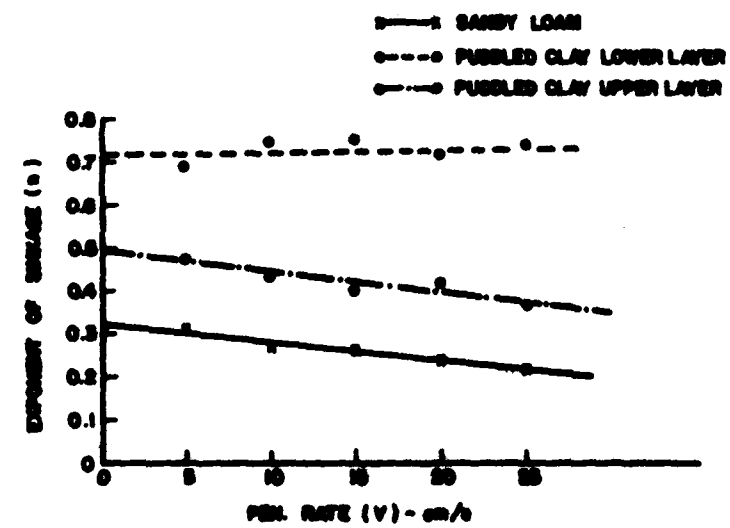

FIG. 6 EFFECT OF PENETRATION RATE ON EXPONENT OF SINKAGE

Soil	Computed value of $k(kN/m^{2+n})$		Computed value of n	
	5 cm/s	25 cm/s	5 cm/s	25 cm/s
Dry sandy loam	518	430	0.3	0.22
Puddled clay (upper layer)	16	20	0.48	0.38
Puddled clay (lower layer)	208	298	0.71	0.71

Table 1 Computed values of sinkage modulus and exponent of sinkage at different penetration rates

The physical significance of the data in Table 1 is not immediately obvious since it is the pressure under a wheel or track which we wish to predict and this involves using both k and n. Figs 7 and 8, using the data from Table 1, show the predicted plate pressure-sinkage curves for the sandy loam and clay soils at 5 and 25 cm/s penetration rate. It can be seen that there is no very strong effect of rate of penetration on plate pressure in the sandy loam soil. Predicted pressure at 30 cm. sinkage at 25 cm/s penetration rate is only 9% less than the value at the same sinkage at 5 cm/s.

There is a very strong effect in the clay soil however. Predicted pressure at 30 cm. sinkage at 25 cm/s penetration rate is 44% greater than the value at 5 cm/s.

4.3 Shear Strength Parameters

The ring shear tests were carried out at deformation rates of from 6.9 to 34.5 cm/s, calculated from the mean radius of the annulus. These corresponded to 5 to 25 cm/s ram velocity. Normal pressure in the sandy loam soil was varied up to a maximum of 123 kPa, however this was found to be quite impossible in the clay soil due to excessive sinkage of the annulus. To avoid this excessive sinkage normal pressure in the tests in the clay soil had to be limited to a maximum of 15 kPa. At each deformation rate and normal pressure, each test was repeated 5 times. Values of the maximum shear torque from each of these tests was used to calculate maximum shear stress at each normal pressure and the sum of all such data at all the normal pressures used to calculate cohesion and angle of internal friction at each deformation rate. The curve of shear torque against angle of rotation showed a clear-cut maximum value in the sandy loam soil, falling off to a constant residual level. No such clear-cut maximum existed in the tests in the clay soil. In these tests the value of shear torque at 30 deg. angle of rotation was taken as indicative of maximum shear stress.

The effect of deformation rate on cohesion and internal friction angle in the two soils is shown in Figs. 9 and 10. There was no significant effect of deformation rate on cohesion in the sandy loam soil but the angle of internal friction decreased very slightly as

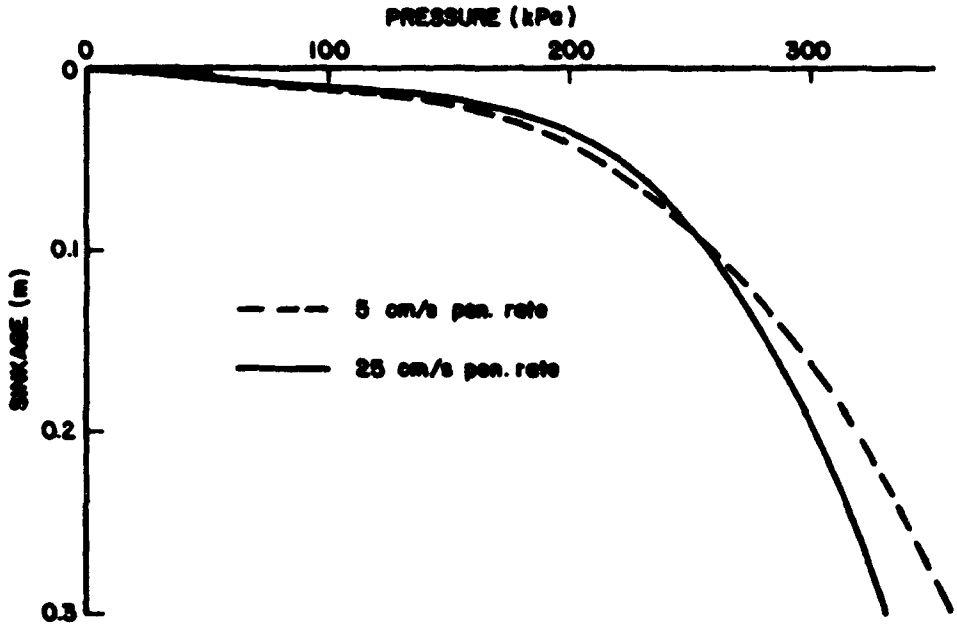

Fig. 7 PREDICTED PLATE PRESSURE - SINKAGE CURVES FOR SANDY LOAM SOIL

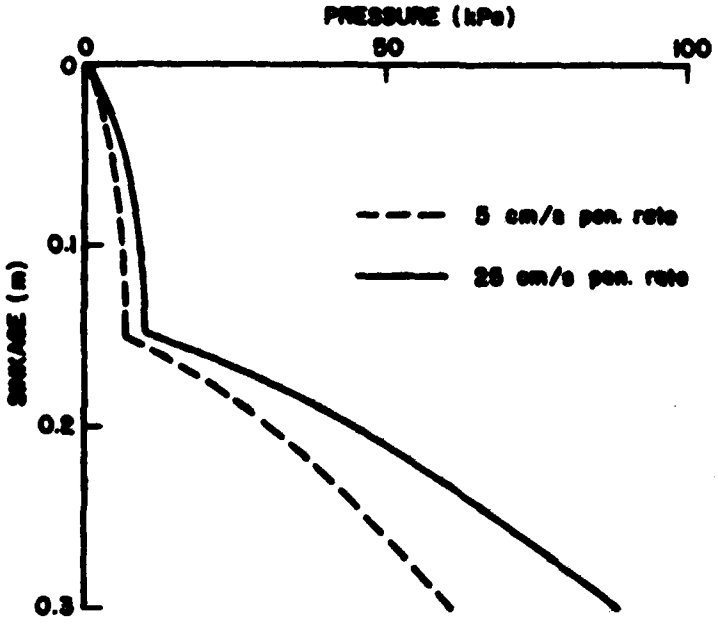

FIG. 8 PREDICTED PLATE PRESSURE - SINKAGE CURVES FOR PUDDLED CLAY SOIL

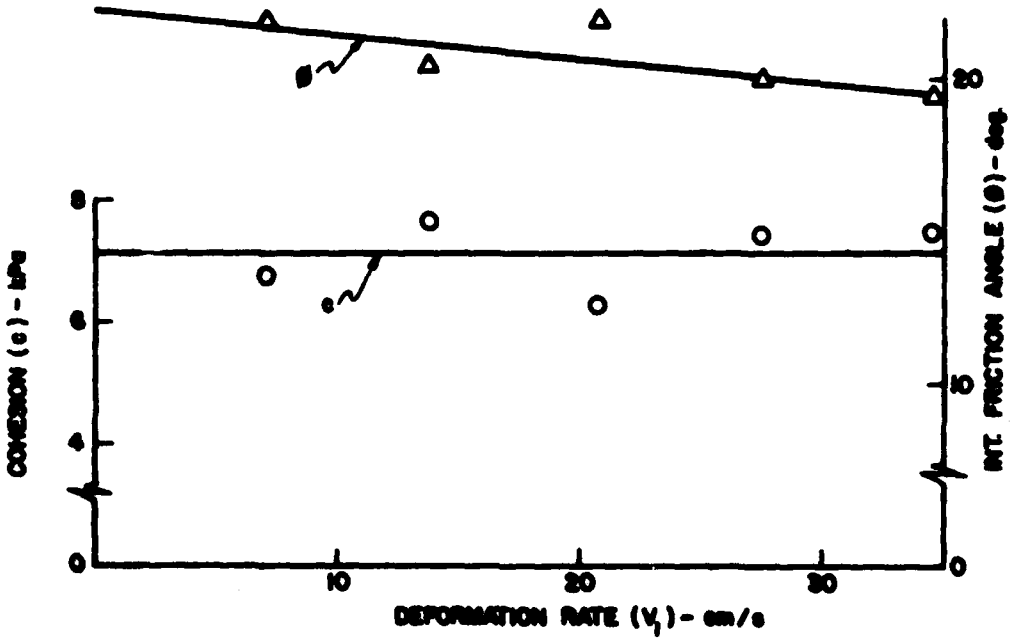

FIG. 9 EFFECT OF DEFORMATION RATE ON SHEAR STRENGTH IN SANDY LOAM SOIL.

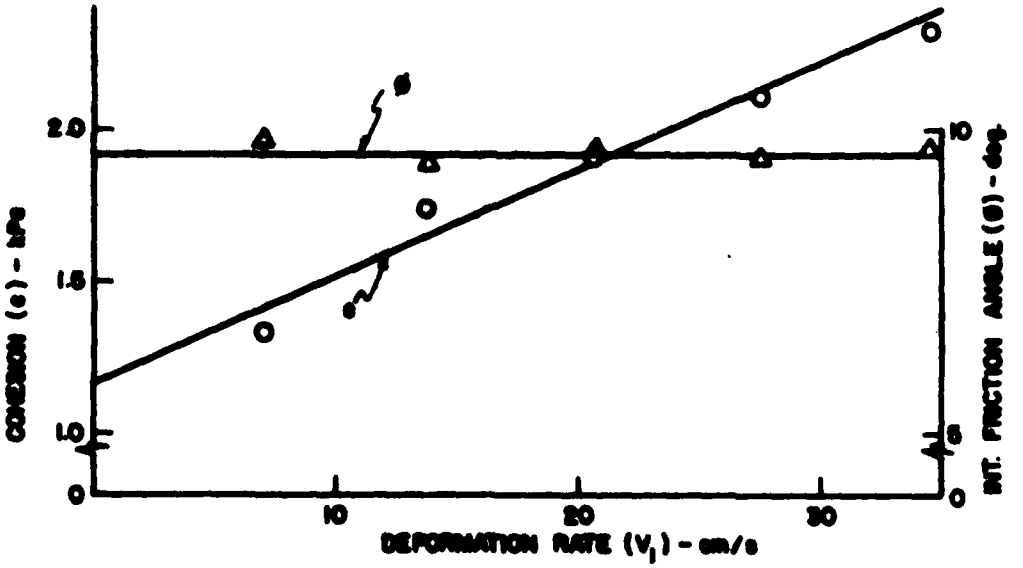

FIG. 10 EFFECT OF DEFORMATION RATE ON SHEAR STRENGTH IN PUDDLED CLAY SOIL.

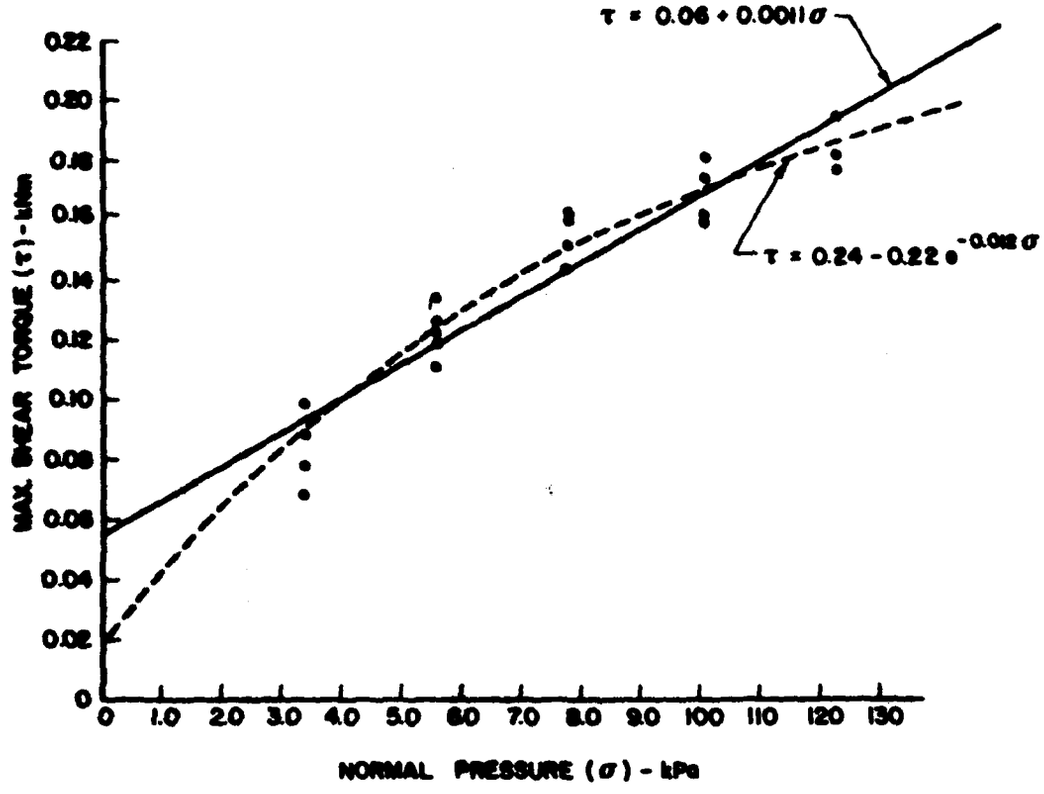

FIG. 11 MAX. SHEAR TORQUE AGAINST NORMAL PRESSURE FOR SANDY LOAM SOIL (21 cm/s DEFORMATION RATE)

deformation rate increased. The relationship was:

$$\phi = 22.3 - 8.2\ V_1 \qquad \ldots\ldots (7)$$

where ϕ = angle of internal friction (deg)

V_1 = deformation rate calculated at mean radius of annulus (m/s)

Using equation (7) the predicted angle of internal friction is 20.2 deg. at 25 cm/s deformation rate as against 21.9 deg. at 5 cm/s, a decrease of 8%.

The angle of internal friction was independent of deformation rate in the clay soil but cohesion was strongly dependent. The relationship was:

$$c = 1.17 + 3.5\ V_1 \qquad \ldots\ldots (8)$$

where c = cohesion (kPa)

Predicted cohesion, using this equation is 52% greater at 25 cm/s deformation rate than at 5 cm/s.

The shear torque against normal pressure curves showed a distinct non-linear tendency in the sandy loam soil. Fig. 11 shows typical data along with the best fitting straight line and exponential curve. The exponential curve gave a much better fit to the data than did the straight line although the straight line fit was statistically significant. Fig. 11 indicates that, as long as the normal pressure used in the ring shear test is close to that exerted by the vehicle on the soil, a linear relationship between shear torque and normal pressure is adequate for calculating c and ϕ. However, if much lower pressures are used, and the resulting calculated c and ϕ used to estimate maximum shear stress at much higher normal pressures than those used in the test, then large errors can be expected.

5. CONCLUSIONS

In the dry sandy loam soil none of the soil properties measured was strongly dependent on penetration or deformation rate in the range used in these experiments. However the plot of shear torque against normal pressure in the ring shear tests indicated that normal pressures used in these tests must be as high as those exerted by the vehicle on the ground otherwise large errors in predicted maximum shear stress can be expected in such soils.

In the saturated,puddled clay soil all the soil properties, with the exception of internal friction angle, were strongly dependent on deformation rate. In such soils it is essential that the deformation rate used in measuring soil properties is close to that imposed by the vehicle on the soil. In the upper layer of this soil it was impossible to apply the required amount of normal pressure in the ring shear tests because of excessive sinkage of the annulus. Measurement of c and ϕ of the lower layer of such soils therefore becomes important. Since

the upper and lower layers of such soils are so different it seems likely that soil properties of each layer will have to be measured separately.

REFERENCES

1. WONG, J.Y. (1978). Theory of Ground Vehicles. John Wiley & Sons.

2. FREITAG, D.R. (1968). Penetration tests for soil measurements. Trans. Amer. Soc. Agr. Engnrs, 11(6): 750-753.

3. EMORI, R.; SCHURING, D. (1966). Static and dynamic penetration tests of soil. J. Terramechanics, 3(1): 23-30.

4. EL-DOMIATY, A.M.; CHANCELLOR, W.J. (1970). Stress-strain characteristics of a saturated clay soil at various rates of strain. Trans. Amer. Soc. Agr. Engnrs, 13(5): 685-689.

5. FLEMMIKEN, J.M.; HEFNER, R.E.; WEBER, J.A. (1977). Dynamic soil strength parameters from unconfined compression tests. Trans. Amer. Soc. Agr. Engnrs, 20(1): 21-25.

6. STAFFORD, J.V.; TANNER, D.W. (1983). Effect of rate on soil shear strength and soil-metal friction. I. Shear strength. Soil and Tillage Research 3(3): 245-260.

7. SARGANA, M.A. (1983). Deformation-rate effects on soil parameters for terramechanics. Asian Inst. Techn. M.Eng. thesis No. AE-83-12 (unpubl).

THE MEASUREMENT OF SNOW PROPERTIES FOR MOBILITY APPLICATIONS: THE UNFROZEN WATER CONTENT.

DR. W.L. HARRISON, DR. G.G. GIMMESTAD, AND DR. S.M. LEE
KRC, MICHIGAN TECHNOLOGICAL UNIVERSITY, HOUGHTON, MICHIGAN 49931

INTRODUCTION

The free water content of snow has been used in over-snow vehicle mobility studies only in a documentary manner. As described by the International Classification for Snow (NRC, 1954), the free water content of snow is indicated by the terms dry, moist, wet, very wet, or slush. The definitions of these categories are shown in table 1.

Throughout the range of conditions, ~~listed in Table 1~~, the variation of free water obviously has a significant effect on the snow strength parameters used in vehicle performance evaluation. During a testing program this past winter (1983-1984) at the Keweenaw Research Center, which involved vehicles attempting to negotiate snow obstacles, free water content was measured and included as snow characterization data along with density, grain size, and snow temperature. Of particular interest to this paper was the difference in test results of two snow obstacles having the same classification under the International system, i.e. "wet". The free water content of the two types of snow used to form the obstacles was measured, by calorimetry, to be 16 ~~percent~~ % and 26 ~~percent~~ %.

Without dwelling on a particular test series as mentioned above, it would be a significant improvement in the characterization of snow if free water content were stated as a quantitative value. This would allow, for example, establishing the relationship between the amount of free water and the snow strength, including the effect of free water content on the snow compaction process, which has an important role in vehicle performance.

FIELD MEASUREMENT OF FREE WATER CONTENT

In field measurements, simplicity and economy are important considerations, because they often determine the ultimate accuracy of a method. Some methods which are suitable in the laboratory are not suitable for field use. In the discussions which follow, it is assumed that basic measurements of mass and temperature are performed in the field, with errors typically of ±0.1 gram and ±0.1 Celsius degree.

A discussion of four calorimetric methods follows, with an appraisal of their usefulness for field measurements. In this discussion, the equations for calculating the free water content are presented without calorimeter correction terms, in the interest of clarity. For each method, at least one reference is given, and the sample calculations are performed using typical values from these references.

1. Melting Calorimetry (Yosida, 1960; Akitaya, 1978)

The equation for melting calorimetry is as follows:

$$F = \left\{1 - \frac{1}{79.4M_2}\left[(T_1 - T_2)\,M_1 - T_2M_2\right]\right\} \times 100$$

where

F = percentage (by weight) liquid water
T_1 = initial temperature of hot water (°C)
T_2 = final temperature of hot water (°C)
M_1 = mass of hot water (grams)
M_2 = mass of snow sample (grams)

A typical numerical example (Akitaya, 1978) is shown as follows:

$$13\% = \left\{1 - \frac{1}{(79.4)\,(25)}\left[(45 - 26)\,125 - (26)\,25\right]\right\} \times 100$$

The sensitivity to errors is as follows:

Parameter	Sensitivity
T_1	-6.3%/°C
T_2	+7.6%/°C
M_1	-1.0%/gram
M_2	+4.8%/gram

The sensitivities to error were found numerically, by varying one parameter at a time while holding the other parameters constant. The melting calorimetry method is rather simple. It requires transporting hot water to the field site, but this is easily done with a thermos type container. Akitaya suggests the additional expediency of transporting prepared (and weighed) bottles of hot water to the test site and returning the melted snow and the water mixture to the laboratory for weighing, so that no weighing is necessary in the field (private communication, 1983).

Both Yosida and Akitaya state an experimentally determined uncertainty in F of approximately ±1%.

II. Freezing Calorimetry (Jones, 1983)

The equation for freezing calorimetry is as follows:

$$F = \left[\frac{M_1\,(T_2 - T_1)C_f}{79.4\,M_2} + \frac{T_2\,C_1}{79.4}\right] \times 100$$

where

T_1 = initial temperature of freezing medium (°C)
T_2 = final temperature of mixture (°C)
M_1^2 = mass of freezing medium (grams)
M_2^1 = mass of snow sample (grams)
C_f^2 = specific heat of freezing medium (cal/g°C)
C_i^1 = specific heat of ice (cal/g°C)

A typical numerical example is shown as follows:

$$7.7\% = \left[\frac{(400)(-17-(38))\ (0.44)}{(79.4)\ (160)} + \frac{(-17)\ (1)}{79.4} \right] \times 100$$

The sensitivity to errors, calculated as for the previous example, is as follows:

Parameter	Sensitivity
T_1	-1.4%/°C
T_2	+2.7%/°C
M_1^2	+0.07%/gram
M_2	-0.18%/gram

It should be noted that sensitivity to errors in the temperature measurements is, in fact, less than that for melting calorimetry. For the interested reader, the reasons for this are discussed by Colbeck (1978). However, in comparison to melting calorimetry, freezing calorimetry is expensive (requiring cold silicone oil), time consuming (requiring a minimum of 20 minutes per test), quite sensitive to operator technique, and it requires considerable data analysis.

The experience of the authors during an extensive series of field measurements was that ±3% is a conservative estimate of experimental uncertainty in free water content measured by this method.

III. Freezing Point Depression (Bader, 1950)

The equation for freezing point depression calorimetry is as follows:

$$F = \frac{1}{M} \left[C_1 - \frac{T(M + C_o)}{79.4} - C_o \right] \times 100$$

where

T = freezing point depression (°C)
M = mass of snow sample (grams)
C_o = mass of liquid water in nitial solution (grams)
C_1^o = mass of liquid water in final solution (grams)

A typical numerical example is as follows:

$$17.4\% = \frac{1}{100}\left[119 - \frac{(1.43)(100 + 98)}{79.4} - 98\right] \times 100$$

The sensitivity to error is given as follows:

Parameter	Sensitivity
M	+0.2%/gram
T	+86%/°C

While this method is the simplest, requiring only the addition of a dilute solution of sodium hydroxide to a known quantity of wet snow and a measurement of the temperature depression, it is not considered suitable for field use. In order to obtain an uncertainty of ±1% in F, T must be measured with an accuracy of ±0.01 °C. This is not realistic for field work. Colbeck (1978) states that the greatest error would probably be introduced by inaccurate measurement of the molal concentration of the sodium hydroxide solution.

IV. Alcohol Mixing Calorimetry (Fisk, 1983)

The equation for alcohol mixing calorimetry is as follows:

$$F = \left\{1 - \frac{1}{79.4M_2}\left[Q_1 - (M_1 + M_2)C_s T_2 - M_1 C_a T_1\right]\right\} \times 100$$

where

T_1 = initial temperature of alcohol (°C)
T_2 = final temperature of solution (°C)
M_1 = mass of alcohol (grams)
M_2 = mass of snow sample (grams)
Q_1 = heat of dilution (calories)
C_a = specific heat of alcohol (cal/g °C)
C_s = specific heat of solution (cal/g °C)

A typical numerical example is as follows:

$$11\% = \left\{1 - \frac{1}{(79.4)\ (25)}\left[625 - (80 + 25)(0.68)(-16)\right]\right\} \times 100$$

The sensitivity to errors is as follows:

Parameter	Sensitivity
M_1	+0.2%/gram
M_2	+2.5%/gram
T_2	+3.6%/°C

The alcohol mixing method is both simple and economical. It requires transporting very little to the field site. The sensitivity to temperature errors is more in line with those of freezing calorimetry than with melting. However, there are some weaknesses in this method, as it has been described in the literature. At the present time, it is not possible to calculate the heat of dilution Q_1 from basic thermochemical data, so the procedure is to fix three parameters (the mass of the snow sample, the mass of alcohol, and the alcohol temperature) and calibrate the method, by using it on prepared snow samples of 0 and 100% free water content. A linear interpolation is then used for data between these two extremes. The systematic error caused by this linear approximation is not known, and the fact that precisely weighed samples of snow and alcohol must be prepared in the field is a disadvantage. The method does, however, appear to hold great promise.

SUMMARY

There are several suitable methods available for measuring free water content under field conditions, for snow-mobility purposes. Although some methods are apparently more accurate than others, a 5% error is probably acceptable. One must be aware that in all cases discussed so far, only wet snow (0°C) is considered. Quantitative values of free water content are a necessity for more detailed analyses such as its effect on strength parameters and critical density (which relates to the compaction process) of <u>dry</u> snow (Harrison, 1981). These analyses will be restricted to laboratory tests, since field calorimetric accuracy is on the order of a few percent.

The other reason that an uncertainty of ±5% is acceptable lies in the inherent variability of snow on the ground. Variations in surface crystals and the surface profile in a rather small area can produce a natural variation in free water content approaching, and in some cases greater than, 5%.

In conclusion, we feel that the quantitative value of the free water content of snow is an important parameter in vehicle performance evaluations, and that there are adequate means available for field measurements.

TABLE 1.

FREE WATER CONTENT

Term	Remarks
Dry	Usually T is below 0°C, but dry snow can occur at any temperature up to and including 0°C. When its structure is broken down by crushing and the loose grains are lightly pressed together as in making a snow ball, the grains have little tendency to cling to each other.
Moist	T = 0°C. The water is not visible even with the aid of a magnifying glass. When lightly crushed, the snow has a distinct tendency to stick together.
Wet	T = 0°C. The water can be recognized by its meniscus between adjacent snow grains, but water cannot be pressed out by moderately squeezing the snow in the hands.
Very Wet	T = 0°C. The water can be pressed out by moderately squeezing the snow in the hands but there still is an appreciable amount of air confined within the snow structure.
Slush	T =0°C. Snow flooded with water and containing a relatively small amount of air.

REFERENCES

Akitaya, E. (1978), "Measurement of Free Water Content of Wet Snow by Calorimetric Method", Low Temperature Science, series A, 36, 103-111.

Bader, H.C. (1950), "Note on the Liquid Water Content of Wet Snow", Journal of Glaciology 1, no. 8, 466-467.

Colbeck, S.C. (1978), "The Difficulties of Measuring the Water Saturation and Porosity of Snow", Journal of Glaciology 20, no. 82, 189-201.

Fisk, D.J. (1983), "Progress in Methods of Measuring the Free Water Content of Snow", S.P.I.E. Proceeding 414, 48-51.

Harrison, W.L. (1981), "Shallow Snow Model for Predicting Vehicle Performance", USACRREL Report no. 81-20, October 1981, p. 10.

Jones, E.B. (1983), "Snowpack Ground-Truth Manual", NASA report CR 170584.

National Research Council (1954), "The International Classification for Snow", Technical Memorandum #31, National Research Council, Ottawa, Canada, August 1981.

Yosida, Z. (1960), "A Calorimeter for Measuring the Free Water Content of Wet Snow", Journal of Glaciology 3, 574-576.

THE MODIFICATION OF SOIL STRENGTH CHARACTERISTICS DUE TO THE PRESENCE OF VEGETATION

I. LITTLETON and J.G. METHERINGTON
ROYAL MILITARY COLLEGE OF SCIENCE, SHRIVENHAM, SWINDON, WILTS. SN6 8LA

INTRODUCTION

Although there has been considerable effort devoted to the study of soil-vehicle interaction and soil working processes, very little attention has been paid to the effect of vegetation on these processes. Greater attention is being given to the reinforcement of soils using geotextiles, and the use of polymer based structural matting to provide temporary refurbishment to weakened soils for vehicle passage over strategically important areas. It is now pertinent therefore to examine the contribution made by fibrous material to soil strength and the possibility of enhancing the strength of soils by the addition of artificial fibres. Clearly the traction that a vehicle is able to mobilise from a soil is determined by certain vehicle parameters (e.g. weight, contact area, tyre tread or track configuration) and certain soil properties. Equally the sinkage and rolling resistance of a vehicle is governed by vehicle characteristics (e.g. wheel size, track size and weight) and certain soil properties. In each case the dominant soil characteristic which affects traction, sinkage and rolling resistance is shear strength. A high shear strength will enhance traction and reduce resistance giving rise to a higher draw-bar pull and generally better cross country mobility. Similarly, the greater the shear strength of soil, the greater will be the forces acting on earth working implements and the energy dissipated during working.

The Fourth Geotechnique Symposium in Print (1) presented several papers on soils containing vegetation but there was no contribution here on the effect of vegetation on shear strength. Beaton (2), working at RMCS, found that experiments performed on naturally occurring soils containing vegetation failed to isolate the contribution of vegetation from the many other variables influencing soil shear strength.

This paper describes a programme of work to investigate the effect on shear strength of the presence of fibrous material. A programme of experimental work examined the effect of adding artificial fibres to clays and a theoretical model of fibre reinforcement was developed to account for the principal findings. The shear box was used throughout, since it most nearly models the enforced failure along a prescribed failure plane, characteristic of soil-vehicle interaction. The theoretical model, whilst derived by specific reference to the shear box, yields a description of shear strength characteristics with wider potential applications.

THEORY

The simple model considers a random distribution of strong, straight fibres of length ℓ and diameter d with a soil of unreinforced quick undrained, shear strength, s, contained in a shear box of height, h, and side length, s. The orientation of a fibre is specified in the vertical

plane by its inclination of θ to the horizontal and with the horizontal plane by its inclination, ψ, to the direction of shear (Fig. 1). If the fibres are strong in comparison with the soil, displacement of the shear box will be accompanied by a combined process of fibre extraction and incision. The model initially examines a straight fibre perpendicular to and symmetrically placed about the surface of intense shear and assumes that the deformed shape of the fibre consists of circular arcs and straight lines. Fig. 2 shows the fibre after a relative displacement, x, of one half of the shear box over the other. Both the surface of intense shear and the original site line of the fibre are tangential to the circular arc, AB. During an increment of shear box displacement the fibre moves to a new configuration shown in Fig. 3. Both

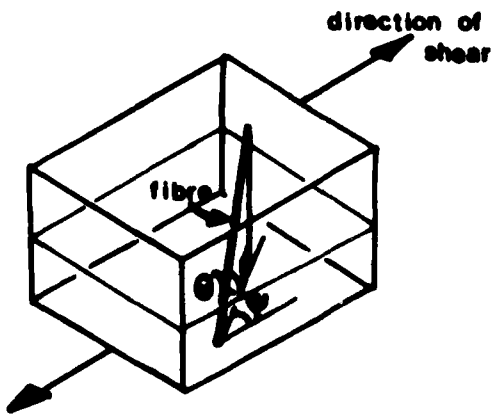

Figure 1

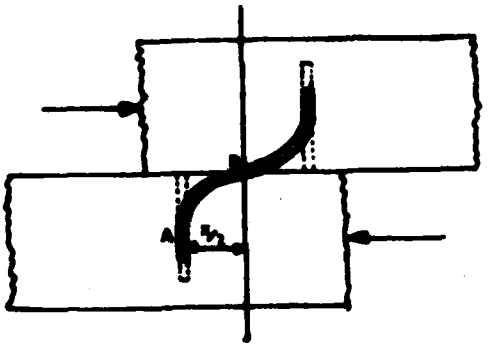

Figure 2

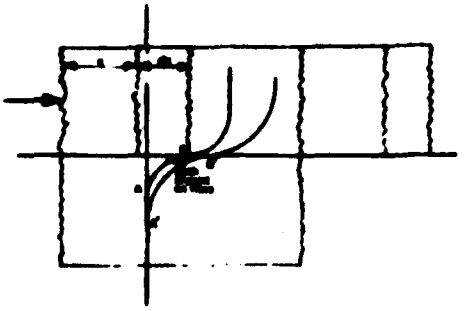

Figure 3

the length of arc, A'B', and the radius of curvature must increase to maintain the condition that both the surface of intense shear and the original fibre site line are tangential to the arc A'B'. From this assumed mode of deformation, the displacements δX and δY of a point on the fibre can be determined and converted into components δn and δt, perpendicular and tangential to the fibre. Clearly then, during an increment of displacement the fibre both slides along its capillary and cuts through the soil.

The resistance to sliding is given by the product of the adhesion and the contact surface area between fibre and its capillary, whilst the resistance to cutting is given by the product of projected contact area

and the bearing capacity. Hence the amount of work done by an element of fibre during an incremental displacement of the shear box is calculated, and summed over the circular arcs above and below the surface of intense shear. To this is added an extra term to account for the work done in extracting the fibre from the straight portion of the capillary. This gives the extra amount of work done during an incremental advance of the shear box due to the presence of a single fibre normal to and symmetrically placed about the shear surface. In reality all fibres with a particular inclination can be sited with their centres at any distance between zero and $\ell/2$ from the shear surface. Those more remote than this will not be counted as intersecting the shear surface and will not contribute to the shear strength of the composite. The energy of deformation associated with a fibre will vary from a maximum when its centre lies in the plane of intense shear to zero when one end lies in that surface. Assuming a linear decrease in energy with eccentricity, it can be shown that the average energy of deformation is one half of that for a symmetrically placed fibre. The above analysis could be extended for a fibre at any inclination, θ, or orientation, ϕ. However, for the purposes of this study an approximation was made by assuming that the effectiveness of a fibre in providing reinforcement was a maximum when it was perpendicular to the surface of intense shear and nil when it was parallel to the shear surface. Moreover it was assumed that orientation in the horizontal plane was immaterial.

Finally it is necessary to obtain an expression for the total number of fibres intersecting the surface of intense shear. By considering a shear box of side length 'a' containing soil with a volume fraction of fibres is 'f', it can be shown that the number of fibres intersecting the shear surface is

$$\frac{2fa^2}{d^2 \ln 2\ell/d}.$$

The details of the entire derivation are contained in reference 3, but for reasons of brevity are omitted here. The final expression for the extra shear strength due to the presence of fibres obtained from the above method is

$$\tau = \frac{fc}{4d \ln(2\ell/d)} \left\{ \left[N_c + (1 - \pi^2 + 2\pi) \frac{c_a}{c} \right] x + 2\ell(\pi - 2)\frac{c_a}{c} \right\} \qquad (1)$$

where f = volume fraction
d = fibre diameter
ℓ = length of fibre
N_c = Terzaghi's bearing capacity factor
c_a = adhesion
c = undrained shear strength
x = shear box displacement

This theory predicts that the extra shear stress which can be mobilised from a soil due to the presence of fibres is proportional to

(i) the volume fraction of included fibres;

(ii) shear deformation.

EXPERIMENTAL WORK

A series of shear box tests were performed on carefully prepared specimens of illite clay containing prescribed fractions of fibres. Moisture content was accurately controlled since the clay composite was formed by adding fixed amounts of water to a mixture of dry powder and fibres. The properties of the illite clay are presented in reference 4. The fibres were fibrillated polypropelene string of average length 30.3 mm (Fig. 4). It can be seen from Fig. 5 that the soil/fibre system produced in this way resembled naturally occurring soil/root systems.

Figure 4

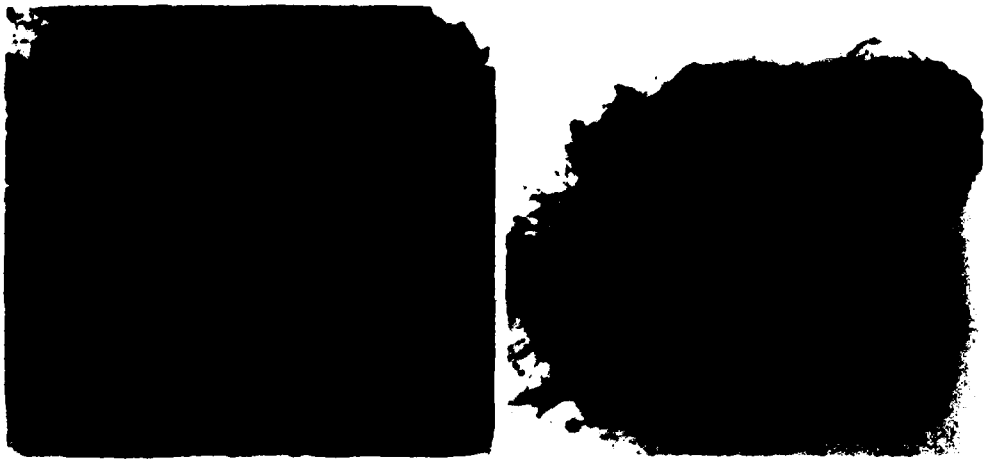

Natural roots

4% artificial fibres in Illite Clay

Figure 5

The principle adopted in forming a range of fibre reinforced clay samples was that the fibres were essentially inert components in the system. The ratio by weight of water to clay powder was maintained at a fixed value, so that the mechanical properties of the matrix material were constant throughout the series of experiments. To this matrix was added a quantity of fibres to provide weight fractions of 1, 2, 3 and 4% fibres. It has been observed (5) that naturally occurring roots seldom occupy more than 5%, by volume, of the surrounding soil. For the materials considered here, a 4% weight fraction equates to 13% volume fraction, so the range of this programme covers that normally found in nature. Further details of the experimental technique are contained in reference 6. A typical set of shear box results are shown in Fig. 6.

DISCUSSION OF RESULTS

Fig. 6 shows that, as predicted, the inclusion of fibres enhances the shear strength of soil. Since equation 1 predicted the extra shear stress which is mobilised due to the presence of fibres as a function of shear box displacement, this is presented from the same data in Fig. 7. These graphs confirm the prediction that the mobilised shear stress increases with shear box displacement. Equation (1) further predicts that the shear

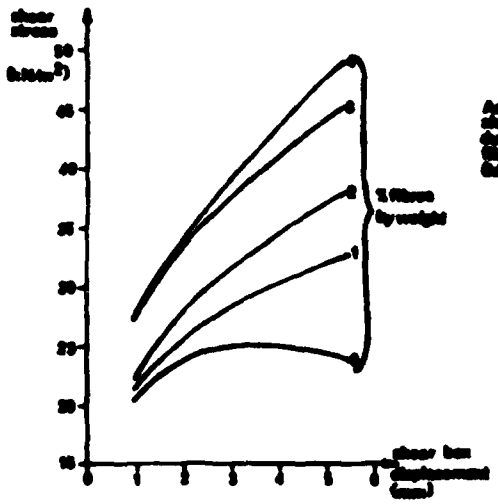

Figure 6

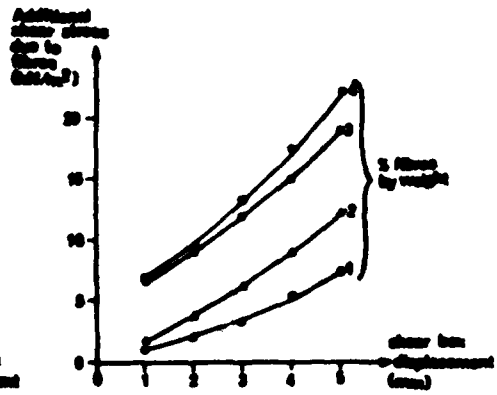

Figure 7

stress at any displacement will be proportional to the volume fraction of fibres present. The experimental results generally confirm this prediction. Fig. 8, for example, shows the extra shear strength mobilised for this set of results at a shear box displacement of 4 mm. Having established broad correlation between the predictions of equation (1) and the observed results, it would be of interest to test the ability of equation (1) to make quantitative predictions of shear strength. The difficulty which arises here is in the evaluation of the quantity $\frac{a}{c}$, the fibre/soil adhesion factor. By taking an estimated figure of 0.1 for this, the predictions of equation 1 can be compared with the results of Fig. 7. These are presented for 2% and 4% fibre content in Fig. 9. The agreement of Fig. 9, albeit dependent upon an estimated value for adhesion factor, is evidence that the theory leading to equation 1 effectively describes the salient phenomena of deformation of soil/fibre composites. This strengthening effect of fibres has also been observed in sands and silts, the results of which are also presented in reference 6.

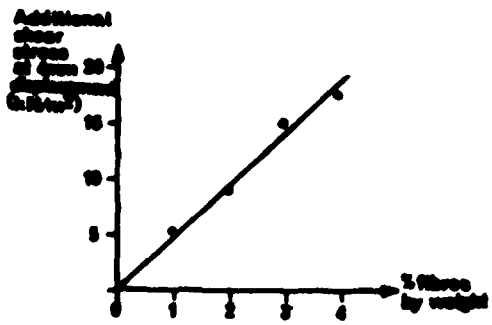

Figure 8

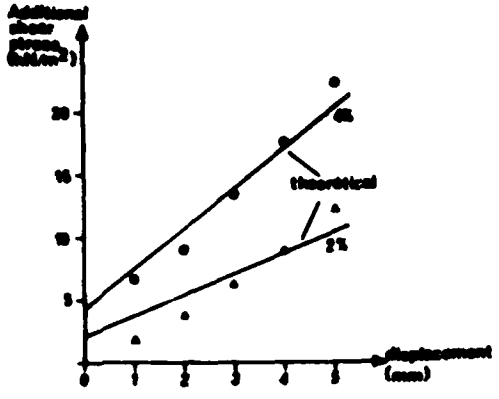

Figure 9

The presence of fibres, either natural or artificial, will increase vehicle traction, reduce rolling resistance, and increase draught forces on earth working machinery. Clearly the presence of vegetation in soils is of importance to both the agricultural and military engineer. It is not difficult, for example, to envisage a scenario in which the deposition of artificial fibres could transform from impassable to passable a strategically important area of terrain, thus ensuring the safe passage of a convoy of vehicles.

In summary, this paper has sought to examine the effect of fibre inclusion on soil strength. Within the limitations and accuracy normally associated with this field of study, it has correctly accounted for the strengthening effect of fibres through a quantitative description of the deformation mechanism.

CONCLUSIONS

1. The inclusion of artificial fibres in real soils provides a useful technique for examining the effect of vegetation on shear stress/deformation properties of soils.

2. A theoretical model based on a combined fibre sliding and cutting mechanism predicts the following:

   (i) Shear stress is proportional to volume fraction of fibres.

   (ii) Shear stress is proportional to shear deformation.

3. Experimental tests on an illite clay containing fibrillated polypropelene provide supportive evidence to confirm the above predictions.

4. An assumed value of adhesion factor enables a reasonable correlation to be established between predicted and observed behaviour.

REFERENCES

1. Various authors. Geotechnique Vol. XXXIII No. 2. June 1983.
2. Beaton, Capt T.R., "Ground Mobility Prediction for Wheels". M.Sc. Thesis, RMCS, Shrivenham, Swindon, Wilts. UK. 1982.
3. Hetherington, J.G., "A theoretical model for the shear deformation of soil/fibre composites". RMCS Technical Note GEOTECH 4.
4. Littleton, I., "Some experimental observations on the ratio of penetration/pull-out stresses for model footings on clay", RMCS Technical Note Geotechnical Note 1, November 1982.
5. Micklethorpe, F.L. and Morby, J., "An introduction to Crop Physiology", Cambridge University Press, 1974.

6. Anderson, Maj J.D.C., Fais Ullah, Maj., "The Effect of Fibre Reinforcement on the Mechanical Properties of Soils", Thesis for ASC Div I Advanced Study. RMCS, Shrivenham, Swindon, Wilts. 1983.

MICROWAVE SENSOR FOR THE TRAFFICABILITY STUDIES OF SNOW

M. SAARILAHTI

UNIVERSITY OF DAR ES SALAAM, DIV. OF FORESTRY, MOROGORO, TANZANIA

1. BACKGROUND

In winter conditions snow is an important mobility factor and studies into the vehicle snow mobility are being intensified (BROWN 1981). Outside the field of transportation, snow properties are widely studied for predicting spring floods. Helsinki University of Technology is actively involved in these studies and a new tool for measuring snow properties has been developed, by Professor M. Tiuri (TIURI and SIHVOLA 1982). This paper discusses the use of a microwave sensor in measuring snow properties for mobility evaluation.

11. Dielectric properties of snow

The dielectric properties of a certain medium determine the propagation of an electromagnetic radiation through it. Shortly these dielectric properties can be described using the real part of the relative dielectric constant (ε_r') which is related to the velocity of the radiowave and the imaginary part of the relative dielectric constant (ε_r''), which describes the energy losses in the medium.

The dielectric properties of snow depend on
- density of snow
- wetness of snow.

Wetness is liquid water, i.e. watér molecules which are not a part of snow chrystals (TIURI and SIHVOLA 1982).

Thus by measuring the dielectric properties the density and wetness of snow can be calculated. The loss factor is proportional to the frequency. Thus, by measuring the resonance frequency and the amount of attenuation using an open resonator, the snow characteristics can be obtained, either by using mathematical models or experimental equations. In Fig. 1 the dependence of ε_r' and the loss factor ($\tan\delta = \frac{\varepsilon_r''}{\varepsilon_r'}$) is presented as a function of snow properties.

12. Microwave snow sensor

The microwave snow sensor is composed of a copper fork-antenna connected to a small metal box at one end containing the electronic circuits. The length of the fork is about 10 cm and the total length of the apparatus is less than 0.5 m. The mass is about 1 kg. The small incorporated battery can be recharged and it supplies the sensor for several hours. The sensor is thus easy to use in the terrain.

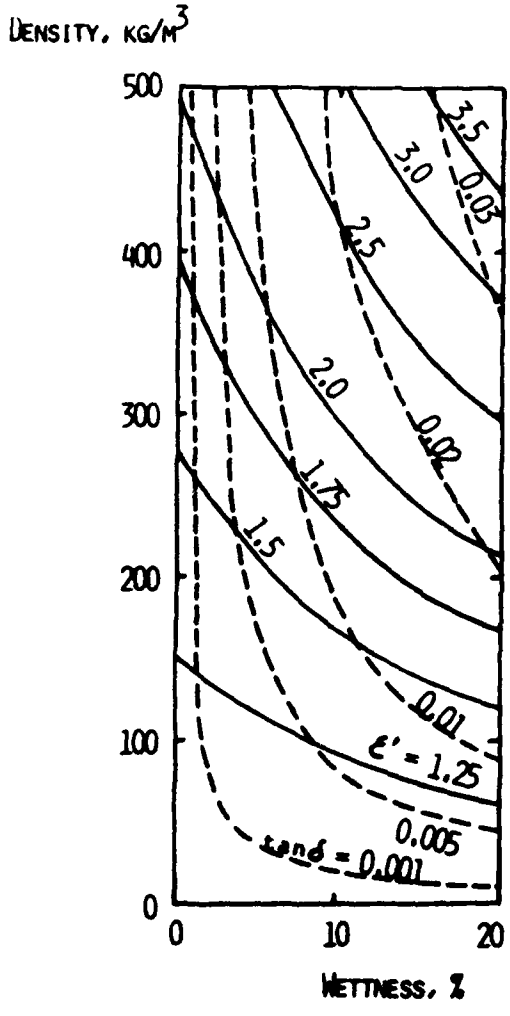

Fig. 1. Dependence of snow properties on dielectric properties (after TIURI and SIHVOLA 1982).

Measurements are made by pushing the antenna into snow. If the sensor is fitted with a displacement transducer and a small cassette recorder, a continuous profile can be registered. Spot-like results can be read on dials.

2. FIELD TESTING OF THE MICROWAVE SNOW SENSOR

A small field test was arranged in April 1982. The spring was advanced, and the air temperature was above 0°C. Snow was coarse grained, wet and many layered. Snow density or wetness were not measured. The cone index was measured using a Farnell-penetrometer. The dial was read at maximum penetration resistances within the penetration depth of about 5 - 10 cm. As known the CI-response during snow penetration is toothed and thus the obtained CI-reading is rather inaccurate. Values less than 10 could not be read.

The microwave snow sensor measurements were made in the horizontal direction in snow walls. The sensor was pushed into the snow and the readings (Fig. 2) were taken. After this the cone penetrometer was pushed into the same layer and the CI reading was taken.

Observations were made at 8 points and of these 4 were on natural snow cover and 4 on packed snow. In total 41 observations were made.

3. RESULTS

A very good correlation between the measured real part of the dielectric constant and the CI-value was found. The best model was

$$CI = 0.0054\,\varepsilon_r^{13.68}\,, \quad r = .904^{xxx} \quad N = 41$$

The scatter diagram is presented in Fig. 3.

If the ε_r-value is under 1.70, no remarkable penetration resistance is found. Above that, the penetration resistance increases rapidly. The scattering of results is partly due errors in CI-readings. As mentioned earlier, the measurement of snow by a penetrometer is difficult. Another source of scattering is the presence of thin icy layers in snow. The snow sensor was pushed into the layer and kept in it, but the penetrometer might have been pushed out of this thin layer. As a comparison, we can give the ε_r-value of ice, which is 3.2 and diminishes a little if there is air inclusion in ice (COOPER et al. 1976). These values seem to fit well, because the ε_r-value of hard packed track was 2.0.

4. APPLICATION OF RESULTS

The snow sensor is a simple and easy device for field measurements. The readings can be converted into
- density and
- wetness

characteristics of snow, and thus the volume-weighing of snow

Fig. 2. Microwave snow sensor measurement.

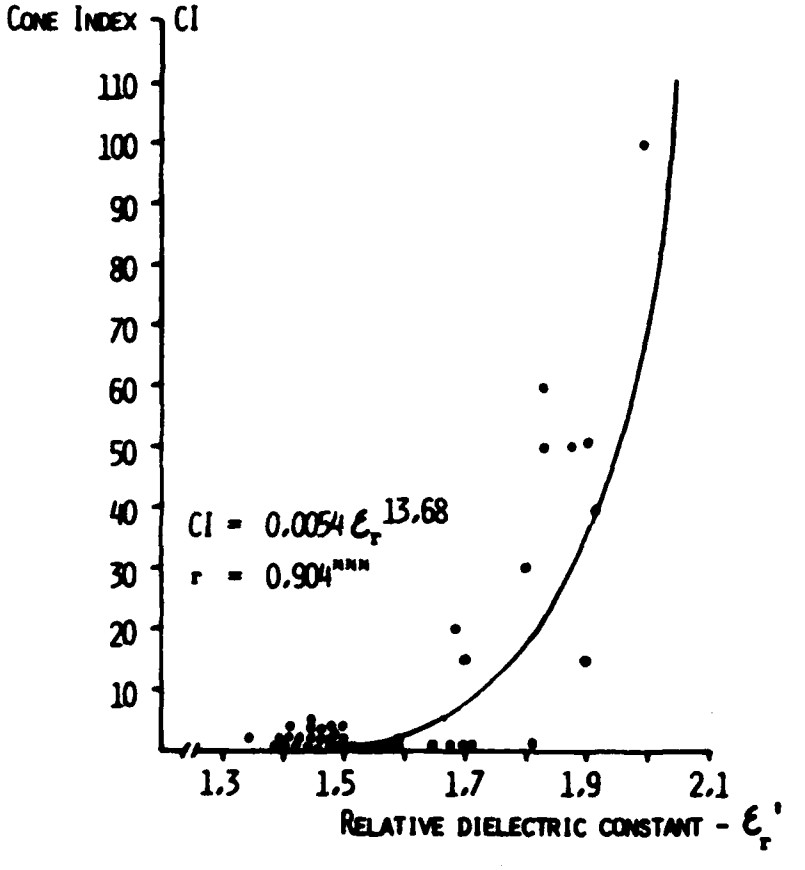

Fig. 3. Dependence of CI-reading on the dielectric properties of snow.

is unnecessary. The penetration resistance and shear strength can be calculated. The wetness is a very important factor in certain conditions, for example when resulting in clogging of steel stracks. Therefore, more detailed studies in the applications of this technique in the field of terramechanics are needed.

REFERENCES

BROWN, R.L. 1981. A comparison of tracked vehicle performance under different snowpack conditions. Proc. 7th ISTVS Congr. Calgary, Alberta. II:531-550.

COOPER, D.W., MUELLER, R.A. & SCHERTLER, R.J. 1976. Measurement of lake ice thickness with a short-pulse radar system. NASA TN D-8189. Cleveland, Ohio.

TIURI, M. & SIHVOLA, A. 1982. Microwave sensor for snowpack wetness and density profile measurement. Proc. 12th European Microwave Conf.: 157-160.

A LUBRICATED CONE PENETROMETER FOR QUANTIFYING THE SOIL PHYSICAL CONDITION

E. W. TOLLNER

AGR. ENGR. DEPT, UNIVERSITY OF GEORGIA EXP. STA., GRIFFIN, GA 30212

INTRODUCTION

The cone penetrometer has for many years been used to characterize soils in terms of cone index in tillage, trafficability and soil-plant interaction studies. The instrument is highly portable and makes possible many measurements in a relatively short period of time. It has, therefore, been used widely to characterize soils where variation is often considerable.

The earliest application of the penetrometer was reported in 1940 for predicting the coefficient of rolling resistance (see McKibben and Hull, 1940). The U. S. Waterways experiment station (1948), considering loose sands and saturated clays, extensively studied trafficability. They introduced the concept of "remolding index" which attempted to account for the impact of subsequent traffic on soil trafficability. Zelenin (1950) presented an empirical relationship relating cone index (with an impact penetrometer) to draft forces of various cutters. Subsequent studies have shown that the coefficients in the relationship change considerably with depth and soil type (Gill and Vandon Berg, 1968). Wismer and Luth (1974) presented a relationship between the cone index (average over 15 cm depth) and traction. Their method performs best in firm soils (Liljedahl, et al 1979). All the results given were largely empirical and should, therefore, be used with caution.

Although cone index is useful for relative comparisons and for correlation with other field data (under consistant soils and soil conditions), this index, in an absolute sense, is difficult to interpret due to uncertainty in the soil reaction. The interpretation of cone index is complicated because its value is dependent on both the soil characteristics and the soil-cone interaction. Soil failure characteristics and soil-cone interaction are complex and depend upon moisture, density, stress history and soil type.

A comprehensive theory or model describing the soil penetration process over a wide variety of soils is yet to appear. Efforts have been made to mathematically describe the penetration process in such specific processes as root growth and small probes (e.g. Greacen et al. 1968), and by sheet piling (e.g. Sangerlat, 1979). Greacen et al. (1968) explained that the soil displacement geometry near penetrating instruments ranged somewhere between cylindrical and spherical, with actual displacement geometry governed by cone angle, cone diameter, soil-metal friction and soil strength parameters. In modelling the penetration process, the assumed soil displacement geometry has a significant effect on the calculated penetration pressure Greacen et al. (1968). In their soils which had high cohesion and high soil friction angles, spherical displacement patterns resulted in a five-fold increase in cone index compared to cylindrical displacement geometry. The interpretation of cone index data would be simplified when the soil failure

geometry is more consistent in a range of soil conditions, as consistant soil displacement enhances development of mathematical models.

A penetrometer was modified (by adding lubrication) with the anticipation of simplifying soil failure geometry and of obtaining two indices; (a) cone index (with reduced soil-metal friction), and (b) "relaxed" penetration pressure (pressure at 1 minute after insertion ceases). It was thought that the modified penetrometer will bring about a radial soil displacement due to reduced soil-metal friction, thereby better defining the soil reaction. For clarity, the new instrument was called an "impedometer.

Results comparing the performance of the impedometer and penetrometer in several soil types found in Southeastern United States are presented and discussed. Cone index and relaxed pressure of penetrometers and impedometers are compared in 4 soil types, 2-4 soil moisture levels (depending on soil workability), 2-3 soil compaction levels, and 4 cone angles. Before presenting results, modifications to the penetrometer are given.

MODIFYING THE PENETROMETER TO BRING ABOUT RADIAL SOIL DISPLACEMENT

The concept of impedometer was based on using lubricating polymers to reduce soil-metal friction associated with a cone penetrometer. Using a 5% polymer-water mixture, Schafer et al. (1975) reported a 55-60% reduction in soil-metal friction. To achieve similar reduction in soil-metal friction in a penetrometer, a hollow cone, with four ports located 90° apart in a circumference as close to the cone tip as structurally possible, was used to introduce lubrication at the soil-cone interface. The base area of the cone was the same as the small ASAE (1982) standard cone penetrometer. The hollow cone, mounted at the end of a hollow shaft connecting the central passage of the shaft with the inside cavity of the cone, permitted the supply of the polymer lubricant under pressure through the four ports at the soil-cone interface.

MATERIALS AND METHODS

Test Apparatus

The penetrometers and impedometers were constructed with four selected cone angles of 15°, 20°, 25° and 30° (ASAE Standard). This range of cone angles was chosen because the desired radial failure pattern was considered most likely within this range of angles. The base area for all four cones was 1.29 cm^2 (0.20 in^2) in accordance with the ASAE Standards (1982). The lubricated cones for the impedometers were constructed by drilling four 1.6 mm dia. ports located 90° apart on a circumference at about 1/3 cone height from the tip. A cavity in the cone was formed by drilling with a 4.8 mm (3/16 in.) drill bit from the base of the cone to a depth where the four ports connected with the cavity. The cone was then attached to a hollow shaft connecting the center passage of the shaft with the cone cavity. This arrangement permitted a lubricant, introduced under pressure in the center passage of the shaft, to flow out through the four cone ports (Tollner and Verma

1983). The lubricant was a 5% mixture of Nalco[1,2] TX270 polymer.

The penetrometer was attached to a 50 kg load cell mounted in the top stationary cross member of an Instron[2] testing machine. A rigid plastic bucket containing a test soil was placed on a platform mounted on the moving crossmember. The crossmember was moved towards the stationary penetrometer to allow the penetration of the cone in the test soil at a fixed rate of 480 mm/minute.

Test Media Preparation

Four test soils, silica sand, Lakeland sand, Tifton sandy loam, and a Cecil sandy clay were employed for the study. The test soils were prepared by air drying and sieving through a 2mm seive for removing debri and adjusting moisture content by either drying or adding water to obtain the desired soil moisture within the selected range of 5-22% (dry basis). Test samples of each soil-moisture level combinations were prepared by pouring 9630 gm. of soil or 15850 gm of sand (air dry equivalent weight) into 19 liter rigid plastic buckets and compacting the sample using a 12 kg. weight falling a distance of 30.5 cm. onto a 1.27 mm thick by 26 mm diameter wooden disc. For each soil-moisture combination, three levels of compaction were obtained by applying either 3, 6 or 12 blows to the loosely filled test sample. Samples were then sealed and stored, undisturbed, for at least 24 hours.

Penetration Procedure

A sample in the bucket was carefully placed on the testing machine so as to not deform the bucket. After mounting the desired cone, the lubrication pump was either switched on for the impedometer tests with hollow cones, or was switched off for the penetrometer tests, and penetration was initiated. Penetration was automatically stopped when the cone reached about 7 cm. from the bucket bottom, resulting in a penetration depth of 12-15 cm. A test plot of penetration depth and penetration pressure was recorded from which the peak value was read. The peak value was denoted as cone index. After the penetration ceased at the maximum penetration depth, pressure readings were recorded for another minute while stress relaxation occurred near the soil-cone interface. The penetration pressure reading at the end of the one minute was denoted as the "relaxed pressure".

Test Conditions

Soil, moisture and compaction combinations utilized in the study, along with corresponding bulk density, are listed in Table 1. Attempts were made to have three compaction levels and four moisture contents (5-25%) for each test soil; however, higher moisture contents frequently resulted in sloppy and unworkable soil conditions. These conditions were responsible for the reduced number of treatments with some soil types. Except for the Silica Sand, the lowest moisture content listed

---

[1]Nalco Chemical Co., 6216 W. 66th Place, Chicago, Ill. 60633.

[2]Trade names are used in this publication solely to provide specific information. Mention of a trade name does not constitute a guarantee of that product by the University of Georgia, nor does it imply an endorsement by the university over comparable products that are not named.

in Table 1 was the air-dried moisture content.

With a given soil-moisture-compaction level combination, three replications with each cone angle were performed for the penetrometer and impedometer. For the penetrometer, the peak cone index (P) was read as was the relaxed pressure (PR). Similarly, for the impedometer, the peak cone index (P_L) and relaxed pressure (PR_L) were obtained. Each dependant variable was analyzed statistically with a completely random factorial (main effects only) design using the SAS package[1].

Visual Observations

Visual observations of soil displacement for both the impedometer and penetrometers were made using the following technique. Approximately 3 cm of loose soil was placed in the bucket and leveled, and a layer of damp tissue paper was carefully laid on the soil layer. The step was repeated until 10-12 layers of tissue paper were present in the soil sample. The loose soil-tissue paper sample was then compacted by applying three blows in the similar manner discussed earlier. The impedometer or penetrometer was then inserted at the center of the soil sample. A 60° segment was then removed to observe soil displacement by noticing the displacement of the tissue paper.

RESULTS AND DISCUSSION

Visual Observations of Soil Displacement

Shown in Figure 1 is the tissue paper displacement by the penetrometer and impedometer for the 15% moisture and 3 blows compaction condition in the Cecil sandy clay soil. Much soil displacement near the path of the cone in the vertical direction is obvious in the case of the penetrometer, whereas with the impedometer, only a slight vertical displacement in the top layer was noticeable. A careful observation of soil displacement indicates that with the impedometer the penetration pressure was nearly all due to radial soil displacement whereas, with the penetrometer, a substantial vertical component was present.

Characteristic Penetration Pressure-Depth Relations

Two characteristic types of relationships of the penetration pressure vs depth were observed. In the Lakeland sand, the silica sand, and Tifton sandy loam and Cecil sandy clay (at the lowest moisture contents), the penetration pressure increased linearly with penetration depth. This trend was consistant for all compaction levels and with all cone angles. When Tifton sandy loam and Cecil sandy clays were sufficiently moist to have compressible aggregates, the penetration pressure vs. depth was non-linear and reached a constant pressure before the maximum penetration depth was reached.

The two different penetration pressure-depth relationships may be best explained by considering the compressibility of the soil. Based on an analysis of various mathematical relationships presented by Sangerlat (1979), the linear penetration pressure-depth relationship could be best

---

[1]SAS Institute, Inc., SAS Circle, Box 8000, Cary, North Carolina 27511.

described by the Terzaghi penetration theory. In this theory, incompressible soil reaches classical coulomb failure, and the failure zone increases with depth of penetration. In the non-linear penetration pressure-depth relationship, soil aggregates presumably were compressed to the point of plastic or compression failure. Greacen et al. (1968) suggest that when aggregate failure occurrs, the radius of soil disturbance by a cone penetrometer is less than 10 cone diameters, which was consistant with our visual observations.

Cone Index and Relaxed Pressures

Means of maximum cone index and means of relaxed pressures for each soil type are presented in Fig. 2 and an overall summary is listed in Table 2. Cone index with the impedometer was always lower. Relaxed pressure was always less than the corresponding cone index. Relaxation was more pronounced with the impedometer, especially in the heavier textured soils. Coefficients of variation in cone index were slightly larger with the impedometer compared to the penetrometer and the coefficients of variation in relaxed pressure were substantially larger with the impedometer.

Tables 3 and 4 list mean cone index and mean relaxed pressure averaged for each moisture content, cone angle, and compaction level within each soil type. In general, moisture effects are complex owing to the fact that moisture can change soil displacement patterns. The higher moisture average appeared to coincide with the moisture content offering the highest real or apparent cohesion value. As cone angle increased penetration and relaxed penetration pressures generally decreased (Figure 3). For Lakeland Sand, Silica Sand and Cecil Sandy Clay, significant differences were noted, with higher cone angles generally resulting in lower cone indices. In the Tifton Sandy Loam there were no significant differences among the cone angles. Effects of compaction level on cone index and relaxed pressures are shown in Figure 3. Compaction had, by far, the greatest effect on the respective cone indices. Each compaction level was statistically significantly different when analysed by soil type.

Penetration Pressure Ratios

Ratios involving cone index and relaxed pressure were computed to aid in further interpretation of the data and are defined as follows: The cone index ratio (P_L/P), penetrometer relaxation ratio (PR/P), impedometer relaxation ratio (PR_L/P) and relaxed pressure ratio (PR/PR). Numerator and denominator cone angles were consistant in all ratios. Calculations are summarized in Tables 2 and 5 and shown in Figure 4.

Cone Index Ratio (P_L/P): This ratio was consistent for the soil types (Figure 4). The same trend held with respect to compaction level (compare appropriate lines on Figure 3). The ratio tended to increase with cone angle (Figure 3). To adequately understand lubrication effects on cone index requires an appropriate mathematical model. Kostritsyn (1956) and Greacen et al (1968) present models which relate cone index to cone geometry variables, soil properties and soil-metal friction. These models should provide a suitable bases for additional investigations.

Relaxation Ratios (PR/P and PR_L/P_L): Mean values of these ratios for each soil type by moisture, cone angle and compaction level are

shown in Figure 4 and Table 2. More relaxation occurred with the impedometer, especially in the heavier soils. For both the impedometer and penetrometer, soil type, compaction level and moisture had considerable influence on cone index and relaxed pressures. The degree of relaxation, indicated by the ratio PR/P in Table 2, is highly dependent on soil type, moisture and compaction level. According to Mitchell (1976) the magnitude of pressure relaxation depends upon the magnitude of applied stress (penetration pressure here) immediately before relaxation begins, soil plasticity and prior stress history. Aggregate compressibility also has a bearing. In other words, relaxation depends on a combination of susceptibility to "work hardening" and the amount of work hardening performed prior to penetration. Low relaxation is indicative of incompressible aggregates or highly compacted plastic soils. Conversely, high relaxation denotes low compaction in plastic soils.

Relaxed Pressure Ratio (PR_L/PR): Effect of moisture content and cone angle was similar on this ratio as was observed on the PR/P and PR/P_L ratios. However, soil type effects were less influential on PR_L/PR ratio compared to other ratios. It was noteworthy that, even when additional compaction (increased number of blows) resulted in only a small change in the measured bulk density, the relaxed PR_L/PR ratio increased indicating a sensitivity to loading. This ratio did exhibit the highest coefficient of variation of all ratios evaluated (Table 5). Pending further evaluation, this ratio may provide an indication of effective compaction important for plant growth, tillage and trafficability studies.

CONCLUSIONS

1) Two types of failure are possible:

   a) In compressible soils where aggregates are plastic, the penetration pressure-depth relation tended towards constant pressure with increasing depth suggesting that soil disturbance was occurring within a relatively smaller zone near the cone.

   b) In incompressible, non-plastic soils the penetration pressure-depth relationship indicated an increasing pressure with depth, suggesting the possibility of classical Coulomb-Rankine failure.

2) Based on the limited visual evidence and on the fact that lubrication always decreased the penetration relaxation ratio (PR_L/PR), it was concluded that lubrication enhances the likelihood of a consistent radial soil failure around the cone, thereby making the soil reaction less variable.

3) Relaxation was least apparent when aggregates were incompressible and compaction was highest. Conversely, relaxation was most apparent when soils were plastic and compaction was least. The relaxation ratio, (PR_L/PR) appears to be useful in predicting the sensitivity of a soil mass to future loading.

It is felt that a measurement system involving an impedometer can be useful for more thoroughly quantifying the soil physical condition. Mathematical models can aid in more completely realizing potential bene-

fits of the soil impedometer. Consideration of soil deformation theories presented by Kostritsyn (1956) and Greacen et al. (1968) suggests a complex relationship between soil-metal friction and cone index. Additional testing is planned to consider not only the Kostritsyn (1956) and Greacen et al. (1968) models but also the Schafer et al. (1969) similitude-based model. The increased consistency of the soil reaction with the impedometer enhances the potential of improving empirical and basic relationships for defining soil conditions, which may be used for determining trafficability and for quantifying effects of tillage operations on soils.

LITERATURE CITED

American Soc. Agricultural Engineers. 1982. Soil Cone Penetrometers, ASAE S313.1. Agricultural Engineers Yearbook. Am. Soc. Agr. Engrs., St. Joseph, MI.

Barley, K. P. and E. L. Greacen. 1967. Mechanical Resistance as a Soil Factor Influencing the Growth of Roots and Underground Shoots. Advances in Agronomy #19, (Ed. by A. G. Norman). Amer. Soc. Agronomy, Madison, WI.

Gill, W. R. and G. E. Vanden Berg. 1968. Soil Dynamics in Tillage and Traction. U. S. Dept. of Agr. Handbook 316. U. S. Dept. of Agric., Washington, D. C.

Kostritsyn, A. K. 1956. [Cutting of a Cohesive Medium with Knives and Cones.] Vsesolvzz/Akad. Sel 'skohozlalstvennykh Nauk. Zeml. Mekh. Shorn. Trudov (Leningrad) 3:247-290, illus. [Natl. Inst. Agr. Engin. Eng. Translation 58].

Liljedahl, J. B., W. M. Carleton, P. K. Turnquist and D. W. Smith. 1979. Tractors and Their Power Units (3rd Ed.) John Wiley & Sons, New York.

McKibben, E. G. and D. O. Hull (1940). Transport Wheels for Agricultural Machines VIII. Soil Penetration Tests as a Means of Predicting Rolling Resistance. Agr. Engineering. 21:231-234.

Mitchell, J. K. 1976. Fundamentals of Soil Behavior. John Wiley-Sons, Inc., New York.

Sangerlat, G. 1979. The Penetrometer and Soil Exploration. (2nd Ed.) Elsevier, Amsterdam.

Schafer, R. L., W. R. Gill and C. A. Reaves. 1975. Lubrication of Soil-Metal Interfaces. Transactions of ASAE 18(5):848-851.

Schafer, R. L., C. A. Reaves and D. F. Young. 1969. An Interpretation of Distortion in the Similitude of Certain Soil-Machine Systems. Transactions of ASAE, 12(1):145-149.

Tollner, E. W. and B. P. Verma. 1983. Modified Cone Penetrometer for Assessing Soil Mechanical Impedance. Transactions of ASAE (In Press).

Waterways Experiment Station (1948). Development of Testing Instruments. Tech. Memo. 3-240. Trafficability of Soils, 3rd. Supp. 66 p. (original not seen. Cited by Gill and Vanden Berg, 1968).

Wismer, R. D. and H. J. Luth. 1974. Off-road traction prediction for wheeled vehicles. Transactions of ASAE 17(1):8-10, 14.

Zelenin, A. N. 1950. Basic Principles of the Theory of Soil Cutting. Moscow (original not seen, cited by Gill and Vanden Berg, 1968).

Table 1.
Test condition of soils: soil type, moisture content, compaction level (blows), and measured dry bulk density.

Soil Type	Moisture Content (%)	Blows	Dry Bulk Density (g/cm^3)
Lakeland Sand	6	3	1.58
		6	1.62
		12	1.68
	10	3	1.61
		6	1.71
		12	1.74
Silica Sand	4	3	1.22
		6	1.27
		12	1.35
	8	3	1.22
		6	1.26
		12	1.30
	14	3	1.30
		6	1.30
		12	1.34
	24	3	1.39
		6	*
		12	*
Cecil Sandy Clay	8	3	1.15
		6	1.28
		12	1.28
	11	3	1.00
		6	1.05
		12	1.10
	15	3	0.90
		6	1.10
		12	1.30
	21	3	1.29
		6	1.35
		12	1.60
Tifton Sandy Loam	6	3	1.43
		6	1.49
		12	1.58
	11	3	1.56
		6	1.64
		12	1.73
	15	3	1.77
		6	1.87
		12	*

*Not run due to poor soil conditions.

Table 2.
Summary of Statistical Parameters on Dependent Variables for the Impedometer (Im) and Penetrometer (Pe).

Soil Type	Dept. Var.*	Error Deg. Freedom		Mean Square Error		Coef. Var.		Mean	
		Im**	Pe**	Im	Pe	Im	Pe	Im	Pe
Lakeland	P	65	65	737	1709	13.9	16.5	184.7	251.1
Sand	PR	64	65	1535	1134	38.0	19.55	103.1	178.2
	PR/P**	64	65	0.012	0.001	24.2	4.96	0.61	0.67
Silica	P	108	109	796	1756	16.2	19.1	173.6	219.2
Sand	DP	107	108	598	1184	23.6	22.56	103.6	150.5
	PR/P	107	108	0.007	0.002	14.6	6.39	0.56	0.68
Cecil	P	128	135	8309	14056	35.1	30.3	259.3	336.8
Sandy	PR	30	29	730	884	32.5	14.2	83.1	208.4
Clay	PR/P	30	29	0.004	0.002	24.5	9.06	0.25	0.56
Tifton	P	88	88	1092	1446	25.9	19.7	150.8	192.5
Sandy	PR	87	88	367	296	45.4	19.8	42.2	87.0
Loam	PR/P	87	88	.007	0.004	34.6	14.6	0.25	0.45

*PR/P refers to relaxed pressure/Cone index, within cone angle.
PR refers to relaxed pressure (kilopascals)
P refers to cone index (kilopascals)

**Note that the tabulated PR/P ratio does not exactly equal values of PR/P calculated using the above data. This occurs because values of PR/P calculated from the above data are not calculated within angle (same cone angle for numerator and denominator). The tabulated PR/P is the appropriate average of values calculated within angle.

Table 3.
Means of Cone Index Over Moist, Cone Angle and Blows for Each Soil Type for the Impedometer (Im) and Penetrometer (Pe).

Soil Type	Moisture Content	Im	Pe	Cone Angle	Im	Pe	No. Blows	Im	Pe
	%	kPa	kPa	degree	kPa	kPa		kPa	kPa
Lakeland Sand	6	196.7	256.2	15	217.0	308.2	3	92.9	131.6
	10	192.7	246.0	20	176.7	243.7	6	170.9	229.7
				25	201.3	227.7	12	313.3	391.5
				30	183.8	224.7			
Silica Sand	4	162.7	203.2	15	179.82	260.7	3	113.8	156.3
	8	174.2	231.6	20	190.53	229.2	6	186.9	237.3
	14	218.7	270.8	25	174.97	195.0	12	237.0	283.4
	24	63.6	77.2	30	149.9	191.2			
Cecil Sandy Clay	8	171.2	249.5	15	277.7	383.1	3	135.8	207.2
	11	351.0	461.6	20	244.2	330.1	6	216.5	316.6
	15	341.9	408.0	25	284.3	317.1	12	433.2	486.8
	21	152.4	228.3	30	230.2	317.0			
Tifton Sandy Loam	6	157.8	189.2	15	157.2	192.9	3	67.6	99.3
	11	230.4	288.4	20	153.9	198.2	6	114.3	155.2
	15	28.3	53.7	25	147.1	199.0	12	330.4	388.2
				30	145.0	189.0			

Table 4.
Relaxed Pressure Over Moisture, Cone Angle and Blows for Each Soil Type with the Impedometer (Im) and Penetrometer (Pe).

Soil Type	Moisture	Im	Pe	Cone Angle	Im	Pe	Blows	Im	Pe
	%	kPa	kPa	degree	kPa	kPa		kPa	kPa
Lakeland	6	113.0	175	15	128.5	215.4	3	32.2	82.9
Sand	10	93.5	169	20	97.2	168.4	6	71.4	155.7
				25	102.5	153.7	12	202.7	278.1
				30	85.6	151.4			
Silica	4	89.7	135.2	15	110.2	188.1	3	56.5	106.6
Sand	8	105.9	162.0	20	120.0	162.5	6	114.3	165.0
	14	140.1	197.0	25	103.1	135.6	12	154.8	200.5
	24	24.3	47.3	30	81.1	122.5			
Cecil Sandy	Relaxed Valves Only			15	132.6	236.8	3	49.5	193.6
Clay	at the 11% Moisture			20	66.7	216.8	6	90.0	278.3
	Level			25	87.3	199.0	12	109.0	15.20
				30	46.0	189.9			
Tifton Sandy	6	51.4	104.2	15	39.4	88.5	3	15.5	43.0
Loam	11	57.64	113.5	20	42.4	86.5	6	25.7	66.0
	15	5.43	21.3	25	43.4	88.9	12	109.7	184.4
				30	43.4	83.8			

Table 5.
Summary of Statistical Parameters on Defined Ratios Combining Impedometer (denoted by subscript and Penetrometer (no subscript) Effects Within Cone Angles.

Soil Type	Dep. Variable*	Error Deg. Fred.	Mean	Mean Square Error	Coef. Var.
Lakeland Sand	P /P	65	0.78	0.022	19.2
	PR /PR	64	0.55	0.04	40.2
Silica Sand	P /P	106	0.73	0.030	21.4
	PR /PR	104	0.68	0.039	29.1
Cecil Sandy Clay	P /P	128	0.73	0.026	22.2
	PR /PR	29	0.43	0.026	37.6
Tifton Sandy Loam	P /P	88	0.74	0.034	25.1
	PR /PR	87	0.41	0.025	38.1

* P_L/P denotes impedometer cone index ratio/penetrometer cone index

PR_L/PR denotes impedometer relaxed pressure/penetrometer relaxed pressure

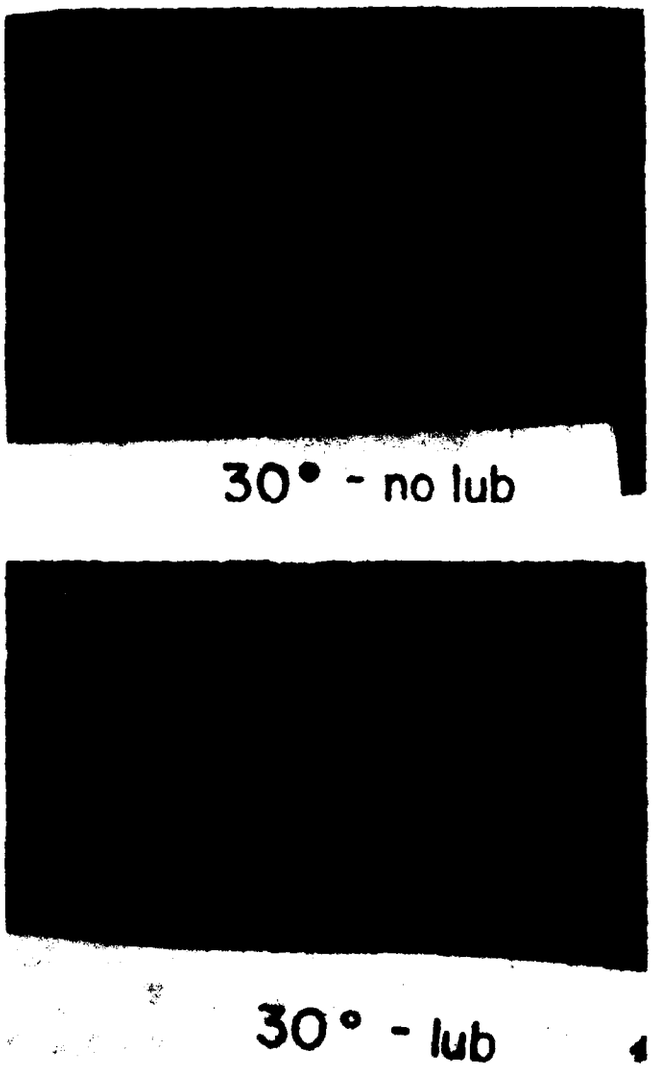

Figure 1. Photographs showing soil displacement patterns resulting from penetrometer (no-lub) and impedometer (lub). The cone angle was 30°; the soil was Cecil Sandy Clay, 15% moisture, 3 blows, for both cone insertions.

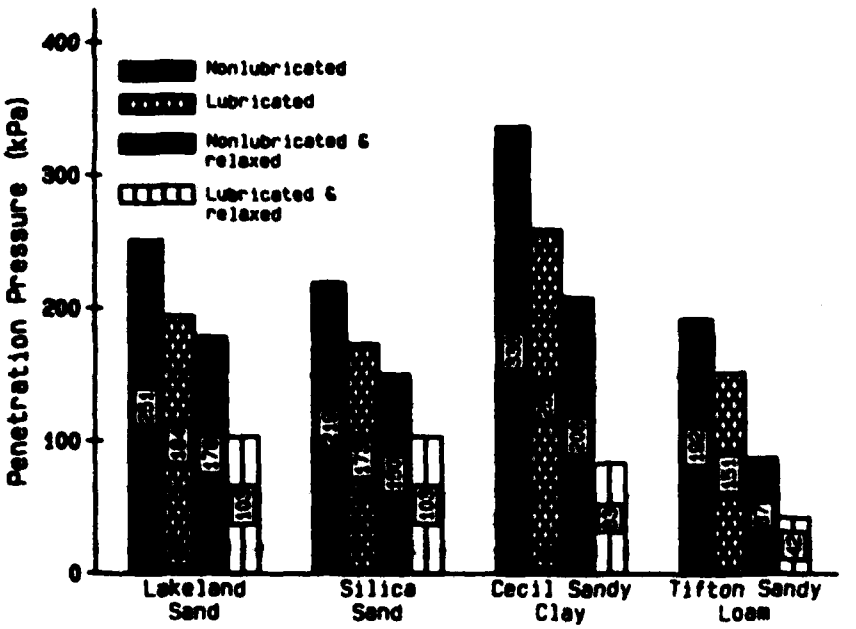

Figure 2. Histogram of cone index means and relaxed pressure means, over all test conditions within soil types for penetrometer (non-lubricated) and impedameter (lubricated), for each soil type tested.

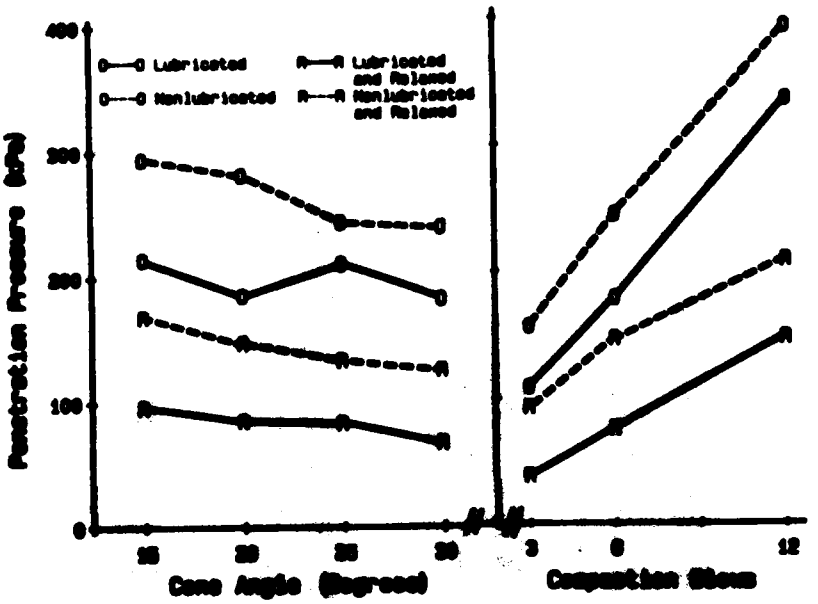

Figure 3. Plots of Penetration Pressure (cone index or relaxed pressure) versus cone angle, and versus compaction level for penetrometers (non-lubricated) and impedometers (lubricated).

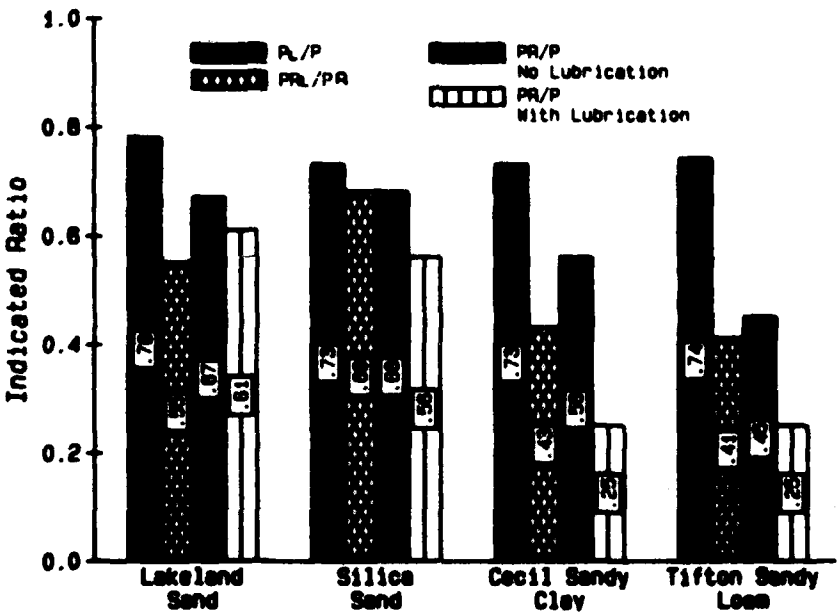

Figure 4. Histogram of cone index ratio (P_L/P) means, relaxation ratios (PR/P and PR_L/P_L) means, and relaxed pressure ratio (PR_L/PR) means, over all test conditions within each soil, for each soil type tested.

A Consideration of Elasto-plastic Model for the Composite Soil

MASAMI UENO

Faculty of Agriculture. The Univ.of RYUKYUS,NISHIHARA,OKINAWA,JAPAN

ABSTRACT

The soil of fields should be regarded as a composite material or composite soil which contains plant's root. By the effect of root, mechanical properties of the composite soil are different from those of usual soil. Then, it may be necessary to estimate and to recognize qualitative and quantitative influences of this difference i.e. root's effect to the trafficability, especially that of low ground contact pressure tractor such as the crawler type. The mechanical properties of composite soil was discussed as a first step to achieve this purpose in this paper. Some experimental results of paddy field's soil as a kind of composite soils showed that the effect of root appeared evidently in the extension and low stress deformation processes. Because plastic deformation also occured remarkably in these stress states, the composite soil was classified mechanically into the elasto-plastic body. Based on these results, an elasto-plastic model, which was modified one for soil, was introduced and examined qualitatively its behaviours. Some parameters were used in this model to account for the characteristics of the plasticity of composite soil. These parameters control the hardening and softening behaviours, which are the function with the volumetric plastic strain and deviatoric plastic strain. Qualitative and quantitative examinations showed that this model properly interpreted the elasto plastic behaviours of composite soil. An example of concrete elasto-plastic constitutive equation was derived from this model. This constitutive equation gave suitable stress-strain curves.

1. Introduction

The main purpose of this paper is to investigate the mechanical properties of composite material with soil and root by the viewpoint of elasto-plastic theory. Although the composite material is a term in the field of industrial materials, that means in this paper the soil includes root. This composite material is named the 'composite soil'.

Off-road vihicles, especially the agricultural machinery, ordinarily run on the ground covered with grass, tree and other plants such as fields. Since this soil contains roots of the plant, its properties are different from the usual soil. In particular the mechanical properties may be more or less influenced by that of roots. Therefore, the trafficability or mobility of off-road vihicles is affected by these roots relating to the mechanical properties indirectly. As shown in recent Japanese type combine harvester tracked crawler shoes, the mean ground contact pressure of some vihicles has gradually decreased to about 2.0 kPa. Under the low ground contact pressure the behaviours of soil may be strongly influenced by the root's effect.

This effect of root has not been regarded as an important factor not only to the studies of trafficability but also to the soil mechanics in the past these studies. At least there was no report to investgate the mechanical properties of the composite soil associated with root's effect. Two main reasons may be thought to this disregard of root's

effect. The one is that this influence is so small to the deformation behaviours of soil under wheel or crawler having the high ground contact pressure relatively. The other is that the soil mechanics has not been sufficiently developed to account for the deformation behaviours of soil included into the composite soil, because soil has very complex mechanical properties. While the importance of soil mechanics to solve the problems related to trafficability has been eagerly insisted, there is a few result of successful application against expectation.

One of the roles of soil mechanics to the study on trafficability is to predict the stress or strain distribution in soil under wheel and crawler. It is necessary for this purpose to describe clearly the deformation behaviours and its resistance of soil. Elasto-plastic theories for soil have been discussed actively in the last two decades to represent the mechanical properties refered to the stress-strain relationships which is called the 'constitutive equation'. It can give mathematical expressions of those stress-strain relationships. Some trials have been treated for applying these results to the problems of sinkage and draft of wheel or crawler by the use of the limit analysis and the FEM (1.Karafiath). Consequently, mechanical properties of composite soil must be clear based on soil mechanics to take consideration into the root's effect upon the problems of trafficability.

Mechanical properties of composite soil perhaps depend on volume and distribution of roots, strength of each root and water contents. But, mechanical properties of component soil, which is called 'matrix soil' in this paper, are most primary factor to those of composite soil. Thus, there are so many factors to influence the mechanical properties of composite soil that the constitutive equation may be very complex. In addition, these factors related to root vary remarkably by the kind of plants, climate etc. So, it may be impossible to take the complete constitutive equation for applying all kinds of composite soil. Therefore, it is rational to discuss the constitutive equation with restriction of application range to the each kind of composite soil.

In this paper, the characteristics of mechanical properties of composite soil were arranged theoretically based on the some experimental results(2.Ueno). As a first step, an elasto-plastic model was assumed and examined its behaviours. Then, an example of elasto-plastic constitutive equation was derived by this model, and some stress-strain curves were calculated to examine this model and equation.

2. An outline of the mechanical properties of composite soil

The mechanical properties of the composite soil called 'Nae Mat' in Japanese as an example which was the paddy field's soil contained roots of rice seedling, were examined experimentally(2. Ueno). Root of rice seedling is small, weak and flexible to the outer force, and constructs the network structure of roots such as fiber reinforced material. Accordingly, the mechanical properties of this composite soil mainly depends on that of matrix soil, but there are some different characteristics compared with usual soil.

These characteristics were summarized as follows on the viewpoints of elasto-plastic theory.

(a) The tendency of shearing and compression characteristics , i.e. dilatancy, strain hardening behaviours and shear strength etc., is near to those of loose packed soil.

(b) Unnegligible extension resistance occurs, which is not observed in most kinds of soil without clay.

(c) The mechanical properties of composite soil is affected by that of soil, weight or volume of roots, strength of each root and water content.

(d) Matrix soil and root show the different responces each other to the mode of applying force. For examples root plays an important role on extension process and soil does on compression process.

(e) The strain is consisted of elastic, plastic and viscostic component. The plastic component is remarkable not only in the finite strain but in the infinitesimal strain.

(f) Stress-strain curves in extension and compression processes represent by the power function.

$$\sigma = a\varepsilon^n \qquad (2.1)$$

the value of exponent is about 0.5 in extension and about 1.0 in compression, within the absolute value of strain 0.3 as shown in Fig.1. In eq.(2.1), σ is stress, ε is strain, a and n are material constants.

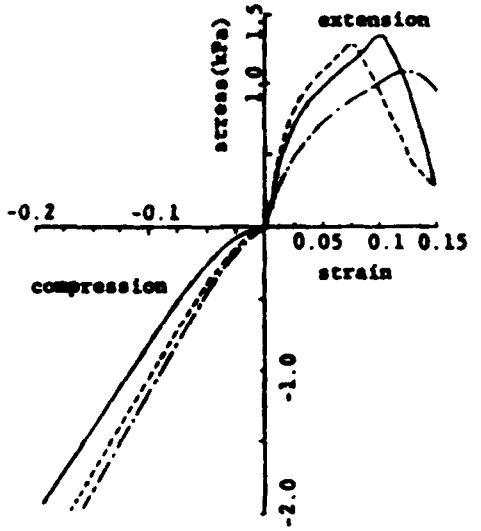

Fig.1 Stress-strain curves of a composite soil

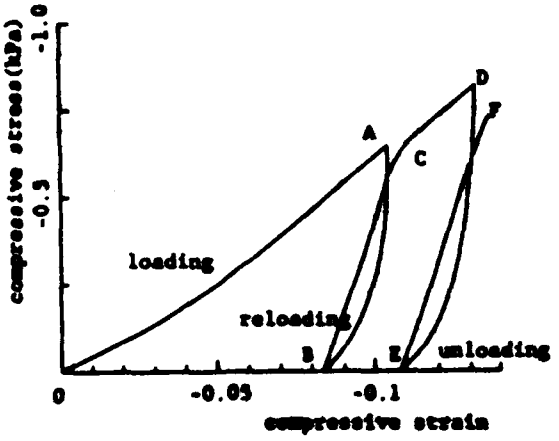

Fig.2 Stress-strain curve in cyclic compression test

In cyclic compression loading process, hysteresis loop appears clearly in the stress-strain curve(see Fig.2).

(g) Shear strength is approximated by Coulomb-Mohr's equation in negative normal stress region.

Taking into consideration with these characteristics, an mechanical model was examined to represent the extension and compression behaviours as shown in Fig.3. This model is consisted of spring, dashpot and slider to account for the elasticity, viscocity and plasticity respectively. This model has three elements A, B and C. The elements A and B are composed of the standard linear solid and slider, the each component has different properties. The fook element C(see Fig.3) distingishes between extension state and compression state, namely in extension state force F acts upon element A, on the other hand in compression state force F acts upon element B apart from A. Thus, the difference of stress-strain curves is possible to describe qualitatively by this model.

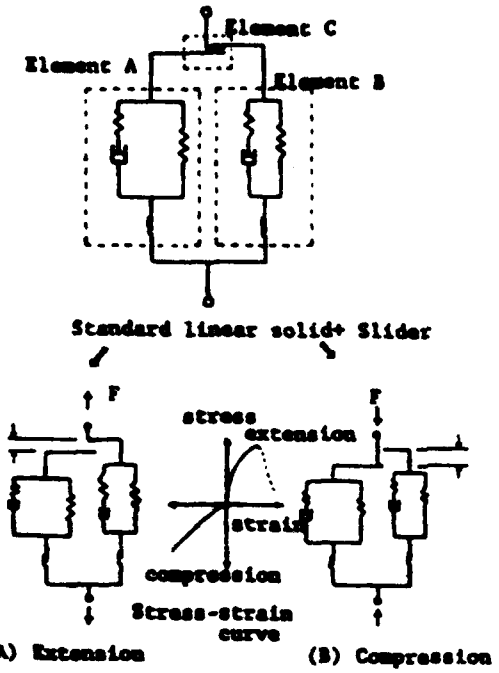

Fig.3 A mechanical model of a composite soil and its behaviours

Although this model can be used to estimate the one dimensional deformation behaviours of composite soil, it can't be applied to general three dimensional deformation problems. So, it is important to do investigate the general mechanical model for applying to the trafficability problems. Because plastic deformation is more remarkable than elastic deformation, mechanical models of composite soil have to be regarded as elasto-plastic models. Viscosity i.e. the time dependency of the deformation behaviours or stress-strain relationships is disregarded in new model. Therefore, this model can be applied to the quasi-static deformation problems.

3. A Plastic Model

While composite soil has some different properties compared with usual soil in the extension and low stress region, elasto-plastic deformation behaviours are generally similar to that of soils. So, most part of deformation behaviours of the composite soil can be expected to represent by the modified elasto-plastic model or constitutive equation for soil. In this section, plastic deformation behaviours are specified by the use of a plastic model.

Based on the above-mentioned experimental outline, following basical assumptions were employed to explain the plastic behaviours of the composite soil.

(a) Yield condition or yield surface exists. This is a function with stress σ_{ij} and plastic strain ε^p_{ij} as follows.

$$f(\sigma_{ij}, \varepsilon^p_{ij})=0. \tag{3.1}$$

or separative form

$$f(\sigma_{ij})-F(\varepsilon^p_{ij})=0. \tag{3.2}$$

where f is a loading function and F is a hardening function which controls the hardening and softening behaviours.

(b) The shape of yield surface in the stress space looks like that of soil which is smooth, outer convex against to the Coulomb-Mohr's surface and closed surface i.e. envelope surface.

(c) The size of initial yield surface is primarily determined by initial

void ratio of composite soil, volume of roots and strength of each root. In this case the influence of water content don't take into consideration, so stress means the effective stress.

(d) Hardening and/or softening behaviours occur with proceeding of plastic deformation, and succeeding yield surfaces are affected not only the plastic volumetric strain ε_v^p but also the second order invariant of deviatoric plastic strain ε_s^p.

(e) Plastic strain increment $d\varepsilon_{ij}^p$, occurs foward to the direction of outer normal unit on the current yield surface. This is generally called the 'associated flow rule' or the 'normality condition', which is represented as follows (3. Drucker).

$$d\varepsilon_{ij}^p = G \frac{\partial f}{\partial \sigma_{ij}} \tag{3.3}$$

where G is a non-negative coefficient which gives the magnitude of plastic strain increment.

(f) Plastic deformation occurs both of the yield stress state and subyield stress state that stress does not reach to the current yield surface(4. Hashiguchi). In the subyield stress state, plastic deformation behaviours are provided by plastic potential φ in similar to the yield surface. In this case the plastic strain increment is taken by the equation that f exchange to φ in eq.(3.3).

These basical assumptions are usually applied to the granular material like as soils without (c) and (d). Assumptions (c) and (d) were introduced to account for the influence of root to the characteristics of plastic deformation behaviours of composite soil.

Based on these assumptions, a concrete plastic model was assumed and the plastic deformation behaviours were analyzed qualitatively as follows.

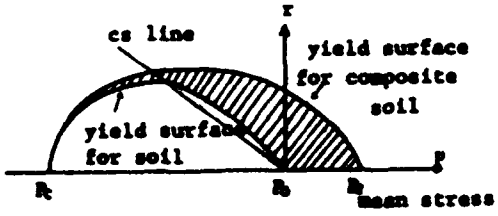

Fig.4 Initial yield surfaces of composite soil and component soil in (p,r) plane

(1) Initial yield surface

Initial yield surfaces for matrix soil and composite soil in the (p,r) plane, where p is pressure and r is second-order invariant of stress deviator, are respectively as shown in Fig.4. Both surfaces and p-axis intersect at the points p_t, p_c and p_0, p_c respectively. These surfaces coincide at the point p_t(<0). If root is relatively strong this surface for composite soil is larger than that for matrix soil. On the other hand, both surfaces apart from each other with increase of the value of p. It means that the composite soil yields higher stress than soil in the hatching zone in Fig.4. Accordingly the strength of composite soil is larger than that of soil within this zone. Value of p_t is mainly influenced by the void ratio of composite soil, and the mechanical conditions of root affect to the value of p_c. If the volume of roots increases and each root becomes strengthen, value of p_c becomes large. Consequently composite soil is reinforced by the root such as fiber reinforced solids in the extension and low stress state.

(2) Yield condition

Yield condition is described by the function f in eq.(3.2).

In many plasticity theories, it is ordinarily assumed that plastic strain increment $d\varepsilon^p_{ij}$ occurs when stress reaches to the yield surface(5. Schofield). In this paper, it is insisted that $d\varepsilon^p_{ij}$ occurs although stress stays within the yield surface(4. Hashiguchi). The plastic potential φ, which is a function with current stress, rules plastic deformation within subyield stress state.

$$\varphi < f \tag{3.4}$$
$$\varphi = f \tag{3.5}$$

Eq.(3.4) gives subyield stress state, and eq.(3.5) gives yield stress state. Normality condition also exists in the subyield stress state as same as the yield stress state.

(3) Plastic strain increment

Plastic strain increment $d\varepsilon^p_{ij}$ is given by following equation derived by the basical assumption (e) and (f).

$$d\varepsilon^p_{ij} = H\,(\varphi/f)^n \frac{\partial \varphi}{\partial \sigma_{ij}}\, d\varphi \tag{3.6}$$

$$\varphi/f < 1 \tag{3.7}$$
$$\varphi/f = 1 \tag{3.8}$$

Eq.(3.7) means subyield stress state and eq.(3.8) means yield stress state. $Hd\varphi$ in eq.(3.6) is non-negative coefficient which corresponds to the coefficient G in eq.(3.3). $(\varphi/f)^n$ controls the magnitude of plastic strain increment $d\varepsilon^p_{ij}$ at the subyield stress state. There is no distinct point to devide subyield and yield stress state, so this transition process is shown smooth. When stress reaches to the yield surface, $f=\varphi$ satisfies in the loading process, and, plastic strain increment in eq.(3.6) equals to that in eq.(3.3).

(4) Hardening, softening and dilatancy behaviours

As discussed by Schofield, Roscoe and Wroth(5.6.7.8), the hardening behaviours of soil are primarily determined by the plastic volumetric strain ε^p_v. Namely, hardening and softening behaviours are associated to the plastic volume change, swelling and shrinking. Especially, the volume change under shear which is called the dilatancy is an important characteristic of deformation of granular materials. Experimental results showed that the composite soil deformed with hardening, softening and dilatancy behaviours same as soil.

Second-order invariant of plastic deviatoric strain ε^p_r is an important measure of those phenomena of composite soil as same as plastic volumetric strain ε^p_v. When the value of ε^p_r or plastic shearing displacement increases, roots contained the composite soil are gradually cut and became weaken. ε^p_r reaches to the critical value ε^p_{rr}, which is a function with the strength of each root and its distribution, then roots are completely cut, so the resistance of shearing deformation decreases rapidly to that of matrix soil. If once are cut, roots don't contribute to the succeeding deformation. This process is equivalent to softening behaviours without the influence of ε^p_v.

Further, positive volumetric plastic strain ε^p_v or swelling causes the softening or weakening of composite soil. If ε^p_v exceeds the critical value ε^p_{vv}, which is a function of the strength of each root and its distribution, roots don't affect the succeeding deformation as same as ε^p_r. Negative volumetric plastic strain ε^p_v, on the other hand, causes hardening, because the void ratio becomes small without cutting of roots.

Plastic deformation behaviours and stress-strain relationships in the simple deformation process such as extension and compression were discussed as follows based on above-mentioned plastic model. Yield surfaces are denoted by circles for simplicity in this qualitative simulation.

(A) Simple extension process

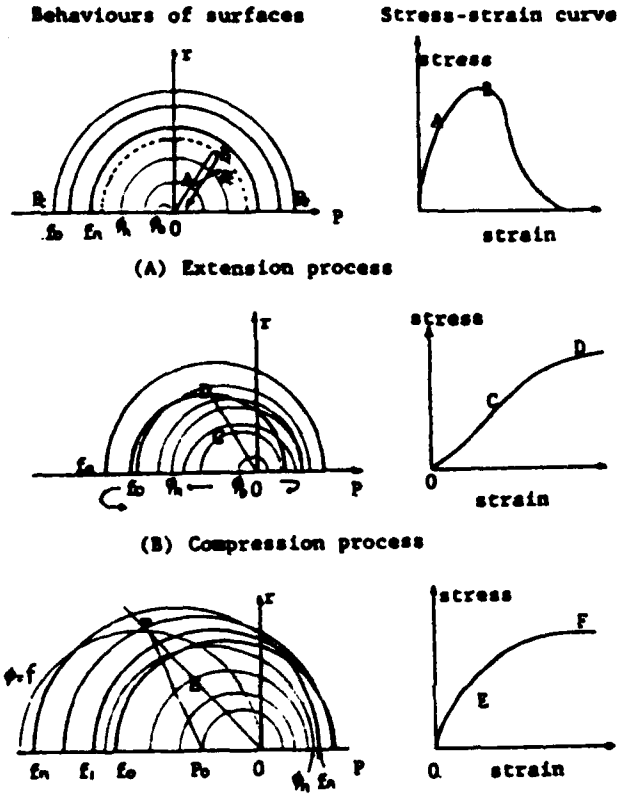

Fig.5 Hardening and softening behaviours of composite soil

The effective stress path of simple extension process draws a line OAB in the (p.r)plane as shown in Fig.5. Initial yield surface and initial plastic potential are denoted by f_0 and φ_0 respectively. After stress reaches to φ_0 plastic strain increment $d\varepsilon_1^p$, occurs along the direction to outer unit normal from the current plastic potentialφ. $d\varepsilon_1^p$, consists of the positive volumetric component $d\varepsilon_v^p$ and deviatoric component $d\varepsilon_s^p$. So, the composite soil is softened with the proceeding of deformation, and the magnitude of $d\varepsilon_1^p$, becomes gradually large. The size of plastic potential φ increases isotropically, and that of yield surface becomes gradually small.

These changes turn remarkable with the elongation, and stress-strain curves drav the shape looks like a mountain (see Fig.5).
The tangential gradient of stress-strain curve decreases with increasing of strain. After the peak of this curve appears at φ_{max}, the value of stress decreases gradually. Then, yield surface f coincides with plastic potential φ, namely yield condition, and both are shirinking rapidly as shown in Fig.5.

(B) Simple compression process

In compression deformation process stress increases from the origin of (p.r)plane and draws a path OCD as shown in Fig.5. Plastic strain increment $d\varepsilon_1^p$, has negative or positive volumetric component $d\varepsilon_v^p$ and deviatoric component $d\varepsilon_s^p$. If negative $d\varepsilon_v^p$ occurs, the hardening behaviours appear in this process. Therefore, the plastic potential φ increases with the proceeding of deformation and the yield surface f becomes large. The increasing rate of plastic potential becomes larger than that of yield surface gradually. Then, the volumetric component of

$d\varepsilon_{ij}^{p}$, decreases gradually in this process and ultimately reaches to the condition $d\varepsilon_{ij}^{p}=0$ which is called 'critical void state'. The deviatoric component $d\varepsilon_{r}^{p}$ increases with the softening behaviours. Until ε_{v}^{p} becomes fairly large, the softening behaviours associated to $d\varepsilon_{r}^{p}$ is not evidence due to the hardening behaviours by ε_{v}^{p}. If stress reaches to the critical void state, that is equivalent to the failure condition, yield surface decreases gradually.

On the other hand, if positive ε_{v}^{p} occurs the softening behaviours appear from the beginning of this process. Because, softening is happened by ε_{r}^{p}, the resultant softening becomes remarkable.

(C) Triaxial compression process

The deformation behaviours in this process are basically similar to those of compression process, although deformation begins arbitrary initial value of p.

4. Elasto-plastic constitutive equation

1) Plastic constitutive equation

In this section, an example of the plastic potential or yield surface of composite soil was firstly assumed to deduce a concrete plastic constitutive equation. Since Schofield and Wroth(8) had established the 'critical soil mechanics', some types of yield surface have been proposed in the field of soil mechanics. An elipse surface proposed by Burland(9) was chosen as an yield surface of composite soil in this paper.

$$f^2 = p^2\left\{1+\frac{1}{M^2}\left(\frac{r}{p}\right)^2\right\} \tag{4.1}$$

Because the composite soil exhibits resistance of deformation against to the extension, the form of this function is slightly modified as follows.

$$f^2 = \varphi^2 = (p-p_0)^2\left\{1+\frac{1}{M^2}\left(\frac{r}{p-p_0}\right)^2\right\} \tag{4.2}$$

where, p is pressure, r is second-order invariant of deviatoric stress $\sigma_{ij}(=\sigma_{ij}-p\delta_{ij})$, M is value of $(-r/p)$ at the critical void state. p_0 represents the coordinate of p-axis at the center of elipse. The notation of stress and strain are as follows.

$$p = \sigma_{ij}\delta_{ij}/3$$

$$r = (\sigma_{ij}\sigma_{ij})^{0.5}$$

$$\varepsilon_{v}^{p} = \varepsilon_{ij}^{p}\delta_{ij}$$

$$\varepsilon_{r}^{p} = ((\varepsilon_{ij}^{p}-\varepsilon_{v}^{p})(\varepsilon_{ij}^{p}-\varepsilon_{v}^{p}))^{0.5}$$

The size of yield surface f equals to the value of hardening function F. The following equation was adopted as an example of F.

$$F = F_s + P \tag{4.3}$$

$$F_s = F_0\exp(-\varepsilon_{v}^{p}/a) \tag{4.4}$$

$$P = P_e\left(1-\alpha\frac{\varepsilon_{r}^{p}}{\varepsilon_{v,r}^{p}}\right)^{n}\left(1-\Delta\frac{\varepsilon_{r}^{p}}{\varepsilon_{r\infty}^{p}}\right)^{l} \tag{4.5}$$

F_s is a hardening function proposed by Hashiguchi(4) for soil, that derived from the $\ln|p|$ - ε_{v}^{p} linear relationships. In eq.(3.4), F_0 is an

initial value of F_s. α is a gradient of the $\ln|p|$ - ε_v^p linear relationships. Function P is introduced to account for the effect of roots to the hardening and softening behaviours of composite soil. P_o is an initial value of P. The second term of right hand in eq.(3.5) represents the effect of ε_r^p, and third term of that does the effect of ε_v^p. m and l in eq.(4.5) are material constants respectively. The denotation + and Δ in eq.(3.5) control the behaviours of yield surface related to hardening and softening. They have following values to simulate the deformation of composite soil.

$$+ = 1 \quad (\varepsilon_r^p \leq \varepsilon_{rr}^p) \tag{4.6a}$$

$$+ = 0 \quad (\varepsilon_r^p > \varepsilon_{rr}^p) \tag{4.6b}$$

$$\Delta = 1 \quad (0 < \varepsilon_v^p \leq \varepsilon_{vv}^p) \tag{4.7a}$$

$$\Delta = 0 \quad (\varepsilon_v^p \leq 0, \varepsilon_v^p > \varepsilon_{vv}^p) \tag{4.7b}$$

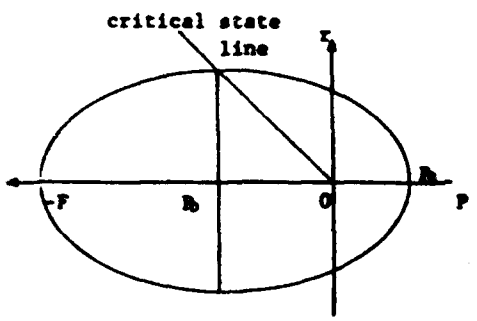

Fig.6 An example of plastic potential and yield surface of composite soil in (p,r) plane

If ε_r^p reaches to ε_{rr}^p, the influence of ε_r^p to the function P vanishes. Also the influence of ε_v^p to the function P is as same as the case of ε_r^p. In addition, if $\varepsilon_v^p \leq 0$, the function P don't affect the hardening function F. Therefore, the role of + and Δ is important on the hardening function F.
Fig.6 shows the above mentioned yield surface in (p,r) plane. Applying eq.(3.2) - (3.5) to eq.(2.6), plastic strain increment is given as follows.

$$d\varepsilon_{ij}^p = \frac{\langle \varphi / F \rangle^n}{(\partial F/\partial \varepsilon_v^p)(\partial \varphi/\partial p) + (\partial F/\partial \varepsilon_r^p)(\partial \varphi/\partial r)} \frac{\partial \varphi}{\partial \sigma_{ij}} \frac{\partial \varphi}{\partial \sigma_{kl}} d\sigma_{kl} \tag{4.8}$$

or

$$d\varepsilon_{ij}^p = \frac{\langle \varphi / F \rangle^n}{(\partial F/\partial \varepsilon_v^p)(\partial \varphi/\partial p) + (\partial F/\partial \varepsilon_r^p)(\partial \varphi/\partial r)} \frac{\partial \varphi}{\partial \sigma_{ij}} \left(\frac{\partial \varphi}{\partial p} dp + \frac{\partial \varphi}{\partial r} dr \right) \tag{4.9}$$

where,

$$\frac{\partial \varphi}{\partial p} = \left\{ 1 + \frac{1}{M^2} \left(\frac{r}{p - p_0} \right) \right\}^{0.5} - \frac{r^2}{\varphi M^2 (p - p_0)} \tag{4.10}$$

$$\frac{\partial \varphi}{\partial r} = \frac{1}{\varphi} \frac{r}{M^2} \tag{4.11}$$

$$\frac{\partial F}{\partial \varepsilon_v^p} = -\frac{1}{\alpha} F_s - \frac{\Delta l}{\varepsilon_{vv}^p (1 - \Delta \varepsilon_v^p / \varepsilon_{vv}^p)} P \tag{4.12}$$

$$\frac{\partial F}{\partial \varepsilon_r^p} = -\frac{+m}{\varepsilon_{rr}^p (1 - + \varepsilon_r^p / \varepsilon_{rr}^p)} P \tag{4.13}$$

When the composite soil yields, φ is replaced by f in these equations.

These equations are so complex that the application to the practical problems is difficult without computer aided calculations. But, these equations are deduced to simple form relatively on the specific deformation processes such as extension, compression etc as follows.
(a) Swelling and shrinking process:

$$d\varepsilon_v^p = \frac{(\varphi/F)^n}{(\partial F/\partial \varepsilon_v^p)(\partial \varphi/\partial p)} \left(\frac{\partial \varphi}{\partial p}\right)^2 dp \tag{4.14}$$

(b) Axisymmetrical compression and extension process:

$$d\varepsilon_a^p = \frac{(\varphi/F)^n}{9(\partial F/\partial \varepsilon_v^p)(\partial \varphi/\partial p) + (\partial F/\partial \varepsilon_\gamma^p)(\partial \varphi/\partial \tau)} \left(\frac{\partial \varphi}{\partial p} + 2\frac{\partial \varphi}{\partial \tau}\right)\left(\frac{\partial \varphi}{\partial p} + \right.$$

$$\left. + \frac{2}{\sqrt{6}}\frac{\partial \varphi}{\partial \tau}\right) d\sigma_a \tag{4.15}$$

$$d\varepsilon_r^p = \frac{(\varphi/F)^n}{3(\partial F/\partial \varepsilon_v^p)(\partial \varphi/\partial p) + (\partial F/\partial \varepsilon_\gamma^p)(\partial \varphi/\partial \tau)} \left(\frac{\partial \varphi}{\partial p} + \frac{2}{\sqrt{6}}\frac{\partial \varphi}{\partial \tau}\right)\frac{\partial \varphi}{\partial p} d\sigma_a \tag{4.16}$$

where $d\varepsilon_a^p$ is axial plastic strain increment and $d\sigma_a$ is axial stress increment.

2) Elastic constitutive equation

In soil mechanics, the plastic deformation behaviours and constitutive equation have been investigated eagerly more than the elasticity. Therefore, the appropriate elastic constitutive equations have not been established. Hooke's law, which is a linear elastic constitutive equation, is used for convenience to the numerical method analysis such as FEM.

Stress-strain curves with elastic deformation of soil show remarkable nonlinearity not only volumetric deformation but shearing deformation. This nonlinearity also appears to that of the composite soil as same as soil. So, following equation was chosen as an elastic constitutive equation for the composite soil, which had been proposed by Hashiguchi(4) as an example of elastic one for soil.

$$d\varepsilon_{ij}^e = \frac{\beta}{3(p_r - p)} dp\delta_{ij} + a N r^{N-1} d\sigma_{ij} \,. \tag{4.17}$$

where, p_r, β, a and N are 'material constants', δ_{ij} is Kronecker's delta, σ_{ij} is deviatoric stress. The first term of the right side of this equation represents the elastic volumetric deformation and the second term of that does the shearing deformation. It is the shortcoming of this equation that can't to describe the difference of elastic behaviours between extension and compression.

3) Elasto-plastic constitutive equation

Strain ε_{ij} (or strain increment $d\varepsilon_{ij}$) is usually assumed as the sum of elastic strain ε_{ij}^e (or $d\varepsilon_{ij}^e$) and plastic strain ε_{ij}^p (or $d\varepsilon_{ij}^p$).

$$\varepsilon_{ij} = \varepsilon_{ij}^e + \varepsilon_{ij}^p \tag{4.18a}$$

$$d\varepsilon_{ij} = d\varepsilon_{ij}^e + d\varepsilon_{ij}^p \tag{4.18b}$$

Plastic strain increment in eq.(4.6) and elastic strain increment in eq.(4.17) apply to those of in eq.(4.18b) to derive an elasto-plastic constitutive equation of composite soil.
Then, the following elasto-plastic constitutive equation was given.

$$d\varepsilon_{ij} = \left\{E^{-1}_{ijkl} + \frac{(\varphi/F)^{*}}{(\partial F/\partial \varepsilon^{p}_{ij})(\partial \varphi/\partial p) + (\partial F/\partial \varepsilon^{p}_{ij})(\partial \varphi/\partial r)} \frac{\partial \varphi}{\partial \sigma_{ij}} \frac{\partial \varphi}{\partial \sigma_{kl}}\right\} d\sigma_{kl} \qquad (4.19)$$

where E^{-1}_{ijkl} is an elastic constitutive tensor given by eq.(4.17). Usually, the matrix expression of this equation is used to the investigation of the general stress-strain relationships and the numerical analyses of three dimensional deformation problems.

4) Examples of stress-strain curve calculated by this equation

Elasto-plastic constitutive equation for simple loading processes, extension and compression, was taken by above discussions. Examples of stress-strain curve in compression process were calculated from these equations(eq.(4.15),(4.16)). The calculation of these curves were used to the numerical integration. The procedure was as follows. Stress increment was calculated by the given plastic strain increment. Then, elastic strain increment and strain increment were estimated by this stress increment. These process were repeated since to take the certain value of stress or strain.

As given in Fig.7 the stress-strain curves varied those forms by the values of "material constants". Those material constants were shown in Table 1. These curves could be approximated by the power function, which was similar to the experimental results as shown in eq.(2.1).

Table-1. material constants used to the calculation

F_0	0.2.	P_e	0.2.	l	1.0.		
m	1.0.	α	0.03.	M	0.5.	n	0.01.
β	0.01.	a	0.001	p_r	0.5.	N	1.0.
c^{p}_{ij}	0.1.						
c^{p}_{ij}	0.2	(curve A)					
	0.5	(curve B)					
	0.1	(curve C)					

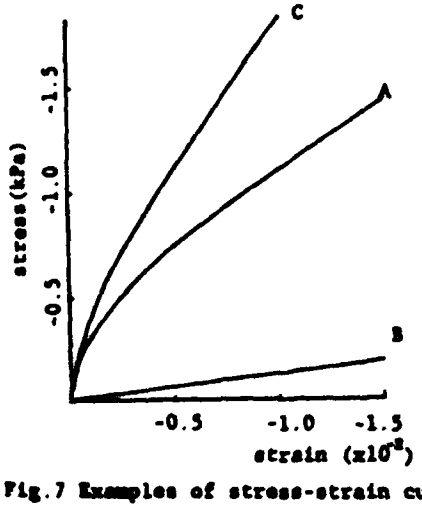

Fig.7 Examples of stress-strain curve by the elasto-plastic constitutive equation

5. Concluding remarks

After the qualitative simulation was treated, an elasto-plastic model for the composite soil was introduced and examined its behaviours as a first step to estimate the influence of root's effect on the trafficability of low ground contact pressure vihicles. An example of the constitutive equation derived by this elasto-plastic model. While the composite soil has vide range of mechanical properties, the elasto-plastic models have to be discussed case by case. Further the efforts may be necessary that to make clear the relationships between the mechanical properties of composite soil and the trafficability.

reference

1) Karafiath L. L. and E. A. Nowatzki: Soil mechanics for off-road vihicle engineering, Series on Rock and Soil Mech., 1978, TRANS TECH S.A. Germany
2) Masami Ueno: Elasto-plastic studies on rice seedling mat(in printing)
3) Drucker, D. C.: Some implications of work hardening and ideal plasticity, Quart. Appl. Math., Vol.7, No.4, 411-458, 1950
4) Hashiguchi K. and M. Ueno: Elasto-plastic constitutive laws of granular materials, Proc. of 9th ICSMFE, Session 9, 73-82, 1977
5) Schofield A. N. and C.P. Wroth: Critical State Soil Mechanics, 1968, Mcgrav-Hill
6) Roscoe F. H. A. N. Schofield and C. P. Wroth: On the yielding of soils, Geotech., Vol.8, No.2, 22-53, 1958
7) Roscoe F. H and A. N. Schofield: Yielding of clays in states wetter than critical, Geotech., Vol.13, No.3, 211-240, 1963
8) Roscoe F. H. and H. B. Poorooshasb: A theoretical and experimental study of strains in triaxial compression tests on normally consolidated clays, Geotech., Vol.13, No.1, 12-38, 1963
9) Burland J. B.: The yielding and dilation of clay, Corres. Geotech., Vol.13, No.3, 211-214, 1965

SOIL BIN FACILITIES: CHARACTERISTICS AND UTILIZATION

R. D. Wismer
Deere & Company Technical Center
Moline, Illinois
USA

ABSTRACT

The results of a survey of soil bin facilities worldwide are summarized. Characteristics and capabilities of the soil bin facilities are cited as well as types of soil-machine tests performed. Research emphasis of the laboratories is discussed. This paper should serve as a valuable reference to soil dynamics specialists by providing a list of soil bin facilities worldwide, their locations, principal investigator, and plans for future research activities.

INTRODUCTION

The development of science and its application—engineering—is very much dependent upon the availability and capability of physical experimental facilities. Without carefully controlled observations of important phenomena, theories cannot be evaluated, modified and evolved. Thus, one measure of an engineering science, such as terrain-vehicle mechanics, is the number and capability of experimental facilities in use. These facilities include both laboratory installations and field test equipment. Laboratory facilities that support soil machine interaction studies—soil bins—were the subject of an international survey conducted in the summer of 1983. Researchers worldwide were contacted to determine the number and capability of soil bin facilities around the world. The results of this survey are summarized in this paper.

LOCATION, STAFF AND GENERAL CHARACTERISTICS

A total of 36 soil bin installations have been located in 12 countries possessing a total of 90 soil bins of varying geometry and sophistication (Table 1). Two-thirds of the soil bin facilities are located in universities with the remainder in technical institutes except for three soil bin installations that are operated by commercial firms. All the commercial soil bins are located in North America. Approximately 80 percent of all the soil bins are "indoor" but only about one-third of these have air temperature or humidity control.

A total of 185 engineers and 96 technicians operate the soil bin facilities reported. As shown in Table 1, the distribution of the number of engineers and technicians among soil bin installations vary widely with one or two per installation being most common. On the average, the facilities have one technician for every two engineers. Complete addresses of the soil bin installations and the names of the principal investigators are presented in the Appendix.

SOIL BIN GENERAL CHARACTERISTICS

The geometry of soil bins reported is presented in Table 2. Although considerable variability is apparent among the soil bin dimensions, some dimensional sizes predominate. Considering only the principal soil bin of each installation a mean

TABLE 1. SOIL BIN INSTALLATIONS

	NUMBER OF		
	SOIL BINS	ENGINEERS	TECHNICIANS
BELGIUM			
Univ. Cath. Louvain	3	1	2
CANADA			
McGill Univ.	3	4	3
Univ. Saskatchewan	1	18	5
Versatile Noble Cultivators Co.	1	3	2
DENMARK			
Royal Vet. & Ag. Univ.	1	1	1
FEDERAL REPUBLIC OF GERMANY			
Tech. Univ. of Munich	3	7	7
Univ. of German Forces	2	10	3
FRANCE			
Estab. Technique D'Angers	2	—	—
JAPAN			
Hokkaido Univ.	3	12	2
Kyushu Univ.	3	3	1
Mie Univ.	2	12	1
THE NETHERLANDS			
IMAG	1	1	1
Tech. Univ. of Eindhoven	2	3	3
POLAND			
Inst. for Bldg. Mech. & Elect.	2	3	2
Warsaw Agricultural Univ.	1	8	2
Warsaw Technical Univ.	1	—	—
PEOPLE'S REPUBLIC OF CHINA			
Chinese Acad. of Ag. Mech'y Science	5	23	16
Jilin Univ. of Technology	4	17	9
Tractor Research Inst. of China	3	7	5
THAILAND			
Asian Inst. of Technology	2	2	3
UNITED KINGDOM			
Cranfield Inst. of Technology	3	5	1
National Inst. of Ag. Engineering	3	2	2
Univ. of Newcastle Upon Tyne	5	5	1
Royal Military College of Science	3	2	2
Scottish Inst. of Ag. Engineering	1	5	4
Transport & Road Research Lab.	5	2	1
UNITED STATES			
Caterpillar Tractor Co.	4	7	2
Deere & Company	1	2	1
Univ. of Illinois	1	—	—
Iowa State University	1	4	1
Kansas State University	1	2	1
University of Kentucky	1	1	0.5
NTML, USDA	12	8	8
North Carolina State Univ.	2	3	1
Purdue University	1	1	0.2
Virginia Polytechnic Inst. & State U.	1	1	1

length of 22 meters, width of 2 meters, and depth of approximately 0.8 meters results. The median values for these principal dimensions are 20 meters, 1.6 meters and 0.6 meters, respectively. There is a high incidence of the larger soil bins, that is length greater than 20 meters, being of an outdoor type.

Test speeds also vary over a broad range with a mean maximum speed of 2.5 meters per second. Minimum speeds are predominantly in the 0 to 0.1 of a meter per second range. A maximum-to-minimum speed ratio of 25 or greater predominates. The median values for maximum test forces are approximately 10 kN for vertical and fore-and-aft forces and less than 5 kN for lateral force.

Functional test capabilities of the soil bin facilities are also presented in Table 2. Tillage is the most common functional test capability with more than two-thirds of all laboratories possessing this capability. Wheel traction is the next most common test capability. It is quite apparent that many laboratories are solely dedicated to either tillage or traction testing. Only six laboratories possess the capability of testing earthmoving devices.

TEST SOILS

Characteristics of the soils used in the soil bins are given in Table 3. A broad variety of soils are reported, ranging from heavy clays to sands, with loams the most common soil type. Moisture, density, cohesion, angle of internal friction and cone index value ranges for the test soils are presented in Table 3. Strength values appear to be quite representative of field conditions with the exception of very high strength soils. Artificial soils are used by six laboratories with an oil-sand-clay mixture being the dominant combination.

Procedures and equipment for processing the soil bin soils are given in Table 4. Tilling followed by leveling and compacting is the most common reprocessing procedure. The rotary tiller, leveling blade and smooth wheel roller are the most commonly used equipment. As with the soil type, a great diversity of procedures and equipment are used in the laboratories.

The laboratories report using a number of soil strength and condition tests for correlating machine performance and for controlling the preparation of test sections. The soil test equipment is listed in the following table by rank order of use:

RANK	SOIL TEST	NUMBER OF LABORATORIES
1	Cone penetrometer	36
2	Ring/plate shear	24
3	Gravimetric moisture and density	23
4	Atterberg limits (liquid and plastic)	23
5	Triaxial shear	22
6	Plate penetration	22
7	Unconfined compression	18
8	Nuclear moisture-density	12
9	Tensile strength	11
10	Vane shear	4

TABLE 2. SOIL BIN GENERAL CHARACTERISTICS

	SOIL BIN DIMENSIONS, m			SPEED, m/s		MAX. FORCES, kN			FUNCTION TEST CAPABILITY		
	LENGTH	WIDTH	DEPTH	MIN	MAX	VERTICAL	FORE & AFT	LATERAL	TILLAGE	TRACTION	EARTH-MOVING
BELGIUM Univ. Cath. Louvain	20.0 2.0 1.8	1.0 0.7 1.6	1.4 0.75 0.39	0	3.0	–	–	–		X	
CANADA McGill Univ.	4.9 9.5 3.6	0.15 1.34 0.13	0.29 0.29 0.41	0	0.3	13	–	–	X	X	
Univ. Saskatchewan	14.0	2.0	0.5	–	–	2	–	–	X		
Versatile Robin Corporation Co.	18.0	3.0	0.6	0.89	2.9	6	6	0	X		
DENMARK Royal Vet. & Ag. Univ.	6.0	1.0	0.7	0	4.5	–	10	–	X		
FEDERAL REPUBLIC OF GERMANY Tech. Univ. of Munich	25.0 12.0 2.0	2.5 1.0 0.5	0.6 0.5 0.4	0	3.0	20	25	10	X	X	
Univ. of German Forces	25.0 25.0	1.5 1.5	1.2 1.2	0	5.0	20	20	2	X	X	
FRANCE Polish Technique D'Angers	69.4 60.0	7.0 7.0	1.2 0.55	–	–	–	–	–			
JAPAN Hokkaido Univ.	22.0	4.0 (three bins)	1.0	0.12	3.5	–	–	–	X	X	
Ryushu Univ.	17.2	1.65 (three bins)	1.0	0.1	2.0	–	–	–	X	X	
Ibiu Univ.	20.0 8.0	1.5 0.5	1.5 0.5	0.05	3.0	3	5	3	X		
THE NETHERLANDS IMAG	20.0	3.0	0.5	0.02	1.8	6	6	6	X		
Tech. Univ. of Eindhoven	44.0 6.0	2.75 0.5	2.2 0.5	0.05	2.2	60	25	20	X		
POLAND Inst. for Bldg. Mach. & Mat.	25.0 4.0	2.0 0.7	1.5 0.45	0	3.0	15	10	–		X	
Warsaw Agricultural Univ.	9.0	1.0	0.5	0.3	3.0	0.5	2	–	X		
Warsaw Technical Univ.	3.0	0.5	0.3	0	0.2	–	5	–	X		X
PEOPLE'S REPUBLIC OF CHINA Chinese Acad. of Ag. Mech'y Sci.	50.0 100.0 12.0	3.0 (two bins) 6.0 (two bins) 0.8	1.0 1.5 0.5	0	3.3	2	15	3	X	X	

Jilin Univ. of Technology	98.0 48.0 38.0 3.0	3.0 2.0 2.0 0.6	1.2 1.2 1.8 0.8	0.3	3.0	—	20	—	X	X	X
Tractor Research Inst. of China	44.8 21.0 88.8	3.0 1.8 4.8	0.8 0.7 1.0	0.17	2.5	20	10	—		X	
THAILAND											
Asian Inst. of Technology	18.0 16.0	2.0 2.0	1.5 1.5	0	1.8	—	—	—			
UNITED KINGDOM											
Cranfield Inst. of Technology	12.0 1.5 5.0	1.7 0.4 1.0	0.4 0.25 0.2	0.02	2.0	5	20	5	X		X
National Inst. of Ag. Engineering	4.5 2.0 16.8	0.9 0.3 1.0	0.4 0.3 0.3	0.005	5.0	2	10	2	X		
Univ. of Newcastle Upon Tyne	6.0 8.0	0.75 (three times) 0.75 (two times)	0.6 0.6	0.01	2.0	2	20	2	X	X	X
Royal Military College of Science	6.0	0.6 (three times)	0.3	0	0.3	—	—	—		X	
Scottish Inst. of Ag. Engineering	18.0	1.8	0.6	0	1.8	—	—	—			
Transport & Road Research Lab.	18.0	8.0 (two times)	1.0	0.6	1.7	—	147	—			
UNITED STATES											
Caterpillar Tractor Co.	17.7 17.7 18.3 22.0	0.8 0.9 1.3 1.3	0.2 0.2 0.5 0.7	0.2	1.0	10	10	—		X	X
Deere & Company	18.0	1.1	0.5	0	3.5	9	9	5	X	X	X
Univ. of Illinois	9.1	0.75	0.3	0	2.0	0.1	0.5	0.1	X	X	
Iowa State University	3.7	0.8	0.2	0	1.8	—	—	—	X	X	
Kansas State University	15.2	1.2	0.5	0.5	2.0	2	4	2	X	X	
University of Kentucky	8.2	1.2	0.9	0.03	4.5	22	11	—		X	
NTRL, USDA	70.2 67.5 17.2	0.1 (zero time) 0.1 (zero time) —	0.01 1.52 0.3	0	4.5	22	45	22	X	X	
North Carolina State Univ.	12.4 1.2	— 0.5	— —	4.8×10^{-5}	1.2	480	—	—	X		
Purdue University	17.1	1.2	0.37	0	1.0	4	4	2	X	X	
Virginia Polytechnic Inst. & State U.	10.0	1.0	0.4	0	1.4	1	2	0.5	X		

TABLE 3. TEST SOIL PROPERTIES

INSTALLATION	SOIL TYPE	MOISTURE CONTENT %	DENSITY (γ) g/cm³	COHESION (C) kPa	ANGLE OF INTERNAL FRICTION (φ) Degrees	CONE INDEX (CI) kPa
BELGIUM Univ. Cath. Louvain	Sand	–	–	–	–	–
CANADA McGill Univ.	Kaolinite Kaolinite–Sand	40–80 30	1.3–1.4 1.6	20–30 50	0 20	– –
Univ. Saskatchewan	–	–	–	–	–	–
Versatile Resin Cultivators Co.	Sand–Silt–Clay	–	–	–	–	–
DENMARK Royal Vet. & Ag. Univ.	Clay Loam Sand	11–14 8–11 0	1.3 1.2 1.2	– – –	– – –	– – –
FEDERAL REPUBLIC OF GERMANY Tech. Univ. of Munich	Sandy Loam Oil–Sand	14.5 8% Oil	1.2–1.7 1.55	5–30 0.3–2	23–34 22–28	130–1320 –
Univ. of Gottingen Forests	Sand Sandy Loam	– –	– –	– –	– –	– –
FRANCE Essais Techniques D'Angers	Clayey Silt (SiL) Sand (SP)	27–33 5–7	1.28–1.35 1.8	15–60 0	10 38	350 420
JAPAN Hokkaido Univ.	Sandy Loam Silt–Loam Clay Sand	40–42 28 28 0.8	1.0–1.2 1.3–1.6 1.6–1.7 1.8	4–10 5–29 68 0	40 30 27 32	680 460–600 800–1200 480
Kyushu Univ.	Sandy Clay Loam Clay Loam	4–34 –	– –	26 –	22–38 –	830 –
Mie Univ.	Sand Clay Loam	– –	– –	– –		
THE NETHERLANDS IMAG	Loamy Clay Sand	20 6	– –	– –	– –	400–800 400–700
Tech. Univ. of Eindhoven	Silt (Loess) Clay–Loam–Sand	15	1.4	2 (Variable)	40	
POLAND Inst. for Bldg. Mach. & Elect.	Sandy Loam	–	–	1.9–2.2	38–42	–
Warsaw Agricultural Univ.	Loamy Sand Heavy Clay	6 20	1.5 2.0	4 30	20 26	300 1000
Warsaw Technical Univ.	Sand Sand	2.2 7.0	1.44 1.60	~0 ~0	28 32	

PEOPLE'S REPUBLIC OF CHINA						
Chinese Assd. of Ag. Mach'y Sciences	Sandy Loam	8.4–19	1.3–1.7	13.6	37	1010–3980
Jilin Univ. of Technology	Clay	35	2.7	0.2–0.25	20	
	Sand	0.2	1.56	0	32	
	Loam	10–20	1.2–1.4	0.1–0.2	28–46	
Tractor Research Inst. of China	Paddy	–				
	Sand	–				
	Clay	–				
THAILAND						
Asian Inst. of Technology	Sandy Loam	3–80	1.0–1.5	0.1–2	10–30	200–1500
	Clay	3–80	1.0–1.5	1–5	5–15	200–1500
UNITED KINGDOM						
Cranfield Inst. of Technology	Sandy Loam	8–12	1.2–1.7	0–7	34–42	–
	Clay–Oil	~20%	1.6	12	5	–
National Inst. of Ag. Engineering	Sandy Clay Loam	10–17	1.2–1.8	–	–	500–2500
	Clay	18–60	0.9–1.5	–	–	300–1500
Univ. of Newcastle Upon Tyne	Sand	–	1.5–2.3	0	32–64	–
	Silt–Clay–Loam	–	–	5	0	–
Royal Military College of Science	Sand	–	–	–		
Scottish Inst. of Ag. Engineering	Sandy Loam	–	1.0–1.5	20–60	35	0–3000
Transport & Road Research Lab	Heavy Clay (CH)	23–34	1.4–1.66	15–120	–	–
	Lean Clay (CL)	16–23	1.6–1.8	15–100	–	–
	Clayey Sand (SC)	7–11	1.8–2.2	15–70	20–46	–
	Clayey Gravel (GC)	8–10	1.8–2.2	15–140	20–35	–
	Sand (SP)	5–12	1.6–1.7	–	–	–
UNITED STATES						
Caterpillar Tractor Co	Oil–Sand–Clay	–	2.4	10	46	600
		–	1.98	3.5	38	300
	Mixtures	–	2.2	15	38	300
		–	1.8	7	21	300
Deere & Company	Sand	~0	1.6–1.7	0–3	35–37	200–700
	Loam	11–15	1.3–1.7	2–10	26–38	80–600
	Clay	32–38	1.3–1.5	13–26	0–<3	150–300
Univ. of Illinois	Oil–Sand–Clay	–	1.88–2.17	5–6.6	41–44	340–670
Iowa State University	Silty Clay Loam	–	–	–		
Kansas State University	Oil–Sand–Clay	–	1.4–1.8	7	27	0–1000
University of Kentucky	Silty Loam	15–35	1.2–1.5	–	–	–
NTAE, USDA	Sandy Loam (SP-SC)			(Variable)		
	Silt Loam (CL-ML)			(Variable)		
	Silty Clay (CH-MH)			(Variable)		
North Carolina State Univ.	Sand to Clay					
Purdue University	NA					
Virginia Polytechnic Inst.	Oil–Sand–Clay	10	2.0	0.3	31	–

TABLE 4. SOIL PROCESSING PROCEDURE AND EQUIPMENT

INSTALLATION	PROCESSING PROCEDURE	PROCESSING EQUIPMENT
BELGIUM		
Univ Cath Louvain	–	–
CANADA		
McGill Univ	(pneumatic comp)	(pneumatic comp)
Univ Saskatchewan	TILL—SUB COMP—LEV—SUR COMP	RT—SHP FT ROL—SPIKE ROL—SM ROL
Versatile Noble Cultivators Co	CUL—HAR—LEV—PACK—WAT	SWP—SPIKE HAR—SM ROL—SPRY
DENMARK		
Royal Vet & Ag Univ	TILL—LEV—COMP	RT—GRD BLD—VIB
FEDERAL REPUBLIC OF GERMANY		
Tech Univ of Munich	(LOAM)—TILL—COMP—TILL—COMP	RC—LD PKR—SWP—VIB TAMP—ROL
	(LOAM)—TILL—COMP	OSC RC—SUB COMP—SM ROL
	(OIL-SAND)—COMP	HAND TAMPER—SM ROL
Univ of German Forces	–	–
FRANCE		
Estab Technique D'Angers	(CLAY)—TILL—WAT—LEV	RIP—TRK COMP
	(SAND)—TILL—LEV	RIP—LEV BLD
JAPAN		
Hokkaido Univ	TILL—LEV—SUB COMP—SUR COMP	RT—LEV BLD—SM ROL—LEV BLD
Kyushu Univ	TILL—LEVEL—COMP—LEVEL	VER RT—LEV BLD—SUB PACK—VIB ROL
Mie Univ	TILL—SPRY—TILL—LEV—COMP	RT—SPRY—RT—LEV BLD
THE NETHERLANDS		
IMAG	TILL—LEV—COMP	RT—GRD BLD—SM ROL
Tech Univ of Eindhoven	TILL—TILL—COMP—LEV	RT—SM ROL—LEV BLD
POLAND		
Inst for Bldg Mach & Elect	TILL—LEV—ROL—WAT	RT—GRD BLD—SM ROL—SPRY
Warsaw Agricultural Univ	TILL—LEV—COMP	RT—LEV BLD—SM ROL
Warsaw Technical Univ	TILL—LEV—COMP	–
PEOPLE'S REPUBLIC OF CHINA		
Chinese Acad of Ag Mach'y Sci	TILL—LEV—COMP—WAT	RT—GRD BLD—VIB ROL—SPRY
Jilin Univ of Technology	WAT—TILL—LEV—COMP—LEV	SPRY—RT—GRD BLD—VIB ROL—LEV BLD
Tractor Research Inst of China	TILL—LEV—COMP	RT—GRD BLD—SM ROL
THAILAND		
Asian Inst of Technology	TILL—COMP—WAT	RIP—RC—SM ROL
UNITED KINGDOM		
Cranfield Inst of Technology	REM SOIL—RECOMP LAYERS	BUCKET—BLADE—SM ROL
National Inst of Ag Engineering	TILL—COMP—LEV	RT—SM ROL—VIB ROT CUT BLD
Univ of Newcastle Upon Tyne	TILL—COMP—LEV	SPADE—STRIP VIB—PLT VIB—GRD BLD
Royal Military College of Science	RAKE—LEVEL—COMP	RAKE—LEV BLD—VIB SM ROL
Scottish Inst of Ag Engineering	TILL—COMP	VIB HAR—VIB SM ROL—SM ROL
Transport & Road Research Lab	TILL—WAT—MIX—COMP	RT—SPRY—RT—SM ROL
UNITED STATES		
Caterpillar Tractor Co	TILL—COMP	RT—SM ROL
Deere & Company	TILL—LEV—COMP	RT—LEV BLD—SM ROL
Univ. of Illinois	TILL—LEV—COMP	RT—LEV BLD—SM ROL
Iowa State University	TILL—LEV—COMP	RT—LEV BLD—SM ROL
Kansas State University	TILL—LEV—COMP	RT—LEV BLD—SM ROL—VIB BLD
University of Kentucky	REM SOIL—REPILL—WAT—COMP	RT—BUCKET—SPRAY—SM ROL
NTMRL, USDA	WAT—TILL—LEV—COMP	SPRY—RT—LEV BLD—SM ROL—V ROL
North Carolina State Univ	–	–
Purdue University	TILL—COMP	RT—SM ROL
Virginia Polytechnic Inst. & State U	TILL—LEV—COMP	RT—LEV BLD—SM ROL

NOTE: CUL = CULTIVATE, HAR = HARROW, WAT = WATER, LEV = LEVEL, SPRY = SPRAY, COMP = COMPACT, SUB = SUBSURFACE, SUR = SURFACE, REM = REMOVE, SM ROL = SMOOTH ROLLER, RT = ROTARY TILLER, GRD BLD = GRADER BLADE, VIB ROL = VIBRATING ROLLER, RIP = RIPPER, LD PKR = LAND PACKER, SWP = SWEEP, RC = ROTARY CULTIVATOR, PLT VIB = PLATE VIBRATOR

The laboratories were also surveyed concerning the primary soil measurement for control of test section preparation. The responses to this question indicated three principal tests are used: cone penetrometer; moisture; and density; with some laboratories using the triaxial shear and Bevameter.

TILLAGE TEST FACILITIES

The tillage test capability of the reported soil bin facilities is presented in Table 5. Twenty-six laboratories reported a tillage test capability and 21 of these can test

TABLE 5. TILLAGE — MAXIMUM TEST CAPABILITIES

INSTITUTION	PASSIVE (DRAWN)			POWERED						
	WIDTH cm	DEPTH cm	DRAFT FORCE, kN	VERT SHAFT	HORIZ SHAFT	TORQUE Nm	ROTATIONAL SPEED, rpm	DIA cm	WIDTH cm	DEPTH cm
CANADA										
McGill Univ.	10	15								
Univ. Saskatchewan	122	150	2							
Versatile Noble Cultivators Co.	100	15	6							
DENMARK										
Royal Vet. & Ag. Univ.				X	X	—	—	—	—	—
FEDERAL REPUBLIC OF GERMANY										
Tech. Univ. of Munich					X	—	—	—	—	—
Univ. of German Forces	50	40	20							
JAPAN										
Hokkaido Univ.	150	50	10		X	340	1200	100	200	50
Kyushu Univ.	50	50	10		X	157	400	50	150	50
Mie Univ.	30	20	3							
THE NETHERLANDS										
IMAG				X	X	200	350	50	20	10
Tech. Univ. of Eindhoven	250	100	25		X	500	1000	—	240	40
POLAND										
Warsaw Agricultural Univ.	23	18	2	X		—	400	12	18	15
Warsaw Technical Univ.	40	15	2							
PEOPLE'S REPUBLIC OF CHINA										
Chinese Acad. of Ag. Mech'y Sci.					X	640	230	40	100	20
Jilin Univ. of Technology	150	150	10							
UNITED KINGDOM										
Cranfield Inst. of Technology	150	30	20	X	X	200	150	30	50	30
National Inst. of Ag. Engineering	60	30	10	X		1000	200	60	60	20
Univ. of Newcastle Upon Tyne	72	40	20							
UNITED STATES										
Deere & Company	60	15	9		X	226	2000	60	23	15
Univ. of Illinois	20	10	0.6							
Kansas State University	38	8	0.4							
NTML, USDA	300	60	45	X	X	—	—	120	75	46
North Carolina State Univ.	5	30	—							
Purdue University	30	10	4							
Virginia Polytechnic Inst. & State U.	10	15	2							

passive tools, 12 powered tools, and 9 both passive and powered tools. The mean of the maximum width test capability for passive tillage tools was 80 cm with a median of 50 cm, while the mean maximum depth was 41 cm with a median of 30 cm. The typical maximum draft force capability for passive tools was 10 kN. The powered tillage tool test capabilities were predominantly horizontal shaft test facilities with six vertical shaft test facilities. The maximum torque test capability was nominally 350 Nm at speeds between 300 and 1000 rpm. Diameter, width and depth of powered tillage test facilities are also presented in Table 5.

TRACTION TEST FACILITIES

Twenty soil bins reported wheel traction test capabilities, six track and five laboritories had both wheel and track facilities. The maximum wheel and track test dimensions and forces are presented in Table 6 for the laboratories reporting. The wheel test facilities had a mean maximum diameter of 101 cm with a median of 80. A corresponding mean maximum wheel width was 38 cm with a median of 30. Maximum vertical load capability for wheel tests varied from 0.3 kN to in excess of 50 kN with similar values for maximum draft. The more limited track test facilities can test tracks of a nominal length of 150 cm and width of 30 cm. Vertical and draft loads for track tests varied over essentially the same range as for wheel tests. Essentially all the wheel and track test facilities could test both powered and unpowered elements. Approximately one-half of the facilities could conduct program-slip and program-load tests as well as constant variable tests. Program-draft capability was more limited with only eight wheel facilities and one track facility possessing this capability.

EARTHMOVING TEST FACILITIES

Earthmoving test facilities were the most limited functional test capability reported by the soil bin laboratories. Only six facilities possessed the capability to test one or more earthmoving devices. A summary of the maximum test capabilities of these laboratories is presented in Table 7. The maximum test dimension of these facilities was limited to approximately 100 cm with bucket volumes of about 0.1 of a cubic meter. The range of scale ratios used for model testing of earthmoving devices range from 1:5 to 1:20 with 1:5 being the most common.

RESEARCH TRENDS

Utilization of the soil bin facilities is impressive. A combination of research, design and teaching predominate in the utilization of the reported facilities. Only two of the 36 soil bin facilities are described as "inactive" by their principal investigator. The major emphasis of all the laboratories was on the conduct of soil-machine research that directly impacts the design of machines. The educational value of the laboratories appears to be concentrated in the training of graduate students within the overall research effort. Only one laboratory reported a "teaching only" function, and only three laboratories reported an "approval or official testing" of manufactured products function. The heavy emphasis of the laboratories on design application is encouraging considering the short term, but disconcerting for the long term.

The range of research subjects addressed by the laboratories is impressive. The traditional subjects of wheel and track traction efficiency, tillage tool shape and force relations, oscillating and powered tool performance, and soil-machine modeling were all cited for past and future research efforts. Some more unusual

AD-A150 653 PROCEEDINGS OF THE INTERNATIONAL CONFERENCE ON THE PERFORMANCE OF OFF ROA.. (U) INTERNATIONAL SOCIETY FOR TERRAIN VEHICLE SYSTEMS M G DWYER AUG 84 4/4

UNCLASSIFIED F/G 13/6 NL

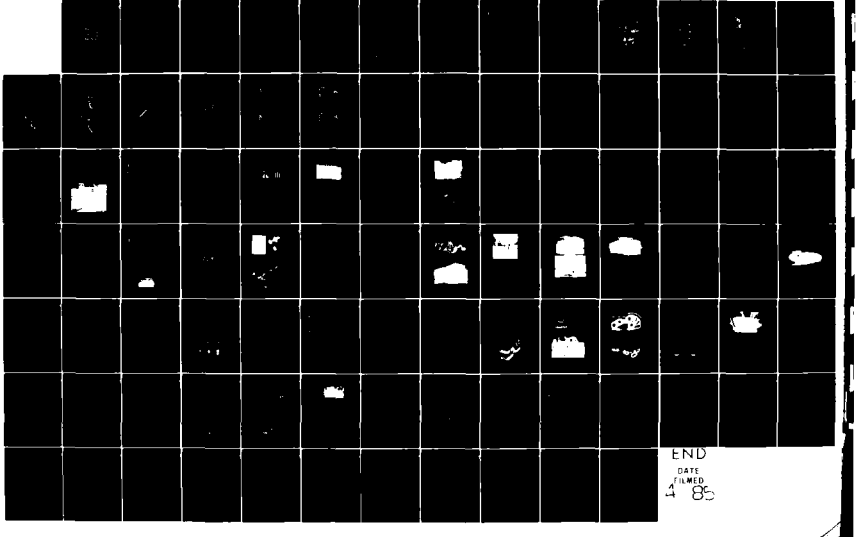

END

DATE FILMED

4 85

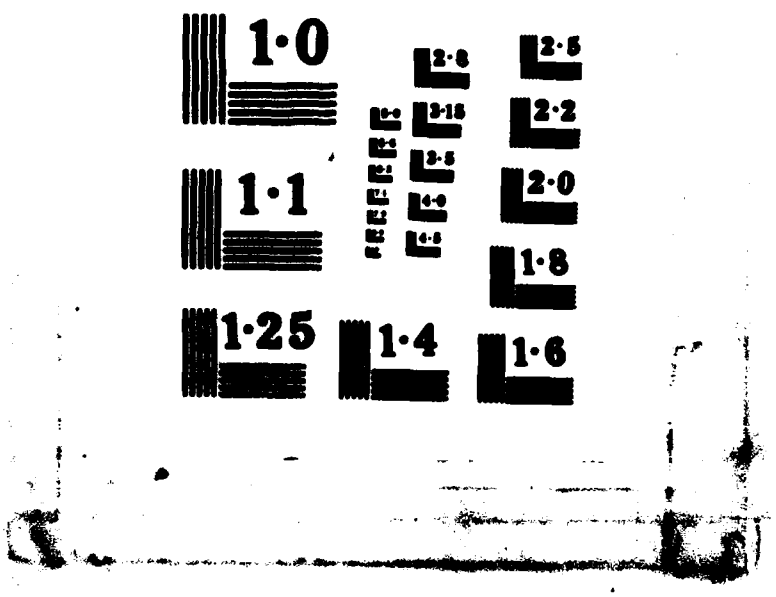
1·0
1·1
1·25
1·4
1·6
1·8
2·0
2·2
2·5

TABLE 6. TRACTION — MAXIMUM TEST CAPACITY

	WHEEL				TRACK			
	DIA cm	WIDTH cm	VERTICAL FORCE, kN	DRAFT FORCE, kN	LENGTH cm	WIDTH cm	VERTICAL FORCE, kN	DRAFT FORCE, kN
BELGIUM								
Univ. Cath. Louvain	200	120	49	9.8	—	—	—	—
CANADA								
McGill Univ.	36	10	1	—				
FEDERAL REPUBLIC OF GERMANY								
Tech. Univ. of Munich	170	50	38	25				
Univ. of German Forces	120	40	30	20				
FRANCE								
Estab. Technique D'Angers	—	—	45	45	—	—	45	45
JAPAN								
Hokkaido Univ.	100	20	3	3				
Kyushu Univ.	60	16	4	1				
Mie Univ.					—	—	—	4.9
POLAND								
Inst. for Bldg. Mech. & Elect.	160	50	15	10	160	30	15	10
Wrocław Technical Univ.					160	30	3	2
PEOPLE'S REPUBLIC OF CHINA								
Chinese Acad. of Ag. Mech'y Sci.	60	30	7	1				
Jilin Univ. of Technology	150	30	12	10				
Tractor Research Inst. of China	150	35	20	10	50	20	15	10
UNITED KINGDOM								
Univ. of Newcastle Upon Tyne	85	30	2	2				
Royal Military College of Science	30	15	—	—	15	15	—	—
UNITED STATES								
Caterpillar Tractor Co.	100	50	10	10	200	50	10	10
Deere & Company	60	25	9	9				
Univ. of Illinois	39	10	0.3	0.2				
Kansas State University	81	25	4	4				
University of Kentucky	38	19	6	4				
NTRL, USDA	188	79	71	44				
Purdue University	61	15	—	—				

TABLE 7. EARTHMOVING TEST CAPACITIES

INSTALLATION	DOZER BLADE		SCRAPER			LOADER BUCKET			EXCAVATOR BUCKET			TYPICAL MODEL RATIOS
	WIDTH cm	DEPTH cm	VOLUME m^3	WIDTH cm	DEPTH cm	VOLUME m^3	WIDTH cm	DEPTH cm	VOLUME m^3	WIDTH cm	DEPTH cm	
POLAND												
Warsaw Technical Univ.	28	2	0.02	30	6				0.027	30	6	—
PEOPLE'S REPUBLIC OF CHINA												
Jilin Univ. of Technology	100	20				0.5	100	20	0.1	30	20	—
UNITED KINGDOM												
Cranfield Inst. of Technology	180	30										
Univ. of Newcastle Upon Tyne	72	40	0.18	60	5							1:5
UNITED STATES												
Caterpillar Tractor Co.*	241–605	74–225	8–34	302–363	—	1–10.3	216–477	—	0.8–2.3	61–137	—	1:5 to 1:20
Deere & Company	48	16	0.0226	38	38	—	82	15				1:6

*Full-scale values not given. Model ratios between 1:5 and 1:20 are used to maintain cutting width between 20 and 25-cm.

research subjects reported are: rimless wheel; boat-type tillage machine; soil reinforcement; and soil anchors. Soil models for soil-machine systems were also the subject of research efforts including critical state soil mechanics principles, cycloidic properties of soils and two- and three-dimensional finite element models. Many studies of seed planter, grain drill, and fertilizer applicator performance and optimization were reported.

Regional emphasis was found in many of the research efforts reported. European and Asian laboratories concentrated on rotary and oscillitory tillage studies. Asian laboratories also emphasize studies of rice paddy tillage and traction. North American laboratories reported numerous studies of soil compaction causes and effects.

The single most common factor present in all the soil bin laboratories was—enthusiasm. The response to this survey was strong and indicated pride and determination among the practitioners of a very special engineering science—terrain-vehicle mechanics. This is undoubtedly our greatest strength and bodes well for the beneficial future use of the soil bin facilities reported in this paper.

APPENDIX

SOIL BIN LABORATORIES ADDRESSES AND PRINCIPAL INVESTIGATORS

BELGIUM

Professor P. F. J. Abeels
Department De Genie Rural
Faculte Des Sciences Agronomiques
University Cath. Louvain
Place Croix du Sud, 3
B-1348 Louvain-La-Neuve
Belgium

CANADA

Raymond N. Yong
Geotechnical Research Centre
McGill University
817 Sherbrooke St. W.
Montreal, PQ., Canada, H3A 2K6

W. B. Read
University of Saskatchewan
Agricultural Engineering Department
Saskatoon, Saskatchewan, Canada
S7N 0W0

Simon Hann
Versatile Noble Cultivators Company
Box 60
Nobleford, Alberta, Canada TOL 1S0

DENMARK

S. Sonne Kofoed
Department of Ag. Engineering
Agrovej 10
2630 Taastrup, Denmark

FEDERAL REPUBLIC OF GERMANY

Prof. Dr.-Ing. K.Th. Renius
Emeritus Prof. Dr.-Ing. W. Sehne
Institute of Agricultural Machinery
Technische Universitat of Munich
8000 Munich 2
Arcisstrabe 21, Germany

Prof. Dr.-Ing. Incobert Schmid
Institut Fur Kraftfahrwesen Und
Kolbenmaschinen
Hochschule Der Bundeswehr
Hamburg
(University of German Forces)
Holsen Hof Weg 85
2000 Hamburg 70, Germany

FRANCE

J. P. Constantin (GCB/MS)
Etablissement Technique D'Angers
Boite Postale n° 4107
49041 Angers Cedex, France

JAPAN

Dr. Matsui, Katsuhiro
Department of Ag. Engineering
Faculty of Agriculture, Hokkaido U.
Kita-9, Nishi-9, Kitaku Sapporo, 060
Japan

Jun Sakai
Agricultural Machinery Laboratory
Faculty of Agriculture
Kyushu University
Hakozaki, Higashi-ku
Fukuoka, 812 Japan

Professor & Chairman Tsutomo Ise
Department of Ag. Machinery
Mie University
Tsu, Mie Japan 514

THE NETHERLANDS

Dr. U. D. Perdok
IMAG
P.O. Box 43
6700 AA Wageningen
The Nethertands

C. F. Peelma
Technical University of Eindhoven
Department of Mech. Engineering
Post Box 513
5600 MB Eindhoven, Holland

POLAND

Prof. Dr. Andrzej Soltynski
Institute for Buildings Mechanization & Electrification in Agriculture
02-532 Warsaw, 32 Rakowiecka Str.
Poland

Prof. Dr. Joret Kuczewski
Institute of Agricultural & Forestry Engineering
Warsaw Agricultural University
02-766 Warsaw, ul. Nowowiyuowsha 166
Poland

Prof. Dr. Gustaw Tyro
Warsaw Technical University
Institute of Cranes & Heavy Construction
Narbutta St. 85
Warsaw, Poland

PEOPLE'S REPUBLIC OF CHINA

Hou Zhiming/Zhu Shenyou
Chinese Acad. of Ag. Machinery Sci.
No. 1 Beishatan Deshengmen Wai
Beijing, China

Prof. Chen Bing-Cong
The Department of Mechanics of Soil-Machine Systems
Jilin University of Technology
Changshun, Jilin
China

Deng Zhuorong
The Tractor Research Inst. of China
Luoyang, Henan
China

THAILAND

Dr. D. Goe-Clough
Division of Ag. & Food Engineering
Asian Institute of Technology
P. O. Box 2754
Bangkok, Thailand

UNITED KINGDOM

Prof. G. Spoor/Dr. R. J. Godwin
Silsoe College
Cranfield Institute of Technology
Silsoe
Bedford MK45 4DT, U.K.

Dr. J. V. Stafford
National Institute of Ag. Engineering
Wrest Park
Silsoe
Bedford MK45 4HS, U.K.

Dr. D. R. P. Hettiaratchi
University of Newcastle Upon Tyne
Department of Ag. Engineering
Porter Building, St. Thomas Street
Newcastle Upon Tyne, NE1 7RU, U.K.

Mr. J. G. Hetherington
Civil Engineering Department
Royal Military College of Science
Shrivenham
Swindon, Wilts, U.K.

D. J. Campbell
Scottish Institute of Ag. Engineering
Bush Estate
Penicuik
Midlothian, EH26 0PH
Scotland, U.K.

A. W. Parsons
Transport & Road Research Lab.
Crowthorne
Berkshire RG11 6AU, U.K.

UNITED STATES

R. J. Sullivan
Caterpillar Tractor Company
100 N.E. Adams Street
Peoria, IL 61629 U.S.A.

L. E. Stephens
Deere & Company Technical Center
3300 River Drive
Moline, IL 61265 U.S.A.

Dr. Carroll E. Goering
Department of Ag. Engineering
University of Illinois
1208 W. Peabody Drive
Urbana, IL 61801 U.S.A.

W. F. Buchele/D. C. Erbach
Ag. Engineering Department
Iowa State University
Ames, IA 50011 U.S.A.

Stanley J. Clark
Ag. Engineering Department
Kansas State University
Manhattan, KS 66506 U.S.A.

Larry G. Wells
Department of Ag. Engineering
University of Kentucky
Lexington, KY 40546-0075 U.S.A.

Robert L. Schafer
National Tillage Machinery Lab.
United States Department of Ag.
P. O. Box 792
Auburn, AL 36831-0792 U.S.A.

Henry D. Bowen/Awatif E. Hassan
Biological & Ag. Engineering Dept.
North Carolina State University
Box 5906
Raleigh, NC 27650 U.S.A.

John B. Liljedahl
Agricultural Engineering Dept.
Purdue University
West Lafayette, IN 47907 U.S.A.

Dr. John V. Perumpral
Agricultural Engineering Dept.
Virginia Polytechnic Inst & State U.
Blacksburg, VA 24061 U.S.A.

PROPERTIES OF DESERT SILTY SOIL IN RELATION TO VEHICLE MOBILITY

ABDEL-FATTAH A. YOUSSEF

ASSOCIATE PROFESSOR OF CIVIL ENG. KING SAUD UNIV, RIYADH, SAUDI ARABIA

Summary - Desert soils covering wadis (valleys) as well as small hills in the wadis are formed from silty-sand soils. A significant part of these soils are wind blown sediments and may be classified as loess. In this study, it was found that the soil in the wadis contains varying amounts of clay, gypsum and salty materials which act as a binder between the soil particles. In their dry state, these soils are brittle, porous and sensitive to moisture and deformation. Laboratory examination of these soils showed that they lost most of their bearing resistance and shear strength upon wetting or deformation. The reduction in bearing resistance and shear strength for these soils was investigated using the plate loading test, the cone penetration test and the direct shear test. The decreases for bearing resistance and shear strength were found to very significantly and at times reached close to 90 percent of the values found in their dry and undisturbed state. In addition the corresponding reduction in trafficability parameters were analyzed based on the reduction of soil strength due to wetting.

INTRODUCTION

Mobility design and trafficability prediction require complete information concerning vehicle supporting elements, supporting soil properties and other terrain characteristics. In their analysis mobility engineers usually depend upon the results obtained from quick and simple field tests. These simple field tests can be performed using plate, cone and vane-cone devices [1, 2 & 3]. The data obtained from these tests are useful to represent the soil trafficability resistance for a short period of time only, where the soil condition is not affected with water or external loads, and where the vehicle speed is relatively low.

The soil is a three phases material and is usually classified by different categories depending upon grain size and material constituents, soil strength parameters and soil behaviour. These soil properties and parameters posses different degrees of sensitivity to changes in both soil-moisture content and application of traffic load which simultaneously compresses and shear the soil. Such sensitivities should be included in any rational analysis.

Relation between factors affecting soil shear parameters, soil properties and vehicle carrying elements is thus essential and should be developed. Part of this relation may be accomplished through identifying the actual soil behaviour and soil strength sensitivity to the region meteorological conditions.

The Middle East desert area is in general characterized by high temperatures, extremely variable humidities, high evaporation rate and low annual precipitation [4]. In such a large area and variable conditions and due to the continuously changing factors such as wind erosion and humidity variation it is difficult to synthesize ground conditions for

mobility engineering purposes. The desert's general topography is dominated with terrain characteristics similar to those illustrated in Figure 1. However in several Middle East desert locations certain unification of conditions may be imposed by the overall climatic regime [4]. Such a climate has been conductive to particular form of erosion, with a dominance of mechanical weathering in the highland which supplies coarse debris that is then transported by occasional streamflood to the low land. In the direction of the low land the fine sediment is transported by wind as well as by water. Through evaporation there is a general upward leaching and surface precipitation of salts and other soluble bonding materials. The ground surface is therefore, commonly covered with granular alluvial sediments, usually without humus, and often saline in character. Figure 2 shows a cross-section for a desert deposition formed by wind and flash floods.

The cross-section along high and low desert land (Figure 2) illustrates the type and distribution of soils in the vertical and longitudinal directions, specially in the surfacial layer which is important for trafficability estimation. The soil formation near the high land area (Zone 1) is composed of angular gravel, sand particles, boulders and cobbles at higher slopes, grading to fine gravel and sand at down slopes. In this zone the soil occur in rough layer and are reasonably compacted and hence usually have good load bearing characteristics except where occasional silt or clay layers or debris flow material occur. In some local areas of this zone the ground roughness may be sufficient to form different degrees of trafficability obstacles. Zones 2 and 3 are composed of finest and farthest travelled sediments - wind blown silts and sands. Significant parts of these two zones are covered with a layer of dry bonded soil sediments. The depth of this layer is varied from 1.0 to 8.0 meter or more depending upon the location of the ground water table. In most cases the bonding materials are soluble. Deposits near the coast may often be partially or completely cemented by carbonate or sulphate. This soil is known as Sabkha, Figures 2, 3 and 4.

Thus based on the above discussion it could be realized that the major mobility engineering problems that these desert conditions can give rise to are:

a) Continuous or scattered obstacles formed by mountaineous areas, local ground roughness, sand dune, ... etc.

b) Reduction of soil bearing resistance and other engineering properties due to the loss of bonding strength upon soil wetting.

This study is mainly concerned with investigating the loss in soil bearing resistance upon wetting in its relation to trafficability prediction. This has been achieved experimentally by investigating the dry soil strength and the wet soil strength using the plate loading test, the cone penetration test and the direct shear test.

EXPERIMENTATION

In this study four soil samples were collected from different places in the Arabian Desert. The soil samples were chosen to represent a good portion of Zones 2 and 3, Figure 2. Sieve analysis, cone penetration, plate load and direct shear tests were carried out for the purpose of soil characterization and performance identification. Figure 5 shows the

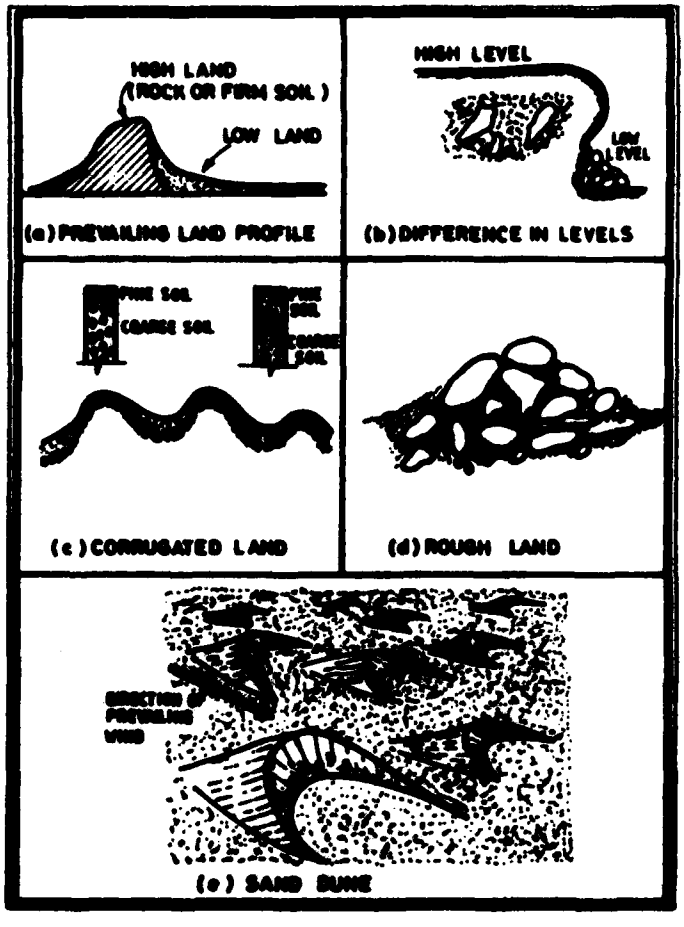

Fig. 1. Schematic diagram showing desert prevailing terrain characteristics

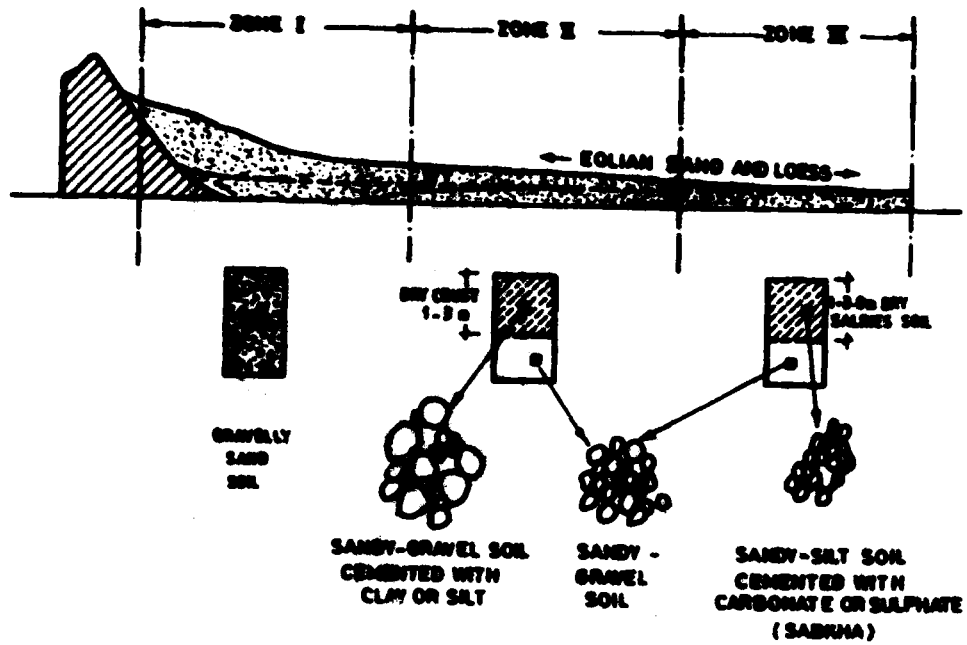

Fig. 2. Cross-section of a desert deposition formed by wind and flash floods.

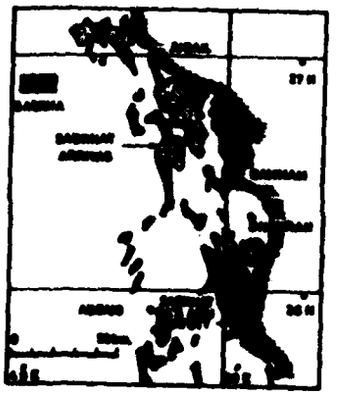

Fig. 3. Sabkha distribution on the west coast of Saudi Arabia [5]

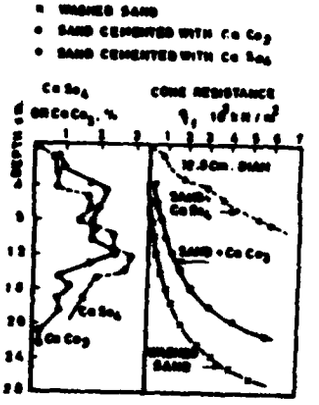

Fig. 4. Salt distribution in Sabkha soil and corresponding soil strength [5]

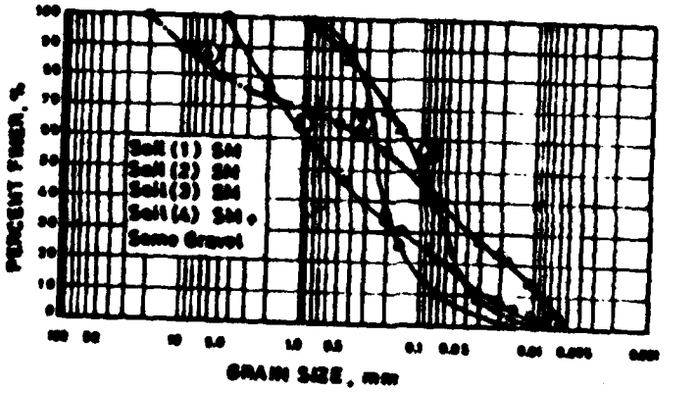

Fig. 5. Grain size distribution for desert soils

gradation curves of the four selected samples where these soils are classified as SM and SM with some gravel according to the Unified Soil Classification System. The soil contains an average of 0.5 percent of gypsum material. The loss in soil shear strength due to the increase in soil moisture content and the corresponding sensitivity of the soil bonding system are tested and discussed.

SOIL PERFORMANCE USING PLATE AND CONE PENETRATION TEST

The first three samples of soils shown in Figure 5, samples (1), (2) & (3) are tested for both dry and wet conditions using cone penetrometer device of 30° apex angle and 28.6 mm diameter. The soil dry densities are chosen to vary within the actual field density range. Also the effect of rate of penetration is partially investigated to explain the effect of vehicle operation over such types of soils.

For these types of soils the cone-penetration test results are presented in Figures 6, 7 and 8. Under natural dry conditions, the soil is found to behave as a normal compressible material. The relationship between the dry density and the cone penetration resistance may likely possess threshold strength-density point below which the soil behaves in a more compressible manner. For a real undisturbed soil, the soil may show a little higher initial cone resistance than that shown in the above figures. Then after this initial stage the soil performance will eventually be the same.

As moisture content changes from 4 to 10-12% (that is, from 6 to 8% moisture increase), the soil may initially gain a little penetration resistance due to apparent shear cohesion, then it gradually loses some of its penetration resistance. The decrease in cone penetration resistance have reached 60% for soils 1 and 2 and 43% for soil 3.

Soil may also lose most of its penetration resistance upon disturbance. This is shown clearly in Figures 6, 7 and 8. As soils (1), (2) and (3) were disturbed to its minimum dry density 14.0, 13.5 and 13.5 kN/m^3, the pressure losses were in the order of 90%, 75% and 88% respectively.

For more understanding of the soil-moisture relation phenomenon in relation to trafficability prediction, soil (4), Figure 5 was tested in dry and soaked (or flushed) condition. The water was flushed in a way that ensures at least 70% saturation. Plate and cone penetration tests were conducted on both natural dry and soaked soils and the results are given in Figures 9 through 12. In these tests the soil dry densities were controlled within a range of 14.4 to 18.4 kN/m^3. To achieve this, the soil bonding property may have been affected and this may have influenced the actual soil behaviour.

The variation in the cone penetration resistance shown in Figures 9 and 10 is obvious. The penetration resistance for soils with 18.4 kN/m^3 density was found to be 9 times higher than that for soils with density of 14.4 kN/m^3. After soils are flushed with water and the moisture content increased from 4 to 14-29% (average degree of saturation is 75%) the soil cone penetration resistances for all soil densities were significantly reduced.

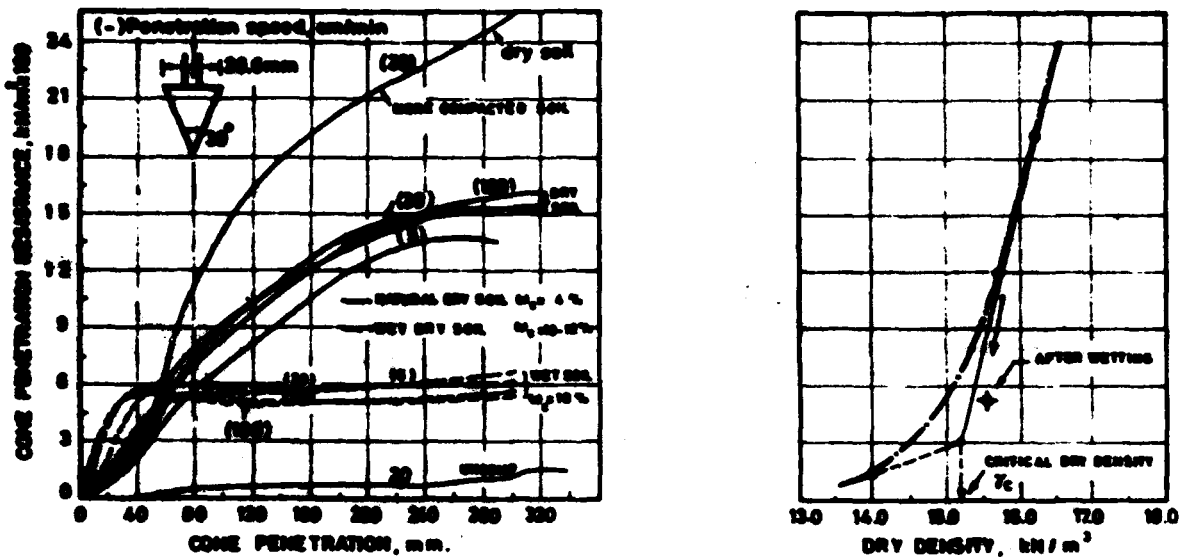

Fig. 6. Cone resistance-penetration relations for different penetration speeds and different dry densities - soil (I)

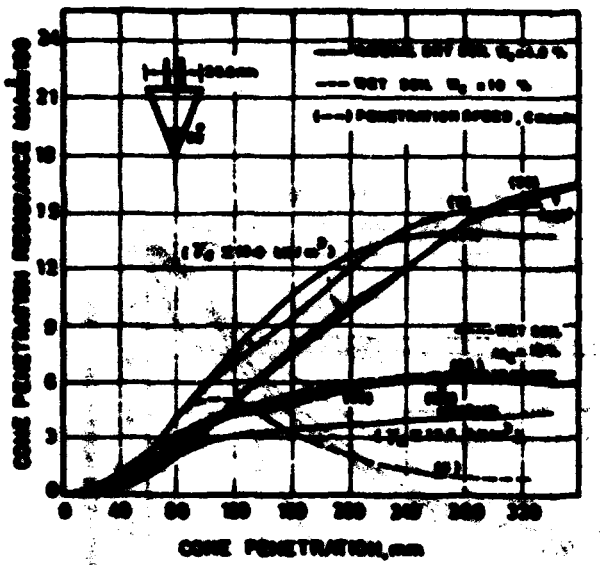

Fig. 7. Cone resistance penetration relations for different penetration speeds and different dry densities - soil (2)

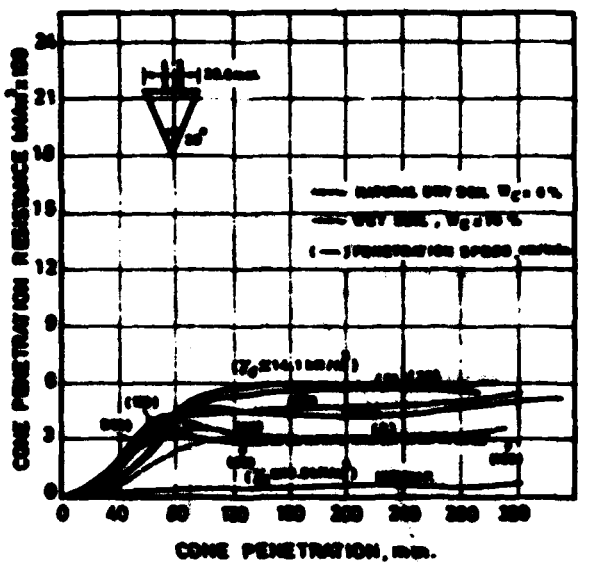

Fig. 8. Cone resistance penetration relations for different penetration speeds and different dry densities - soil (3)

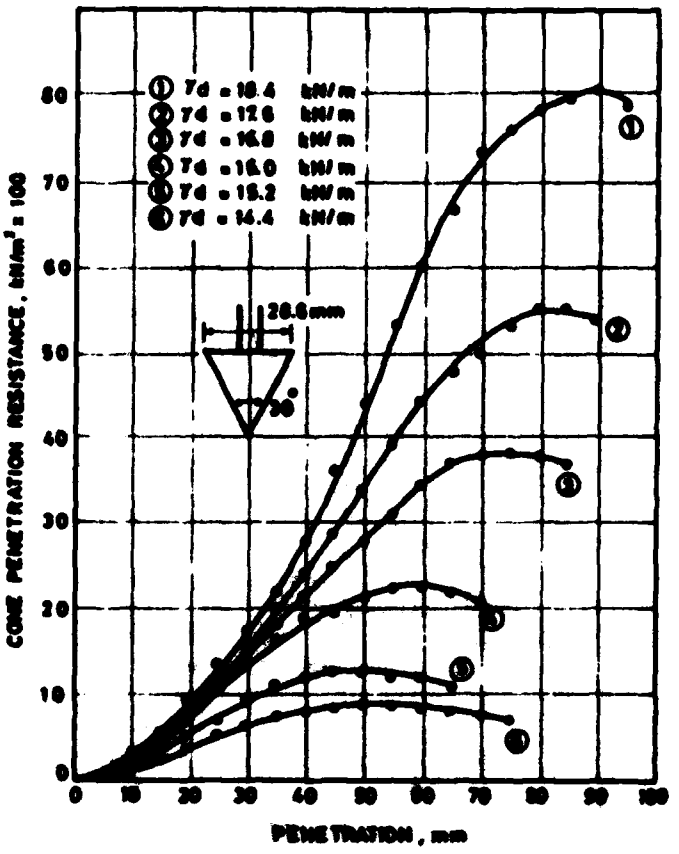

Fig. 9. Cone resistance-penetration relations for different dry densities - soil (4)

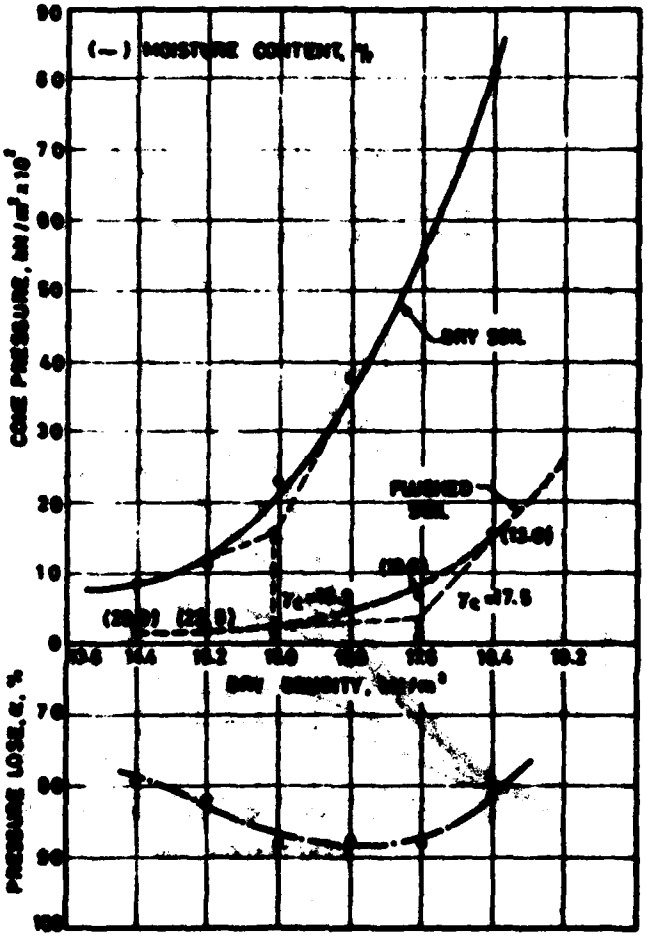

Fig. 10. Cone resistance dry density relations for dry and flushed soil and the corresponding pressure lose - soil (4)

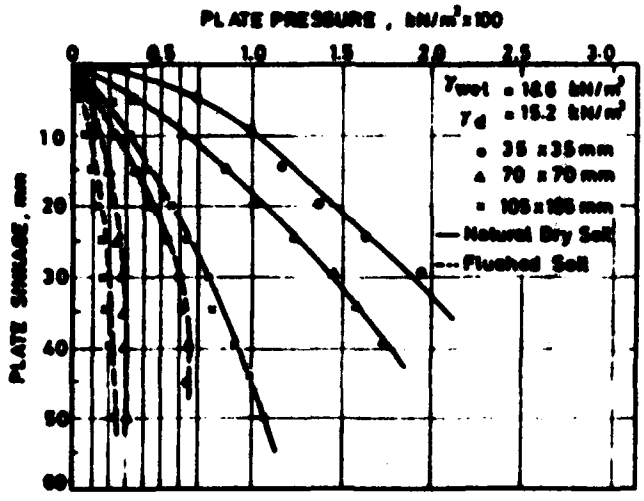

(a) Plate pressure-sinkage relations for natural and flush soil - square plates - soil (4)

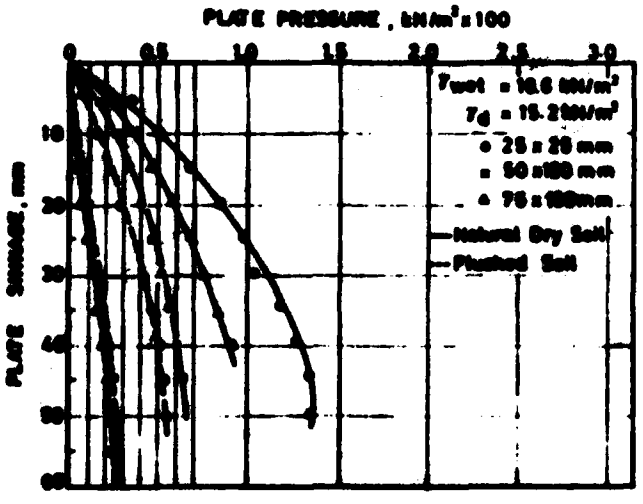

(b) Plate pressure-sinkage relations for natural and flush soil - Rectangular plates - soil (4)

Fig. 11. Plate pressure - sinkage relation - γ_{dry} = 15.2 kN/m^3 - soil (4)

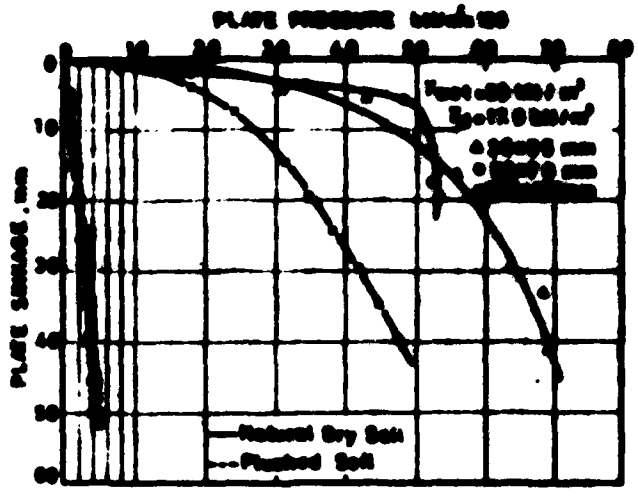

(a) Plate pressure-sinkage relations for natural and flushed soil - square plates - soil (4)

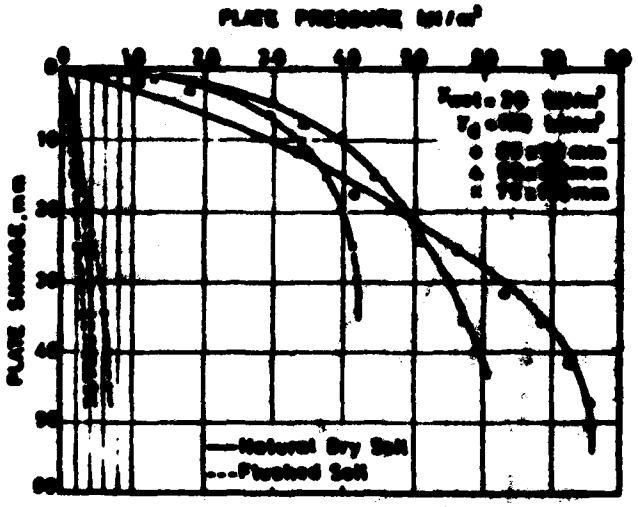

(b) Plate pressure-sinkage relations for natural and flushed soil - Rectangular plates - soil (4)

Fig. 12. Plate pressure-sinkage relation - γ_{dry} = 17.6 kN/m^3 - soil (4)

Figure 10 summarizes the cone penetration test results for these two cases; cone penetration resistances for natural dry soil with different dry densities; and cone penetration resistances for soaked soils with different dry densities. In both cases the cone penetration resistance-density relations show threshold density values of 15.9 and 17.5 kN/m^3 for dry and soaked soils respectively. Below these threshold values the improvement in the soil strength is very nominal and above which the improvement in the soil strength is very significant and may exhibit a linear relationship. The loss in cone penetration resistances due to water soaking is determined in the above figure and was found to be in the order of 85%. The highest reduction value was found to be about 88% at the threshold points.

The soil cone penetration resistance loss were determined from the following relationship;

$$a = \frac{CI_d - CI_F}{CI_d} \cdot 100 \qquad (1)$$

where

a = cone-penetration resistance loss, %

CI_d = cone-penetration resistance for a natural dry soil

CI_f = cone-penetration resistance measured for flushed soil

The plate load tests were conducted on two chosen soils with predetermined dry densities 15.2, 17.6 kN/m^3. These soils were tested in dry and flushed conditions by using two sets of plates with different sizes.

The plate load tests were carried under a slow penetration rate 5 mm/min, and the plate pressure-sinkage relationship is determined as shown in Figures 11 and 12. From these two figures the plate penetration resistance can be easily compared for natural dry and soaked soil conditions. Analysis of these test results may indicate not only the significant loss in soil strength after the soil is flushed with water but also the change in soil behaviour. The average pressure losses were found to be as follows:

(a) For soil with dry density of 15.2 kN/m^2, the average pressure loss is 75%

(b) For soil with dry density of 17.6 kN/m^2, the average pressure loss is 90%

However there are some differences between the pressure loss values measured by cone and plate load tests; the average value may still be the same. Also, in general such a significant bearing pressure loss reflects the importance of this study.

ANALYSIS AND DISCUSSION

Based on the test results and the accompanying discussion it is now clear that the loss in desert soil bearing resistance will affect vehicle mobility over such a soil. To evaluate this loss the soil strength values for natural dry and wet soils were determined using three plate load-sinkage formulae. The Bekker plate-sinkage equation [1] is:

$$P = \left(K_\phi + \frac{K_c}{b}\right)(Z)^n \qquad (2)$$

where P and Z are plate pressure and sinkage respectively and K_ϕ, K_c and n are soil strength values. The Hansel plate-pressure equation [8] is:

$$P = K_1' + K_2' \frac{S}{A} \qquad (3)$$

where P is soil pressure; K_1' and K_2' are soil strength values and S, A are plate perimeter and area respectively. And the author's plate-sinkage equation [7] is:

$$P = \left(K_1 + \frac{1}{2} b K_2\right)\left(\frac{Z}{A/S}\right)^n \qquad (4)$$

where P = soil pressure; Z = plate sinkage; b = plate width; A = plate area; S = plate perimeter and K_1, K_2, n = soil shear value.

The soil shear strength parameters C and ϕ were determined from direct shear test. The determined soil bearing strength values and the determined shear strength parameters are summarized in table (1), for natural dry and flushed soils.

The effect of changes in soil bearing values and soil shear strength parameters on the wheel motion resistance and wheel traction formula (equations 5 and 6 developed by Bekker [1])for the natural dry soil and the flushed or wet soil can be easily determined and is presented as follows:

$$R_c = \frac{1}{\frac{2n+2}{2n+1}\sqrt{(3-n)}\;\sqrt{(n+1)(K_c + b K_\phi)}^{\frac{1}{2n+1}}}\left(\frac{W}{\sqrt{b}\,D}\right)^{\frac{2n+2}{2n+1}} \qquad (5)$$

$$H = [bLC + W\tan\phi]\left[1 - \frac{K}{iL}\left(1 - e^{-\frac{iL}{K}}\right)\right] \qquad (6)$$

where R_c = motion resistance; H = maximum soil thrust; W = wheel load; D = wheel diameter; b = wheel width; L = wheel contact length; i = wheel slip and K = slip coefficient.

Table 1. Soil bearing strength values and shear parameters

Dry Density	Shear Parameters		Equation (2)			Equation (3)		Equation (4)		
	c	ϕ	k_c	k	n	k_1'	k_2'	k_1	k_2	n
kN/m^3	kN/m^2		$\times(100)^n$ kN/m^{n+1}	$\times(100)^{n+1}$ kN/m^{n+2}		$\times 100$ kN/m^2	kN/m	$\times 100$ kN/m^2	$\times 10000$ kN/m^2	
Case (1) Natural dry soils										
15.2	0	36	1.09	0.14	0.68	0.52	0.58	0.67	0	0.99
17.6	5	41	7.35	2.63	0.38	3.00	0.53	4.18	0.11	0.32
Case (2) Flushed soils										
15.2	3	30	0.65	-0.01	0.98	0.10	0.36	0.18	0.01	0.87
17.6	5	30.5	0.17	0.23	0.80	0.33	0.31	0.02	0.10	0.81

In general the significant decrease of the soil bearing values and shear strength parameters will result in the decrease of traction force and the increase in motion resistance. The outcome of these changes will be a reduction in the vehicle drawbar pull or may cause a vehicle immobilization. It should also be noticed that the soil bearing value given in equation 4 can be used with Bekker analysis [1] to yield an equation similar to equation (5) and consequently the same conclusion can be reached.

CONCLUSIONS

Desert soil can be characterized by its many particle structure systems and is composed of different materials. In many cases it may be described as a brittly bonded material sensitive to water and deformation actions. Performed tests and analyses on this soil have led to the following conclusions:

(1) Desert soil classified as silty sand soil (SM) which is sensitive to both water and deformation.

(2) Desert silty soil may lose up to 90% of its bearing or penetration resistance after it becomes wet.

(3) Desert silty soil will lose most of its bearing and shear strength if deformed or disturbed.

(4) Desert silty soil possess threshold density values below which the soil is lacking in strength and may not support heavy vehicles.

(5) For desert silty soil it has been found that by increasing the soil moisture content, there is a reduction in the soil bearing values as determined by the plate loading test and, in the shear strength parameters, as determined by the direct shear test. This reduction in soil strength will cause a significant increase in vehicle motion resistance as well as a significant decrease in the maximum traction force.

ACKNOWLEDGMENTS

The author wish to acknowledge Mr. Abdulaziz A. Al-Othman, teaching assistant, and all Soil Mechanics Laboratory staff at the College of Engineering, King Saud University, for their help in the experimental work.

REFERENCES

[1] M. G. Bekker, Introduction to Terrain-Vehicle Systems. Ann Arbor, The University of Michigan Press, U.S.A. (1969).

[2] G.W. Turnage, Using Dimensionless Prediction Terms to Describe Off-Road Wheel Vehicle Performance. American Society of Agricultural Engineers, Paper No. 72-634, Chicago, Illinois, U.S.A. (1972).

[3] R.N. Yong, A.F. Youssef, Application of Vane-Cone Tests on Soil for Determination of Trafficability. Proceeding of the 6th International Conference, ISTVS, Vienna, Austria (1970).

[4] P.G. Fookes, Middle East-Inherent Ground Problems, Proceeding of the Conference on Engineering Problems associated with Ground Conditions in the Middle East, Teh Geological Society, London (1978).

[5] W. Akili, On Sabkha Sands of Eastern Saudi Arabia. Symposium on Geotechnical Problems in Saudi Arabia, King Saud University, Riyadh, Saudi Arabia (1982).

[6] J.E. Bowles, Foundation Analysis and Design, McGraw-Hill Ltd. (1977).

[7] A.F. Youssef, G.A. Ali, Determination of Soil Parameters Using Plate Test, Journal of Terramechanics Vol.19. No. 2, pp 129-147, 1982.

TOPIC 12

VEHICLE DESIGN

CUTHBERTSON TRACKS

JAMES A. CUTHBERTSON, O.B.E.
MANAGING DIRECTOR, JAMES A. CUTHBERTSON LTD., BIGGAR, SCOTLAND.

The equipment described in this paper is the result of some 33 years of work in producing full track tractors and half track tractors, for wheeled tractors. All of the systems have been manufactured and proved in various areas. Since experimental work was first started, many different types of vehicles have been equipped.

The original concept of the track was to make a sectional track which linked together; the drive plate and the outside grouser plate were bolted or rivetted together, with wire rope loop arrangement, outside rubber moulded pads. This eliminated completely the hinge pin operation since the bending moment on the track was entirely taken through the rubber enclosed wire rope system and lengthening or shortening the track was dependant on the number of track pads employed.

This type of track was used continually for about 20 years. Its main weakness was found to be in the fact that puncture or leakage could occur in the rubberised wire rope and water, especially sea water, could enter at those punctures and, eventually, cause failure, by rusting.

At this point, a search was undertaken for a medium which had sufficient tensile strength to transmit HP at up to 200 HP and had not the serious disadvantage of rusting. The eventual outcome of this research was the development of rayon and nylon woven belts. The weaving of these belts was designed to give transverse as well as longitudinal strength and was ample, in the first tracked vehicle, for 100 HP full tractor on peat land, swamp land, rough mountain areas and in all weathers, including snow and heavy frost conditions. Although this type of track, in its triangular form, has been used on muskeg in Canada, I do not think it was ever supplied for work in perma frost conditions in the North of Canada, but, if these extreme types of condition were to be met, it is perfectly simple to obtain the proper type of tracking of woven belt to the required standard, since these are common in Canada with the Snowmobile and, say, Nodwell and

Bombardier. Certainly, it does not seem to be affected by the very serious frost conditions, in the North of Canada.

A further development of this tracking is the triangular tracks fitted to 4WD vehicles which we now produce. The great advantage we claim for this type of track and which has been proved in practice, is the greater length of ground contact of the vehicle, their ability to have high ground clearance, self cleaning properties of the tracking and the low wear which has been attained through eurethane sprockets.

The general conception of this track was for a central rocking bar which had, at its extremities, either single or twin wheels and a polythene sprocket which forms the drive on the inside of the track. The system allows complete oscillation, in irregular land or areas where ditching has taken place and the necessity to cross these ditches, without damage, and has an advantage since the basic concept of the track is to reduce ground pressure and, at the same time, produce reasonable tractive effort. This arrangement has proved to be extremely good and is adaptable for many 4WD applications.

The steering of this equipment is the normal hydraulic steering attachment to the original steering wheel, so that the full controls of the vehicle are from the conventional steering wheel. In fact, steering of this tractor is, if anything, lighter than the wheeled version.

Another very interesting advantage is that the torque supplied at the sprocket is at least half and sometimes only one third of the torque which would be supplied to the wheels, the reason being that the sprocket arrangement is normally at least half or one third less in diameter, than the wheeled version.

It is attached to the vehicle by the same stud method as is used for wheels and the main attachment to the undercarriage is a simple straightforward bolt system which can readily be removed and by removing the sprocket and replacing the wheels, the vehicle is returned to its original wheeled state. Depending on the width of the tractor, the ground pressure of the vehicle can be reduced to one psi, and the construction of the outside track cleats, in standard form, allows the vehicle to travel without damage on tarmacadam

roads, as well as performing in an outstanding manner in very rough or swamp terrain.

The Land-Rover conversion, shown in Fig. 1, which is applicable to the majority of 4WD tractors has been thoroughly tested over the last 15 years.

The purpose of this paper is mainly to advertise the very considerable advantage of being able to create very low pressure machinery for under-developed countries, where, in paddy land rice cultivation, and transport problems, it is necessary to have a lower ground pressure than from a wheeled tractor and this track application has a great advantage in that it is interchangeable, with the wheeled adaption, while the wheeled vehicle is of some advantage on hard land work. Also, the low cost of production of specialised equipment is made feasible by the use of already tested 4WD tractors, thus avoiding the extremely expensive commitment of producing the whole mechanics of a new tractor. Standard, proved 4WD vehicles can be used, without strain on other mechanism.

SPECIFICATION

Short wheel based Land Rover

Overall length	13 ft.
,, width	6 ft. 6 ins.
Unladen weight	3 tons 10 cwt.
Pay load	10 cwt.
Ground pressure—unladen	1.9 p.s.i.
,, ,, —laden	2.3 p.s.i.
Climbing ability	1 in 1
Side stability controllable	30°
Tipping angle	45°
Top speed	35 m.p.h.
Steering	Hydraulic power assisted articulation
Turning radius	25 ft.
Controls	Standard Land Rover

Tracks: 4 tracks 12" wide, each consisting of 48—1½" broad steel track shoes, riveted on to 2—4" 6-ply Nylon/Cotton reinforced rubber belts. The belts and track shoes are independently renewable.

All models of Land Rover can be converted.

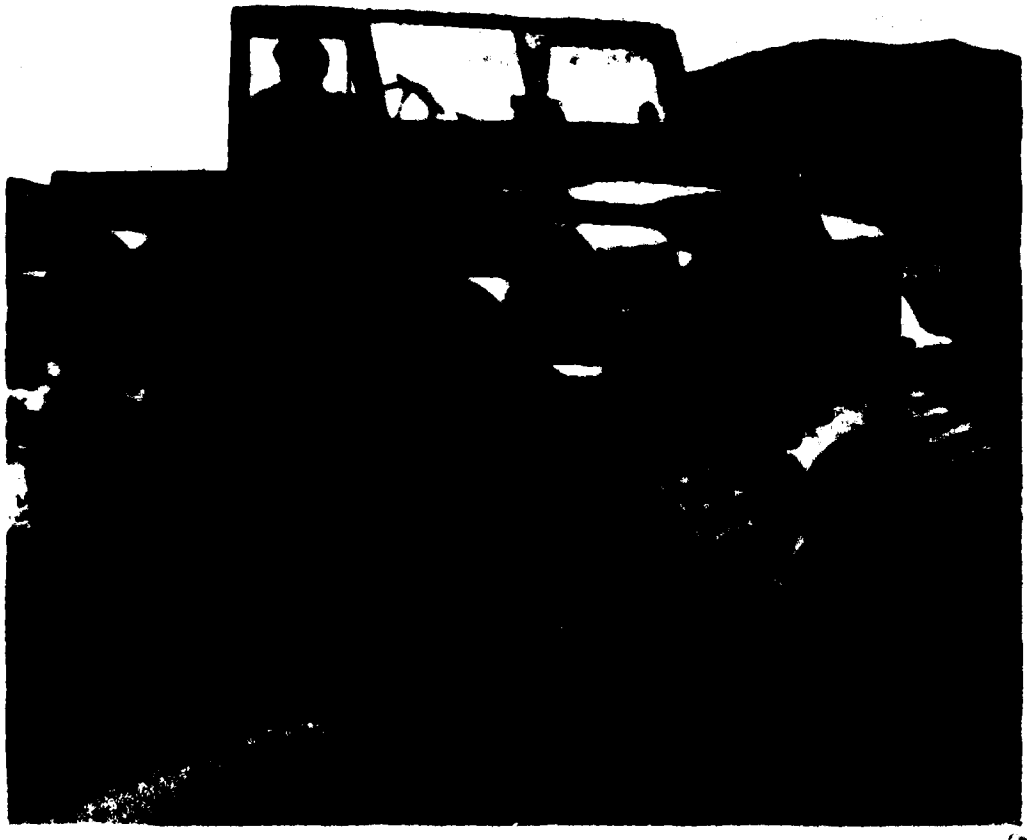

Fig. 1 Land Rover conversion

AN ALL TERRAIN VEHICLE EQUIPPED WITH CTIS

AWATIF E. HASSAN

NORTH CAROLINA STATE UNIVERSITY, RALEIGH, NORTH CAROLINA, USA

ABSTRACT

An all terrain vehicle designed and developed at North Carolina State University in 1980 was modified to incorporate a central tire inflation system (CTIS) composed of an air compressor, solenoid valves and controls to provide the proper air inflation pressure to the powered wheels. A radar unit for ground speed/slip measurements was employed to detect the vehicle mobility. The unit's slip data were erratic and could not be recommended for automatic control of the tire inflation pressure. Conversely, the radar ground speed outputs were within ±2% of the actual measured speeds and will be used in future circuitry control of the CTIS.

INTRODUCTION

Performance of off-road vehicles, such as skidders and tractors, depends on their flotation which is dependent on tire size and inflation pressure. Resistance to motion and vehicle mobility are usually affected by wheel sinkage and tire contact areas (footprints) which in turn affect rolling resistance and tractive effort. Kaczmarek (1981) reported that the footprint of the ZIL-157 military vehicle increased from 0.04 to 0.092 m^2 when the tire inflation pressure was reduced from 294 to 55 kPa under a constant loading condition.

The use of a central tire inflation system (CTIS) has been limited to military vehicles (Czako, 1974) and has been widely used in the USSR and Eastern Europe since World War II. All air systems used on these vehicles are manually controlled from the cab by the vehicle operator. Czako (1974) listed 31 models using central tire inflation systems developed by six nations from 1942-1970. Of these 31 vehicles, 19 are production and 12 prototype/experimental models. There is no production vehicle in the U.S.A. while the USSR has 12 models. The internal axle slip ring commonly used on the production vehicles to allow the compressed air to enter and leave the tires was designed and developed by the U.S. Army on the M54, 5-ton experimental truck.

In agriculture, tire inflation pressure has been one of the most important factors affecting motion resistance and tire performance. Zoubori (1967) reported a significant increase in tractive power efficiency as a result of a reduction in inflation pressure of tractor tires at constant drawbar pull. The same results were demonstrated in Czako's study (1974) on military vehicles where a definite increase in vehicle mobility and drawbar pull was achieved with central tire inflation reduction from 240 to 103 kPa on loam soil.

Burt and Bailey (1982) reported an improvement in the tractive efficiency of a powered radial tire equipped with a CTIS, operating under controlled soil bin conditions, by the selection of appropriate levels of inflation pressure and dynamic load. They also concluded that net traction in future field applications can be improved with automatic control of inflation pressure of tires and dynamic loads on wheel axles for constant travel reduction ratio under varied soil conditions.

Grevis-James and Bloome (1982) developed and tested a tractor power monitor to measure ground speed, wheel slip, and drawbar pull using two magnetic pickups for ground and wheel speeds and a strain-gauge drawbar dynamometer. A fifth wheel unit was used to measure ground speed on the four-wheel tractor which might not be applicable under forestry conditions. The use of a radar unit for ground speed measurements eliminates the fifth wheel and is very attractive in field application. Many radar units are equipped with sensors to detect ground speed as well as slip (Tsuha, et al, 1982, Richardson, et al, 1982). Under laboratory conditions, Tsuha, et al, reported that the accuracy of the ground speed measurements using radar units was $\pm 5\%$. Several tractor performance monitors using radar based true ground speed sensors for agriculture and off-highway equipment are available on the market for installation on vehicles to monitor field performance and production.

The great variability in the road/terrain conditions represents the main difficulty in the use of manually operated central tire inflation/ ground speed control systems. Several questions are in order:

1. How does the *operator* know that the tire pressure needs adjustment?

2. How can he interpret the control console readings from the radar ground speed sensor to inflation pressure alteration?

3. How does the operator know to what extent and in what direction the pressure should be adjusted?

4. How often and how fast can the operator respond to terrain variation in a certain time interval?

A logical answer to all these questions leads to the need for full automatic control of the central tire inflation pressure system using various sensors. Therefore, the ultimate goal of this research program is to develop an automatic central tire inflation system to assure vehicle mobility under various forestry terrain/soil conditions. However, the main objectives of this paper are to present an all terrain vehicle equipped with a CTIS, to discuss the various means and sensors for automatic control of tire inflation pressure, and to present the results of field evaluation studies using different tire inflation pressures.

DESIGN OF THE ATV

Site Characteristics

The forestry environment includes many extremes. One of the more severe of these extremes is wet sites that have been bedded in preparation for tree planting (Hansen, 1978). Figure 1 shows soil strength and

a typical bed profile in the Coastal Plain region of North Carolina. Soil strength is very low and hence requires a low ground pressure vehicle for tree planting and subsequent forest operations. The use of a trailed planter on these sites requires at least a minimum of a 45-kW crawler tractor which tracks to either side of the bed causing clearance and bogging problems and resulting in losses in machine productivity.

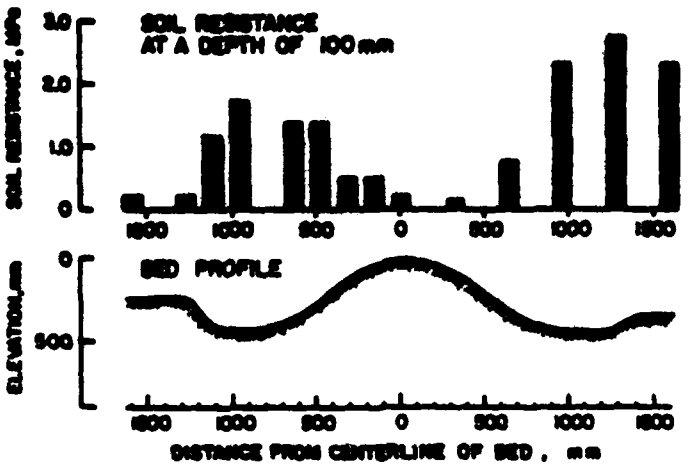

FIG. 1. Profile and soil strength measurements of a typical bed prepared by a bedding plow without packer drum.

Basic Design of the ATV

The above limitations and other considerations led to the development of a light-weight, all terrain vehicle (Fig. 2) at North Carolina State University in 1980 (Hassan and Whitfield, 1982). The ATV is equipped with a 12 kW, air-cooled engine, hydrostatic transmission and terra tires.

Field Testing and Evaluation

The ATV was operated on various beds of histosal soils in the Hofmann Forest, Maysville, N.C. and on oxisol soils of Federal Paper Board Co., Inc. at Lumberton, North Carolina. The vehicle proved to be adequately powered and displayed good maneuverability and stability.

A traction (pull) test of the ATV was conducted on a bedded site and a dirt road at Lumberton, where the load was applied by a skid pan and was increased by adding dead weights to the pan. The line pull was measured by a hydraulic dynamometer. For each load, advance and time per five revolutions for each of the two powered wheels were recorded to determine the travel reduction and ATV forward speed. The average moisture contents on a dry weight basis of the bedded site and the road were 80% and 20% respectively. The pull-travel reduction curves for this test are shown in Fig. 3 for a tire inflation pressure of 42 kPa. A total of 1000 N pull was available at 15 percent travel reduction on the bedded site. This

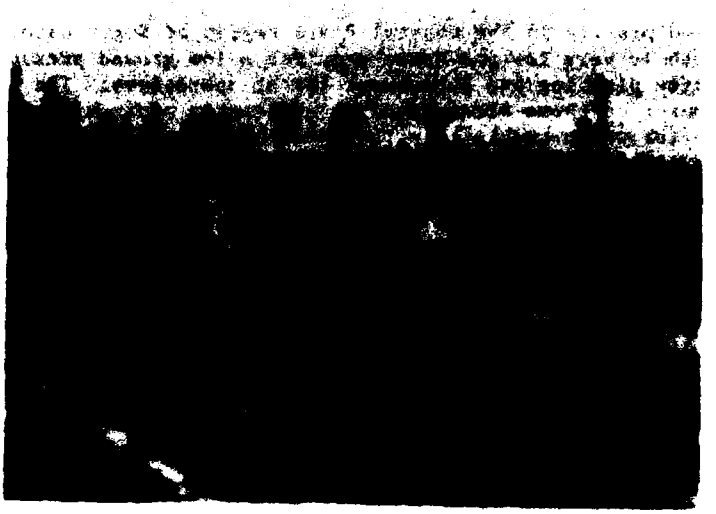

FIG. 2. The ATV with A-frame suspension is shown operating on a bedded site at the Hofmann Forest, N.C. - May 1980.

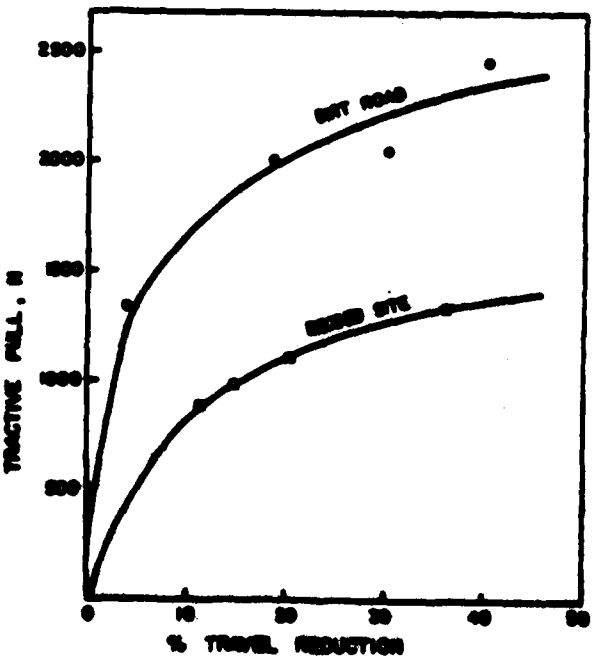

FIG. 3. Tractive pull-travel reduction curves for the bedded site and dirt road at Lumberton, N.C., May 1980.

pull force should be sufficient for light forestry operations. The results of the pull test also indicated that the overall tractive power efficiency of the ATV was only 25% at a ground speed of 5.4 km/h.

The control mechanism for the hydraulic pumps allowed the driver to turn easily and control the speed of the vehicle. Total mass of the vehicle and two operators, one driver and one instrument reader, was 692 kg. The mass distribution was 78% on the front drive wheels and 22% on the rear caster wheels. However, on rough terrain, the caster wheels tended to lose contact with the ground and swirl which caused excessive drag and lateral rear-end swings. This phenomenon was most evident when the ATV was attempting to travel across the beds. By increasing the trailing angle of the rear wheels, this problem was eliminated except in very rough terrain.

The suspension system on the front wheels of the vehicle was helpful in maintaining wheel to ground contact, but the suspension A-frame caused clearance problems in some instances. Stiffer springs than those on the machine should allow for more equal movement of the suspension frame above and below its static no-load position.

CENTRAL TIRE INFLATION SYSTEM

Physical Parameters of the ATV

The use of skidder tires or similar large size tires was not possible due to the large volume of air to be controlled or to the need to redesign the tire so that a small portion of its volume would be controllable.

The results of field testing of the ATV in North Carolina in 1980 indicated that the light weight vehicle, when properly designed, should be suitable for forestry applications and suggested further development, (Hassan and Whitfield, 1982). Therefore, it was decided to use the ATV in the development of an automatically controlled CTIS suitable for off-road vehicles. The original design of the ATV was limited to a total mass of 692 kg. The addition of the CTIS and radar unit increased the vehicle mass to 860 kg (Fig. 4) with weight distribution of 74 and 26 percent on the front and rear axles respectively. The front axle springs were strengthened to accommodate the additional weight. The caster rear wheel inflation pressure was maintained constant at 48kPa throughout the entire study.

Central Tire Inflation Pressure Circuit

The ATV tire inflation system circuit shown in Fig. 5 is composed of two normally closed solenoid valves for inflating and deflating the air pressure of the front powered tires. A portable compressor equipped with a 3-kW gas engine supplies compressed air at 670 kPa. When air is to be added to the tire, the inflation solenoid valve is activated, and subsequently air flows from the compressor tank through the valve to the swivel elbow joints and enters the tires. When air is to be removed, the deflation solenoid valve is activated and the air flows from the tires through the valve where it is vented to the atmosphere. A muffler is used on the valve outlet to reduce the air pressure before discharge for safety and noise control. Four safety relief valves set at 137 kPa are used in the inflation/deflation circuit to protect the tires against

FIG. 4. The ATV equipped with the CTIS and radar speed unit operating on sodded field at NCSU, June 1983, where (1) inflation solenoid valve, (2) deflation solenoid valve, (3) safety relief valves, (4) radar monitor mounted 60 cm above ground at 37° depression angle with the horizontal plane, (5) radar console for direct readout, (6) manual pressure switch circuit, (7) elbow pivot joint connecting the CTIS to the drive wheel, (8) portable air compressor with 3-kW engine.

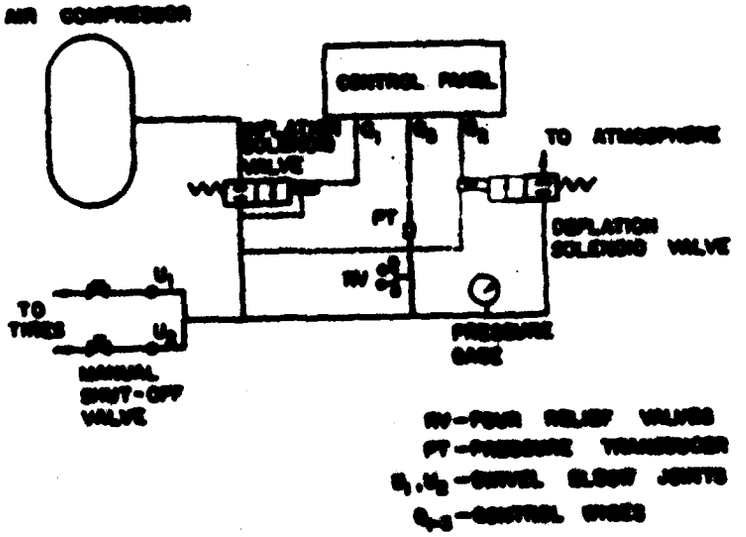

FIG. 5. ATV central tire inflation/deflation system equipped with pressure transducer for controlling tire inflation.

high pressures. The normally open manual shut-off valves are used to prevent air leakage from the tires when the vehicle is not in use for an extended period.

A manual switch circuit composed of two push button battery-operated switches controlling the inflation and deflation solenoids was necessary to investigate the operational characteristics of the tire pressure system and to the development of the control system.

Central Tire Inflation System Tests

Tests of three to five replications were conducted to determine the characteristics of the CTIS under different conditions. The compressor tank fillup rates were 13.8, 11.8, and 10.3 kPa/s with air pressure rising from 0-207, 0-414 and 0-620 kPa respectively. A total of 60 seconds was needed to fill the tank to 620 kPa and five seconds to discharge it completely to the atmosphere.

The average inflation and deflation rates of the ATV tires at different tank pressure settings for three trials are shown in Table 1. The tests were conducted stationary due to difficulties of recording the data while in motion, and the data were consistent and almost identical for all trials. When the compressor tank was pressurized to 207 kPa, the air solenoid valves were inoperable because their pilot pressure has to be greater than 207 kPa to activate the solenoids. The rate of inflation of the ATV tires decreased in general with a decrease in the air compressor pressure and for higher tire pressure settings (Table 1).

The results of the tire and tank pressure tests indicate that the CTIS was adequately designed for the ATV and will provide fast pressure response to tolerate difficult terrains and wet conditions.

INSTRUMENTATION FOR AUTOMATIC CONTROL OF THE CTIS

As in any automatic control system, the pertinent objective is to select sensing and control devices to maintain the most suitable level of inflation pressure. Policies for a particular terrain condition will depend on the inputs and sensitivity of the transducers used.

Sensing and Control Devices

Sensing devices can be a function of ground contact pressure, depth/sinkage of wheels, applied external load, dynamic load on tires, ground condition, ground speed/wheel slip or a combination of any of these variables.

A sensor based on tire-ground contact pressure might be ideal for direct feedback needed for vehicle mobility. Strain gauges imbedded into the tire periphery would provide continuous recording of ground contact pressure that may be sensitive to soil/terrain variations. However, because of the terrain roughness and the severe punishment of the tires under field conditions, the strain gauges would not be able to function properly, which will eliminate this approach.

TABLE 1. CHARACTERISTICS OF THE ATV CENTRAL TIRE INFLATION SYSTEM. SEPTEMBER 1982 - NCSU.

Tire Pressure	Compressor Tank Pressure		Required Time	Average Pressurization Rate
	Initial	Final		
kPa	kPa	kPa	Sec	kPa/s
A. Tire Inflation Test				
0- 35	620	540	0.5	70
0- 69	620	478	0.9	77
0-103	620	402	1.4	74
0-138	620	206	2.5	55
0- 35	414	341	0.5	70
0- 69	414	207	1.0	69
0-103	414	115	1.5	69
0-138	414	0	17.3	8
0- 35	207	103	1.0	35
0- 69	207	35	3.3	21
0-103	207	0	22.0	5
B. Tire Deflation Test				
103- 0			2.16	48
138- 0			3.16	44
C. Tire Pressurization at Constant Intervals				
0- 35	620	517	0.5	70
35- 69	517	414	0.5	68
69-103	414	310	0.6	57
103-138	310	207	1.5	23

Internal tire pressure would vary with tire deflection and deformation on different surfaces. Therefore, under soft terrain conditions where sinkage takes place, tire deformation will differ, resulting in a change in the tire inflation pressure. A pressure transducer in line with the tire pressure lines (Fig. 5) can predict tire pressure variations within $\pm$1.0 kPa*. A logic circuit comparing the pressure transducer output with a predetermined window of acceptance composed of

*Personal communication with the National Tillage and Machinery Laboratory staff, USDA, Auburn, Alabama.

maximum and minimum air pressure values, is necessary for the success of this sensing method. Whenever the pressure transducer signal is outside of the window, an appropriate comparator pulse is generated to activate the respective solenoid valve for either deflating or inflating the tires (Fig. 5). The inflation pressure sensing method was discarded because of complexity and time needed for debugging the logic circuit.

A load sensing device can predict the change in resistance due to terrain variation. Unfortunately, under most field conditions the load drags behind the vehicle, therefore, the machine will be immobile before a signal is generated. A change in axle load distribution due to operating on steep terrain might be useful for adjusting the inflation pressure of all tires. Electronic axle load cells are available for heavy truck application and might be utilized in this application.

A sensor based on ground condition measurements such as cone penetration resistance moisture content of soil, depth of snow, or soil density, equipped with a time delay circuit for proper timing will be useful in automatic control of the CTIS. Unfortunately, these soil parameters are not independent of each other and also vary with soil type and structure.

A sensor based on ground speed/slip measurement will provide direct information needed for tire inflation pressure control. The ground speed/slip sensors, normally utilize a microwave Doppler radar unit or a fifth wheel in front of the vehicle for monitoring the slip. Several devices are available and can be readily installed on farm tractors for controlling wheel slip and measuring productivity. It was felt that the speed/slip control technology is well established and can be implemented on the ATV with the CTIS for automatic control of tire inflation pressure.

RADAR GROUND SPEED MEASUREMENTS

Principle of Radar Measurements

The radar sensor provides a true measure of vehicle speed over the ground using the Doppler principle (Fig. 6). Illuminating the ground below the vehicle, the reflected beam is compared with the transmitted beam to derive a difference of Doppler frequency proportional to the vehicle speed.

The Doppler frequency shift is expressed by (Hyltin, et al, 1973):

$$f_d = \frac{2 V_g}{\lambda} \cos \theta$$

where:

- f_d = Apparent Doppler frequency shift in Hertz.
- V_g = Velocity vector (vehicle velocity).
- λ = Wavelength of transmitted beam.
- θ = Angle between the velocity vector and center of the antenna beam (depression angle).

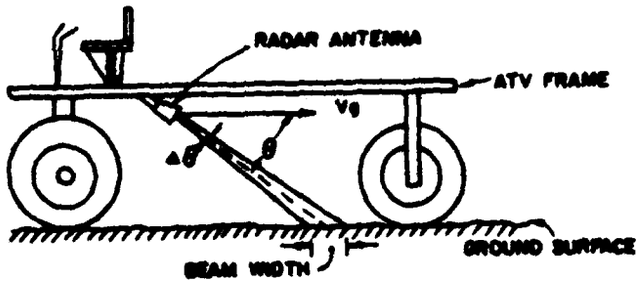

FIG. 6. Geometry of single beam Doppler frequency measurements.

The vehicle velocity is calculated from:

$$V_g = \frac{f_d \lambda}{2 \cos \theta} \qquad (1)$$

For an antenna depression angle of 37° and transmitted frequency of 24.125 GHz, a vehicle velocity of 1.609 km/h (1 mph) is equivalent to a Doppler frequency shift of 57.5 Hertz (Tsuha, et al, 1982). The output of the radar sensor is a square wave whose frequency is directly proportional to the vehicle velocity. The frequency to speed conversion factor is approximately 35.7 Hz/km/h (57.5 Hz/mph) when the sensor is mounted at a depression angle of 37°, approximately at 0.6-1.0 m (24-39") above the ground. It will operate satisfactorily while facing in either direction; forward or rearward.

A Radar Sensor for the ATV

A radar unit (Dickey-John TPMII) was installed on the ATV as close as possible to its center of mass, approximately 60 cm above the ground with depression angle of 37° and transmitted frequency of 10.535 GHz resulting in calibration factor of 1 Hz/cm/s (44.7 Hz/mph). The unit monitor console displays ground speed, wheel slip, engine rpm, and area covered. A 10-tooth sprocket based on the radar pulse rate of 223.5 pulses/s for the wheel slip measurement was first evaluated but because the ATV was hydrostatically driven and operated at low speeds, a 96-tooth sprocket and a magnetic pickup transducer mounted on the right wheel axle to determine wheel slip were most suited for this application.

The output signals on the radar console are at the rate of one read-out per second, which is very slow because of the time delay in processing the signals. An interface circuit with the input signals to the TPM II-MD43328 registers will be constructed and fed to an external computer for controlling the tire inflation pressure based on slip and/or ground speed inputs. When developed, this automatically operated ground speed

central tire pressure system will represent a great revolution in vehicle mobility and in optimizing field operations which will result in substantial energy and cost savings.

Radar Performance & Evaluation

The main components of the radar unit are an antenna, a microwave transceiver, an estimator and a microprocessor. The horizontal speed is calculated from the radar transmitted signal (Eqn. 1) and the slip is calculated either from the engine rpm for direct drive vehicles or from wheel rpm for hydrostatically driven vehicles such as the ATV used in this study.

Tests of the radar unit to determine its characteristics were conducted in Fall, 1982 on a paved road andon a sodded football field, NCSU campus, Raleigh. The vehicle was operated at constant full throttle with constant rear tire pressure of 48 kPa and front tire pressure ranging from 13.8 to 110.3 kPa. The trails were approximately 30 meters long on nearly straight and level ground. The data shown in Table 2 are the average of all recorded points along the trails for each tire inflation pressure. The ground speed on the paved surface was fairly constant at all tire pressures, however, it increased slightly with an increase in tire inflation pressure on the sod. The slip percent readings were erratic and constantly changing. After repeating the tests at tire pressures of 27.6 and 110.3 kPa, it was concluded that the slip measurements were not sufficiently accurate for controlling tire inflation pressure. Contrarily, the ground speed readings were within $\pm$ 0.15 km/h for the same test run (Table 2).

Calibration of the radar ground speed measurements was conducted on two 152.4-m trails, one on paved road and the other on sod, on the NCSU Campus by recording the time for each 30.5 meters (station) along the trail and at least four radar console readings for each station. The results of this calibration indicated that the radar recorded ground speed measurements (V_r) were less than the average recorded speed using a stop watch (V_t); the error is within + 3.5 percent. The statistical equation of all data points obtained from this calibration test was:

$$V_t = 1.036\ V_r \qquad (2)$$

Traction/Slip Test Results

Relationships between slip and ground speed under different loading conditions have been established by several investigators in the agriculture and off-road vehicle fields. A pull test was conducted on a heavy sandy clay soil at the Schenck Memorial Forest, 8 km west of NCSU campus. A 152.4-m trail was established with five stations marked every 30.5 m. The average moisture content of the soil was 52.4 percent on dry weight basis. A skid pan loaded with pulpwood was used to load the ATV during the traction test. The test was conducted at four tire inflation pressures (Table 3). The radar speed and slip data were read directly from the console and recorded on a microcassette recorder by one operator riding on the ATV and the time travelled per station for

TABLE 2. PERFORMANCE OF THE RADAR UNIT AT DIFFERENT INFLATION PRESSURES AND NO LOAD. NOVEMBER 1982.

Tire Pressure kPa	Rolling Radius mm	Engine RPM mean	Engine RPM σ*	Ground Speed km/h mean	Ground Speed km/h σ	Slip % mean	Slip % σ
A. Paved Surface							
13.8	316	3256	6	8.0	0.08	3.6	0.6
27.6	337	3211	13	8.0	0.14	3.2	0.8
41.4	348	3218	10	8.1	0.08	3.2	0.8
55.2	352	3223	7	8.2	0.13	1.6	0.6
68.9	357	3232	13	8.5	0.08	2.4	0.6
82.7	360	3226	6	8.5	0.14	2.4	0.6
96.5	364	3234	6	8.5	0.06	3.0	0
110.3	365	3231	4	8.5	0.06	2.8	0.5
B. Sod Surface							
13.8	316	3175	4	7.6	0.14	5.8	0.4
27.6	337	3199	7	7.7	0.13	4.4	0.9
41.4	348	3218	15	7.9	0.18	3.8	1.1
55.2	352	3209	6	8.1	0.18	4.6	1.3
68.9	357	3223	9	8.2	0.11	3.4	1.1
82.7	360	3220	4	8.3	0.08	2.0	0.7
96.5	364	3253	4	8.5	0.13	2.0	0
110.3	365	3248	3	8.4	0.08	2.4	0.6

*Standard Deviation

speed and travel reduction measurements was recorded by another operator on the ground.

The results of these tests indicated again the reliability of the ground speed measurements and unacceptability of the slip readings obtained by the Dickey-John unit. The radar data output prior to processing was monitored on an oscilloscope and found consistent. Calibration of the radar unit to relate pulse counts to ground speeds will be conducted in the laboratory using a variable speed belt unit. A logic circuit is under investigation to control the tire inflation pressure.

TABLE 3. RESULTS OF THE PULL TEST AT THE SCHENCK MEMORIAL FOREST, NCSU WITH THE ATV OPERATING AT FOUR TIRE PRESSURES. NOVEMBER 1982.

Tire Pressure kPa	Pull N	Travel Reduction %	Ground Speed km/h	Radar Measurements Speed km/h	Radar Measurements Slip %
27.6	0	0	7.7	7.4	4.7
	111	2.7	7.5	7.1	5.9
	313	6.9	7.1	6.9	5.8
	644	14.5	6.6	6.4	9.2
55.2	0	0	7.9	7.6	3.2
	111	4.2	7.5	7.1	4.6
	327	5.4	7.5	7.2	4.5
	859	16.2	6.6	6.5	10.4
82.7	0	0	8.1	7.8	3.1
	111	3.9	7.8	7.3	3.7
	367	5.3	7.7	7.4	3.7
	862	17.7	6.7	6.6	11.8
110.3	0	0	8.1	7.8	2.9
	111	4.1	7.8	7.2	3.2
	433	5.4	7.6	7.4	4.4
	865	17.3	6.7	6.8	12.9
	1376	21.2	6.4	6.2	12.1

CONCLUSIONS AND RECOMMENDATIONS

1. The radar speed measurements are suitable and accurate for detecting ground speed of forestry and off-road vehicles.

2. The central tire inflation system design was adequate and can be extended to larger vehicles and skidders.

3. Work is in progress to interface with the radar console speed and wheel rpm signals to automatically control the tire inflation pressure.

REFERENCES

1. Burt, E. C. and A. C. Bailey. 1982. Load and inflation pressure effects on tires. Transactions of the ASAE 25(4):881-884.

2. Czako, T. F. 1974. The influence of the inflation pressure on cross-country performance. Journal of Terramechanics 11(3 & 4):13-23

3. Grevis-James, I. W. and P. D. Bloome. 1982. A tractor power monitor. Transactions of the ASAE 25(3):595-597.

4. Hassan, A. E. and J. K. Whitfield. 1982. Student design of an all-terrain vehicle for forestry operations. SAE Technical Paper Series #821041, 7 P.

5. Hassan, A. E. 1978. Effect of mechanization on soils and forest regeneration. I. Coastal Plain organic soil. Transactions of the ASAE 21(6):1107-1111.

6. Hyltin, T. M., T. D. Fuchser, H. B. Tyson, W. R. Regueiro. 1973. Vehicular radar speedometer SAE Paper Series #730125, 36 P.

7. Kaczmarek, R. W. 1981. Innovative mobility designs utilized on foreign wheeled and tracked vehicles. Proceedings of the 7th International Conference, ISTVS, Calgary, Alberta, Vol. 1: 263-296.

8. Richardson, H. A., R. L. Lanning, K. A. Kopp and G. J. Carnegie. 1982. True ground speed measurement techniques. SAE Technical Paper Series #831058. 10 P.

9. Tsuha, W., A. M. McConnell and P. A. Witt. 1982. Radar true ground speed sensor for agricultural and off-road equipment. SAE Technical Paper Series #821059. 9 P.

10. Zombori, J. 1967. Drawbar pull tests of various traction devices on sandy soils. Journal of Terramechanics 4 (1):9-17.

CENTRAL TIRE INFLATION SYSTEMS (CTIS) - A MEANS TO ENHANCE VEHICLE MOBILITY.

ROBERT W. KACZMAREK

US ARMY TANK-AUTOMOTIVE COMMAND, WARREN, MICHIGAN

For the vehicle designer there are numerous considerations that must be taken into account. Based upon the type of requirements which are to be placed upon a vehicle, a variety of alternatives are usually available to achieve the final design goal. The nature of modern warfare places an additional responsibility and somewhat more difficult burden on the designer of military wheeled vehicles.

Probably one of the most demanding features hoped for in modern military wheeled tactical vehicles is to achieve a high degree of mobility. If a wheeled vehicle is mobile it can function in a broader range of roles, therefore providing it with a higher degree of utility.

Since there are numerous ways of increasing a wheeled vehicles overall mobility and effectiveness it then becomes a choice of which mobility features to incorporate into a vehicle design and how effective each of these features are from a performance and a cost effectiveness standpoint.

One of the most effective and well proven systems that has been adapted to wheeled tactical vehicles to improve the overall vehicle mobility is CTIS. In general these systems, feature relatively simple designs, are a highly effective and convenient method of enhancing vehicle mobility and are relatively simple to operate.

The intent of this paper is to discuss the issue of CTIS from the advent of the technology to the state-of-the art.

A CTIS can be defined as, "A system incorporated in a wheeled vehicle which permits the vehicle tire pressures to be regulated by the vehicle driver/crew member from within the vehicle cab while on the move". If the vehicle tires are deflated from 50psi to 15psi the tire footprints will increase substantially. Whenever the area of the footprint is increased the ground pressure which that vehicle experiences is reduced. Assuming that the soil strength conditions are identical, the tractive effort and overall mobility for a vehicle will increase at the lower pressure level, hence allowing this vehicle to accomplish a high level of mobility performance.

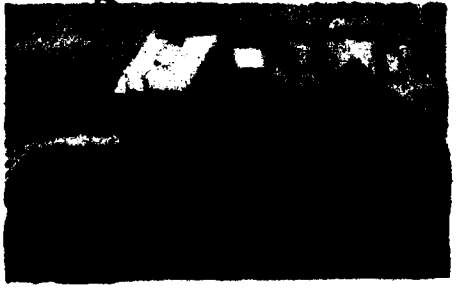

Fig. 1 BTR-152 Soviet Armored Car

The BTR-152 Soviet Armored Car (Fig. 1) utilized CTIS. The CTIS design for the BTR-152 was of the "Pentagraph" type which had exposed air lines that led to the wheel hubs. On the overall, the CTIS operation on the BTR-152 did improve overall vehicle mobility; however when the vehicle negotiated rough terrain or heavy vegetation the "Pentagraph" lines were damaged and adversely effected the operation of the CTIS. Fig. 2 basically illustrates the system layout for the CTIS which the BTR-152 vehicle employed.

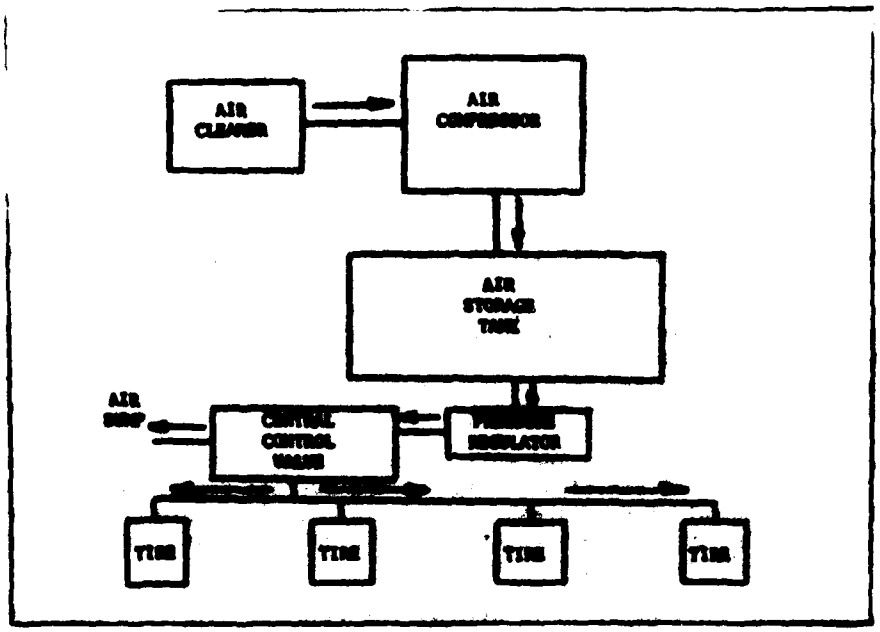

Fig. 2 BTR-152 CTIS System

The operation of this system was very simple. As shown in figure 2, air entered the system thru an air cleaner, was compressed into an air storage tank and regulated at a pre-set working system pressure. When it was desired to increase tire pressure levels the inflation control valve was positioned in the inflate mode and the vehicle tires were inflated, when deflation was desired the vehicle operator simply positioned the control valve to the deflation position, permitting the tires to "dump" air past the control valve.

After World War II both the United States and the Soviet Union experimented with CTIS to include utilizing slip rings on the axles as a means of transfering air from the [illegible] axles to the vehicle tires. (Fig. 3) illustrates a typical slip ring assembly and its relationship to the vehicle axle housing.

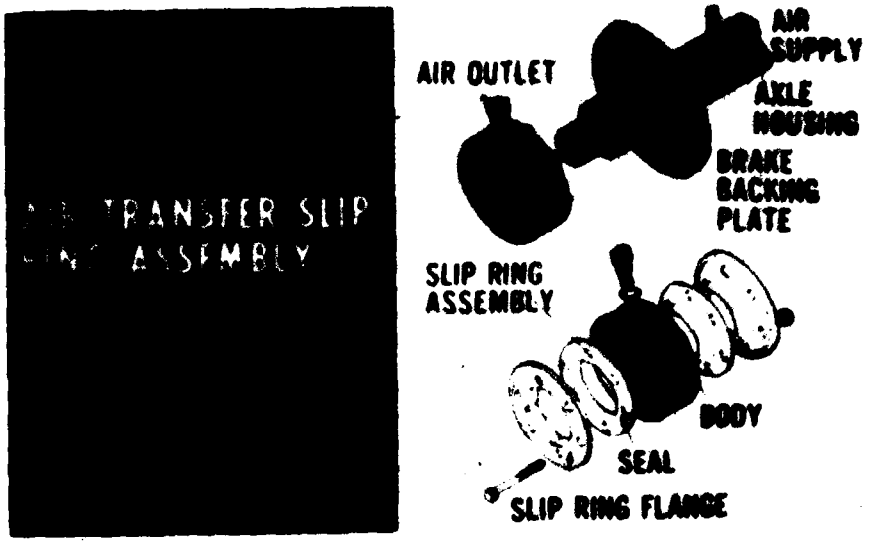

Fig. 3 Air Transfer Slip Ring Assembly

Since World War II the Soviet Union and Warsaw Pact Countries have emphasized the use of CTIS on all tactical wheeled vehicles. Fig. 4 is a diagram of a CTI System utilized on an early Soviet 2½ tonne cargo truck (ZIL-157). The ZIL-157 was a departure from the earlier vehicles utilizing CTIS in that it did employ slip rings on the axles as a means of air delivery. Each slip ring assembly is fitted with seals to help prevent air leakage. By observing Fig. 4 it is evident that the basic difference between the CTIS on the BTR-152 and the ZIL-157 is the utilization of the slip ring.

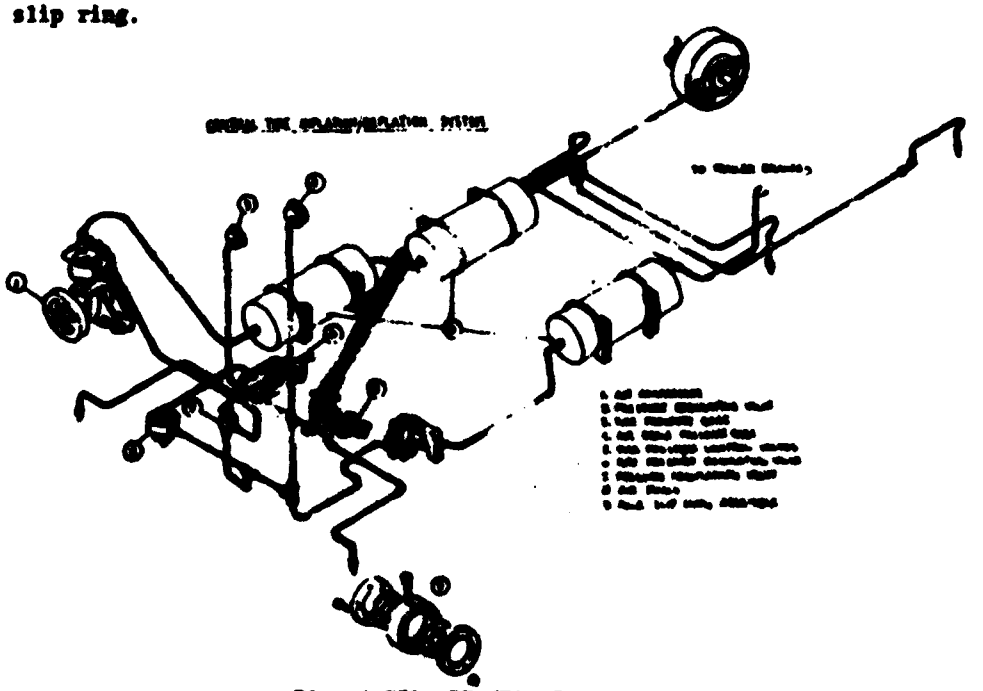

Fig. 4 ZIL-157 CTIS System

Since CTIS is usually installed on vehicles which have an air brake system, the air pressure for CTIS and air brake operations is supplied from a common vehicle air tank supply system. Being that vehicle safety is more important than vehicle performance a valve is installed on the vehicle air tank supply system which assures that the air pressure required to operate the vehicle air brakes is satisfactory prior to diverting air pressure to operate CTIS. If the vehicle air tank supply pressure level is relatively low, this valve will regulate air pressure to the air brakes for operation but no air pressure will be delivered for CTIS usage.

It was emphasized earlier in this paper that the primary intent of CTIS from a mobility standpoint is to lower vehicle tire pressure levels in an effort to increase the tire ground contact area which will lower the overall ground pressure and help increase vehicle drawbar pull and mobility. Figure 5 is a graph of the changes in tire footprint areas for the ZIL-157 vehicle utilizing a 12:00 X 18 bias ply agressive tread tire. Both the net and gross footprint areas more than double when the tire pressures are dropped from 50psi to 10psi. This footprint area increases primarily in the length dimension.

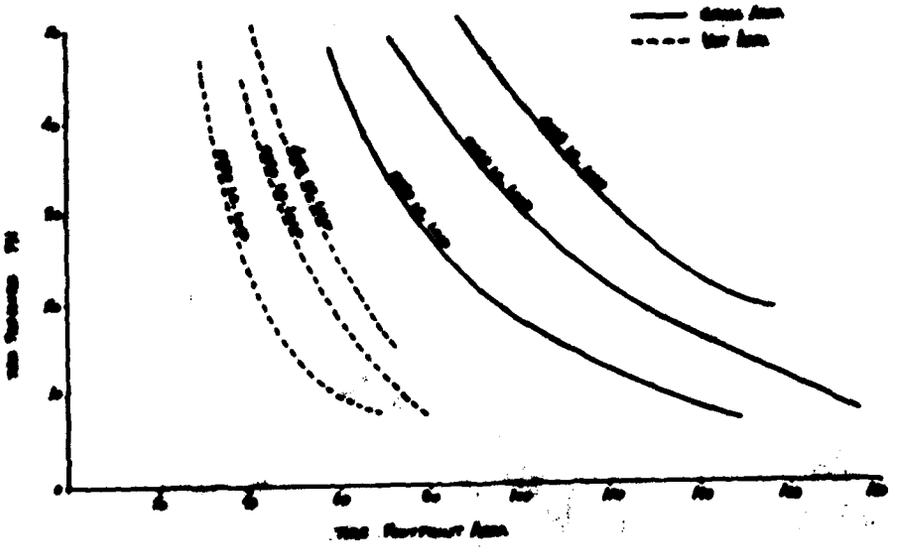

Fig. 5 ZIL-157 Footprint Areas

Figure 6 is a table which illustrates the maximum increase in Drawbar-Pull while reducing inflation pressure levels on the ZIL-157 vehicle. It is interesting to note the percent increase in drawbar-pull when tire pressure levels are reduced.

Tires used on vehicles utilizing CTIS can be standard type tires, bias or radial ply, tube or tubeless design. If a tube is used within the tire, the valve core must be removed to allow for deflation of the tire when the CTIS control valve is activated from within the vehicle cab.

The wheels that are used for CTIS design are of the "split" type configuration to allow for a bead spreader to be installed within the tire. A bead spreader must be used to compress the tire bead against the inner wheel rim surface so that when operating at low tire pressures the tire bead does not separate from the inner wheel rim and deflate the vehicle tires. A locking device is also installed in the tire/wheel assembly to prevent the tube from rotating in relation to the wheel at low tire pressures. Figure 7 illustrates the tire/wheel assembly with bead spreader which is employed on the TATRA 813 vehicle.

SOIL	VEHICLE	INFLATION PRESSURE psi	DRAWBAR PULL lbs.	DRAWBAR PULL INCREASE %
WET LOAM	ZIL-157	35	3600	- -
		15	4300	19 -
		7	5000	39 16
FINE SAND	ZIL-157	35	5000	-
		15	6300	26
COARSE SAND	ZIL-157	35	3000	-
		15	5000	66
DRY LOAM	ZIL-157	35	8500	-
		15	9200	8

Fig. 6 ZIL-157 Drawbar Pull At Varying Tire Pressures

The Czechoslovakian TATRA 813, 8X8, 8 tonne Tactical Cargo Truck (Fig. 8) produced in the 1980s timeframe, utilizes CTIS. The configuration of the CTIS inflation/deflation controls and the manifold for the tire pressure control valves on the TATRA 813 vehicle are an improved design but the overall system functions in basically the same manner as earlier systems (Fig. 9)

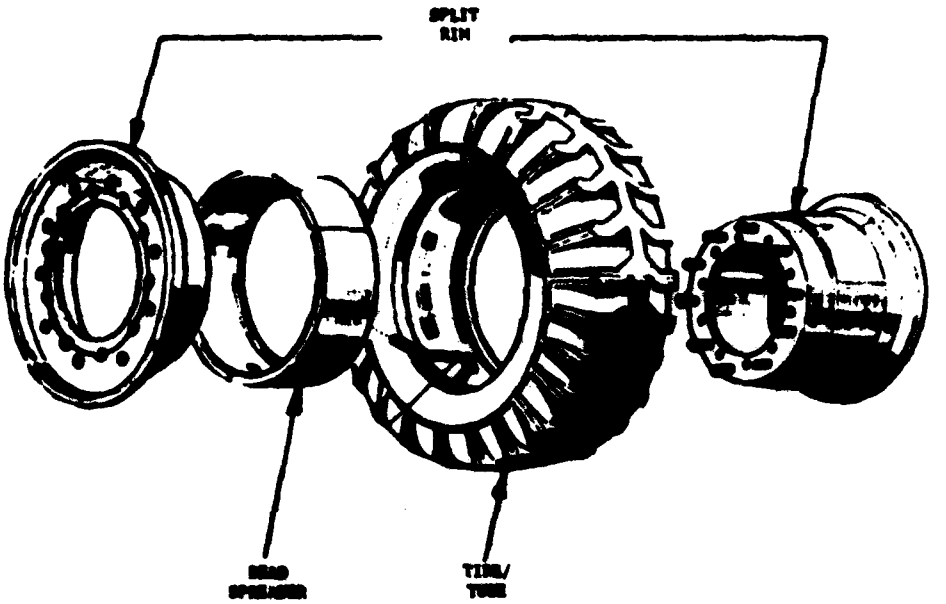

Fig. 7 TATRA 813 Tire/Wheel Assembly

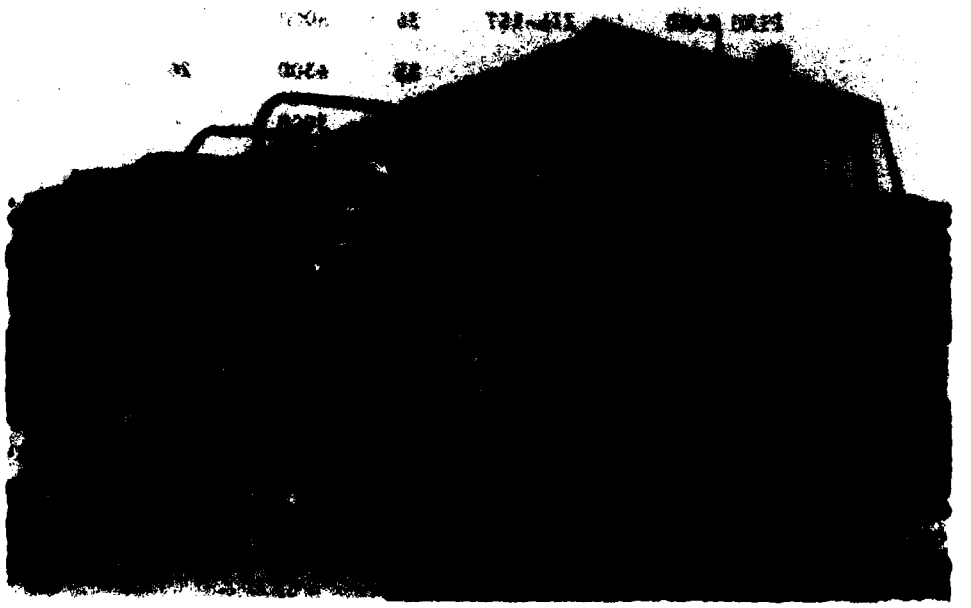

Fig. 8 TATRA 813 Vehicle

Fig 9 TATRA 815 CTIS Controls

The Yugoslavian FAP 2026, 6X6, 6 tonne Tactical Truck (Fig. 10) produced in the 1977 timeframe, also utilizes CTIS. In the authors opinion, the FAP 2026 CTIS control console represents a clear departure in design from other Soviet/Warsaw Pact vehicle systems. On previously known vehicles of this type, there were central manifolds designed into the system which allowed for isolating leaks or "blown out" vehicle tires by the use of valving from within the vehicle cab. Some systems allowed the vehicle operator to monitor the pressure of an individual tire or the entire CTIS from within the cab. On the FAP 2026 vehicle (Fig. 11) the only two controls are the control for activating/deactivating the CTIS, and the pressure control valve which allows the driver/operator to pre-select the vehicle tire pressures according to the terrain which the vehicle will be subjected to. The graduations on the pressure control are labeled in bars of pressure.

Judging from the known employment of CTIS on tactical vehicles it is apparent that since World War II the Soviet Union & Warsaw Pact countries have dominated this technology area. However, in recent years the emphasis on ways to increase a vehicles overall mobility has resurfaced the issue of CTIS in the free world.

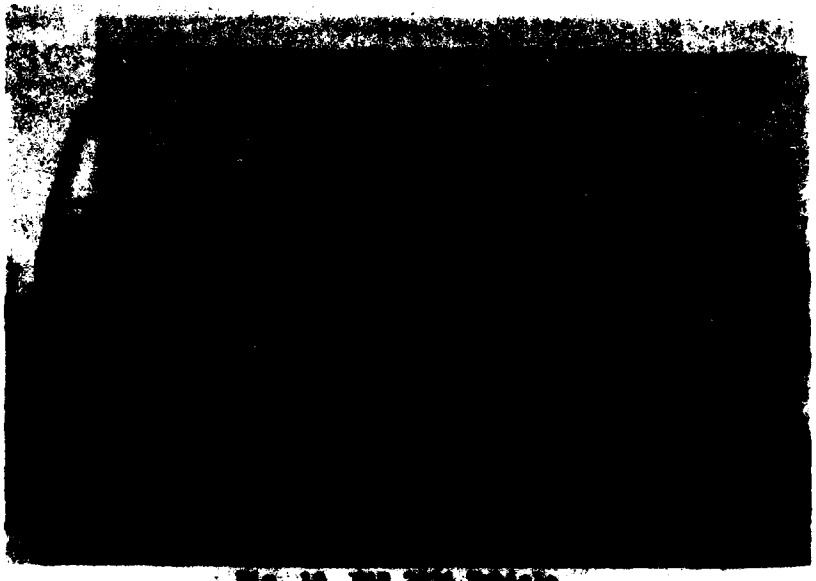

Fig. 10 PAP 2026 Vehicle

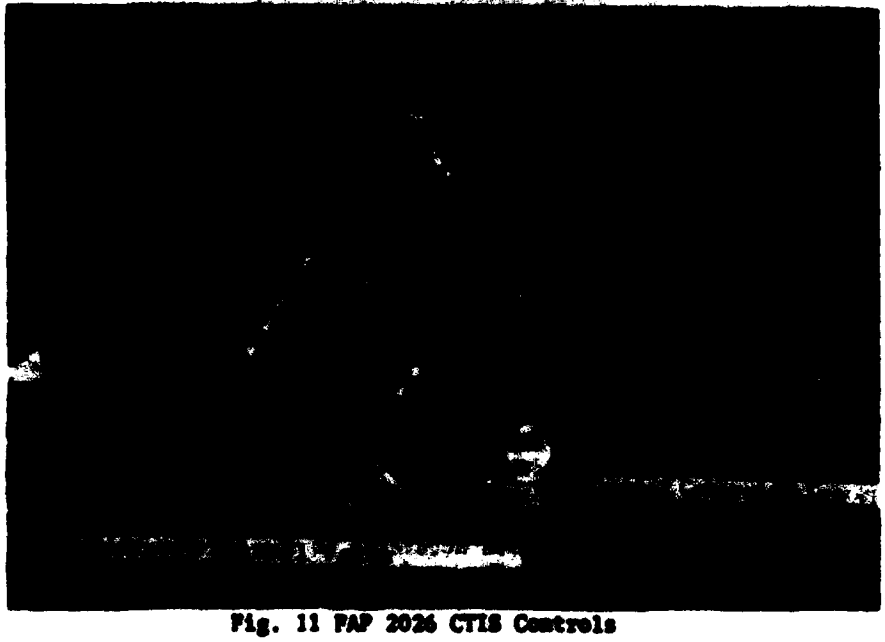

Fig. 11 PAP 2026 CTIS Controls

A system which is currently being marketed by the AM General Corporation is adapted to a five ton tactical truck (Fig. 12) and is fitted with radial ply tires. All previously known applications of CTIS have utilized bias ply tires, so the change to a radial tire certainly should add a dimension to enhancing a vehicles overall mobility. Fig. 13 illustrates the general layout of the CTIS utilized by AM General Corporation.

Fig. 12 AM General 5 Ton Cargo Truck

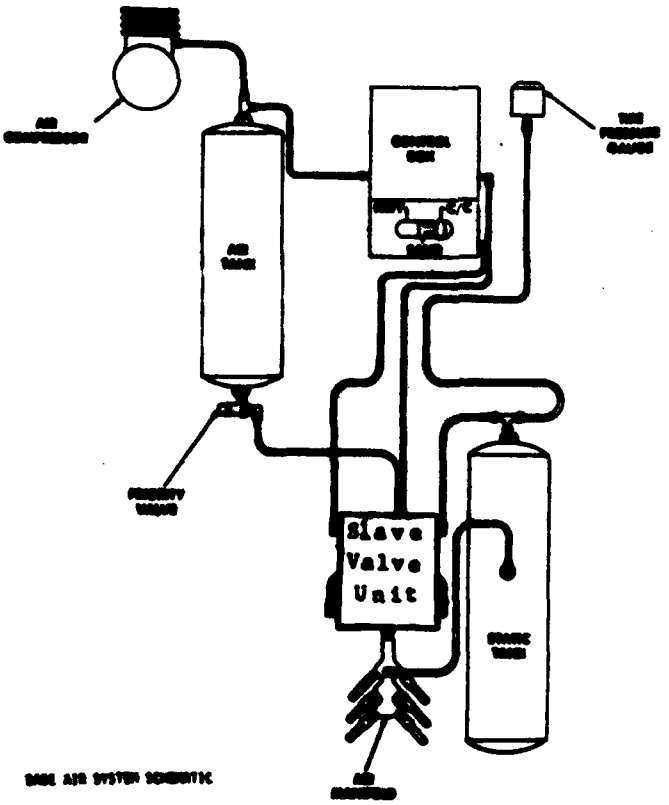

Fig. 13 AM General CTIS System

The design of AM General's patented system incorporates some definite improvements to previously known systems. In an effort to reduce tire inflation times a large 16.1 CFM air compressor is used. For comparative purposes the ZIL-157, an earlier Soveit 6X6 vehicle utilized a 5.5 CFM air compressor. The AM General system incorporates a single air tank (for air brakes and CTIS) instead of two or three interconnected tanks as observed in earlier generation system designs. A straight forward and simple to use pressure control valve is also utilized on the AM General design for the various terrains which a vehicle may have to negotiate.

In the authors opinion, the AM General CTIS design represents the state-of-the-art- in the CTIS technology area. Nevertheless, there are other technical approaches worth mentioning which could have merit in varying vehicle tire pressure levels as a means to increase overall vehicle mobility.

Currently there are R&D efforts underway to design and manufacture charged cartridges that can be adapted to a vehicle axle hub with hose connection between the charged cylinder and the vehicle tire. An electronic signal from the vehicle driver/operator activates a valve on the charged cylinder for inflating/deflating a vehicle tire. This system would eliminate the need for a vehicle compressor and the associated controls and plumbing but would be limited from the standpoint of the number of times it could inflate a vehicle tire prior to being re-charged or exchanged for a new cylinder. In a combat environment the charging of these cylinders could also prove to be hazardous.

Due to the characteristically strong flexible sidewall of a radial ply tire, the quality of the vehicle ride and handling are substantially better than that of a vehicle utilizing conventional bias ply tires. In the past several years an extensive amount or progress has been made on advanced radial tire designs. It would be ideal to assume that a radial tire could be designed to operate at one standard pressure level for both soft soil and primary road application. Such a design would allow a vehicle to have low ground pressure and high traction in the off road terrain and then be able to operate at high speeds on primary roads with relatively low rolling resistance to prevent high heat build-up. Some current tire designs have been offered as candidates for use as a standard pressure tire but to date have not received overall approval for this type of usage. In the event that a currently produced larger size radial tire were used to fulfill this requirement it would probably prove to be too heavy for the application. As a result vehicle ride and handling would be degraded and the tires would probably have a tendency to overheat during high speed driving on primary roads, hence destroying the tire.

It is also reasonable to assume that a completely unique automatic CTIS could be designed which would require no driver/operator input or judgment. Such a system would automatically sense and continually monitor the terrain conditions and adjust the vehicle tire pressures to an optimum pressure level. In addition, such a system could activate/deactivate the vehicles differential locking mechanisms on an "as needed" basis; depending on the terrain being negotiated.

Up to this point various CTI systems have been discussed with an attempt to generally describe what type of hardware has been developed as well as introducing some alternatives approaches to increasing vehicle mobility by varying tire pressure/profile relationships.

If a component is to be designed into a vehicle configuration, regardless if it concerns the vehicles mobility, survivability or maintainability; it must focus around the original intent or mission of the vehicle itself. Depending on how well these components are chosen and engineered into the vehicle design is somewhat dependent upon how successful the vehicle will fulfill this mission.

Webster's Dictionary defines a mission as "an assigned duty or task". This definition can be exemplified upon when we attempt to define the mission of a vehicle. A very general definition of the mission of a wheeled cargo truck could be "to transport personnel and equipment over various terrains in an effective manner". Hence, when designing such a vehicle it would seem practical to place the most concern on those factors or components which would provide the vehicle with the highest probability of completing its intended purpose. Such a vehicle must possess certain engineering performance characteristics or potentials (i.e. specific acceleration, top speed, grade climbing) in order to negotiate the obstacles throughout the vehicle mission. The vehicle should be designed to a high degree of reliability so that failures are kept to a minimum so as not to interfere with mission completion. Last but not least, time required to fulfill a mission must be taken into consideration.

The performance characteristics of a vehicle must always be highly regarded during a vehicle design phase. Certifications concerning engine horsepower, vehicle step climbing capability, minimum braking distance, soft soil mobility performance, etc. are all somewhat common requirements for modern military wheeled vehicles.

Whenever CTIS is considered for adaptation to a wheeled vehicle it is probably viewed as a system which enhances a vehicles mobility performance. However, it should also be noted that by utilizing CTIS, the ride and handling characteristics of the vehicle can also be improved, therefore labeling it as an impressive side benefit. The more energy that is absorbed by a vehicle operator or the vehicle components, the more fatigue occurs, causing overall degraded vehicle performance and eventual component failures.

A CTIS was adapted to some 15 and 16 ton US Goer Vehicles (Fig. 14). Since the Goer vehicles did not have a suspension system, the flexing of the sidewalls of the large 16 ply, 29.5 X 25.00 earthmover type tires provided the only means of absorbing the shock between the terrain and the vehicle. In a tactical truck, if the tire design is properly chosen, it too will reduce shock and have a cushioning effect upon the vehicle driver and the suspension components.

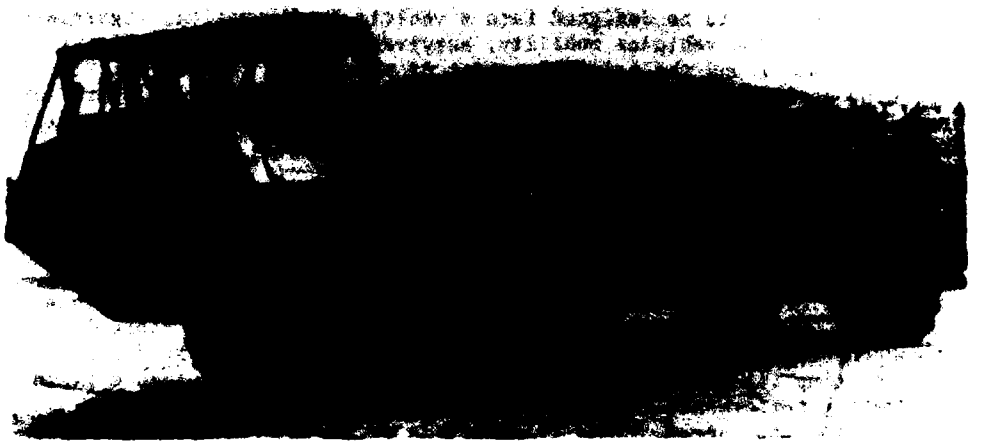

Fig. 14 US Goer Vehicle (16 Ton)

On a vehicle that employs CTIS the tire pressure levels can be adjusted when negotiating rough terrain. The lowering of the tire pressures will then allow greater flexing in the tire sidewall which will decrease the amount of energy normally experienced in the vehicle suspension system components thereby increasing component life and improving the overall reliability and maintainability of the vehicle.

Fig. 15 graphically displays the relationship between surface roughness/ vehicle tire pressures at various vehicle speeds.

If CTIS is properly utilized and consequently does improve the overall reliability and maintainability of a vehicle then it can prove to be a very cost effective system. Fig. 16 graphically displays the relationship between maintenance costs and usage of vehicles over various surface roughness courses.

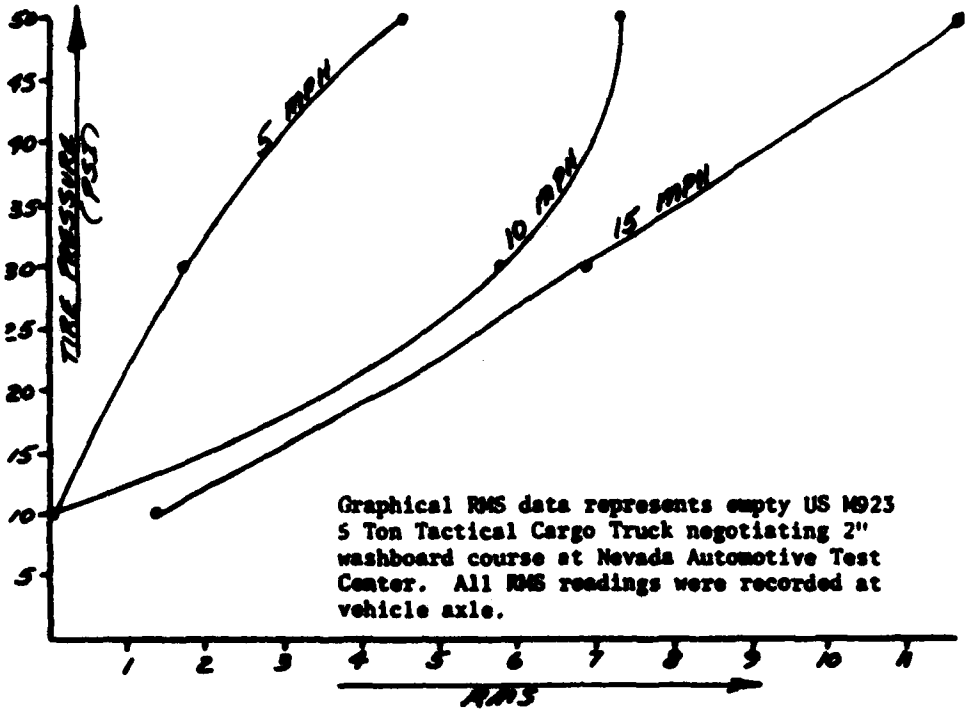

Fig. 15 Surface Roughness Vehicle
Tire Pressures At Various Vehicle Speeds

Utilization of CTIS can also have a positive impact from the Human Engineering/Psychological viewpoint. If a vehicle driver has been operating a vehicle which has a somewhat rough ride, this driver will experience most of the accelerations/decelerations when the vehicle is negotiating rough terrain. Driving a vehicle under these conditions will increase driver fatigue and will most likely also increase the time required to negotiate a given terrain. From a psychological viewpoint, an operator will become disgruntled with a vehicle that has a marginal performance level. A driver needs to have confidence in the equipment he/she is operating or the level of accomplishment will be relatively low.

In general, whenever the time element to complete a given task can be reduced, the more efficient an operation becomes. Likewise whenever we increase the time it takes to complete a given mission, the overall effectiveness of that mission decrease accordingly.

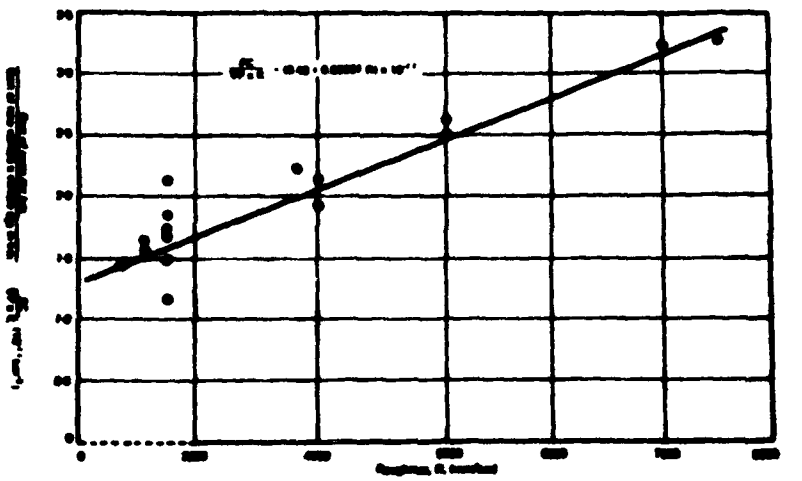

(Reproduced from British Department of Transport, Transport Road and Research Laboratory Report 672. The Kenya Road Transport Cost Study: Research Vehicle Operating Costs)

Fig. 16 Vehicle Maintenance Cost/Terrain Surface Roughness

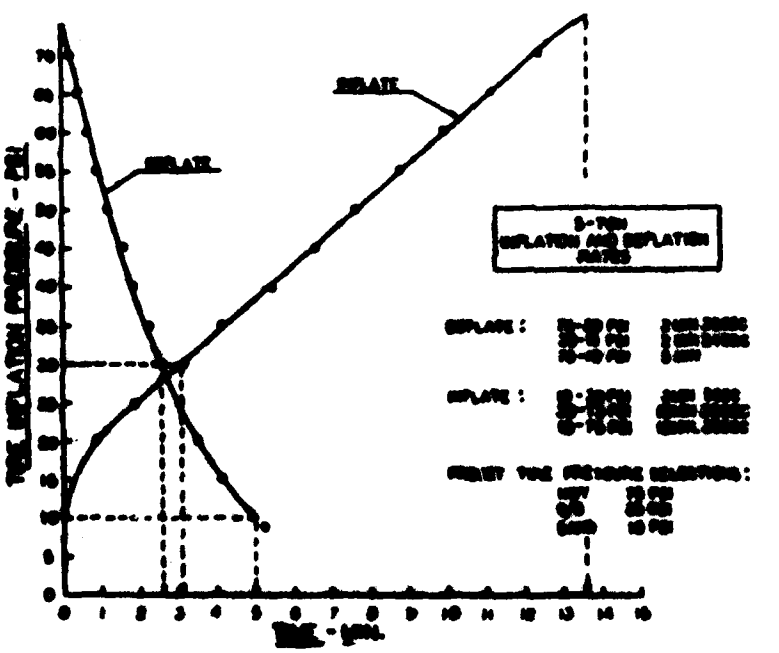

Fig. 17 Inflation/Deflation Times For AM General CTIS

Since the time factor can be such an important element when viewing a vehicle mission, it would seem practical and cost effective to incorporate those features/components into the overall vehicle design package which will help minimize the elapsed mission time.

Assuming that we have two identical wheeled vehicles, one with CTIS and one without; in all probability the vehicle equipped with CTIS will function in a more effective manner.

From the standpoint of negotiating adverse terrain the vehicle with CTIS will adapt to a given situation (varying tire pressure levels) in a quicker, more organized manner than the vehicle without CTIS. A vehicle with CTIS can have the tire pressures altered from within the vehicle cab while on the move. A vehicle without CTIS must first be stopped and the crew must physically exit the cab and manually inflate/deflate each vehicle tire. Depending on the type of CTIS employed the tire inflation/deflation times may vary but on the overall it takes considerably longer for a vehicle without CTIS to have tire pressures adjusted manually to the same pressure level of a vehicle utilizing CTIS.

Fig. 17 is a graphical display of the times recorded to inflate/deflate the AM General CTIS utilizing the Michelin 14.00 X 20 XS tires.

Since the tire size (volume) and number of tires on a vehicle (drive mode) are directly related to inflation/deflation times, the air compressor capacity is a critical factor. Hence, the best ways of decreasing inflation times is to increase the air compressor capacity and have it operating at optimum RPM. Likewise, the most logical means of decreasing tire deflation times is to provide for larger air exhaust ports and associated plumbing.

In a combat environment vehicle tires can be very vulnerable. If a vehicle employs CTIS the probability of completing missions in a timely manner and increasing a vehicles survivability is enhanced. Depending on the system design various corrective procedures can be followed for a punctured or blown out tire. On some of the Soviet/Warsaw Pact designs the wheel which has a leaking tire is isolated from the overall system by closing of a valve within the cab. Most systems also employ valves at the vehicle wheel which can be physically turned off in the event of puncture or leakage. Another approach could be to utilize a larger size air compressor which could accomodate a considerable amount of leakage.

The following is the authors opinion of some of the necessary general characteristics for an ideal CTIS.

a. In order to provide air pressure for both the vehicles air brakes and CTIS an adequately sized air compressor should be fitted into the design package. Such a compressor would account for inflating vehicle tires from minimum to maximum pressures in a relatively short timeframe as well as providing for an occasional leakage or blown out tire.

b. The CTIS cab controls should incorporate a straight forward and simple design and be convenient for the vehicle driver to operate. Such features as a range of positions to place the tire pressure control lever, depending on the terrain that is to be negotiated (i.e. mud, gravel, paved highway, etc.) can help reduce driver confusion and error and enhance overall mission effectiveness.

c. A well designed CTIS will incorporate a high degree of safety. From the standpoint of adequate vehicle air brake pressure, proper valving should be fitted to the vehicle air tank system to ensure that the air brakes have priority over CTIS.

d. Because of the obvious advantages radial ply tires have over bias ply tires regarding vehicle ride, handling & overall performance it would seem logical to fit a vehicle utilizing CTIS with radial ply tires. Fig. 18 illustrates the footprint areas of both the standard US M35C and the newer Michelin XS tires at varying pressure levels.

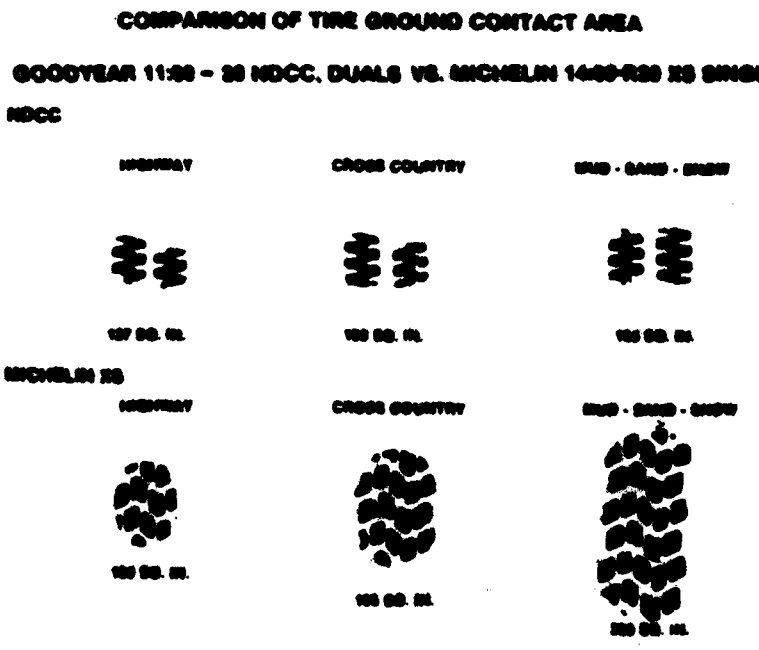

Fig. 18 M35C/Michelin Tire Footprint Areas

SUMMARY & CONCLUSIONS

The modern day pneumatic tire is designed to fulfill a broad range of requirements for numerous vehicle applications. Due to the characteristics of tire sidewall flexibility, vehicle designers are capable of employing CTIS on a vehicle to enhance its mobility and ride dynamics. By deflating the tires on a vehicle, the tire sidewall flexibility functions as a shock and vibration damper for the vehicle over rough terrain. In effect, by using CTIS, the vehicle suspension system can be optimally tuned for a broad range of terrain conditions. The installation and proper usage of CTIS can therefore optimize a vehicles overall tractive-dynamic performance, allowing a vehicles power parameters to be utilized in the most practical and cost effective manner.

ACKNOWLEDGMENTS

The author would like to express appreciation to the following organization for the use of technical information applicable to this paper:

US Army Tank Automotive Command
US Army Foreign Science and Technology Center
AM General Corporation
Nevada Automotive Test Center

RUBBER TRACKS FOR MACHINERY AND VEHICLES IN FORESTRY AND AGRICULTURE

PER IVAR NICKELSON, Technical Manager of Skega AB, Ersmark, Sweden

Summary

In agriculture and forestry it is important to increase mobility and lower the ground pressure to avoid soil compaction and damages to the ground. Rubber tracks have flexible sides which give a much more lenient behaviour to the ground than steel tracks. A special track system, the twin-bogie with rubber tracks, evens out obstacles and increases the mobility on all types of surfaces. This system together with a variation of vertically adjustable bogies has a big potential in the military sector. A light and thin rubber track reduces soil compaction in agriculture and is very useful in all ecologically sensitive areas.

The experiences gained when developing fully moulded rubber tracks (fig. 1) for the all-terrain vehicles BV 202 and later on BV 206 (fig. 2) are the base on which we rely when designing new tracks for different purposes. It is necessary to cooperate with a manufacturer of vehicles when designing tracks because the total track system must be looked upon as a unit. The design then depends on working conditions and demands.

Always when the soil is wet the farmers face problems with mobility on the fields and at the same time the soil is most liable to compaction. The vehicles tend to become bigger and heavier which is contrary to the demands on low ground pressure and reduction of soil compaction. There is no question that soil compaction reduces yield, so rubber tracks can be one solution to overcome the problem.

Also for forestry machines the demands are good mobility, low ground pressure and environmental leniency. Particularly when thinning out forests, it is essential to cause as little damage to the ground as possible as well as to roots of trees which should be left.

Rubber has special properties and behaves quite differently from steel. Rubber is flexible and elastical and has the ability to dampen forces. To get a good result when using rubber, all properties have to be utilized to their full extent. Different rubber compounds give different properties why it is important to evaluate conditions under which rubber has to work and use a compound meeting these demands. Important properties for rubber used in tracks are resistance to tearing, cutting and chipping and a high cut-through value.

When using rubber it is possible to design tracks with flexible sides which will give a much more lenient behaviour to the ground than steel tracks (fig. 3). These tracks have stiff and sharp sides and cut the root system which makes the sinking much deeper. Rubber tracks do not cut the reinforcing mat of roots close to the surface and act like a suspension bridge. On very soft ground it could mean the difference between success and failure.

The design of rubber tracks must be made in close cooperation with the design of the total track system. Total load and speed of the vehicle as well as width, length and weight of the track together with tension system and number of road wheels are the most important factors to consider. A rubber track is reinforced to stand the traction forces without elongation but also to give side stability. Together with a suitable width to length ratio and the arrangement of wheels, the side stability determines the degree of reliability in performance and prevention of track shedding. Height and shape of grousers depend on conditions and type of terrain where the vehicle is to be used.

Together with a manufacturer of forestry machines, Kockums Industrier AB, Söderhamn, Sweden, a special track unit, the twin-bogie with rubber tracks, is being developed. The system is being tested on a vehicle for transportation of logs, type forwarder (fig. 4). The twin-bogie consists of a primary and a secondary bogie giving the vehicle special attributes. The vehicle has eight tractive tracks. The bogie system balances the distribution of the weight of the vehicle and the surface pressure will thus be lower, particularly in heavy terrain. The twin-bogie system improves the rate of balance and the rate of swaying is reduced to a fraction compared with that of a conventional vehicle. The driver experiences this as very favourable and the obstacles as only one fourth of their actual height. The vehicle manages obstacles as high as the diameter of the wheels and climbs over higher obstacles by means of the secondary bogie flipping over (fig. 5). The mobility and manoevrability on all types of surfaces, be in forest ground, block terrain, swamps or on snow, are without comparison. It has also been possible to considerably increase the rate of speed in heavy terrain.

A variation of this track unit is bogies connected to movable arms which are vertically adjustable by hydraulic cylinders (fig. 6). It means that the clearance to the ground is adjustable and the vehicle can run horizontally in a side slope.

We think that the potential for both of these systems is much bigger in the military than in the civilian sector.

The twin-bogie system increases the price of course, but this will be compensated for by higher speed in heavy terrain, no downtime and cost for removing tracks when running on general roads and all advantages mentioned before.

The tracks for the twin-bogie are rather short, 3500 mm, and relatively wide, 580 mm. This eliminates the risk of track shedding. The road wheels are standard pneumatic tyres which lower the price and also give an increased flexibility to the system. The traction force is transferred by friction only. Thanks to the rubber to rubber contact it works perfectly even in snow conditions. The track is built up by two heavy reinforced endless traction belts connected with transversal "grousers" or pads bolted to the belts. Inside the track there are guiders to center the track to the wheels (fig. 7). The pads are reinforced and designed to stand a high load in very rough terrain and of course permit driving on general roads as all rubber tracks do. The rubber is rather thick to prevent cut-through damages and has a high resistance to tearing, cutting and chipping.

For agricultural purposes we expect tracks to reduce damages to the ground but also to give a low ground pressure and thus reduce soil compaction. As the degree of soil compaction depends on specific contact pressure, it is important to distribute the pressure under the track as uniformly as possible, for instance by adjusting the tensioning.

A thin and light track is designed to suit in agriculture. It is fully moulded with very low grousers and flexible sides. Twin mounted pneumatic tyres are used and the short centre to centre distance between the wheels makes it possible to use a low and relatively weak steel bar. These cross bars are combined with the inside guiders in the centre of the track (fig. 8). The width of the track is 450 mm and the length is 4500 mm. A test to find out the difference between such a track and a wheel is carried out in cooperation with NIAE, Silsoe, UK. The track unit is shown in fig 9. When writing this paper no results are available.

We think that this type of tracks can be used also in forestry work, when thinning out the forest, since the flexible sides will not cause damages to the roots. The design of the track means low ground pressure and the low grousers give only little damage to the ground.

Use of rubber tracks is of course not restricted to forestry and agriculture only but will come to use wherever special demands are made on mobility and environmental leniency.

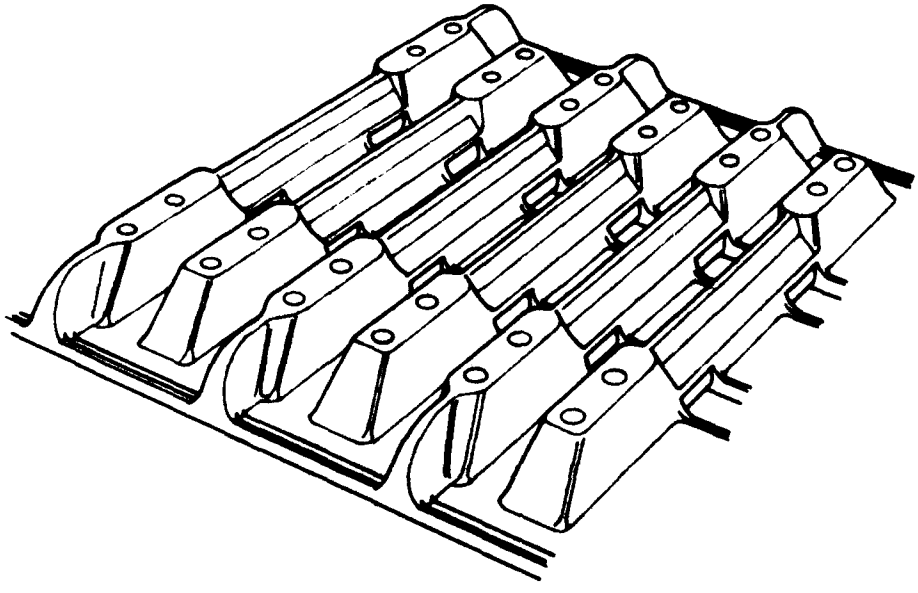

Fig. 1 Fully moulded rubber-track

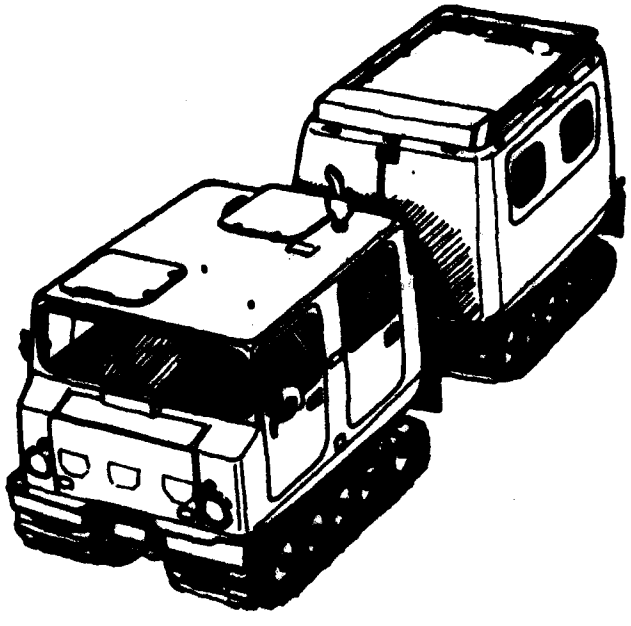

Fig. 2 All-terrain vehicle BV 206

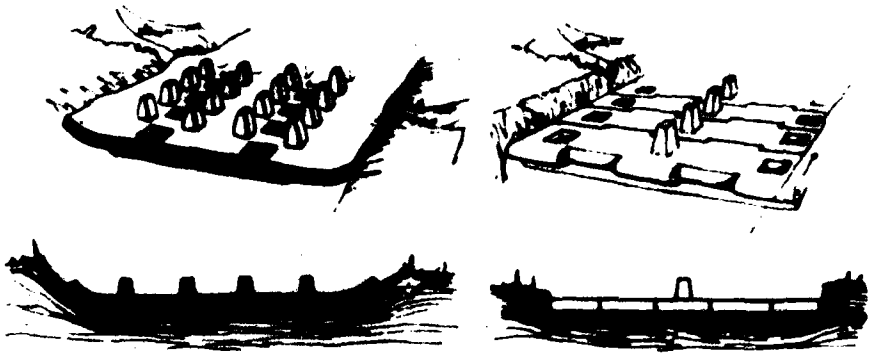

Fig. 3 Rubber-track contra steel-track

Fig. 4 Twin-bogie system

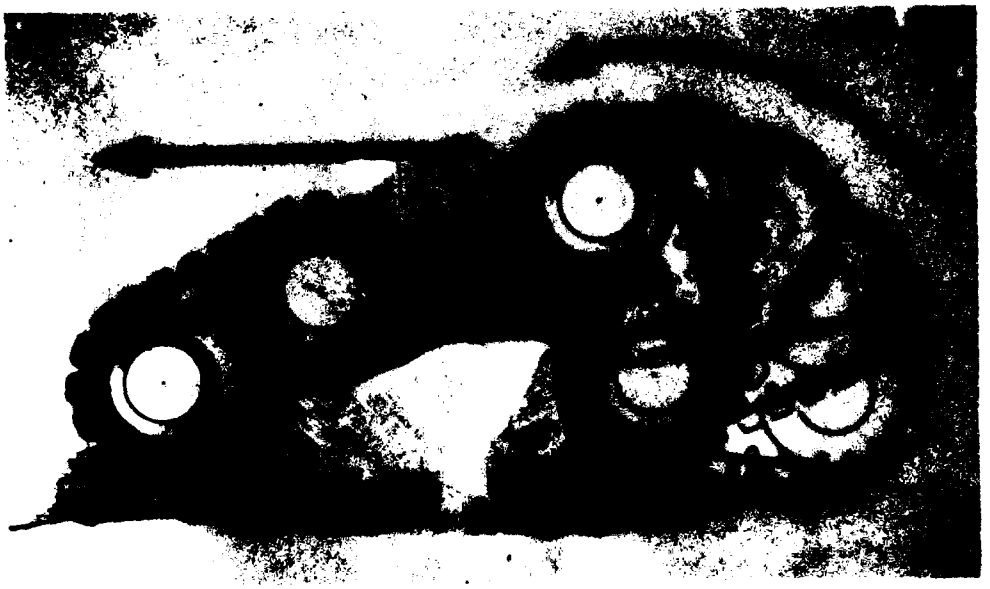

Fig. 5 The bogie is flipping over

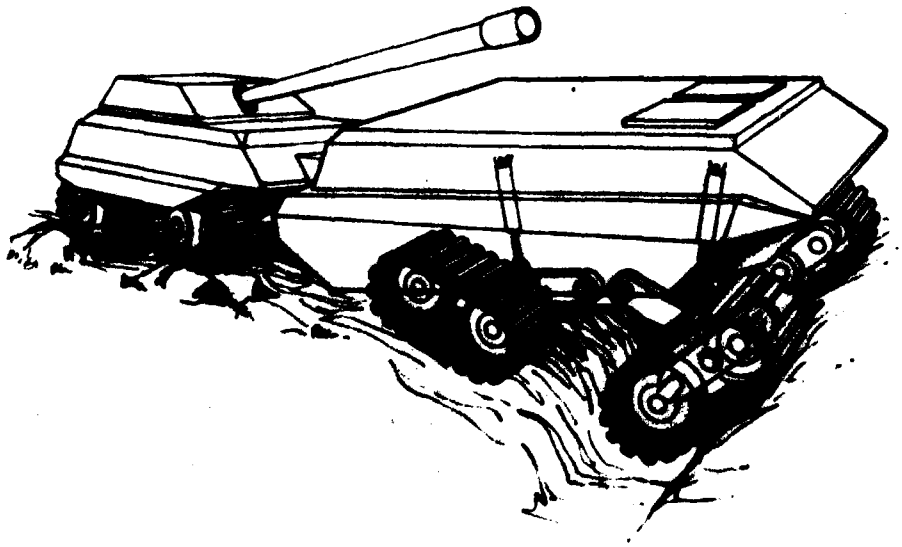

Fig. 6 Vertically adjustable bogie

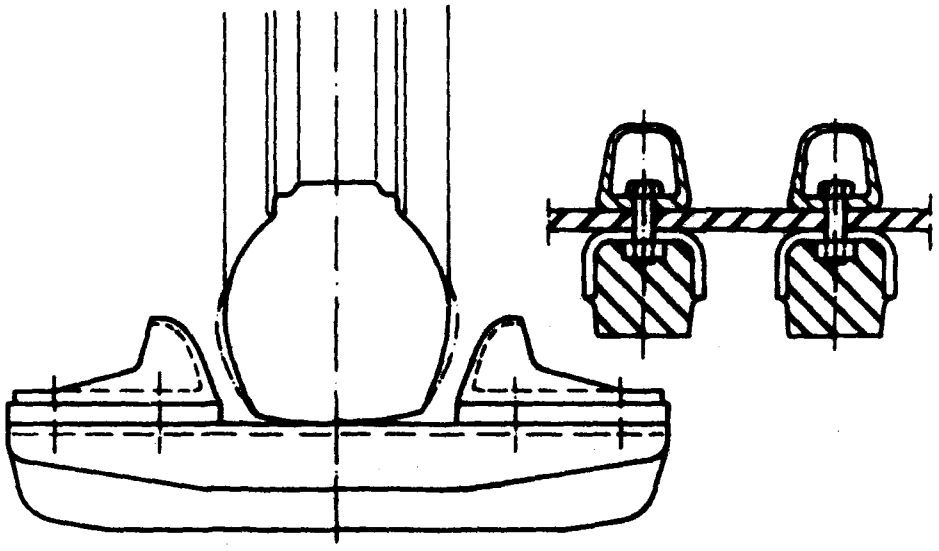

Fig. 7 Rubber-track for twin-bogie

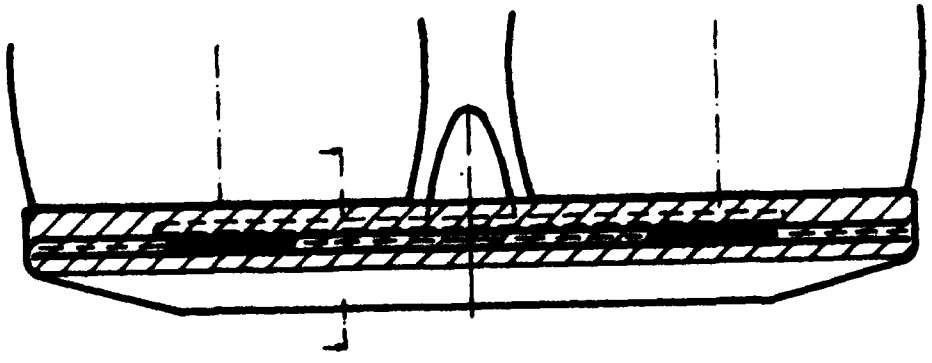

Fig. 8 Light and thin rubber-track

Fig. 9 Test unit

IMPROVEMENTS IN CRAWLER TRACTOR TRACTION

KOJI.OGAKI, YUKIO.TAMURA
KOMATSU LTD, HIRATSUKA, JAPAN

INTRODUCTION

Large traction has to be produced at the undercarriage of the bulldozers to overcome the horizontal resistance caused by digging up and moving earth or ripping rocks, therefore, improvement in traction is one of the most efficient approaches to upgrade the performance of bulldozers.

So far, many theoretical and experimental works have been accomplished and formulas have been introduced to predict traction and slippage of a tractor under given soil conditions.

If all the hypotheses which those formulas are based on rightly explain the actual phenomena, there would be no room to improve the traction except to change parameters appearing in formulas. To improve the traction performance from another point of view, we have to find discrepancies in these theories or modify the formulas by adding new parameters.

By the way, coefficient of traction, μ, may be expressed as follows;

$$\mu = \frac{\int \tau dx / \int \sigma dx - \theta}{1 + \theta \cdot \int \sigma dx / \int \sigma \cdot dx}$$

Abbreviations are shown schematically in Fig.1.

Among these parameters, ℓ and θ are determined by the average contact pressure, backtilt moment, and so on, which are independent of the crawler, and $\int \tau dx / \int \sigma dx$ is the foundamental parameter relating with the interaction between ground and crawler. To find another approach to improve this parameter, $\int \tau dx / \int \sigma dx$, we

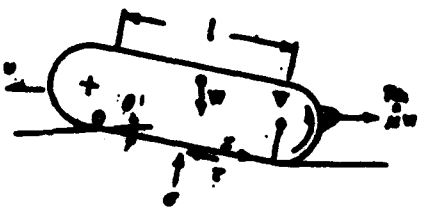

Fig.1.Force acting to crawler

measured traction performance, vertical and tangential force acting on a shoe, tilting angle between neighboring two shoes, soil deformation and stress distribution beneath the crawler to find another approach to improve traction. Obtained data are examined closely with the result that tilting motion of shoes and dynamic load on shoes reduce traction considerably.

Based on this conclusion, the new crawler has been developed which prevents shoes tilting and reduces dynamic load acting on shoes which are unfavorable for traction. Also traction performance of the new crawler is compared with that of conventional crawler. It is concluded that this new crawler improves the traction considerably and also reduces travelling resistance and vibrations.

PHENOMENA UNFAVORABLE FOR TRACTION

1. ON SOFT GROUND

Fig.2 shows experimental results of normal and tangential ground force acting on a single grouser shoe of a tractor pulling constant load on soft loam. These forces are devided by projected area of a shoe providing normal and tangential stress respectively.

The normal stress fluctuates a little but tends to increases linearly as the track frame travels. On the other hand, tangential stress fluctuates very much. The high stress appears at half a shoe pitch backward of a

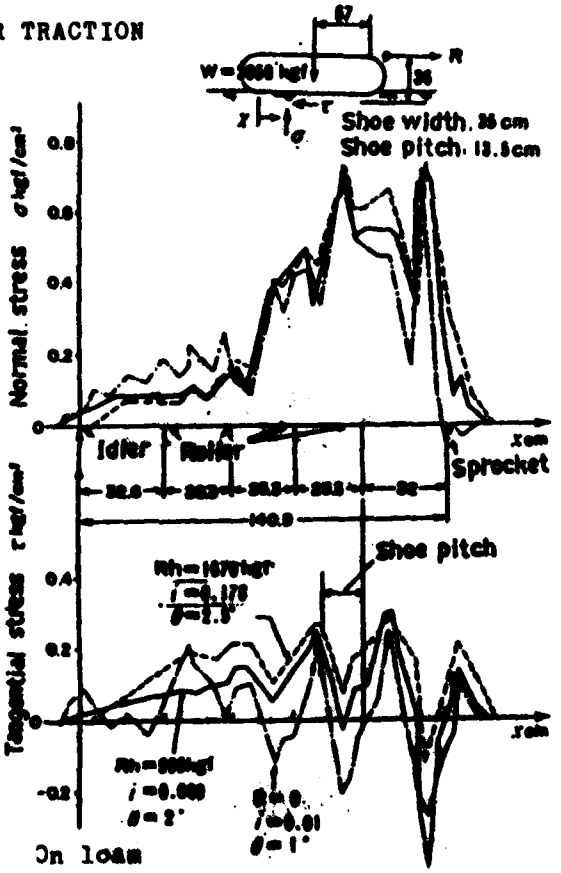

Fig.2. Normal and tangential stress at various track frame position

track roller and low at half a shoe pitch in front of a track roller. It is generally observed that the fluctuation of tangential stress decreases, but average stress increases as the traction increases. Tangential stress is calculated from measured normal stress, shear properties of soil obtained by ring shear test, and horizontal deformation of soil at surface estimated from measured travel reduction. The result is compared with the measured tangential stress in Fig.3. The maximum stress measured is similar with the calculated but minimum stress measured is lower than calculated stress. This suggests the existence of unfavorable phenomena for traction.

As the track roller traverses on the link surface, the vertical load deflects the track links from the horizontal around each pin joint. Fig.4 shows the experimental results of tilting angle between neighboring two shoes.

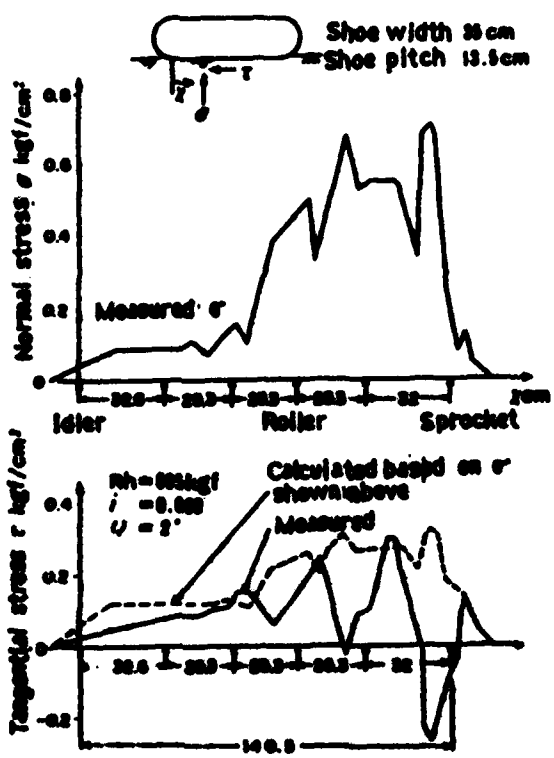

Fig.3.Comparison between measured and calculated tangential stress

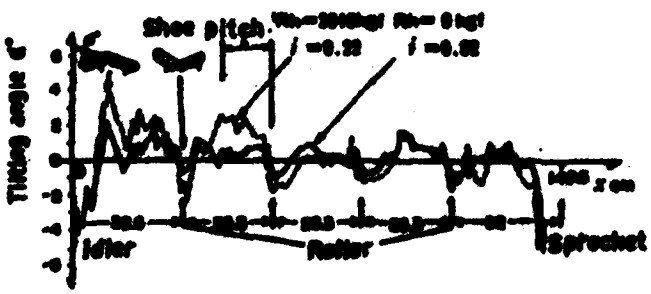

Fig.4.Measured tilt angle on lean

The tendency of the measured tilt angle agrees well with that of tangential stress so that disagreement between measured and calculated tangential stress is deduced to be caused by this deflection or tilting motion of shoes.

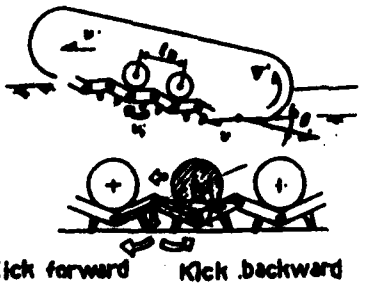

Fig.5.Fluctuation of shoe link

As shown in Fig.5, as a track roller travels closer to a pin, a front shoe tilts back and kick the soil forward, conversely, when this roller passes through that shoe, this shoe kicks the ground backward. A close observation of a pinjoint and neighboring two shoes shows that a front shoe kicks the soil forward and a rear shoe kicks backward when a track roller is on that pin joint. As this roller travels onto the next pin, shoes tilt reversely.

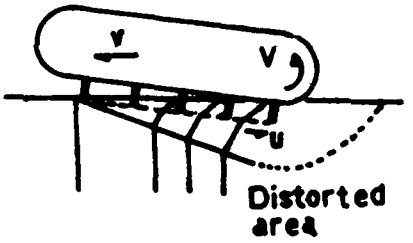

Fig.6.Deformation of soil beneath crawler

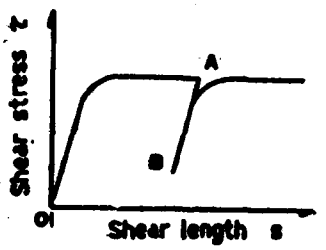

Fig.7.Shear properties of ground soil

Let this kicking velocity be v_0 with respect to joint pin. This pin moves at V with respect to track frame. Also the tractor itself travels at v in fixed cordinates. Therefore, a shoe kicks soil forward at $V-v-v_0$ or backward at $V-v+v_0$ in fixed cordinates. On the other hand, the deformation of white powder put into the vertical hole in test track, as the tractor travels is measured as shown in Fig.6. At the distorted region, these lines deformed to be inclined but straight and parallel. This indicates that soil in this region moves backward uniformly at u. Therefore a shoe kicking soil forward moves backward with respect to soil beneath the shoe at $V-v-v_0-u$. Whenever this velocity $V-v-v_0-u$ becomes negative, a shoe kick soil forward, hence, as shown Fig.7, shear

stress condition changes from A to B.

At low travel reduction (low V-v), negative velocity at the tip of the shoe may become large enough to cause negative tangential stress at a moment. Next instance this shoe kicks the soil backward, thus recovers positive stress. The tendency of Fig.3 may be explained as described above. From these reasons, it is concluded that tilting motion of shoes around pin joint reduces traction of the conventional crawler.

2. ON HARD GROUND

Measured normal and tangential ground force acting on a shoe of a tractor pulling constant load on concrete ground are shown in Fig.8. Dotted line indicates calculated tangential stress for comparison. It is observed that intermittent spike-like normal stress acts on the shoe, thus the tangential stress in phase. Calculated tangential stress is much lower than the measured. From this reason, it is infered that there would be some phenomena unfavorable for traction.

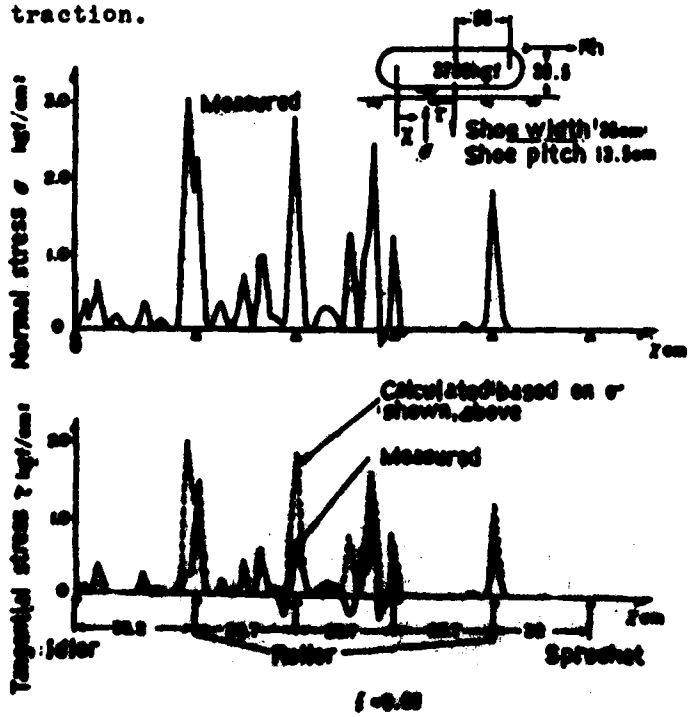

Fig.8.Stress distribution of crawler running on concrete road

Suppose a shoe is pulled horizontally with constant normal load, resultant tangential stress would be as shown in Fig.9 (a). On the other hand, tangential stress will be as shown in Fig.9 (b) under cyclic normal load. Therefore, cyclic normal stress reduces average tangential force by shaded area in Fig.9(b). AT low travel reduction, the slip length during a touch-and-leave cycle of shoes to ground becomes short, consequently, larger reduction of traction takes place. This way, intermittent spike-like normal stress reduces integrated tangential stress or traction. The sharp fluctuation of normal stress occures with rollers position as shown in Fig.10.

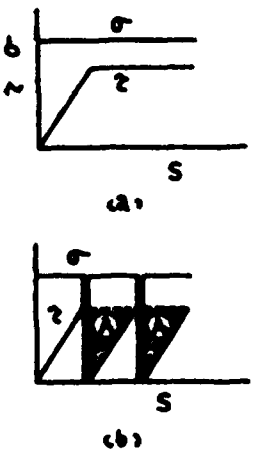

Fig.9.Relationship among normal, tangential stress and deformation of a shoe

PRINCIPLE OF THE NEW CRAWLER

The basic principle of the new crawler is shown schematically in Fig.11. And picture 12 is a photographic view of the tractor equipped with the new crawler. A track rail attached to the track frame rolles over multirollers mounted on each track pin joint. The teeth of aprockets

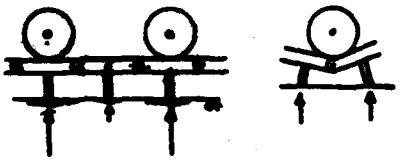

Fig.10.Ground force with various roller positions

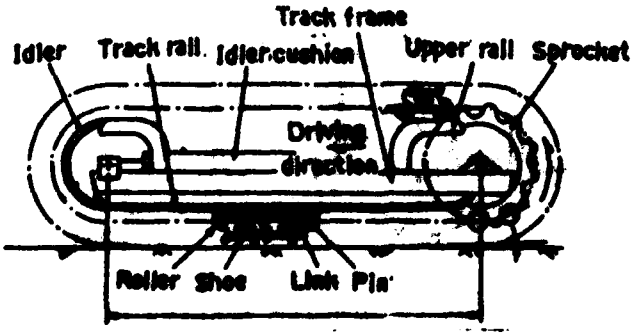

Fig.11.Schematic view of new crawler

meet with those rollers. When a shoe contacts with ground, rollers on two neighboring pin joints are pushed against the track rail so that the tilting motion of shoes is restrained.

Fig.12. Photographic view of the tractor equiped with the new crawler

Measured tilting angle of shoes of the new crawler is shown in Fig.13. Since track frame is supported by only two shoes on hard ground surface, track frame does not jolt except when a ground contacting shoe is placed on a higher spot or the center of the gravity of vehicle passes through supporting shoe. Hence, less fluctuation of normal stress acting on shoes is anticipated. Measured normal stress acting on a shoe of the new crawler shown in Fig.14 supports this principle. Also less travelling resistance and dynamic load enable us to expect dependability of components of the new crawler.

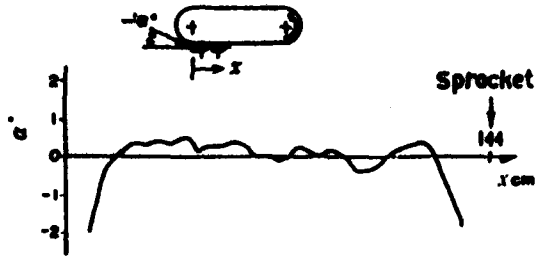

Fig.13. Tilt angle of new crawler

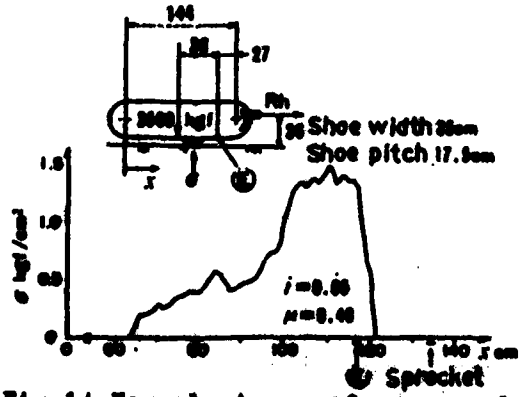

Fig.14. Normal stress of new crawler on concrete

TRACTION PERFORMANCE OF THE NEW CRAWLER

The traction performance of the conventional and the new crawler are compared in Fig.15 and specification of the tractor used is in Table 1. On both soft and hard ground, the new crawler improves traction especially at low travel reduction.

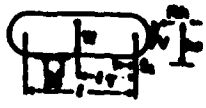

Table.1.Specification of tractor

Type		W kgf	l cm	p_0 cm	h_p cm	Shoe	d_g cm	l_t cm	V km/h	b cm	h_0 cm
New	A	3900	144	17.3	—		65	27	2.8	51	36
	B	4100	164	13.5	—	▽	65	7	2.8	51	36
Conv.	C	4100	164	13.5	—		65	7	2.8	51	37
	D	3700	166	13.5	25.7	▽	67	—	2.8	51	36

Rubber

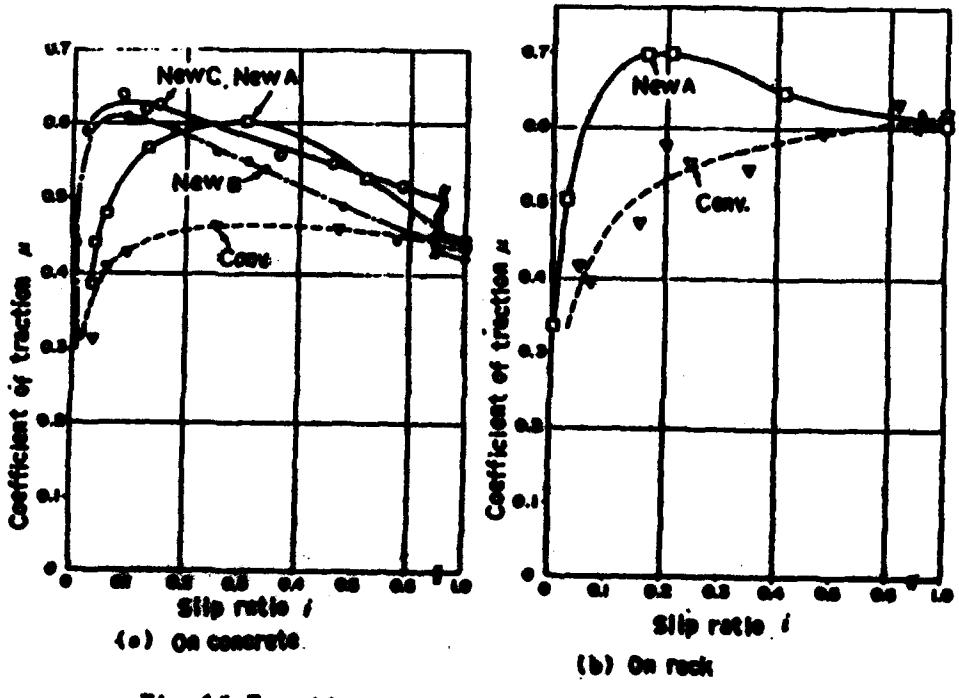

Fig.15.Traction performance of new crawler

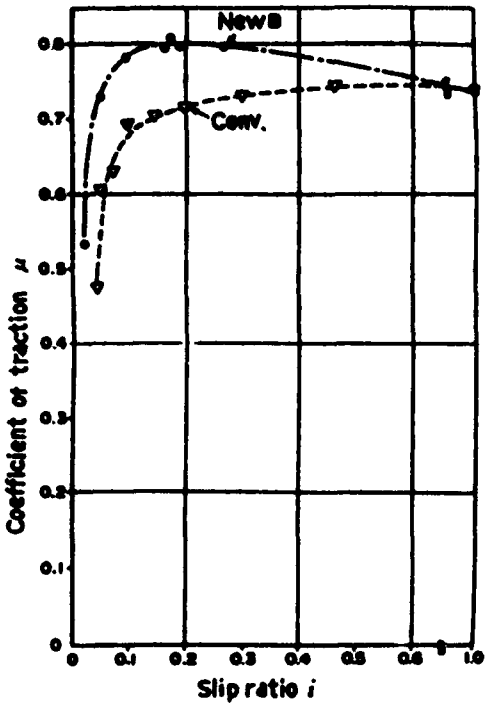

(c) On loam

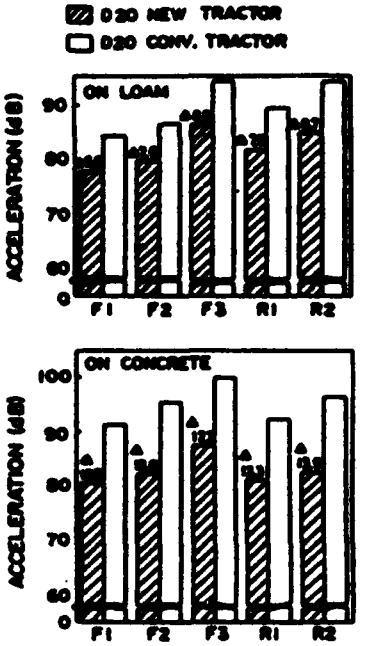

Fig.16. Acceleration of vibration at operater's seat

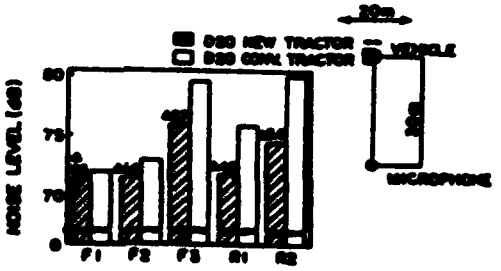

Fig.17. Noise level

OTHER ATTRACTIONS OF THE NEW CRAWLER

The vibration and noise at the operater's seat of the new crawler is measured and compared with that of conventional crawler in Fig.16 and 17 respectively. It is also confirmed that the new crawler reduces the vibration and noise considerably.

CONCLUSION

Authers improve the traction performance of tractor by eliminating unfavorable phenomena for traction from crawler. The new crawler also reduces dynamic load, hence, is dependable. And on the process of this research, unfavorable phenomena of crawler are clarified. By taking those facters into account, the prediction of traction and slipping under given soil condition is carried out with much better accuracy. This will be reported on another opportunity.

NOISE REDUCTION IN THE TERRAIN-VEHICLE T 11

V. TANDARA, DR.-ING.

TECHNICAL CONSULT AND EXPERT, D-1000 BERLIN 19, POSTFACH 1323

1. Introduction

Noise has negative effects on the human organisms, i.e. it reduces the capability for work. Permanent exposure to traffic noise can probably increase the cardiovascular risk /1/.

There is an increasing tendency of tightened up legal prescriptions for noise reduction in order to improve the steadily deteriorating quality of life. Vehicles are the most important noise sources in the street traffic. To decrease their influence, lower limiting values for the external noise of vehicles are aimed at. In the second half of the eighties the external noise of utility cars in Europe will be limited to 80 dB(A). These limits are low and will not without difficulties be achieved in all motor-vehicles, especially not in utility cars (lorries and buses, but terrain-vehicles as well). This is not only a result of the situation in the driving aggregate, the combustion engine, but in other direct and indirect noise sources too.

In the vehicle the driver and the passengers are subject to noise, that is why efforts are made to achieve the lowest possible values of inner noise. At the moment, only laws exist which limit the level of noise at the place of work, that is the driver's seat.

2. Description of the terrain-vehicle T 11

The terrain-vehicle T 11 has three axles and is designed for the transport of people and different materials up to an overall tonnage of 5000 kg. The fully loaded vehicle can easily move on regular streets and heavy ground. The ground can be soft, swampy, snowed up or sandy. For this reason the T 11 has a pneumatics with which the tyre pressure can be changed between 0,7 and 3,5 bar in a very short time. The front and rear tyres are of the same type.
The T 11 works at an outside temperature from 243 K to 313 K. It can move through water with a depth of one metre. The maximum speed of the terrain-vehicle T 11 is 92 km/h on the street. It can haul a trailer up to an overall weight of 5000 kg.

The driving aggregate of the vehicle is the six-cylinder, four-stroke, air-cooled V-Diesel engine F 6L 413 V with direct injection.

The engine output is transmitted by a dry single-plate clutch, a five-gear synchromesh transmission, a two speed transfer box for on-the-road and cross-country gear, cardan shafts and

final drives.

The chassis consists of two U-side-rails which are connected with crossbeams. All three axles are connected with the chassis by leaf springs, rubber bufflers and hydraulic shock absorbers. They grant, together with the elastic chassis, a good adaptation of the vehicle on any ground.
The vehicle has a hydropneumatic two-circuit brake, a handbrake, and an engine brake.
The terrain-vehicle is equipped with a hydro-servo-steering.
There is an open and a closed type of the vehicle cabin. The platform has a canvas cover. A closed superstructure may be installed instead of the platform.

The most important data of the terrain-vehicle are given in Table 1.

Table 1: Technical data of the terrain-vehicle T 11

Denotation	Dimension	
overall length	mm	~ 6060
overall width	mm	~ 2270
overall hight (unladen)	mm	~ 2470
effective length of the platform	mm	~ 4420
effective width of the platform	mm	~ 2120
payload on the ground	kg	3000
on the road	kg	5000
number of gears		5
electric equipment	V	24
tyres		12.00-18 PR 10

The technical data of the Diesel engine F 6L 413 V are given in Table 2.

Table 2: Technical data of the air-cooled, six-cylinder V-Diesel engine F 6L 413 V

Denotation	Dimension	
automotive rating to DIN 70020	kW	110.2
at a engine speed of	1/min	2650
number of cylinders		6
displacement	cm^3	8482
cylinder bore	mm	120
stroke	mm	125
max. engine speed at idle running	1/min	2830
max. torque	Nm	491
at a engine speed of	1/min	1400
average effective pressure	bar	5.89
compression		18
mean piston speed	m/s	11.04
length	mm	990
width	mm	1180
hight	mm	935

This engine is not only installed as a driving aggregate in

the terrain-vehicle T 11, but in buses and lorries as well. Additionally it is used with reduced engine speed as an aggregate motor.

3. Noise sources of the terrain-vehicle T 11

The most important noise sources of the terrain-vehicle are:
- the driving aggregate
- the transmission
- the rolling noise of tyres
- the vehicle body
- the noise of air on the surfaces of the vehicle and in the ports.

3.1 Noise sources of the driving aggregate

In a driving aggregate, here a Diesel engine, are:
- inner and
- external noise sources.

The most important inner noise sources are:
- the combustion
- strokes of the piston
- the motor control
- the driving wheels etc.

The external noise sources are:
- the suction system
- the exhaust gas conduct
- the cooling fan
- the motor surface
- the motor brake
- the auxiliary aggregates etc.

Although a number of noise sources are mentioned, their influence on the noise level of the engine will differ. One or another noise source can be more prominent. Then a higher expense of labour will be necessary to reduce its influence. This leads to the conclusion that there can be no universal solution which would have the same results in all combustion engines. As an example a comparison between a suction engine and an engine with a precombustion or turbulence chamber might serve. The combustion pressures in the engines are different and so the influence of the combustion pressure will be different. The different combustion pressures inevitably cause different intensities of the strokes of the piston in the working cylinder /2/.

3.2 Transmission

The transmission is an important part of the terrain-vehicle T 11. It consists of a mechanic synchromesh gear, a transfer box, cardan shafts and the final drives which are installed over the overall length of the vehicle. In all these parts different cogwheels and bearings are noise sources. Similar to combustion engines, the noise level of a gear depends on the speed, the performance, the production and the accuracy of manufacture /3,4,5/. Then this holds true for the transfer box as well. The influence of the transmission is stronger, when the external noise of the terrain-vehicle is below 85 dB(A) and the inner noise below 80 dB(A). The influence of

the gear and the transfer box can be direct or indirect. It is direct, if they themselves are noise sources as a result of high strain, indirect, if by the chosen gear the driving aggregate runs at propititious or nonpropititious speed.

3.3 Rolling noise of tyres

The rolling noise of tyres is made by the tyres and depends on the speed of the vehicle. In the terrain-vehicle T 11 it is caused by six big tyres with coarse tyretread and a large plane of contact on the road. In this connection one has to take into consideration the influences of the quality of pavement and the direct surroundings of the road.

3.4 Vehicle body

The lower part of the driver's cabin and the platform are made of sheet-steel. The cabin roof consists either of plastics parts or of a canvas cover. If the weather-conditions make it necessary, the platform as well can be covered with a canvas cover. Although the whole structure of the terrain-vehicle is sturdy, it could not be avoided that, especially on uneven ground, uncomfortable noise appears. This is considerably increased by the construction of such a type of vehicle.

3.5 Noise on the surfaces of the terrain-vehicle

One must not ignore the noise which appears on the surfaces of the terrain-vehicle and in the ports for the cooling of the engine. This plays an important role, because terrain-vehicles are generally built nonpropititions to air streams. Many salient corners of the vehicle body and even the canvas cover become unpleasant noise sources at higher travelling speed or strong streamings of air. Generally, everything that has negative results on the value of resistance of the terrain-vehicle is a potential noise source.

4. Possibilities of noise reduction of the driving engine

For a long time combustion engines as driving aggregates had been regarded as the most important noise sources of motor vehicles. This was less because their noise level could not be reduced, but because the existing limiting values admitted such a high noise level of engines. This situation might be compared with the problem of the emission of pollutants in the exhaust gas or the high fuel consumption of combustion engines. When it became necessary, the emission of pollutants and the fuel consumption of engines have been remarkably reduced. This is similar to the noise reduction. Because of high nondeductible costs this improvement in quality could not be carried out earlier.

A necessary noise reduction of the driving engine in the terrain-vehicle can be achieved by a noise reduction of single inner and external noise sources of the engine /6,7/, as well as by its complete encasing /8,9/. A complete encasing of the engine can only diminish the influences of the inner noise sources of the combustion engine, of its surface, and of the auxiliary aggregates. The influences of the external noise sources have to be solved additionally.

4.1 Inner noise sources of the combustion engine

4.1.1 Combustion

Every combustion in a reciprocating engine is accompanied by a sudden increase of pressure that leads to a formation of primary gas powers. These powers act on the cylinder wall and the cylinder head. Their intensity increases the higher and steeper the increase of pressure is. For instance, in a one-cylinder Diesel engine an intensity of combustion up to 90times of the acceleration due to gravity was registred on the cylinder wall /2/.

4.1.2 Strokes of the piston

Besides the primary gas powers, secondary powers owing to the effect of interia of moving parts of the driving apparatus lead to strokes of the piston on the cylinder wall. They are caused by piston slapping as a result of the piston clearance and desaxation. The intensity of the strokes of the piston depends mainly, besides on the forces due to mass, on the connecting rod proportion, the piston clearance, the piston length, the lucibrating film on the cylinder wall, and last but not least on the bearing clearance of the connecting rod on the piston axle end and the piston wrist. A detailed interpretation of these conditions is given in the study /2/.

4.1.3 Motor control

Parts of the control system of the combustion engine are:

- the cam shaft
- the tapoets
- the push rod
- the valve rockers
- the inlet and outlet valves with springs and
- the driving cogwheel on the camshaft.

The important noise sources are the inlet and outlet valves and the driving cogwheel of the camshaft. The valves steadily move to and fro and thereby strike metal surfaces. The intensity of the strokes depends on the lifting speed of the valves, the engine speed, and the length of the way the valves have to go. It is highly important that the control mechanism is well synchronized and any resonance on the valve stem guide is prevented. Here one mainly thinks about the spring where an ageing of the spring material can lead to an alteration of the characteristic curve of the spring. There are examples known where a reduction of the critical speed of 8% and great damages in engines were the result of the alteration of the characteristic curve of the spring /10/.

4.1.4 Driving cogwheels

The driving cogwheels of the crankshaft and of the auxiliary aggregates can be important noise sources. The camshaft and the oil-pump are driven by the cogwheel of the crankshaft. The noise of the cogwheels is caused by the influence of the variable forces, therefore, even with the highest accuracy of manufacture, certain sounds cannot be eliminated. It appears under the influence of the radial force P_p which effects the teeth of the cogwheels, the bearings and by them the engine

crankcase. As soon as the force changes, vibrations of the crankcase walls emerge and these are radiated by the outer surface. High strain leads to unavoidable deformations of the crankcase, the bearings, the crankshaft and the camshaft etc. and these are very important for the noise of cogwheels. The deformations lead to faults of meshing of the cogwheels.

The bending vibrations and rotary oscillations of the crankshaft can be high and cause, as it was the case in one type of engine, damages of the driving cogwheels, the crankshaft, and the oil-pump /11/. These vibrations had been the result of a lower stiffness of the crankshaft, its bearings and the crankcase.

One should only work on the inner noise sources of the driving engine, when all opportunities on the external noise sources are exhausted or when further development or new construction work of the engine is done. This is less the case because such work is difficult, but because of the high expense of time and costs in the following realization in series. Study /12/ reports extensive alterations of an engine which caused a noise reduction of the passing vehicle to values of 83-85 dB(A). Since work on the external noise sources was done simultaneously, it cannot with certainty be said which improvement can be traced back to the reduction of the inner noise sources. It is supposed that the changes made on the engine had the effect of a noise reduction of 3,5 - 4 dB(A).

5. External noise sources

5.1 Suction and exhaust systems

The noise of the suction and exhaust systems springs from the working medium exchange and is regarded as a result of the combustion of the gas-air mixture and of the streaming pulsations. The latter are caused by the periodical work of the systems for the supply with air and the carrying off of the combustion gases. The pulsating stream is, because of the flexible medium, always connected with a sound wave. It spreads in the pipe system of the exhaust as an overpressure wave and in the suction system as a low pressure wave with a level wave front and in free air in the first approximation as a ball wave.
The suction and exhaust noise is reduced by sound absorbers. In most cases higher attention is paid to the exhaust muffler. Most likely this is done because of the higher sound pressure in the exhaust system. But the noise of the suction system of installed engines can, in spite of its lower sound pressure, influence the inner noise of vehicles very badly. This mainly depends on the layout and the fitting of the suction system. The negative influence of the suction system especially in the region of low frequency (at low engine speed) as soundpressure waves which cause an unpleasant feeling in the passengers.

5.2 The cooling fan

The cooling fan is installed to cool the engine. It may become an important noise source, especially if little attention in its design has been paid to the stream conditions in it or in the inlet and outlet. Such a situation can arise, if the layout speed of the fan proves inadequate and has to be in-

creased by a new gear ratio. Every increase of the numbers of revolutions simultaneously means an increase of the circumferential speed of the fan blades. The stream conditions in the inlet and the outlet and those in the fan change. By an alteration of these conditions the noise of the fan increases too. The noise or the frequency spectrum can be influenced, besides by construction alterations of the fan and the blades, by altering the number of blades or their arrangement.

5.3 The motor surface

The noise on the motor surface has its origin in the inner noisesources of the engine. The influence of the motor surface on the noise depends considerably on its conception, its design, and its properties of material.
On the basis of many experiments on vehicles and engines as well as the achieved noise reduction in vehicles and engines /3,6,7,9/ could be recognized that the influence of the surface had not been that important. The external noise level of these vehicles according to ISO was nevertheless about 80 dB(A).

5.4 Auxiliary aggregates

Among the auxiliary aggregates, the compressor has to be mentioned above all. The noise of it is caused by the control elements and might be compared with the noise of the suction and exhaust systems. This noise especially appears at low engine speed and can increase the total noise of the engine considerably. The switchings on and off are especially disadvantageous, they can lead to resonances in the case of badly harmonized conditions at the chassis and the car body.

6. Carried out tests

As long as there had been high limiting values of the external noise of vehicles, it was possible to ignore some noise sources because the level of other noise sources was very high. The situation is changed in vehicles in which the external noise has been reduced. The influence of the overloud noise sources of the driving engine has been eliminated in those vehicles, thus an additional noise reduction of the vehicles could only be achieved by working on other noise sources. The aim of all efforts was to achieve external noise values of 80 dB(A), a value which will be in force for utility cars in Europe in the second half of the eighties.

What 80 dB(A) mean can be seen by the fact that if there were only four most important noise sources of a vehicle none must have a higher noise level than 74 dB(A). After all, two noise sources of the same intensity cause an increase of noise of 3 dB(A). Supposing that the driving engine F 6L 413 V had only eight noise sources, none of them must have a higher noise level than 71 dB(A), if the noise level should be limited to 80 dB(A). If there are 16 different noise sources, which is more probable, the noise level must not be higher than 68 dB(A). At a lower noise level of the engine, the level of the different noise sources has to be lower in proportion.
From the number of noise sources can be seen that below a certain noise level improvements of single noise sources are hardly recognizable. This makes noise reduction very difficult.

Additionally, other noise sources have to be taken into consideration. These are above all:

- the engine cooling
- tolerances of measurement.

In connection with the engine cooling one thinks of the fan of the engine. Its speed does not only depend on the temperature of the engine, respectively the oil temperature, but on the outside temperature as well. The mass of air and not the volume of air is decisive for the cooling of the engine. That means that according to the outside temperature, a remarkable difference may be in the necessary volume of air, i.e. the fan speed. In the case of the tested engine, special working conditions (303 K outside temperature) make additional 58% volume of air necessary, compared with the outside temperature of 273 K. But a larger quantity of air does not only mean a higher speed of the fan, but a higher velocity of flow too. Higher velocities of flow, not only inside the fan but on the cooling surfaces of the engine as well, are accompanied by higher losses of pressure in the cooling system. The varying working conditions necessarily influence not only the noise level of the engine but the fan performance too.

In connection with the tolerances of measurement one thinks not only about the tolerances which are a result of the accuracy of manufacture of the measuring instruments, but mainly about the influences of the outside and engine temperature which can cause different fan speed at the same engine speed. Thus certain differences of the noise level of the engine can appear.

7. Extent of made alterations

Before it was possible to make noise reduction, necessary extended measurements had to be carried out on the terrain-vehicle T11. The influences of different noise sources could be estimated by an analysis of the results of measurement and the possibilities of their reduction could be discussed. Before one thinks about extended alterations, it is advisable to analyse in how far a noise reduction of a vehicle or a driving engine may be achieved by simplest means.

After thorough consideration we came to the conclusion that firstly work should be done on the driving engine, i.e. on its external noise sources. This is especially so, because with the same type of engine, but with changed characteristic values, good results could be achieved in other vehicles /6,7/. By working on the suction and exhaust systems of the engine, its cooling, on the engine compartment etc., but without encasing the engine, the external noise of the passing vehicle could be reduced to values according to ISO of 80-81 dB(A) and the inner noise to values of 70-75 dB(A) in coaches, buses and suburban traffic buses. These alterations can be realized in series very quickly and without much effort.

There were the following possibilities on the terrain-vehicle T 11:

- the reduction of the influences of the exhaust system
- the reduction of the influences of the suction system
- alterations of the engine compartment

- alterations of the tiltable cabin
- the reduction of the influences of the cooling fan
- the reduction of the direct and indirect influences of the driving engine on other parts of the vehicle (resonances etc.).

A reduction of the influences of the exhaust system is possible between the exhaust collectors and the end of the exhaust gas pipe. Much can be achieved by the installation of a more effective exhaust muffler. But the loss of pressure in the system must not be higher than the allowed values, because this would cause, among other things, a reduction of the engi output. The influence of the exhaust system on the measured noise level of the vehicle was not so important, because the noise level of other noise sources was higher.

The suction system mainly influences the inner noise level, because it is installed below the tiltable cabin. It consists of two suction collectors, two air filters and the necessary pipes. Because originally no suction sound absorber had been planned, by a reconstruction of the suction system which now has a bigger air filter, a suction sound absorber and an appropriate layout of pipes, positive results could not only be achieved concerning a noise reduction but concerning the engine output and the increase of the moment of rotation (torque) of 3-5% too /13/.

Only smaller alterations have been made in the engine compartment. For instance, aprons with absorbtion material were installed at the sides of the engine, and the opening on the back-wall of the tiltable cabin was slightly diminished.

8. Results of measurement

In the tests a terrain-vehicle T 11 with a cabin roof of plastics parts and without a platform was used. The inner and external noise of the vehicle was measured before and after alterations had been made.

The measurements of the inner noise in the vehicle cabin were taken according to DIN 45639 and of the external noise according to ISO. The different measured values were put into a diagram and connected with another. In almost all diagrams the measured values of the original condition and the final condition are given. The original condition is the terrain-vehicle with a cabin roof of canvas cover, the interim and final condition mean the tested vehicle with a cabin roof of plastics parts.

9. Inner noise

The level of the inner noise in the vehicle cabin was measured in the standing and moving vehicle on the driver's seat and above the driving engine. In the standing vehicle the measures were taken in relation to the engine speed, in the moving vehicle in relation to the vehicle speed and to the gear.

Figure 1a gives the measured values in the standing terrain-vehicle T 11 on the driver's seat in relation to the engine speed. In all phases an almost linear rise of the noise level

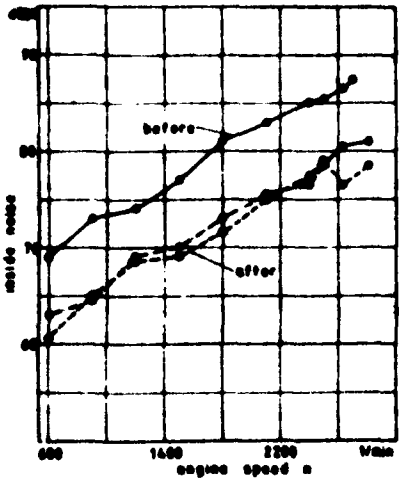

Fig 1a: Noise of stationary terrain vehicle T11, driving seat

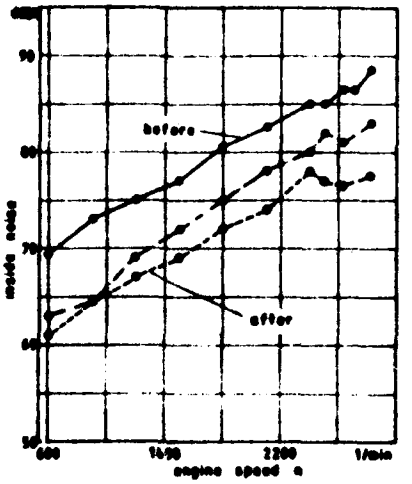

Fig.1b: Noise of stationary terrain vehicle T11, above engine

can be observed at increasing engine speed. A deviation happens in the final condition at an engine speed between 2400-2500/min, which is a result of resonances. An improvement between 5,5-9,5 dB(A) can be stated in the whole range of engine speed. At the maximum engine speed of 2830/min the noise level has been reduced from 87 dB(A) to 78,5 dB(A) and at idle running at 600/min from 69 dB(A) to 60,5 dB(A). Similar results were observed in the cabin above the driving engine, Figure 1b. In comparison with the results on the driver's seat, here a greater improvement could be achieved than it had been in the interim condition.

Figure 2a gives the noise level in the driving terrain-vehicle on the driver's seat. The noise level of the vehicle moving by engine drive was measured in the fifth gear. For the sake

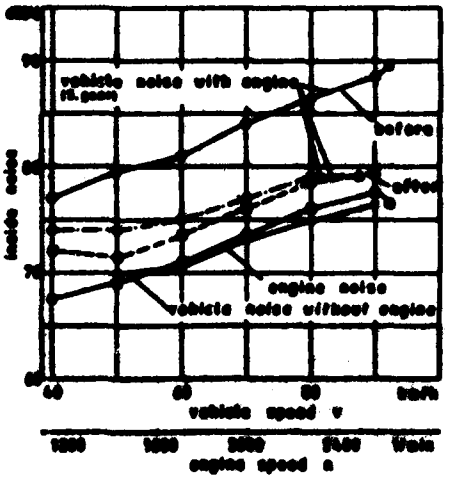

Fig.2a: Noise of terrain-vehicle T11 in motion, driving seat

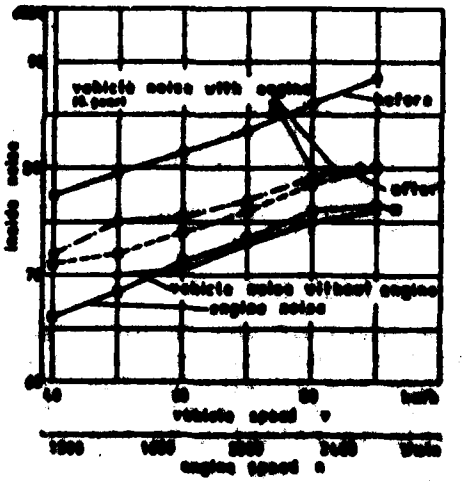

Fig.2b: Noise of terrain-vehicle T11 in motion, above engine

of comparison, the noise level of the driving engine at the corresponding vehicle speed is given. The linear rise of the noise level with increasing vehicle speed, i.e. increasing engine speed, is here evident too. At all vehicle speeds a remarksble noise reduction between 6-9 dB(A) has been achieved. At a vehicle speed of 40 km/h the noise level could be reduced from 77 dB(A) to 72 dB(A), at 92 km/h from 89,5 dB(A) to 79,5 dB(A). In all driving ranges the noise level of the engine was about 2-4,5 dB(A) less than that of the vehicle. The noise of the engine was only 1-1,5 dB(A) higher than that of the vehicle without engine.

Therefore can be seen that the increased noise of the vehicle is not only a result of the driving engine but of other influences as well. These influences were at least as strong as that of the driving engine. Similar results were measured above the engine, Figure 2b. The noise level of the vehicle has been reduced in the whole driving range about 6-8 dB(A). The noise of the engine was about 3-5 dB(A) less than the noise of the vehicle and is almost the same than that of the vehicle without engine. This once more underlines the influence of other noise sources on the inner noise of a vehicle.

Figures 3a and 3b give the inner noise in the cabin of the moving vehicle in the different gears at maximum engine speed.

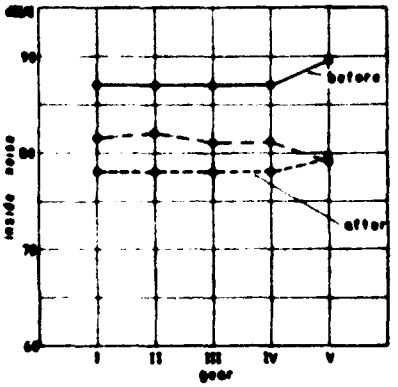

Fig.3a: Noise of terrain vehicle T11 in motion, driving seat

I,II,III,IV - engine speed 2830/min

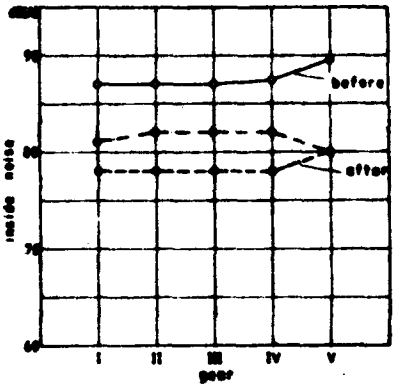

Fig.3b: Noise of terrain vehicle T11 in motion, above engine

I,II,III,IV - engine speed 2 830/min

In the first, second, third and fourth gear an engine speed of 2830/min was reached, in the fifth gear 2500/min in the interim condition and 2565/min in the final condition. In the first four gears the measured noise level is the same as the noise level of the engine. On the other hand, in the fifth gear the noise of the engine was about 2-2.5 dB(A) less, thus the higher noise level in the vehicle can be attributed to other influences. Here the rolling noise of tyres and the transmission mainly come to the mind. In the first four gears the influence of the rolling noise of tyres could not be important because of low vehicle speed.
The noise level in the whole driving range was 9-10 dB(A) less than in the original condition.

10. External noise

The external noise was measured on the standing vehicle. It was done at a distance of 7m and in relation to the engine speed. The distribution of measuring points is given in Figure 4.

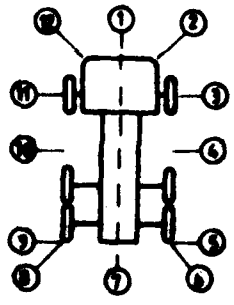

Fig. 4: Measuring points the external noise at a distance of 7m

Figure 5a and 5b give the measured values of the original, the interim and the final condition. The original and the interim condition were measured at a maximum engine speed 2830/min, Figure 5a, and the final condition at engine speeds of 2500/min and 2830/min, Figure 5b. At the maximum engine speed the noise level of the vehicle has been reduced about 1,5-6 dB(A). The greatest reduction could be measured in the front region, that is near the installed engine. There the highest values of 82 dB(A) were measured.

A reduction of the engine speed to 2500/min would lead to an additional noise reduction about 2-3 dB(A). The influence of the engine speed on the noise level of the standing vehicle is given in Figures 6 and 7. The measured values were taken on the measuring points 3 and 11, that is on the the driving engine, Figure 4. From this it can be seen that an almost parallel shift of the noise values about 4-6 dB(A) downwards has resulted in the whole range of speed. Maximum values of about 80 dB(A) were measured at the maximum engine speed.

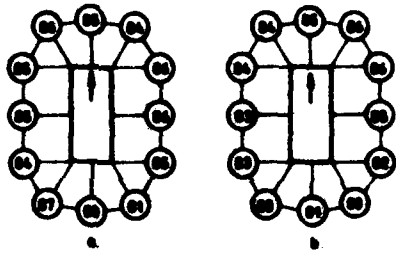

Fig. 5a: Noise of stationary terrain-vehicle T11 a distance of 7m, 110kW
a, b - engine speed 2830 1/min

Whereas in a standing vehicle mainly direct and indirect influences of the engine are measured, there will be other influences of a passing vehicle. In connection with the indirect influences one mainly thinks about the various resonances which are a result of the engine performance. The measurements of the passing terrain-vehicle were taken according to DIN at a distance of 7,5m from the roll axis of the vehicle.

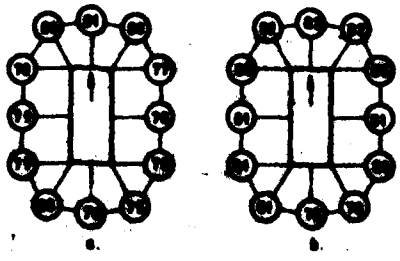

Fig. 5b: Noise of stationary terrain-vehicle T11 a distance of 7m, 110kW
a - engine speed 2500 1/min
b - engine speed 2830 1/min

Figure 8 gives the external noise of the terrain-vehicle with and without engine drive in relation to the vehicle speed(orig. condition). The noise of the vehicle without engine was measur. with the engine switched off and moving, notstationed trans-

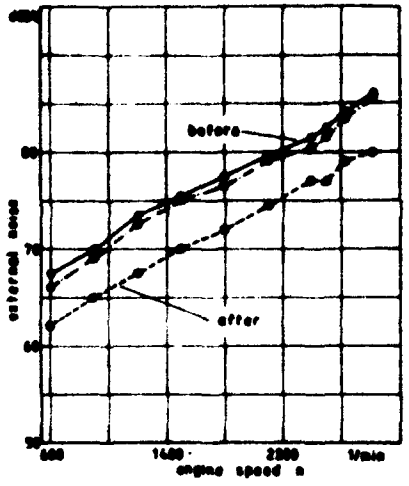

Fig. 6: Noise of stationary terrain vehicle T11, right side, point 3

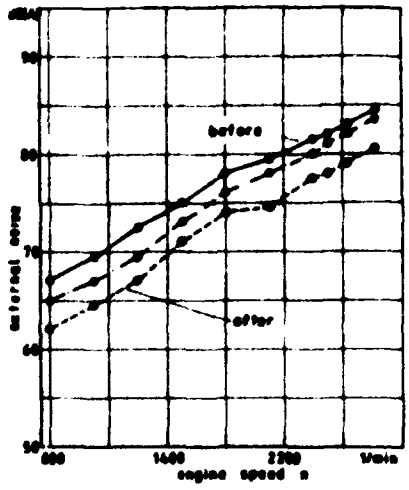

Fig. 7: Noise of stationary terrain vehicle T11, left side, point 11

nission which was driven by the wheels. The noise level of the terrain-vehicle without engine drive was higher than the noise of the combustion engine (final condition). At a vehicle speed up to 60 km/h the difference was 3,5-4,5 dB(A) and above 60 km/h 5-6,5 dB(A). At the maximum vehicle speed of 88 km/h a noise level of 82,5 dB(A) was measured.

From all these results can be concluded that the influence of the driving engine was not very high and certainly other influences have to be considered. Here the rolling noise of tyres and the transmission have to be mentioned.

The influence of the transmission is heightened because of the open design of the vehicle. It is especially high in lower gears at high engine speeds and under high strain. These results are as well shown in the measurements of the external noise of the passing vehicle in the third gear according to ISO, where a value of 85 dB(A) was taken.

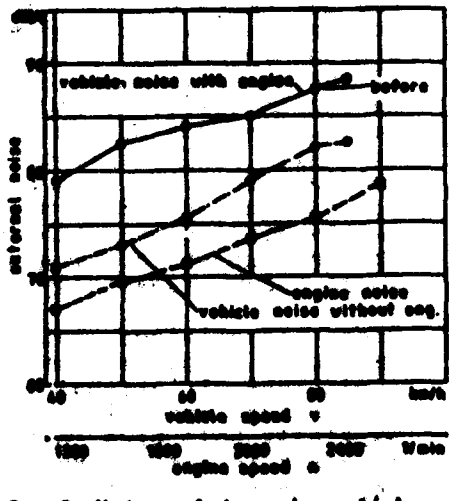

Fig. 8: Noise of terrain-vehicle T11 in motion

11. Possibilities of additional noise reduction of the terrain-vehicle

An additional noise reduction of the vehicle is possible, but can not only be achieved by a further reduction of the noise of the engine, but mainly by working on other noise sources

of the vehicle.

There are several possibilities for a reduction of the noise level of the engine, above all a reduction of the engine speed and alterations of the external noise sources of the engine. A complete encasing of the engine will hardly produce a remarkable improvement, which is proved by the results of the study / 9/. A real encasing of an engine means that the characteristic lines of the engine remain constant at the beginning and the end of the experiments. This is not the case in most of the works reported. Mostly other alterations are additionally made, only some of them shall be mentioned here. These are:

- speed reductions
- the installment of an supercharged engine
- alterations of the external and internal noise sources etc.

Supercharging means that an engine with the same output but lower speed is installed. This has necessarily effects on the noise level. Positive results of these alterations are completely attributed to the motor encasement. This is not founded on facts and has led to a wrong estimation of the whole situation of vehicles and to a determination of limiting values for the external noise of utility cars which in reality can not or only under greatest efforts be achieved. It could especially be studied in the case of buses that the limiting values aimed at for the second half of the eighties could not be kept. That is why they have again been increased from 80 dB(A) to 83 dB(A). It is said that the reason for it lies in the influence of the transmission which cannot be argued straight away. The studies /3,6/ have commented on this fact. A motor encasement produces no remarkable reduction of noise of the engine because all external noise sources of the engine remain unaltered and the noise level of the engine increases as a result of a higher operating temperature and a more intensive performance of the cooling fan. Moreover, a motor encasement is the most expensive solution and gives rise to a lot of other problems which have to be regarded. These are mainly difficulties that arise in repairing and the proneness of the complete cooling system of the engine. The problems would become especially apparent in series cars.

There are opinions that state a fuel saving as a positive result of a complete encasement. But this is said under wrong conditions. Frictional losses of the engine would be kept low by constant operating temperatures. This opinion can only partially hold true in the cold season and short drives with frequent interruptions, whereas at a higher surrounding temperature a more intensive performance of the cooling fan can be expected. The more intensive performance of the cooling fan does not only mean a higher noise level but an increased fuel consumption of the engine as well. The disadvantages of a motor encasement are now recognized by other authorities too. This is shown by existing solutions where additional ventipanes are installed to protect the engine from overheating. Regularly, the noise level of these vehicles had to be measured with open ventipanes. But in a normal test the engine will hardly heat up to a degree where the ventipanes open automatically.
It is known that a reduction of the fuel consumption can be

achieved my minimizing the value of resistance of the vehicle. A lining of the lower parts of the engine would prove useful. But this result can as well be achieved without a motor encasement, if the front part of the vehicle is modelled with more care than it is now usual.

12. Conclusions

The inner noise of the standing terrain-vehicle T 11 at maximum engine speed has been reduced to 78,5 dB(A) and the external noise to about 80 dB(A). The values of the inner noise remained in the moving terrain-vehicle at maximum engine speed in all gears below 80 dB(A). This noise level in a cabin of such a type of vehicle is low.

The external noise level of the passing vehicle was according to ISO 85 dB(A). These values have been achieved on a vehicle without a platform by working on the external noise sources of the engine and by small alterations in the engine compartment. The alterations have not been carried out to the optimum. By an additional improvement of the alterations, with a platform and especially by small alterations of the transmission, a noise level of 82-83 dB(A) might be achieved at the same engine speed. But in this type of vehicle an additional noise reduction can only be achieved by reducing the influence of the transmission and other noise sources. A combustion engine encasement would hardly lead to an improvement of the condition.

13. References

/1/ H. Ising, Ch. Havestadt "Gesundheitliche Auswirkungen von Verkehrslärmbelastung", Bundesgesundhbl. 26, 3.3.1983

/2/ W.Pflaum, V. Tandara "Zur Kavitation an Zylinderlaufbüchsen von Dieselmotoren", MTZ 30(1969)3
also
W. Pflaum, V. Tandara "On the cavitation of cylinder liners in diesel engines", Scientific Information Consultants Limited, London, England,1969.

/3/ V. Tandara "Getriebe als Lärmquelle in einem Minibus A 6" 6th IFTOMM-Congress, Des. 15-20, 1983, New Delhi /I/.

/4/ VDI-Richtlinien 2159 "Getriebegeräusche", Beuth Vertrieb GmbH, Berlin und Köln.

/5/ H. Pettig "Dynamische Zahnkraft", Diss. TH München, 1955.

/6/ V.Tandara "Lärmminderung bei Nahverkehrsbussen und der Einfluß der Transmission", Jahrestagung der VDI-Gesellschaft Fahrzeugtechnik, 1978, Nürnberg. Fortschritts-Bericht der VDI-Zeitschriften Nr. 54, Reihe 12.

/7/ V. Tandara "Lärmminderung am Versuchsreisebus AS 3500 E", ATZ 81(1979)7-8.

/8/ H.K. Beuer "Geräuscharme Nutzfahrzeuge mit Motorkapselung", JUMV-Conference 1979, Bled /YU/.

/9/ V. Tandara,"Noise reduction of air-cooled Diesel engine F 6L 413 V", Inter-noise '83, 1983, Edinburgh /UK/.

/10/ V. Tandara, "Probleme im Steuerungssystem des Verbrennungsmotors X", 1972 / unpublished/.

/11/ V. Tandara, "Schäden an Antriebszahnrädern im Motor Y", 1973 /unpublished/.

/12/ I. Summerauer, N. Bösch, "Möglichkeiten aktiver Lärmbekämpfung an Fahrzeug-Dieselmotoren", Fisita-Congress 1978, Budapest.

/13/ V. Tandara, "Verbesserung der Leistung und des max. Drehmoments am Dieselmotor F 6L 413 V mit angepaßtem Saugsystem", Technika-Mašinstvo 26(1977)1, Beograd /YU/.